



University of Novi Sad
Faculty of Technical Sciences

DEPARTMENT OF GRAPHIC
ENGINEERING AND DESIGN

GRID
2012

6TH INTERNATIONAL SYMPOSIUM ON
GRAPHIC ENGINEERING AND DESIGN
www.grid.uns.ac.rs/symposium/grid2012.html

Proceedings - The Sixth International Symposium GRID 2012

Publisher:

FACULTY OF TECHNICAL SCIENCES
DEPARTMENT OF GRAPHIC ENGINEERING AND DESIGN
21 000 Novi Sad, Trg Dositeja Obradovića 6

Editorial committee:

PhD Dragoljub Novaković
PhD Igor Karlović
MSc Sandra Dedijer

Technical secretary:

MSc Gojko Vladić

Editor:

PhD Dragoljub Novaković

Layout and production:

GRID team

Print:

Futura, Novi Sad

Circulation:

300 copies

CIP - Каталогизacija у публикацији
Библиотека Матице српске, Нови Сад

655(082)
7.05:655(082)

INTERNATIONAL Symposium on Graphic Engineering and Design GRID (6 ; 2012 ; Novi Sad)

Proceedings / 6th International Symposium on Graphic
Engineering and Design GRID 2012, Novi Sad, 15-16.11.2012. ;
[organizer] Faculty of Technical Sciences, Department of
Graphic Engineering and Design, Novi Sad ; editor Dragoljub
Novaković . - Novi Sad : Fakultet tehničkih nauka, Grafičko
inženjerstvo i dizajn, 2012 (Novi Sad : Futura). - 320 str.
: ilustr. ; 29 cm

Tiraž 300. - Bibliografija uz svaki rad.

ISBN 978-86-7892-457-6

1. Faculty of Technical Sciences (Novi Sad). Department of
Graphic Engineering and Design
а) Графичка индустрија - Зборници б) Графички дизајн - Зборници

COBISS.SR-ID 275040263



GRID 2012

UNIVERSITY OF NOVI SAD
FACULTY OF TECHNICAL SCIENCES
DEPARTMENT OF GRAPHIC ENGINEERING AND DESIGN

6TH INTERNATIONAL SYMPOSIUM ON
GRAPHIC ENGINEERING AND DESIGN

PROCEEDINGS

November 15-16, 2012
Novi Sad, Serbia

Scientific Committee

Prof.PhD Wolfgang Faigle, *HDM, Stuttgart (GER)*
Prof.PhD Thomas Hoffman-Walbeck, *HDM, Stuttgart (GER)*
Prof.PhD Malferd Werfel, *IFRA, Darmstadt (GER)*
Prof.PhD Mladen Lovreček, *Faculty of Graphic Arts, Zagreb (CRO)*
Prof.PhD Miroslav Gojo, *Faculty of Graphic Arts, Zagreb (CRO)*
Prof.PhD Diana Milčić, *Faculty of Graphic Arts, Zagreb (CRO)*
Prof.PhD Diana Gregor - Svetec, *Faculty of Natural Sciences and Engineering, Ljubljana (SLO)*
Prof.PhD Tadeja Muck, *Faculty of Natural Sciences and Engineering, Ljubljana (SLO)*
Prof.PhD Marie Kaplanova, *Faculty of Chemical Technology, Pardubice (CZE)*
Prof.PhD Georgij Petriaszwili, *Warsaw University of Technology, Warsaw (POL)*
Prof.PhD Tome Jolevski, *Technical faculty, Bitola (MKD)*
Prof.PhD Erzsébet Novotny, *Faculty of Light Industry and Environmental Engineering, Budapest (HUN)*
Prof.PhD Csaba Horváth, *Faculty of Light Industry and Environmental Engineering, Budapest (HUN)*
Prof.PhD Livija Cvetičanin, *Faculty of Technical Sciences, Novi Sad (SRB)*
Prof.PhD Ilija Ćosić, *Faculty of Technical Sciences, Novi Sad (SRB)*
Prof.PhD Slobodan Nedeljković, *Academy of Arts, Novi Sad (SRB)*
Prof. Boško Ševo, *Academy of Arts, Novi Sad (SRB)*
Prof.PhD Vera Lazić, *Faculty of Technology, Novi Sad (SRB)*
Prof.PhD Miloš Sorak, *Faculty of Technology, Banja Luka (BIH)*
Prof.PhD Katarina Gerić, *Faculty of Technical Sciences, Novi Sad (SRB)*
Prof.PhD Dragoljub Novaković, *Faculty of Technical Sciences, Novi Sad (SRB)*
Prof.PhD Jelena Kiurski, *Faculty of Technical Sciences, Novi Sad (SRB)*
Prof.PhD Branko Milosavljević, *Faculty of Technical Sciences, Novi Sad (SRB)*
Prof.PhD Siniša Kuzmanović, *Faculty of Technical Sciences, Novi Sad (SRB)*
Prof.PhD Rossitza Velkova, *Printing Industry Union of Bulgaria, Sofia (BUL)*
Prof.PhD Salim Ibrahimfendić, *Faculty of Graphic Arts, Sarajevo (BIH)*
Ass.Prof.PhD Igor Karlović, *Faculty of Technical Sciences, Novi Sad (SRB)*

Organizational Committee

Dragoljub Novaković, *Faculty of Technical Sciences, Novi Sad (SRB)*
Živko Pavlović, *Faculty of Technical Sciences, Novi Sad (SRB)*
Igor Karlović, *Faculty of Technical Sciences, Novi Sad (SRB)*
Željko Zeljković, *Faculty of Technical Sciences, Novi Sad (SRB)*
Sandra Dedijer, *Faculty of Technical Sciences, Novi Sad (SRB)*
Magdolna Pal, *Faculty of Technical Sciences, Novi Sad (SRB)*
Nemanja Kašiković, *Faculty of Technical Sciences, Novi Sad (SRB)*
Uroš Nedeljković, *Faculty of Technical Sciences, Novi Sad (SRB)*
Ivan Pinčjer, *Faculty of Technical Sciences, Novi Sad (SRB)*
Ivana Tomić, *Faculty of Technical Sciences, Novi Sad (SRB)*
Neda Milić, *Faculty of Technical Sciences, Novi Sad (SRB)*
Vladimir Zorić, *Faculty of Technical Sciences, Novi Sad (SRB)*
Srđan Draganov, *Faculty of Technical Sciences, Novi Sad (SRB)*
Ivana Jurič, *Faculty of Technical Sciences, Novi Sad (SRB)*

Bojan Banjanin, *Faculty of Technical Sciences, Novi Sad (SRB)*
Irma Puškarević, *Faculty of Technical Sciences, Novi Sad (SRB)*
Rastko Milošević, *Faculty of Technical Sciences, Novi Sad (SRB)*
Jelena Vladušić, *Faculty of Technical Sciences, Novi Sad (SRB)*

Technical Secretary

Gojko Vladić, *Faculty of Technical Sciences, Novi Sad (SRB)*

Reviewing Committee

Prof.PhD Miroslav Gojo, *Faculty of Graphic Arts, Zagreb (CRO)*
Ass.Prof.PhD Sanja Mahović - Poljaček, *Faculty of Graphic Arts, Zagreb (CRO)*
Prof.PhD Csaba Horváth, *Faculty of Light Industry and Environmental Engineering, Budapest (HUN)*
Prof.PhD Diana Gregor - Svetec, *Faculty of Natural Sciences and Engineering, Ljubljana (SLO)*
Prof.PhD Tadeja Muck, *Faculty of Natural Sciences and Engineering, Ljubljana (SLO)*
Prof.PhD Marie Kaplanova, *Faculty of Chemical Technology, Pardubice (CZE)*
Prof.PhD Dragoljub Novaković, *Faculty of Technical Sciences, Novi Sad (SRB)*
Ass.Prof.PhD Igor Karlović, *Faculty of Technical Sciences, Novi Sad (SRB)*
Ass.Prof.PhD Živko Pavlović, *Faculty of Technical Sciences, Novi Sad (SRB)*
Ass.Prof.PhD Nemanja Kašiković, *Faculty of Technical Sciences, Novi Sad (SRB)*

WITH SUPPORT OF:

Ministry of Education, Science and Technological Development,
Republic of Serbia

Provincial Secretariat for Science and Technological Development,
Vojvodina, Republic of Serbia

Faculty of Technical Sciences, Novi Sad, Republic of Serbia

CEEPUS III RS-0704-01-1213

CO - ORGANISER:

Faculty of Graphic Arts, Zagreb, Croatia

EQUIPMENT AND MATERIAL DONORS:

KBA, Germany

Alois Carmine KG, Austria

Horizon, Germany

Perfecta, Germany

Flint Group, Germany

Foliant, Czech Republic

Dalim Software, Germany

StudioRIP, England

Merus, Slovenia

Rotografika, Subotica, Serbia

Forum, Novi Sad, Serbia

Systemic, Belgrade, Serbia

Centropapir, Sremski Karlovci, Serbia

TABLE OF CONTENTS

FOREWORD	11
----------------	----

INTRODUCTORY LECTURES

1. Horváth, C.: Lean and green printing ... Hit or Myth?	13
2. Novaković, D., Karlović, I.: Drupa and post Drupa trends in graphic arts technology in the time of economic crisis.	19

SPECIAL PRINTING APPLICATIONS AND MATERIALS

3. Đokić, M., Kavčič, U., Mraović, M., Pivar, M., Pavlović, L., Muck, T.: Printed passive electronic structures on recycled papers, cardboards and foils	29
4. Friškovec, M., Mandelj, T., Vasić Stepančić, Š., Klanjšek Gunde, M.: The influence of physical parameters on the dynamic color of thermochromic printing inks	37
5. König, S., Gregor-Svetec, D.: Optical properties and UV/VIS spectra of aged papers	45
6. Jašúrek, B., Vališ, J.: UV/EB Inks and varnishes in printing Industry	51
7. Krstić, J., Kiurski, J., Obadović, D., Oros, I., Cvetinov, M.: Absorption characteristics of magenta sheet-fed offset printing ink as an indicator of ink pollution	59
8. Možina, K., Rutar, V.: Modifying natural CaCO_3 to effect on quality of ink-jet prints	65
9. Novotny, E., Szentgyörgyvölgyi, R.: Examination of nanocomposites	69
10. Panák, O., Syrový, T., Szöllősiová, L.: Production of security printing patterns by means of thermochromic and conventional offset inks	77
11. Pashich, R., Andonovska, S., Markoski, A.: Changes of spectrophotometric characteristics of offset printing substrates under the external factors influence	85
12. Simendić, V., Vukić, N., Simendić, B.: The influence of printing inks viscosity on the colorimetric properties of screen printed samples	91
13. Syrový, T., Pál, M., Peřinka, N., Jašúrek, B., Vališ, J.: Electrical properties of printed conductive polymer layers	99
14. Vališ, J., Jašúrek, B., Panák, O., Svobodová, J.: Drying of UV and hybrid inks after inline varnishing.	107

PRINTING FORMES AND IMAGE CARRIERS

15. Cigula, T., Poljak, J., Peko, V., Tomašegović, T.: Sodium metasilicate solution as a developer for CtCP offset printing plates	115
16. Dedijer, S., Cigula, T., Novaković, D., Gojo, M.: The contact angle of reference liquids on flexographic printing plates as a function of time.	121

17. Hudika, T., Tomašegović, T., Mahović Poljaček, S.: Offset printing plates: alternative method for quality control	129
18. Mahović Poljaček, S., Tomašegović, T., Gojo, M.: Influence of UV exposure on the surface and mechanical properties of flexographic printing plate	135
19. Milić, N., Dedijer, S., Pal, M., Pavlović, Ž.: The statistical analysis of processing conditions' influence on the surface roughness of flexo printing plate	141

PRINT QUALITY

20. Balaban, P.: The significance of color and its color characteristics on printed flexible packaging.	153
21. Gazibarić, Z., Živković, P., Živojinović, D.: Determining the correlation between total hardness of water and spectro-densitometric characteristic of printing quality	157
22. Kašiković, N., Vladić, G., Milić, N., Avramović, D.: Influence of ink layers and different materials on the colour fastness to rubbing.	165
23. Stančić, M., Karlović, I., Jurić, I.: Influence of digitally printed self adhesive foils on print quality parameters.	171
24. Szentgyörgyvölgyi, R.: Printing of folding carton by digital technologies	179

COLOUR SCIENCE

25. Agić, D., Rudolf, M., Agić, A., Stanić Loknar, N.: Case study carbon black separation extended features	187
26. Gebeješ, A., Tomić, I., Huertas, R., Stepanić, M.: A preliminary perceptual scale for texture feature parameters.	195
27. Jurić, I., Karlović, I., Tomić, I.: The possibility of using G7 method for calibration and characterization of Xerox docucolor digital press	203
28. Samu, K., Veres, Z.: Comparison of industrial and non automated color calibration created color profiles.	209
29. Vladić, G., Kašiković, N., Avramović, D., Milić, N.: Colour differences of process colors as predictors of secondary mixtures, red, green, and blue in digital textile printing	213

DIGITAL AND WEB MEDIA

30. Avramović, D., Kašiković, N., Vladić, G., Zeljković, Ž.: HTML5 and SVG driven methods for data presentation in scientific publishing	221
31. Bareis, V., Artemieva, I., Dörsam, B., Hoffmann-Walbeck, T.: JDF-PDF preflight software	231
32. Hladnik, A.: Digital image compression using principal components analysis	237
33. Iskra, A., Možina, K.: Analyzing different elements of web galleries	243

34. Zorić, V., Milosavljević, B.: Digital publishing formats	251
---	-----

DESIGN AND TYPOGRAPHY

35. Nedeljković, U., Banjanin, B., Puškarević, I., Pinćjer, I.: Empirical findings on feature distinctiveness: legibility based on differentiation of characters	261
36. Nedeljković, S., Pinćjer, I., Nedeljković, U.: Principles of art nuovo and it's reflection on contemporary type forms	271
37. Pušnik, N., Možina, K., Podlesek, A.: Comparison of processing words presented at various positions on display	279
38. Radivojević, R., Pejić, S.: Communication through design: transfer of ideas - creation of context	285

PACKAGING AND ENVIROMENTAL PROTECTION

39. Adamović, S., Rajić, Lj., Prica, M., Milošević, R., Puškarević, I., Zorić, V.: Electrocoagulation/electroflotation treatment of offset printing developers	293
40. Milčić, D., Donevski, D., Šefer, M.: Assessing print production process capability	299
41. Milošević, R.: Mechanical models for creasing and folding behaviour of paperboard and cardboard: state-of-the-art	303
42. Pál, M., Koltai, L., Novaković, D., Dedijer, S., Draganov, S.: Characterisation of fold-crack resistance of coated papers by Tensile and Mullen burst test.	311
43. Prica, M., Dalmacija, B., Pešić, V., Milošević, R., Banjanin, B., Zorić, V., Adamović, S.: Possibility of using cardboard mill sludge in immobilization of copper from contaminated sediment	317

Foreword

Dear readers,

It is my great pleasure to introduce You the research papers of the Sixth Symposium on Graphic Engineering and Design. With this proceeding we continue the works of previous symposiums which have been held biennial since year 2002.

We're delighted that this international symposium has again a great number of the papers and participants coming from many countries.

The papers include the achievements of researches in the field of technology and scientific areas relevant to graphic technology and graphic design. Through the work of the symposium GRID we continued significant scientific cooperation with educational institutions all over the world, especially with the neighbouring countries in the region. With them we are continuing good cooperation which is the driving force for the creation and display of new developments, both individual and common.

I want to thank everyone who participated with their paper and presentation in the symposium. Your contribution is significant for the improvement of the Symposium on Graphic Engineering and Design GRID 12. The research achievements here presented are also valuable to the scientific and professional community and are highly appreciated.

Prof. PhD Dragoljub Novakovic

LEAN AND GREEN PRINTING ... HIT OR MYTH?

*Csaba Horváth, Óbuda University, Rejtő Sándor
Faculty of Light Industry and Environmental Engineering,
Institute of Media Technology, Budapest*

*Corresponding author: Csaba Horváth
e-mail: csaba.horvath@nyt.hu*

1. ABSTRACT

On commission of a packaging printing company, the author has launched a research work in order to find a methodology by which the necessary steps can be explored to turn the application of this modern technology into a business success. The lean manufacturing studies have primarily focused on the human-machine environment, analyzing all the activities that are connected with the operation and servicing of the machines. Step by step, the research has tried to expose those hindering factors, superfluous or less efficient organizational and management process elements that now increase costs. Today, profitable printing production is not feasible by means of price increases; the only expedient way to follow is to cut costs. In this respect, lean management can be supportive.

Keywords: *lean printing, lean and green strategy, improving value chain performance, sustainability*

2. OBJECTIVES OF THE RESEARCH

Even the procurement of brand new equipment or the provision of base materials of the highest standards is not a guarantee for the printing business to produce printed products of consistently outstanding quality at a profit. The struggle against electronic communication, the global economic crisis and the sharp competition with the existence of excess capacities put a pressure on printers. One should ensure quicker lead times for the products, offer regulated and cheap prices, and besides steadily excellent quality is to be maintained.

Printers tend to see the source of the growth of production and profit in new investments, which is mostly not true. It is not enough to buy modern printing machines, but they are to be operated with high efficiency in order to see the return of the investment. In the conventional approach, if the printing machine features high printing speed, then it will necessarily boast of significant efficiency and utilization rate. In fact, however, additional parameters should also be considered when the utilization rate and efficiency of a printing machine is examined. Such parameters include the setup time, the time loss, the generation of rejects, the competence level and certainly the speed of the machine.

It is a legitimate question how a favourable situation can be achieved, how we can generate more profit from the given production process?

Recently, a company manufacturing packaging materials (cardboard boxes) has purchased and commissioned new sheet-fed presses with state-of-the-art accessories. However, the expected profit has not been pocketed.

On commission of this company, we have launched our research work in order to find a methodology by which the necessary steps can be explored to turn the application of this modern technology into a business success.

Our studies have primarily focused on the human-machine environment, analyzing all the activities that are connected with the operation and servicing of the machines. Step by step, we have tried to expose those hindering factors, superfluous or less efficient organizational and management process elements that now increase costs.

3. RESEARCH METHODS

The exploration of the human-machine environment principally calls for the methods of organizational studies.

Google the words “Lean Printing” and you will find a wide range of advice on new manufacturing techniques and methodologies, which will allow your business to operate more productively,

more effectively, and more profitably. However, you may be disappointed with how much of what you find is new, or original – the reason being that the underlying premise of Lean is based on the principles of sound business sense, and these principles have been around a very long time. The following research explores what “Lean” is and how applicable. “

Lean management is a systemic methodology that identifies, eliminates all forms of losses, as well as all such activities that do not represent any added value for the customer, client. Its aim is to provide the product with ongoing drift and continuous added value. It perfects the process with which the business is able to satisfy the client’s demands; it improves production efficiency, and thus opens the way to the generation of further profit. In the past few years, the *lean* work methodology has been applied by several companies involved in graphic communication. As these companies have had hardships and witnessed varied successes in adopting the system, just little published experience is available.

At our printer client manufacturing packaging materials, we got down to implement the *lean* work methodology back in 2010. First, we structured the necessary knowledge base. We elaborated a system for the company as based on the *lean* work methodology, and called it the *SBS (step by step) way*. This method basically follows the *lean* thinking, but in a substantially simpler design. We considered the simplification of the system to be justified, because the company had not relied on such organizational methods before that would have at least been slightly similar to the *lean* system. We deemed the leap from the actual situation of the company to the desired position to be too large, and therefore we wanted to walk this considerable distance in smaller steps in order to avoid failure.

The *SBS way* program aims at the optimization of the printing process. The goal of the project is to improve the utilization rate of the printing machines, minimize time losses (faults, setup times), enhance performance (printing speed) and reduce reject sheets generated in production.

First, the reduction of the setup time and the number of the reject sheets generated in production was targeted. These were the fields where the necessity to transform the human–machine environment seemed to be the most obvious. In the framework of the investment, the company purchased such state-of-the-art technology whose application allowed the fastest possible setup times. Still, the system failed to operate with sufficient efficiency.

To cut setup times, the SMED (Single Minute Exchange of Die) method has been applied. When the setup process is optimized, in fact the following actions are taken:

- reduction of the number of steps/components to be completed,
- reduction of the number of setups,
- improvement of the accuracy of setups,
- reduction of the generation of rejects.

To clarify the setup time and unveil the processes, causes of the excess time demand, the Fishbone/Ishikawa Diagram was used (Figure 1).

The SMED makes a distinction between so-called external and internal operations that jointly form the setup process. Internal operations can be executed when the press is in standstill, for instance during the replacement of the die plate. External operations can be completed in the course of the printing of the actual copies, when the printing machine generates marketable products, for example during the preparations for the replacement of the die plate.

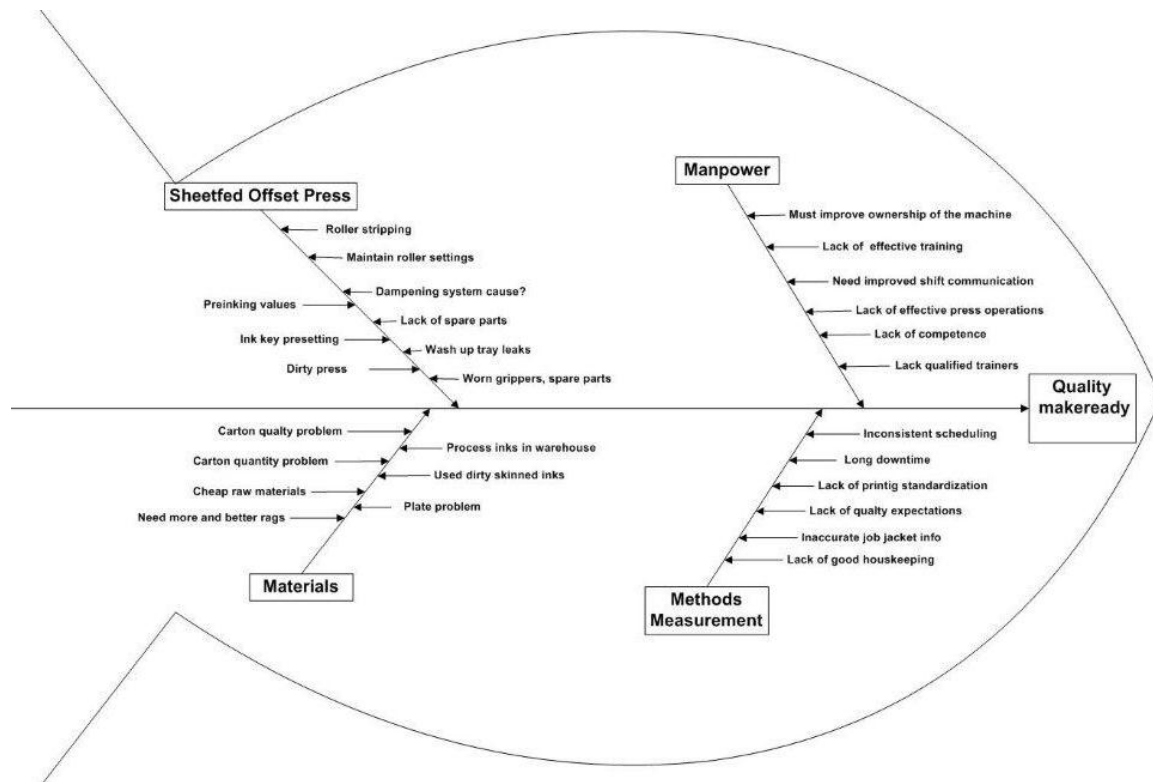


Figure 1: Makeready Fishbone diagram

The optimization of the setup time consists of three main phases:

- Phase 1: Separation of internal and external operations.
- Phase 2: Conversion of internal operations into external operations.
- Phase 3: Harmonization of all the elements of the setup operations.

To *separate internal and external operations*, the process of changeover was subjected to value stream analysis by way of making and evaluating a video recording. After the making of the recording, the video shots were replayed in the presence of the work team, each of the operations performed was identified, and they were also determined quantitatively (in terms of time). In addition to the video recording, a motion diagram was also compiled (Figure 2) in order to visualize and easily recognize losses.

During the conversion of internal operations into external operations, the following questions need to be answered in the light of the steps that have already been identified.

- What is the purpose of the operation?
- Why should the machine be in standstill to perform the actions?
- Is the operation convertible from internal setup to external setup?

We tried to form the largest possible number of operations in the external setup, as irrespective of the weight of the operation, thereby minimizing the time loss.

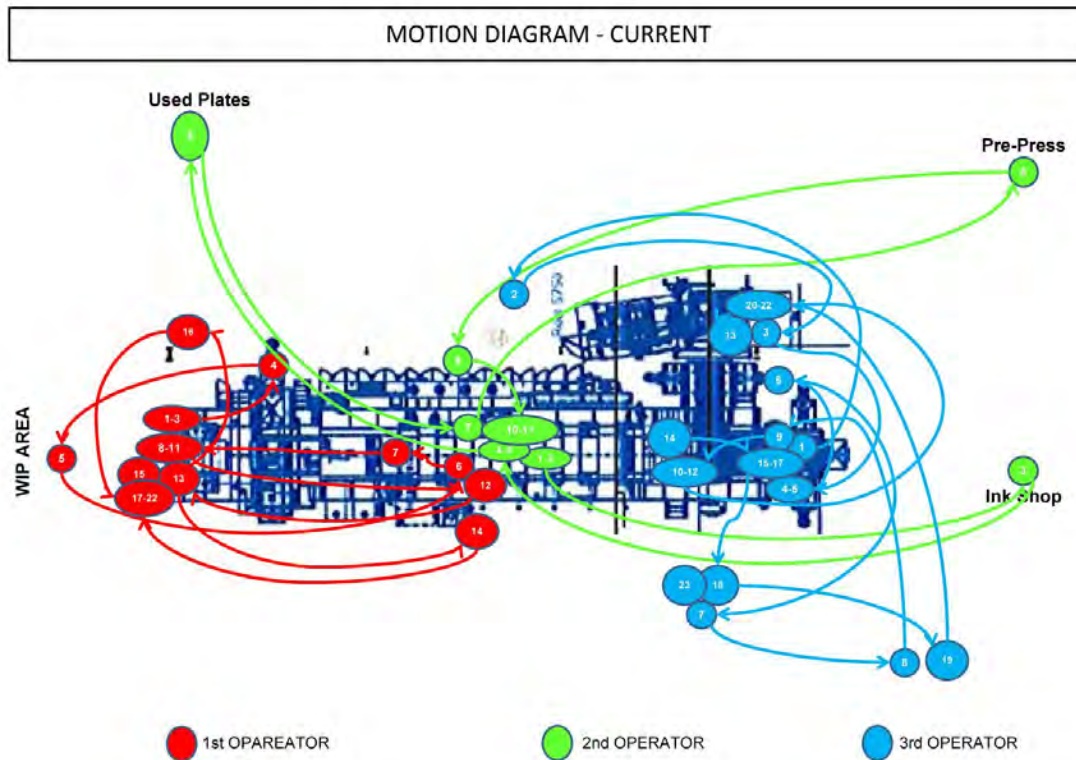


Figure 2: Spaghetti map - current

The steps included here are:

- documentation steps (completion of the work dossier),
- preparation of the die plate, bending, checking, preparations for the replacement of the plate,
- uploading, checking CIP3 data,
- interpretation of the work dossier,
- preparation of the lacquer form,
- preparation, unwrapping of the print carrier,
- preparation of detergents, materials,
- preparation of printing colours, etc.

Once we had a clear view as to which operations should be performed when and where, we started to *harmonize the operations* and simplify more complex steps. Conventional tasks, such as the development of the die plate and the machine washing process, did not result in considerable challenges, because the printing presses included in the target group feature a significant level of automation. On the other hand, the synchronization of the work steps of printing engineers proved to be a more difficult task. It brought about changes, and initially they were hardly accepted. Nevertheless, they recognized that if they were working as a team, more steps could be performed concurrently, in parallel. As they also watched the video recording, i.e. how they had been working, it was easier to convince them. The losses were shown before their own eyes. During the SMED project, merely joint team work contributed to the success, because the workers themselves planned work processes, and optimized their operations. Such difficulties were experienced as the differing competence levels. Certain printing engineers were capable of performing only certain steps, thereby deteriorating flexibility, but within the framework of the lean training program the differing competence levels could also be resolved. We tested the newly framed work processes in practice, with success. The same steps were taken by the printing engineers, but in a different order, and thus materially cut the time demand of setup (Figure 3).

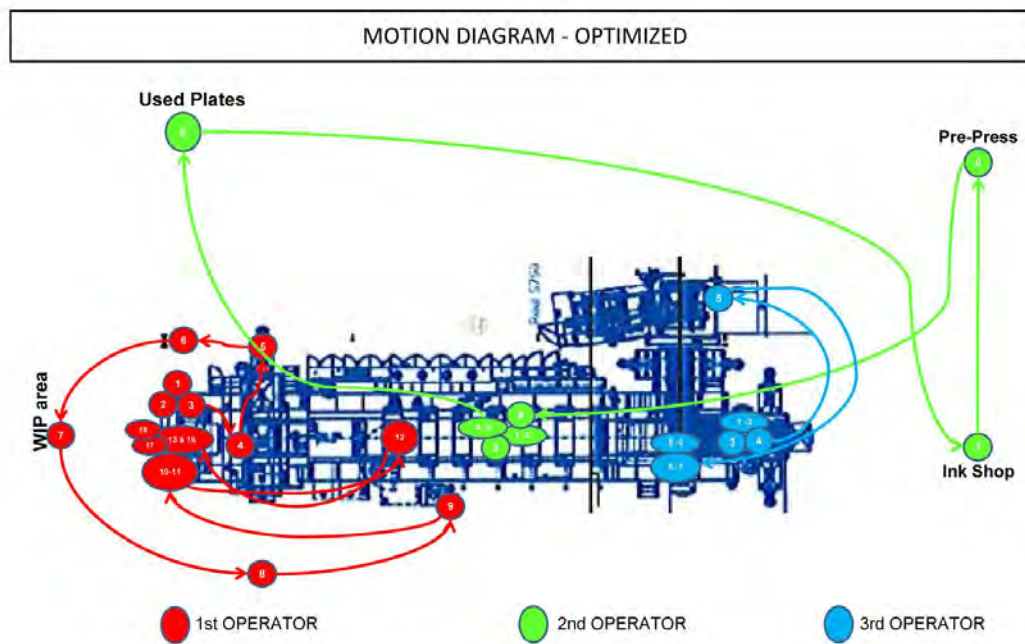


Figure 3: Spaghetti map - optimized

4. SUMMARY OF RESULTS

In 2011, the optimization of the printing process proved to be the key achievement in the life of the plant. Our aim has been accomplished, as the setup times and the numbers of reject sheets have been substantially reduced and permanently minimized (Figure 4). This Figure also shows that the problems associated with the speed of the machine and time losses are still to be tackled. However, it is again an outcome corresponding to our step-by-step approach. For the upcoming year, we should make progress in this latter field, as well. Our successes so far underline the efficiency of the application of *lean management*, and as a consequence there is rising trust in our researches and the related, practical organizational work.

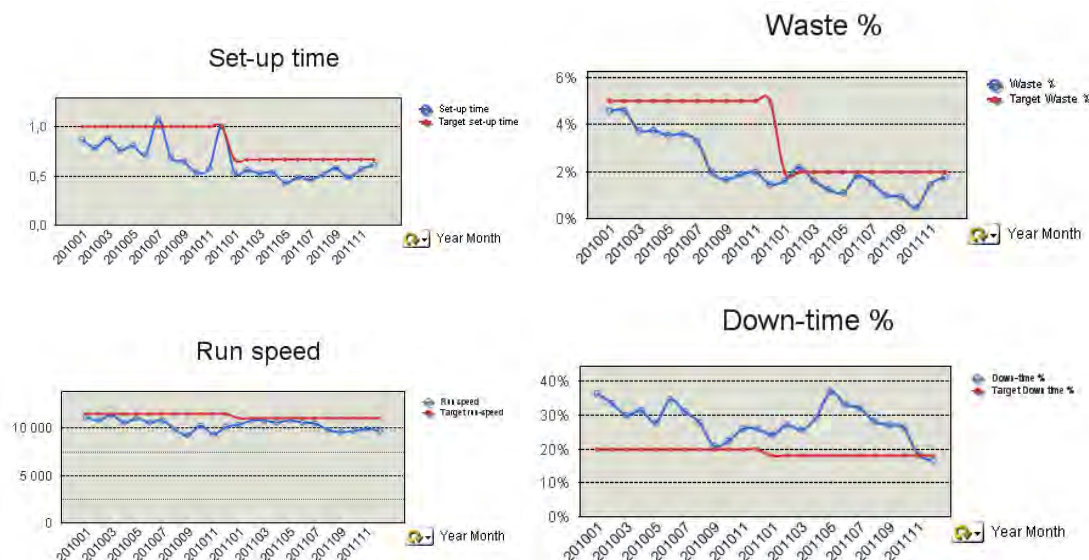


Figure 4: Utilization properties of the printing presses taken as the target group

5. CONCLUSION

Printing production is not feasible by means of price increases; the only expedient way to follow is to cut costs. In this respect, *lean management* can be supportive.

The *lean* simplification we have elaborated, i.e. the SBS (Step by Step) way method has proved its efficiency in making the first achievements, which demonstrates that the printing business is a proper scene for the application of the method, and further cost-cutting solutions can be expected from the continuation of the work.

6. LITERATURE

- [1] Cooper, K. - Keif, M. G.- Macro Jr. K. L.: "Lean Printing: Pathway to Success", PIA/GATFPRESS, Pittsburgh, , 2007, ISBN: 0-88362-586-5
- [2] Cooper, K.: Lean Printing: "Cultural Imperatives for Success PIA/GATFPRESS", Pittsburgh, 2010, ISBN: 9780883626887
- [3] Rizzo, K.E.: " Total production Maintenance: A guide for the printing industry", PIA/GATFPRESS, Pittsburgh, (3rd ed.), 2008, ISBN: 0883626209
- [4] Rothenberg, S. – Cost, F.: " Lean Manufacturing in Small- and Medium-sized printers" Printing Industry Center, 2004
- [5] Wells, N.: "Leaner & Greener, Value Chain" (presentation), Lean & Green, International Environment Conference, DRUPA, Düsseldorf, May 12, 2012
- [6] Weather, J.P.: "Lean & Green, Economic and Environmental benefits of Lean (presentation)", Lean & Green, International Environment Conference, DRUPA, Düsseldorf, May 12, 2012
- [7] Behringer, R.: Sustainability as a Success and Competitive Factor (presentation) Lean & Green, International Environment Conference, DRUPA, Düsseldorf, May 12, 2012
- [8] Wells, N. (ed.): "PRINT: seen lean & green", Book 1, PrintCity GmbH & o. KG, Gröbenzell, Germany, 2012
- [9] Wells, N. (ed.): "PRINT: seen lean & green", Book 2, PrintCity GmbH & o. KG, Gröbenzell, Germany, 2012
- [10] Keif, M.G.: "Setup Reduction for Printers: A Practical Guide to Reducing Makeready Time in Print Manufacturing, FLEXO, 2009 September, pp. 49-52.

DRUPA AND POST DRUPA TRENDS IN GRAPHIC ARTS TECHNOLOGY IN THE TIME OF ECONOMIC CRISIS

Dragoljub Novaković, Igor Karlović
Faculty of Technical Sciences, Graphic Engineering and Design, Novi Sad

Corresponding author: Dragoljub Novaković
e-mail: novakd@uns.ac.rs

1. ABSTRACT

The world still at financial crisis and many industries are trying to hold their positions. The printing industry as a service industry especially in Europe was also severely hit by the shrinking economy and aims to find new markets and possibilities in the changing world. Drupa as the prime trend show for the graphic arts with shrinking attendances showed some global megatrends and few surprises. Digitalization is a mega trend with possibilities to print packaging, RFID tags and personalized low print run jobs. Digital printing systems mainly based on electro photography and ink jet dominate the field while other sectors aim for maximizing the efficiency and automation. The main attraction of Drupa was the Landa nanography technology which promises some new ink application possibilities on a wide variety of substrates. This only proves that innovation and technological breakthroughs are the main driving forces for economical growth and problem solving. Also there is a clear trend of diversification of the printing industry where the written words are more and more reproduced by the digital media devices like tablets and on the other hand printing is used more and more for model making, electronic circuit printing and even human body parts printing with 3D bio printers.

Key words: *Drupa, nanography, digitalization, future trends*

2. INTRODUCTION

The printing and graphic arts industry was always a good indicator of the wider and deeper changes in our society. The rise of the newspapers with the industry revolution, the proliferation of books with the rise of literacy and newly the shift from printed to digitalized publications are best seen through the changes in the technologies used in the media and printing industry. The paralysation of the global economic system which is nowadays called the Great Recession (recession is defined as two quarters of consecutive contraction of GDP (Gross Domestic Products) off all sectors, print is perhaps hit the hardest by recessions. On one front, it is reliant on consumer confidence, GDP growth and the subsequent advertising investments made by large companies. On the other it is a manufacturing industry, reliant on bank lending to invest in equipment. For printers, the financial crisis was a perfect storm (Mitting, 2012). But before the economic crisis the printing industry had already some turmoil. This was due in part to the sudden and significant changes that have occurred industrially and economically. Prior to the current economic crisis, the printing industry had already been facing significant challenges. This was exacerbated by the fact that the print industry was already suffering when the downturn hit. Many companies in the sector had reacted slowly to the advent of the Internet and were operating business models better suited to the heyday of print with high overheads and often inefficient machinery and internal processes. Since then, advertising levels, retail sales and the performance of the business services and finance sector have all negatively impacted the printing industry and, thus, demand for commercial printing machinery. The printing industry is directly dependent on advertising, and thereby on the overall economy. Advertising products account on average for over 60 percent of print shop production. A glance at the capacity utilization of print shops in the US makes clear the considerable extent that companies cut back on expenditures during the crisis, especially in their advertising outlays. In the industrialized countries, this resulted in a historic low volume of expenditures. The transition to digital products has impacted this industry more than any other. Printed advertisements used to be the major medium. Today, advertisers are transitioning to digital formats, leveraging everything from the Internet to vending machines. Declining retail sales not only impact demand for the equipment able to produce full colour catalogues and brochures but also the labels, invoices and other packaging materials used on the goods themselves. Finally, the troubled state of

business services and the finance sector means less business forms, preprinted contracts, annual reports and stationary are needed (AccuVal 2012). The initial findings in the “EU Manufacturing Industry: What are the Challenges and Opportunities for the Coming Years?” monitored by the EU Commission (EU, 2010) found that in printing all the subsectors have been confronted by now to the effects of the crisis. Compared to previous recessions, the decline in investments during the current recession was particularly huge. It is unlikely that the printing industry returns to a “business as usual” situation after the crisis. The printing industry did not benefit from specific State Aid aiming at mitigating the effects of the crisis. Printing companies continue exploring restructuring developments for their business: the medium and large size companies continue a merging and acquisition process, which have started several years ago. SMEs develop further efforts towards specialization and niche markets, where they have a significant advantage due to their flexibility and adaptability.

Packaging print shops have been able to benefit to a greater extent from the recovery of the economic situation – and they suffered considerably less from the crisis, even though their orders also declined in 2009. Due to their extremely low capacity utilization, demand by print shops in the industrialized countries for consumables was lower than in the past. The crisis considerably accelerated the trend towards consolidation of the printing industry in the industrialized countries. The print shops that remained are undergoing a process of transformation from traditional workshops to modern industrial enterprises. They are industrializing their processes and specializing in profitable business models. In order to meet the competition, they are investing in the optimization of their overall processes – for example, by means of software- based process integration. The crisis has temporarily put a brake on the growth of the printing industry in most of the emerging markets (Heidelberg ,2011).

3. DRUPA TRENDS

The Drupa print fair was always sending out key impulses for the worldwide print and media industry and laying down foundations for future trends. Drupa 2012 which held this year while the Great Recession is still impacting the industry and the whole European society Drupa still managed to bring some positive signals about a brighter future. The recession impacted mostly the attendances which totalled at 314,500 and this makes Drupa 2012 figures about 75,000 down from Drupa 2008. In Figure 1. we can see the that from 2000 there is a decline trend with a sharp drop between the two last Drupas.

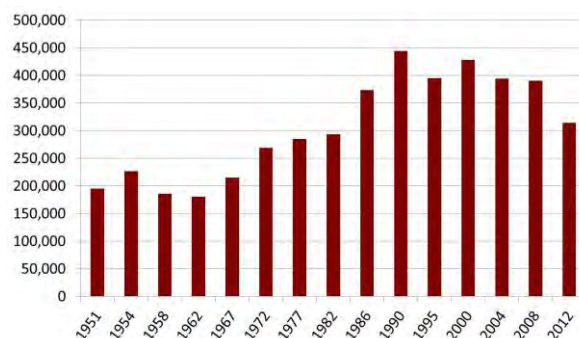


Figure 1. Drupa fair attendance thousands/year

According to Werner Matthias Dornscheidt the President & CEO of Messe Düsseldorf “This drop does not come as a surprise for us and the sector as a whole. In Germany alone the printing industry lost some 3,900 operations with over 61,000 employees between 2000 and 2011. In the USA over the same period more than 7,700 printing operations closed; However – and this is the key point – customers now no longer come to drupa as large delegations or on group corporate trips; it is much more top managers who travel to Düsseldorf. Drupa is clearly the decision-makers’ trade fair and the trade fair for business.” (Messe Dusseldorf, 2012). This comes as no surprise as, after all, the proportion of top managers amongst visitors has grown significantly since 2008 (50.8% compared with 44.4% in 2008) according to Drupa officials. Also according to Drupa final report the dominating themes at Drupa 2012 were automation, packaging printing, digital printing, hybrid technologies, web-to-print applications and environmentally sound printing. All previous Drupa fairs had some keyword like the 1990 Drupa

which was labelled Digital drupa, the improved productivity drupa (1995), the press and workflow automation drupa (2000), JDF drupe (2004), Inkjet Drupa (2008). This year's Drupa has not yet been clearly defined through one label but there are some suggestions as nanography drupa, hybrid drupa, digitalization drupa and even inkjet drupa again. These labels show the trends which dominated the fair show. The technology which was maybe the most amazed and talked about was the Landa nanography. Landa is pushing this new technology and challenging the mainstream of offset printing in terms of quality and costs and with signed partnerships with Heidelberg, manroland and Komori makes it a digital printing technology which impact will be closely observed by all in the industry. One of the several models presented at Drupa 2012 is shown in Figure 2.



Figure 2. Landa S10 nanographic printing press (Copyright by HSPR media)

At the heart of the Nanographic Printing™ process are Landa NanoInk™ colorants. Comprised of pigment particles only tens of nanometres in size (1 nanometer is about 100,000 times thinner than a human hair), these nano-pigments are extremely powerful absorbers of light and enable unprecedented image qualities. Landa Nanographic Printing is characterised by ultra-sharp dots of extremely high uniformity, high gloss fidelity and the broadest colour gamut of any four-colour printing process. Nanographic Printing begins with the ejection of billions of microscopic droplets of water-based Landa NanoInk onto a heated blanket conveyor belt. Each droplet of aqueous NanoInk lands at a precise location on the belt, creating the colour image. As the water evaporates, the ink becomes an ultra-thin dry polymeric film, less than half the thickness of offset images. The resulting image is then transferred to any kind of ordinary paper, coated or uncoated, or onto any plastic packaging film – without requiring pre-treatment. The NanoInk film image instantaneously bonds to the surface, forming a tough, abrasion-resistant laminated layer without leaving any residual ink on the blanket. Since NanoInk images are already dry, there is no need for post drying. Two-sided printing becomes simple and printed goods can be immediately handled, right off the press, even in the most aggressive finishing equipment (Nanowerk,2012). The print results in sharp dots with no bleeding as can be seen in Figure3.

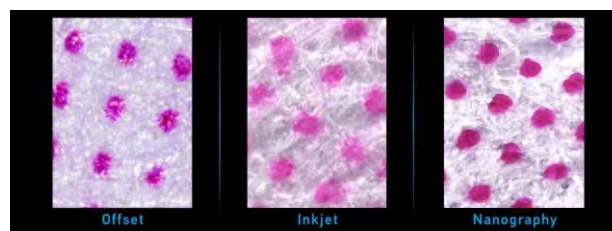


Figure 3. Nanography and other printing technology dot comparison (Copyright by HSPR media)

Beside these technological benefits the main attraction of the nanographic printing press was the user interface and console with a large touch screen panel which enables ultra modern user experience and easiness of using a touch screen mobile phones. Due to the high degree of automation on Landa Nanographic Printing Presses, a single operator can manage two, three or even four presses at a time. When the operator leaves the press, the display switches to Vital Signs Mode, in which key indicators are presented in large fonts that can be easily read from 50 metres away. In addition, the entire user interface is duplicated on a portable touchscreen tablet that is magnetically attached to the press at any convenient location. According to Benny Landa the founder of Landa corporation "Landa Nanographic Printing Presses are intended not to

replace offset printing, but to complement it. For the foreseeable future, offset printing will continue to be the preferred method for producing run lengths of tens of thousands or hundreds of thousands, and " But the market is demanding shorter and shorter run lengths – and that's where Nanography comes in – to enable print service providers to produce those short to medium run lengths economically – at offset speeds. That's what we mean when we say that Landa Nanographic Printing brings digital to the mainstream." (Nanowerk, 2012).

4. DRUPA AND POST DRUPA TRENDS IN DIGITAL PRINTING

Beside the nanography there were also some new improvements in other fields of the digital print sector (Tribute, 2012):

- The well-established toner based sheet fed presses are reaching a level of maturity where progress is slowing up. There were some speed improvements, such as the Xerox iGen 150 and Konica Minolta bizhub PRESS C1100, and we may be getting to close to the full speed such dry toner presses using ground or chemically grown toners can achieve. What we are likely to see in the future with these presses is increased functionality, such as the longer sheet sizes as shown on the Xerox iGen4 EXP and the Kodak Nexpress Platform, and extra functionality through extra printing stations, again as seen on the Kodak Nexpress Platform.
- Liquid toner presses move forward in functionality and speed. This was seen with the launch of the new HP Indigo Series 3 platform as shown with the HP Indigo 10000, 20000 and 30000 presses. These new presses have an increased imaging width of nearly 30 inches (75 cm). This width is easier to achieve with liquid toner than with dry toner. This extra width allows for larger sheet sizes increasing productivity and adding increased flexibility. It also allows for a reel fed press for the flexible packaging market to challenge flexo printing, and also a single sided press for the folding carton market.
- The arrival of a number of new high-speed continuous feed inkjet presses to compete with the range of presses already successfully operating in the market. These included the KBA Rotajet 76, the Komori Impremia IW20, the Founder EagleJet P5200 and the Fujifilm Jet Press W. These presses used either Kyocera or Panasonic print heads. Of these only the Founder and Fujifilm products are already in the market, the Fujifilm product having great similarities to some Océ JetStream presses as they all come via Miyakoshi.
- The B2 sheet fed press market. This is a market that was previewed at the previous drupa with the Fujifilm JetPress 720, the Dainippon Screen Truepress JetSX and the Jadason QPress. These presses are now available for sale unlike every other B2 digital sheet fed press introduced at drupa. For these new introductions is expect that most of them becoming available for sale after IPEX in 2014. The other new presses that were previewed were all inkjet based and included the following. The Komori Impremia IS29 built upon a Komori press chassis with Konica Minolta print heads (also being introduced as the Konica Minolta KM-1 press); the Delphax Elan press using Memjet print heads; the Fujifilm Jet Press F folding carton press that uses the same Dimatix Samba print heads as the Jetpress 720. Most lack true digital functionality like duplex printing, inline finishing and multiple input paper sources and because of these imitations will have to compete against the latest very efficient B2 format offset presses like the Heidelberg SM75 Anicolor for conventional printing work.

Inkjet technology is gaining a new momentum with numerous improvements. The inkjet printing market is valued at \$33.4 billion in 2011 and forecast to grow to \$67.3 billion in 2017, according to Smithers Pira, the worldwide authority on the packaging, print and paper supply chains (Smyth, 2012). The developments shown at drupa further cement and will accelerate more widespread adoption. Inkjet printing is not a discrete market, and the technology is used in many diverse graphics, packaging and industrial applications using very different types of equipment and materials. Inkjet is used in textile printing, in industrial decoration for glass, ceramics, flooring and synthetic building materials. It is used in manufacturing display screens, photovoltaics and some electronic products and there is great potential for inkjet to be used as a manufacturing process for precisely applying small quantities of material in additive deposition processes. Inkjet is currently a small proportion of global print and printed packaging. In 2011 it accounted for some 4.2% of print value and just under 0.5% of the volume. It is attractive to

suppliers because the sector is growing strongly while conventional print volumes fall. It will still account for less than 1% of print volume by 2017, but significantly it will be nearly 7% of the market value. Inkjet is well established in visual communications using wide-format equipment, but the really dynamic sector is in high-speed inkjet, with many print providers moving away from high-volume mono laser printing. In 2011 HP reported that the print volume from its inkjet presses was 459% higher than in 2010, with well over 8 billion pages printed across the year with volumes accelerating steeply. Inkjet is being used in magazine production, with 300,000 copies of the November edition of Popular Mechanics magazine sent to US subscribers with a personalized cover. An outsert from HP greeted the subscriber by name and showed a scene specific to their home town. Inside the issue was a 16-page advertising section, printed by O'Neil Data, which gave readers locations where they could buy HP products near their homes. One reasonably new ink jet technology which enables high speed ink jet printing is the already mentioned Memjet technology. At its base level it is a thermal drop on demand (DoD) system. However, Memjet delivers an entire inkjet solution to its OEMs for integration into front end and transport system at a relatively low cost. The base solution includes printheads, control chips, software, and ink, with optional components available depending upon the individual OEM need. The 'Waterfall' inkjet technology currently centers around the 8.77" wide printhead that can deliver up to 700 million 1-2 picoliter drops per second. It prints through 70,400 nozzles at either 6 inches per second at 1600 x 1600 dpi or 12 inches per second at 1600 x 800 dpi, making it one of the fastest inkjet systems available.



Figure 4. Memjet printhead includes 70,400 nozzles (Copyright by Memjet)

The head includes 11 integrated circuit chips (IC) and five ink channels that can print CMYK +1, or 5 different spot colors. The fixed head requires minimal warm-up time and prints in one pass without moving back and forth across the sheet as some other printheads do. The controller chips are optimized for the system to support delivery of up to 12 inches per/sec., or 60 continuous pages per minute. The 'total' solution comes with a software development kit that minimizes the work required for OEM development and integration into transport and front-end systems. The basic consumables for all of the OEM devices are the ink and the printheads. Currently Memjet inks are water-based dye inks that are specifically designed to work with Memjet printheads. The inks and drop size allow significant ink laydown and quick drying on inkjet compatible papers. The ink densities and resultant print contrast provide an impressive production print product. Printhead life expectancy for production print is estimated at up to 4 liters of ink printed at 70% coverage (Zwang, 2012). One other market where digital technologies are making progress is the folding carton applications. This is a market that was first previewed at the previous drupa by Xerox working with Stora Enso. Xerox has been relatively successful in specialized niche carton applications with their technology. The global market for digital printed packaging and labels is worth \$4.8 billion globally in 2011, according to new research by Smithers Pira (Smyth, 2012). The study *The Future of Digital Printing for Packaging* shows the market is growing quickly; by 2016 it will be worth nearly \$12.2 billion, a compound annual growth rate (CAGR) of 20.6% during 2011–16. This equates to 37 billion A4 prints in 2011 and 75.9 billion in 2016. The growth is driven by the changing demands of packaging buyers – more varieties and pack sizes is fragmenting the market, leading to shorter runs that digital technology can produce economically. Digital printing and finishing technology manufacturers are improving the performance of their equipment in terms of speed, quality and reliability, and these improvements are moving the economic breakeven point of digital ever higher against conventional printing. The latest HP Indigo and Xeikon narrow-web presses claim to be more cost effective than flexo up to runs of some 7,000 linear metres; this cut-off represents an ever growing proportion of the market as runs decline. The new B2 sheetfed inkjet and toner engines will be aimed at cartons, for example the Fujifilm JetPress F offering a novel water based UV ink that will significantly push the achievable quality level. Labels have the greatest penetration, followed by corrugated with small amounts of cartons, flexible packaging, metals and rigid plastics. Digital has limited penetration in the wider \$300 billion packaging market, with just 1.59% of the value and 0.63% of the print volume in 2011. This will

grow, but in 2016 it is expected to be still just over 1% of printed packaging volume. Today electrophotography in high value label applications dominates the digital packaging market. We forecast inkjet will catch up in both volume and value terms by the end of 2016. Instead of completing and stocking batches of product for subsequent order, many pharmaceutical suppliers are producing larger quantities of generic products, than customizing the packs for a particular application or product. In Europe this is becoming quite common, with blister packs, cartons or vials being digitally printed in the destination language on bespoke lines. The benefit is reduced stock in the supply chain, with potential for redundancy and waste as well as reducing the working capital tied up in stock. In the past couple of years many sectors have reduced their stock holdings. Inkjet technology is increasingly being added onto existing packaging lines, replacing slow and limited thermal transfer systems to provide better quality and flexibility. Digital printing can be useful in brand protection, with clear and UV fluorescent toners and inks providing covert and overt security features. Variable data capability can provide unique text and code identifiers resulting in pack traceability across the whole supply chain to point of use.

5. PRINTED ELECTRONICS AND 3D PRINTING

With price pressure and volume reductions being forecast for print, the industry it is on the lookout for new opportunities. Adding electronic capability has been on the horizon for many years. After a hiatus instigated by the global slowdown, there are encouraging examples of how print might evolve to create new high-value print products. The printing of products like packaging labels is now incorporating capability for adding electronic functionality directly to the printed media. RFID technology is gradually turning into an authentic and reliable option for identification. Applications like item level tagging and supply chain applications are key growth drivers of this industry, which are increasingly becoming popular. There is still a long way to go before RFID achieves penetration in the apparel sector, but JCPenney, Wal-Mart and other companies' already tagging apparel are considering new categories, including automotive parts, cosmetics, electronics and jewellery. Also there are reports on using RFID tags to monitor laboratory samples and as an anti theft tool. The RFID market will continually rise with wider and wider adaption models. 3D printing is expanding its possibilities and as just one very special application it can be mentioned that scientists at the Massachusetts Institute of Technology claim that they are one step closer to creating a synthetic liver using 3D printing to replicate the human organ and build a network for the blood vessels to grow into. This maybe can't be directly connected with graphic arts but the process of printing is definitively evolving in some earlier unforeseen directions (Inquisitr Ltd., 2012).

6. DIGITAL PUBLICATIONS AND MEDIA TRENDS

Print service providers, like many other businesses, are being impacted by mobile technology. Smartphones and tablets are now an integral part of peoples' daily lives; the pervasiveness of mobile technology continues to influence the "consumerization" of business, and the printing industry is not immune to this trend. Customers increasingly request access to services via their mobile devices, and internal business and production operations are going mobile, as well. Ultimately, the role of mobile technology is going to be increasingly important in business—and not just when it comes to marketing services. More and more print suppliers are taking advantage of the digital revolution to add to their portfolio of client services in areas such as managing mailing lists and customer data, handling stock and fulfilment, designing and managing customers' websites, and running campaigns that integrate all media, new and old. The traditional print business model, price-driven and product-focused, is no longer fit for purpose. With the industry's customers now looking for cost-effective campaigns rather than just cut-price commodity print, printers can no longer rely solely on manufactured products and low prices to differentiate themselves: print must adapt if it is to survive. In an Infotrends survey (Little and Yeager, 2012) which result is presented in Figure 4. it can be seen that more and more print service provider expand their business to online and mobile platforms.

With the advent of mobile devices and tablet as well dedicated ebook readers some production volumes of classic printed books and magazines go through changes. There is a steady rise of sold ebooks in the UK of 366% (Flood, 2012) drawing its data from information provided by 250 publishers, the Publishers Association's Statistics Yearbook put the value of consumer ebook

sales – fiction, non-fiction and children's digital titles – at £92m in 2011. This is a 366% increase on the previous year, the Publishers Association said, and consumer ebooks are now equivalent to 6% of consumer physical book sales by value.

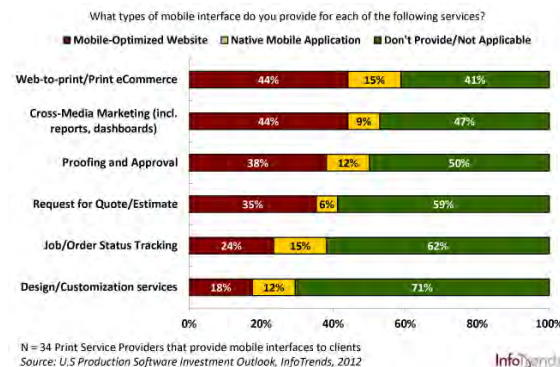


Figure 5. Types of Mobile Interfaces Provided to Clients (Copyright by Infotrends)

The shift from printed to electronic media is also noted in two details from the 9th State of the News Media 2012 (report which states that more than four in ten American adults now own a smartphone. One in five owns a tablet). New research released in this report finds that mobile devices are adding to people's news consumption, strengthening the lure of traditional news brands and providing a boost to long-form journalism. Eight in ten who get news on smartphones or tablets, for instance, get news on conventional computers as well. People are taking advantage, in other words, of having easier access to news throughout the day – in their pocket, on their desks and in their laptops. The problems of newspapers also became more acute in 2011. Even as online audiences grew, print circulation continued to decline. Even more critically, so did ad revenues. In 2011, losses in print advertising dollars outpaced gains in digital revenue by a factor of roughly 10 to 1, a ratio even worse than in 2010. When circulation and advertising revenue are combined, the newspaper industry has shrunk 43% since 2000. One very striking information is also that Google had revenues (\$37.9 billion) of \$4 billion greater than those of the entire newspaper industry in 2011. That gap will keep growing in 2012 and the years to follow. Accelerated demand from advertisers for internet advertising is having an impact on print advertising, with revenues from print advertising expected to decline across all media over the forecast period. New techniques of multichannel communications to engage with consumers are developing, while the return on advertising expenditure is being monitored carefully. The developments in communications technology are moving towards a connected world through computers, tablets and smartphones. Internet usage figures show that the medium is growing consistently generally resulting in a downward impact on print readership. These changes cause advertisers to rethink their overall marketing strategies and to devote more resources to experimenting with electronic media. On the other hand some quite new digital formats like "tablet only magazines" failed to keep profit for their owners and many of them were shut down this September (Moses, 2012) for several reasons like the lack of support from the advertisers and low subscription numbers. This does not mean that in the future there is no place for these kind of publications but that maybe it was too early for a major part of the population.

7. CONCLUSION

Summarizing the presented new hardware's and software's which were marketed under the shadow of the economic crises it can be said that technological innovation like nanography, smart packaging and intelligent software solution and cloud computing still manages to drive the printing industry progress. These new applications in combination with some other presented innovations at the Drupa show that printing has a future, not maybe as we have imagined but in a much more diversified ways. This proves that only new ideas and solution can provide answer to the economic challenges of the days. On the other hand as other parts of the technological devices improve and spread mainly the portable smartphones and tablets with a very wide interconnection of people through social sites new layers of communication and information channels are opening. As print evolves and becomes integrated with digital media channels, the industry as a whole will require individuals to have a holistic understanding of all media types

and they the roles that they play in supporting one another. As earlier paper was the only courier of human thoughts and ideas it will be joined by other digital electronic media mainly online and mobile devices which will partly takeover the task, but printing on paper is still here to stay.

Acknowledgments

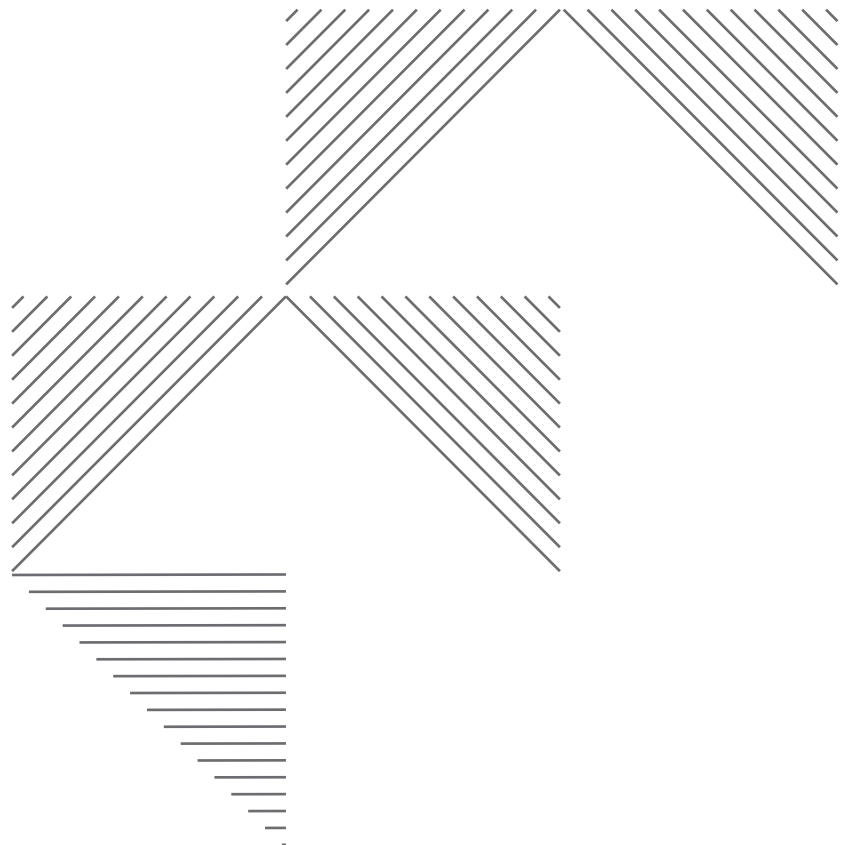
This work was supported by the Serbian Ministry of Science and Technological Development, Grant No.:35027 "The development of software model for improvement of knowledge and production in graphic arts industry"

8. LITERATURE

- [1] AccuVal Associates:" Industry Factors Weaken Printing Equipment's Secondary Market" URL <http://www.accuval.net/insights/featuredarticle/detail.php?ID=65> (last request: 2012-08-24).
- [2] European Commission: "EU Manufacturing Industry:What are the Challenges and Opportunities for the Coming Years?" URL http://ec.europa.eu/enterprise/policies/industrial-competitiveness/economic-crisis/files/eu_manufacturing_challenges_and_opportunities_en.pdf (last request: 2012-07-21).
- [3] Flood A.:" Huge rise in ebook sales offsets decline in printed titles",URL <http://www.guardian.co.uk/books/2012/may/02/rise-ebook-sales-decline-print-titles> (last request: 2012-09-09).
- [4] Heidelberg:" Underlying conditions Printing industry suffering heavily from the global economic crisis" URL http://www.ca.heidelberg.com/nz/www/en/binaries/files/investor_relations/reports/2010-11/100804_conditions_pdf (last request: 2012-08-21).
- [5] Inquisitr Ltd.:" Printing A New Liver: Scientists At MIT Use 3D Printing To Create New Human Organs" URL <http://www.inquisitr.com/268381/printing-a-new-liver-scientists-at-mit-use-3d-printing-to-create-new-human-organs/> (last request: 2012-09-09).
- [6] Little C., Yeager B.:" More Print Providers Offering Mobile-Enabled Services, Solutions" URL <http://blog.infotrends.com/?p=8828> (last request: 2012-10-09).
- [7] Messe Dusseldorf: "drupa 2012 sends out Trendsetting Impulses for the Print Sector", press realase 16.05.2012 URL http://www.drupa.de/cgi-bin/md_drupa/custom/pub/content.cgi?lang=2&oid=16479&ticket=g_u_e_s_t&ca_page=en%2F1410_4639.htm (last request: 2012-08-21).
- [8] Mitting W.:" How the economic crisis will shape the future and impact drupa" URL <http://www.printerspost.com.au/printingnews/2516/how-the-economic-crisis-will-shape-the-future-and-impact-drupa.aspx> (last request: 2012-08-22).
- [9] Moses L.:" Nomad Editions Calls it Quits Mobile publisher shuts three remaining titles"URL <http://www.adweek.com/news/advertising-branding/nomad-editions-calls-it-quits-143659> (last request: 2012-13-09).
- [10] Nanowerk ::" Landa's Breakthrough Nanographic Printing Press Changes the Face of Mainstream Print Markets with Versatility of Digital and Qualities of Offset" URL <http://www.nanowerk.com/news/newsid=25272.php> (last request: 2012-09-1).
- [11] Smyth S.:" The Future of Inkjet Printing – post drupa review" URL <http://whattheythink.com/articles/58279-future-inkjet-printing-post-drupa-review/> (last request: 2012-08-22).
- [12] Smyth S.:" Outlook for Digital Printing for Packaging" URL <http://whattheythink.com/articles/58799-outlook-digital-printing-packaging/> (last request: 2012-08-22).
- [13] Tribute A.:" Digital Printing at drupa – Part 1" URL <http://whattheythink.com/articles/58201-digital-printing-drupa-part-1/> (last request: 2012-09-2).
- [14] Zwang D.:" Drupa 2012, the Inkjet Drupa...again? A closer look at Memjet and three unique OEMs" URL <http://whattheythink.com/articles/56686-drupa-2012-inkjet-drupaagain-closer-look-memjet-three-unique-oems/> (last request: 2012-08-22).



Special Printing Applications and Materials



PRINTED PASSIVE ELECTRONIC STRUCTURES ON RECYCLED PAPERS, CARDBOARDS AND FOILS

Miloje Đokić¹, Urška Kavčič², Matija Mraović^{3, 4}, Matej Pivar¹,
Leon Pavlovič⁴, Tadeja Muck¹

¹University of Ljubljana, Faculty of Natural Sciences and Engineering, Ljubljana

²Valkarton Rakek d.o.o., Rakek

³Pulp and Paper Institute, Ljubljana

⁴University of Ljubljana, Faculty of Electrical Engineering, Ljubljana

Corresponding author: Miloje Đokić
e-mail: milojeus@yahoo.com

1. ABSTRACT

Printed electronics is expected to replace many conventional electronic systems. It is already used in the manufacture of RFID tags, various sensors, OLED displays, batteries, solar cells etc. The goal of printed electronic industry is to print electronic systems in roll-to-roll technology, as cheap as possible.

Printed electronics can be divided into three parts: Wafer part, printed part and hybrid part. Wafer technology is not classic printed electronics and it is characterised by the procedures of production which are applied with the classic chip production (vacuum coating, photolithography, etching, etc.) This technique has the possibility of designing high resolution so that is applied in OLED displays, electroluminescent films, photovoltaic films, etc.

Printed electronics is based on the additive process of printing (flexo, screen, digital printing...) where the various substrates were printed with functional inks. This type of printed electronics can be fully printed by roll-to-roll technology that allows mass production, which significantly affects the favorable price of products. Hybrid technology of printing electronics combines the first two mentioned techniques. Flexible materials can be used with printed and hybrid technology.

This research was focused on printing RFID antennas and sensors on recycled papers, cardboards and foils. RFID (HF and UHF) antennas, humidity and temperature sensors were printed with the semi-automatic screen printing machine. Monofilament polyester plain weave mesh with 120 l/cm was used. These structures were printed using conductive (thermal drying and UV drying) and dielectric inks and dried under hot air, UV and Heat&Press drying conditions to obtain the lowest resistivity.

In the first part of our research UHF antenna was designed according to the chips specification and printed. The radiation patterns of antennas were evaluated and finally the chips were integrated onto the printed antennas to produce RFID tags. Measurements showed that tags on all recycled papers and cardboards operate well.

The second part of our active research has already started. The humidity and temperature sensors were printed and first analysis for humidity sensors were performed. Results are optimistic.

Key words: HF, UHF, RFID, antenna, sensor, temperature, humidity, recycled paper, cardboard, foil

2. INTRODUCTION

Radio frequency identification RFID is rooted in discoveries made by Faraday and discoveries in radio and radar technologies. The RFID tags can be subdivided into active and passive tags; active tags have a longer reading/writing range and passive tags a shorter one. The latter are much simpler and cheaper than active tags and are more widely used [1]. The RFID system can work at low (LF: 125/134 kHz), high (HF: 13.56 MHz) or ultrahigh (UHF: 860–960 MHz) frequency ranges [2]. The LF and HF tags operate with inductive coupling and have short reading range, on the other hand the UHF tags use radiative coupling and have longer reading range [3].

The integration of RFID tags in different applications is important in order to gain greater functionality in the products. With traditional manufacturing techniques the integration of RFID tags may not be technically and economically competitive in mass production. Etching is typically used in RFID tag manufacturing to produce conductive antenna pattern. Although it is an efficient process, it has a few drawbacks. It contains many process phases and uses different chemicals which are not environmentally friendly and are expensive [3]. Because of that, investigations are focused on the use of conventional printing technologies for mass production of printing electronics directly on different materials. Among the printing technologies, the most popular are screen printing [4–6], inkjet [7], flexography [8] and gravure [9]. The performance of printed RFID antennas was characterized by many researchers [10–15].

In the first part of our research the goal was to optimize the printing process conditions for screen printing of passive HF and UHF RFID antenna on coated cardboard, on uncoated recycled paper and on foil. The UHF antenna was designed regarding to chip specification and the antenna's impedance and radiation pattern were simulated with a commercial 3D numerical solver. The antennas were printed using semi-automatic screen printer. For coated cardboard and uncoated recycled paper thermal drying silver based conductive ink, and for foil UV drying silver based conductive ink were used. For HF antenna dielectric, UV curing printing ink was also used. Drying conditions have been varied in order to obtain good print quality on all printing materials. The analysed influences of drying conditions of printed conductive layers have been proven to be significant. After printing and heating the UHF antennas printed on cardboard and recycled paper were evaluated by a measurements of radiation pattern. In that moment we didn't have right results of relevant electrical parameters on the foil, and because of that the radiation pattern for antenna printed on foil were not performed.

The second part of the research relates to the printed sensors, as part of the printed electronics that are applicable in wide range of products, but mostly to smart packaging. Smart packaging can be defined as packaging that contains an external or internal indicator to provide information about aspects of the history of the package and/or the quality of the product. It may be divided into three parts: sensors (gas, bio and fluorescence based oxygen sensors), indicators (integrity, freshness and time temperature indicators) and RFID. [16]

Smart packaging usually involve the ability to sense or measure an attribute of the product, the inner atmosphere of the package, or the shipping environment. This information can be communicated to users or can trigger active packaging functions. The goal of the second part was to be attempted to print moist and temperature sensors directly on the substrate, and to optimize the printing process conditions. The sensors were printed with semi-automatic screen printing system, using thermal drying silver conductive ink. As a printing material coated cardboard, foil and uncoated recycled paper were used.

3. MATERIALS AND METHODS

The research was done according to the procedure presented on Figure 1.

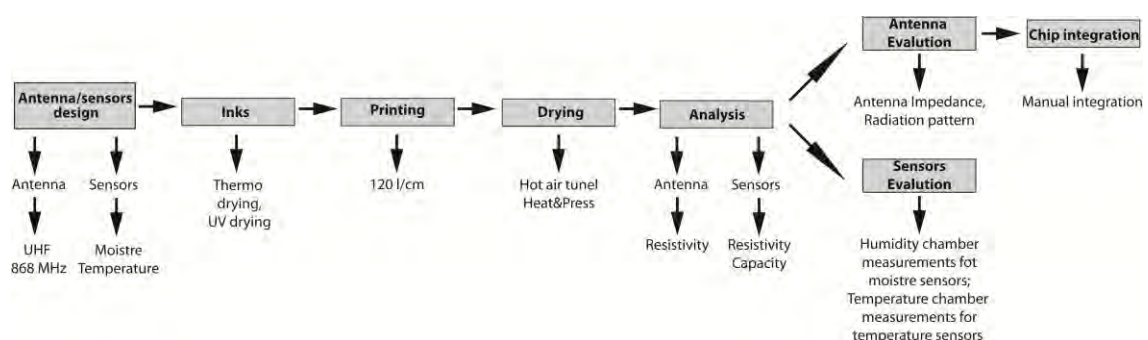


Figure 1: Scheme of research

3.1 Printing inks

Table 1: Printing inks

Printing inks	Drying (for a moving belt drier)	Printed on:	Use for:
CRSN2442 Suntronic Silver 280 (Sun Chemical)	thermal; 30–90 s on 110°C–130°C	Coated cardboard and recycled paper	Antennas (UHF and HF) and sensors
DuPont 5064H (DuPont)	thermal; 120 s on 140°C	Coated cardboard and recycled paper	Antennas (UHF and HF) and sensors
REXALPHA RA FD 076 FS (Toyolnk)	UV, >200 mJ/cm ²	Foil	Antennas (UHF and HF)
CFSN6057 Suntronic Dielectric 681 (SunChemical)	UV, 650mJ/m ²	Coated cardboard and recycled paper	Antennas (HF)

Printing was performed with a semi-automatic screen printing machine “Roku print SD 05”. Monofilament polyester plain weave mesh with 120 T/cm was used for screen printing process.

3.2 Printing materials

Three types of printing materials were used; conventional coated cardboard and uncoated recycled paper and foil. Coated cardboard had thickness of 400 microns (grammage 245 g/m²), recycled uncoated paper had 75 µm and grammage of 80 g/m². The thickness of the foil was 160 µm (grammage 265 g/m²).

3.3 Drying

At first drying conditions were determined. All printed samples were dried under different conditions in order to determine optimal drying process. Drying (Figure 2), for coated cardboard and uncoated recycled paper, was performed in hot zone at different temperatures, starting from 100°C till 170°C with 10°C step, applying the same speed of the moving belt (45 seconds in hot zone)(I phase). Optimization of drying conditions were achieved with two-stages drying process. While the resistance of prints after first phase was still high, the prints were dried under Heat&Press (II phase).

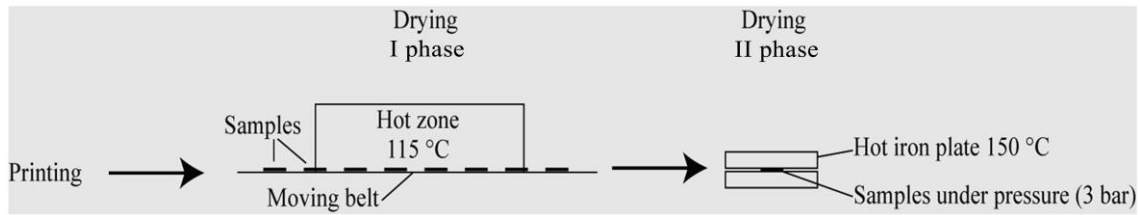


Figure 2: Schematic representation of two phases combined drying process

By analogy with cardboard and recycled paper, foil was also subjected to two-stage drying. The difference is in the first stage where instead of heat tunnel UV tunnel was used. The reason for UV drying is use of hybrid UV ink which is used as printed conductive layer on PETG films. The problem, which was prevalent during the whole research print electronics on plastic film, was finding the appropriate UV conductive ink. All previous inks used, before Toyolnk inks, were not sufficiently conductive, i.e. had a high resistance. At the end of the study was successfully acquired Toyolnk REXALPHA RA FS FD 076 hybrid conductive ink, which has met all the necessary criteria. After successfully drying, resistance was measured using the digital multimeter DT-890G.

3.4 Antenna design

The UHF antenna was designed regarding to SL900A EPC Class 3 Sensory Tag Chip chips specification. The main terms for the antenna design were the RFID chip impedance (approx.

$20 - j325 \Omega$), and material properties used for the printed antenna. For modification and simulation of the antenna, as substrate cardboard and recycled paper were used, because in that moment printed ink on foil did not have good conductivity.

The UHF printed antenna was designed as a resonant planar structure and the type of the antenna was chosen to be the capacitive-loaded dipole, which fits the standard credit-card size (Figure 3) at the operating frequency of 868 MHz. The antenna properties (impedance and radiation pattern) were first simulated with a commercial 3D numerical solver (Ansoft HFSS) and then also evaluated by a measurement. The relative permittivity of the base of the printed antenna (paper or cardboard) used for the simulation was 3.2 with a loss tangent of 0.003. The radiation efficiency of 87% was obtained. The radiation pattern was measured also on printed antennas on both materials. The foil did not have enough good conductivity results, and because of that measurements weren't performed for foil. The measurements were done in order to find out how the antenna works regarding to printing material.



Figure 3: Design of UHF antenna

3.5 Design of sensors

Humidity content sensor was realised in the form of a parallel plate capacitor. Square electrodes (1×1 cm, 2×2 cm, 3×3 cm) (Figure 4A) were screen printed on both sides of a dielectric material (paper or cardboard sheet), and thus forming a simple parallel plate capacitor. Since capacitance of a capacitor is proportional to the dielectric constant (ϵ_r) of the dielectric between its plates, it is possible to indirectly measure humidity content in the dielectric material (printing material). Capacitance is changing because of a change in ϵ_r of the dielectric due to humidity amount in the dielectric material. Such sensor is able to track humidity level in the material.

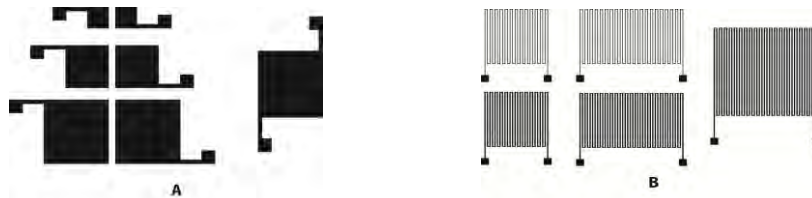


Figure 4: Printed sensors A-capacity sensors; B-temperature sensors

Temperature sensor (Figure 4B) was printed as an electrical resistor in the form of long and thin conducting lines. Resistor in the form of conducting lines exhibits a change in its resistance value due to temperature change, and this can be measured with a simple Ohm-meter.

3.6 Measurements of printed layer resistance

For all substrates resistances measurements were done using the digital multimeter DT-890G, and applying the two-point method for measurements. Measurements were taken on test element showed on figure 5 between points 1 and 2 with normal length of $L = 22$ mm and width $W = 3$ mm. The nominal number of squares in that print area is $N_{sq} = L/W = 10.3$.

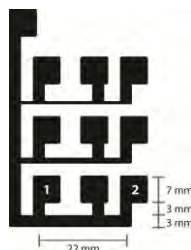


Figure 5: Test element for measurements of resistivity

3.7 Measurements of antenna's radiation pattern

Outdoor antenna measuring polygon was used for radiation pattern measurements in E (electric field) and H (magnetic field) direction. Measurements of antenna's radiation pattern were done on printed antennas on coated cardboard and uncoated recycled paper. As mentioned earlier, the foil at the time of measurement antenna's radiation pattern did not have good enough conductivity results.

3.8 Analysis of printed sensors

Measurements were conducted in a humidity chamber at constant temperature of 23°C in three separate series. Prior to each series the samples were conditioned at a specific relative humidity level for 24 hours. Before the first series of measurement the samples were kept at 50% relative humidity for 24 hours, for the second series they were kept at 43% relative humidity and for the third series they were kept at 93% relative humidity for 24 hours. First series was conducted with increasing the relative humidity from 50% to 80% in 10% steps and waiting time between the steps was 1 hour. Second and third series were made in the opposite direction from 80% relative humidity to 50% relative humidity in 10% decreasing steps, waiting time was 1 h between each step. Capacitance was measured every hour with HP LCR-meter with impedance method at 1 kHz.

4. RESULTS AND DISCUSSION

4.1 Drying

To get the lowest values of resistance and to achieve better conductivity is necessary to provide optimal drying process. For thermal drying of inks with a moving belt drier the manufacturer recommends temperature from 100°C to 130°C over 30–90 seconds in the hot zone. We proved that effective drying – with short drying time can be achieved with two-stage drying process, conventional thermal drying (hot air channel) and Heat&Press drying. Optimal drying conditions were different for all printing materials.

- cardboard, 135 seconds thermal drying at 115°C with successive Heat&Press drying at 150°C (10s)
- recycled paper, 90 seconds thermal drying at 115°C with successive Heat&Press drying at 150°C (10s)
- foil, 4 passing through UV tunnel at about 1200 mJ/cm² with successive Heat&Press drying at 150°C (80s), which is equivalent to 60 min thermal drying in oven at 70°C after UV curing

4.2 Electrical properties

After a successful drying, which consisted of two phases, the resistance between point 1 and 2 of the test structure measured on uncoated recycled paper and coated cardboard was the same (Figure 6) - final resistivity is very low on both materials, below 100 mΩ/sq. Coated cardboard and recycled paper were printed with SunChemical ink, and foil with Toyolnk.

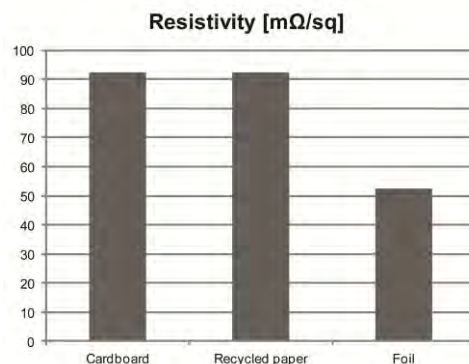


Figure 6: Resistivity after successful drying on all materials

4.3 Measurements of radiation pattern

The radiation pattern is nearly the same in E and H directions for simulated UHF antenna and also for printed antennas on both materials – coated cardboard and uncoated recycled paper (Figure 7). Prints that were used for the measurements of radiation pattern were printed with SunChemical ink. The foil did not have enough good conductivity results, and because of that measurements aren't performed for foil.

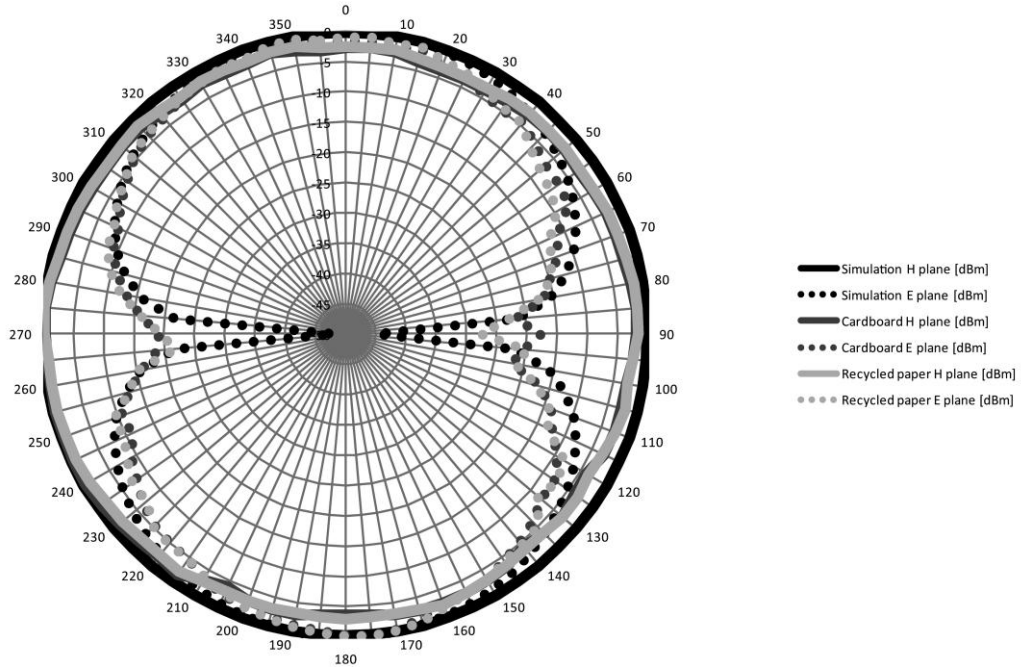


Figure 7: The radiation pattern for simulated UHF antenna and printed on cardboard and recycled paper materials

4.4 Results of the analyzed sensors

Humidity content sensor exhibits great change in capacitance when recycled paper is used as a dielectric material as shown in figure 8A for a 2×2 cm sensor. Change in minimum and maximum measured values is of the 10^3 pF order, this is by far the greatest change for any material under test. The response is almost flat under 60% relative humidity which is the low range limit. Thickness of the recycled paper was around 80 μm . Figure 8B shows response of a sensor with cardboard as a dielectric material. Response is more uniform than in the recycled paper based sensor and is almost linear. Cardboard thickness was around 520 μm .

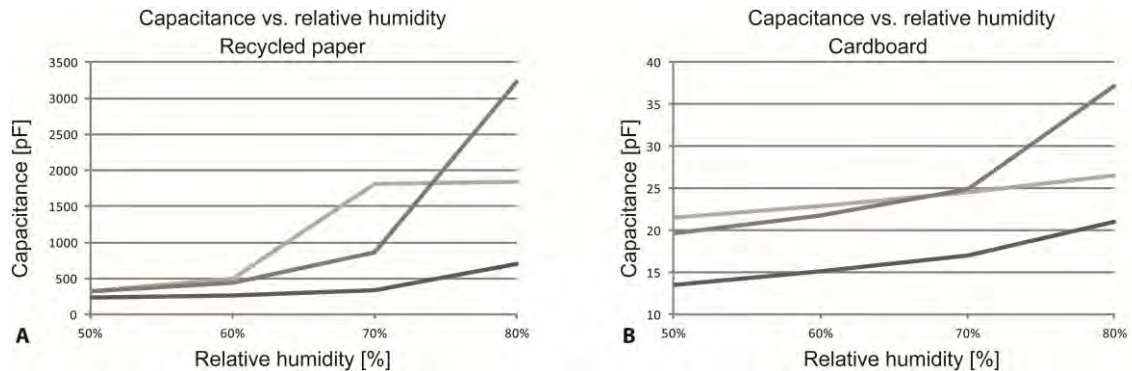


Figure 8: A – Recycled paper based sensor (3 series); B – Cardboard based sensor (3 series)

5. DISCUSSION

The crucial condition needed to fulfill for printing RFID antennas is lower resistance of printed layer. In order to achieve this it is necessary to choose the optimal drying conditions that lead to a reduction of resistance to minimum values - evaporation of solvents (conventional printing ink) or increased / accelerated cross linking monomer (UV ink).

During the research drying conditions varied to obtain minimum resistance of conductive elements – antenna. It was concluded that, in addition to various high temperatures in the heat tunnel, pressure, under the printed samples were exposed after the first phase of thermal drying, has effect that further reduce the resistance. The optimal dose for each of the drying material for printing was established, for each material it was different.

Cardboard and recycled paper were selected for antenna simulation. At the time of simulation and measurement antenna's radiation pattern – the foil did not have enough good conductivity results, and because of that measurements aren't performed for foil. The measurements mentioned at last were done in order to find out how the antenna works regarding to printing material and to determine antenna quality factor and its resonant frequency.

Capacitance is increasing with increasing content of humidity in the dielectric material (paper/cardboard). Repeatability of measurements in a recycled paper based sensor is poor. Both types of sensor have memory for humidity and it is very important for the measurement how the samples were conditioned prior to the start of the measuring cycle and as well as the starting relative humidity level. Resolution is better in measurements going from high relative humidity values (80% relative humidity) to low, that is in a material with a higher humidity content.

6. CONCLUSION

Acceptable electrical properties of screen-printed conductive layer require optimization of drying process, in order to have the lowest resistance. The main benefit of two-stages drying is shorter drying time and energy savings.

The resistivity of conductive ink based on silver is very low and is independent of printing material. This statement is also proved by measurements of radiation patterns. Printed antennas on both printing materials show very similar radiation pattern. The design of UHF antenna is appropriate for cardboard and recycled paper – no differences on radiation pattern were shown between simulated one and antennas printed on those printing materials.

Unfortunately parallel plate sensor suffers from humidity accumulation between the electrodes and it's response is not in accord with actual level of humidity present in the dielectric at given time. Improved designs have already been completed and manufacture (printing) is currently under way. This will improve the response and prevent humidity to accumulate in the sensor itself. One idea of such improvement is to perforate the electrode plates or use a comb variant sensor, or some other geometry of electrodes to allow for better passing of humidity to and from the dielectric material.

The sensor at this stage is able to distinguish between three levels of humidity (< 60%; 60%–75%; > 75% relative humidity), which could be satisfactory for simple applications, where for example only levels over 75% relative humidity are critical for product or operation.

Acknowledgements

Urška Kavčič acknowledges the Slovenian Technology Agency for young researcher support, operation part financed by the European Union, European Social Fund. Operation implemented in the framework of the Operational Programme for Human Resources Development for the Period 2007–2013, Priority axis 1: Promoting entrepreneurship and adaptability, Main type of activity 1.1.: Experts and researchers for competitive enterprises.

7. LITERATURE

- [1] M. Bolić, D. Simplot-Ryl, I. Stojmenović (2010): *RFID Systems – Research Trends and Challenges*, Wiley.
- [2] U. Bogataj, M. Maček, T. Muck, M. Klanjšek Gunde (2011): Readability and modulated signal strength of two different ultra-high frequency radio frequency identification tags on different packaging. *Packag. technol. sci.*, pp. 1-12.
- [3] S. L. Merilampi, T. Bjorninen, A. Vuorimäki, L. Ukkonen, P. Ruuskanen, L. Sydanheimo (2010): The Effect of Conductive Ink Layer Thickness on the Functioning of Printed UHF RFID Antennas. *Proceeding of the IEEE*, vol. 98, (9), pp. 1610 – 1619.
- [4] M. Słoma et al. (2011): Investigations on printed elastic resistors containing carbon nanotubes, *Journal of Material Science: Materials in Electronics*, published on line 9.02 2011-04-01.
- [5] K. Janeczko et al. (2010): Screen printed UHF antennas on flexible substrates, *Proc. of SPIE*, vol. 7745, (77451B).
- [6] M. Jakubowska et al. (2011): Printed transparent electrodes containing carbon nanotubes for elastic circuits applications with enhanced electrical durability under severe conditions, *Materials Science and Engineering: B*, vol. 176, (4) , pp. 358-362.
- [7] K. Futera et al. (2010): Printed electronic on flexible and glass substrates, *Proc. of SPIE*, vol. 7745, (77451B).
- [8] A. Blayo, B. Pineaux (2005): Printing processes and their potential for RFID printing, *Proc. of the 2005 Joint Conference on Smart Objects and Ambient Intelligence: Innovative Context-Aware Services: Usages and Technologies*, Grenoble, pp. 27–30.
- [9] M. Pudás et al. (2005): Gravure printing of conductive particulate polymer inks on flexible substrates", *Progress in Organic Coatings*, vol. 54, (4) , pp. 310–316.
- [10] D. Y. Shin et al. (2009): Performance characterization of screen printed radio frequency identification antennas with silver nanopaste, *Thin Solid Films*, vol. 517, (21), pp. 6112-6118.
- [11] A. Syed et al. (2007): Effects of Antenna Material on the Performance of UHF RFID Tags, *Proc. of IEEE International Conference on RFID*, Grapevine, 26-28, pp. 57 – 62.
- [12] P. V. Nikitin et al. (2005): Low cost silver ink RFID tag antennas, *Proc. of IEEE Antennas and Propagation Society International Symposium*, vol. 2B, pp. 353 – 356.
- [13] S. Merilampi et al. (2007): Analysis of Silver Ink Bow-Tie RFID Tag Antennas Printed on Paper Substrates, *International Journal of Antennas and Propagation*, ID 90762, p. 9.
- [14] A. Rida et al. (2007): Design and Integration of Inkjet-printed Paper-Based UHF Components for RFID and Ubiquitous Sensing Applications, *Proc. of 37th European Microwave Conference*, (<http://users.ece.gatech.edu/~etentze/EuMC07.pdf>).
- [15] L. Yang, M. M. Tentzeris (2007): Design and Characterization of Novel Paper-based Inkjet-Printed RFID and Microwave Structures for Telecommunication and Sensing Applications, *Proc. of IEEE/MTT-S International Microwave Symposium*, pp. 1633 – 1636.
- [16] Robertson G.: Recent Innovations in Packaging Technology to Ensure Safety and Quality of Food and Ingredients, Southeast Asian Food and Agricultural Science and Technology (SEAFast) Center, URL <www.seafast.ipb.ac.id/unduh/00-keynote-GRobertson.pdf> (last request: <8.10.2012.>)

THE INFLUENCE OF PHYSICAL PARAMETERS ON THE DYNAMIC COLOR OF THERMOCHROMIC PRINTING INKS

Mojca Friškovec¹, Tina Mandelj², Špela Vasić Štepančič², Marta Klanjšek Gunde³

¹ Cetis d.d. Celje

² University of Ljubljana, Faculty of Natural Sciences and Engineering, Ljubljana

³ National Institute of Chemistry, Ljubljana

Corresponding author: Mojca Friškovec

e-mail: mojca.friskovec@cetis.si

1. ABSTRACT

Thermochromic printing inks are different from conventional ones, since they change colour with temperature. At low temperatures they appear in a coloured state but at high temperatures they become transparent. The decolouration and the re-colouration don't occur at the same temperature; therefore the ink exhibits a colour hysteresis loop. For the development of thermochromic inks and their use in precise applications, it is necessary to carefully analyse the dependence of their dynamic colour on different extrinsic parameters which could influence the colour response of the complex system inside functional pigment capsules. Research work was focused on two commercial screen printing thermochromic inks. The dynamic colour was characterized by five parameters – the total colour contrast, the openness and the width of the colour hysteresis loop, yellowness and the area of the hysteresis loop described by the corresponding colour change in the CIELAB colour space. The dependence of the parameters on the layer thickness, the repeatability of the colour hysteresis loops of 3 consecutive heating-cooling cycles and the influence of storage conditions of the sample prior to measurement were studied. The results show that variation in ink film thickness has an effect on all parameters. The starting temperature of the measurement can impact the colour hysteresis loop, i.e. if the sample is firstly heated or cooled. The hysteresis loop in the first heating-cooling cycle in some cases differs from those obtained in the second and third consecutive cycle. The analysis shows that some parameters could influence the colour of thermochromic samples as a function of temperature. These results are important for every advanced application of thermochromic inks.

Key words: thermochromism, thermochromic inks, hysteresis loop, dynamic colour, physical parameters, characterization.

2. INTRODUCTION

Thermochromic (TC) inks are different from conventional once, since they change colour with temperature (White and LeBlanc, 1999). Because of their dynamic colour they are frequently applied on security printed matter, innovative packaging and promotional products (Phillips, 2000; Kerry and Butler, 2008). Most frequently used TC inks are microencapsulated organic TC composites mixed in a suitable binder. Most TC organic composites are mixtures consisting of a colour former (leuco dye), a colour developer and a solvent (Seeboth and Löttsch, 2008). Their colour change is reversible and depends on two competing reactions; the one between the dye and the developer, which prevails below the melting point of the solvent, and the other between the solvent and the developer when the solvent melts (MacLaren and White, 2003; MacLaren and White, 2003). The complex chemistry of the organic TC composite provides materials with a unique dynamic colour that can be easily recognized by the naked eye and is difficult to reproduce.

TC inks typically discolour at higher temperatures than they recolor. Between the totally coloured and fully discoloured states, the colour of a TC sample depends on the temperature and also on the thermal history, which results in a colour hysteresis (Kulcar, Friskovec et al., 2010). The loops of commercial TC inks have varying widths and shapes – some of them are approximately symmetrical but highly asymmetric ones also exist (Kulčar, Friškovec et al., 2009; Gunde, Friškovec et al., 2011).

Changes to the colour hysteresis might be important in any advanced application of a TC ink where the dynamic colour is of considerable importance. Important issues to be addressed are

the repeatability of the colour hysteresis, the influence of storage conditions and ink layer thickness of the sample on the colour hysteresis. These are the research subjects of our present work.

3. EXPERIMENTAL PART

3.1. Materials

Two commercially available UV based screen printing TC inks printed on OBA-free gloss coated paper (150 g/m²) were tested (Table 1). Prints were made with the SD 05 machine (RokuPrint, Germany) employing a SEFAR PET 1500 monofilament polyester mesh 120/34Y. Both inks were printed in one, two and three layers. Corresponding thicknesses for Sicpa green samples are 12, 23 and 36 μm and for the TCX blue samples 16, 28 and 43 μm as measured with micro-TRI-gloss μ machine (BYK Additives & Instruments). Each layer was cured with energy of $\sim 400 \text{ mJ/cm}^2$.

Table 1: Selected data of applied inks: sample name, producer, drying method, activation temperature (T_A), the size of the largest pigment particles (grindometer value) and specular gloss evaluated at 60° (gloss units, GU).

sample	producer	drying method	T_A (°C)	grindometer value (μm)	gloss (GU)
TCX blue	Coates Screen, Germany	UV curing	31	11	35
SICPA green	Sicpa, Switzerland	UV curing	33	1,5	63

3.2. Measurements

Spectral reflectances were measured with the i1 Pro spectrophotometer (X-Rite). The CIELAB values were calculated with the KeyWizrad (X-Rite) software using 2° standard observer and D50 illuminant. The colour differences were calculated according to the CIEDE2000 colour difference equation (CIE-Publication, 2004). The samples were heated/cooled on the Full Cover water block (EK Water Blocks, EKWB d.o.o., Slovenia). Temperature of its flat copper plate surface was varied by circulating thermostatically controlled water in channels inside the water block. Three consecutive heating-cooling cycles were measured for every sample in a temperature range from 5 to 50 °C. The results were recorded continuously in 1 °C steps without stopping the heating-cooling processes. The average heating and cooling rates were around 2.6 °C/min and 2.2 °C/min, respectively.

Firstly the samples were measured from low to high temperatures and then cooled back again (HC cycle) and then they were measured in revers cycle; from high to low temperatures and then heated back again (CH cycle). For these measurements the samples were stored at room temperature (21 °C) then placed on the cooled/heated copper plate and immediately measured. These measurements were done on samples with a single ink layer.

Secondly the samples were left at low temperature (5 °C) for one hour and 24 hours prior to the measurements and compared to the sample measured from the room temperature. Here only three consecutive HC cycles were made.

Thirdly samples with different layer thickness were measured. One, two and three ink layers were used. Here only three consecutive HC cycles were made.

3.3. Evaluation of the dynamic colour

The dynamic colour of TC samples was analysed through the corresponding colour hysteresis. Each colour hysteresis has two different sigmoidal-like curves which represent the heating and cooling of the sample. Five parameters were applied to describe the most important properties of the hysteresis loops and of the colour trajectory described during the heating-cooling cycle in the CIELAB space. The parameters TCC, Y, O, W and Area_{Lab} of a typical colour hysteresis loop are shown on Figure 1.

The total colour contrast (TCC), yellowness (Y) and openness (O) are defined for the static states. The TCC is the colour difference between the completely coloured and totally decolourised states of the sample, Y represents the colour difference between the totally decolourised sample and the substrate and O represents the colour difference between the first

and last measurement of one measuring cycle. The width of the hysteresis loop (W) describes temperature-dependant states. W is the temperature difference between the decolourisation and colouration of the sample and is given only for the L^* value, since values for a^* , b^* and C^* are approximately the same.

During the entire measuring cycle, the sample's colour describes two trajectories in the CIELAB colour space, one on heating and another one on cooling. They are, in general, not the same but are usually connected at both ends (in the totally coloured and fully decolourised states, see Figure 1, right). The area of the surface between the colour trajectories provides a measure of difference in colour obtained during heating and cooling of the TC sample. We named this parameter $Area_{Lab}$; it becomes zero when both colour trajectories are the same. The $Area_{Lab}$ was calculated using the equation:

$$Area_{Lab} = \frac{1}{2} \sum_i |H_i H_{i+1} \times H_{i+1} C_{i+1}| + |C_{i+1} C_i \times C_i H_i| \quad (1)$$

H_i and C_i represent colour points in the CIELAB space at i -th temperature during heating and cooling, respectively. $H_i H_{i+1}$ is the vector between the colours H_i and H_{i+1} . The size of each vector product is used to express the corresponding area.

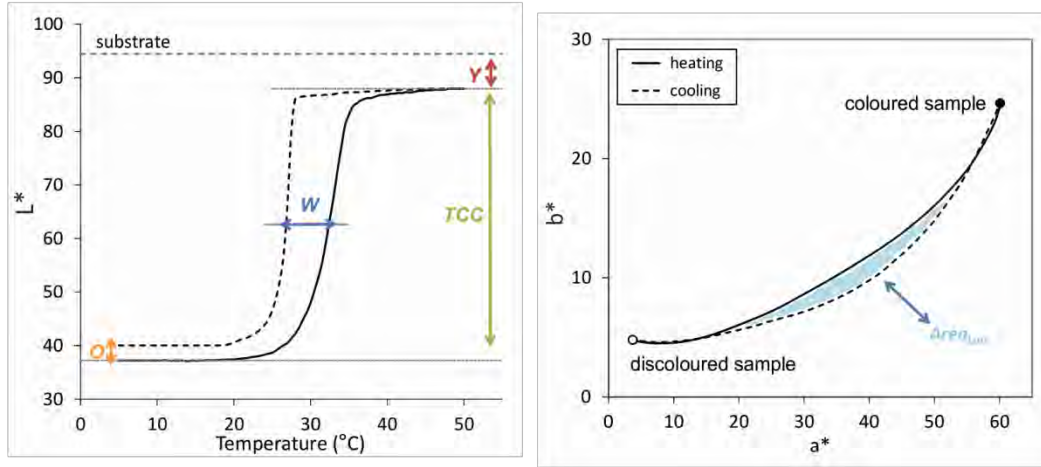


Figure 1: The parameters used for colorimetric characterisation of the dynamic colour of TC inks: total colour contrast (TCC), yellowness (Y), width of the loop (W), openness (O) (left). The colours describe two different trajectories in the CIELAB space, as shown by a projection on the (a^*, b^*) plane (right).

4. RESULTS & DISCUSSION

The paper deals with repeatability of the colour hysteresis loops, the influence of storage conditions of the sample prior to measurement on the hysteresis loop and dependence of the colour hysteresis parameters on the layer thickness. Results are represented in the form of colour hysteresis loops and values of the corresponding parameters.

4.1. Repeatability of the colour hysteresis loop

For this research only samples with a single layer of ink were measured. We tested how the starting measuring temperature affects the colour hysteresis and its repeatability. One measurement started at the lowest temperature, 5 °C (HC cycle) and the other at the highest temperature, 50 °C (CH cycle). Prior to the measurements the samples were at room temperature (21 °C). To see the repeatability of the colour hysteresis we measured three consecutive cycles. All corresponding $L^*(T)$ hysteresis loops for SICPA green sample are represented in Figure 2 and for TCX blue in Figure 3.

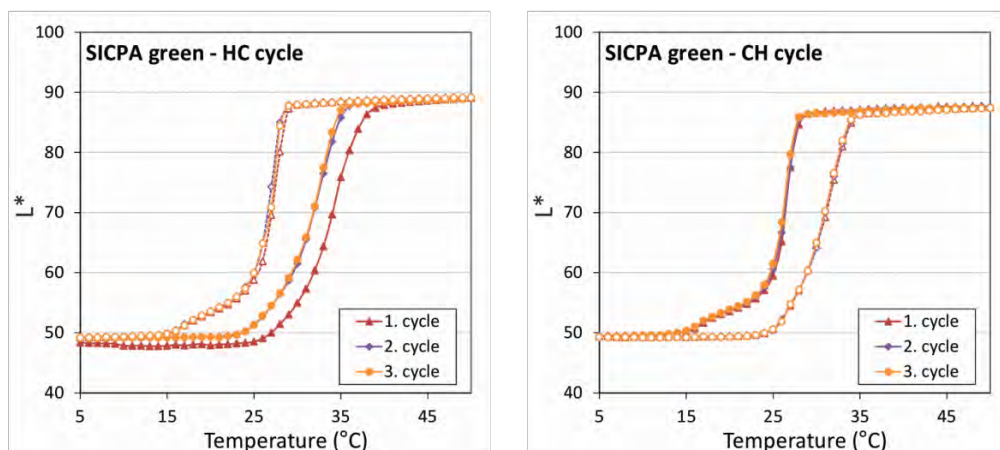


Figure 2: The $L^*(T)$ hysteresis loops of three consecutive HC cycles (left) and CH cycles (right) for the SICPA green sample.

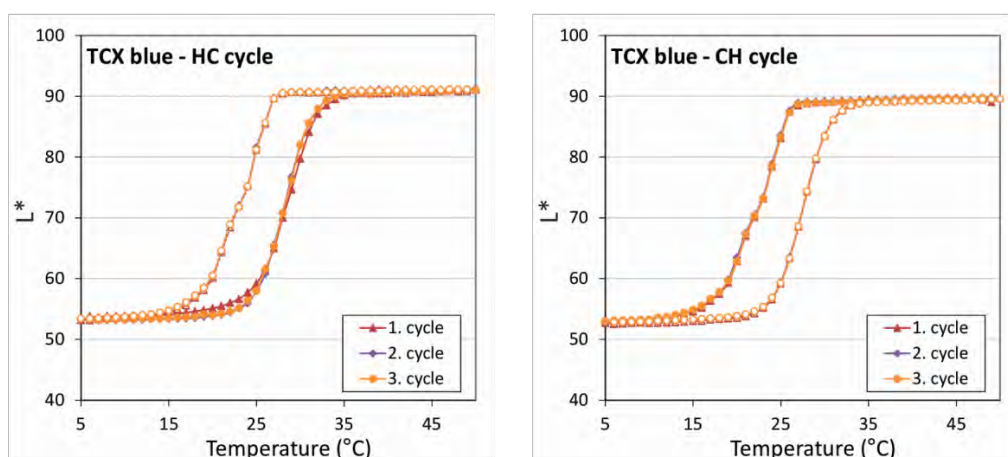


Figure 3: The $L^*(T)$ hysteresis loops of three consecutive HC cycles (left) and CH cycles (right) for the TCX blue sample.

It can be seen from the results in Figure 2 and Figure 3 that all the loops are almost identical when the sample is first cooled and then heated (CH cycle). When measuring HC cycles sometimes the first loop differs from the second and third one which are always the same or very similar. The difference in the first cycle in comparison to other two is large for the SICPA green sample and insignificant for TCX blue sample. Parameters describing the properties of the loops are represented in Table 2.

Table 2: Values of the parameters used to evaluate the dynamic colour of SICPA green and TCX blue samples measured in three consecutive HC and CH cycles.

parameter cycle type	TCC		Y		W		O		Area _{Lab}	
	HC	CH	HC	CH	HC	CH	HC	CH	HC	CH
SICPA green										
1. cycle	34,7	33,1	8,4	8,6	6,9	5,4	1,4	0,2	230	163
2. cycle	34,3	33,3	8,2	8,4	5,2	5,3	0,1	0,1	163	170
3. cycle	34,4	33,2	7,9	8,5	4,9	5,6	0,1	0,1	158	172
TCX blue										
1. cycle	39,0	38,8	4,1	4,4	5,4	5,9	0,4	0,2	133	165
2. cycle	39,4	38,6	4,1	4,2	5,2	6,0	0,3	0,1	146	157
3. cycle	39,1	38,4	4,1	4,5	5,3	5,9	0,0	0,1	142	154

TCC and Y parameters are the same regardless the cycle type and number. O can vary for the first loop in the HC cycle, but differences are small. W and Area_{Lab} are the parameters with the most significant difference between consecutive cycles. For the SICPA green sample they are larger for around 35 % for W and 45 % for Area_{Lab}.

4.2. Influence of exposure time at low temperatures on the colour hysteresis loop

Effect of exposure to low temperatures before the measurement on the colour hysteresis loop was evaluated. We compared the hysteresis loops of the sample that was put on the cooled cooper plate and measured immediately (0 h), the sample that was on the cooled copper plate for one hour before the measurement (1 h) and the sample that was placed in the refrigerator for 24 hours at 5 °C and then measured (24 h). For this test only samples with a single layer of ink were measured and only HC cycles were done. All corresponding $L^*(T)$ hysteresis loops for SICPA green sample are represented in Figure 4 and for TCX blue in Figure 5.

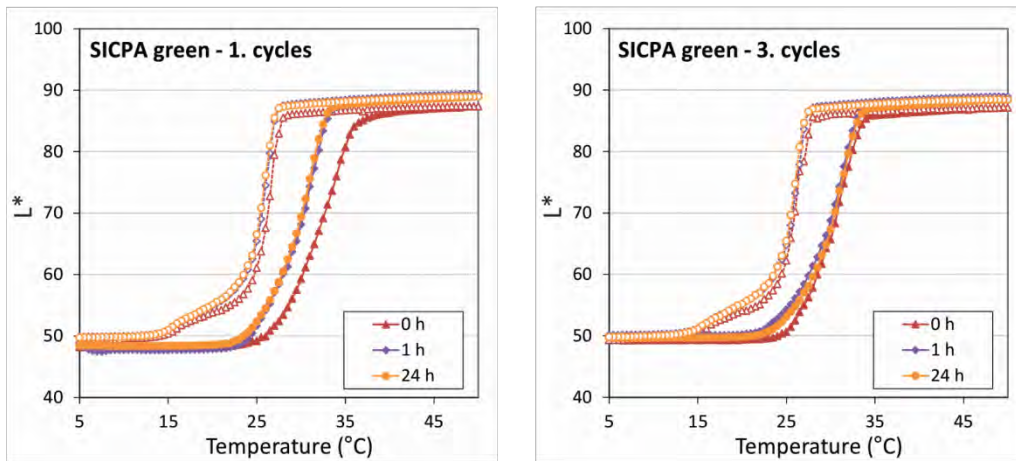


Figure 4: First (left) and third (right) colour hysteresis loops for the sample SICPA green measured after different exposures to low temperatures.

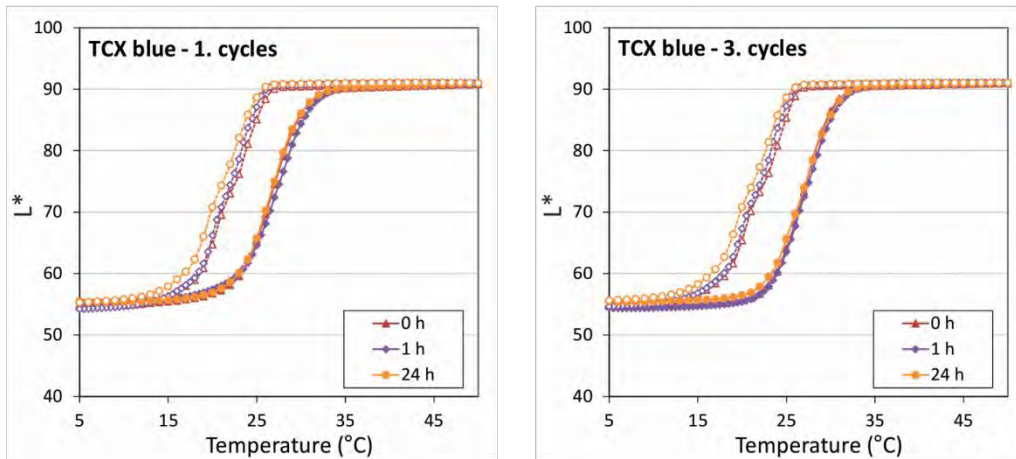


Figure 5: First (left) and third (right) colour hysteresis loops for the sample TCX blue measured after different exposures to low temperatures.

Longer exposures to low temperature have an effect on the hysteresis loops. SICPA green sample has narrower loops (no more the so-called “first cycle effect”) while TCX blue has slightly wider ones. Otherwise the shape of the L^*/T loop remains the same.

Table 3: Values of the parameters used to evaluate the dynamic colour of SICPA green and TCX blue samples measured after different exposure to low temperatures.

parameter cycle	TCC		Y		W		O		Area _{Lab}	
	1.	3.	1.	3.	1.	3.	1.	3.	1.	3.
SICPA green										
0 h	34,0	33,1	8,5	8,4	6,9	4,9	1,3	0,1	227	160
1 h	34,9	32,5	8,1	8,2	4,5	4,6	1,2	0,2	180	146
24 h	35,0	33,5	8,2	8,3	4,8	4,5	1,3	0,2	152	154
TCX blue										
0 h	38,1	38,0	4,2	4,2	5,6	5,9	0,4	0,1	102	129
1 h	37,0	38,4	4,3	4,2	6,3	6,3	1,0	0,2	124	150
24 h	37,6	37,6	4,3	4,1	6,7	6,8	0,4	0,1	142	146

TCC and Y parameters are the same regardless the exposure to low temperatures and number of cycle. O can be slightly larger for the first cycles but differences are small. W and Area_{Lab} are the parameters with the most significant difference between various measurements. Parameters are most similar between consecutive cycles for the sample that was left at 5 °C for 24 hours.

4.3. Influence of layer thickness on the colour hysteresis loop

For each TC ink samples with one, two and three ink layers were measured. Only HC cycles were performed. The corresponding hysteresis loops for SICPA green and TCX blue are represented in Figure 6.

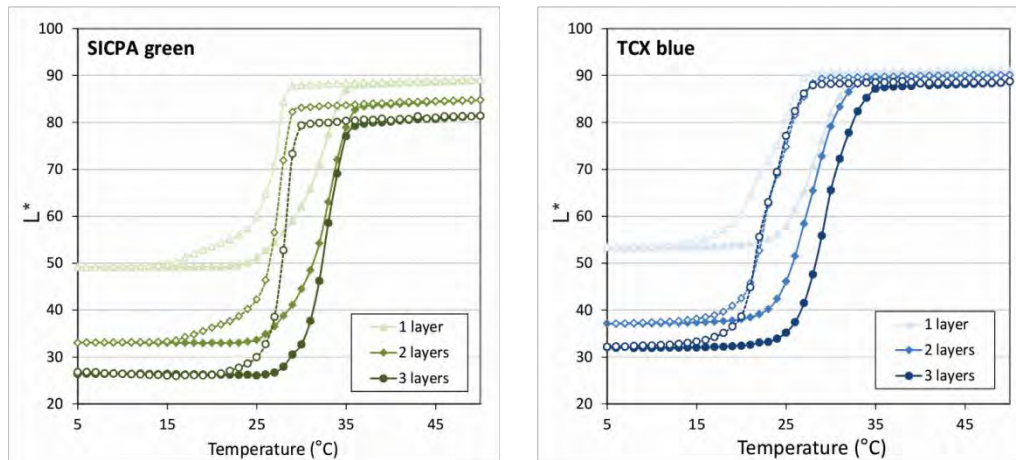


Figure 6: Colour hysteresis loops for SICPA green (left) and TCX blue samples (right) with different ink layer thickness.

Layer thickness has a big influence on the hysteresis loops. Thicker samples have bigger and wider loops and lower discoloration ability in comparison to samples with thinner layers. Values for the parameters of the hysteresis loops are given in Table 4.

Table 4: Values of the parameters used to evaluate the dynamic colour of SICPA green and TCX blue samples with different ink layer thickness.

	TCC	Y	W	O	Area_{Lab}
SICPA green					
1 layer	34,4	7,9	4,9	0,1	158
2 layers	47,3	12,4	5,4	0,1	486
3 layers	53,7	14,2	5,9	0,1	794
TCX blue					
1 layer	39,1	4,1	5,3	0,0	142
2 layers	54,3	5,9	6,6	0,0	580
3 layers	59,3	7,6	6,6	0,1	946

All the parameters increase with layer thickness apart from O. From the Y results it is obvious that SICPA green has lower discoloration ability than TCX blue sample. SICPA green has also a bit narrower loop than TCX blue, which means that the difference (in °C) between discoloration and re-colouration is smaller.

5. CONCLUSION

Dynamic colour of TC inks is represented with the colour hysteresis loop and characterized with five parameters: the total colour contrast (TCC), yellowness (Y) openness (O) and width (W) of the hysteresis loop and the surface area between the heating and cooling colour trajectories in the CIELAB space (Area_{Lab}). In this paper it was evaluated how different physical parameters influence on the colour changing properties of TC inks.

We researched the repeatability of colour hysteresis loop within three consecutive measuring cycles. We measured two different cycles, one from the lowest to the highest temperature and then back to lowest one (HC cycle), and the other from the highest to the lowest temperature and then back to the highest one (CH cycle). It was found out that repeatability is better for the CH cycle.

Effect of exposure to low temperatures before the measurement on the colour hysteresis loop was evaluated. Longer exposures to low temperature have an effect on the hysteresis loops, especially on the width of the loop. For some inks the loop can become narrower, but for others slightly wider. Otherwise the shape of the L*/T loop remains the same.

Layer thickness has a big influence on the shape of the hysteresis loops. Thicker samples have bigger and wider loops and lower discoloration ability in comparison to samples with thinner layers.

Acknowledgements

Mojca Friškovec acknowledges the Slovenian Technology Agency for young researcher support, operation part financed by the European Union, European Social Fund. Operation implemented in the framework of the Operational Programme for Human Resources Development for the Period 2007–2013, Priority axis 1: Promoting entrepreneurship and adaptability, Main type of activity 1.1.: Experts and researchers for competitive enterprises.

6. LITERATURE

- [1] CIE-Publication: "Colorimetry", 3rd edition (CIE Central Bureau, Vienna, 2004),
- [2] Gunde, M. K., M. Friškovec, et al.: "Functional properties of the leuco dye-based thermochromic printing inks", proceedings of 64th Annual Technical Conference TAGA (Pittsburgh, Pennsylvania, USA, 2011), 216
- [3] Kerry, J. and P. Butler: "Smart packaging technologies for fast moving consumer goods", 1st edition (John Wiley and Sons Inc., Chichester, 2008), 356
- [4] Kulcar, R., M. Friškovec, et al.: "Colorimetric properties of reversible thermochromic printing inks" *Dyes and Pigments*, 86 (3), 271-277, (2010)

- [5] Kulčar, R., M. Friškovec, et al.: "Colour changes of UV-curing thermochromic inks", proceedings of 36th International research conference of IARIGAI (Stockholm, Sweden, 2009), 429
- [6] MacLaren, D. C. and M. A. White: "Competition between dye-developer and solvent-developer interactions in a reversible thermochromic system" *Journal of Materials Chemistry*, 13 (7), 1701-1704, (2003)
- [7] MacLaren, D. C. and M. A. White: "Dye-developer interactions in the crystal violet lactone-lauryl gallate binary system: implications for thermochromism" *Journal of Materials Chemistry*, 13 (7), 1695-1700, (2003)
- [8] Phillips, G. K.: "Combining thermochromics and conventional inks to deter document fraud", proceedings of Optical Security and Counterfeit Deterrence Techniques (San Jose, California, USA, 2000), 99-104
- [9] Seeboth, A. and D. Löttsch: "Thermochromic phenomena in polymers", 1st edition (Smithers Rapra Technology Limited, Shrewsbury, 2008),
- [10] White, M. A. and M. LeBlanc: "Thermochromism in commercial products" *Journal of Chemical Education*, 76 (9), 1201-1205, (1999)

OPTICAL PROPERTIES AND UV/VIS SPECTRA OF AGED PAPERS

Silva König, Diana Gregor-Svetec
Faculty of Natural Sciences and Engineering, Ljubljana

Corresponding author: Silva König
e-mail: silva.koenig@ntf.uni-lj.si

1. ABSTRACT

Change of optical properties is often the most obvious characteristic during paper ageing. The decrease of brightness or the increase of yellowness occurs because of sunlight, high humidity and high temperature. The moist heat and light treatments of accelerated ageing were applied to investigate the ultraviolet/visible (UV/VIS) spectroscopy of non-recycled, recycled, uncoated and coated papers. In addition to spectroscopy, the optical properties were measured to evaluate cellulose and paper degradation. The results reveal different stability of aged papers. The effect depends on the type of accelerated ageing and on paper characteristics.

Key words: recycled paper, accelerated ageing, moist heat treatment, light fastness, UV/VIS spectroscopy, optical properties

2. INTRODUCTION

Papers are susceptible to colour changes during storage. This is easily seen as a yellowish or brownish colour of old printed materials, such as old books and newspapers (Jääskeläinen, Liitiä, 2007). The loss of brightness during ageing is attributed to the presence of chromophores that are formed by the degradation of paper components (cellulose, hemicelluloses and lignin). Paper yellowing depends to the paper structure and surface coating (Debeljak, Gregor-Svetec, 2010). The speed of paper ageing depends especially on its fibre components, and increases with rising lignin contents. Organic additions used as optical brighteners are also chemically unstable and have a negative influence on the oxidation reaction. Recycled papers are less stable compared to papers made of virgin fibres because of the different recovered paper rows, which can have poor quality and unwanted components. Moreover, chemical agents are used during the deinking process. This process can result in shorter cellulose fibres and worse chemical and mechanical paper properties (Černič, 2010; Grilj et al., 2012).

UV/VIS spectroscopy enables the measuring of reflectance and transmittance of solid or liquid materials. The measurements are performed using collimated beam; when it is detected in collimated form, specular reflectance or directional transmittance is measured. The integrating sphere enables the collecting of the light emerging from the sample in arbitrary direction; thus, the diffuse reflectance or diffuse transmittance could be obtained. Such analysis enables the surface characterisation of glossy or rough solids or the photometric analyses of turbid, colloidal, transparent and translucent samples in solid or liquid forms. Most common are the measurements of textiles, dyes, papers and glass. The spectra give information about electronic shells of the material in the investigated sample, which is of great importance in many applications in the material science and in several applications (Perkinelmer, 2010; Grilj et al. 2011). UV/VIS reflectance spectroscopy is also a practical method to study the chemistry of pulp yellowing (Jääskeläinen, Liitiä, 2007).

The main reason of this research was to investigate paper changes during two different accelerated ageing. We analyse optical properties and UV/VIS spectra of non-recycled, recycled, uncoated and coated papers.

3. MATERIALS AND METHODS

In the research, four different commercially produced papers with similar grammage (100 g/m²) were analysed. Slovenian paper mill Papirnica Vevče supplied two wood-free papers: uncoated (VUP) and matt-coated (VCP) papers made of virgin fibres. The other two papers were bought from the Danish paper manufacturer Dalum Papir A/S. These papers were 100 % recycled, uncoated (RUP) and matt-coated (RCP). Paper properties were determined according to the appropriate standards and are presented in Table 1.

Papers were exposed to the two different accelerated ageing methods for 12 days. A conditional chamber was used for the moist heat treatment (ISO 5630-3, 1996), where the specimens were exposed to a temperature of 80 °C with 65 % relative humidity without light exposure. A Xenotest Alpha (Atlas) was used for the light fastness (ISO 12040, 1997) analysis. The specimens were exposed to the xenon arc light at a temperature of 35 °C with 35 % relative humidity. The temperature of the black standard was 50 °C. A Xenochromo 320 nm filter and turning mode illumination were used.

Untreated papers and papers treated with both mentioned accelerated ageing methods were evaluated using spectrophotometric measurements.

A Color Digital Swatchbook (X-Rite) spectrophotometer with UV light was used to measure ISO brightness (ISO 2470, 1999) of papers under standard light D65 and 2° observer. Instrument was calibrated on white standard. ISO brightness was measured as reflectance of opaque sheet wisp at 457 nm wavelength 6 times for each sample.

The yellowness index was calculated as follows:

$$YIE313 = \frac{100(C_X X - C_Z Z)}{Y} \quad (1)$$

where X, Y, Z are the CIE tristimulus values, and C_X and C_Z are coefficients (D65/10°: $C_X = 1.3013$, $C_Z = 1.1498$) (Debeljak, Gregor-Svetec, 2010).

An Eye-One Pro (X-Rite) spectrophotometer was used to measure the $L^*a^*b^*$ values of papers under the following condition: D50 illumination, 2° observer, density standard DIN, absolute white base, no filter and reflectance measuring mode. Measurements were repeated 3 times for each sample.

Using the UV/VIS spectrometer Lambda 800 with PELA-1000 integrated sphere accessory (PerkinElmer), we measured the reflectance values in the wavelength region 200–900 nm. The measurements of all samples were conducted in 5-nm steps, preparing 5 specimens for each sample, the average values of reflectance and transmittance of which was calculated with software UV WinLab 6.0.2.0723.

Optical properties and UV/VIS spectra of the papers were determinate at the upper side of the papers only.

Table 1: Properties of the papers

Properties	Standard	Treatment	VUP	VCP	RUP	RCP
Grammage [g/m ²]	ISO 536	–	99.6	96.5	97.3	101.7
Thickness [μm]	ISO 534	–	126	88	106	92
Specific volume [cm ³ /g]	ISO 534	–	1.26	0.91	1.08	0.90
Roughness, Bendtsen [ml/min]	ISO 5636-3	Untreated	156	44	213	91
		Moist heat*	184	47	215	87
		Xenon lamp*	217	50	252	106
Air permeance, Bendtsen [ml/min]	ISO 5636-3	Untreated	865	< 5	335	9
		Moist heat*	883	< 5	282	11
		Xenon lamp*	930	7	420	15

*After 12 days of treatment

4. RESULTS AND DISCUSSION

4.1. Optical properties

Reduction of ISO brightness due to different accelerated ageing is shown in Figure 1. ISO brightness for moist heat treatment reduces the least for paper VUP (4 %), followed by RCP (5 %), RUP (7 %) and VCP (8 %). Differences for light ageing are higher in comparison with moist heat treatment. Papers VCP, RCP and VUP have at light ageing similar reduction (about 20 %). Meanwhile ISO brightness for paper RUP reduces for 33 %.

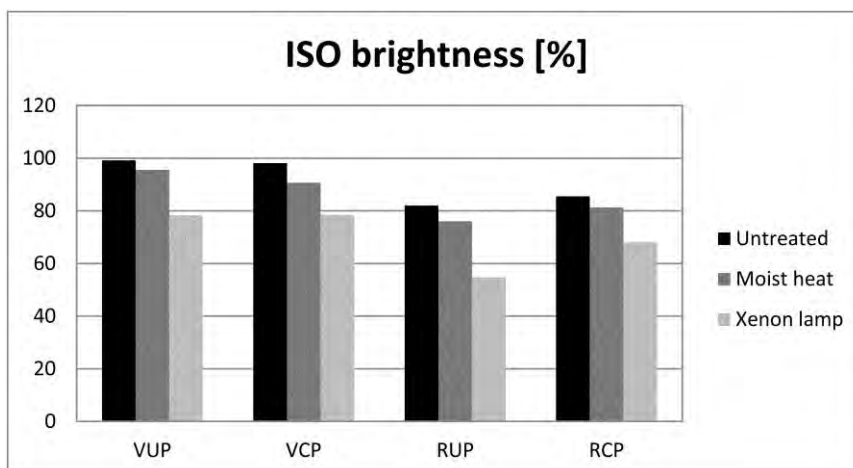


Figure 1: Reduction of ISO brightness

Figure 2 shows the rising of paper yellowness according to accelerated ageing. Yellowness index for moist heat treatment increased 5 units for paper VUP, following by RCP (6), RUP (7) and VCP (8). Yellowness index for papers VCP and RCP increased 12 units, for RUP 22 units and for VUP 24 units at light ageing. Trend for moist heat treatment is similar to those of ISO brightness; meanwhile for light ageing the difference between uncoated and coated papers can be detected because the change for the first one is larger. Coated papers are subject to yellowness a bit less than uncoated papers. Figure 3 supplements the findings in Figure 2. Paper colours shift from blue to yellow region for papers made of virgin fibres (VUP and VCP) and from neutral to yellow region for recycled papers (RUP and RCP).

Increasing yellowness and decreasing ISO brightness of aged papers occurs due to degradation of optical brighteners. Substrates without optical brightener agents can achieve better light fastness performance (Chovanцова-Lovell, Fleming III, 2006). Paper yellowing is the natural ageing process because of sunlight, high humidity and high temperature. The loss of brightness during ageing is attributed to the presence of the chromophores formed by the degradation of paper components (cellulose, hemicelluloses, lignin) (Debeljak, Gregor-Svetec, 2010). Such effect partly occurs also because of increased air permeance and roughness during ageing which can be seen in Table 1. Differences in surface properties happened due to larger holes, spaces between fibres and fillers, and therefore different light scattering.

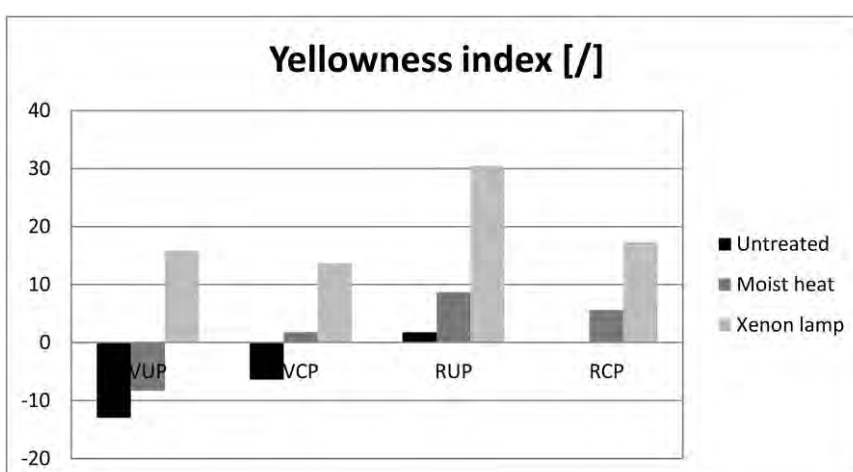


Figure 2: Increasing of yellowness

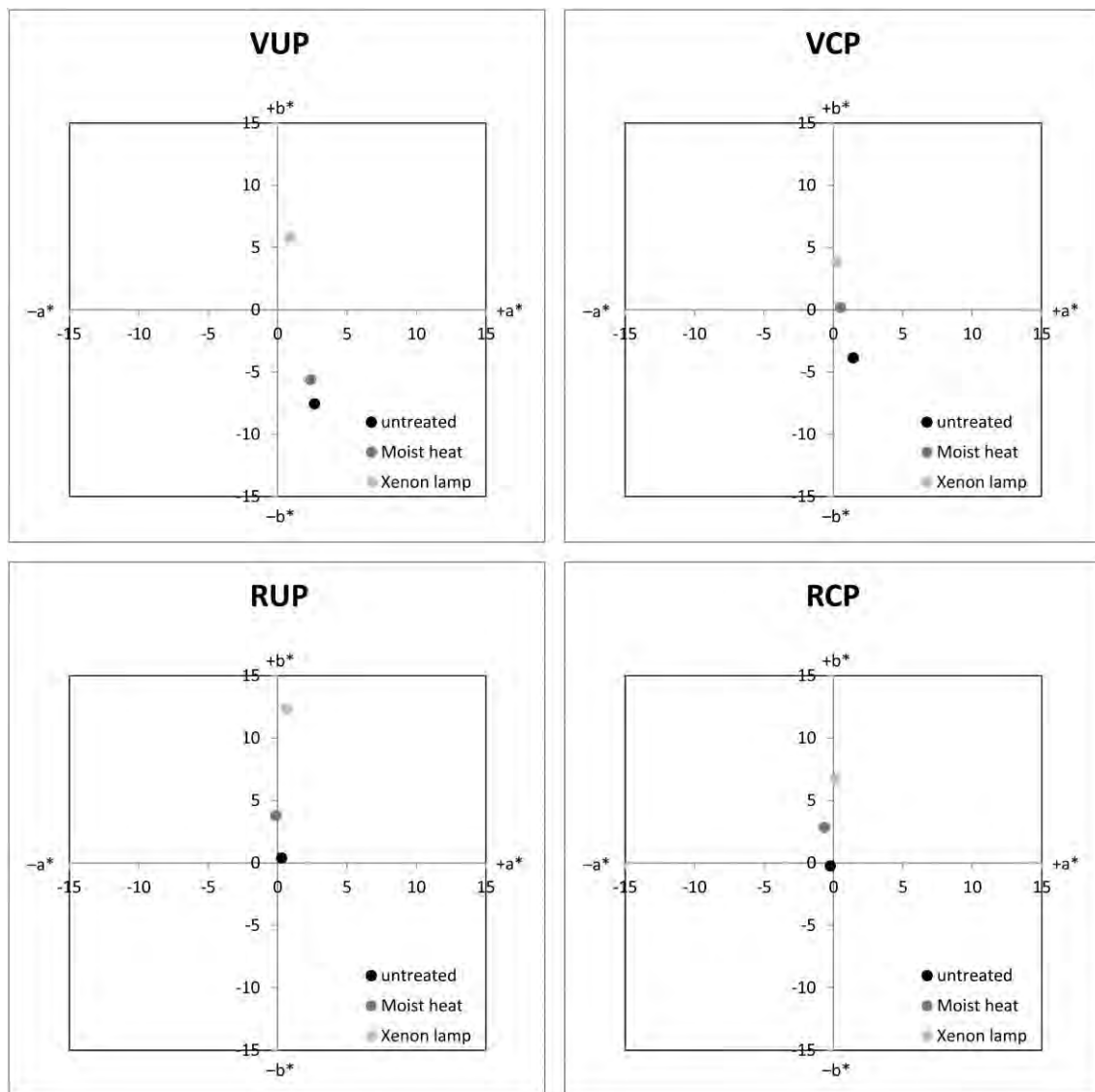


Figure 3: Change of CIE a^*b^* components

4.2. UV/VIS spectroscopy

Figure 4 show the reflectance of untreated and treated papers in dependence of the wavelengths. Particularly interesting are the reflectance values of papers made of virgin fibres, the values of which exceed 100 %. This is a typical phenomenon of papers which contain optical brighteners, due to which paper emits light even more in the UV spectral region. The phenomenon is the strongest at uncoated paper made of virgin fibres (VUP), where the maximum reflectance value equals 240 %. The coating on paper partially suppress the effect of brighteners. Maximum reflectance value for coated paper made of virgin fibre (VCP) equals 105 %. Recycled papers have smaller reflectance value which mean less optical brighteners in paper surface.

Degradation of optical brighteners during ageing is visible also from reflection in the UV spectral region (Figure 4). A small degradation of optical brighteners occurs at moist heat treatment and large at light treatment. Different papers have almost the same spectra after ageing with light treatment which indicates that their optical brighteners completely degrade.

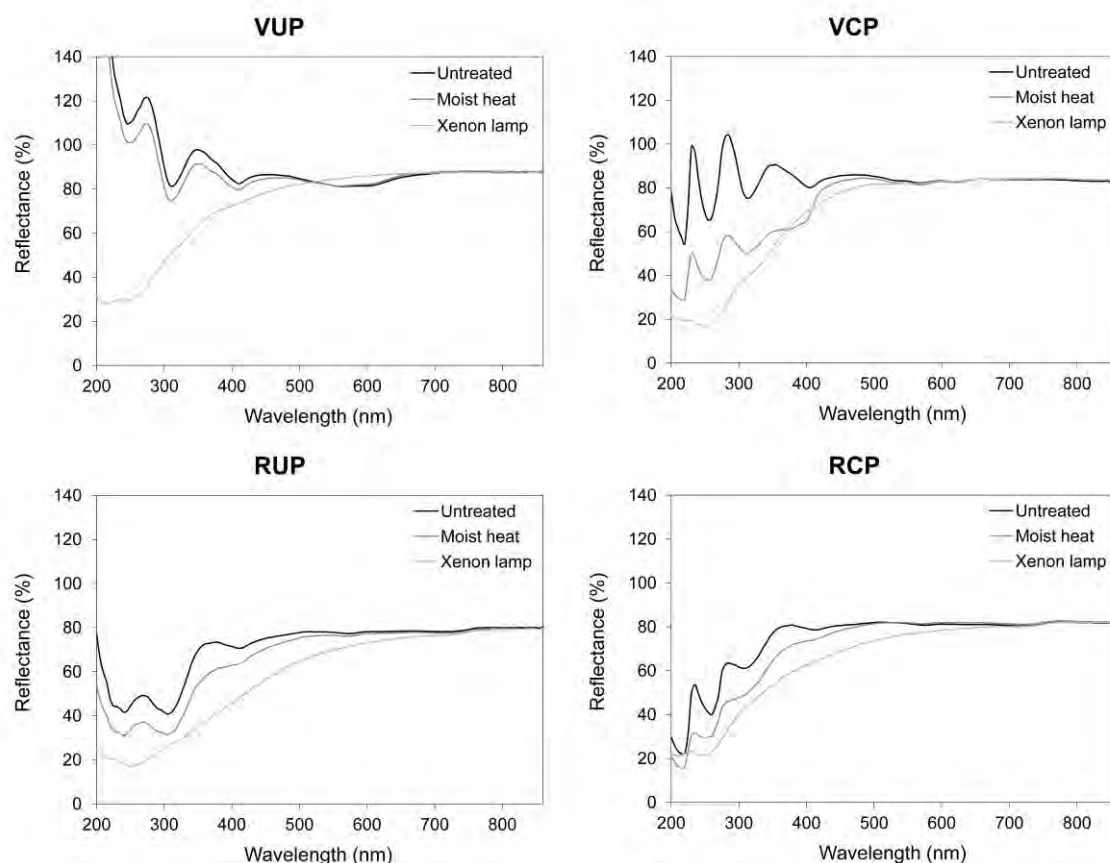


Figure 4: Change of UV/VIS spectra

5. CONCLUSIONS

The article presents optical properties and UV/VIS spectra of aged papers. The results reveal the different stability of papers. The effect depends on the type of accelerated ageing and paper characteristics. Moist heat ageing has less influence on optical properties and UV/VIS spectra than light ageing. The better light fastness of coated papers in comparison with uncoated ones has been indicated from yellowness index and CIE a^*b^* components. Meanwhile the reflectance at UV spectral region reveals larger amount of optical brighteners in papers made of virgin fibres than in recycled papers and therefore greater decrease of reflectance during ageing at those papers.

Acknowledgements

The financial support for the PhD grant from the Slovenian Research Agency is gratefully acknowledged.

6. LITERATURE

- [1] Jääskeläinen, A.-S., Litiä, T.: "UV/vis reflectance spectroscopy reveals the changes in fibre chemistry during ageing", *SpectroscopyAsia* 3 (4), 11–13, 2007.
- [2] Debeljak, M., Gregor-Svetec, D.: "Optical and colour stability of aged specialty papers and ultraviolet cured ink jet prints", *J. Imaging Sci. Technol.* 54 (6), 060402-1, 2010.
- [3] Černič, M.: "Kemijska in fizikalna razgradnja papirja in dokumenta", *Tehnični in vsebinski problem klasičnega in elektronskega arhiviranja*, Radenci, 2010, pages 209–225.
- [4] Grilj, S., Muck, T., Gregor-Svetec, D.: "The ageing resistance of offset and electrophotographic prints", *Nord. Pulp Paper Res. J.* (in print), 2012.
- [5] PerkinElmer: "Applications and Use of Integrating Spheres with the Lambda 650 and 850 UV/Vis and Lambda 950 UV/Vis/NIR Spectrophotometers", URL

http://shop.perkinelmer.com/content/ApplicationNotes/APP_LAMBDA650IntegratingSpheres.pdf (last request: 2010-02-01).

- [6] Grilj, S., Muck, T., Hladnik, A., Gregor-Svetec, D.: "Recycled papers in everyday office use", Nord. Pulp Paper Res. J. 26 (3), 349, 2011.
- [7] ISO 5630-3: "Paper and board – Accelerated ageing – Part 3: Moist heat treatment at 80°C and 65 % relative humidity", 1996.
- [8] ISO 12040: "Graphic technology – Prints and printing inks – Assessment of light fastness using filtered xenon arc light", 1997.
- [9] [9] ISO 2470: "Paper, board and pulps – Measurement of diffuse blue reflectance factor (ISO brightness)", 1999.
- [10] [10] Chovancova-Lovell, V., Fleming III, P. D.: "Effect of Optical Brightening Agents and UV Protective Coating on Print Stability of Fine Art Substrates for Ink Jet", Proceedings of the IS&T NIP22: International Conference on Digital Printing Technologies, Denver, 2006.

UV/EB INKS AND VARNISHES IN PRINTING INDUSTRY

*Bohumil Jašůrek, Jan Vališ
University of Pardubice, Faculty of Chemical Technology,
Department of Graphic Arts and Photophysics, Pardubice*

*Corresponding author: Bohumil Jašůrek
e-mail: bohumil.jasurek@upce.cz*

1. ABSTRACT

This paper reviews the different mechanisms of UV inks curing (free radical, cationic and hybrid polymerization). The advantages and disadvantages of these various types of UV inks are discussed together with their applications areas. Next, the various UV sources used for curing of these inks are outlined. The text describes mercury lamps, doped mercury lamps, excimer lasers and also UV LEDs. UV LEDs are potentially very interesting UV source, which may in the future replace existing sources in some applications. The last part is focused on EB inks. In the text the curing mechanism, applications areas and their comparison with UV inks are explained.

Key words: *UV ink, EB ink, UV source, cationic polymerization, radical polymerization*

2. INTRODUCTION

Photoinitiated polymerization (mostly by UV radiation) of multifunctional monomers and oligomers is one of the most efficient methods to produce highly cross-linked polymer networks. The beginning of UV curing industry can be found in the 1960. [1] Since then much effort was given to develop these systems (photoinitiators, monomers and oligomers, additives, optimization of formulations, UV sources, reflectors, etc.). In these days this technology has many commercial applications (printing inks and varnishes, coatings, adhesives, dielectric layers, etc.), because of its unique advantages. The most important advantages are:

- Rapid curing time (fractions of a second) with obvious production benefits in today's high speed production lines. The final product can be further processed immediately after printing.
 - Low operating costs, lower energy consumption.
 - Enhanced material properties that allow manufacturers to make their products more attractive and durable. Finished products exhibit very good abrasion and solvent resistance coupled with superior toughness. Another important benefit is that the UV inks and varnishes allow to achieve the highest gloss not attainable by any coating method.
 - Low VOCs (volatile organic compounds) is certainly the most discussed aspect of UV curing (not always the most important). UV inks and coatings release virtually zero VOC, although photoinitiators may have some solvents and the formulations contain some volatiles (weight loss of the applied cured film is usually in the range from 1 to 3 % versus 70 % and higher for low solids and even waterborne systems).
 - Pot life. Because the inks and coatings do not contain volatiles, evaporation of the inks in inking unit does not occur. This in turn leads to increased stability on the press, reduction of downtime for cleaning, faster set ups and job changeovers, etc. [2, 3]
- In the printing industry are UV systems used mainly as printing inks and varnishes. They are often used in offset printing, flexography, inkjet and screen printing.

3. THE UV CURING PROCESS

UV formulations generally contain five types of substances (monomers, oligomers, photoinitiators, pigments and additives). Monomers are low molecular weight materials and their main function is to adjust required viscosity of final formulation. Oligomers are higher molecular weight materials with higher viscosity. Usually, the type of oligomer backbone determines the final properties of cured film such as flexibility, toughness, etc. Photoinitiators are substances that initiate the polymerization process. The UV curing process requires a radiation source (UV or visible light). Photoinitiators absorb this radiation and decompose onto reactive species (free radicals or cations). These reactive particles start polymerization reaction of monomers and

oligomers that they are quickly (in fractions of second) converted from a liquid formulation into a solid, cured film. Pigments are substances that provide given colour and additives modify the inks properties (surfactants, defoamers, light stabilizers, etc.) or modify properties of final cured film (waxes, etc.).

There are three different UV curing systems: free radical, cationic and hybrid polymerization. UV curing systems are dominated by acrylate chemistry and free radical polymerization with many various types of binders and photoinitiators for precise setting of final properties of cured materials and are relatively well known. The cationic curing is alternative curing technology and is not as widespread as free radical polymerization, but it offers several advantages over more commonly used free radical polymerization. Hybrid polymerization, which combines the advantages of free radical and cationic polymerization, is currently very limited.

3.1. Free radical polymerization

Photoinitiators exposed to an UV radiation spontaneously decompose into free radicals initiating polymerization reaction. These radicals react with double bond of oligomers or monomers resulting in further growing macroradicals. A quickly growing chain is finally stopped by chain-breaking reaction. The polymerisation results in three-dimensionally cross-linked, insoluble and rigid macromolecules. All this happens within fractions of second so immediately after curing a highly resistant film is obtained.

The disadvantage of these systems is mainly oxygen inhibition that is carried out in air (oxygen reacts with radicals and not reactive peroxyradicals are produced). The oxygen inhibition is manifested by an induction period, lower rates and lower degrees of polymerization producing partially cured film. This effect is most pronounced in the curing of thin layers, where high surface area to volume ratio supports fast oxygen diffusion into film. Therefore some UV-driers are equipped by inert gas (mostly nitrogen) what results in significantly increased production speed of printing machines or amount of photoinitiators in ink formulation can be reduced. Another disadvantage of these systems is volume contraction during polymerization (shrinkage). The result of this shrinkage is lower adhesion of inks to some substrates (especially to plastic foils and metals) and also "edge curl effect" (mainly for thin materials like labels). Systems that polymerize by free radical polymerization have typically shrinkage about 5–15 %. [4]

3.2. Cationic polymerization

Cationically curable inks have quite a different reaction mechanism. The monomers and oligomers are based on epoxides, vinylethers and other electron-rich vinyl compounds. Cationic formulation can contain also alcohols in combination with epoxides (alcohols act as chain transfer agent). The initiating species is in this case the Lewis or Brønsted acid. This acid is produced by decomposition of cationic photoinitiator after UV exposition. The proton contained in the acid induces opening of the epoxide ring with a continuous chain growth. Contrary to polymerisation initiated by free radicals here the breakdown products of the photoinitiators are long-lasting and reaction continues after exposure. The average lifetime of cationic active centres has been found to be in order of tens of minutes in comparison to free radicals which have very high termination rate constant and subsequently short lifetimes of active center—typically less than second [5]. First curing takes place mainly at the surface, and then slowly continues. The acid can diffuse through the still liquid layer and cure layers that had not yet been directly exposed by UV radiation. This process can be of advantage when highly opaque inks are printed, as the UV radiation does not penetrate all the way to the substrate (this cause the insufficient curing of inks cured by free radical polymerisation).

Shrinkage of cationic formulations is much lower and usually is about 3–5 %. [4] Low shrinkage minimizes internal stress and this is one of the reasons why cationic formulations have excellent adhesion to a wide variety of substrates. The combination of epoxides with polyols or vinyl ethers allows large-scale adjustment of film properties from rigid to flexible depending on individual requirements. Additions of polyols also increase depth of cure of thick coatings. Another important advantage of cationic formulations is that there is no inhibition by air oxygen, because it involves positively charged species and not radicals. Generally cationic inks have lower potential for skin and eye irritation or sensitization than radical curing inks and also odor of liquid and cured ink is very low. The cationic inks are also characterized as inks with enhanced barrier properties. All mentioned aspects are mainly important for food packaging.

Despite these certainly excellent properties there are following limitations. The curing speed is lower and final properties of catatonically cured inks are developed up to 24 hours or more after UV curing (referred as dark cure). Amines or other basic materials, including some pigments and additives tend to neutralize the initiating acid, resulting in poor cure response and subsequently by poor adhesion or micro-wrinkling (or both). The inks cured by cationic polymerization are negatively affected by high ambient humidity. This can be suppressed by infrared dryers that decrease relative humidity and on the other hand increase cure speed due to increased temperature of ink. Advantages and disadvantages of these two types of inks are summarized in Table 1.

Table 1: Comparison of cationic and free radical systems

Parameter	Free radical	Cationic
Cure speed	High	Moderate to high
Initiation	UV radiation	UV radiation and heat
O ₂ sensitivity	Yes	No
Humidity sensitivity	No	Yes
Base sensitivity	No	Yes
Shrinkage	Large	Low
Adhesion	Moderate to good	Excellent
Post cure	Limited	Strong
Chemical resistance	Good	Moderate to good

3.3. Hybrid polymerization

Relatively new are hybrid systems that combine the advantages of free radical and cationic polymerization. The main advantage of hybrid systems is that they often synergistically combine the properties of the two constituent homopolymers (glass transition temperature, melting temperature, strength and toughness, etc.) [6] Another important advantages of the radical/cationic hybrid systems is that they reduce oxygen and humidity sensitivity in the respective free radical and cationic polymerization, favourably affect shrinkage as well as stress development (in comparison to free radical systems), improved film-forming properties, increased cure speed and final properties are developed much faster. [6, 7] In work [8] a positive effect of epoxide monomer on polymerization of acrylate monomers in hybrid system was proved. The reaction rate of free radical polymerization was much faster in the presence of epoxides (against pure free radical system) and also higher conversion of acrylate monomers was reached (free radical polymerization is faster than cationic and due to the cationic monomers act as a plasticizers during early polymerization of acrylate monomers). The reached conversions of acrylate double bonds were about 15 % higher in monomer mixture than in pure acrylate monomer. The conversion of cationic monomer was only slightly lower (few percent) in hybrid mixture than in pure epoxide system. The using of hybrid polymerization in coatings and printing inks is currently very limited and is mostly subject of research. In future, it could be a powerful tool to achieve tailor-made properties, in particular to produce hard and flexible polymeric materials well suited for coating applications.

4. UV SOURCES

For UV curing is important not only UV radiation, but also near visible spectrum from 400 to 450 nm (mainly for pigmented systems). The UV region can be split into to three parts: UVA (400–315 nm), UVB (315–280 nm) and UVC (280–100 nm). Selecting the right UV source (spectral output, power, heat, input power, lifetime, etc.) is crucial for efficient UV curing performance. Each photoinitiator has its unique spectral absorption pattern. Additionally, other compounds in the ink or coating (such as oligomers, diluents, and mainly pigments) have their own impact on

the overall absorption characteristics of the cured system. Besides the above mentioned parameters are for successful curing also important some other aspects: production speed, type of printed material (paper, polymer foils, etc.), type of reflectors, thickness of cured ink, rheology of ink, etc. Short wave UV around 250 nm has little penetrative power and is mainly used to provide surface cure. Long wave UV and near visible light penetrate much further and is more useful for depth cure. [1]

4.1. Medium pressure mercury lamp

The most common used UV source for UV curing is medium pressure mercury lamp. Besides medium pressure mercury lamps, there are also low and high pressure mercury lamps. Mercury lamps provide significant advantages over other approaches, such as lower cost, faster process speed and higher UV power. On the other hand they have some fundamental limitations such as, high electrical power, relatively short lifetime, use of mercury which is now considered environmentally hazardous, high production of infrared radiation and also production of ozone. The mercury vapour may be energised by an electric arc discharge or by microwave radiation (the lamp output in both cases is similar). Parameters of these two types of mercury lamps are summarized in the Table 2. Typical spectrum of medium pressure mercury lamp is shown on Figure 1 (often marked as H-bulb). For pigmented systems is better to use doped mercury lamps due to shift of spectral output to longer wavelengths (D-bulb is doped by iron, V-bulb by gallium, Figure 2 and 3).

Table 2: Comparison of medium pressure mercury lamps (arc and microwave lamps)

	Arc lamp	Microwave powered lamp
Power (W/cm)	80–300	120–240
Length (cm)	up to 180	25 (max)
Start-up time	2–3 minutes	10 seconds
Lifetime (hour)	1 000	3 000

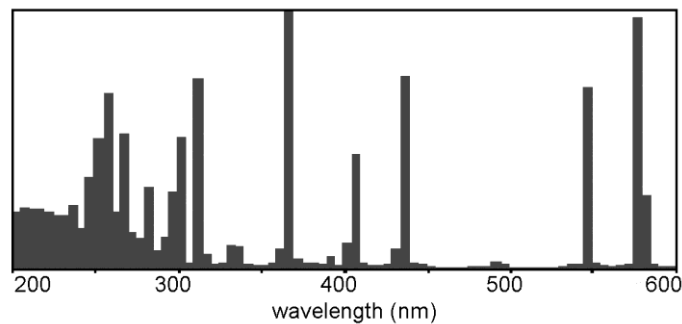


Figure 1: Spectrum of medium pressure mercury lamp (H-bulb)

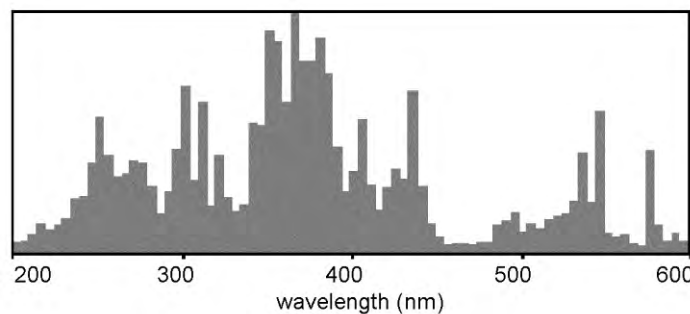


Figure 2: Spectrum of medium pressure mercury lamp (D-bulb)

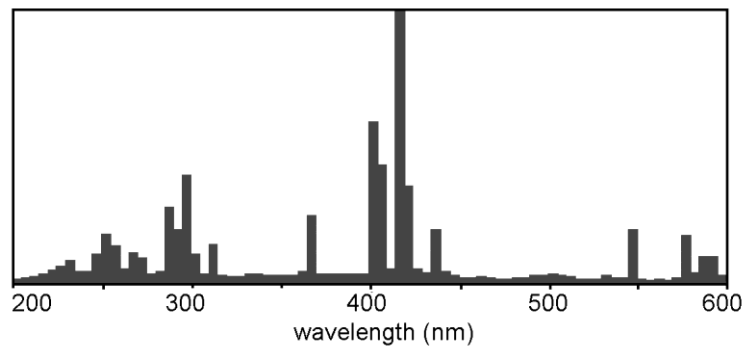


Figure 3: Spectrum of medium pressure mercury lamp (V-bulb)

H-bulb has strong output in the UVC (200–280 nm) and the UVB (280–320 nm). It is typically used for curing offset inks and overprint varnishes. D-bulb has much higher percentage of its output in the UVA (320–400 nm) and this lamp is used where deeper penetration is required. Applications include thick pigmented inks and very thick clear coatings. V-bulb has strong output in the violet region of the visible spectrum (400–420 nm) and it makes this lamp well suited to cure white pigmented coatings.

In addition to mercury lamps also xenon lamps are used, which are characterized by lower heat production and are supplied in smaller sizes.

4.2. Excimers

An excimer laser is a form of ultraviolet laser. The term excimer is short for “excited dimer”. Excimers can be formed by noble gases and noble gas/halogen mixtures, for which the term excimer is incorrect (since a dimer refers to a molecule of two identical parts/atoms). The correct but less commonly used name for noble gas/halogen mixture is exciplex laser. Under the appropriate conditions of electrical stimulation and high pressure, a pseudo-molecule called an excimer (or exciplex) is created. The excimer state is of short duration. When the excimer breaks up, UV radiation is emitted in a very narrow, quasi monochromatic spectral range. Depending on the used gas, different narrow-band UV spectrums are emitted, mainly in a single spectral line (Table 3). An excimer laser typically uses as noble gas argon, krypton, or xenon and as halogen fluorine or chlorine. [9]

Table 3: The wavelength of an excimer lasers

Excimer	Wavelength (nm)	Excimer	Wavelength (nm)
(ArAr)*	126	(KrF)*	248
(KrKr)*	146	(ClCl)*	259
(FF)*	157	(XeBr)*	282
(XeXe)*	172	(XeCl)*	308
(ArF)*	193	(XeF)*	351
(KrCl)*	222	(NN)*	337

Company Heraeus Noblelight produces excimer lamps under the name Bluelight with emission maximums of 172, 222, 282 and 308 nm [9]. The most used wavelength is 308 nm (excimer XeCl*). [10]

Using excimer UV sources provide a number of indisputable advantages:

- no heating of the printed substrate as radiation does not involve any infrared radiation (important mainly for polymer foils),

- better utilization of electrical power for drying process and effective curing process, because only activating radiation is emitted (no visible or infrared radiation) and wavelength can be chosen to match the maximum of photoinitiator absorption,
- no ozone generation (excimers with emission bands in UVA or UVB region),
- the presence of inert gas prevents the quenching process caused by atmospheric oxygen and thus significantly increases the yield of polymerization and the degree of conversion,
- suitable combination of excimer lamps can create matt surfaces without special matting additives (for example short wave excimers with emission bands at 172 or 222 nm cure only thin layer on the top and this fast-curing surface film cracks and causes diffuse scattering of light. Consequently the excimer with longer wavelength (308 nm) cures the rest of the varnish.

Between disadvantages belongs:

- higher purchase costs,
- excimers power (up to 50 W/cm) that is still considerably lower than the power of mercury lamps,
- the ink photoinitiator system needs to be adapted to the particular wavelength of excimer. Conventional UV lamps are polychromatic and therefore cover a greater bandwidth of photoinitiator. [10]

4.3. UV LED

Over the past few years the irradiance of commercial UV-LED (light emitting diode in UV range) devices increased from a few hundred mW/cm² to approximately 10 W/cm². [11] This leads to a wide range of UV-LED applications (printing inks and varnishes, curing adhesives, coatings etc.) Due to fundamental semiconductor material processing issues, present LEDs are limited to wavelength longer than 355 nm (commercially available UV LEDs operating at 365, 385, 395 and 405 nm). [12] UV-LEDs can offer substantial benefits, such as, instant on-off, mercury free, longer lifetime (> 20 000 hours), low energy consumption, lower production cost, no generation of ozone and heat, maintenance free, etc. Main disadvantages of UV-LED systems are: lower UV power in comparison with mercury lamps and the lack of suitable chemistry. Over the past ten years, most UV chemistry has been formulated to react with broad band mercury spectrums. Not all systems from previously formulated UV chemistry is compatible with monochromatic UV-LEDs and has to be reformulated to react and accomplish similar cure results as are achieved with mercury lamps. UV-LED inks and coatings require specific photoinitiator types that absorb at longer wavelengths. Only three groups of commonly used photoinitiators absorbed at long wavelengths (Phosphine oxides, Thioxanthenes and Ethyl Michlers ketone). It is also important to choose much more reactive oligomers and monomers to achieve suitable reactivity levels. [13] With reformulation another disadvantage of these inks is connected, the higher price. With longer wavelengths and lower power of UV-LEDs often relates insufficient surface cure due to oxygen inhibition (better full cure results can still be achieved with a broad-spectrum mercury lamps). Oxygen inhibition can be eliminated by using of inert gas (nitrogen), but is connected with increased running costs.

In the graphic arts industry are UV-LEDs used mainly in inkjet printing and it could be soon the preferred choice compared to mercury lamps. UV-LEDs are also used in offset printing (narrow web presses) and flexography, but they are not as widespread as in inkjet printing. An example of offset printing machine with UV-LEDs can be Ryobi 525GX LED-UV from a Japanese company Ryobi. With existing LED sources, careful optimisation and high photoinitiator loadings the offset inks can be cured at 100 m/min. [13]

5. EB INKS

EB is the abbreviation for electron beam curing. Electron beam is an ionizing radiation of such high energy that molecules of monomers and oligomers of printing inks or coatings are ionized, thus causing the release of free radicals. In principle, the same monomers and oligomers can be used for EB and UV curing. Owing to high energy, a sufficient number of initial radicals are released and therefore there is no need to add expensive photoinitiators. [10] The absence of photoinitiator has three major advantages. 1) economical aspect due to elimination of expensive photoinitiators from formulations, 2) environmental aspect, because photoinitiators are usually variously modified aromatic substances that can migrate from cured film and 3) better storage stability of the inks.

The use of EB curing for printing inks and varnishes, particularly in the packaging industry is growing rapidly (mainly in the USA, Western Europe, but also in emerging markets of China, India, etc.). The driving forces are ecology, economy and development of low voltage EB systems operating in the 80–125 kV range (these low voltage EB equipments were introduced in early 2000). The electron energy of these systems is lower and more efficiently deposited to the thin layers to be cured. Low voltage EB systems are thus smaller and more compact than traditional EB equipment and, due to their effective generation of energetic electrons, they also consume considerably less energy. In Table 4 there is shown a comparison of energy consumption of web offset press equipped with UV and EB drying (UV: IST 6 lamps, each 200 W/cm, 3 chill drums; EB: ESI EZCure I EZ110/90/1200 DF, no chill drum). [14]

EB systems are due to their high penetrating power of electrons especially well-suited to cure thick, multiple and heavily pigmented layers of inks and coatings. EB curing enables wet-on-wet curing of several layers of inks at the end of printing machine with just one EB station. EB curing of inks and varnishes is very fast (printing speed can be up to 600 m/min) and due to high penetrative power of electrons a “100%” cure is achieved without residual uncured monomers and oligomers. This high effectiveness of printing process favours using of EB systems mainly in web offset and flexo printing. Other areas, where these low voltage systems are used, are for the curing of overprint varnishes and high gloss lacquers on gravure and flexo printed materials and in applications where lamination is replaced by an EB cured varnish. [14] For food packaging is also important that during the curing any microorganism in the substrate is destructed by electrons. Main drawbacks of EB curing are higher investment costs, radiation inside a protective atmosphere (e.g. nitrogen) and higher cost for printing inks.

Table 4: Energy consumption UV vs. EB (web offset press) [14]

Item	UV	EB
Electric power	215 kW	58 kW
Cooling capacity	113 kW	21 kW
Cooling water	9750 l/h	3660 l/h
Exhaust air	1940 m ³ /h	Not required
Inert gas	100–120 m ³ /h	80–100 m ³ /h

6. CONCLUSIONS

The use of UV inks and varnishes in printing industry is growing up due to their obvious benefits such as rapid curing time and possibility of further processing immediately after printing, enhanced material properties (high gloss, excellent scratch and chemical resistance), low VOC, etc. Today, most of UV cured inks and coatings are based on free radical polymerization, but in future, with continuing development proportion of cationic systems (better adhesion, no oxygen inhibition, more flexible cure film) or hybrid systems will increased.

Still the most widespread UV source is mercury lamp, but in close future can be the preferred choice LEDs (for example in inkjet printing). LEDs are probably the most promising UV source (low energy consumption, instant on/off, longer lifetime, environmental aspect, etc.) and with continuing development it can be assumed, that their main drawbacks will be overcome (lower radiation intensity and need to reformulate existing UV systems designed for mercury lamps).

Alternative method to UV curing is system cured by accelerated electrons (EB curing). With development of low voltage EB sources increased number of print houses using EB inks (EB systems have been installed and are now in operation mainly in the USA and Western Europe). Due to the obvious advantages of EB curing (absolute and very fast drying, lower energy consumption) and with decreasing prices of EB units a larger expansion of these systems to other parts of the world it can be expected.

7. LITERATURE

- [1] Green, A. W.: Free radical photoinitiators: A Review and Primer, RadTech Europe 2007, Wien, Austria, 2007.
- [2] UV Curing... More than a Solventless Technology, Union Carbide Corporation, URL <http://www.fusionuv.com/news_events/technical_papers/cyracure_book.pdf> (last request: 2003-09-15).
- [3] UV Curing – Technical principle and mechanism, Ciba Specialty Chemicals, URL <http://www.mufong.com.tw/Ciba/ciba_guid/rz_uv_curing_brosch%EE%BB%AAe07%5B1%5D.pdf> (last request: 2012-09-04).
- [4] Tafelmeier, E.: UV-radiation curing technology, Coates Screens, URL <<http://www.coates.de/sne/uvradiation.pdf>> (last request: 2012-09-10)
- [5] Sipani, V., Scranton A.: "Kinetic studies of cationic photopolymerizations of phenyl glycidyl ether: termination/trapping rate constants for iodonium photoinitiators", J. Photochem. Photobiol. A: Chem. 159, 189-195, 2003.
- [6] Lin, Y., Stransbury, J. W.: Kinetics studies of hybrid structure formation by controlled photopolymerization, Polymer 44 (17), 4781-4789, 2003.
- [7] Uvacure® Cationic Cure Technology, UCB, URL <http://www.chemicals.ucb-group.com/b_units/b2indust/radcure/uvacure/uvacure.html> (last request: 2003-12-16).
- [8] Jasurek, B., Valis, J., Weidlich, T.: Hybrid photoinitiator based on arene-iron complex and α -hydroxy alkyl phenone, Proceedings of RadTech Europe 2007 (CD), (Vincentz Network: Vienna, Austria, 2004).
- [9] Excimer lamps, Heraeus Noblelight, URL <http://www.heraeusnoblelight.com/en/products_1/uvprozesstechnik_1/uvp_excimer.aspx> (last request: 2012-09-13).
- [10] Kipphan, H.: Handbook of Print Media, (Springer, Berlin, 2001), 174–175, ISBN 3-540-67326-1.
- [11] Peil, M., Langenscheidt, A., Hertsch, S., Simon, J., Maiweg, H.: Curing behavior of UV-LED curable inks: Influence of dose, irradiance and wavelength, Proceedings of RadTech Europe 2011 (CD), (Vincentz Network: Basel, Switzerland, 2011).
- [12] Swain, P. K., Harbourne, D., Leonhardt, D., Bao, R.: Advancements in UV LED technology and its impact on UV curing applications, Proceedings of RadTech Europe 2011 (CD), (Vincentz Network: Basel, Switzerland, 2011).
- [13] Herlihy, S., Karsten, R.: Can UV LED breakthrough into graphic arts printing applications?, Proceedings of RadTech Europe 2011 (CD), (Vincentz Network: Basel, Switzerland, 2011).
- [14] Lauppi, U. V., Rangwalla, I.: Low voltage electron beam curing an update, Proceedings of RadTech Europe 2011 (CD), (Vincentz Network: Basel, Switzerland, 2011).

ABSORPTION CHARACTERISTICS OF MAGENTA SHEET-FED OFFSET PRINTING INK AS AN INDICATOR OF INK POLLUTION

Jelena Krstić¹, Jelena Kiurski¹, Dušanka Obadović², Ivana Oros¹, Miroslav Cvetinov²

¹Faculty of Technical Sciences,

Department of Graphic Engineering and Design, Novi Sad

²Faculty of Sciences, Department of Physics, Novi Sad

Corresponding author: Jelena Kiurski
e-mail: kiurski@uns.ac.rs

1. ABSTRACT

The ultraviolet-visible spectroscopy was used to determine the absorption characteristics of magenta sheet-fed offset printing ink. Two samples of printing ink, fresh and used, after 20,000 printed sheets, were investigated. The recorded spectrum showed the maximum absorption in regions characteristic for Lithol Rubine B pigment. The intensity changes of the absorption maximum is due to the energy shifts to lower values, while an increased band with occurs at higher temperatures of printing processes associated with an increasing resonance energy. This phenomenon could be useful as an indicator of ink ageing process.

Keywords: UV-VIS, Lithol Rubine B, sheet-fed offset printing, pollution

2. INTRODUCTION

The most common carriers of color for magenta inks are typically acid or alkaline salts of iron, barium, calcium and copper [1, 2]. The Lithol Rubine B is commercial name for organic dye, calcium (4Z)-4-[(4-methyl-2-sulfonatophenyl)hydrazono]-3-oxo-2-naphthalenecarboxylate, which is widely used in production of sheet-fed offset printing ink. Lithol Rubine B is a reddish synthetic azo dye (Figure 1) in form of red powder.

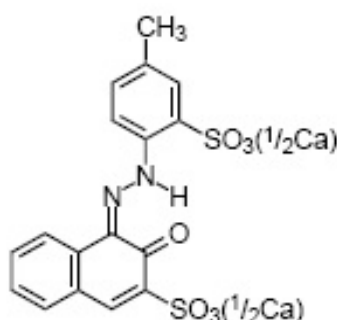


Figure 1: Lithol Rubine B pigment (LRB)

It is slightly soluble in hot water, and insoluble in cold water and ethanol [3, 4]. LRB is used as dye for plastics, paints, printing inks, and textile printing. When it is used as a food dye, LRB has E number E180 in the EU. Beside in food, sodium and calcium salt as red pigment are generally use in cosmetics and printing. In the US both salts are approved for usage in drugs and cosmetics (with the exception of eye area use). Similar, in Japan both salts are approved for OTC-drugs (Over-the-Counter Drugs) and cosmetics for external application. According to FDA (Food and Drug Administration) a maximum daily dose of 5 mg is considered to be safe and a group ADI (Acceptable Daily Intake) of 0.15 mg/kg bw/day was established (FDA 1982). In the EU an ADI of 0-1.5 mg/kg was deduced by the SCF (Scientific Comity for Food) in 1983 (EG Doc III/9280/90) [5].

None of the available studies for magenta ink, either sodium or calcium salt, gave any indication that the azo dye might be a reproductive toxin up to the highest dose tested. Although none of the reported studies is in line with current guideline requirements and the available information

is rather limited for all reported studies, including a 3-generation study and teratogenicity studies in 2 species support the overall conclusion, that Lithol Rubine B does not have to be considered as a reproductive toxic substance [5].

The main source of environmental exposure to Lithol Rubine B pigment would occur through the treatment and disposal of waste paper, particularly recycling. During the recycling process, some of the pigment may be discharged in the aqueous waste from recycling plants. However, only small amounts are to be used annually, and it is therefore unlikely that toxic concentrations would result, even before dilution of any discharges by the receiving water [6].

In this paper magenta printing inks were investigated in order to determine differences in chemical composition and physical structure of pigment particles after 20,000 printed sheets, as an indicator of early ink ageing.

3. MATERIALS AND METHODS

Two magenta printing inks were sampled from a offset printing facility of Novi Sad, Serbia. A fresh sample was taken from the original ink packaging and a used magenta was taken after 20,000 printed sheets from the ink unit of Heidelberg SM 74 2-P-H offset machine. Physico-chemical and fastness properties of Lithol Rubin B are presented in Table 1.

Table 1: Physical, chemical and fastness properties of Lithol Rubine B pigment [7]

Property	Value
Molecular formula	C ₁₈ H ₁₂ N ₂ O ₆ SCa
Molecular weight	424.46 g/mol
pH value	7-8
Density	1.8 g/cm ³
Oil Absorption	45-55 ml/100g
Heat Resistance	180 °C
Printing resistance	Light Full Shade (5-6), Light Tint Shade (3-4), Water (3), Acid (1-2), Alkali (1), Paraffin Wax (2-3)
Solvent Resistance	Ethanol (3-4), Butanol (3), Ethyl Acetate (3), Isopropanol (2), M.E.K.(3-4), Toluene (4-5), Linseed Oil (4)
Synonyms: C.I. Pigment Red 57:1; C.I. 15850:1; Lithol Rubine BK; 3-hydroxy-4-[(4-methyl-2-sulfophenyl)azo]-2-naphthalenecarboxylic acid, calcium salt (1:1); 3-hydroxy-4-[(4-methyl-2-sulfophenyl)azo]-2-naphthalene carboxylic acid, calcium salt; 3-hydroxy-4-[(2-sulfo-p-tolyl)azo]-2-naphthalene carboxylic acid, calcium salt (1:1)	

Absorption spectra were recorded using UV-VIS spectrophotometer SPECORD 205, Analytik Jena. For this purpose, the ink samples were prepared by dilution in appropriate organic solvent.

The elemental composition of magenta ink was determined by AAS method (PerkinElmer's AAnalyst 300 Spectrometer), Table 2.

Table 2: The AAS elemental composition of magenta printing ink

Sample	Element amount (mg/kg)								
	Pb	Cr	Zn	Cu	Fe	Ni	Al	Co	Mn
Fresh magenta	<0.1	<0.1	0.29	0.40	0.54	0.02	19.79	6.48	25.90
Used magenta	0.24	0.00	9.82	0.88	2.19	0.34	28.45	103.78	4.18

The granular structure and composition is confirmed by using SEM/EDS JEOL JSM 6460LV operating at 20 kV, Figures 2 and 3.

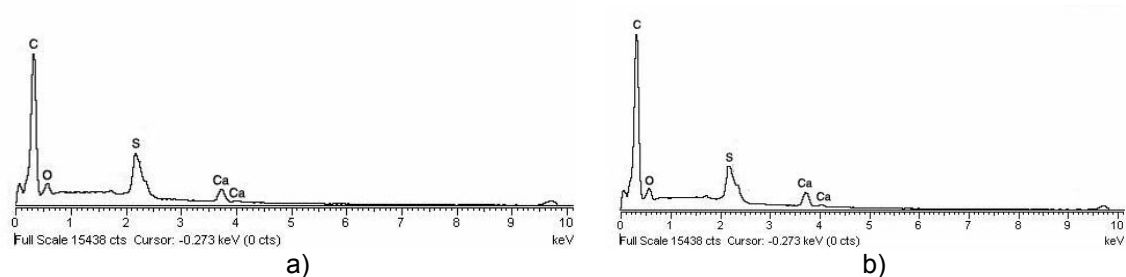


Figure 2: EDS spectra of magenta ink samples: a) fresh and b) sample after 20,000 printed sheets

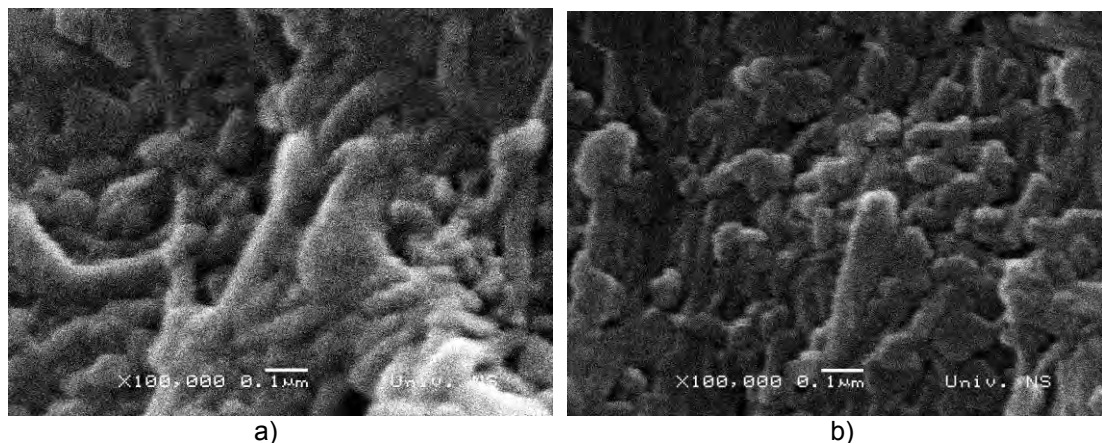


Figure 3: SEM image of magenta ink samples (x 100,000): a) fresh and b) sample after 20,000 printed sheets

A granular red pigment contains calcium present as an oxide, Figure 3, with the primary particle diameter of 50 nm.

4. RESULTS AND DISCUSSION

Absorption or emission of ultraviolet or visible light by a molecule depends on electron transitions between molecular orbital energy levels, just as absorption or emission of electromagnetic radiation by an atom is determined by electron transitions between different energy levels in the atom and the difference in energy, DEs, for those transitions [8].

Molecular orbital theory provides a model for the way electromagnetic radiation interacts with molecules. An electron in the π bonding molecular orbital (MO) of an organic part of Lithol Rubine B can be excited to an π antibonding MO. This is described as a $\pi - \pi^*$ transition. Molecular orbital theory predicts that the energy difference, DE, between levels will decrease if the double bond is conjugated with another double bond. Conjugation exist when series of alternating double and single bond.

High surface area in the presence of Ca^{2+} ions proved efficient hosts for bulky dye molecules of Lithol Rubine B [9]. A mechanism involving the dual interaction of CaO particles with the acidic sites located on dye molecule. Any high temperature of the CaO substrate generates Ca silicate islands where Ca^{2+} ions are more completely surrounded by oxygen ligands and therefore less available for any particular interaction with the dye molecules, Figure 3.

Also, there are two important properties of dyes that are paramount in controlling their oxidation. The first property to note is that reactivity of dyes is frequently controlled by one of its tautomeric forms. Indeed, dyes that adopt the hydrazones tautomeric form tend to be most sensitive to oxidation and are characterized by their deeper colors. Thus, it is commonly assumed that the hydrazones tautomeric form is the reactive dye species. However, dye tautomeric equilibrium is of fundamental importance to oxidation/reduction. In particular, tautomeric equilibrium is set up when there is a naphthenic hydroxyl group conjugated with the azo linkage. The equilibrium mixture of two tautomeric forms, azo or hydrazones forms has characteristically different visible spectra: azo absorbing typically at 400-440 nm and hydrazones at 475-510 nm [10].

The recorded spectra of magenta ink samples showed the maximum absorption in regions which are characteristic for Lithol Rubin B pigment (255, 345, 402, 540 and 552 nm). The characteristic band of $\pi - \pi^*$ transitions, with absorption maximum at 255 nm, in both samples of magenta ink (fresh and used) splits into two bands with maxima at ~220 and 270 nm, which confirmed the presence of Ca^{2+} ion with absorption maximum at 239.9 nm, Figure 4. The other absorption maxima of Lithol Rubin B pigment in magenta inks are shifted at 325, 402, 527 and 575 nm. These maxima could be attributed both to the $\pi - \pi^*$ and $n - \pi^*$ transitions of the imino, carboxylic and aromatic functional groups present in magenta dye structure, respectively (Figure 4).

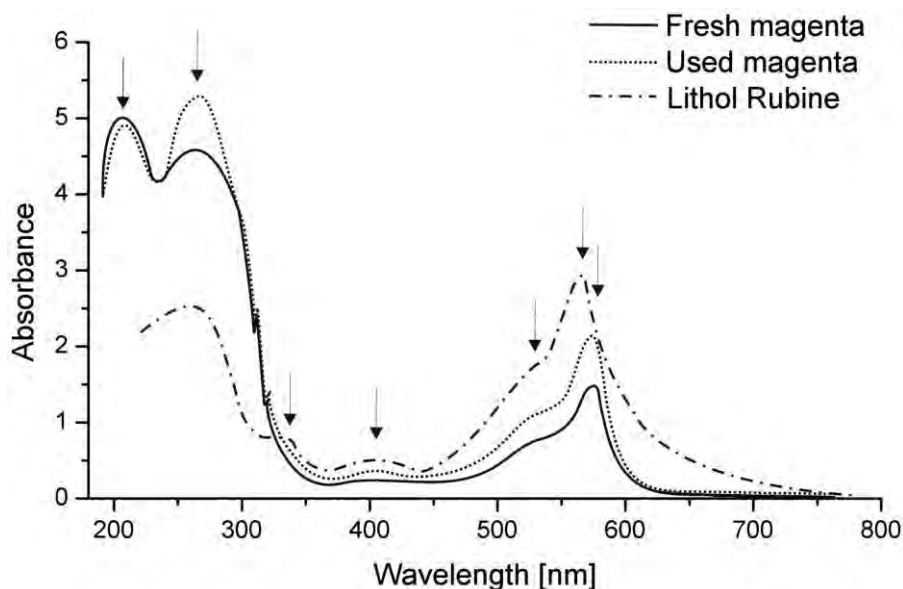


Figure 4: UV-VIS spectra of sheet-fed offset magenta ink

The intensity changes of the absorption maximum is due to the energy shifts to lower values, while an increased band with occurs at higher temperatures of printing processes associated with an increasing resonance energy. However, wider bands would indicate a particle growth with increasing of the processing temperatures above 60°C, Figure 3b. Also, the obtained changes in absorption spectrum are useful as an indicator of ink ageing process which can produce an inconvenience of ink usage as a prevention step of environmental protection.

5. CONCLUSION

Magenta (Lithol Rubine B) as sheet-fed offset printing ink was investigated using UV-VIS spectroscopy in order to determine the start of aging process. The obtained spectra showed the typical absorption profile of Lithol Rubine B as a main structure of magenta ink. The spectra of the fresh and used inks were similar but with different intensity of absorption maxima and quantity of particles. The characteristic band of $\pi - \pi^*$ transitions, with absorption maximum at 255 nm, splits into two bands with maxima at ~220 and 270 nm, which confirmed the presence of Ca^{2+} ion with absorption maximum at 239.9 nm. The intensities of absorption maxima are smaller after 20,000 printed sheets, and the phenomena could be the indicator of magenta ink aging process starting. With increasing the printing process the maximum of the UV peak is shifted to higher wavelengths.

Acknowledgement

The authors acknowledge the financial support of the Ministry of Education and Science of the Republic of Serbia (Projects No. TR 34014, III 46009 and ON 171015).

6. LITERATURE

- [1] Kiurski, J., Radin Oros, I., Krstić, J., Adamović, S., Vojinović Miloradov, M., Mihailović, A., Grujić, S.: "The spectrochemical analysis of waste printing inks", Proceedings of XVIII International Scientific and Professional Meeting „ECOLOGICAL TRUTH“ ECO-IST '10, (Apatin, Serbia, 2010), pages 126-132.
- [2] Koleske, V. J.: "Paint and Coating Testing Manual: Fourteenth edition of the Gardner-Sward Handbook", (ASTM International, 1995.), pages 191-192.
- [3] Craver, D. C., Carraher E. C. Jr.: "Applied Polymer Science: 21st Century", (Elsevier Science, UK, 2000.), pages 496-498.
- [4] Kiurski, J., Krstić, J., Oros, I., Adamović, S., Vojinović Miloradov, M.: "Waste printing inks as a pollutant of graphic environment", Proceedings of the 5th International Symposium on Graphic Engineering and Design (GRID '10), (Novi Sad, Serbia, 2010), pages 207-210.
- [5] The Scientific Committee on Consumer Products (SCCP), "Opinion of the Scientific Committee on Cosmetic Products and Non-Food Products Intended for Consumers", Pigment red 57, SCCNFP/0795/04, Adopted by the SCCNFP during the 28th plenary meeting of 25 May 2004, pages 1-17.
- [6] National Industrial Chemicals Notification and Assessment Scheme, "Magenta pigment", Full public report, 1991, pages 1-10.
- [7] Chemicalland21, "Lithol Rubine B", URL <http://chemicalland21.com/specialtychem/finechem/LITHOL%20RUBINE%20B.htm> (last request: 2012-07-18).
- [8] Volland, W.: "Electronic Spectra of Molecules: The Absorption of UV and Visible Light", (Bellevue Community College, 1999.)
- [9] Roper, M T., Kwee T., Lee, Y. T., Guymon, A. C., Hoyle, E. C., "Photopolymerization of pigmented thiol-ene systems", Polymer 45, 2921-2929, 2004.
- [10] Kroschwitz, I. J.: "Kirk-Othmer Encyclopedia of Chemical Technology", 5th Ed., (John Wiley & Sons, Inc., New York, 2007.), page 349.

MODIFYING NATURAL CaCO_3 TO EFFECT ON QUALITY OF INK-JET PRINTS

Klemen Možina¹, Vera Rutar²

¹University of Ljubljana, Faculty of Natural Science and Engineering, Ljubljana

²Pulp and Paper Institute, Ljubljana

Corresponding author: Klemen Možina

e-mail: klemen.mozina@ntf.uni-lj.si

1. ABSTRACT

Paper is the most common graphic material because of their traditional sustainability and biodegradability. Coatings and surface treatment with natural components and additives can replace unfriendly and more expensive synthetic materials, normally with special properties. However, special properties can be obtained with surface functionalization by chemical or surface geometry modification. Surface geometry modification can be achieved by the application of the pigments and coating formulations with appropriate properties, granulation, particle size distribution and particle shape. The ground calcium carbonate (i.e. GCC) usage in papermaking industry is more and more widely used. Beside optical properties, the trends of lightweight materials, i.e. reducing grammage by using nano materials and products (i.e. NMP), lower specific energy requirement and costs, forces increasing of pigments usage. After all, as everything has its own limits, the resemblance happens with GCC pigment. Following the stated above, the pigment engineering appears with the idea of particles modification to increase its applicability and particularity. Modified GCC particles, e.g. TCC (i.e. treated calcium carbonate) enable wide range spectrum of the GCC raw material application. In the article, the right technological procedure to treat wet grinded GCC and the effect on the changes of the particle geometry, that at the same time, influence on increased functional properties, i.e. paper structure and its surface are presented. Results of survey showed that properties of GCC coated printing paper, required for ink-jet printing with water-based inks had improved.

Key words: GCC, modified pigments, coated paper, ink-jet printing, bleeding, wicking

2. INTRODUCTION

The paper industry has realized high-speed inkjet printing as a vast new business opportunity. To provide high goals the R&D activities are going into a new, i.e. modified coating pigments, mostly on the bases of GCC development with special properties as the answer on the increasing market demands. [1, 2, 3] Ink-jet printing is non-contact printing technique. The only contact is in the moment of ink transfer on the paper surface. For good reproduction and print quality, the coated papers are used, where the coated layer serves as micro-porous substrate. Dye in ink penetrates into the micro-porous substrate along the capillaries and the depth of the penetration is the criteria for the printout quality. [4, 5] An ink-jet printing test for the vaterite-coated papers resulted in high print quality, without bleeding or wicking problems because of the good wettability tendency (similar with silica). In the paper coating substrate, the fixing agent, i.e. poly-DADMAC was added. [6] For liquids, e.g. ink or printing color, their penetration into the paper is more important than flow through the paper structure. Liquid penetration takes place by capillary flow in capillaries between particles in coated layer structure. The penetration flow is expressed by the Lukas-Washburn (Equation 1) and Young-Laplace equations (Equation 2). [7, 8]

Liquid transfer on/in paper surface is represented with *Young-Laplace equation*:

$$\Delta p = 2\gamma_{\lambda} \cos(\theta) \frac{1}{r} \quad (1)$$

while wettability or liquid penetration is expressed by *Lukas-Washburn – equation*:

$$h^2 = \frac{r^2 t}{4\eta} \left(\frac{2\gamma \cos \theta}{r} + \Delta p \right) \quad (2)$$

where is:

Δp – external pressure difference,

γ_{λ} – surface tension,

θ – contact angle between the liquid and the capillary wall,

r – pore radius,

η – fluid viscosity,

p – liquid pressure in the nip, and

h – distance travelled.

Solely surface tension and gravity effects drive the flow of the liquid. In printing and converting processes the nip pressure forces liquid to penetrate into the paper. Regarding printing process, we can talk about liquid transfer and wettability of the printing substrate. On the other hand, in printing and converting processes the nip pressure forces liquid to penetrate into the paper. Further, surface tension is small compared to external pressure. *Lucas-Washburn* equation (e.g. Equation 2) can be rewritten in Equation 3, where, p , is liquid pressure in the nip.

$$h^2 = \frac{2r^2 p}{k\eta} \quad (3)$$

The Kozeny constant, k , is included to account for irregular and tortuous pores. *Kozeny-Carman* equation (e.g. Equation 4) gives a quantitative relation between permeability and porosity. The model assumes a uniform bed of packed particles that have an effective particle diameter (d_{eff}).

$$K_v = \frac{\Phi^3 d_{\text{eff}}^2}{36(1-\Phi)^2 k} \quad (4)$$

where is:

Φ – porosity,

d_{eff} – effective diameter (influence on pore volume and shape), and

k – Kozeny constant.

Equations 3 and 4 express the phenomena of liquid transfer in to the printing substrate. The Lukas-Washburn equation predicts the depth of liquid penetration. In converting process, e.g. calendaring, paper surface, mostly coated surface, the external pressure compresses paper structure, which reduces pore volume and consequently reduces liquid penetration.

3. EXPERIMENTAL PART

In laboratory scale some trials of preparing and coating colour with modified GCC pigment were done. The main purpose of all trials was to find out the procedure of pigment modification to encounter the market demands for the ink-jet printing papers and paperboards. Cationic treatment captures the anionic dye and keeps it from spreading and wicking. The GCC, with special procedure, the charge as well as the shape and size of the pigment particles were also modified. The specific surface area increased and at the same time, the particles charge increased from 17 to 12 mV at pH 7.85. With the addition of weak and/or strong acids, we changed the specific surface area from 8 to 33 m²/g (i.e. table 1).

Table 1. Modified pigment preparation

Trials, No.	Modification procedure	Addition		BET [m ² /g]
/	Raw material – dry			8.10
5	Material with 10 % s.c. + weak acid	Ca(OH) ₂	CO ₂	29.10
8 – TCC2	Material with 10 % s.c. + weak acid	Ca(OH) ₂	CO ₂	32.93

The trials of coating base wood free paper with three coating colours, with standard wet grinded GCC pigment quality, modified pigment TCC2 and reference pigment, were done. The main differences between used materials, like specific surface area and mean particle diameter are shown in the table 2.

Table 2. Pigments characteristics

Pigment sample	D50 [%]	BET [m ² /g]
standard	0.686 µm	12.24
quality TCC 2	1.241 µm	32.93
Ref.	1.353 µm	60.74

The following SEM pictures (i.e. Fig 1–3) of calendered coated paper surface show the effect of the particles shape and size on micro porosity of the coating layer.

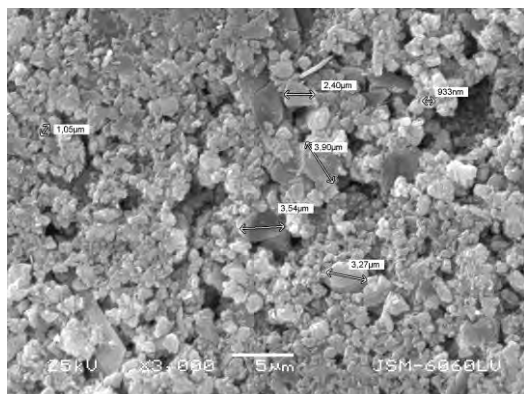


Fig 1. Standard product.

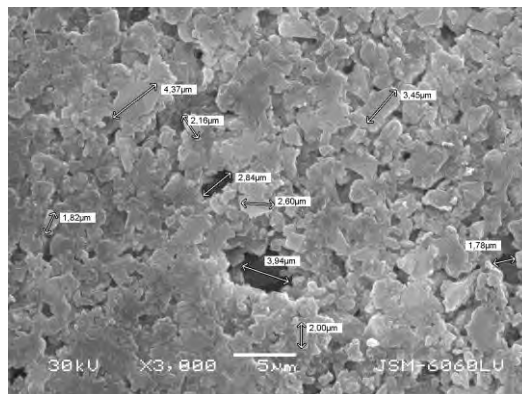


Fig 2. Modified product TCC2.

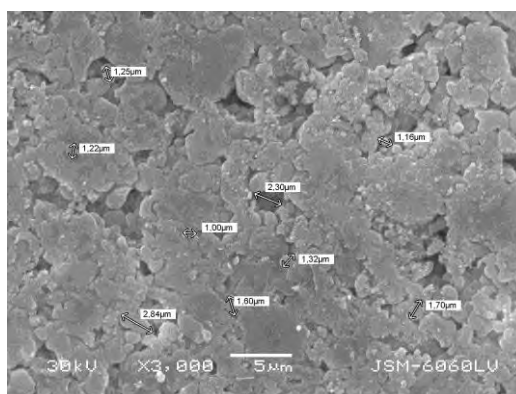


Fig 3: Reference product.

Coated papers were tested on inkjet printing. Pre-presses were done on the printer HP Officejet 6000 Printer (thermal 4800 x 1200 dpi, dye-based inks, min 1.3 pl). In the table 3, 4 and 5 are presented results of bleeding and wicking, determined by image analysis. The effect of the pigment particles modification on micro porosity and successful capturing anionic dye showed significantly clear, so spreading and wicking, evaluated by image analysis was minimized.

Table 3. Bleeding of black 8 on yellow

Specimen	Picture of bleeding	Area [%]	Increment [%]	Share [%]
standard		38.95	- 5.72	- 12.81
TCC2		55.56	10.89	24.38
reference		44.68	0.01	0.02
ideal		44.67		

Table 4. Bleeding of yellow 8 on black









Specimen	Picture of bleeding	Area [%]	Increment [%]	Share [%]
standard		38.16	1.86	5.12
TCC2		36.37	0.07	0.19
reference		36.29	- 0.01	- 0.03
ideal		36.30		

Table 5. Wicking

Specimen	Picture of wicking	Area [mm ²]	Perimeter [mm]	Increment of Perimeter [mm]	Share [%]
standard		21.82	60.50	- 2.80	- 4.42
TCC2		24.68	63.93	0.63	1.00
reference		24.13	63.86	0.56	0.88
ideal		23.30	63.30		

4. CONCLUSION

Ground calcium carbonate (GCC) is the main component in the coating color. The successful pigment engineering, like finer particle size distribution, effective dispersing system and other procedures that are reflected in modified specific area, charge etc., provide a satisfactory high values of significant properties of the coated paper surfaces that are used as a main graphic material in many different printing technics. Results of development work are studying the impact of modified GCC pigment on micro-porosity of the coated paper surface and effect on capturing anionic dye in ink-jet printing technique.

Acknowledgement

Many thanks to Rok Rutar and Janja Juhant Grkman, from the company Calcit Stahovica, Slovenia, for samples of modified pigments and their participation in trials.

5. LITERATURE

- [1] The future of specialty papers to 2013, Leatherhead, UK: Intertech Pira, 124 pp, 2008.
- [2] Frisk R., Kukamo V., Varney D.: "Keeping up with the printer", PPI, p. 39–42, 2010.
- [3] Rutar R., Rutar, V., Možina K.: "Finer pigment for better print", 14th International conference on printing, design and graphic communication Blaž Baromić, Senj 6th–9th October 2010, Croatia.
- [4] Gane, P. A. C.: "Viewing paper coating formulations as nano composites open the door to a new materials technology", Przegł. Papier, 66 (8), abstract, 2010.
- [5] Patrick, K.: "A tailored approach to kaolin products", Paper 3600, Nov/Dec, p. 40–42, 2010.
- [6] Mori, Y, Toshiharu, E, Akira, I.: "Application of Vaterite-Type Calcium Carbonate Prepared by Ultrasound for Ink Jet Paper", Journal of Imaging Science and Technology, 54 (2), abstract, 2010.
- [7] Niskanen, K.: "Paper Physics", Papermaking Science and Technology, Book 16, p. 287–294, 1998.
- [8] Holik, H.: "Handbook of Paper and Board", Wiley-VCH, 2006.

EXAMINATION OF NANOCOMPOSITES

Erzsébet Novotny¹, Rozália Szentgyörgyvölgyi²

¹State Printing Company, Budapest

²Óbuda University, Faculty of Light Industry and Environmental Engineering, Budapest

Corresponding author: Erzsébet Novotny

e-mail: novotny@any.hu

1. ABSTRACT

Significant progress can be expected in the field of the production of high quality and varied printed products thanks to nanotechnology, which exploits their new properties. Our work focused on the measurement of the electric conductivity of nanocomposites. For the experiments we prepared flexo inks with special composition, which contained multi-walled carbon nanotubes. In the inks, we varied the % ratio of short and long nanotubes and the layer thickness. According to the results of the examination the presence, length and percentile distribution of nanotubes in the composite have a fundamental effect on conductivity. We also analysed pictures of carbon nanotubes made with Genetic digital microscope and high-resolution CM10 transmission electron microscope. Due to their very strong density these inks not need other black pigments.

Key words: nanotubes, nanocomposites, electric conductivity

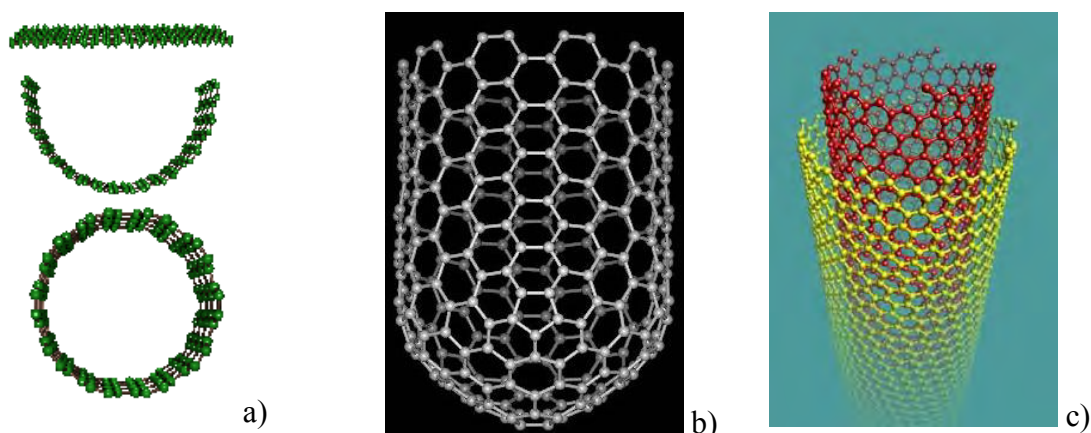
2. INTRODUCTION

Nanotechnology has been slowly seeping into our day-to-day life almost imperceptibly, and is becoming part of our life. The research of atomic sized objects started in earnest during the last decades of the 20th century. It was at that time that the devices (electron microscopes) that made possible the observation of nanometric or even smaller objects for the human eyes became available. Moreover, in 1981 Swiss scientists developed a new device which operated on the basis of a completely different principle than the electron microscope or the optical microscope. This device was the scanning tunneling microscope, which has a resolution in the order of a tenth of the atomic dimensions. There are basically two nanotechnologies. One of them is the evolution, the other the revolution nanotechnology. The revolution (or bottom-up) nanotechnology is the „bottom-up view, where complete functional plants and complete manufacturing systems are built from atom to atom, from molecule to molecule. The evolution (or top-down technology) nanotechnology covers the field of technological procedures already in existence, where material particles in the nano order of magnitude were already used. Nanotechnology includes the production, accurate handling, and planned arrangement of materials smaller than 100 nanometres. The 100 nanometres threshold is important, because this is the threshold where effects that cause new kinds of properties in comparison to the traditional macroscopic size became dominant in the behaviour of the materials.

Most products are manufactured using silver nano-particles or fullerene and carbon nanotubes. The fullerene and carbon nano-objects have special mechanical and electronic properties, and these products exploit those properties.

Carbon has been well known for a long time. Other forms of carbon with different properties are diamond and graphite. The difference in properties is caused by the difference in the bond between carbon atoms. The third form, the fullerene type material was discovered in 1985. During spectrometric mass measurements Sir Harry Kroto and his co-workers discovered that there is a perfectly spherical molecule with a diameter of 1 nm, consisting of sixty atoms, the fullerene, C₆₀. [1] Within nanotechnology, one of the fastest developing trend focuses on the carbon nanotubes (Figure 1). This increased interest is due to the promising electric and mechanical properties of the carbon nanotubes. The tensile strength of a carbon nanotube is a hundred times of that of an equal sized steel filament, while only weighting one sixth as much. It is convenient to think of the mono-walled carbon nanotube as a single atom thick graphite sheet rolled up to form a perfect tube, with a diameter in the one nanometre scale while it could be tens of micrometres long. Multi-walled carbon nanotubes consist of mono-walled nanotubes concentrically nested into each other, and the distance between tube walls is equal to the

distance measured between the graphite layers (0.34 nm). Nanotubes have potential use in reinforced composites, nanoelectronics, sensors, and nanomechanical devices. The most recent member of the carbon nanomaterial group is the „graphene”. Graphene, which was discovered in 2004, is a flat, one atom thick carbon sheet [2].



*Figure 1: Carbon nanotube - a) Rolling one atom thick graphite (grapheme layer)
b) Mono-walled carbon nanotube capped with fullerene half spheres.
c) Open-ended multi-walled nanotube [1]*

3. MATERIALS AND METHODS

To treat flexo inks as nanosystems has by now become everyday practice. In the examination part, we too have studied the novel properties of a new nano-composite. Composites are also called associated materials. Composites are compounds made of two or more materials with different structures and different macro, micro, or nano dimensions in order to emphasise advantageous and reduce disadvantageous properties, because the base material of the composites gets better properties with the aid of the reinforcing phase. Base materials are called matrix, the other elements are called second (or reinforcing) phase. [3]

The purpose of our examinations was to determine the effect of the use of multi-walled carbon nanotube on the conductivity of flexo inks. In the course of the experiments we have used the method of frequency response analysis in two ways: in the case of the special flexo inks we have measured mass resistance, while in the case of the materials applied to thermo paper surface resistance was measured.

In the course of the analysis, we have examined in detail a new nano-composite system. Since carbon nanotubes have good electric conductivity, a significant increase of electric conductivity was expected for the flexo inks used in the experiments.

The flexo ink samples used for the examinations were prepared with the aid of a laboratory size VMA-GETZMANN type bead mill. (Figure 2) During the preparation of the ink, the carbon nanotubes were added directly to the binding material, and were dispersed into the binding material with the aid of the bead mill. The product used in the bead mill was Sigmund Lindner GmbH “SiLibeads” brand, type “S”, article number 40505, size between 1.25-1.55 mm.



Figure 2: VMA-GETZMANN GMBH D-51580 Reichshof type bead mill

We noted that the nanotubes behave as black pigments in the binding material, though this was not the reason why no additional pigment was necessary (Black pigment e.g.: black, black iron oxide, bone coal) [4] in the nanocomposite, what we wanted to examine after the addition of the nanotubes was the conductivity of the ink system as this was the objective of the experiment. The samples were prepared using special flexo ink into which short (50-150 nm) and long (500-1500 nm) carbon nanotubes were mixed in the rate of 2-5%, which was applied to the thermo paper in 12 and 24 μm thick layers. (Table 1)

Table 1: Properties of samples

Number of sample	Concentration of nano parts	thickness (μm)	Other
1	2,5% long carbon, 20% Silver	12	
2	2% long carbon 20% Silver	12	20% dilution
3	2% long carbon, 16,2% Silver	12	20% dilution
4	4% long carbon	12	cross-linking
5	3,4% long carbon	12	cross-linking
6	4% long carbon	12	
8	3,39% long carbon	12	
9	5% short carbon	24	
10	5% short carbon	12	
11	1% short carbon	24	
15	Silver	24	
16	Wersnitt	12	
17	Wersnitt	24	

Since carbon nanotubes are not easily wettable, it is very difficult to mix them with the base materials; they settle in the finished ink, do not bind to the other components, therefore they must be made hydrophilic by adding hydroxyl groups, to make them wettable and processable. It was necessary to vary short and long nanotubes in the ink, because the wettability of the shorter nanotubes is better. The concentration had to be varied, because the higher the percentage of nanotubes the more it settles later in the ink. The goal was to avoid the sedimentation of the nanotubes in the ink but still improve conductivity. Silver pigment was actually aluminium powder, not spherical in form, but irregular plates with a diameter of 0.5-1 micrometre. Wersnitt is a dispersed system, where synthetic resin is dispersed in water media. Samples 16 and 17 were made by applying wersnitt in layers of 12 μm and 24 μm respectively. Inks no. 1, 2 and 3 contain silver pigment and all three samples contain long nanotubes in 2 and 2.5%, the thickness of the ink layer is 12 μm . The layer thickness of samples 4, 5, 6 and 7 is identical but the concentration of long nanotubes is around 4%. Samples number 9, 10, and 11 contain short nanotubes and the layer thickness is 12 μm and 24 μm . Samples number 4 and 5 contain cross-linking agent. Print number 15 is a simple silver ink with an ink layer thickness of

24 μm . Samples number 9 and 10 contain 5% nanofibre but their layer thickness is different. Short nanotubes have a higher percolation threshold; therefore, bigger amounts must be used to improve the conductivity of the prints.

In the case of long nanotubes, we could not use 5% pigment concentration, because at that concentration the ink would agglomerate in the bead mill, adhere to the glass beads and became unsuitable for use. We should use 20% dilution in this case.

The purpose of preparing prints samples was to examine the conductivity and resistance of the ink samples in dry condition too with Frequency response analysis method. The prints were prepared using standard sample holders and ink squeegee wand. The prints were made on 90g/m² topcoat quality thermo paper. The threaded cuts in the wands were of different depths; therefore ink samples they squeezed, after settling made layers of different thickness. The layer thickness was 6 micrometres made by wand number 1, 12 micrometres by wand number 2 and 24 micrometres by wand number 3.

4. RESULTS AND DISCUSSION

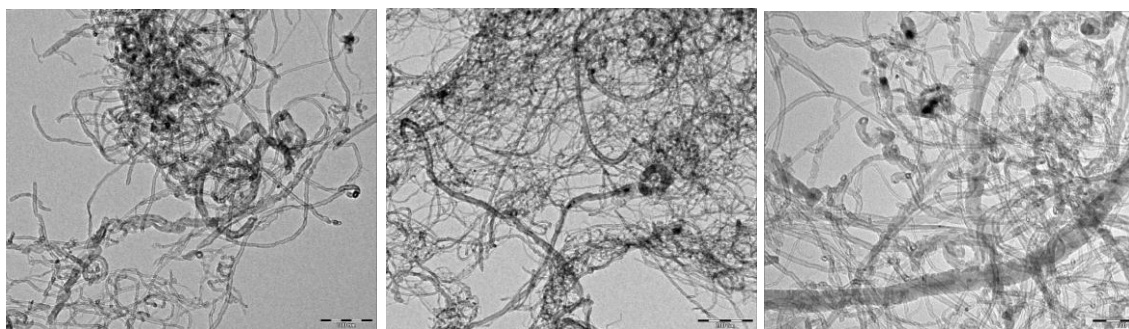
4.1. Microscopic results

For examination of carbon multi-walled nanotubes microscope pictures were taken of the nanotubes used in the ink. The pictures show the twisted multi-walled carbon nanotubes and the contour of the nanofibres. During the preparation of the samples and the microscope pictures, we noted that the carbon nanotubes have very good coverage properties and behave as excellent black pigments. Pictures made with Genetic digital microscope show the structure of the nanotubes and how the nanofibres look like in mass. The nanotubes are clogged and are difficult to process in the course of ink preparation. (Figure 3)



*Figure 3: The structure and density of the nanotubes
(Genetic digital microscope, 1000x)*

The fibres shown in the picture are the transilluminated multi-walled carbon nanotubes. There are some regular circles at different spots; these are pictures of the cross sections of the nanotubes. The clogged structure of the nanotubes and that shorter and longer nanotubes are present together can be observed. (Figure 4)



*Figure 4: The structure of the nanotubes
(Philips CM10 electron microscope, scale 200nm, 100nm)*

4.2. Results of conductivity measurement of the samples

The inks were measured in a homemade liquid cell fashioned after a Novocontrol BDS1307 sample holder. This is a concentric cylinder condenser with earthed protective electrodes. The electrodes were made of stainless steel, the insulating components of Teflon. The measurement was aimed at determining the capacity of this special condenser. [5]. In the course of preliminary measurements we have established that when the relative humidity of the ambient increases so does the water content of the sample, and thus conductivity as well. Therefore, it is to be expected that humidity will have a significant effect on the results of electric measurements. For this reason, we have measured the resistance of the bare thermo paper in ambient with 9%-100% relative humidity. The 7 samples were kept in stable humidity conditions at 25°C for one week, and then we measured the dependence of their conductivity from the water content with impedance spectroscopy. (Figure 5)

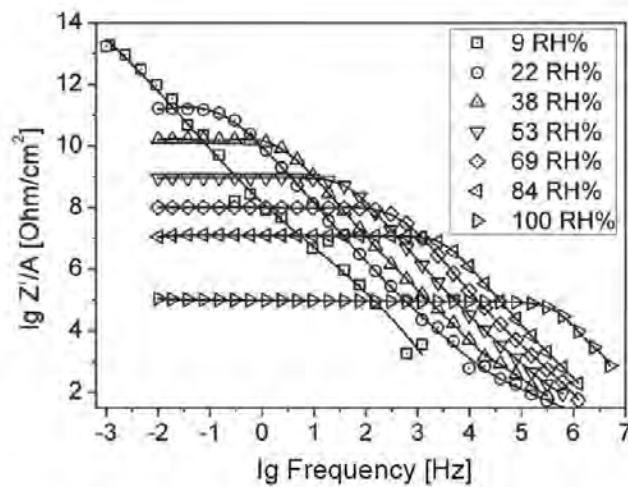


Figure 5: The change of the impedance spectrum of the thermo paper with ambient humidity

The resistance of the samples decreased by several orders of magnitude with the increase of the water content. In the case of the samples kept at low humidity, especially at high frequencies we were able to measure only the spectrum resulting from the inner structure of the instrument. At lower frequency ranges, this converted to ohm-ic behaviour: the samples measured as simple resistors. With the increase of the water content, this transition range moves towards higher frequencies. (Figure 6)

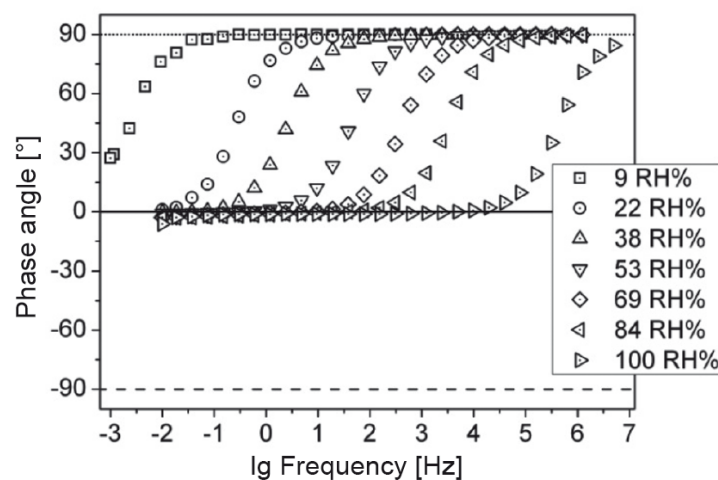


Figure 6: Frequency dependence of the phase angle with increasing humidity

The samples were measured with both direct current (DC) and alternating current (AC) method. We were able to carry out more accurate measurements with direct current at the lowest and highest relative humidity. An exponential function was laid on the data series measured. The resistance of the paper used changed by more than six orders of magnitude with the change in the relative humidity of the ambient. The AC and DC resistances measured in the thermo paper can be shown in Figure 7 and Table 2.

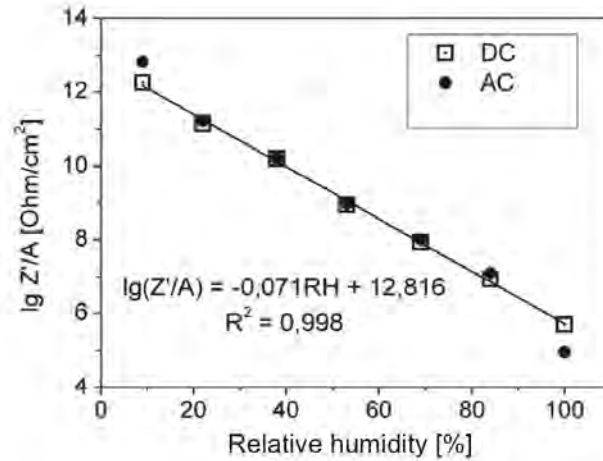


Figure 7: The change in the resistance of the thermo paper with the relative humidity of the ambient

Table 2: The AC and DC resistances of thermo paper

RH	R/A DC [Ohm/cm ²]	R/A AC [Ohm/cm ²]
9	1.786E+12	6.800E+12
22	1.412E+11	1.656E+11
38	1.587E+10	1.641E+10
53	8.726E+08	9.245E+08
69	8.635E+07	1.002E+08
84	8.354E+06	1.262E+07
100	4.970E+05	9.050E+04

Since part of the samples has such high resistance that they can only be measured at very low frequencies, we used direct current measurement method. [6] (Table 3)

Samples number 15, 16, and 17 have the highest resistance. These three samples are the silver ink, and two wernitts with different layer thickness. So their conductivity is the lowest. Their resistance is higher than 6.4 GΩ/cm². The values measured for samples number 9, 10 and 11, which contained type A short, nanotubes was close to that measured for silver and wernitt. Samples 9 and 11 had the same thickness, but there was a 4% difference in nanotube contents between them, still their resistance value was not significantly different. We found the same thing in the case of samples number 9 and 10. Though the concentration of nanotubes was 5% in both samples, layer thickness was reduced from 24 μm to 12 μm.

A significant difference can be observed between samples number 10 and 8 at identical thickness of 12 μm. Sample number 8 contains long nanotubes, as opposed to sample 10. Resistance changed between the two samples by four orders of magnitude, which is a very significant. The big difference can be explained by the fact that sample 8 contains long nanotubes which causes lower percolation threshold. This is the critical concentration which, if exceeded, will result in the sharp decrease of resistance of the composite (e.g. ink containing carbon nanotubes) in consequence of the adjoining (percolating) conducting fibres.

Examining sample 5 and 8 we have made the same observation, namely that the resistance of sample number 5 exceeds the resistance of sample number 8 by two orders of magnitude. Both samples contain about 4% of long, type B nanotubes, with a difference between the samples of

only 0.01% and both have a thickness of 12 μm . The difference between the two samples is in the cross-linking agent present in sample number 5 but absent in sample number 8. Thus, the cross-linking agent causes the relatively big difference in resistance. Similar tendency has been observed between samples number 4 and 6. Both samples contain about 4% of long nanotubes, and both have a thickness of 12 μm . The only difference is the cross-linking agent present in sample number 4, which caused a one order of magnitude difference in the measured value.

Table 3: The AC resistance of the special prints

Number of sample	Concentration of nano parts	thickness (μm)	Other	R/A [Ohm/cm^2]
1	2,5% long carbon, 20% Silver	12		1.093E+08
2	2% long carbon 20% Silver	12	20% dilution	1.510E+07
3	2% long carbon, 16,2% Silver	12	20% dilution	1.944E+07
4	4% long carbon	12	cross-linking	1.724E+06
5	3,4% long carbon	12	cross-linking	5.556E+07
6	4% long carbon	12		6.556E+04
8	3,39% long carbon	12		1.185E+06
9	5% short carbon	24		2.857E+09
10	5% short carbon	12		4.464E+09
11	1% short carbon	24		4.445E+09
15	Silver	24		8.001E+09
16	Wersnitt	12		6.452E+09
17	Wersnitt	24		1.429E+10

The data showed a difference of three orders of magnitude between samples number 1 and 6. Sample number 1 contained only 2.5% of long nanotubes; as compared to the 4% nanotube concentration in sample number 6 but in addition, it also contained 20% silver pigment. Actually, the silver pigment is aluminium powder, which is not spherical in shape but irregular, 0.5-1 micrometre pellets. Aluminium has good conductivity but at this concentration with the shape described above, it will not change conductivity significantly, that is, its concentration in the sample was below the percolation threshold. When comparing samples number 6 and 10 it becomes evident that there is a significant difference in the capacity of short and long nanotubes to affect conductivity. Sample number 10 contains 5% short nanotubes, sample number 6 contains about 4% long carbon nanotubes, and still there is approximately a difference of five orders of magnitudes between the resistances of the two samples. The best conductivity was observed with sample number 6m where we have measured a resistance of $6.556 \times 10^4 \Omega$. We can safely state that at these concentrations short nanotubes hardly change the conductivity of the ink in comparison to the wersnitt, as the shorter fibres have a higher percolation threshold. (Figure 7)

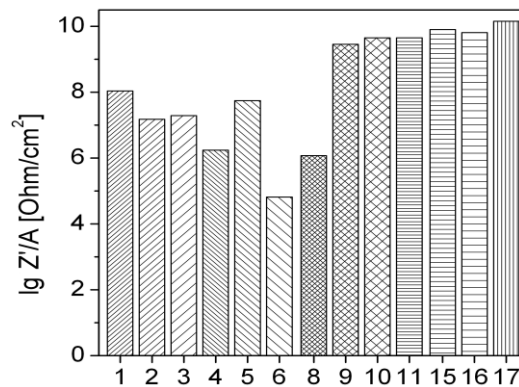


Figure 7: The AC resistance of the special prints (samples 1-17)

Based on the differences it can be inferred that the presence, concentration and length of nanotubes affect conductivity fundamentally.

However, the results of the examination also indicate that the traditional wernitt currently used in flexo inks is not suitable for the preparation of conductive inks. To prepare the composite required to achieve proper conductivity the binder used should display a measure of conductivity in itself after drying. In its present form the composite is not yet suitable to control electronic processes, but with some development work and experiments it could be used through printed electronics as useful element in electric circuits.

As a result of their good covering capacity, multi-walled short and long carbon nanotubes are suitable to be used as pigments; therefore the future study of their printing properties would also be advantageous.

5. CONCLUSIONS

For the experiments we prepared flexo inks with special composition, which contained multi-walled carbon nanotubes. In the inks, we varied the % ratio of short and long nanotubes and the layer thickness. We also analysed samples of carbon nanotubes made with Genetic digital microscope and high-resolution CM10 transmission electron microscope. We prepared the ink samples we have made for the surface resistance measurement tests. The measurements were carried out with the thermo papers printed with the nanocomposite. We obtained the following results. The conductivity of the samples prepared with inks that contained short nanofibres was low; the measurement results were in the order of GΩ. Better results were obtained with long carbon nanotubes. In these samples it could be observed that cross-linking agents reduce the electric conductivity of the material to a great extent. The best result was achieved with sample number 6, a resistance of $6.556 \times 10^4 \Omega$. According to our classification, this value was classified as semiconductor. In the course of examining surface resistance the examined samples proved that the presence of nanotubes in the composite increases conductivity. According to the results of the examination the presence, length and percentile distribution of nanotubes in the composite have a fundamental effect on conductivity. Nevertheless, more experiments are necessary in order to prepare a binding material, which will display certain conductivity in itself after drying. This wernitt is not suitable for the production of conductive inks. Further experiments and tests in this direction could lead to far better results than the above and to the preparation of a flexo ink with good conductivity.

Acknowledgements

We thank Mr. Gyula Lángos and Mr. Csaba Nagy their contribution in this work, which is a part of a collaborated research program between institutes and companies on nano-inks.

6. LITERATURE

- [1] Bíró, L. P.: "Mi a nano és mi a nanotechnológia", MTA, Budapest, 2010
- [2] "New materials – the rise of carbon nanostructures"
<http://www.nanowerk.com/nanotechnology.php> (last request: 2010-12-07).
- [3] Lévai, Z.: "Gyakorlati tanácsok flexonyomtatáshoz", Magyar Grafika, Flexo különszám, Budapest, 2004
- [4] "Patikamédia, szakkifejezések", <http://patikamedia.hu/pigment>.
(last request: 2011-03-22)
- [5] Novocontrol Technologies GmbH et. Co. KG, Alpha-A High Resolution Dielectric, Conductivity, Impedance and Gain Phase Measurement System USER's Manual, Hundsangen/ Germany, 2005
- [6] Hevesi, I.: "Elektromosság", Nemzeti Tankönyvkiadó, Budapest, 2007

PRODUCTION OF SECURITY PRINTING PATTERNS BY MEANS OF THERMOCHROMIC AND CONVENTIONAL OFFSET INKS

Ondrej Panák, Tomáš Syrový, Linda Szöllősiová
University of Pardubice, Faculty of Chemical Technology,
Department of Graphic Arts and Photophysics, Pardubice

Corresponding author: Ondrej Panák
e-mail: ondrej.panak@upce.cz

1. ABSTRACT

The aim of this work was to create patterns consisting of two parts. One part is a selected combination of CMY fractional area coverage with full overprint of thermochromic (TC) offset ink and second part is a computed CMY simulation to match the first part in colour appearance. As first, different binary combinations of C, M, Y were printed with overprint of TC ink with full area coverage. The patches were measured by spectrophotometer to obtain reflectance spectra and consequent colorimetric parameters. To be able to simulate the overprints with TC ink just by CMY combination, simple colorimetric Neugebauer model, simple spectral Neugebauer model, and also their Yule-Nielsen modifications were used. By iteration techniques, fractional area coverage of CMY simulations was obtained. In second step, security patterns consisting of CMY combination with TC ink overprint and their computed simulation were printed and evaluated in terms of colour difference. For the study coated and uncoated paper and two TC inks (green and red) were used. The results show, that spectral Neugebauer model with Yule-Nielsen modification was in average the best predicting model in case of uncoated paper. The results for coated paper show, that simulations computed by simple colorimetric Neugebauer model resulted in lowest colour difference. However, the colour differences of simulations were above 4, regardless of computing method of CMY dot area coverage of the simulation.

Key words: thermochromic, Neugebauer model, colour simulation

2. INTRODUCTION

2.1. Thermochromic inks

By applying dynamic colours to the print, visual impact on customer's attention is increased. Such an added value can be done by using special inks, like reversible thermochromic. These inks change their colour by temperature change. The pigments, which are used in offset reversible thermochromic inks work on principle of a leuco-dye based thermochromic system. The system is encapsulated in polymeric envelope, and particles of size several micrometres are incorporated in to the binder (Seeboth, Löttsch 2008, Small, Highberger 1999).

The offset thermochromic inks differ significantly from conventional inks, in terms of rheological and tack properties (Panák, Kaplanová et al. 2010), moreover these properties are highly influenced by emulsification process in the inking unit of a printing press (Panák, Jašúrek et al. 2011). Offset thermochromic inks are pale in colours and much higher amount of the ink has to be dosed toward inking unit. Thicker ink layers exhibit also higher gloss of printed layer (Kulčar, Panák et al. 2010). However, the maximum thickness, which could be printed by conventional offset printing press, corresponds to the thickness, where the gloss of printed ink layer does not increase significantly (Panák, Jašúrek et al. 2011, Kulčar, Panák et al. 2010).

The activation temperature is usually one value specified by producer. It is temperature, at which the colour change appears. However, the reversible leuco-dye based thermochromic inks exhibit a temperature interval, in which the total colour difference appears and this interval during heating and cooling is shifted – the colour change in dependence of temperature exhibit a hysteresis loop. As Kulčar et al suggest, the colour change should be thus specified more than one temperature (Kulčar, Friškovec et al. 2010).

Thermochromic inks can be used in mixtures with conventional printing inks. By this way, the printed pattern has the colour of the mixture at lower temperatures, and when the colour is high enough, the thermochromic part become colourless and the pattern will have the colour of conventional ink, with relatively good characteristic (Kulčar, Friškovec et al. 2011). Other

method of combining thermochromic with conventional inks is to print a special pattern consisting of two parts. One is printed by thermochromic ink, and another is printed by conventional CMYK printing. These two parts should match in appearance at typical office temperature. When the heat is applied, the thermochromic part of the pattern disappears, and only part printed by conventional inks is apparent. By this technique a special antifraud pattern could be produced (Phillips 2000).

The open question is how to find the proper CMY combination, to match the colour of thermochromic overprint. In this paper, we have investigated, how well some mathematical models can predict the colour of thermochromic and conventional ink overprints.

2.2. Fractional area coverage models used for prediction

The Murray-Davies model defines relationship between fractional area coverage and reflectance of this area if single colorant is printed by equation (Wyble, Berns 2000, Green 2003):

$$R_{\lambda} = a_{teor} \cdot R_{\lambda,solid} + (1 - a_{teor}) R_{\lambda,paper} \quad (1)$$

Where R_{λ} is computed spectral reflectance of theoretical fractional area coverage a_{teor} at wavelength λ , $R_{\lambda,solid}$ is spectral reflectance at full area coverage and $R_{\lambda,paper}$ is spectral reflectance of a substrate. The unknown effective fractional area coverage a_{eff} can be computed by equation:

$$a_{eff} = \frac{R_{\lambda-min,meas} - R_{\lambda-min,paper}}{R_{\lambda-min,solid} - R_{\lambda-min,paper}} \quad (2)$$

Where $R_{\lambda-min,meas}$ is reflectance of that particular fractional area coverage. The index with $\lambda-min$ defines a reflectance at wavelength with minimum value at full area coverage. Theoretical fractional area coverage a_{teor} is an actual image send to the printer or image setter. Effective fractional area coverage a_{eff} is an estimated value of a print, which contains mechanical and optical dot gain. Equation 2 can be extended to a spectral form (Wyble, Berns 2000):

$$\begin{aligned} a_{eff} &= \mathbf{R}_{meas,adj} \mathbf{R}_{solid,adj}^T (\mathbf{R}_{solid,adj} \mathbf{R}_{solid,adj}^T)^{-1} \\ \mathbf{R}_{meas,adj} &= \mathbf{R}_{meas} - \mathbf{R}_{paper} \\ \mathbf{R}_{solid,adj} &= \mathbf{R}_{solid} - \mathbf{R}_{paper} \end{aligned} \quad (3)$$

Where $\mathbf{R}_{meas,adj}$ and $\mathbf{R}_{solid,adj}$ are row vectors of spectral measurements.

To model colour print with multiple colorants, Neugebauer model can be used (Wyble, Berns 2000, Green 2003, Tzeng 1999, Gerhardt 2007). The reflectance of an area R is a sum of a product of fractional area coverage of each Neugebauer primary A_i and its reflectance at full area coverage R_i (Wyble, Berns 2000, Green 2003):

$$R = \sum_{i=1}^m A_i R_i \quad (4)$$

Neugebauer primaries are all possible overlap combinations of primary colorants used in printing. If n primary colorants are used in printing, the model needs $m = 2^n$ of Neugebauer primaries. When CMY colorants are used, eight Neugebauer primaries have to be considered: white (w), cyan (c), magenta (m), yellow (y), blue (b), green (g), red (r), and black (cm). If the fractional area coverage of primary colorants is known (a_c, a_m, a_y), the fractional area coverage (A_i) of Neugebauer primary is computed by Demichels equations:

$$\begin{aligned}
A_w &= (1-a_c)(1-a_m)(1-a_y) \\
A_c &= a_c(1-a_m)(1-a_y) \\
A_m &= a_m(1-a_c)(1-a_y) \\
A_y &= a_y(1-a_c)(1-a_m) \\
A_b &= a_c a_m (1-a_y) \\
A_g &= a_c a_y (1-a_m) \\
A_r &= a_m a_y (1-a_c) \\
A_{cmy} &= a_c a_m a_y
\end{aligned} \tag{5}$$

The equation can be rewritten in matrix form (Gerhardt 2007):

$$\mathbf{A} = \mathbf{M} \cdot \mathbf{c} \tag{6}$$

Where \mathbf{A} is vector of fractional area coverage of Neugebauer primaries, \mathbf{M} matrix of coefficients:

$$\mathbf{M} = \begin{bmatrix} 1 & -1 & -1 & -1 & 1 & 1 & 1 & -1 \\ 0 & 1 & 0 & 0 & -1 & -1 & 0 & 0 \\ 0 & 0 & 1 & 0 & -1 & 0 & -1 & 1 \\ 0 & 0 & 0 & 1 & 0 & -1 & -1 & 1 \\ 0 & 0 & 0 & 0 & 1 & 0 & 0 & -1 \\ 0 & 0 & 0 & 0 & 0 & 1 & 0 & -1 \\ 0 & 0 & 0 & 0 & 0 & 0 & 1 & -1 \\ 0 & 0 & 0 & 0 & 0 & 0 & 0 & 1 \end{bmatrix} \tag{7}$$

and \mathbf{c} is vector of colorant combinations:

$$\mathbf{c} = [1 \quad a_c \quad a_m \quad a_y \quad a_c a_m \quad a_m a_y \quad a_m a_y \quad a_c a_m a_y] \tag{8}$$

The same approach applied in Eq 4. Can be also applied to tristimulus values:

$$\begin{aligned}
X &= \sum_{i=1}^m A_i X_i \\
Y &= \sum_{i=1}^m A_i Y_i \\
Z &= \sum_{i=1}^m A_i Z_i
\end{aligned} \tag{9}$$

Better results of colour prediction are achieved by Yule-Nielsen modification of previously described models (Rolleston, Balasubramanian 1993, Tzeng 1999, Wyble, Berns 2000, Gerhardt 2007, Rolleston, Balasubramanian 1993). The modification introduces n -value, which accounts for light scattering in paper. Equation 1 and 3 are extended by an $1/n$ exponent (Wyble, Berns 2000, Green 2003):

$$R_{\lambda}^{1/n} = a_{teor} \cdot R_{\lambda, solid}^{1/n} + (1-a_{teor}) R_{\lambda, paper}^{1/n} \tag{10}$$

$$\begin{aligned}
a_{eff} &= \mathbf{R}_{meas, n} \mathbf{R}_{solid, n}^T (\mathbf{R}_{solid, n} \mathbf{R}_{solid, n}^T)^{-1} \\
\mathbf{R}_{meas, n} &= \mathbf{R}_{meas}^{1/n} - \mathbf{R}_{paper}^{1/n} \\
\mathbf{R}_{solid, n} &= \mathbf{R}_{solid}^{1/n} - \mathbf{R}_{paper}^{1/n}
\end{aligned} \tag{11}$$

The Yule-Nielsen modification of Neugebauer model is then:

$$R^{\frac{1}{n}} = \sum_{i=1}^m A_i R_i^{\frac{1}{n}} \quad (12)$$

$$\begin{aligned} X^{\frac{1}{n}} &= \sum_{i=1}^m A_i X_i^{\frac{1}{n}} \\ Y^{\frac{1}{n}} &= \sum_{i=1}^m A_i Y_i^{\frac{1}{n}} \\ Z^{\frac{1}{n}} &= \sum_{i=1}^m A_i Z_i^{\frac{1}{n}} \end{aligned} \quad (13)$$

Another modification can be done by spectral n $n(\lambda)$ -value, where every wavelength in spectral measurement has its number (Wyble, Berns 2000):

$$R^{\frac{1}{n(\lambda)}} = \sum_{i=1}^m A_i R_i^{\frac{1}{n(\lambda)}} \quad (14)$$

The acquisition of fractional area coverage of primary colorants can be done by spectral or colorimetric reproduction (Rolleston, Balasubramanian 1993, Tzeng 1999, Gerhardt 2007). In spectral modelling the reflectance spectrum of modelled combination of $a_{c,teor}$, $a_{m,teor}$ and $a_{y,teor}$ should match the desired reflectance spectrum of CMY combination with thermochromic overprint. For this reason a difference of two reflectance spectra (R_1 , R_2) has to be computed using spectral root mean square (sRMS) difference (Gerhardt 2007):

$$sRMS = \sqrt{\frac{1}{N} \sum_{i=1}^N (R_1(\lambda_i) - R_2(\lambda_i))^2} \quad (15)$$

where N represents no. of samples in one reflectance spectrum.

In colorimetric reproduction a colour difference is used to compare desired and modelled colorimetric characteristics:

$$\Delta E_{ab} = \sqrt{(L_1^* - L_2^*)^2 + (a_1^* - a_2^*)^2 + (b_1^* - b_2^*)^2} \quad (16)$$

where L^* , a^* , b^* are coordinates of CIELAB space computed from reflectance spectra as described in (CIE 2004). In CIEXYZ space the colour difference can be also described by Euclidean distance:

$$\Delta XYZ = \sqrt{(X_1 - X_2)^2 + (Y_1 - Y_2)^2 + (Z_1 - Z_2)^2} \quad (17)$$

3. EXPERIMENTAL

All prints were done by a printing press Man-Roland 500, with conventional printing inks of series Maxxima produced by Huber. Thermochromic inks used in presented paper were red thermochromic ink produced by Chromatic Technologies (denoted as TC red) with activation temperature 31 °C, and green thermochromic ink produced by Sicpa with activation temperature 27 °C. Printing masters were prepared without any colour management, with amplitude modulated screening at 120 lpi. Two substrates were used: matt coated paper 200 g/m² and uncoated paper 100 g/m². The experiment was divided into two parts. The first part consisted of preparing and printing the first testing pattern and mathematical modelling of CMY simulations of chosen overprints. The second part consisted of printing previously computed CMY simulations next to the corresponding patches with overprints and evaluation of obtained

differences. The first testing pattern contained colour ramps of C, M, Y, with theoretical fractional area coverage (a_{teor}) ranking from 10–100 % with 10 % interval and values with 25 % and 75 % fractional area coverage in addition. The pattern contained also 100% areas of thermochromic inks. The testing pattern comprised 16 square fields. Every square field consisted of 144 patches. The square fields were Cyan + Magenta , Magenta + Yellow, Cyan + Yellow combinations of colour ramps as shown in figure 1a (4 copies of each square in the pattern). Every patch in the square field had its own specification determining his position (see figure 1b). Three of each binary combination were overprinted by full area coverage of one single thermochromic ink (TC red or TCgreen). Patches chosen for further modelling are specified in Table 1.

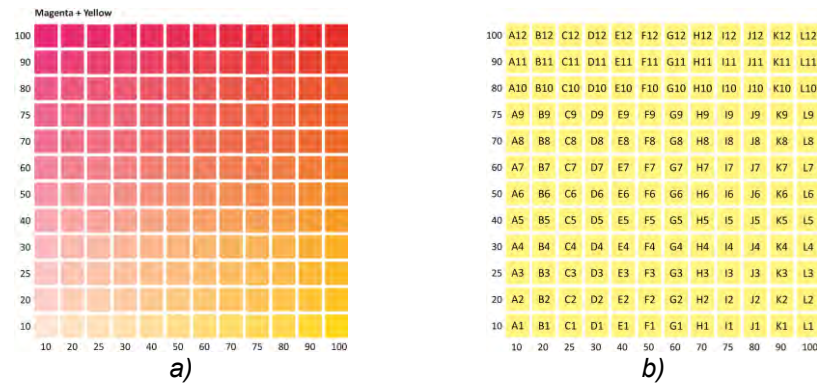


Figure 1. Example of Magenta + Yellow square field (a) and specification of its colour patches (b)

Table 1. Colour patches selected for modelling CMY simulations

Cyan + Yellow + TC Red	A1	A6	A9	F1	F6	F9	L1	L6	L9
Magenta + Yellow + TC Green	A1	A3	F1	F3	F6	L1	L3		
Magenta + Yellow + TC Red	A3	F3	F6	L1	L3				

Theoretical fractional area coverage of three primary colours ($a_{c,teor}$, $a_{m,teor}$, $a_{y,teor}$) was computed to match the colour of selected colour patch. These theoretical values of CMY simulations were computed by 5 methodologies described below. The second testing pattern consisted of square patches, where next to each overprint specified in Table 1. all five simulations were printed. Moreover, some of the simulations were chosen to produce security printing patterns shown in Figure 2.

Every colour patch of the first testing pattern was measured on 5 sheets chosen from whole print load. All measurements were performed by spectrometer i1pro and colorimetric parameters were computed using D50 and 2° observer.

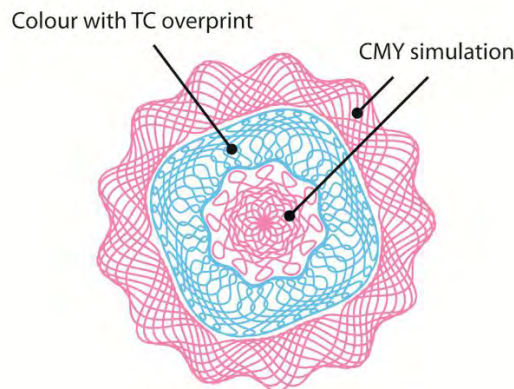


Figure 2. Structure of security printing pattern.

3.1. Colorimetric Neugebauer model (CNB)

At first, the effective fractional area coverage (a_{eff}) of all patches in C, M, Y colour ramps were computed using equation 3. Then the transfer function $a_{eff}=f(a_{teor})$ for each primary colorant were defined. Using Equation 9 and 6, optimum parameters a_c , a_m , a_y of modelled CMY simulation were found by iteration process using GRG nonlinear method satisfying conditions: $0 \leq a_c$; a_m ; $a_y \leq 1$ and $\Delta XYZ = min$. (the difference between XYZ of measured colour patch specified in Table 1 and its corresponding CMY simulation). Parameters a_c , a_m , a_y were effective fractional area coverage of CMY simulation, and from the transfer curves theoretical fractional area was computed.

3.2. Spectral Neugebauer model (SNB)

The transfer curves were in this case the same as in case of CNB model. In the iteration process equations 4 and 6 were used to find a_c , a_m , a_y . fractional area coverage of CMY simulation. Limiting conditions were in this case: $0 \leq a_c$; a_m ; $a_y \leq 1$ and $sRMS = min$. (the difference between reflectance spectra of measured colour patch specified in Table 1 and its corresponding simulated spectra).

3.3. Yule-Nielsen modified colorimetric Neugebauer model (YNCNB)

In this model, the n -value had to be found first. The process was again iterative. The effective fractional area coverage of colour patches in C, M, Y colour ramps was computed by equation 11. Computed value of a_{eff} was substituted for a_{teor} in equation 10. From obtained reflectance spectrum XYZ values were computed and compared to measured XYZ values of each patch of colour ramp by means of ΔXYZ . These 12 values (one colour ramp contained 12 patches) were summed and the optimal n -value was found to satisfy conditions $\sum \Delta XYZ = min$. This process was done for each C, M, Y colour ramp separately and average value of three n -values was taken to compute a_{eff} by eq. 11 in order to specify transfer functions. Averaged n -value was used in equation 13, to find the a_c , a_m , a_y of CMY simulation. The satisfying conditions and computations of a_{teor} was analogous as for CNB model.

3.4. Yule-Nielsen modified Spectral Neugebauer Model (YNSNB)

The n -value was found as follows. The effective fractional area coverage of colour patches in C, M, Y colour ramps was computed by equation 11. Computed value of a_{eff} was substituted for a_{teor} in equation 10. Obtained reflectance spectrum was compared with measured spectrum in terms of $sRMS$. Twelve values of $sRMS$ were summed and the optimal n -value was found to satisfy conditions $\sum sRMS = min$. This process was done for each C, M, Y colour ramp separately and average value of three n -values was taken to compute a_{eff} by eq. 11 in order to specify transfer functions. Averaged n -value was used in equation 12, to find the a_c , a_m , a_y of CMY simulation. The satisfying conditions and computations of a_{teor} was analogous as for SNB model.

3.5. Spectral Yule-Nielsen modified Spectral Neugebauer Model (SYNSNB)

In his model the n -value was found for each wavelength of the spectra separately. The computational process was analogous to YNSNB. In addition optimum $n(\lambda)$ of one colour ramp had to satisfy also condition: $|n(\lambda_{i+1}) - n(\lambda_i)| \leq 0.2$. Three $n(\lambda)$ sets were averaged on each wavelength to obtain one set of $n(\lambda)$. They were used in further computation using equation 14. and fractional area coverage of CMY simulation were found.

4. RESULTS AND DISCUSSION

Estimation of a_c , a_m , a_y of CMY simulations by CNB and YNCNB models were problematic especially for colour patches of TC overprints on uncoated paper, where the colour patch contained 100% area coverage of yellow (with marking Li in Table 1). Optimal values of a_c , a_m , a_y were found for conditions, where minimal ΔXYZ were above 1.2. Moreover all selected colour patches of Magnta + Yellow + TC Red square field exhibited the similar problems, but only when CNB model was used. In all other simulation the optimum a_c , a_m , a_y were found for

conditions, where minimal ΔXYZ were well below 0.0004. This problem did not occur in modelling of simulations printed on coated paper.

Optimal values a_c , a_m , a_y estimated by SNB, YNSNB and SYNSNB models were found for conditions, where minimal $sRMS$ was below 0.06.

The optimal n -values for each of C, M, Y ramp, found by match of colorimetric parameters or reflectance spectra are shown in Table 2. As can be seen, the optimal n -value of YNCNB model for yellow ramp is very high in comparison to cyan and magenta ramp. Therefore only cyan and magenta n -values were averaged.

Table 2. Optimal and average n -values

	Cyan	Magenta	Yellow
Uncoated			
Optimal n -value YNCNB	3.54	3.91	20.81
Optimal n -value YNSNB	3.38	4.78	6.53
Average n -value YNCNB	3.73		
Average n -value YNSNB	4.9		
Coated			
Optimal n -value YNCNB	1.68	1.52	1.43
Optimal n -value YNSNB	1.66	1.59	1.5
Average n -value YNCNB	1.54		
Average n -value YNSNB	1.58		

According to procedures described in previous chapter, five CMY simulations were computed for every patch selected in Table 1. Colorimetric parameters were measured on five sheets from whole printing load. On every sheet, simulations computed by CNB, SNB, YNCB, YNSNB, SYNSNB were compared to the colour patch with corresponding thermochromic overprint in terms of ΔE_{ab} . The results from all selected colour patches are summarized in Figure 3, where average colour difference obtained by specific model, with 95% confidence interval is illustrated. As can be seen, the best prediction in case of uncoated paper was achieved by YNSNB and SYNSNB, which are significantly better than all other models, but the difference between those two is almost none. Therefore YNSNB is in general the best model in prediction on uncoated paper. On coated paper is the situation opposite. The best predictions on coated paper are by CNB model. The extension of CNB model by n -value of YNCNB model did not cause significant improvements. These results are a summarization from all colour patches. In some of the prints, the final security pattern was produced according to intention, to have same apparent colour of TC overprint and its simulation.

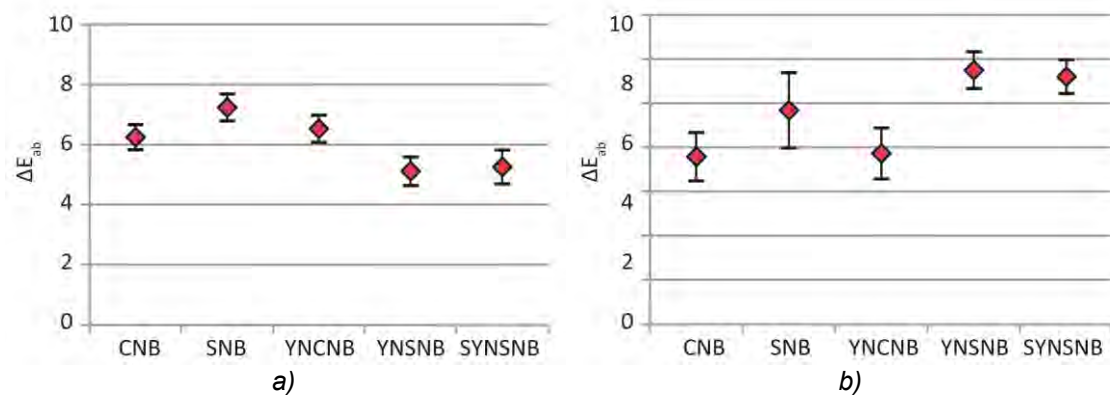


Figure 3. Average colour difference of selected patches with colour overprints and their simulations on uncoated paper (a) and coated paper (b)

5. CONCLUSIONS

To simulate colour of overprints of two thermochromic inks over CMY combination, five models were used. The best results were obtained by Yule-Nielsen modified spectral Neugebauer model for prints on uncoated paper, and by simple colorimetric Neugebauer model on coated substrate. These results summarize the models predictions from all chosen colour patches. The average colour difference is more than 4, thus the prediction of simulations is not sufficient. However, some simulations resulted in desired effect. For better results, more primary inks should be used, like hexachrome offset prints. Since it was difficult to obtain exact colour match of TC overprints and their simulations, another approach should be considered. To avoid any disappointment, the proposed graphical design should have already a combination where the TC overprint is intentionally different from CMY combinations.

Acknowledgements

Special thanks are due to Studio Kozel s.r.o., Czech Republic for performing the prints and enthusiasm to test thermochromic inks in real conditions.

6. LITERATURE

- [1] CIE TECHNICAL COMMITTEE 1-48, 2004. Colorimetry. 15:2004. Vienna, Austria: CIE.
- [2] GERHARDT, J., 2007. *Spectral Color Reproduction: Model based and vector error diffusion approaches*, Ecole Nationale Supérieure des Télécommunications.
- [3] GREEN, P., 2003. Characterizing hard copy printers. In: P. GREEN and L. MACDONALD, eds, *Colour Engineering: Achieving Device Independent Colour*. Chichester, England: John Wiley & Sons Ltd, pp. 221-243.
- [4] KULČAR, R., FRIŠKOVEC, M., GUNDE, M.K. and KNEŠAUREK, N., 2011. Dynamic colorimetric properties of mixed thermochromic printing inks. *Coloration Technology*, 127(6), pp. 411-417.
- [5] KULČAR, R., FRIŠKOVEC, M., HAUPTMAN, N., VESEL, A. and GUNDE, M.K., 2010. Colorimetric properties of reversible thermochromic printing inks. *Dyes and Pigments*, 86(3), pp. 271-277.
- [6] KULČAR, R., PANÁK, O., OTÁHALOVÁ, L., FRIŠKOVEC, M., KAPLANOVÁ, M. and GUNDE, M.K., 2010. *Dynamic Colour and Appearance of Thermochromic Offset Inks*, B. [1] SIMONCIC, ed. In: *5th International Symposium on Novelties in Graphics*, May 27–29 2010, Faculty of Natural Sciences and Engineering, Department of Textiles, pp. 795-800.
- [7] PANÁK, O., JAŠÚREK, B., VALIŠ, J., KAPLANOVÁ, M. and GUNDE, M.K., 2011. Printability of thermochromic offset inks and their interactions with dampening solution. In: N. ENLUND and M. LOVREČEK, eds, *Advances in Printing and Media Technology*, XXXVIII. Darmstadt, Germany: IARIGAI, pp. 277-283.
- [8] PANÁK, O., KAPLANOVÁ, M., GUNDE, M.K. and FRIŠKOVEC, M., 2010. Rheological properties of thermochromic offset inks, B. SIMONCIC, ed. In: *5th International Symposium on Novelties in Graphics*, May 27–29 2010, Faculty of Natural Sciences and Engineering, Department of Textiles, pp. 529-533.
- [9] PHILLIPS, G.K., 2000. Combining thermochromics and conventional inks to deter document fraud, R.L. VAN RENESSE and W.A. VLIEGENTHART, eds. In: , April 7, 2000 2000, SPIE, pp. 99-104.
- [10] ROLLESTON, R. and BALASUBRAMANIAN, R., 1993. *Accuracy of various Types of Neugebauer Model*. SPRINGFIELD; 7003 KILWORTH LANE, SPRINGFIELD, VA 22151: SOC IMAGING SCIENCE & TECHNOLOGY.
- [11] SEEBOTH, A. and LÖTZSCH, D., 2008. *Thermochromic phenomena in polymers*. Smithers Rapra.
- [12] SMALL, L.D. and HIGHBERGER, G., 1999. Thermochromic ink formulations, nail lacquer and methods of use. 424/61 edn. US: A61K 7/04.
- [13] TZENG, D.Y., 1999. *Spectral-based color separation algorithm development for multiple-ink color reproduction*, Rochester Institute of Technology.
- [14] WYBLE, D. and BERNIS, R., 2000. A critical review of spectral models applied to binary color printing. *Color Research and Application*, 25(1), pp. 4-19.

CHANGES OF SPECTROPHOTOMETRIC CHARACTERISTICS ON OFFSET PRINTING SUBSTRATES UNDER THE EXTERNAL FACTORS INFLUENCE

*Roberto Pashich, Snezana Andonovska, Aleksandar Markoski
Faculty of Technical Sciences, Bitola*

*Corresponding author: Roberto Pashich
e-mail: roberto.pasic@uklo.edu.mk*

1. ABSTRACT

Paper is the most used printing substrate which is subject of many external influences. Hydrolytic degradation of cellulose molecules is the most often destructive process during the paper natural aging. In this paper the spectrophotometric characteristics of four types of offset printing substrates have been examined: Offset paper (70 gr/m²), Kunstdruck Matt (115 gr/m²), Kunstdruck Matt (200 gr/m²) and Chromokarton (280 gr/m²). Test form is printed on KOMORI SPICA 429P.

The analysis includes measuring of spectrophotometric characteristics of the mentioned printing substrates after printing process, accelerated aging in thermal chamber with working controlled conditions and repeated measurement of spectrophotometric characteristics of accelerated aged prints.

Accelerated aging was performed in thermal chamber following the recommendations of ISO 5630 which provides chamber controlled conditions (temperature of 80 °C and 72 – 75 % relative humidity). The intervals of accelerated aging are set of 6, 12 and 24 days. The measurement was performed by spectrophotometer X-rite SpectroEye.

Key words: *printing substrates, spectrophotometric characteristics, ISO 5630 - 3, accelerated aging.*

2. INTRODUCTION

Paper as the most commonly used printing substrate is subject to many degradation changes. In those processes acid and alkaline hydrolysis, oxidation or thermolysis reactions occur. The most common reaction, however, is hydrolysis degradation of cellulose molecules, as an essential component of the paper composition. In addition, the values of these degradation changes are associated with temperature. Therefore, it is considered that the results of accelerated aging can be used to create a conclusion of the mechanism and legalities in terms of natural aging. Such an approach enables monitoring and analysis of the consequences mentioned appeared on the paper and print.

2.1. Types of artificial aging of paper

Aging of the paper can be performed in three ways:

- Thermal aging of the paper, which is performed under the influence of increased temperature and relative humidity;
- Light aging of paper which is performed under the influence of UV-radiation and by using fluorescent lamps through UV-reflection spectral analysis and
- Aging of paper using pollutant gases at temperatures up to 25°C and relative humidity up to 50%.

Thermal aging of the paper is the most used method of artificial aging of the paper, which is performed at a temperature of 80°C and relative humidity of 65 - 75%.

3. EXPERIMENTAL PART

The printing of test forms was performed on four color Komori Spica 429 machine, with colors from Sun Chemical and ColorPrint manufacturers and density of solid CMYK colors according to ISO12647 - 2.

Four types of papers printed with offset printing technology are examined:

- Offset paper 70 g/m²;
- Kunstdruck Matt 115 g/m²;
- Kunstdruck Matt 200 g/m²;
- Chromokarton 280 g/m².

In the experimental installation shown in Fig.1 the examined samples are set to thermal aging for a period of 6, 12 and 24 days, corresponding to the approximate lifetime of paper from 50, 100 and 180 years.



Figure 1: Experimental installation



Figure 2: Paper samples

3.1. Description of experimental installation

The examined samples of paper are subjected to thermal aging duration of 24 days in the experimental installation shown in Fig.3, specially constructed for that purpose.

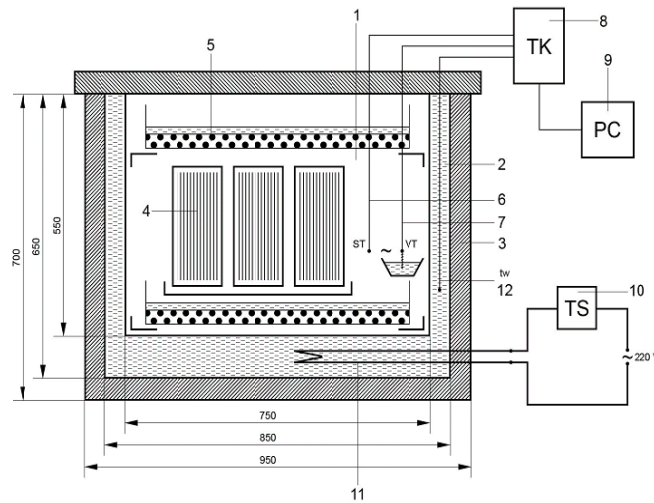


Figure 3: Experimental installation description

(1. installation box, 2. duplicator, 3. insulation – polyurethane, 4. sheet of papers, 5. saturated solution, 6. dry thermometer, 7. wet thermometer, 8. temperature card, 9. PC, 10. digital thermostat, 11. electrical heater)

The experimental installation (1) for thermal aging of paper, shown in Fig.3, is constructed in the form of duplicator (2), which is well-insulated container whereby partition walls by heating water with electric heat (11) with power of 1000 W, serving as heaters. The inner space of installation is insulated with polyurethane compartment with 50 mm thickness. The examined samples of paper (4) are placed inside the container, which is insulated from external influences and which reached a temperature of 80°C and 72 – 75% relative humidity. The temperature is measured and regulated with a digital thermostat (10) and relative humidity is determined as a function of temperature difference between dry and wet thermometer. These thermometers, by temperature card (8) are connected to personal computer (9), which read the temperature values for dry and wet thermometer. Under and over the measured samples of paper (4) there are two vessels with saturated solution of sodium chloride (NaCl) and water (H₂O), for evaporation and generating humidity in internal space insulated from external influences.

3.2. CIE L*a*b* results

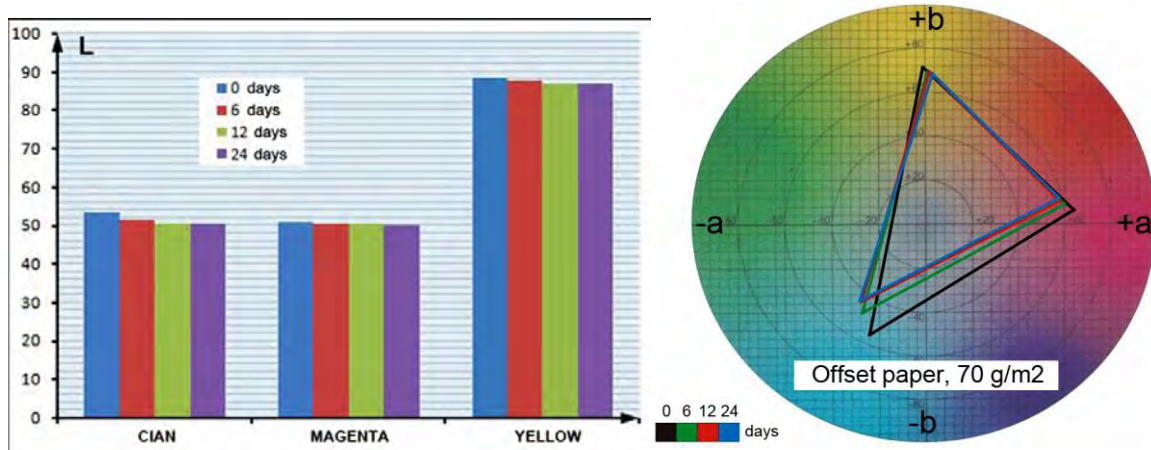


Figure 4: CIE L*a*b* result, offset paper, 70 g/m²

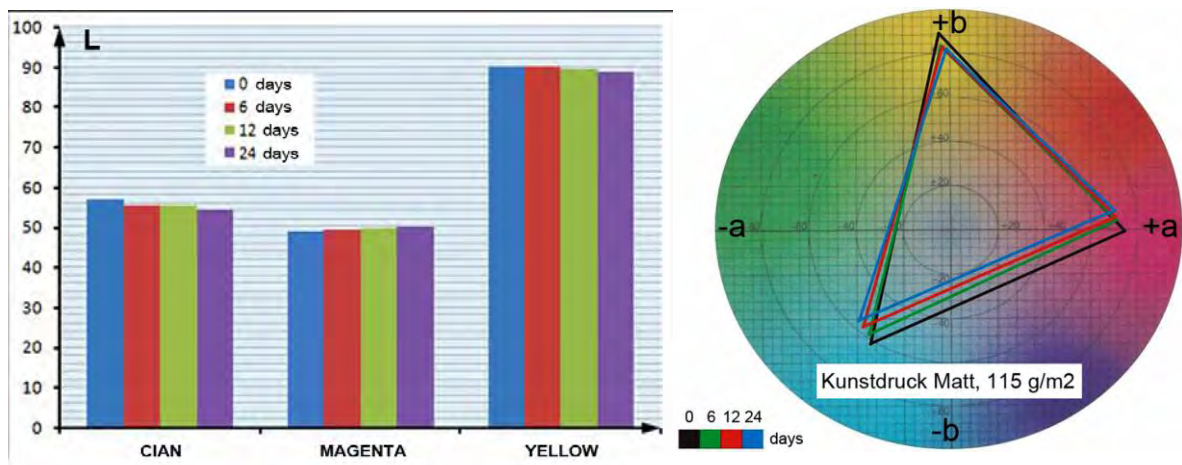


Figure 5: CIE L*a*b* result, kunstdruck matt, 115 g/m²

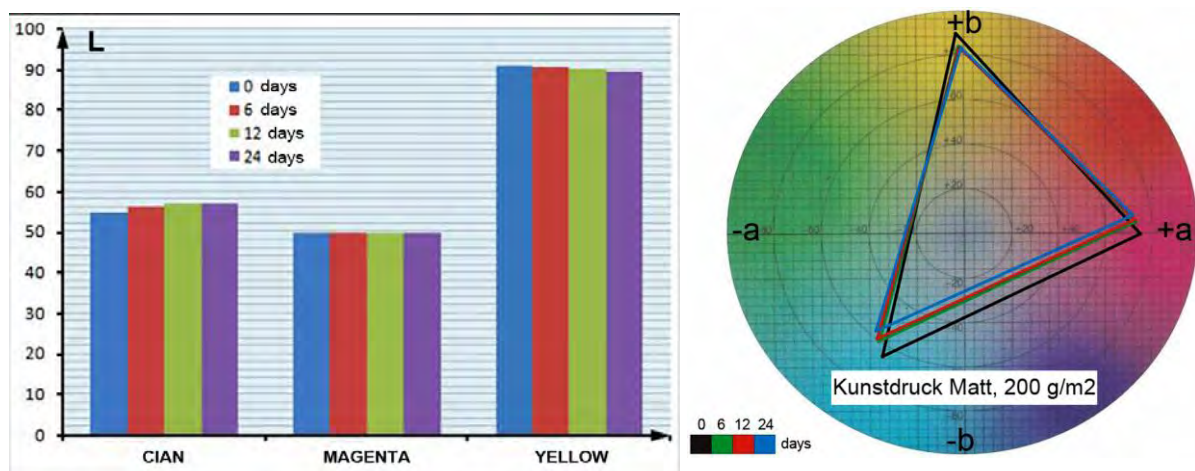


Figure 6: CIE L*a*b* result, kunstdruck matt, 200 g/m²

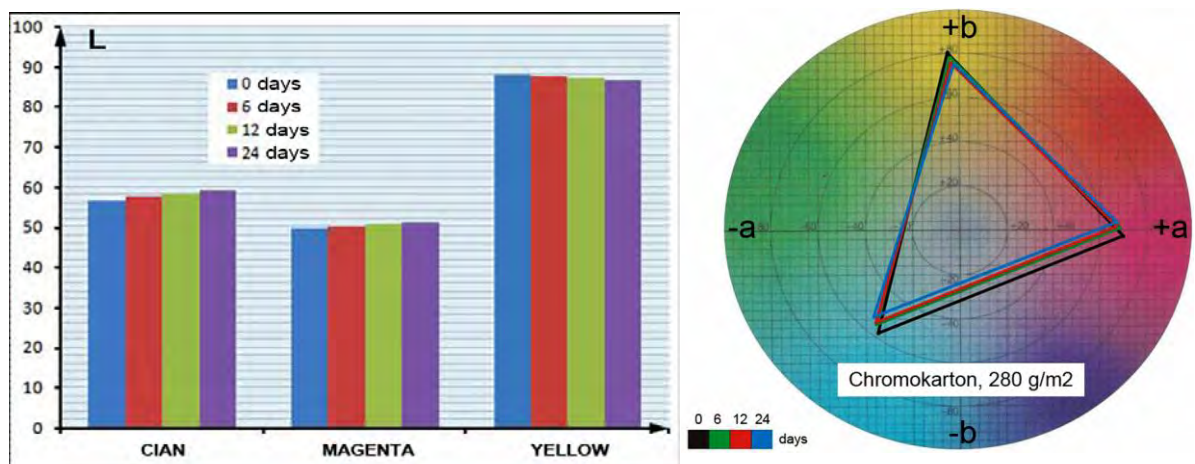


Figure 7: CIE L*a*b* result, chromokarton, 280 g/m²

4. DISCUSSION AND CONCLUSION

Fig. 4 to Fig. 7 shows the CIE L*a*b* values of fresh printed samples with offset printing technology. The following changes are noted after artificial aging of printed papers :

- On aged Offset prints of offset paper 70 g/m² are noted the following color differences (ΔE):

Table 1:

Offset paper 70 g/m ²			
ΔE	Cian	Magenta	Yellow
0 - 6	9.6	4.1	2.1
0 - 12	14.4	5.4	3
0 - 24	14.6	8.5	4.4

Cyan shows the greatest change of thermal aging, magenta shows lees change, while the yellow color remains app. unchanged.

- At Kunstdruck Matt 115 g/m² paper, are noted the following color differences (ΔE):

Table 2:

Kunstdruck Matt 115 g/m ²			
ΔE	Cian	Magenta	Yellow
0 - 6	8.2	5.2	3.5
0 - 12	10	6.5	3.8
0 - 24	13.2	8.4	5.8

Cyan shows maximum change in the first 6 days of thermal aging of paper, while the changes after 12 and 24 days are significantly lower. Magenta and yellow color shows minor deviations which are also maximal after the first 6 days of thermal aging.

- At Kunstdruck Matt 200 g/m² paper, are obtained the following values in color differences (ΔE):

Table 3:

Kunstdruck Matt 200 g/m ²			
ΔE	Cian	Magenta	Yellow
0 - 6	8.1	4.9	3.1
0 - 12	9.6	5.9	3.6
0 - 24	12.5	7.2	4.7

Cyan shows the largest deviation, while deviations at magenta and yellow color are significantly small.

- At Chromokarton 280 g/m² paper, color differences (ΔE) are as follows:

Table 4:

Chromokarton 280 g/m ²			
ΔE	Cian	Magenta	Yellow
0 - 6	3.3	4.1	2.2
0 - 12	5	5.3	3
0 - 24	7.2	6.6	4.1

Considerably small deviations are observed in cyan and magenta, while the deviations at yellow color are remained virtually unchanged.

5. LITERATURE

- [1] Eski, K., Bucher, B. L., Sloneker, J. H.: *"Sensitized Photo Degradation of Cellulose and Cellulosic Wastes"*, USA, 1973;
- [2] Noris T.O.: *"Proceeding of the Workshop of the Effect of Aging on Printing and Writing Papers"*, ASTH Institute for Standards Research, Philadelphia, 1994;
- [3] Bolanča Z., Agić D.: *"Colorimetric Properties of the Model Offset Inks and the Durability of the Prints"*, Proceedings of 28th International Conference of IARIGAI, Montreal, 2001;
- [4] Krgović, M., Ošap, D., Konstantinović, V., Perviz, O., Uskoković, P.: *"Ispitivanje grafičkih materijala"*, Tehnološko-metalurški fakultet, Beograd, 2006;
- [5] Bolanča S., Mikota M., Mrvac N., Majnaric I.: "Comparison of the Quality Limits of some Printings Papers in Offset and Digital Printing", *Advances in Printing Science and Technology*, A.(Ed) Bristow, Surrey, UK, 177 - 182, 2001;
- [6] ISO 5630: Paper and board - Accelerated ageing;
- [7] ISO 186: Paper and board - Sampling to determine average quality;
- [8] ISO 302: Pulps - Determination of Kappa number;
- [9] DIN 6738: Paper and Board: Lifespan Classes.

THE INFLUENCE OF PRINTING INKS VISCOSITY ON THE COLORIMETRIC PROPERTIES OF SCREEN PRINTED SAMPLES

Vesna Simendić¹, Nevena Vukić¹, Borislav Simendić²

¹University of Novi Sad, Faculty of Technology, Novi Sad

²Higher Education Technical School of Professional Studies, Novi Sad

Corresponding author: Vesna Simendić
e-mail: vesnavele@gmail.com

1. ABSTRACT

The screen printing technique is different from other printing techniques, primarily because of its simplicity and ability to print on substrates of any shape, size, material and thickness. Since solvent-based inks are used in this technique, it is very important to reduce the level of volatile compounds contained in solvents in order to protect the environment. This paper presents the results of the influence of different viscosity values of screen printing inks on the colorimetric properties of samples printed on plastic and ceramic substrates. Changing of viscosity was determined by adding the solvent, and measured using a rotational viscometer. Inks were printed on polycarbonate (PC) and ceramic substrates. Colorimetric properties of printed samples were determined using the spectrophotometer Vipdens 2000. Since ink viscosity directly depending on the amount of solvent, considering rheological properties, it is possible to determine the minimum amount of solvent, without changing colorimetric properties of printed samples. By determining the optimum amount of solvent in ink it is possible to avoid excessive evaporation in the process of screen printing.

Key words: screen printing ink, volatile organic compounds, viscosity, colorimetry.

2. INTRODUCTION

History of inks starts in 2500 B.C., when Egyptians and Chinese invented ink. Recipe was simple: carbon residue made from burning oil, etc., was mixed with water or gum. During the time ink has evolved. Constantly changing printing technologies and demands from the printers and end users are forcing modern ink industries to continually change formulation of inks. Nowadays, ink has to adapt to faster printing speeds, more cost-effective processes, and tougher environmental regulations.

For all types of inks, two properties: cohesion and adhesion, are significant. Cohesion is force that keeps the ink together; adhesion is power to stick to a different material, e.g., a substrate. Printing is possible because the ink adheres more to a different material than to itself. Ink is consisted of: 1) pigment, which gives color, and 2) vehicle, which provides the ink's cohesive and adhesive properties. Pigments are finely ground powders made from mostly inorganic compounds. Pigments are in solid form both in the ink and on the substrate. Liquid part of the ink is vehicle, and it's job is to support the pigments in a printable medium and make them adhere to the substrate. The vehicle is a combination of binders and solvents. Solvents have to keep the ink liquid enough to be printable, but also have to control drying of the ink. Solvents have to evaporate slowly so that the ink doesn't dry in the screen, but as soon as the ink is printed, solvents must dry very fast so that drying time does not slow down production. Almost all solvents used in inks that dry by evaporation are volatile substances and flammable to some degree. Water-based inks are non-toxic and non-flammable, but they need more time for drying. The binder is a solid or heavy liquid that provides body to the ink. Its most important job is getting the pigment to adhere to the substrate. Binders are film-forming resins such as ethylcellulose and nitrocellulose that are used in most screen printing inks. The vehicle undergoes changes as the ink dries. Solvents evaporate, and only resins and pigments remain on the surface of the substrate. [1]

2.1. Viscosity of Inks

Rheological properties of inks play an important role in the process of printing graphic products [3-5]. Rheology is consisted of four general categories: elasticity, plasticity, rigidity and viscosity. Rheology of liquids, follows the changes in the liquid shape after physical force is applied, and it mostly focuses at viscosity. Viscosity is the ratio of shear stress to shear rate (viscosity = shear stress/shear rate).

Viscosity of screen-printing inks range from 1000-10,000 cp for graphics and as high as 50,000 cp for some highly loaded polymer-thick film (PTF) inks and adhesives.

Most inks abide a "shear thinning" phenomenon during mixing or running on a press. The ink viscosity drops with increasing of shear rate, which looks simple, apart from two additional properties: 1. Yield point. This is the amount of shear stress necessary for the initial flow. Erstwhile the yield point is surpassed, the solid-like behavior vanishes and the loose network structure of the liquid is torn up. Inks also display this property, but slightly less. Yield point is one of the most important ink properties. The second factor is time dependency. The viscosity of some inks changes over time even when a constant shear rate is applied. This means that viscosity can depend on the amount and duration of applied mechanical force. When shearing forces are removed, the ink will return to its viscosity. That is rate of return, another important ink property, and it can vary from seconds to hours.

Other two factors that can dramatically change viscosity are temperature and solvent content. Rheological additives, particularly thickeners, are important as well.

Temperature: Rising the temperature will reduce the viscosity of virtually all inks. With cold inks often will not be possible to print, and refrigerated inks must be conveyed to room temperature before printing. Temperature of ink must be maintained during printing process. The likely thinning of inks during a printing process can be caused by rise of temperature. Rise of thermal energy results in more molecular movement and less resistance to flow.

Solvents: Aim of true solvents is to reduce viscosity. Latent or partial solvents have lower effect. But non-solvents will generally increase viscosity, and it is used in some ink formulations. Yet, too much solvent will remove the binder from solution. For that reason, change of viscosity depends on the type and amount of solvent. Viscosity of most of inks, especially vinyl, will increase substantially and partially gel during storage. High-shear mixing in the most cases can bring them back to a usable range.

Thickeners: A different range of silicas and other fillers are used for viscosity increase and building of inks. This usually increases the thixotropic behavior of the inks, which can be significant. Inks with excessive bleed can be improved with thickeners and the yield point will often increase. Even though many ink suppliers are beginning to provide thickeners and formulating guidelines, it is best if the use of thickeners is left to experienced ink formulators. [2] Since inks contain solvents, there are additional risks to the health of employees and the creation of smog in the atmosphere. Therefore, measures must be taken to control the vapor and collect it. The problem is usually caused by the nature of pigments and their low ability to absorb oil in the mixing process. Therefore, it is important to determine the minimum amount of solvent that contributes to the formation of suitable rheological properties of ink with regard to the printing process. This minimum amount is possible to determine by controlling ink viscosity depending on the amount of the solvent.

The use of solvent-based inks is particularly evident in the process of screen printing. Solvent-based inks are made of polymer resins in powder or granular form (acrylic, vinyl, polyester, urethane and epoxy polymers). They form the chemical basis of inks and give them final appearance. Polymeric resins are dissolved in a mixture of volatile organic solvents, and the result is a fluid of viscosity suitable for printing. The share of solvent in conventional inks for screen printing is up to 75%. Legal restrictions in the use of organic solvents in screen printing come from the fact that during mixing, printing and drying of ink the evaporation of solvent occurs, so that the volatile organic compounds (VOC) enter the atmosphere. Then sunlight acts as a catalyst in a photo-chemical reaction that converts the organic substance in smog.

Smog has become a serious problem endangering the environment, but it is also a health problem in many industrial cities in the world. Although national regulations to reduce smog in the environment differ considerably, reducing emissions of volatile solvents into the atmosphere has become an increasingly important factor in protecting the environment.

3. EXPERIMENTAL

This paper focuses on formulating inks for screen printing on polycarbonate and ceramic substrates with satisfying optic properties, but with less amount of solvent contents due to hazard risks of volatile organic compounds.

3.1. Methods

Methods used for characterization of inks and printed samples are: 1. Brookfield rotational viscometer for determination of viscosity of inks, 2. Vipdens 2000 colorimeter for determination of optical properties of printed samples.

3.1.1. Determination of viscosity of non-Newtonian fluids

To determine the viscosity of non-Newtonian fluids, which include printing inks, rotational viscometers are used allowing control of the shear stress applied to the fluid and measuring of the resulting shear displacement. Shear stress can be increased and reduced in a very small measurement area, which provides testing and evaluation of rheological and viscoelastic properties.

The principle of operation of the rotating cylinder viscometer: the cylindrical bob rotates in the fixed cup filled with the ink. Shear displacement of the ink is proportional to the torsional moment (torque) required to cause rotation. Since the shear stress (measured torque) and the shear displacement (rotation speed) are known, one can calculate the viscosity η . The ability of continuous speed control of ink rotation allows the examination of behavior of the fluid over time, i.e. thixotropy [5].

3.1.2. Optical properties of inks

To control an ink, or to determine its optical properties, it is necessary to know its colorimetric properties. Colorimetric measurement provides parameters through which are determined psychophysical properties of ink color. The psychological values that describe color are:

- Hue,
- Saturation, and
- Lightness.

These properties are subjective and depend on the observer and the conditions of observation. In the three-dimensional system, the color is represented as a point, determined by three coordinates. Hue is determined by the amplitude, or the angle between the polar axis and the diameter to a point on the circumference of the circle. Saturation is shown as a certain length on this diameter, whereas lightness is the distance of vertical projection of points B on the vertical axis from the point O, which represents black color. The display of color properties of the ink is provided by using the CIE color system. Such systems use three coordinates to determine the color in the color space. CIE color spaces include [6]:

3.1.2.1. CIE $L^*a^*b^*$ color system (CIELAB)

The $L^*a^*b^*$ acronym refers to the three values that the system uses to describe the color, L^* (luminance = lightness) is the level of lightness in color, while a^* and b^* are the chromaticity values of color, i.e. coloration from the following relationships: green in relation to red (a^*) and blue relative to yellow (b^*). CIELAB color model (Figure 2) was developed by the International Organization for Standardization CIE (Commision Del'Eclairage Internationale). CIELAB provides a system of defining colors by using existing standards for colorimetry, instead of binding to specific devices. Therefore, this model is often referred to as universal as it is independent of a color processing device, unlike RGB and CMYK, which were developed specifically for the needs of different devices for color processing. RGB is a color model of the computer screen, and CMYK a color model of the reflecting sheet of paper with colored pigment applied onto its surface, and CIELAB does not depend on either the light or colored pigment.

3.1.2.2. Colorimetric measurement

Colorimetric measurement is based on a comparison of one color with another obtained through the additive or subtractive synthesis of color in the colorimeter. During measurement, two parameters of color, hue and saturation, which jointly create the property called chromaticity are determined. Colorimetric measurements are determined by the spectral composition of light illuminating the sample, the user and spectral properties of filters used to obtain the primary colors (X for red, Y for green and Z for blue stimulus).

3.1.2.3. Color difference

Determination of color is more than a numerical representation. The most common color difference standard of CIELAB system is used to compare colors of two objects. Color difference is represented with the ΔL^* , Δa^* , Δb^* or DL^* , Da^* , Db^* (where Δ and D symbolize the difference). The obtained differences ΔL^* , Δa^* , Δb^* represent the total difference or distance between the CIELAB diagram and can be represented with a unit value known as the absolute color difference ΔE .

$$\Delta E^* = \sqrt{\Delta L^{*2} + \Delta a^{*2} + \Delta b^{*2}} \quad [7]$$

3.2. Materials

Ink used for printing on polycarbonate surface was the olive green ink for screen printing PY284 (Sericol), and it was prepared with different amounts of the petroleum-based solvent ZV557 of the same manufacturer. Viscosity was determined for each level of ink dilution by using a rotational viscometer. The tested ink was applied to the polycarbonate substrate using the screen printing technique. After the required time a solid coating was formed on the substrate, and its colorimetric properties were tested using colorimeter/ spectrophotometer function of the reflection densitometer Vipdens 2000. The results of measured viscosity are shown in Table 1, whereas Figure 3 shows a diagram of dependence on solvent percentage.

Table 1: Viscosity of samples 1, 2, 3 and 4

Sample name	Total sample weight [g], Container mass 59.29 g	Ink weight PY284 [g]	Solvent weight ZV557 [g]	Ink percentage [%]	Solvent percentage [%]	Viscosity [mPas]	Scale range [%], 10-90%
Sample 1	120.53	120.53	0.00	100	0	10362	66.0
Sample 2	124.55	118.35	6.20	95	5	6070	34.0
Sample 3	92.08	83.94	8.14	91.5	8.5	2130	13.3
Sample 4	80.90	73.54	7.36	90.0	10.0	1430	11.3

During measurements, the percentage of utilization of the viscosity scale ranged from 11.3% to 66%. Since the measured viscosity values are in the range from 10% to 90%, the measurement is valid. From the results shown in Table 1. it can be seen that viscosity of PY284 decreases with increasing percentage of solvent in the total mass of the sample. In the first measurement there was no solvent, and viscosity was 10362 mPas. The first adding of the solvent to the ink (5%) reduces the viscosity to 6070 mPas, and finally it drops to 1430 mPas for the solvent percentage of 10%. Dependence of viscosity of ink on solvent percentage is shown in the Figure 1.

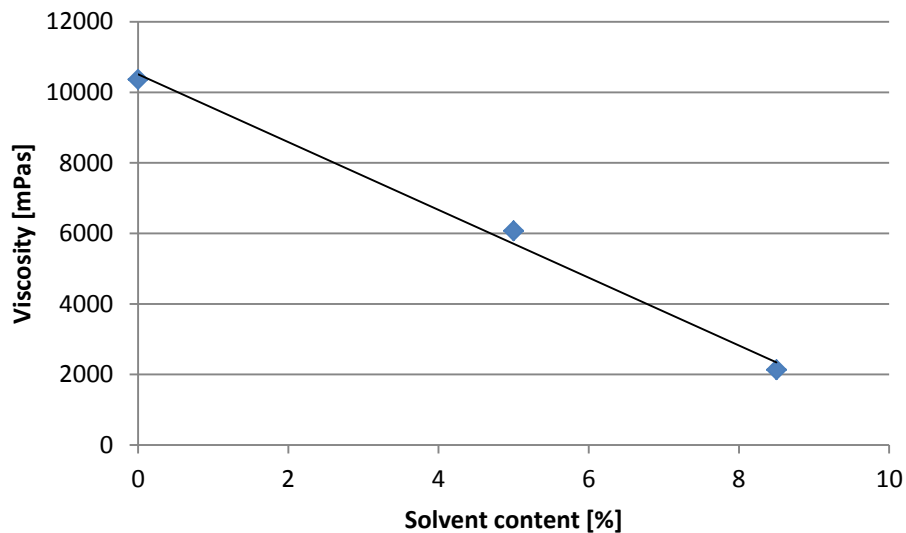


Figure 1: Dependence of viscosity of ink on solvent percentage

Ink used for printing on ceramic substrate was cobalt blue H64 (Heraeus). It is powdered ink, consisted of different sized pigment particles. Deviation of pigment particle size of the same ink depends on two factors:

1. Pigment particles should be 2-3 times smaller than mesh openings in the aim of avoiding screen getting clogged (8-15 μ m).
2. On the other hand particles shouldn't be too small. Amount of too small particles decreases intensity of color and makes process of mixing into paste more difficult.

Percentages for mixing pigments with medium:

- Sample 5: 65 wt% of medium
- Sample 6: 78 wt% of medium

Appropriate medium should provide clear print by keeping quality of halftone during printing process. It is necessary to reproduce the same quality of halftone as on the film. Therefore, for mixing the paste for the four color process printing should be used medium that is specially designed for halftone printing. Recommended medium of the same producer Thix (thixotropic) medium for screen printing nr. 221/thix/2.2. Recommended varnish is L 406 or L 407 (same producer). Dynamic viscosity of two ink samples and pure medium are presented in Table 2.

Table 2. Dynamic viscosity of two ink samples and pure medium

	Sample 5		Sample 6		Sample 7
Medium	75.48 [g]	65%	79.95 [g]	78%	100%
Pigment	40.84 [g]	35%	22.75 [g]	22%	0%
Dynamic viscosity	2562.5 [mPa·s]		928.9 [mPa·s]		560.5 [mPa·s]

4. RESULTS AND DISCUSSION

4.1. Determination of colorimetric properties for screen printing on polycarbonate

Table 3 presents the measured values and colorimetric properties of samples 1, 2, 3 and 4 of the coating on the polycarbonate substrate in CIELAB color system, obtained in measurements using the instrument Vipdens 2000. Viscosity values shown in Table 1 refer to viscosity of samples 1, 2, 3 and 4 .

Table 3: Colorimetric values of ink samples in CIELAB color system

	Sample 1	Sample 2	Sample 3	Sample 4
L*	24.3	24.4	24.7	25.1
a*	-96.8	-97.4	-98.6	-99.2
b*	-30.7	-31.4	-31.0	-31.2

As a reference sample was selected the first sample. It is a solvent-free ink sample and color difference (ΔE) with samples 2, 3 and 4 was made considering Sample 1. The results of obtained color differences are shown in Table 4.

Color difference ΔE is the difference in the measured field in relation to the reference color (in this case, sample1). Color differences of samples 2,3 and 4 compared to sample1 are shown in Table 4.

Table 4: Color difference (ΔE) of samples 2, 3 and 4 compared to sample 1

	Sample 2 - Sample 1	Sample 3 - Sample 1	Sample 4 - Sample 1
ΔL^*	$24.4 - 24.3 = 0.1$	$24.7 - 24.3 = 0.4$	$25.1 - 24.3 = 0.8$
Δa^*	$-97.4 - (-96.8) = -0.6$	$-98.6 - (-96.8) = -1.8$	$-99.2 - (-96.8) = -2.4$
Δb^*	$-31.4 - (-30.7) = -0.7$	$-31 - (-30.7) = -0.3$	$-31.2 - (-30.7) = -0.5$
ΔE	$\Delta E^* = \sqrt{(-21.4)^2 + 70.1^2 + 2.5^2} = 73.3$	$\Delta E^* = \sqrt{(-21.2)^2 + 69.5^2 + 1.7^2} = 72.8$	$\Delta E^* = \sqrt{(-21)^2 + 68.3^2 + 2.1^2} = 71.5$

Adding 5% of solvent to the ink gives values of $\Delta E = 0.93$. Increasing percentage of solvent to 8.5%, the color difference increases the value to 1.87. These values are within tolerances. From the examination of ink differences it can be concluded that the adding of solvent ZV557 to ink PY284 of 8.5% does not significantly change its optical properties ($\Delta E < 2$). In the case when the amount of 10% of the solvent is added, the change in colorimetric properties becomes significant ($\Delta E > 2$). [8]

4.2. Determination of colorimetric properties for screen printing on ceramic substrate

Table 5. presents the measured values and colorimetric properties of samples 5 and 4 of the coating on the ceramic substrate in CIELAB color system, obtained in measurements using the instrument Vipdens 2000. Viscosity values shown in Table 2 refer to viscosity of samples 5 and 6.

Table 5: Colorimetric values of ink samples in CIELAB color system

	Sample 5	Sample 6
L*	21.6	29.4
a*	-86.4	-115.8
b*	-46.8	-38

Color difference ΔE is the difference in the measured field in relation to the reference color. Color differences of samples 5 and 6 are shown in Table 6.

Table 6: Color difference (ΔE) of samples 5 and 6

	Sample 5	Sample 6
ΔL^*	6.6	14.4
Δa^*	-86.4	-54
Δb^*	-46.8	65.3
ΔE	62	86

From Table 6 it can be seen that ink with higher viscosity showed better results compared to ink with lesser amount of viscosity.

5. CONCLUSIONS

The screen printing technique differs from other printing techniques, mainly because of its simplicity and ability to print on substrates of any shape, size, material and thickness. Since solvent-based inks are commonly used in this technique, it is very important to minimize the level of volatile compounds contained in order to protect the environment. It is shown that changes in viscosity modify optical properties of ink, thus establishing the dependence of viscosity of ink on its optical properties. The results of viscosity tests demonstrate a correlation between the amount of solvent and ink viscosity, and show that the addition of solvents into ink up to 8.5% reduces ink viscosity from 10352 mPas to 2130 mPas. Considering optical properties of the obtained coating on the polycarbonate substrate, by adding the solvent up to 8.5%, it is possible to keep the color difference in the allowed range. By determining the viscosity of ink it is possible to assess the optimal amount of solvent for which the color difference ΔE does not exceed the limit, and in the case of screen printing it is $\Delta E=2$. After determining the optimum amount of solvent, it is possible to avoid excessive evaporation during the process of screen printing. For printing on ceramic substrate it is concluded that reducing viscosity of ink by increasing percent of medium in paste cannot improve quality of prints. Therefore it is necessary to investigate if increasing viscosity by mixing, or rising temperature of the paste would improve quality of prints.

6. LITERATURE

- [1] D. H. Dalwadi, C. Canet, N. Roye, and K. Hedman: "Rheology: An Important Tool In Ink Development", American Laboratory, 2005.
- [2] K. Gilleo: "Rheology and Surface Chemistry for Screen Printing", Screen Printing, pp. 128-132, February 1989.
- [3] Lin H.W., Chang C.P., Hwu W.H., Ger M.D., Journal of Materials Processing Technology, 197, 284-291, 2008.
- [4] Rose A.: "Electrocomponent Science and Technology", 9 (1981) 43-49.
- [5] Thompson B.: "Printing materials Science and Technology", Pira 2002.
- [6] Kipphan H.: "Handbuch der Printmedien, Technologien und Produktionsverfahren" Springer, 2000.
- [7] Pešterac Č., Novaković D.: "Denzitometrija i kolorimetrija priručnik za vežbe", Fakultet tehničkih nauka, Novi Sad, 2004.
- [8] Simendić B., Barić D., Simendić V., Vukić N.: "Korišćenje reoloških karakteristika pri određivanju optimalnog sadržaja rastvarača u bojama za sito štampu", Bezbednosni inženjering, Kopaonik, Zbornik radova, 373-378, 2012.

ELECTRICAL PROPERTIES OF PRINTED CONDUCTIVE POLYMER LAYERS

*Tomáš Syrový, Michal Pál, Nikola Peřinka, Bohumil Jašúrek, Jan Vališ
University of Pardubice, Faculty of Chemical Technology,
Department of Graphic Arts and Photophysics, Pardubice*

*Corresponding author: Tomáš Syrový
e-mail: tomas.syrový@upce.cz*

1. ABSTRACT

The goal of this study was to evaluate the influence of several factors on electrical parameters of printed conductive polymer PEDOT:PSS layers. The main factors studied were the temperature conditions, the thickness of polymer PEDOT:PSS layers, the width of conducting lines and contact arrangements of electrodes made by silver composite inks and carbon paste. Prints were made on polymer substrate Melinex[®] ST 504.

Key words: PEDOT:PSS, screen printing, conductivity, sheet resistance

2. INTRODUCTION

Research and technological progress in the last twenty years has brought new discoveries and insights from the field of conductive inks and their practical usability. New types of materials have begun to be applied for the use in several printing techniques, both conventional (screen printing, flexography, gravure) and digital printing (inkjet). This new direction in the printing industry, which is called "printed electronics", means that conventional printing techniques are used to create layers that have meaning not only as a mediator of visual perception, but often have functional properties such as conductive, luminescent, thermochromic and other properties. Under this concept it can be imagined a wide range of electronic components and complex multilayer systems such as transistors, capacitors, printed circuits, RFID, printed batteries, electroluminescent displays, optoelectronic switching devices, etc.

For the preparation of the printed electronic devices, printing materials with various properties (electrical, physical, etc.) are usually used. For preparation of functional layers there are used printing formulations based on conductive or semiconductive materials. By using these printing materials, layers with properties close to pure metal conductivity, semiconductive materials and materials having high electrical resistance – (dielectrics) can be made. For good printability by several printing techniques, the printing inks/pastes must have corresponding electrical properties, and also suitable physico-chemical properties (rheology, surface tension, etc.) to be applicable using such techniques. Materials suitable for the printing of electrically conductive layers can generally be divided into two groups: conductive polymers and electrically conductive inks based on metal composites.

2.1. Conducting polymers

Before the second half of the 20 century, the polymeric materials have been due to its dielectric properties almost invariably regarded as insulators. Fundamental change in the perception of the electrical properties of polymers was started by the discovery of the conducting polymers. Conductive polymers conduct electric current due to the presence of conjugated bonds. These types of polymers are soluble in common solvents, or it is possible to create a stable dispersion which can be applied on the substrate by printing. In comparison to conventional silicon and germanium semiconducting polymers, they have good mechanical flexibility and allow the preparation of conductive films on flexible substrates. The advantage is their low cost in comparison with other types of conductive and semiconductive materials, good environmental degradability and in many cases the possibility of preparing highly transparent conductive layers. For these and other reasons, the current trend is to prepare functional layer based on semiconducting polymers using various printing techniques.

Currently the most practically used conductive polymers are polythiophene derivatives, which are applied on the basis of polymeric complex PEDOT:PSS (poly(3,4-ethylenedioxythiophene)-poly(styrenesulfonate),). The PEDOT:PSS is industrially synthesized monomer of EDOT where

PSS acts as counter ion component. The degree of polymerization of PEDOT-u is limited and its oligomers usually have about 20 monomer units. The PSS molecules, which have significantly higher molecular weight compared to PEDOT, form counter ion and also stabilize the aqueous dispersion of PEDOT.

The solids phase of PEDOT:PSS aqueous dispersions is in the range 1-4%. Polymeric layers created using conductive polymers can be used for many applications such as antistatic coating of polymers and glasses, formation of conductive surfaces, conductive layers for OLED, PV applications and organic thin film transistors (OTFT).

Besides polythiophene derivatives, many various kinds of conductive polymers are synthesized, whose structure is influenced depending on the application. These applications are usually solar cells photovoltaic (PV), OLED, electroluminescent panels, OTFT, etc. Because to this group of polymers, or rather oligomers, there are included compounds that are characterized by a complex structure, their long structural formulas are replaced with abbreviations - P3HT, PCBM C60, PCDTBT, PCPDTBT, F8TBT.

2.2. Electrically conductive inks based on metal composites

Electrically conductive inks based on metal composites inks can be generally classified according to applied printing technique. The ink properties and their composition depends on printing technique. This is related to the choice of liquid or volatile component of an ink, binding system, and other additives. In the domain of metal composite inks currently dominate thermally curable systems, usually based on epoxy resins (curing temperature of 100-200 °C). The metal (Ag, Au, C, etc.) content is relatively high and usually is about 50 to 90 wt.%. Besides the classical particle based composites, which are in form of microstructured particles, there are also offered metal composites based on nanoparticles and colloidal particles. These inks are formulated to fit specific requirements determined by printing technique and application. The next development of conductive inks is toward reducing the temperature necessary for their sintering after print. This allows using large variety of printing substrates that are sometimes not compatible with high temperature.

2.3. Electrically conductive inks based on silver particles

At the market, the most used conductive inks are based on silver particles. It is primarily due to the fact that silver has the highest conductivity of the metals and also good stability on air. The conductivity of the printed layers is near to conductivity of bulk silver. A disadvantage of the use of silver is its high price.

Another disadvantage of the composite inks based on silver particles is the migration of silver, but in present time this problem should be solved by the combination of silver and palladium. Current types of conductive inks based on silver should be resistant to migration of silver.

3. EXPERIMENTAL

The printing of electrically conductive layers was performed using semi-automatic screen printing machine HF S 200 with pneumatic actuator. The squeegee with rectangular profile of width 95 mm is made from three-layer polyurethane with a hardness of 75/90/75 Shore A. The stencils were obtained by polyester mesh with mesh count 120 lines/cm.

For the preparation of layers based on PEDOT:PSS, commercial screen printing ink Clevios™ S V3 was used. The electric contacts were printed using silver ink ECM CI-1001. As the printing substrate PET foil Melinex® ST 504 was used. All printed samples were dried at 130 °C for 10 minutes.

The measurement of electrical properties was performed using the special probe with four-point contact electrode arrangement. The measuring probe is equipped with a thermostatic table for measuring electrical properties in dependence on the temperature. This device is equipped with a chamber for the liquid nitrogen, which allows measuring the temperature dependence of the electrical resistance in the range of -180 to 200 °C. The dependence of electrical resistivity on temperature was measured in the temperature range -180 to +80 °C for the prepared samples. The current at the current contacts was set to 100 µA and the voltage was monitored at voltage contacts. To measure the electrical resistance Keithley 2602 multimeter was used, as well as for

the measurement of sheet resistance by Van der Pauw method. Measurement of sheet resistance was carried out in an inert atmosphere of Argon under reduced pressure to ~ 5 Pa. To measure the thickness of printed layers a mechanical profilometer Veeco Dektak 150 was used.

3.1. Layout of testing patterns

The essential parameters for the characterization of electrical properties of the conductive materials are the sheet resistance, volume resistivity and conductivity. To determine these quantities, following test patterns were prepared.

3.2. The system of lines

Lines are used as a basic element in printed electronics to produce conductive connection, electrodes, etc. To evaluate electrical characteristics in dependence of area of conductive lines, several patterns of various sizes were prepared (see Figure 1). Length of lines was set to: 20, 15, 10 and 5 mm, width: 5, 4, 3, 2, 1 and 0.5 mm. The following figure illustrates the dimensions, where the first value indicates the line width and the second value is the line length between contacts in millimetres.

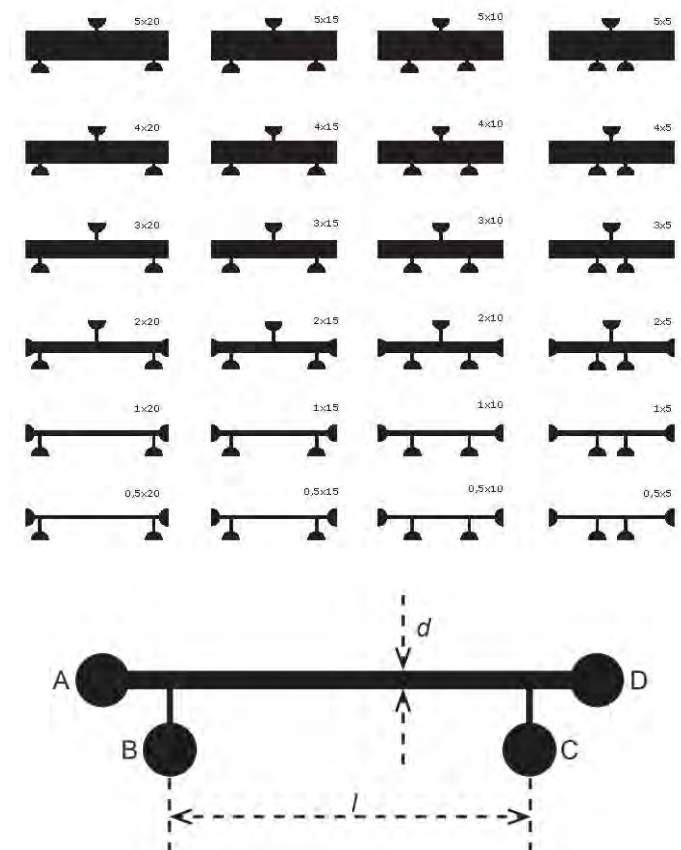


Figure 1: From the left: Lines with contacts for two-point and four-point method; functional part of the line and its dimensional parameters; A, D current contacts; B, C voltage contacts, d - line width, l -active line length

Besides the influence of the geometrical parameters of lines on resistance characteristics, the influence of print order of layers, the polymer layer, contact silver electrodes (eAG), or deposited graphite electrodes -colloidal graphite (EG), on the measured electrical characteristics was observed. The aim was to assess what is the most appropriate combination of the print order to achieve the highest conductivity of printed layers. By print were prepared various combinations of electrical layers and their ordering are described in Table 1.

3.3. The system of squares

Squares with dimensions of 10×10, 20×20, 30×30 mm for determination of the sheet resistance as the material constants were printed. As in the case of the system of lines, combination of numbers layers and the printing order of PEDOT:PSS layer and the silver layer had varied.

Table 1: Order of printed electrically conductive layers

Sequence or order	Description mark/ The system of lines	Sequence or order	Description mark/ The system of square
PEDOT:PSS 1 ×	—	PEDOT:PSS 1 ×, silver electrode	⊥
PEDOT:PSS 2 ×	=	PEDOT:PSS 2 ×, silver electrode	⊥
PEDOT:PSS 1 ×, silver electrode	⊥	PEDOT:PSS 1 ×, silver electrode, PEDOT:PSS 1 ×	⊥
PEDOT:PSS 2 ×, silver electrode	⊥	Silver electrode, PEDOT:PSS 1 ×	⊥
Silver electrode, PEDOT:PSS 1 ×	⊥	Silver electrode, PEDOT:PSS 2 ×	⊥
Silver electrode, PEDOT:PSS 2 ×	⊥		

4. DISCUSSION

4.1. Determination of conductivity of printed layers in dependence of temperature

The temperature dependence of conductivity of layers (PEDOT:PSS and also silver) was measured on the line patterns of different width and one active length. The results of one and two layer prints of PEDOT:PSS lines with width 5, 4, 3, 2, 1×20 mm are shown in Figure 2. The thickness of printed lines was estimated by mechanical profilometer. For a single layer of PEDOT:PSS, the mean thickness of 230 nm was determined. The thickness of two layers, printed wet-on-dry was 400 nm. In following text, various thicknesses of polymer layers will be labelled by their mean values of thickness. Temperature dependence of conductivity of silver lines is presented in Figure 3.

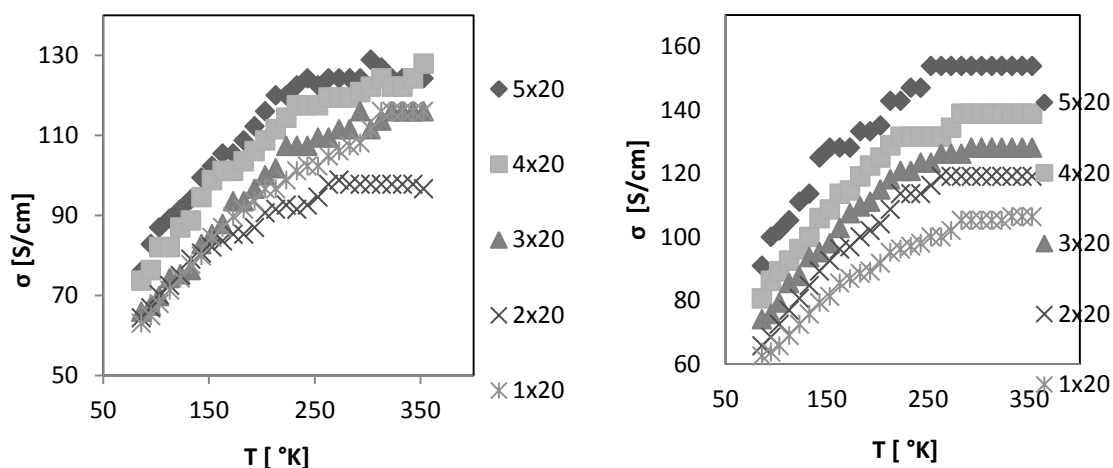


Figure 2: The temperature dependence of conductivity of printed layers PEDOT:PSS; from the left: 230 nm, 400 nm

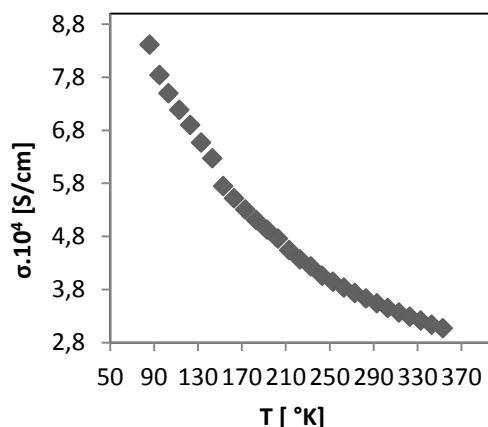


Figure 3: The temperature dependence of conductivity of printed silver layers

The temperature dependence was measured from the temperature of liquid nitrogen, i.e. -183 °C to +80 °C. The graphs show a different course of the temperature dependences of conductive polymers compared to exponential course of layers based on silver composite ink. The difference in values of conductivity for the composite silver ink is also evident.

The results clearly show, that there is negligible influence of temperature on the conductivity of PEDOT:PSS layers in temperature interval -20 – +80 °C. This conclusion can be said especially for measuring electrical characteristics in the temperature range of +15 to +25 °C, which can be considered a region room temperature.

4.2. Influence of the thickness and width of the lines on the conductivity of PEDOT:PSS layers

The four-point method was used to obtain the dependence of the conductivity on the layer thickness and the width of the lines. Measurements were performed at 20 °C. Conductivity was measured at a constant current $I = 100\mu\text{A}$ and voltage at the voltage electrodes was monitored.

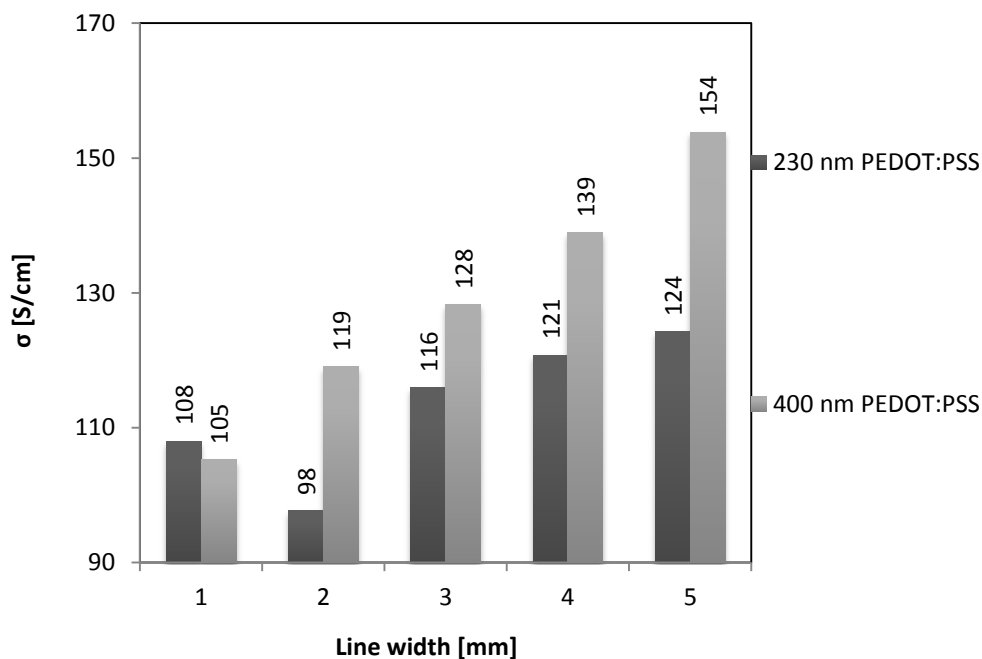


Figure 4: Results of the electrical conductivity of line systems estimated by four-point method for PEDOT: PSS printed on Melinex® ST 504

The dependence of conductivity on width of the PEDOT:PSS lines, printed as 2 layers with layer thickness ~ 400 nm, was confirmed (see Fig. 4). The results of conductivity in dependence of width in case of one layer print are probably affected by the presence of the one outlier point, which can be caused by non-uniform thickness of printed line.

4.3. Effect of arrangement of the contact electrodes and effect of their materials on measured electrical characteristics

The line pattern, printed with different order of polymer and electrodes layer, with different amount of printed material, was tested in order to determine, how these parameters affect the measured electrical properties. Measurements were performed at a current $I = 100 \mu\text{A}$.

In the case, when the conductive polymer layer PEDOT:PSS was printed as a first and the contact electrodes \perp eAG + eG as second layer, the lowest value of the conductivity was measured. This phenomena is due to the formation of contact when silver ink dried on top of PEDOT:PSS layer. Smooth surface of PEDOT:PSS layer caused, that the contact area between the silver layer - eAG and polymer layer PEDOT:PSS is smaller than in the case, when layers were printed in the opposite arrangement. In the case, when layers are arranged that PEDOT:PSS is printed on top of \top EAG + eG, the higher roughness of silver contact electrode surface has positive effect, because the interface is larger and the contact resistance is lower. When contact electrodes were made by colloidal graphite (eG) in the layer order PEDOT: PSS \perp eG, the results are comparable with the arrangement of PEDOT:PSS \top eAG + eG. This can be caused by lower contact resistance between the PEDOT:PSS and eG.

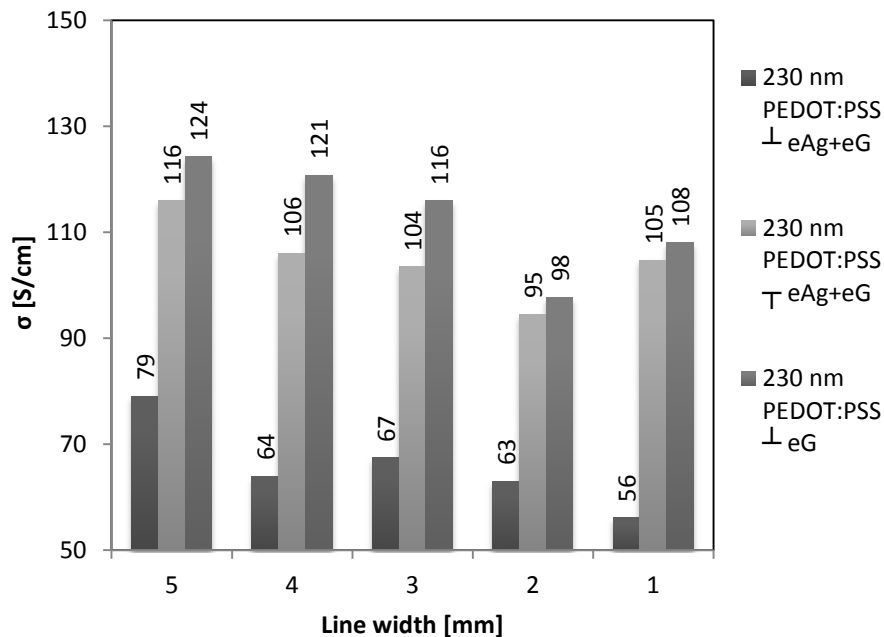


Figure 5: The influence of contacts arrangement and materials on measured conductivity of PEDOT:PSS layers printed on substrate Melinex® ST 504

4.4. Temperature dependence of the sheet resistance of the PEDOT:PSS

In these experiments, the four-point Van der Pauw method was used to estimate values of sheet resistance of two different thicknesses of conductive polymer layer (Fig. 6). It is clear that the influence of temperature on the sheet resistance of material is very small (Fig. 7). The sheet resistance of PEDOT:PSS layer with a thickness of 230 nm has a mean value about $1445 \Omega/\text{sq}$ for the temperature range from 23°C to 93°C . In the case of 400 nm thick layer, the sheet resistance was $431 \Omega/\text{sq}$ within a similar temperature range. Significantly higher sheet resistance of 230 nm thick layer of PEDOT:PSS is caused by higher layer inhomogeneity compared to 400 nm thicker layer, which can be observed by visually or image analysis.

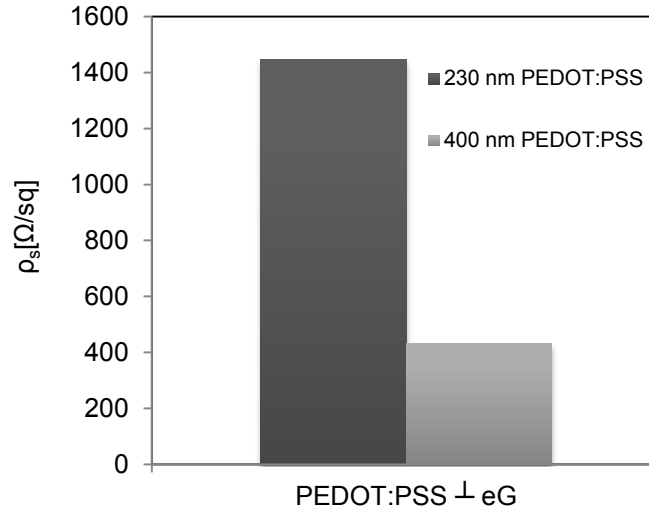


Figure 6: The sheet resistance estimated using Van der Pauw method

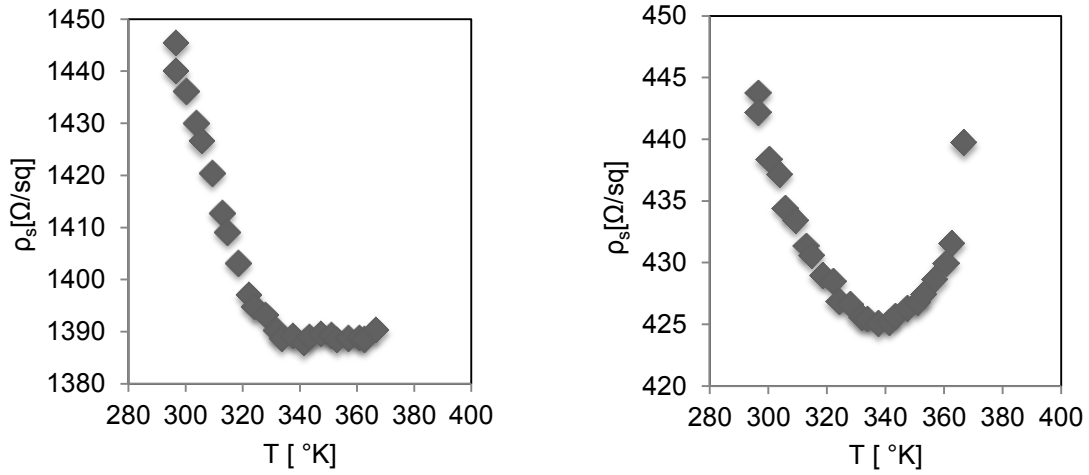


Figure 7: Dependence of sheet resistance of PEDOT:PSS layer on temperature determined by the Van der Pauw method; from the left: thickness 230 nm, respectively 400 nm.

5. CONCLUSION

The test patterns were prepared on the substrate Melinex® ST 504 by screen printing techniques. In dependence on the printing conditions, the 230 nm or 400 nm thickness of PEDOT:PSS layer was achieved. The impact of polymer layer thickness and the width of lines on conductivity was determined. It was found, that the conductivity (measured by four-point method) of the films at temperature close to room temperature (20 °C) is very little temperature dependent. The same effect was observed in the case of sheet resistance (van der Pauw) measurements.

The aim of this study was also to assess the influence of layer order and materials of layers on the measured electrical characteristics. It was found that the higher value of conductivity was achieved when the first printed layer was the silver conductive layer overprinted by PEDOT:PSS layer. Similar electrical parameters were measured for layers overprinted by colloidal graphite paste eG as contact electrodes. The results suggest, that the thickness of the layer, its topology, width of lines, the order and material of contacting conductive polymer layer has a significant influence on the measured electrical characteristics, and therefore all these relevant variables can and must be taken into consideration when electrical parameters of conductive PEDOT:PSS polymer layers are evaluated. The findings of this work will be used in further applications, where PEDOT:PSS layers are used in multilayer functional systems.

6. LITERATURE

- [1] PAUW, L. J. van der. A method of measuring the resistivity and hall coefficient on lamellae of arbitrary shape. Philips Tech. Rev. 1958, vol. 20, s. 220-224.
- [2] ASTM F1896 - 10. Test method for Determining the Electrical Resistivity of Printed Conductive Material. June 2010.
- [3] ASTM D257 – 07. Standard Methods for DC Resistance or Conductance of Insulating Materials. June 2007.
- [4] HEANEY, Michael B. Electrical Conductivity and Resistivity. Boca Raton: CRC Press, 1999.
- [5] BLYTHE, T; BLOOR, D. Electrical properties of polymers. New York: Cambridge University Press, 2005.

DRYING OF UV AND HYBRID INKS AFTER INLINE VARNISHING

Jan Vališ, Bohumil Jašůrek, Ondřej Panák, Jitka Svobodová
University of Pardubice, Faculty of Chemical Technology,
Department of Graphic Arts and Photophysics, Pardubice

Corresponding author: Jan Vališ
e-mail: jan.valis@upce.cz

1. ABSTRACT

The aim of this study was to monitor drying of hybrid and UV curable offset printing inks with additional UV varnish overlay. FTIR was used to monitor the curing of the inks and varnishes, depending on UV dose (exposition time). Another considered parameter was the abrasion resistance of ink layers depending on the time elapsed after press and irradiation. Measurements were carried out on the varnished and unvarnished samples. Three different substrates were used (cardboard, polymer foil and cardboard with metallic foil).

Key words: UV polymerization, abrasion resistance, FTIR

2. INTRODUCTION

Printing inks cured by UV radiation are widely used in different printing techniques for decades. Their main advantage is immediate curing which leads to short process time between print and following finishing. Another advantage is absence of nonreactive solvents (volatile organic compounds) resulting better toxicological and environmental aspects, moreover there is not a distinct difference of thickness comparing to a wet film. Thus the layers printed by these inks exhibit a relatively high gloss.

Disadvantage of UV cured printing inks is their price and further investments to additional necessary devices. In case of multi colour printing press special rollers (made of EPDM) for each inking unit are required. Each printing unit should also contain UV curing unit. Different chemical composition (see Table 1) has strong impact on physical properties and their behaviour during the print. Inks cured by UV radiation have generally lower viscosity and they are less thixotropic, what might result in higher dot gain and lower contrast. [1, 2, 3, 4]

Tables 1: General inks compositions [5]

Conventional sheetfed ink		UV offset ink	
Mineral oil (280–320 °C)	0–30 %	Polyester acrylates	0–30 %
Semi drying vegetable oil and esters thereof	15–30 %	Diluted polyesters	0–40 %
Drying alkyd	10–20 %	Epoxy acrylates	10–40 %
Hard resin (rosin mod)	20–35 %	High func. urethane acrylates	0–10 %
Pigment	14–24 %	Pigment	14–24 %
Fillers	0–5 %	Fillers	4–8 %
Wax	3–5 %	Wax	1–2 %
Driers	2 %	Monomers	5–15 %
Anti-oxidants	0–2 %	Photoinitiator blend	6–12 %

The high gloss leads to a relatively big popularity of UV varnishes. Their application does not require using inking unit of an offset printing press; the only additional investment is UV source. Unfortunately, the compatibility of conventional (drying process is driven by oxypolymerization) offset inks with UV varnish is very low. The UV varnish can be applied only on a dried surface of conventional ink, and also in this case there are problems with anti set-off powders. By application of a primer, usually a disperse varnish, the problems can be solved. The printing press has to contain then two units for varnishing. Using hybrid inks is another possibility how to overcome above mentioned problems. These inks combine binders which are cured by oxypolymerisation and also binders cured by polymerization initiated by photoinitiators (see

Table 2) [5]. After UV irradiation, the layer of the ink is enough cured and the varnish can be applied. The compatibility of hybrid ink with UV varnish is enough for maintaining the final gloss of the surface. The conventional part of the ink ensures the compatibility with common rollers of an inking unit based on NBR material, so the conventional and hybrid inks can be alternated in the printing press.

Table 2: General hybrid ink composition [5]

Hybrid ink	
Vegetable oil and esters thereof Semi drying alkyd	5–15 %
Polyester acrylates	0–50 %
Epoxyacrylates	0–10 %
Vegetable oil acrylates	0–50 %
Pigment	14–24 %
Fillers	4–8 %
Wax	1–2 %
Monomers	5–15 %
Photoinitiator blend	4–8 %
Stabilizers, inhibitors	<1 %

The quality of final print significantly depends on the substrate; especially the penetration of the ink in to the substrate determines the quality of final layer (gloss, dot gain, rubbing resistance) [6]. In practical application of overprinting hybrid inks by UV varnish, there was observed a lower rubbing resistance during following finishing. The aim of this work was to investigate the rubbing resistance of prepared layers.

3. MATERIALS AND METHODS

3.1. Printing Inks and varnish

Hybrid UV ink – Magenta UV Hybrid Plus/Litho UOH30080 (XSYS Print Solution)

UV ink – Magenta Suncure Starlux (Sun Chemical)

UV varnish – Excure 90006 (Arets Graphics)

3.2. Printed materials

Achilles – cardboard with laminated metallic foil (Alto)

Ensocoat – two side coated SBS cardboard (Storaenso)

Primex Gloss – PP foil (Exten)

3.3. The surface tension measuring

The surface tensions of the printed materials were determined by measuring of contact angles of standard liquids (water, diiodomethane). Device CAM 100 for measuring the sessile drop was used. Three drops of both liquids on all printed materials were measured. The surface tension was calculated by Owens-Went method.

3.4. Preparation of printed samples

Printing was carried out on proofing device IGT C1. Amount of printed ink was chosen so that the resulting print fit to $L^*a^*b^*$ coordinates, as is defined in ISO 12467 (ink transfer approximately 0.7 gm^{-2} i.e. 0.005 g of ink on area of $22 \times 3.3 \text{ cm}$). Printed samples were cured in a UV tunnel Aeroterm Miniterm (medium pressure Hg lamp); UV dose for hybrid ink was 1300 mJ/cm^2 and for UV ink 1750 mJ/cm^2 . UV dose was measured by UV-integrator from uv-technik. Printed samples with a higher ink transfer (approximately 3.1 gm^{-2}) were also prepared to simulate overprint of four layers (process colour printing). These samples were cured with high UV dose, approximately 5700 resp. 7300 mJ/cm^2 .

Part of printed uncured samples was overprinted by UV varnish (approximately 3.0 gm^{-2}). Curing of ink and varnish layers was carried out simultaneously with UV dose 1600 mJ/cm^2 for thinner layer of hybrid ink and UV varnish, 2000 mJ/cm^2 for thinner layer of UV inks and UV varnish and 5500 mJ/cm^2 for thicker layer of both types of ink and UV varnish.

3.5. FTIR

The degree of curing of inks and varnishes was monitored by IR spectra (FTIR spectrometer Avatar 320, Nicolet Instrument Corp.). Samples were printed on cardboard Achilles (cardboard with laminated aluminium foil). The curing of UV and hybrid ink was monitored by the peak 810 cm^{-1} (acrylate double bound). As reference peak was used band with maximum at 860 cm^{-1} . For irradiation of samples were used above mentioned UV tunnel Minitherm and also UV source Greenspot (high-pressure Hg lamp).

3.6. Test of abrasion resistance

The test was carried out on the Ink Rub Tester (Testing Machines Inc.). Prepared samples were rubbed by using weight 1.8 kg , with 20 movements at 85 movements/min. As counterpart the reverse sides of the tested materials were used. To be able to compare the abrasion resistance of different materials a standard material was also used as counterpart (APCO paper). Abrasion test was carried out immediately after irradiation, after 1 hour, 24 hours and after 168 hours. The degree of abrasion was determined by measuring the colour changes on the used counterpart. For all colorimetric measurement the spectrophotometer X-Rite 530 was used and CIELAB colour difference ΔE was evaluated.

4. RESULTS

As can be seen from table 3, the surface free energy of the tested materials is quite different. In the case of cardboard Esocoat there was found a significantly lower value of surface free energy than is recommended by ink manufacturers ($38\text{--}44 \text{ mNm}^{-1}$).

Table 3: Surface energy of printed substrates

Printed material	Surface energy [mN.m^{-1}]	Polar comp. [mN.m^{-1}]	Disperse comp. [mN.m^{-1}]
Achilles	50,34	10,60	39,75
Ensocoat	34,26	1,22	33,04
Primex	44,86	10,36	34,50

Figures 1 and 2 show the IR spectra of uncured and cured hybrid and UV inks. The conversion degree of hybrid ink was almost 100 % compared to UV inks, where the degree of conversion reached about 93 % (medium-pressure Hg lamp) and 96 % (high-pressure Hg lamp). The presence of UV varnish did not influence the degree of conversion neither hybrid nor UV ink.

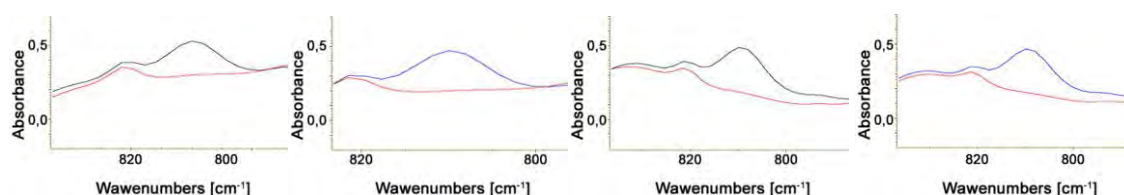


Figure 1: The curing of hybrid ink in terms of IR spectra
a) UV dose 1800 mJ/cm^2 , medium-pressure Hg lamp
b) UV dose 1500 mJ/cm^2 , high-pressure Hg lamp
c) Overprint by UV varnish, UV dose 1500 mJ/cm^2 , medium-pressure Hg lamp
d) Overprint by UV varnish, UV dose 1500 mJ/cm^2 , high-pressure Hg lamp

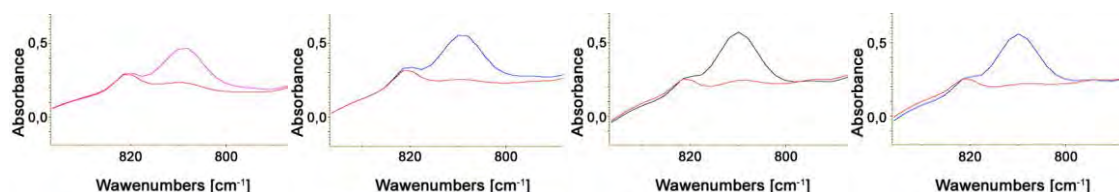


Figure 2: The curing of UV ink in terms of IR spectra
a) UV dose 1700 mJ/cm², medium-pressure Hg lamp
b) UV dose 1550 mJ/cm², high-pressure Hg lamp
c) Overprint by UV varnish, UV dose 1500 mJ/cm², medium-pressure Hg lamp
d) Overprint by UV varnish, UV dose 1500 mJ/cm², high-pressure Hg lamp

Table 4 summarizes results of abrasion resistance of prints. In the case of hybrid ink the results are not much different among tested substrates. In the case of UV ink printed material plays a significant role. The lowest abrasion resistance was found for cardboard Ensocoat, the highest for PP film Primex. When rubbing was performed by using APCO coated paper, very similar results were found for all tested materials. In all cases, the use of varnish increased resistance to abrasion. Time dependence of abrasion resistance was not found out.

Table 4: Abrasion resistance of samples with higher ink deposition (0.023 g, irradiation 5700 resp. 7300 mJ/cm²) expressed as ΔE

Printed material	Ink	Rubbing material	UV varnish	ΔE			
				immediately	after 1 hour	after 24 hours	after 168 hours
Achilles	Hybrid	Achilles	no	0.3	0.3	0.4	0.7
			yes	0.5	0.6	0.7	0.8
		APCO	no	2.9	2.8	2.3	2.3
			yes	1.6	1.2	1.3	1.3
	UV	Achilles	no	4.1	3.8	4.9	5.9
			yes	1.6	1.7	2.0	2.2
		APCO	no	1.5	1.4	1.7	2.4
			yes	1.3	1.1	1.7	1.5
Ensocoat	Hybrid	Ensocoat	no	0.9	1.5	1.3	1.5
			yes	0.5	0.4	0.4	0.4
		APCO	no	2.1	2.3	2.3	2.0
			yes	2.0	1.6	1.3	1.6
	UV	Ensocoat	no	8.0	6.9	6.1	7.1
			yes	4.0	4.9	4.8	4.6
		APCO	no	1.4	1.7	1.6	2.0
			yes	1.6	1.5	1.5	1.6
Primex	Hybrid	Primex	no	0.6	0.6	1.2	0.6
			yes	0.6	0.5	0.5	0.5
		APCO	no	2.1	2.8	1.8	2.2
			yes	1.2	1.4	1.6	1.3
	UV	Primex	no	2.3	0.9	0.6	1.1
			yes	0.5	0.9	0.7	0.7
		APCO	no	1.4	4.4	1.7	2.7
			yes	1.5	2.0	1.3	1.8

5. CONCLUSIONS

It was confirmed that the abrasion resistance of prints is affected by printed material and also significantly by material, that is used as counterpart for rubbing test. There were no effects of the UV varnish layer on degree of curing of UV or hybrid inks. Abrasion resistance of prints did not change over time

6. LITERATURE

- [1] Anon.: "Hybrid inks: emerging or enduring technology?",
URL http://www.americanprinter.com/alt/mag/printing_hybrid_inks_emerging/
(last request: 2012-09-18).
- [2] Štěpánová, A.: "Fyzikální vlastnosti UV hybridních ofsetových barev", Diploma Thesis, University of Pardubice, 2008.
- [3] Remenárová, K.: "Vlastnosti hybridních tiskových barev", Diploma Thesis, University of Pardubice, 2006.
- [4] Kaplanová, M., Remenárová, K., Jašůrek, B., Vališ, J.: "Study of the rheological behaviour of conventional, hybrid and UV offset inks", Advances in Printing Media Technology, Vol. XXXIV, pages 101–108, IARIGAI, Grenoble, France 2007, ISBN 978-953-7292-04-1
- [5] Gevaert, P.: "Ink Performance Properties of UV, Conventional and Hybrid Inks", RadTech Europe 2003, Conference Proceedings, vol. 1, p. 515, November 3–5, 2003, Berlin, Germany.
- [6] Rousu, S., Gustafsson, J., Preston, J. and Heard, P.: Interactions between UV curing, hybrid-UV and sheetfed, offset inks and coated paper – commercial print trials, TAGA Journal, Vol. 2, pages 174–186, 2006.



Printing Forms and Image Carriers



SODIUM METASILICATE SOLUTION AS A DEVELOPER FOR CTCP OFFSET PRINTING PLATES

Tomislav Cigula, Jelena Poljak, Vedrana Peko, Tamara Tomašegović
University of Zagreb, Faculty of Graphic Arts

Corresponding author: Tomislav Cigula
e-mail: tomislav.cigula@grf.hr

1. ABSTRACT

Many printing techniques increase their market share, but offset printing is still market leader in printing of many graphic products. It is a very complex process in which printing plate has significant influence on the final reproduction quality. Offset printing plates are in most cases built of aluminium foils which are processed in order to enhance needed surface characteristics and ensure stability and durability in the printing process.

One of the key processes in the plate making is developing which must remove ink receptive photoactive layer, but in the same time minimizes change of the hydrophilic aluminium-oxide layer. Therefore, chemistry free and low chemistry plates are being developed, but they are still not used when it comes to the high quality products and reproduction of long runs, so improvement of the chemical developing processes is of high importance.

This research was conducted in order to investigate application of developers based on the sodium metasilicate of various concentrations. For that purpose samples of printing plates coated with positive diazo photoactive layer were exposed in same condition and then developed in developers with five different concentration of sodium metasilicate. Determination of influence on the aluminium-oxide layer was made by observing profilometric roughness parameters and the contact angle values when applying two different fountain solutions.

Results of the investigation have shown that concentration of the sodium metasilicate has an impact on the aluminium-oxide roughness and consequently wetting properties, but comparing it to the other investigated developers, the impact is smaller. Results have showed high correlation between contact angle roughness parameters values, showing high influence of surface structure on wetting properties.

This research has proved the influence of investigated developing process on the non-image area surface, which could cause problems in printing plate exploitation. In addition, the sodium metasilicate proved to be possible chemical compound to be used for developing of investigated printing plate type, but prior to that there must be further research conducted to determine its behaviour in other process parameters.

Key words: lithography, roughness parameters, contact angle, developing, sodium metasilicate

2. INTRODUCTION

Offset printing plates are mostly built of aluminium foils. To enhance fountain solution adhesion on the aluminium oxide film in the printing process and to ensure better adhesion of the photosensitive coating on the foil's surface (Limbach et al., 2003, Hutchinson, 2001), the aluminium foil needs to be roughened by electrochemical processes of graining and anodic oxidation (Gobbetti, 1991, Lin et al., 2001). The anodic oxidation is usually conducted in a two step process in which aluminium foil is first cathode and then anode (Nishino et al., 2004, Cigula, 2011).

In these processes, specific anodic layer is formed on the aluminium foil, which consists of a thin non-porous compact oxide layer (barrier layer) and an outer extremely porous oxide layer (Figure 1). Size and quality of the grained microstructure, i.e. of the porous layer, will influence the printing performance and durability of the printing plates (Dimogerontakis, 2006, Rivett, 2011). In the final step, the formed layer of aluminium oxide is coated with a photosensitive layer which enables image transfer on the printing plate.

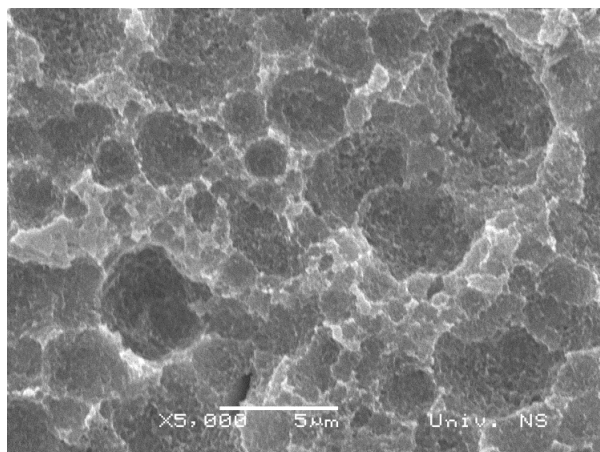


Figure 1: Aluminium oxide porous layer at magnification of 5000× (Cigula, 2011)

The plate making process consists of two main processes, exposure and developing (Mac Phee, 1998). Electromagnetic energy of certain wavelengths will in the exposure induce photochemical reaction in the photoactive layer and change its solubility in defined solution. Developing is process in which soluble parts of the photoactive layer are removed from the aluminium foil, and open the aluminium-oxide surface. The remains of the photoactive layer on the aluminium foil represent image areas, while the opened aluminium-oxide layer builds non-image areas. As previously mentioned, the structure of the aluminium-oxide layer has an important role in printing quality and therefore should not be influenced by the plate making process. Nevertheless, majority of the photoactive layers which are chemically processed in the plate making process use highly alkaline solutions as a developer, which could impair surface of the amphoteric aluminium-oxide (Mahovic Poljacek et al., 2011, Cigula, 2011).

Previous research (Cigula et al., 2012, Baracic, 2009) showed high influence of the potassium and sodium hydroxide solution on the surface change of the aluminium-oxide. This research was made to determine influence developers made of different concentration of the sodium metasilicate solution, as silicate and phosphate salts are used in fountain solutions to improve its better adsorption on the non-image areas (aluminium-oxide). On the other hand, sodium metasilicate is a white powder soluble in water even at room temperature and the resulting solution is alkaline (Greenwood and Earnshaw, 1997), so it could be used as a developer for some types of offset printing plates.

3. MATERIALS AND METHODS

To conduct this research, samples of conventional printing plates coated with positive diazo photoactive layer were prepared. These plates could be used in conventional and Computer to Conventional Plate (CtCP) making process. In both plate making processes developing of the printing plate is carried out in an alkaline solution.

Samples of the printing plate were exposed with PlurimetEXPO74 unit equipped with 3.5 kW metal-halide lamp for 60 pulses (the unit measures the pulse energy and compensates reduction of lamp intensity over time). After exposure, samples were developed in the developers of different sodium metasilicate (Na_2SiO_3) concentrations, from 0.1 to 0.5 mol dm^{-3} . Developers were prepared by dissolving Na_2SiO_3 p.a. crystals in distilled water (INA, ISO 9001, ISO 14001, OHSAS 18001). In order to eliminate influence of temperature and saturation of developer (Mahovic Poljacek, 2007), all samples were developed at temperature of $25 \pm 0.1^\circ\text{C}$ in freshly prepared developer. Samples were immersed in the developer for a period of 60 s. After developing process all samples were washed in distilled water and dried at room temperature.

In order to determine influence of the developing process on the aluminium-oxide layer, measurements of the contact angle and roughness parameters were performed. The contact angle measurements were performed by Dataphysics's OCA30 goniometer. Contact angle was determined using Sessile drop method. Analysis of the liquid drop was performed by Dataphysics' SCA20 software using ellipse/Laplace-Young fitting depending on the drop shape (Dataphysics, 2006). The volume of the applied liquid drop was 1 μl . In order to rule out the contact angle dynamics, measurement of the contact angle was conducted with same delay

from the first liquid-solid contact for all samples (Cigula et al., 2010). Two different fountain solutions were prepared for this research. FS1 was alcohol based and prepared from demineralised water in which 2.5 %vol buffer, 1 %vol additive for conductivity correction and 11 %vol 2-propanol were added. Due to bad influence on environment and people health of 2-propanol (Inchem, 2012), alcohol free fountain solutions are present on the market. Second fountain solution used for this research (FS2) was alcohol free, prepared from demineralised water in which commercial additive in concentration of 4 %vol and 0.7 %vol additive for conductivity correction were added.

Profilometric roughness parameters – R_a , R_q , R_p and R_v were measured by the Portable Surface Roughness Tester TR 200. The unit is compatible with ISO 4287, DIN 4768, ANSI B 46.1 and JIS B601 standards. The selected profilometric parameters were chosen among others as they were previously used in the lithographic printing plates surface characterization (Risovic et al., 2009, Pavlovic et al., 2012).

4. RESULTS AND DISCUSSION

Measurements of the roughness parameters were performed ten times on the one sample and results showed in Figures 2 and 3 are mean values.

Figure 2 shows influence of the sodium metasilicate (Na_2SiO_3) concentration on the profilometric parameters R_a and R_q . The values of both parameters have similar dependence to the Na_2SiO_3 concentration, high increase from first to the second concentration after which one could notice slight, but constant decrease. The lowest values of the both parameters were measured at the first investigated concentration (0.1 mol dm^{-3}), while highest values were at Na_2SiO_3 concentration of 0.2 mol dm^{-3} .

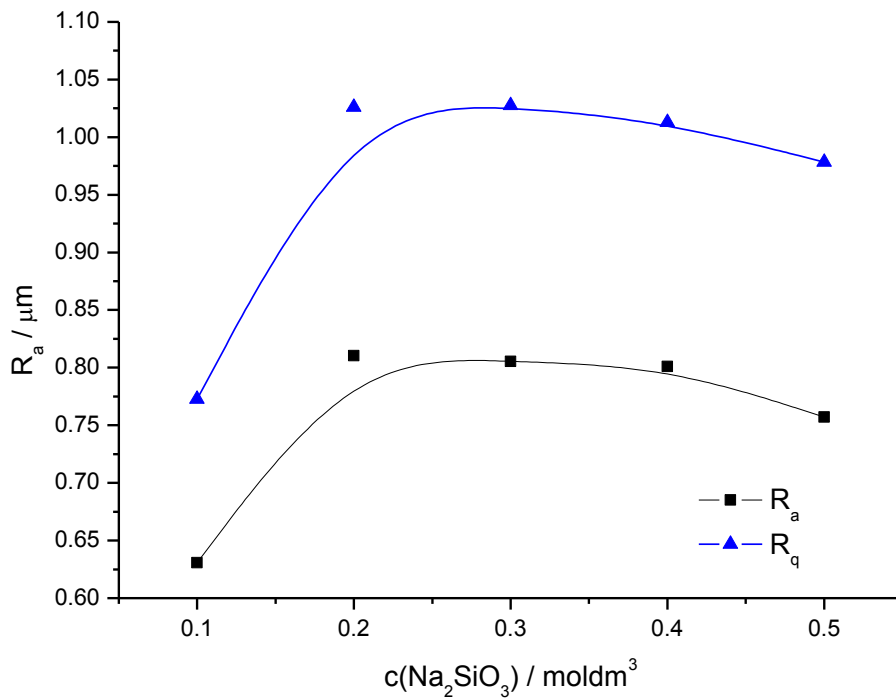


Figure 2: R_a and R_q depending on the Na_2SiO_3 concentration

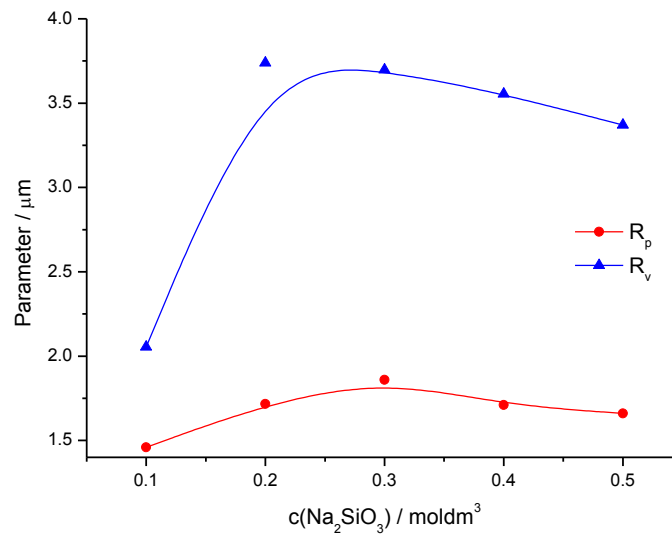


Figure 3: R_p and R_v depending on the Na_2SiO_3 concentration

Similar behaviour could be seen in Figure 3, which shows dependence of the profilometric parameters R_p and R_v on Na_2SiO_3 concentration. Different to the other parameters is behaviour of the R_p , which has highest value at Na_2SiO_3 concentration of 0.3 moldm^{-3} , and its values are more monotonous throughout monitored concentrations.

This behaviour suggests that lowest concentration of Na_2SiO_3 (0.1 moldm^{-3}) does not completely remove photoactive coating from the aluminium-oxide surface in the proposed time period. Parts of that coating stay in the valleys resulting with lower R_v value. On the other hand, decrease of the parameter values after reaching maximum is probably consequence of dissolving of aluminium-oxide in alkaline solution and possible sedimentation of some chemical products in the surface valleys. Higher difference between R_a and R_q values at first and second concentration could indicate slight shift of base line in profilometric roughness parameters definition.

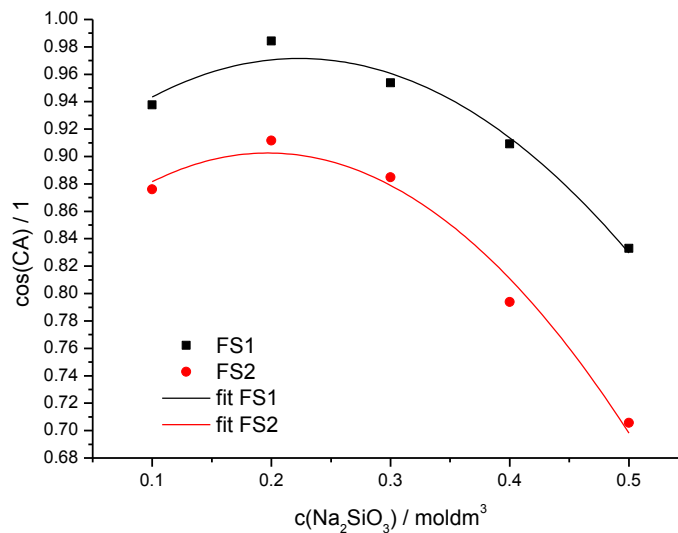


Figure 4: Cosine of contact angle value when applying fountain solutions

In Figure 4 one could see influence of Na_2SiO_3 concentration on cosine of contact angle ($\cos(\text{CA})$) between prepared fountain solutions and non-image areas of the printing plates. One could see that the dependence of $\cos(\text{CA})$ on concentration of Na_2SiO_3 is square polynomial with maximum value at Na_2SiO_3 concentration of 0.2 moldm^{-3} . One could also notice that

dependence of $\cos(\text{CA})$ for both fountain solutions is nearly the same, but values of $\cos(\text{CA})$ for FS1 are higher than of $\cos(\text{CA})$ for FS2. This means that there is better wetting of printing plate's non-image areas with FS1.

There is high correlation coefficient, calculated according to Pearson, between results of contact angle measurement and presented roughness parameters (R_a , R_q , R_p and R_v), highest between R_a and $\cos(\text{CA})$ for FS2 (0.976) and lowest between R_p and $\cos(\text{CA})$ for FS1 (0.773) which shows high connection between surface texture and wetting properties of investigated surfaces. On the other hand, although lowest values of the roughness parameters were measured on the sample developed in developer of lowest Na_2SiO_3 concentration, lowest $\cos(\text{CA})$ were measured at sample developed in developer of highest Na_2SiO_3 concentration. This behaviour is probably the consequence of different methods measuring range. The diameter of the diamond tip on the TR200 portable tester is 5 μm , meaning it could sense remains of the photoactive coating in the valley of that size, while droplets which are applied on the surface in the contact angle measurement are of millimetre scale. Nevertheless, both measuring methods pointed out the same sample on which maximal values are reached.

5. CONCLUSIONS

The aim of this research was to investigate application of sodium metasilicate (Na_2SiO_3) as a developer for the positive diazo printing plates. For that purpose, developers with Na_2SiO_3 concentrations of 0.1 to 0.5 mol dm^{-3} with step of 0.1 were prepared. Influence of the Na_2SiO_3 concentration on the non-image areas was determined by measuring contact angle and roughness parameters.

Results of the research showed that Na_2SiO_3 could be used as a developer for the positive diazo printing plates. Lowest Na_2SiO_3 concentration is at investigated developing process parameters (temperature, developing time) insufficient for total removal of photoactive coating, meaning lowest values of roughness parameters. The maximal values of the roughness parameters are reached at the Na_2SiO_3 concentration of 0.2 mol dm^{-3} and further concentration increase causes dissolution of the aluminium-oxide and decrease of the roughness.

Results of the contact angle measurements are in good correlation with the results of roughness parameters, meaning the best wetting of the non-image areas with fountain solution was achieved at sample with highest roughness. Regardless of the developing solution used, better wetting results on samples were obtained by application of alcohol based fountain solution (FS1).

This research has proved that sodium metasilicate is acceptable as a developer of positive diazo printing plates and the optimal concentration of Na_2SiO_3 is 0.2 mol dm^{-3} , when using other developing parameters as proposed in this research. To get better insight into the usability of this solution, further research must be conducted to define influence of other developing process parameters, such as temperature, developing time and developer saturation, on the printing plate quality. Furthermore, this solution could be tested in developing of other photoactive coatings which use alkaline developers.

6. LITERATURE

- [1] Baracic, M., Cigula, T., Tomasegovic, T., Zitinski Elias, P. Y., Gojo, M. (2009) Influence of Plate Making Process and Developing Solutions on the Nonprinting Areas of Offset Printing Plates, Proceedings, 20th International DAAAM Symposium: "Intelligent Manufacturing & Automation: Theory, Practice & Education", Viena, pp. 0599-0600.
- [2] Cigula, T. (2012) Quality analysis of the nonprinting areas on printing plates, Dissertation, University of Zagreb, Faculty of Graphic Arts, Zagreb
- [3] Cigula, T., Fuchs-Godec, R., Gojo, M., Slemnik, M. (2012) Electrochemical Impedance Spectroscopy as a tool in the plate making process optimization, Acta Chimica Slovenica, 59, pp. 513-519
- [4] Cigula, T., Mahović Poljaček, S., Gojo, M. (2010) Influence of Drop Volume on Time-dependant Contact Angle", in "DAAAM International Scientific Book 2010", DAAAM International Vienna, Vienna, pp. 195-202.
- [5] Dataphysics (2006) OCA30 instruction manual
- [6] Dimogerontakis, T., Van Gils, S., Ottevaere, H., Thienpont, H., Terryn, H., (2006) Quantitative topography characterisation of surfaces with asymmetric roughness induced by AC-graining on aluminium, Surface and Coatings Technology, 201, pp. 918-926.

- [7] Gobbetti, O. (1991) Electrochemical Graining of Aluminum or Aluminum Alloy Surfaces, Patent No.: US5064511.
- [8] Greenwood, N.N., Earnshaw, A. (1997) Chemistry of the Elements (2nd ed.). Butterworth–Heinemann. Oxford
- [9] <http://www.inchem.org/documents/pims/chemical/pim290.htm>, 14.9.2012.
- [10] Hutchinson, R. (2001) Surface engineering for lithography, Transactions of the Institute of Metal Finishing, 79, pp. 57-59
- [11] Limbach, P. K. F., Amor, M. P., Ball, J. (2003) Aluminium Sheet with Rough Surface, Patent No.: US6524768 B1.
- [12] Lin, C. S., Chang, C. C., Fu, H. M. (2001) AC electrograining of aluminum plate in hydrochloric acid, Materials Chemistry and Physics, 68, pp. 217–224.
- [13] MacPhee, J., (1998) Fundamentals of Lithographic Printing, Volume I Mechanics of Printing, GATFPRESS, Pittsburg
- [14] Mahović Poljaček, S., (2007), Surface structure characterization of the offset printing forms, Dissertation, University of Zagreb, Faculty of Graphic Arts, Zagreb
- [15] Mahovic Poljacek, S., Risovic, D., Cigula, T., Gojo, M. (2012) Application of electrochemical impedance spectroscopy in characterization of structural changes of printing plates, Journal of Solid State Electrochemistry, 16, pp. 1077-1089
- [16] Nishino, A., Masuda, Y., Sawada, H., Uesugi, A. (2004) Process for Producing Aluminum Support for Lithographic Printing Plate, Patent No.: US6682645 B2.
- [17] Pavlovic, Z., Novakovic, D., Cigula, T. (2012) Wear analysis of the offset printing plate's non-printing areas depending on exploitation, Technical gazette, 19, pp. 543-548
- [18] Risovic, D., Mahovic Poljacek, S. Gojo, M., (2009) On correlation between fractal dimension and profilometric parameters in characterization of surface topographies, Applied Surface Science, 255, pp. 4283-4288
- [19] Rivett, B., Koroleva, E.V., Garcia-Garcia, F.J., Armstrong, J., Thompson, G.E., Skeldon, P. (2011) Surface topography evolution through production of aluminium offset lithographic plates, Wear, 270, pp. 204-217

THE CONTACT ANGLE OF REFERENCE LIQUIDS ON FLEXOGRAPHIC PRINTING PLATES AS A FUNCTION OF TIME

Sandra Dedijer¹, Tomislav Cigula², Dragoljub Novaković¹, Miroslav Gojo²

¹Faculty of Technical Sciences, Graphic Engineering and Design, Novi Sad,

²Faculty of Graphic Arts, Zagreb

Corresponding author: Sandra Dedijer
e-mail: dedijer@uns.ac.rs

1. ABSTRACT

Wetting and spreading of a liquid on a solid surface are two surface phenomena which highly influence many processes in various industrial fields. The wetting properties of the printing areas on a printing plate have an important role in gaining high quality imprints since they influence ink transfer from a printing plate onto the printing substrate. In flexography are that properties even more important as the printing inks are of lower viscosity and the pressures in the printing process are lower in comparison to the other printing techniques. Although wetting properties could be observed by measuring static contact angle, the time dependant contact angle is of high importance as time for the ink transfer from the anilox roller onto the printing plate and finally to the printing substrate is very short. This paper shows results of determining wetting characteristics of two flexographic printing plates by measuring the dynamic contact angle of reference liquids and its influence on the surface free energy calculation. The obtained results have shown that contact angle values of two reference liquids are slightly influenced by the time of measurement, meaning they reach equilibrium state very fast. Furthermore, it could be seen that printing plate type also influences the dynamic contact angle values. Surface free energy of printing areas at investigated printing plates has not been significantly changed. This research proved that time of the measurement has slight influence on the value of the contact angle which means that reference liquids reach equilibrium state quickly and therefore surface characterization of the flexographic printing plates could be made by observing only static contact angle. On the other hand, when the most viscous liquid of the ones used (glycerol) was applied on the surface, contact angle changed in time so further research should be directed to determining the dynamic contact angle of the printing ink on the printing plate's printing areas.

Key words: contact angle, wetting, surface free energy, flexographic printing plate

2. INTRODUCTION

Flexography is a printing technique with highest increase of the market share in graphic arts industry due to substantial technological development. Ability to produce relatively high quality imprints on number of various substrates has put flexography in the leading position when it comes to the packaging printing. Increase in the usage of flexography in printing has induced more researches of the flexographic printing plates and printing ink as those two parameters are highly important in achieving imprints of high quality. In order to make a high quality imprint one must assure good ink transfer from the printing plate to the printing substrate. There are many parameters influencing that transfer, among others printing press, impression, and the interaction between printing ink and printing plate. This made research of wetting and spreading characteristics rather frequent (Johansson, 2008).

The wetting of a solid surface by a liquid can be described through equilibrium (static / Young) contact angle (Shuangying et al., 2011, Kubiak et al., 2011, Bormashenko et al., 2011). On the other hand, the contact angle depends on the speed and direction of the contact line movement. Wetting front of a liquid may change the properties of the substrate and as the wetting front advances the contact angle varies with the velocity of the front (Hamraoui et al., 2000). Thus the determination of the static contact angle can be used if the droplet of the liquid stabilizes immediately after application on a solid surface (Cigula et al, 2009). When the change of the contact angle value in time after application is significant, which is common in industrial processes, the dynamic contact angle must be calculated.

This research was made to define the change of the liquid droplets on the surface of the printing area on the flexographic printing plate over a defined period of time. The conducted research had given valuable information about the liquid droplet behavior and its stabilizing abilities after application on the surface of the flexographic printing plate.

3. THEORY

Wetting and contact angle, in particular the contact angle dynamic, remain as a standard methods for characterization of the different surfaces, since they play an important role in many technological processes (De Ruijter et al., 1998, Kwok and Neumann, 1999, Cigula et al., 2009). Measurement of contact angle between liquids of known surface free energy and a solid surface enables defining surface free energy of a solid surface, its wetting properties, homogeneity and roughness characteristics (Cigula et al., 2009, Prabhu et al., 2009).

Wettability (or wetting) can be defined as the tendency of a liquid to spread on a solid substrate depending on the solid surface properties and the type of used liquid (Cigula et al., 2010, Shuangying et al., 2011, Kirchberg et al., 2011, Meng et al. 2011., Kubiak et al., 2011). It is conditioned by surface tension decrease in solid - liquid system (Cigula et al., 2010, Kubiak et al., 2011). The liquid will spread on the solid surface until the balance between cohesion (internal forces) of liquid, capillary (surface tension) forces and gravity is reached (Cigula et al., 2010, Kubiak et al., 2011). The achieved state of equilibrium corresponds to the minimal energy state among the three phases and the contact angle at this state is called equilibrium (static) contact angle or Young angle (Kubiak et al., 2011, Bormashenko et al., 2011, Shuangying et al., 2011). The determination of the Young angle is important for the characterization of solid-liquid interfacial systems (Rodríguez-Valverde et al., 2010, Kubiak et al., 2011) and it is closely related to the specific interfacial energies, through the Laplace-Young equation (1), (Figure 1) (Rodríguez-Valverde et al., 2010):

$$\sigma_s = \gamma_{sl} + \sigma_l \cdot \cos \Theta \quad (1)$$

where σ are the surface tension coefficients of solid-gas (s) and liquid-gas (l) interfaces, γ_{sl} is solid-liquid interface, Θ is the Young angle.

Thus, contact angle (CA) is the angle between the solid surface and liquid-gas interface, measured through the liquid phase (Farshid Chini and A. Amirfazli, 2011), i.e. it is the angle between tangent on the liquid drop (t_1) and the tangent on the solid surface (t_2) in the point where all three phases (solid, liquid and gas) meet (Figure 1) (Cigula et al., 2010). When applying water droplets, if the angle value is between 0° and 90° , solid surface is hydrophilic, and if CA value is between 90° and 180° degrees the surface is hydrophobic (Kemling, 2003).

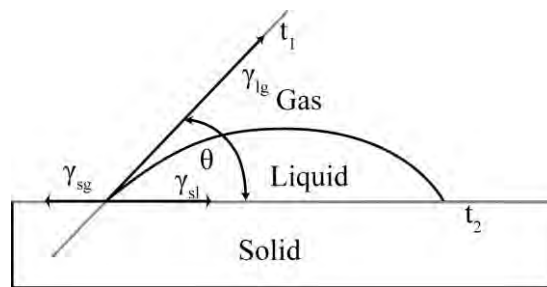


Figure 1: Contact angle between liquid and solid surface

It also can be stated that a liquid will spread on the solid surface of higher surface free energy and would not on the solid surface of lower surface free energy (Bormashenko et al., 2011).

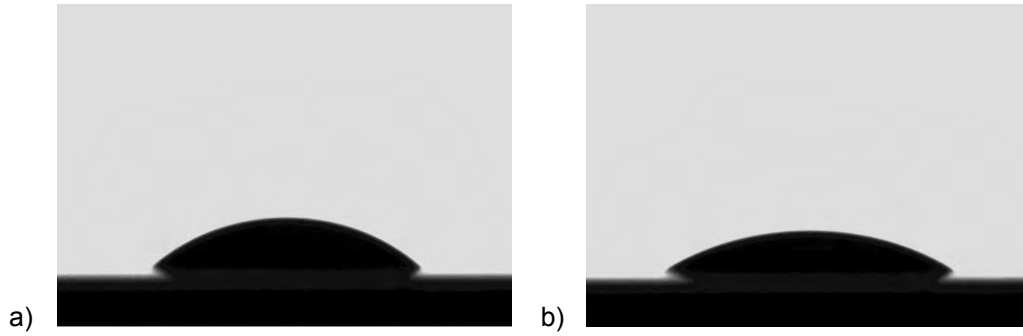


Figure 2: Contact angle between liquid and solid surface a) 0.3 seconds after solid-liquid initial contact and b) 1.3 seconds after solid-liquid initial contact

In most situations equilibrium state of contact angle cannot be reached. Due to the dependence of CA values on the speed and direction of the contact line movement, the non-ideal features of nearly all solid surfaces, an adequate description of the wetting process becomes quite complex and the Young angle experimentally becomes inaccessible (Hamraoui et al., 2000, Rodríguez-Valverde et al., 2010). Namely, once the contact line begins to move the conditions at the contact line are greatly complicated due to the dynamic forces generated by the motion which change the surface tensions, altering the balance in Young's equation (Sciffer, 2000). In order to characterize a solid surface the one can measure the dynamic contact angles as the finite number of different contact angles. The dynamic contact angle describe the processes at the liquid/solid boundary during the increase in volume (Θ_a - advancing angle) or decrease in volume (Θ_r - retreating angle) of the drop (Kruss, 2012). This difference between Θ_a and Θ_r , is called contact angle hysteresis (Grancarić et al., 2008, Rodríguez-Valverde et al., 2010, Pinterich et al., 2011) which is influenced by surface roughness of a solid surface, heterogeneity and metastable states (Grancarić et al., 2008, Pinterich et al., 2011). Calculations based on contact angle hysteresis can be denoted as an empirical approach since the current theoretical framework in surface thermodynamics is not sufficiently developed to enable the closed-form calculation of the Young angle from hysteresis measurements on real surfaces (Rodríguez-Valverde et al., 2010).

Advancing angles are normally used in order to determine the surface free energy of a solid since usually no liquid film is present in the movement direction of the liquid/solid interface (Pinterich et al., 2011, Kruss, 2012). The dynamic properties of a contact angle can be also observed through monitoring the changes in CA values of a liquid drop of known volume on a solid surface measured in the defined time after initial liquid-surface contact (Figure 2) (Cigula et al., 2009).

Surface free energy can be defined as the energy of particles in the surface layer in comparison to the particles in the mass of the chemical substance (Cigula et al., 2009). It provides a measure of the mutual affinity of interacting surfaces to a liquid drop. Surface free energy could be calculated from measured values of contact angle (Dimitrios et al. 2010). Although there are many different method for calculating surface free energy of a solid, for calculation of surface free energy of polymers one could use the universal method proposed by Owens, Wendt, Rabel and Kaelble (Dataphysics, 2006). According to Owens, Wendt, Rabel and Kaelble the surface tension (the value of the surface tension is equal to the value of the surface free energy) of each phase can be split up into a polar (σ^P) and a disperse (σ^D) part (Kruss, 2012):

$$\sigma = \sigma^P + \sigma^D \quad (2)$$

Owens and Wendt combined surface tension equation (2) and solve Laplace-Young equation using (3) (Kruss, 2012):

$$\gamma_{sl} = \sigma_s + \sigma_l - 2\sqrt{\sigma_s^D \cdot \sigma_l^D} - 2\sqrt{\sigma_s^P \cdot \sigma_l^P} \quad (3)$$

where γ_{sl} is surface free energy on solid – liquid phase interface, σ_l is surface tension of a liquid phase and σ_s is a surface tension of a solid phase, σ_s^P and σ_l^P are polar parts of the surface tension, σ_s^D and σ_l^D are dispersive parts of the surface tension.

Combining (1), (2) and (3) one could calculate contact angle of know liquid and solid. Kaelble solved the equation combining two liquids and calculating the mean values of the calculated surface energy values (Kruss, 2012). Rabel made it possible to calculate the polar and disperse parts of the surface energy with the aid of a single linear regression from the contact angle data of various liquids (Kruss, 2012). He combined equations (2) and (3) and enabled calculation of polar and disperse part of the surface tension (4)

$$\frac{(1 + \cos \theta) \cdot \sigma_l}{2\sqrt{\sigma_l^D}} = \sqrt{\sigma_s^P} \sqrt{\frac{\sigma_l^P}{\sigma_l^D}} + \sqrt{\sigma_s^D} \quad (4)$$

where θ is contact angle between liquid and solid phase, σ_l is surface tension of a liquid phase, σ_s^P and σ_l^P are polar parts of the surface tension, σ_s^D and σ_l^D are dispersive parts of the surface tension. As equation (4) is a linear function, $y = ax + b$, one could calculate surface free energy of a solid surface by drawing a diagram of (4) for a number of contact angles measured by applying liquids of known surface tension and its polar and dispersive part (Figure 3).

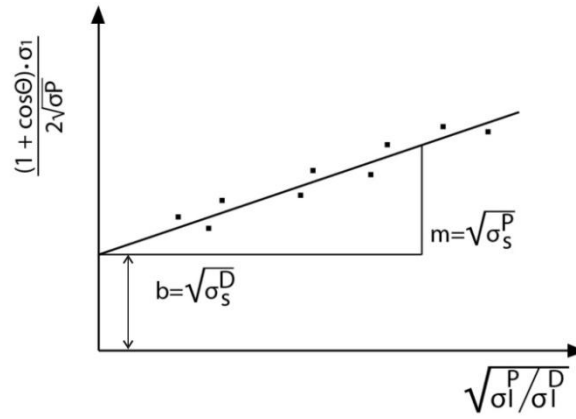


Figure 3: Determination of the disperse and polar part of the surface tension of a solid

4. MATERIALS AND METHODS

For conducting this research two digital (CtP) flexo printing plates 1.14 mm thick were prepared, A – printing plate with thermal developing process and B – printing plate with organic solvent based developing process. Processing parameters for printing plate making were:

A - back exposure for 50 s, main exposure for 720 s, UVA exposure for 420 s, UVC exposure for 7 s, developing using 10 rotations of the developing drum.

B - back exposure for 40 s, main exposure for 600 s, UVA exposure for 600 s, UVC exposure for 600 s, developing speed of 155 mm/minute, drying for 6000 s. The measurements were conducted on the samples of solid tone areas (dimensions: 120 × 15 mm) taken from the central part of the printing plate.

Video based, optical contact angle measurements were performed by Data Physics OCA30 goniometer. Contact angle was measured using the sessile drop method for applying liquid drop and Laplace – Young calculation method for drop analysis, i.e. contact angle measurement. The surface free energy value was calculated by using Owens, Wendt, Rabel and Kaelble (OWRK) analysis method by measuring the contact angle of three liquids of known surface free energy and viscosity (Table 1).

The measuring was conducted at the temperature of round 25°C using the drop volume of 1.5 µl. Contact angles of liquids were defined from average values of eight liquid droplets placed at different areas of the same printing plate sample. Contact angles of liquids were determined at various steps after initial contact (t = 0 s). The contact angle was measured in period from 0.5

– 3 s at every 0.5 s and from 3 – 30 s at every 3 s as it is assumed that spreading of the liquid is higher at the beginning of the solid-liquid interaction.

Table 1: Surface free energy (γ_{lv}) and their dispersive (γ_{div}) and polar (γ_{plv}) components and viscosity of liquids

Liquid	Surface free energy γ (mNm ⁻¹)			Viscosity (mPas)
	γ_{lv}	γ_{div}	γ_{plv}	
Diiodomethane (Ström)	50.8	50.8	0.0	2.78
Glycerol (van Oss)	64.0	34.0	30.0	1412
Water (Ström)	72.8	21.8	51.0	1.002

5. RESULTS AND DISCUSSION

The results of the contact angle measurement are presented in figures 4 to 6. The measured values are presented with points and lines in a diagram present trend values.

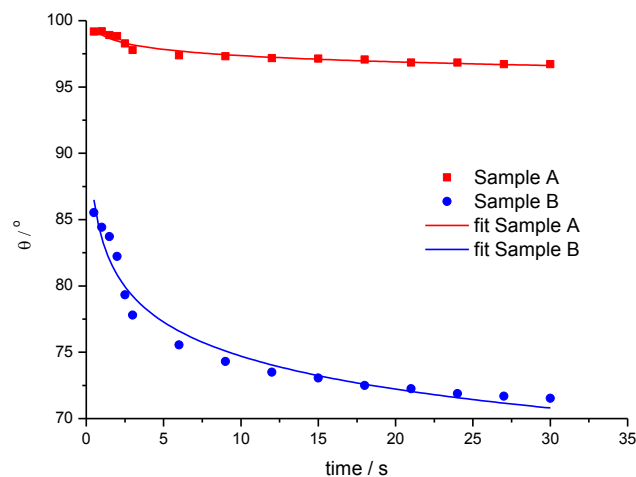


Figure 4: Contact angle values of glycerol as function of time

In Figure 4 one can see that the change of contact angle value are depicted by decreasing power function ($y=ax^b$). It can be seen that change of the contact angle is smaller when applying glycerol on the sample A surface in comparison to the application on the surface of sample B printing plate. The change in the contact angle value between first and last measurement at sample A is less than 2.5° while at sample B the difference is nearly 20°. In addition, values of the contact angle of glycerol on sample A are significantly higher than those on the sample B (15 – 20° depending on the measuring time period from initial contact) meaning better wetting properties of sample B.

Change of the contact angle values of water is shown in Figure 5. One could see that the functional dependence of the contact angle on time is similar to the one seen at glycerol on sample A. Water droplets show similar behavior on both surfaces (sample A and B) but with different values. Like at glycerol, contact angle on sample B is lower and decrease slightly more through time. Furthermore, results indicate stabilization of the contact angle value for both printing plates after time period of 3 seconds. Namely, difference between measured contact angles at 3 and 30 seconds is 0.53° for printing plate A and 1.59° for printing plate B.

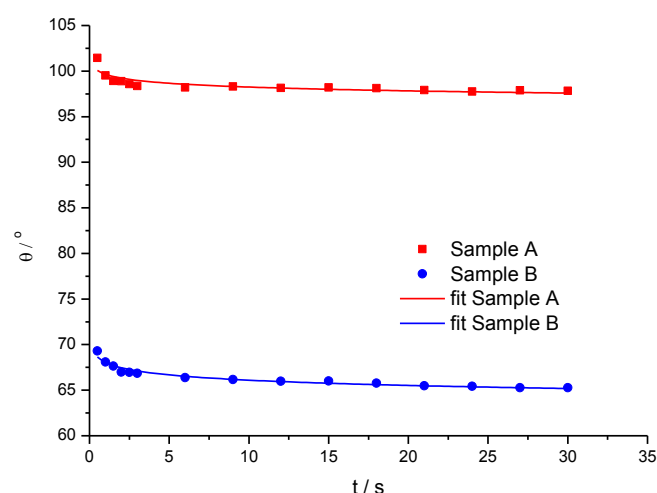


Figure 5: Contact angle values of water as function of time

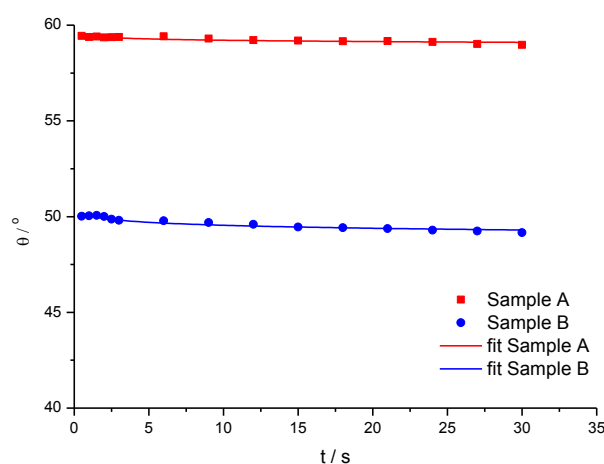


Figure 6: Contact angle values of diiodomethane as function of time

Observing diagram presented in Figure 6 one could see that contact angle values of diiodomethane on both printing plate samples are nearly independent on the time period of measurement. This behavior indicates that equilibrium state of diiodomethane is reached almost momentarily after application on the solid surface. Nevertheless, contact angle value slightly decreases in the observed time period with change of 0.47° for printing plate A and 0.86° for printing plate B between first and last measurement.

The results presented in figures 4 – 6 indicate that printing plate B shows better wetting for all three applied liquids and in the same time is more sensitive to the time when contact angle is measured. Although contact angle decreases with time for all observed liquid-solid interactions, highest change is measured when applied glycerol on printing plate B. On the other hand, contact angle value of diiodomethane is stable in the whole observed time period.

The printing plates are built of polymer which is organic based (Thompson, 2004) and therefore has larger dispersive part of surface free energy meaning better wetting with dispersive liquids (Figures 5 and 6). This is probably also the reason for small impact of measurement time on the contact angle values as liquids with similar (diiodomethane) or opposite (water) composition reach equilibrium state quickly. On the other hand, glycerol has dispersive and polar part of the surface free energy nearly the same and furthermore it has significantly higher viscosity of all used liquids which lead to the fact that there is more time needed to reach equilibrium state. Regardless of the applied liquid, contact angle value is influenced by time of measurement on the sample B which could be the consequence of higher homogeneity of printing plate's A surface.

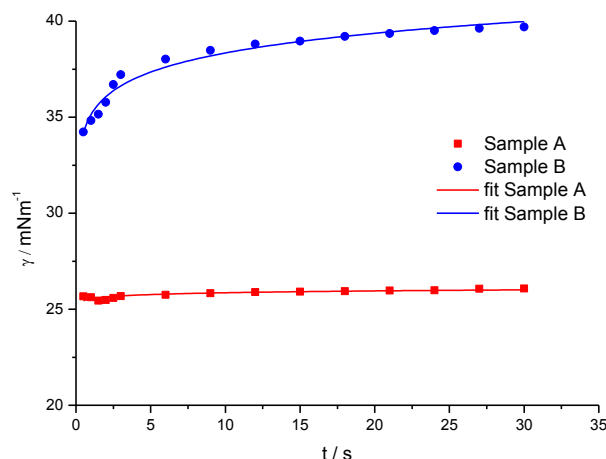


Figure 7: Dependence of surface free energy on time of contact angle measurement

Measurements of the contact angle of standard liquids are made in order to determine surface free energy of a solid surface. Results of the surface free energy calculation can be seen in Figure 7. It can be seen that these results are in correlation with changes in contact angle values. Since the changes in contact angle in case of printing plate B are higher than in case of printing plate A, there is also a greater increase in surface energy over observed time period. Correlation coefficients calculated according to Pearson show that contact angle of glycerol is best correlated with the surface free energy value of the printing plate (-0.90191 for Sample A and -0.99898 for sample B) meaning that those values most significantly influence calculation of the surface free energy, which is expected as other contact angle values (water and diiodomethane) are nearly unchanged over observed measurement's time period.

6. CONCLUSIONS

Wetting characteristics of a printing plate's surface has significant role in achieving high imprint quality as the ink transfer from the anilox roller to the printing plate and then to the printing substrate. This makes research and characterization of the printing plate's surface rather important. This paper was aimed on defining the influence of time passed from the initial contact of liquid drop with the solid to the measurement of the contact angle on its value and surface free energy calculation.

Obtained results showed that contact angle values are rather stable when applying diiodomethane. Contact angle of water stabilizes after nearly 3 second from initial contact of liquid with the solid surface while only at application of glycerol on printing plate B there is a difference of nearly 20 percent between first and last measurement, measurement time of 0.5 s and 30 s, respectively. In addition, results of the surface free energy calculation showed that values of the glycerol and its change over measurement's time period had influenced its value.

This research proved that determination of the time dependant contact angle on a flexographic printing plate is important as results showed there is significant change when applying liquid like printing ink, which is not predominantly polar or dispersive. Furthermore, there is high difference between surface energy values of observed plates which indicate their different behavior in the printing process although all other parameters of the printing process would be constant. Therefore, one should not forget to determine surface properties of the printing plate and if needed make the proper adjustments of the plate making process or ink preparation to obtain needed quality level of the imprints and to keep it in similar range.

Acknowledgements

This work was supported by the Serbian Ministry of Science and Technological Development, Grant No.:35027 »The development of software model for improvement of knowledge and production in graphic arts industry«

7. LITERATURE

- [1] Bormashenko, E., Musin, A., Zinigrad, M. (2011) Evaporation of droplets on strongly and weakly pinning surfaces and dynamics of the triple line, *Colloids and Surfaces A: Physicochemical and Engineering Aspects*, pp. 235– 240
- [2] Cigula, T., Gojo, M., Novaković, D., Pavlović, Ž. (2010) Influence of Various Concentrates on Quality of Printing Plates' Wetting Process, *Machine Design*, pp. 325-330
- [3] Cigula, T., Mahović-Poljaček, S., Gojo, M. (2009) Defining of time-dependent contact angle of liquids on the printing plate surfaces, *Proceedings of the 20th international DAAAM Symposium, "Intelligent Manufacturing & Automation: Theory, Practice & Education"*, 25-28th November 2009, Vienna, Austria
- [4] Dataphysics, OCA30 instruction manual, 2006.
- [5] De Ruijter M., Kolsch, P., Voue, M., De Coninck J., Rabe, J.P. (1998) Effect of temperature on the dynamic contact angle, *Colloids and Surfaces A: Physicochemical and Engineering Aspects* 144, pp. 235–243
- [6] Farshid Chini, S., Amirfazli, A. (2011) A method for measuring contact angle of asymmetric and symmetric drops, *Colloids and Surfaces A: Physicochemical and Engineering Aspects*, 388, pp. 29– 37
- [7] Grancarić, A.M., Tarbuk, A., Chibowski, E. (2008) Slobodna površinska energija tekstila, *Tekstil* 57 (1-2), pp. 28 -39
- [8] Hamraoui, A., Thuresson, K., Nylander, T., and Vassili Yaminsky, V. (2000) Can a Dynamic Contact Angle Be Understood in Terms of a Friction Coefficient?, *Journal of Colloid and Interface Science*, 226, pp. 199–204
- [9] Johnson, J. (2008) Aspects of Flexographic Print Quality and Relationship to some Printing Parameters, *Doctoral Dissertation, Karlstad University Studies*
- [10] Kemling, F. (2003) The effect of surface roughness on capillary inhibition, *Dissertation, Department of mathematics, Lulea university of technology, Stockholm*
- [11] Kirchberg, S., Abdin, Y., Ziegmann, G. (2011) Influence of particle shape and size on the wetting behavior of soft magnetic micropowders, *Powder Technology*, pp 311–317
- [12] Kruss (2011), Contact angle models [Online] Available from: <http://www.kruss.de/en/theory/measurements/contact-angle/models/owrk.html>, [Accessed: 3rd April 2012]
- [13] Kubiak, K.J., Wilson, M.C.T. , Mathia, T.G. Carval, P. (2011) Wettability versus roughness of engineering surfaces, *Wear*, pp. 523–528
- [14] Kwok, D.Y., Neumann A.W. (1999) Contact angle measurement and contact angle interpretation, *Advances in Colloid and Interface Science*, 81, pp. 167-249
- [15] Lamprou, D. A., Smith, J. R. Nevell, T. G., Barbu, A., Stone, C., Willis, C. R., Tsibouklis, J. (2010), A comparative study of surface energy data from atomic force microscopy and from contact angle goniometry, *Applied Surface Science*, 256, pp. 5082–5087
- [16] Meng, X.L., Wan, L.S., Xu, Z.K. (2011) Insights into the static and advancing water contact angles on surfaces anisotropised with aligned fibers: Experiments and modeling, *Colloids and Surfaces A: Physicochemical and Engineering Aspects*, pp. 213– 221
- [17] Pinterich, T., Winkler, P.M., Vrtala, A.E., Wagner, P.E. (2011) Experiments on the contact angle of n-propanol on differently prepared silver substrates at various temperatures and implications for the properties of silver nanoparticles, *Atmospheric Research*, 101, pp. 510–518
- [18] Prabhu, K. N., Fernades, P., Kumar, G. (2009) Effect of substrate surface roughness on wetting behaviour of vegetable oils, *Materials and Design*, 30, pp. 297–305
- [19] Rodríguez-Valverde, M. A., Montes Ruiz-Cabello, F. J. Gea-Jódar, P. M., Kamusewitz, H., Cabrerizo-Vílchez, M. A. (2010) A new model to estimate the Young contact angle from contact angle hysteresis measurements, *Colloids and Surfaces A: Physicochemical and Engineering Aspects*, 365, pp. 21–27
- [20] Sciffer, S. (2000) A phenomenological model of dynamic contact angle, *Chemical Engineering Science*, 55, pp. 5933-5936
- [21] Shuangying, W., Shi, J., Gu, J., Wang, D., Zhang, Y. (2011) Dynamic wettability of wood surface modified by acidic dyestuff and fixing agent, *Applied Surface Science*, article in press
- [22] Thompson B. (2004) *Printing Materials: Science and Technology*. 2nd edition, Pira International

OFFSET PRINTING PLATES: ALTERNATIVE METHOD FOR QUALITY CONTROL

Tomislav Hudika, Tamara Tomašegović, Sanja Mahović Poljaček
Faculty of Graphic Arts, University of Zagreb

Corresponding author: Tamara Tomašegović
e-mail: ttomaseg@grf.hr

1. ABSTRACT

In this paper the differences of results obtained by three measuring systems for determining surface coverage value of the printing plates were presented. The aim of this research was the introduction of image analysis as an alternative method for the characterization of surface coverage and tone reproduction of printing plates. Results have shown that different measuring systems for image analysis (IC Plate, ImageJ and Stream motion) obtain a different result in coverage values calculation. IC Plate is automated device for capturing the printing plate's area and automatically calculating coverage value, while ImageJ and Stream motion are programs supported by software which analyzes imported images that need to be captured by the microscope. Based on the results, one can say that ImageJ and Stream motion are more complex methods for coverage calculation, but they enable greater control of the imported images by means of manual adjustment.

Key words: printing plates, image analysis, quality control

2. MONITORING THE TONE REPRODUCTION IN OFFSET PRINTING

Standardization of all stages in the graphic reproduction process and monitoring the potential problems that may occur enables the production of high quality printing plates in order to obtain optimal reproduction of the original work. Measurements and characterization of printing plate's surface structure are a challenge for different science and technical fields. The main reason for that statement is a complex workflow that consists of different processes, for example, adjustment of a digital file for reproduction, an imaging of the printing plates, their chemical processing and finishing of the plates (Adams&Romano, 1996; Gemeinhardt 2001; Daimond, 1991).

Since the printing plate is one element in the graphic reproduction process, with the imprint as a final product, its quality and stability during the printing process directly influences quality of the imprint. In order to avoid quality reduction of printing plates and the imprints, errors in printing plate production must be timely detected and corrected. For this reason, a systematic and standardize control should be conducted on each printing plate. Nowadays, a number of methods for the analysis of material surface properties exist. In printing technology, where precise measurements are important, one must have in mind tracking of accuracy of reproduction in each segment of the reproduction process (Foley et al., 1992; Seydel, 1996).

The all segments in printing process are connected to each other, and are mutually conditioned. One of the basic parameter for monitoring the quality of the printing plate and printing process is the information about the tone reproduction. Tone reproduction provides information about the transfer of a digital file to the printing plate, and furthermore, from the printing plate to the printing substrate. In an ideal reproduction conditions, digital information in the file and the image on the printing plate and substrate should be uniform. Unfortunately, due to technological limitations, tolerances in the reproduction process are inevitable. In order to obtain an optimal quality of the reproduction all limitation and tolerances should be defined and adjusted before the reproduction starts (Mahovic et al., 2003; Born, 1983; Ihme, 1982).

Monitoring of the reproduction of tones can be realized in several ways, but is commonly conducted by means of surface coverage characterization. The assumption is, that even though different measuring devices and methods have a different system of data processing, they will provide a uniform, and in some cases, same results (Tomasegovic et al., 2011). This fact should be imposed as a widely accepted standard, not only in theory. In practice, the necessity of automation and equalization of applicable processes and methods of measurement should be adjusted.

This paper will present three methods for characterization of printing plate surface with the aim of introducing image analysis as an alternative method for the characterization of tone reproduction.

3. MATERIALS AND METHODS

Printing plates used in this investigation were offset CtP printing plates with raster Maxton CMYK 15-75-0-45 of 150 lcm^{-1} , a screen angle of 45° and Elliptical IP shaped raster. The thermo-negative "preheat" type of printing plate, with sensitivity of 800-850 nm were used (Goodman&Nüssel, 1999). For this paper a computer-generated control wedge with group of fields of 1% to 5%, 10%, 20%, ..., 95% to 100% coverage value for tone reproduction control was generated (Figure 1).

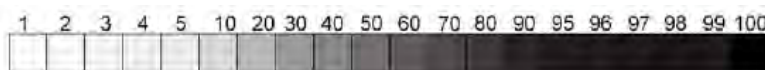


Figure 1. Control wedge with control fields of different coverage value

Imagesetter used in this paper was KODAK Magnus VLF, with imaging speed of 28.2 printing plates/h for printing plate with dimension of 2700mm, and 52.6 printing plates/h for the plates of 1030 mm. Printing plate making process was conducted according to the standardize procedure (ISO 12218:1997; ISO 12647-2:2004).

Characterization of printing plate reproduction and determination of coverage values transfer from the file to the printing plate by different methods was the objective of this investigation. Firstly, coverage values on the printing plate samples were measured by means of portable plate reader Gretag Machbeth IC Plate II, with adequate software support. This device is one of the most widely used methods for coverage values measurement because it enables process automation and fast control of the printing plates. Therefore, it was used as referent method in this paper. Each field on the wedge was measured ten times. When measuring, measured data can be carried out through a software algorithm, processed, and shown as middle-value results in diagrams.

As defined in the title, the aim of this paper was to introduce alternative methods of image analysis, as a new technique for characterization of surfaces in various research fields. Those methods require a capturing of images of measured samples in order to get a digital file of an image. The printing plate samples was snapped and digitalized by means of Metallurgical Microscope Olympus BX51, the industrial version of a microscope designed for the study of metal and polymer surfaces. The microscope is equipped with UIS2 Optical System and is connected to the computer. UIS2 lens system has a wide magnification spectrum with the accuracy of 0.1 mm.

After capturing images by means of a microscope, in the second procedure step was the analysis of the obtained images in software for image analysis. For this purpose, different image analysis software was used. First one was ImageJ, free on line image analysis software, and the second one was Stream motion – program supported by Olympus BX 51.

For image analysis with ImageJ the TIFF format images were processed and converted from multitone images in duotone images in order to obtain 2-byte pictures and maximize the contrast between the nonprinting and printing elements. Furthermore, for image analysis in Stream motion the digital images were adjusted by means of different applicable tools (contrast and lighting correction). After image adjustments, coverage value was calculated in given software. Analysis of these results was conducted, and the dependence of nominal and measured values were shown in diagrams. Schematic presentation of the coverage value measurement workflow can be seen in Figure 2.

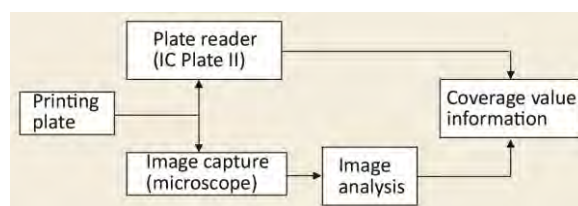


Figure 2. Coverage value measurement workflow

4. RESULTS AND DISCUSSION

Based on the measurement results, diagrams of dependence of measured on nominal coverage values were presented, and relations between the values obtained by plate reader and image analysis software were calculated.

In Figure 3 one can see captured images of characteristic fields on printing plate samples. The differences between images are visible. Wedge presents the digital data which was generated for this paper. IC Plate presents images processed by IC Plate software. ImageJ and Stream motion present bitmap-images obtained by tone and contrast adjustments. Therefore, one can conclude that each system uses different types of algorithms for image analysis, and expect deviations in the measurement results.

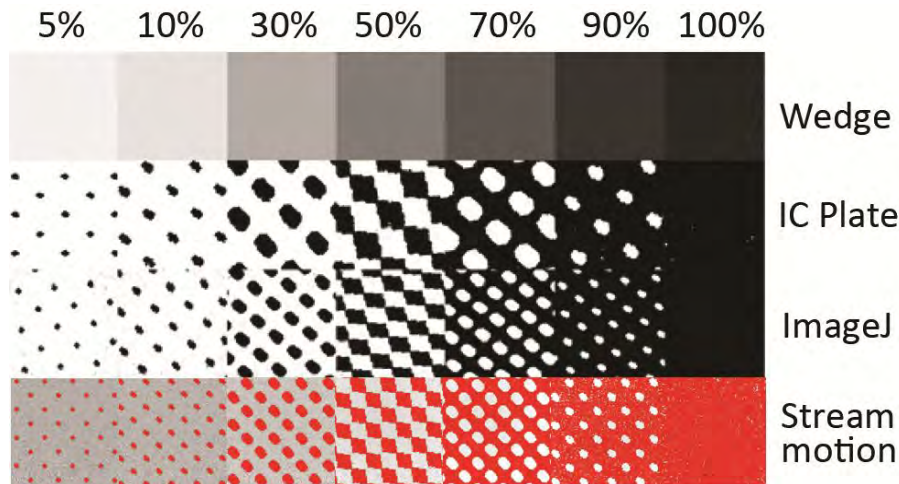


Figure 3. Images of printing plate's coverage values obtained by different measuring systems

Results of coverage values measurement obtained by using three different measuring systems can be seen in Figures 4 and 5.

As we can see in Figure 4, the differences measured below 10% of coverage values are minor. In coverage area from 0% - 50%, one can see that ImageJ shows largest differences in measured samples in comparison to the results of the IC Plate and Stream motion. Opposite to the values of the lower nominal coverage, higher coverage values (50% - 100%) show greater differences on measurement by Stream motion (Figure 5). In addition, all methods show that differences in coverage values on investigated printing plate's samples are highest between 90% and 100%.

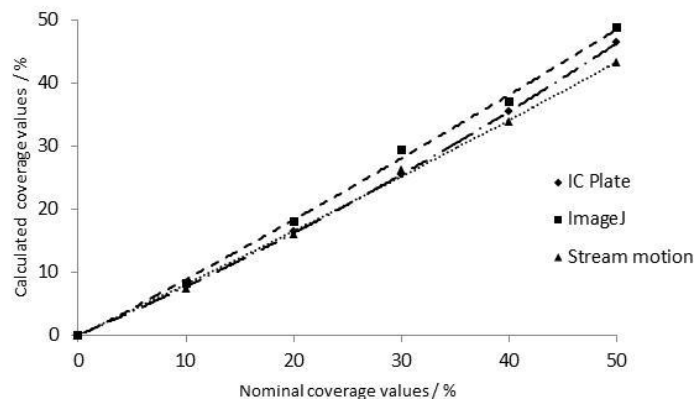


Figure 4. Comparison of nominal and measured coverage values obtained with different measuring methods from 0% - 50% coverage values

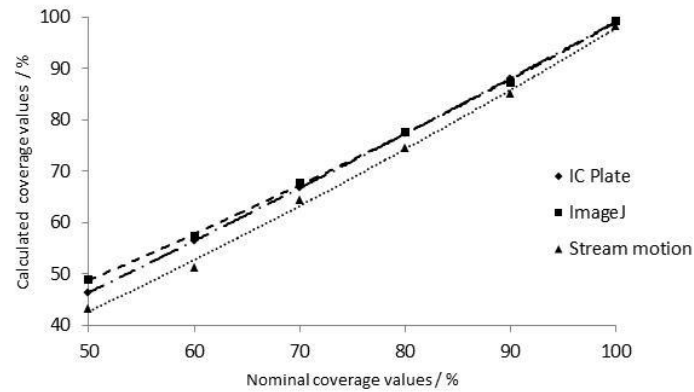


Figure 5. Comparison of nominal and measured coverage values obtained with different measuring methods from 50% - 100% coverage values

After calculating of mean coverage value for each field measured by IC Plate, ImageJ and Stream motion, results were compared and difference between coverage values was determined. In figure 6 one can see the difference in coverage values measurements performed by different measuring systems. Δd presents difference between coverage values measured by IC Plate and calculated by ImageJ and Stream motion:

- Δd = coverage value (ImageJ) - coverage value (IC Plate);
- Δd = coverage value (ImageJ) - coverage value (Stream motion);
- Δd = coverage value (IC Plate) - coverage value (Stream motion).

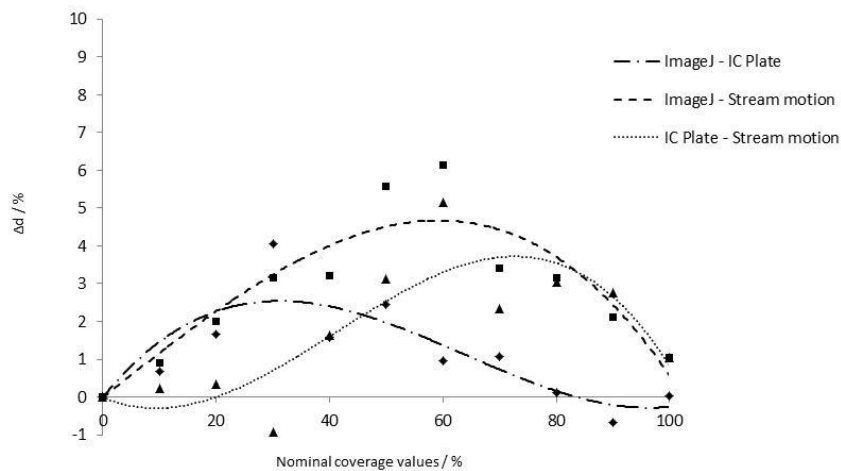


Figure 6. Comparison of coverage values calculated by ImageJ, IC Plate and Stream motion

One can see that Δd value is positive in almost whole coverage area, which implies the accuracy of measurements. In coverage area under 50%, because of automatic median adjustment, ImageJ detects higher coverage values than IC Plate and Stream motion. ImageJ calculates higher values in general, but at higher coverage values (> 50%) analyzes the image as a negative image. This means that further correction was made on the nonprinting areas, resulting as decrease of calculated coverage values and approaching the values measured by IC Plate. On the other hand, Stream motion calculates lower values than IC Plate in coverage area from 35% - 100% because of the different algorithm and chosen median value than one used by IC Plate. Median value in Stream motion was manually set, and was increased in higher coverage area in order to remove noise from image.

Comparing alternative measuring systems - ImageJ and Stream motion – one can conclude that ImageJ calculates higher coverage values in general. Differences in calculated values are maximal in midtone area, indicating that median value is set differently.

5. CONCLUSION

In this paper the differences of results obtained by three measuring systems for determining surface coverage value of the offset CtP printing plates were presented. The aim of this research was the introduction of image analysis as an alternative method for the characterization of tone reproduction on printing plates.

Results showed that different measuring systems for image analysis (IC Plate, ImageJ and Stream motion) obtain a different result in coverage values calculation. IC Plate is automated device for capturing the printing plate's area, storing the information and automatically calculating coverage value, while ImageJ and Stream motion are programs supported by software which analyzes imported images that need to be captured by the microscope.

Based on the results and experience, one can say that ImageJ and Stream motion are more complex method for coverage calculation, but they enable greater control of the imported images by means of manual adjustment. In addition, comparing ImageJ and Stream motion, one can notice deviation from values measured by IC Plate, up to 6% for Stream motion. This fact indicates that manual control of median value must be carefully set in order to gain as accurate results as possible. Furthermore, ImageJ, as free software, proved to provide optimal results with automatic setting of median value.

According to the results presented in this paper, image analysis software with portable camera could be used as a powerful and an economical tool for quality control of the printing plates, furthermore imprints, recycled papers and other similar products (materials) used in graphic arts reproduction.

6. LITERATURE

- [1] Adams, R.M., Romano, F.: "Computer to Plate: Automating the Printing Industry", Graphic Arts Technical Foundation, 1996, USA.
- [2] Born, E.: "Handbuch der Rasterphotographie", Verlag Ambripress Basel, (1983), 13-19.
- [3] Diamond, A. S.: "Handbook of Imaging Materials", Marcel Dekker, Inc. 1991, NY, Basel, Hong Kong, 61-157.
- [4] Foley, J. D., van Dam, A., Feiner, S. K., Hughes, J. F.: "Computer Graphics – Principles and Practice", 2nd edition, Addison – Wesley Publishing Company, 1992.
- [5] Gemeinhardt, J.: "Belichter und Plattentechnologie", Fachhefte Grafische Industrie Bulletin Technique 4, 2001, 14-17.
- [6] Goodman, R., Nüssel B.: "The Technology Generations of Digital Thermal Printing Plates", TAGA Proceedings, 1999, Rochester (NY), 264-279.
- [7] Ihme, R., "Lerhbuch der Reproduktionstechnik", VEB Fachbuchverlag, 1982, Leipzig, 30-39.
- [8] Mahović, S., Agić, D., Gojo, M.: "Mechanical and Optical Differences in Long Run Printing in Conventional and CtP Offset Systems", Proceedings of the 30th International Iarigai Research Conference, 2003, Croatia, 219-227.
- [9] ISO 12218:1997 Graphic technology - Process control – Offset platemaking
- [10] ISO 12647-2:2004 Graphic technology - Process control for the production of halftone colour separations, proof and production prints - Part 2: Offset lithographic processes
- [11] Seydel, M.: "Computer to Plate: Digital Workflow and Integration into Quality Offset Printing", TAGA Proceedings, 1996, Rochester (NY), 634-348.
- [12] Tomašegović, T., Cigula, T., Mahović Poljaček S., Gojo, M.: "Comparison of different measuring systems for printing plate's coverage values evaluation", Printing future day's proceedings 2011, Reinhard R. Baumann (ur.), 2011, Chemnitz: VWB - Verlag für Wissenschaft und Bildung 39-44.

INFLUENCE OF UV EXPOSURE ON THE SURFACE AND MECHANICAL PROPERTIES OF FLEXOGRAPHIC PRINTING PLATE

Sanja Mahović Poljaček, Tamara Tomašegović, Miroslav Gojo
University of Zagreb, Faculty of Graphic Arts

Corresponding author: Sanja Mahović Poljaček
e-mail: sanja.mahovic@grf.hr

1. ABSTRACT

Flexographic printing plates are widely used in packaging printing and are therefore a subject of number of studies. Since the properties of the flexographic printing plate significantly influence properties of the final product, the impact of different plate processing conditions were investigated in this paper.

Samples of flexographic printing plate used in this research were made from liquid photopolymer, and the influence of main exposure (UV radiation) on mechanical and physical-chemical properties was studied. Contact angle, surface energy and hardness changes were measured. Information about changes that occur on the surface and in the volume of a flexographic printing plate as a result of different processing conditions was provided. Results obtained in this paper are relevant for the flexographic reproduction process for two reasons: they point to the absorption of the printing ink and they define possible deformations that occur due to the pressure in printing process.

Key words: flexography, photopolymer, UV radiation, hardness, contact angle, surface energy

2. INTRODUCTION

Flexographic printing plates are characterised by a geometrical difference between printing and nonprinting areas and a flexible material which is elastically deformed for each imprint. The printing plate's printing areas adsorb printing ink and transfer the ink to the printing substrate under the pressure. Reproduction of graphic products printed in flexography requires a complex and detailed approach, especially from the printing plate production aspect. Flexographic printing plates are mainly made from photosensitive monomers, functionalized polymers and additives, such as photo initiators and plasticizers. They are compressible, which enables printing on different types of printing substrates - paperbacks, labels, flexible packaging paper, corrugated board and cartons (Page Crouch J., 1998., Lanska David J., 2007.).

In the last decade a great improvement has been made in the computer-controlled printing plate making process. Application of new types of materials increased the quality of the printing plates and made the plate making procedure ecologically friendlier.

Quality of flexographic printing depends on several parameters, such as ability of printing plate to adsorb printing ink from the anilox roller and ability of printing substrate to assimilate printing ink from the printing plate. Hardness of printing plate and pressure in the printing process are the most influenced parameters, too. Therefore, in order to monitor changes in flexographic printing plate's quality, the aim of this paper was to investigate changes in hardness and surface energy of flexographic printing plates produced under different main exposure conditions.

3. MECHANICAL AND PHYSICAL-CHEMICAL PROPERTIES OF FLEXOGRAPHIC PRINTING PLATE

Mechanical and physical-chemical properties of flexographic printing plate are influenced by the type of printing plate material (photopolymer), photopolymerization process and duration of exposure, which can result in particular printing plate hardness and polar and dispersive components of surface energy (Mahović Poljaček S. et al., 2012., Brajnović O., 2011.).

When exposed to UV radiation, photopolymerization occurs and exposed parts of the plate become insoluble in defined processing solution. However, after the last step of flexographic printing plate making process, in the plate can still remain unpolymerized monomers. This can result with reduced hardness of the plate and thus larger compression and deformations in the printing process.

Compressibility of the photopolymer printing plate can be characterised as plate's advantage and weakness. It enables printing on ragged materials. On the other side, the images transferred to the printing substrate can be deformed.

Duration of exposure also affects surface energy of photopolymer. With prolonged exposure, UV radiation causes polymerization of residual monomers and increases degree of polymerization (DP_n) (*composite.about.com*):

$$DP_n = \frac{M_n}{M_0} \quad (1)$$

M_n – Total molecular weight of the polymer;
 M_0 – Molecular weight of the monomer unit.

By increasing the duration of exposure, molecular weight of the photopolymer increases. The surface tension of polymers tends to increase with increasing molecular weight. Therefore, surface energy value also ascends. Polar and dispersive components of the surface energy change as a result of physical-chemical changes that occur on the photopolymer surface under the influence of UV radiation. These changes can affect the adsorption of the printing ink on the printing plate in the graphic reproduction process.

4. EXPERIMENTAL

In this paper, five samples of full-tone liquid photopolymer printing plate with variations in main exposure were prepared. Liquid photopolymer TRODAT i40 was used. Back exposure time was set at 32 seconds, post-exposure at 900 seconds, and main exposure was varied (126, 153, 180, 207 and 234 seconds). The duration of exposures was defined according to the manufacturer's recommendations.

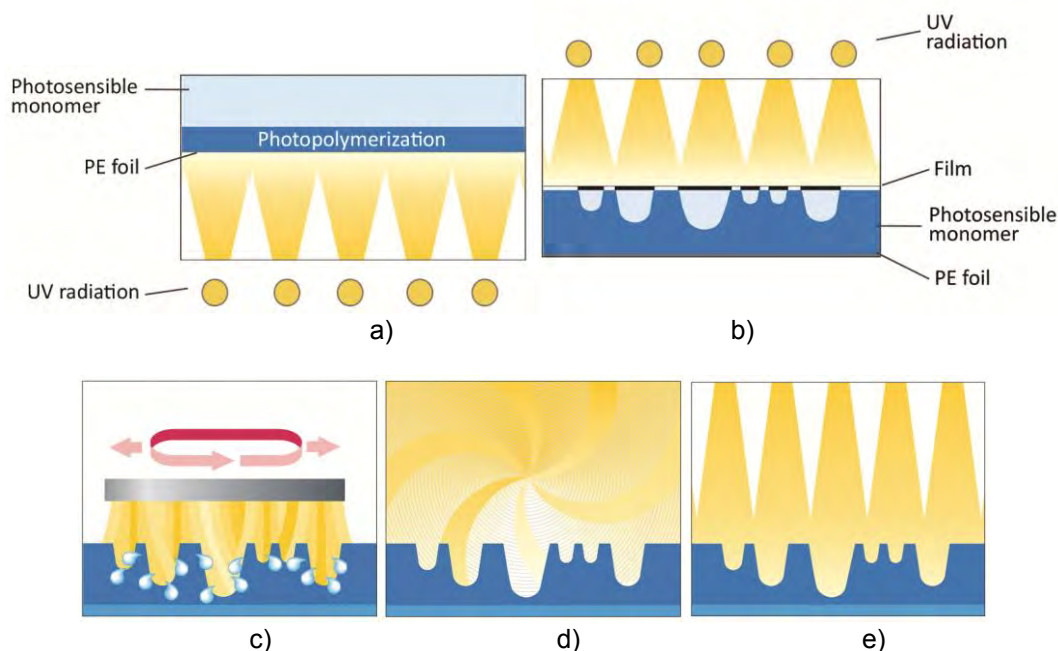


Figure 1: Production of liquid photopolymer flexographic printing plate

On Figure 1(a) – e)) one can see the processes which should be proceeded with the liquid photopolymer:

- a) back exposure - creation of basis layer;
- b) main exposure - definition of printing and nonprinting areas;
- c) chemical and mechanical developing;
- d) drying;
- e) post-exposure - finishing the photopolymerization process and improving printing plate's mechanical properties.

Samples of printing plates were made in AZ 1500 N3 device for production of liquid photopolymer flexographic printing plates. The device consist of the unit for UV exposure, developing unit and drying unit.

After production of printing plate samples, two kinds of measurement were conducted – hardness and contact angle/surface energy measurement. Hardness of printing plate samples was measured by means of Zwick durometer, using Shore A method (www.ides.com). Seven measurements were conducted on each sample and mean values were calculated.



Figure 2: Data Physics - OCA30

Contact angle and surface energy were measured by means of gonimeter Data Physics OCA 30 (Figure 2) (*DataPhysics Instruments GmbH, 2006.*). Three probe liquids were used for measurements: water, glycerol and diiodomethane.

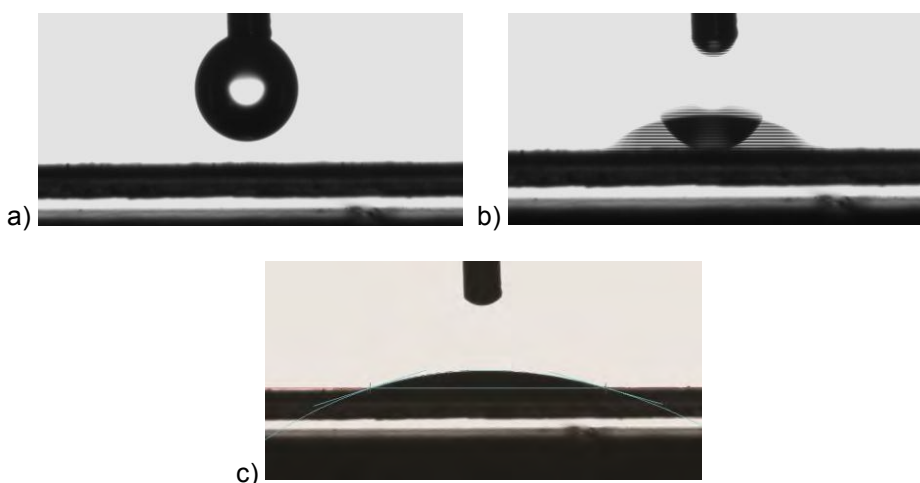


Figure 3 (a) - c)): Contact angle and surface energy measurement using Sessile drop method

Contact angle was measured using Sessile drop method, ten times on each sample. When using the sessile drop method, one applies liquid with a known surface energy on the substrate. Contact angle and surface energy of the probe liquid are the parameters which are then used to calculate the surface energy of the solid sample. The liquid used for such experiments is referred to as the probe liquid, and the usage of several different probe liquids is required. Mean value of contact angle for each sample was calculated. Surface energy was measured using OWRK (*Owens-Wendt-Rabel and Kaible*) method, applicable for polymer, aluminium and coatings characterization (adsabs.harvard.edu).

5. RESULTS AND DISCUSSION

In Figure 4 one can see the relation between the hardness of flexographic printing plate and the main exposure. With prolonged main exposure, printing plate hardness increases. Overall, 90% increase of main exposure time results with 10% increase of printing plate's hardness. That relation is probably a result of higher degree of monomer space-bounding due to longer exposure which more compact and solid material structure (web.mit.edu).

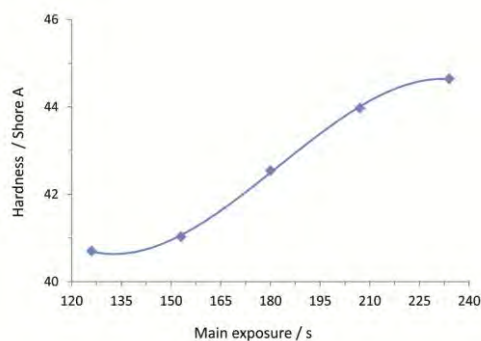


Figure 4: Dependence of printing plate's hardness on main exposure

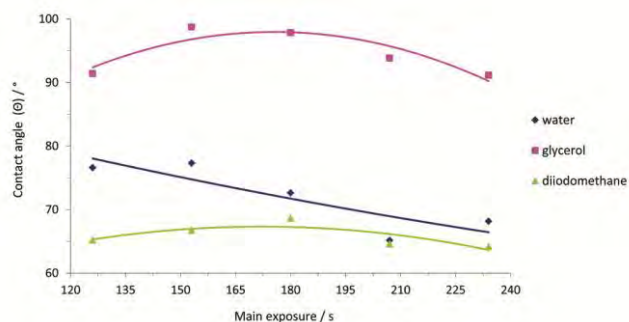


Figure 5: Dependence of contact angle on main exposure

Water (polar liquid), glycerol (liquid with equable proportion of liquid and dispersive phase) and diiodomethane (primarily dispersive liquid) were used as a probe liquids with known surface energy values.

Dependence of contact angle on main exposure for each probe liquid can be seen in Figure 5. Contact angle values of glycerol are highest and vary from 91° to 98°. For water, contact angle values vary from 66° to 76°, and contact angle values of diiodomethane are lowest, with variations from 65° to 77°. One can also see that all contact angle values show decreasing tendency with prolonged main exposure. Obtain results indicate that changes occur in the surface properties of phopopolymer, which are the result of increased degree of polymeriaztion caused by main exposure.

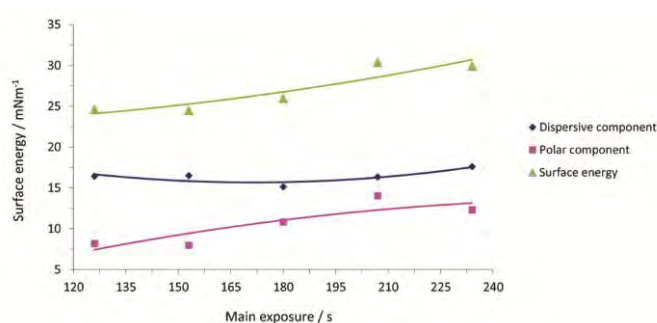


Figure 6: Dependence of printing plate's surface energy on main exposure

After contact angle measurements, surface energy and its dispersive and polar component were calculated by means of SCA 20 program support. Results of surface energy calculations can be seen in Figure 6.

Based on obtained surface energy results, one can conclude that the overall increase of surface energy is caused by increase of the polar component, while dispersive component does not change significantly. This type of surface energy changes in dependence on main exposure time could be caused by migration of oxygen in the surface layer of photopolymer. Namely, with prolonged exposure time, greater amount of photoinitiator activates and reduces the oxygen amount in the photopolymer volume (Andzejewska, E., 2001.). That oxygen diffuses in the surface of the photopolymer, influencing the polar component of surface energy. Enhancement of polar component of surface energy could influence the adsorption of printing ink on the flexographic printing plate (Dedijer S. et al., 2011.).

In Figure 7 one can see the diagram of correlation between flexographic printing plate's hardness and surface energy. Correlation number is 0,952647. Same trend of hardness and surface energy values on the printing plate indicates that photopolymerization process has uniform impact on both properties.

Prolonged duration of main exposure results with increase in polymerization degree and molecular weight, which also directly influences surface tension and energy (Andzejewska, E., 2001.).

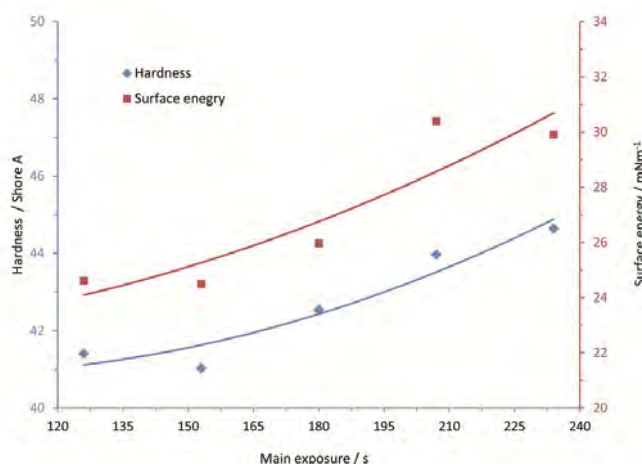


Figure 7: Correlation between printing plate's hardness and surface energy

6. CONCLUSION

Demands of the modern packaging design and technology are most often to distinguish the product from the other similar ones. Therefore, one of the requirements in packaging printing is optimal quality of the printed product.

This study was performed in order to determine the influence of the main exposure on the surface energy and hardness of the photopolymer flexographic printing plate, since these two properties can significantly influence the quality of the imprint.

Results of measurements have shown high correlation between changes in hardness and surface energy of the printing plate with increase of main exposure duration. Results indicate that prolonged UV radiation leads to higher degree of polymerization, which causes increase of hardness. Furthermore, UV radiation activates photo initiators, which cause the migration of the oxygen from the volume of the sample to the surface, therefore increasing the polar component of the surface energy. This can result with changes in printing plate's properties of ink adsorption.

In addition, high correlation number between measurements indicates that possible changes which happened with the printing plate's surface energy can be defined through hardness measurement, too. After that, if needed, further measurements can be performed.

Correlation of the hardness and surface energy on several types of flexographic printing plates will be studied in the future. Hardness measurement could appear to be quick alternative method for obtaining basic information about changes of printing plate's physical-chemical surface properties.

7. LITERATURE

- [1] Lanska David J.: „Common- Sense Flexography, PIA/GATF Press Pittsburgh, 2007.
- [2] Page Crouch J.: „Flexography Primer”, 2nd edition, PIA/GATF Press, Pittsburgh, 1998.
- [3] Andzejewska, E.: „Photopolymerization kinetics of multifunctional monomers“, Progress in Polymer Science, 26 (4), 2001., 605-665.
- [4] Dedijer S., Apro M., Pavlović Ž., Cigula T., Obrenović B., „Influence of ink solvent concentration on wetting of flexo printing plate and PE foil“, Proceedings of the 2nd International Joint Conference on Environmental and Light Industry Technologies (ed. Á. Borbély), Budapest, 2011., 143-150.
- [5] Mahović Poljaček S., Cigula T., Tomašegović T., „Meeting the quality requirements in the flexographic plate making process“, Proceedings of the 44th conference of the International Circle of Educational Institutes for Graphic Arts Technology and Management, Budapest, 2012. , 8.
- [6] Brajnović O.: „Prilagodba izrade fotopolimerne tiskovne forme novim kvalitativnim zahtjevima“, Magistarski rad, Grafički fakultet Zagreb, 2011.
- [7] <http://adsabs.harvard.edu/full/1953AuJPh...6...86Z> (last request: 2012-19-09).
- [8] <http://composite.about.com/library/glossary/d/bldef-d1507.htm> (last request: 2012-28-09).
- [9] <http://web.mit.edu/nnf/education/wettability/summerreading-2005short.pdf> (last request: 2012-15-09).
- [10] http://www.ides.com/property_descriptions/ISO868.asp (last request: 2012-06-09).
- [11] DataPhysics Instruments GmbH, Operating manual OCA, 2006.

THE STATISTICAL ANALYSIS OF PROCESSING CONDITIONS' INFLUENCE ON THE SURFACE ROUGHNESS OF FLEXO PRINTING PLATE

Neda Milić, Sandra Dedijer, Magdolna Pal, Živko Pavlović
Faculty of Technical Sciences, Graphic Engineering and Design, Novi Sad

Corresponding author: Neda Milić
e-mail: milicn@uns.ac.rs

1. ABSTRACT

The ink transfer from the flexo printing plate to the printing substrate, which determines the quality of imprints, is highly influenced by the surface topography of printing plate. The aim of study was to investigate the correlation between roughness characteristics of solid printing areas and different plate processing conditions. For this purpose, eight samples of CtP flexo plate with thermal developing were made varying two factors: the main exposure time (8, 10, 12 and 14 minutes) and the number of rotations of developing drum (8 and 10 rotations). For comparing roughness parameters from all eight plates, a two-factorial ANOVA was applied. Since obtained results showed the significant main effect of exposure time, but also the interactive (join) effect of two factors, for the further analysis of the separate influences one-factorial ANOVA and T tests were used. Discovered significant influence on the surface roughness of the printing plate implies the importance of specifying and monitoring values of investigated processing conditions.

Key words: flexo printing plate, surface roughness, statistical analysis, processing conditions

2. INTRODUCTION

In flexographic industry, flexible printing plate and usage of various printing inks provide production of high quality imprints on a variety of substrates (coated and uncoated papers and cardboards, metallised and paper foils and polymer films) with high volume runs. Flexographic printing plates are relief plates with printing (image) elements raised above non printing areas. The main prerequisite for imprints with fulfilling quality demands is well-defined and controlled ink transfer from ink tank to the printing substrate. One of the parameters which directly influence the ink transfer is the surface topography of the printing plate. In the case of flexo printing plates, the analysis of surface topography will give relevant information to make possible prediction of behaviour of the flexo plate surface during printing process (Barros, 2009).

2.1. Thermal processing

Flexo plates with thermal processing are prepared using heat. The uncured photopolymer (the areas of the photopolymer which were not exposed to UV light) will melt or substantially soften while the cured photopolymer will remain solid and intact at the chosen melting temperature (Choi and O'Brate, 2010). There should be a substantial difference in the melt temperature between the cured and uncured polymer since that allows the creation of an image in the heated photopolymer by selectively removing the uncured parts. This way thermal processing eliminates development solvents and the lengthy plate drying times needed in chemical processing to remove the solvent (Choi and O'Brate, 2010). The speed and efficiency of thermal processing allow flexo plate production for printing jobs where quick turnaround times and high productivity are important (Choi and O'Brate, 2010).

In a typical thermal development process, the uncured photopolymer layer is melted or substantially softened by passing the printing plate over a heated drum. The exact temperature of drum depends on the properties of the particular photopolymer being used and it is set between the melt temperature of the uncured photopolymer on the low end and the melt temperature of the cured photopolymer on the upper end (Choi and O'Brate, 2010). While rotating with the drum in the heated condition, the plate is contacted with an absorbent sheet material that will absorb or otherwise remove the softened or melted uncured photopolymer.

This removal process called "blotting" is typically accomplished using a screen mesh or an absorbent woven or non-woven fabric (polymer or paper – based). After cooling, the resulting flexo plate can be mounted on a printing plate cylinder.

2.2. Roughness analysis

In order to quantify the topography of material surfaces, profilometric methods, like MSP-mechanical stylus contact profilometry or non – contact laser profilometry can be used (Risović, 2009). In the case of contact profilometry, the measuring unit is equipped with sharp diamond tip mounted on a cantilever which moves along a line on the surface of the material. The surface irregularities (peaks and valleys) cause the displacement of the tip in direction opposite to the moving direction. These displacements are recorded and the corresponding peaks and valleys are directly measured. For a given specimen, several test lines need to be recorded to get precise determination of surface texture (Chappard et al., 2003, Dedijer and Novaković, 2010). The surface roughness parameters are influenced by the instrument type, instrument settings, the post processing of measured data and the microstructure of the measured surface (Ramón-Torregrosa, 2008).

2.3. Roughness parameters

The characterisation of surface topography of printing plate is made by measuring roughness parameters. There are many roughness parameters which can be used for the surface characterization, but most commonly used are amplitude ISO roughness parameters (ISO 4287:1997 and ISO 12218:1997): R_a (average surface roughness), R_q (R_{ms} , root-mean-square deviation), R_{zDIN} (mean value of the single roughness depths Z_i), R_p (leveling depth) and R_v (Mahović, 2007; Dedijer and Novaković, 2010).

R_a is the average value of the absolute profile's data inside an evaluation length, divided by the total length. In other words, it represents the arithmetic mean of the absolute values of profile deviation of mean within sampling length (Dedijer and Novaković, 2010, Pavlović, 2010):

$$R_a = \frac{1}{l} \int_0^l |y(x)| dx \quad (1)$$

R_q (R_{ms}) is the square root of the arithmetic mean of the squares of profile deviation from mean within sampling length (Mahović, 2007, TR 200 Manual, 2010, Dedijer and Novaković, 2010):

$$R_q = \sqrt{\frac{1}{l} \int_0^l y^2(x) dx} \quad (2)$$

R_{zDIN} is mean value of the single roughness depths Z_i or, in other words, average maximum height of the profile (average of all vertical distances between the highest and the lowest point for a sampling length) (Mahović, 2007, TR 200 Manual, 2010, Dedijer and Novaković, 2010):

$$R_{zDIN} = \frac{1}{n} (Z_1 + Z_2 + \dots + Z_n) \quad (3)$$

R_p is the height from the highest profile peak line to mean line within the sampling length (Mahović, 2007, TR 200 Manual, 2010).

R_v is the height from the lowest profile peak line to mean line within the sampling length (Mahović, 2007, TR 200 Manual, 2010).

When it comes to thermally processed flexo plates, the most significant factors influencing surface roughness during thermal developing include (1) developing drum temperature; (2) main exposure time; (3) blotter process; and (4) the type of photoresin used. Thermally developed printing plates may have problem with high surface roughness due to the blotting materials used to remove uncured photopolymer. With excessively course blotting material and inadequate number of rotations of developing drum, patterns of the blotting material can be embedded in the cured photopolymer relief, especially on the solid areas. Furthermore, it was found that increasing of the developing drum temperature and main exposure time decreases surface roughness (Choi and O'Brate, 2010). That means that inadequate exposure time will lead to too low or too high surface roughness of the printing plate.

While moderate surface roughness is desirable since an increased surface roughness leads to high ink transfer and, thereby, to high optical density, the excessive roughness of the solid areas cause low solid ink density on the printed solid areas due to failure to make contact between the printing plate surface and a given substrate (Choi and O'Brate, 2010).

In this study, two production parameters were varied (4 different main exposure times x 2 different rotation numbers of the developing drum) in order to establish the correlation between named ISO surface roughness parameters and production conditions. This roughness measurement data is very important since it influences the further printing process. Defining the significance and nature of the correlation between surface roughness of printing plates and production condition will provide better understanding of plate making process and guidelines for adequate values for those production parameters.

3. EXPERIMENTAL PART

3.1. Materials and methods

For the purpose of this study, a CtP 1.14 mm thick flexographic printing plates (DuPont™ Cyrel® DFH 045) with thermal processing were used, which means that plates have the LAM layer intended to develop thermally, without using any solvents and without drying process. Processing phases for thermal plates are back exposure, laser ablation, main exposure, thermal developing, post exposure and light finishing. Thermal developing phase is characterized by the number of rotations of plate cylinder in developing device (developing drum). The laser ablation (imaging) of printing plates (1100 x 900 mm format) was done by CDI Spark 4835 Esco expozé device (with external drum and a single laser beam) using AM screening (resolution 5080 ppi) and screen ruling of 50 l/cm. The UV exposures (back, main, post and light finishing) were made with DuPont™ Cyrel® 1000 ECLF device, while plate developing was done with device for thermal developing DuPont™ Cyrel® FAST 1000 TD. According to research goal, the set of eight printing plates was made with following characteristics:

1. Back exposure time: 50 seconds;
2. Main exposure time: 8, 10, 12, 14 minutes;
3. Post exposure and light finishing: UVA – 7 minutes, UVC -7 minutes;
4. Developing conditions : 8 and 10 rotations of developing drum (for each variation of main exposure time – 8, 10, 12 and 14 minutes);

Produced plates were used for investigating influence of different main exposure time and different developing conditions on surface roughness. Profilometric roughness parameters - R_a , R_p , R_v , R_q and R_z were measured using the Portable Surface Roughness Tester TR 200. The unit is compatible with ISO 4287, DIN 4768, ANSI B 46.1 and JIS B601 standards. The measurement's parameters were: sampling length: 0.80 mm, traversing speed: $V_t = 0.135 \text{ mm s}^{-1}$, RC filtering method, measuring range: $\pm 20 \text{ } \mu\text{m}$ and resolution: $0.01 \text{ } \mu\text{m}$ compatibility with ISO 4287 standard.

Measurements of the roughness parameters of the investigated printing plates were made on the solid printing areas on 18 different spots in both printing and cross printing directions in order to avoid possible variations due to measuring direction.

4. RESULTS

Tables 1 and 2 show mean values (of 36 measurements – 18 in printing direction and 18 in cross printing direction) and corresponding standard deviations of all five roughness parameters, while the graphs of mean values for each roughness parameter are presented in Figure 1.

Table 1: Mean arithmetic value and standard deviation of the roughness parameters in the case of different main exposure time and developing process with 8 drum rotations

Main exposure time	Roughness parameters	Ra (μm)	Rq (μm)	Rz (μm)	Rp (μm)	Rv (μm)
8 min	Mean value (Standard deviation)	0.41(0.06)	0.51 (0.08)	2.21(0.40)	1.11(0.28)	1.11(0.17)
10 min		0.49(0.05)	0.61(0.06)	2.64 (0.29)	1.33 (0.22)	1.31 (0.17)
12 min		0.48(0.05)	0.59 (0.06)	2.48 (0.32)	1.25 (0.20)	1.23 (0.20)
14 min		0.48(0.07)	0.58(0.08)	2.42(0.37)	1.19(0.24)	1.23(0.17)

Table 2: Mean arithmetic value and standard deviation of the roughness parameters in the case of different main exposure time and developing process with 10 drum rotations

Main exp. time	Roughness parameters	Ra (μm)	Rq (μm)	Rz (μm)	Rp (μm)	Rv (μm)
8 min	Mean value (Standard deviation)	0.48(0.04)	0.59(0.06)	2.51(0.32)	1.31(0.40)	1.26(0.16)
10 min		0.48(0.06)	0.60(0.08)	2.59(0.45)	1.37(0.32)	1.22(0.20)
12 min		0.42(0.06)	0.51(0.08)	2.16(0.32)	1.07(0.19)	1.08(0.17)
14 min		0.44(0.07)	0.54(0.08)	2.30(0.39)	1.17(0.23)	1.12(0.20)

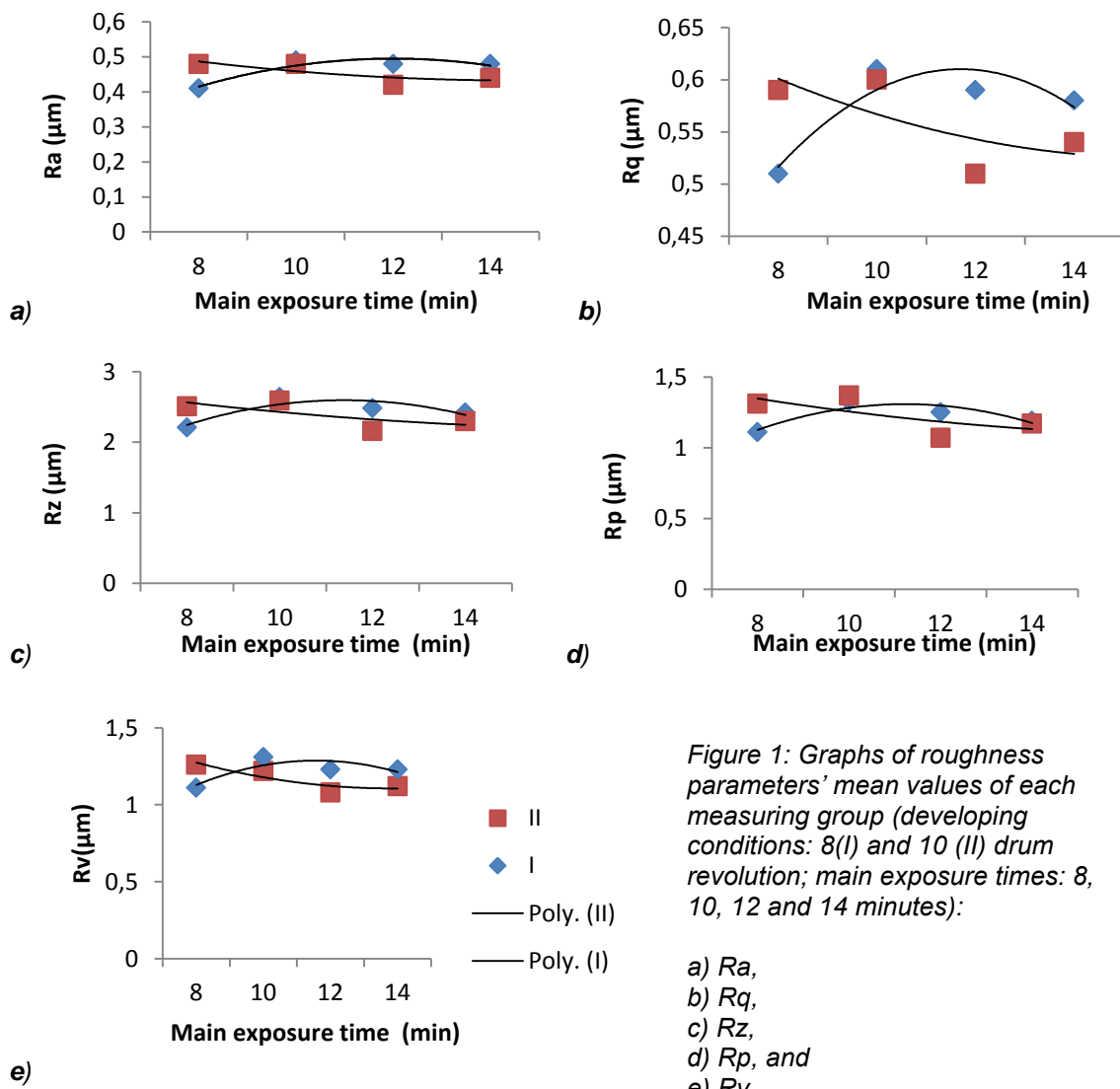


Figure 1: Graphs of roughness parameters' mean values of each measuring group (developing conditions: 8(I) and 10 (II) drum revolution; main exposure times: 8, 10, 12 and 14 minutes):

a) Ra,
b) Rq,
c) Rz,
d) Rp, and
e) Rv.

While the use of a graph does not tell whether the impact of different main exposure period and drum revolution numbers on roughness parameter value is statistically significant, it can give information about trend of parameters' changes. According to results showed in Figure 1 it is clear that all five observed roughness parameters have the same behaviour and, for both developing conditions the trends of roughness changes due to different exposure time have the polynomial character, but with the opposite direction. The roughness parameters have a slight value increase in the case of developing with 8 rotations, while, in the case of 10 rotations, values are decreasing with longer exposure periods.

In order to determine the statistical significance of the differences in the roughness parameters, obtained from the plates processed with different main exposure time and different number of drum rotations during thermal developing, the statistical analysis were done. All statistical tests were conducted using the software SPSS (Statistical Package for Social Science) with a 0.05 significance level (the significances bellow 0.05 are marked in tables with *). Beside statistical significance, the effect size (the practical significance) is also calculated for each test using partial eta squared, where Cohen classifies 0.01 as a small effect (in tables marked with *), 0.06 as a medium effect (in tables marked with **), and 0.14 as a large effect (in tables marked with ***) (Pallant, 2007).

For investigating both the individual „main“ effects and the joint „interactive“ effect for two independent factors (main exposure time and number of drum revolutions) on the surface topography of the solid areas a two-factorial ANOVA is used. Table 3 gives an overview of two-factorial ANOVA results for all roughness parameters.

Table 3: Results of statistical analysis (two- factorial ANOVA) for all roughness parameters

<i>Roughness parameter</i>		<i>F value</i>	<i>Statistical significance p</i>	<i>Partial Eta Squared</i>
<i>Ra</i>	<i>Exposure (time) effect</i>	7.960	0.000*	0.08**
	<i>Developing (rotation number) effect</i>	2.416	0.121	0.01
	<i>Exposure x Developing (interactive) effect</i>	16.805	0.000*	0.15***
<i>Rq</i>	<i>Exposure (time) effect</i>	8.949	0.000*	0.09**
	<i>Developing (rotation number) effect</i>	2.390	0.123	0.00
	<i>Exposure x Developing (interactive) effect</i>	14.602	0.000*	0.14***
<i>Rz</i>	<i>Exposure (time) effect</i>	10.141	0.000*	0.10**
	<i>Developing (rotation number) effect</i>	1.279	0.259	0.00
	<i>Exposure x Developing (interactive) effect</i>	9.208	0.000*	0.09**
<i>Rp</i>	<i>Exposure (time) effect</i>	7.539	0.000*	0.08**
	<i>Developing (rotation number) effect</i>	0.132	0.716	0.00
	<i>Exposure x Developing (interactive) effect</i>	5.975	0.001*	0.06**
<i>Rv</i>	<i>Exposure (time) effect</i>	4.885	0.003*	0.06**
	<i>Developing (rotation number) effect</i>	4.793	0.029*	0.02*
	<i>Exposure x Developing (interactive) effect</i>	10.379	0.000*	0.10**

The obtained results show the significant main effect of exposure time, but also the significant interactive effect of two factors in the case of all five roughness parameters with effect sizes from medium (for Rz, Rp and Rv) to large (for Ra and Rq) (see Table 3).

Because of the significant interactive effect, the results could not be simply and easily interpreted, so the further statistical analysis of separate influences was done. The one-factorial ANOVA tests followed by post hoc Tukey tests were applied in order to more precisely define the exposure time influence and the results with all corresponding variables relevant to test are presented in Tables 4-7.

For the printing plates developed with 8 drum rotations, the one-factorial ANOVA results show significant difference between mean values of all five roughness parameters in dependence of different main exposure time with large effect sizes (see Table 4). Since with significant ANOVA result it is known that groups differ, but it is not known where these differences occur, the post hoc Tuckey HSD test was used for comparing each pair of groups (see Table 5).

Table 4: Results of statistical analysis (one-way ANOVA) for all roughness parameters in the case of developing with 8 drum revolutions (main exposure times are 8,10,12 and 14 minutes)

Roughness parameter		Sum of squares	F value	Statistical significance	Partial Eta Squared
Ra (I)	Between groups	0.148	15.092	0.000*	0.24***
	Within groups	0.459			
	Total	0.607			
Rq (I)	Between groups	0.195	12.539	0.000*	0.21***
	Within groups	0.726			
	Total	0.921			
Rz (I)	Between groups	3.345	9.138	0.000*	0.16***
	Within groups	17.082			
	Total	20.428			
Rp (I)	Between groups	0.968	5.733	0.001*	0.11**
	Within groups	7.878			
	Total	8.846			
Rv(I)	Between groups	0.771	8.005	0.000*	0.15***
	Within groups	4.495			
	Total	5.266			

Table 5: Results of statistical analysis (post-hoc Tukey HSD test) for all roughness parameters in the case of developing with 8 drum revolutions (main exposure times are 8, 10, 12 and 14 minutes)

Roughness parameter	Time (min) I	Time (min) J	Mean difference (I-J)	Statistical significance	95% Confidence interval	
					Lower bound	Upper bound
Ra (I)	8	10	-0.082611*	0.000	-0.12	-0.05
		12	-0.069278*	0.000	-0.10	-0.03
		14	-0.066444*	0.000	-0.10	-0.03
	10	12	0.013333	0.756	-0.02	0.05
		14	0.016167	0.629	-0.02	0.05
	12	14	0.002833	0.997	-0.03	0.04
Rq (I)	8	10	-0.097417*	0.000	-0.14	-0.05
		12	-0.077111*	0.000	-0.12	-0.03
		14	-0.071750*	0.000	-0.12	-0.03
	10	12	0.020306	0.630	-0.02	0.06
		14	0.025667	0.433	-0.02	0.07
	12	14	0.005361	0.989	-0.04	0.05
Rz (I)	8	10	-0.425361*	0.000	-0.64	-0.21
		12	-0.267111*	0.008	-0.48	-0.05
		14	-0.205528	0.065	-0.42	0.01
	10	12	0.158250	0.224	-0.06	0.37
		14	0.219833*	0.042	0.01	0.43
	12	14	0.061583	0.877	-0.15	0.28
Rp (I)	8	10	-0.224194*	0.001	-0.37	-0.08
		12	-0.141722	0.059	-0.29	0.00
		14	-0.082500	0.455	-0.23	0.06
	10	12	0.082472	0.455	-0.06	0.23
		14	0.141694	0.059	0.00	0.29
	12	14	0.059222	0.715	-0.09	0.20
Rv (I)	8	10	-0.204639*	0.000	-0.31	-0.09
		12	-0.125278*	0.018	-0.24	-0.02
		14	-0.123028*	0.021	-0.23	-0.01
	10	12	0.079361	0.242	-0.03	0.19
		14	0.081611	0.219	-0.03	0.19
	12	14	0.002250	1.000	-0.11	0.11

The post hoc test (Tuckey HSD test) results show where are differences between groups (see Table 5). In the case that there is statistical significant result with a 0.05 significance level, the numeric value of corresponding mean difference (I-J) is marked with *.

Post-hoc comparisons using Tukey HSD test indicated that the mean score for 8(I) group was significantly different from other three groups (10(I), 12(I), and 14(I) minutes) in the case of parameters Ra, Rq, and Rv. Mean values of parameters Ra, Rq and Rv of 10(I), 12(I), and 14(I) groups did not differ significantly from each other. In the case of parameter Rz, 8(I) group was significantly different from 10(I) and 12(I) groups and 10(I) group from 14(I) group. All these significances were with large effect size. For parameter Rp, significant difference with medium effect size was found only between 8(I) and 10(I) groups.

Table 6: Results of statistical analysis (one- factorial ANOVA) for all roughness parameters in the case of developing with 10 drum rotations (main exposure time are 8,10,12 and 14 minutes)

Roughness parameter		Sum of squares	F value	Statistical significance	Partial Eta Squared
Ra (II)	Between groups	0.105	9.880	0.000*	0.17***
	Within groups	0.497			
	Total	0.602			
Rq (II)	Between groups	0.189	11.078	0.000*	0.19***
	Within groups	0.796			
	Total	0.984			
Rz (II)	Between groups	4.205	10.148	0.000*	0.18***
	Within groups	19.336			
	Total	23.540			
Rp (II)	Between groups	1.939	7.419	0.000*	0.14***
	Within groups	12.195			
	Total	14.134			
Rv (II)	Between groups	0.712	7.266	0.000*	0.13***
	Within groups	4.576			
	Total	5.288			

For the printing plates developed with 10 drum rotations, the one-factorial ANOVA results also showed significant difference between mean values of all five roughness parameters in dependence of different main exposure time with large effect sizes (see Table 6). The post hoc Tuckey HSD test was used for comparing each pair of groups (see Table 7).

Table 7: Results of statistical analysis (post-hoc Tukey HSD test) for all roughness parameters in the case of developing with 10 drum revolutions (main exposure times are 8,10,12 and 14 minutes)

Roughness parameter	Time (min) I	Time (min) J	Mean difference (I-J)	Statistical significance	95% Confidence interval	
					Lower bound	Upper bound
Ra (II)	8	10	-0.003667	0.994	-0.04	0.03
		12	0.060500*	0.000	0.02	0.10
		14	0.039750*	0.027	0.00	0.08
	10	12	0.064167*	0.000	0.03	0.10
		14	0.043417*	0.013	0.01	0.08
	12	14	0.020750	0.454	-0.02	0.06
Rq (II)	8	10	-0.011861	0.909	-0.06	0.03
		12	0.076750*	0.000	0.03	0.12
		14	0.050333*	0.027	0.00	0.10
	10	12	0.088611*	0.000	0.04	0.13
		14	0.062194*	0.003	0.02	0.11
	12	14	-0.026417	0.448	-0.07	0.02
Rz (II)	8	10	-0.079556	0.800	-0.31	0.15
		12	0.351778*	0.001	0.12	0.58
Rz (II)	8	14	0.214139	0.074	-0.01	0.44
		12	0.431333*	0.000	0.20	0.66
		14	0.293694*	0.006	0.07	0.52
	10	14	-0.137639	0.398	-0.37	0.09
		12				
	12	14				

Table 7 (Continue)						
Rp (II)	8	10	-0.067528	0.766	-0.25	0.11
		12	0.231444 [*]	0.006	0.05	0.41
		14	0.133639	0.224	-0.05	0.31
	10	12	0.298972 [*]	0.000	0.12	0.48
		14	0.201167 [*]	0.023	0.02	0.38
	12	14	-0.097806	0.498	-0.28	0.08
Rv (II)	8	10	0.043361	0.739	-0.07	0.15
		12	0.175972 [*]	0.000	0.07	0.29
		14	0.136139 [*]	0.009	0.03	0.25
	10	12	0.132611 [*]	0.012	0.02	0.24
		14	0.092778	0.135	-0.02	0.20
	12	14	-0.039833	0.786	-0.15	0.07

From Table 7 can be noticed that post-hoc comparisons using Tukey HSD test indicated that the mean value for 8(II) and 10(II) groups were significantly different from 12(II) and 14(II) groups, but not from each other in the case of parameters Ra and Rq. In the case of parameters Rz and Rp, group 8(II) was statistically different from 12(II) group, and 10(II) group from 12(II) and 14(II). All these significances were with large effect size. For parameter Rv, significant difference with medium effect size was found between following pairs: 8(II) and 12(II), 8(II) and 14(II), 10(II) and 12(II) groups.

For defining the developing condition influence t-tests were applied and the test results are presented in Table 8.

Table 8: Results of statistical analysis (T test with independent samples) for all roughness parameters in the case of different developing conditions – 8 and 10 drum rotations (main exposure times are 8, 10, 12 and 14 minutes)

Expo sure time	Roughness parameter	t value	Statistical significance	Mean difference	95% Confidence interval		Partial eta squared.
					Lower bound	Upper bound	
8 min	Ra	-5.495	0.000*	-0.068	-0.093	-0.043	0.30***
	Rq	-4.780	0.000*	-0.077	-0.109	-0.045	0.25***
	Rz	-3.499	0.001*	-0.298	-0.468	-0.128	0.15***
	Rp	-2.244	0.017*	-0.198	-0.360	-0.0363	0.07**
	Rv	-3.995	0.000*	-0.156	-0.233	-0.078	0.18***
10 min	Ra	0.821	0.415	0.011	-0.016	0.037	0.01
	Rq	0.496	0.622	0.009	-0.026	0.043	0.00
	Rz	0.536	0.594	0.048	-0.130	0.226	0.00
	Rp	-0.643	0.522	-0.041	-0.170	0.087	0.01
	Rv	2.107	0.039*	0.092	0.004	0.180	0.06**
12 min	Ra	4.659	0.000*	0.062	0.035	0.088	0.24***
	Rq	4.691	0.000*	0.077	0.044	0.110	0.24***
	Rz	4.245	0.000*	0.321	0.170	0.472	0.20***
	Rp	3.796	0.000*	0.175	0.083	0.267	0.17***
	Rv	3.392	0.001*	0.146	0.060	0.231	0.14***
14 min	Ra	2.401	0.019*	0.038	0.006	0.070	0.08**
	Rq	2.322	0.023*	0.045	0.006	0.084	0.07**
	Rz	1.361	0.178	0.122	-0.057	0.300	0.03
	Rp	0.326	0.745	0.018	-0.093	0.129	0.00
	Rv	2.364	0.021*	0.103	0.016	0.191	0.07**

For plates with main exposure time of 8 minutes, there were statistical differences between mean scores of groups 8(I) and 8(II)), developed with 8 and 10 rotations of developing drum in the case of all five roughness parameters with effect sizes from medium (for Rp) to large (for Ra, Rq, Rz and Rv) (see Table 8). The same result, but with large effect sizes for all parameters, was obtained with main exposure time of 12 minutes. In the case of 14-minute exposure, the number of rotations of developing drum had significant influence with medium size effect on Ra, Rq and Rv parameters, while in the case of 10-minute exposure, the significant difference between 10(I) and 10(II) groups was only found for Rv parameter (see Table 8).

5. DISCUSSION

According to result presented in Tables 3-8, both factors (main exposure time and number of rotations of developing drum) have the influence on surface roughness characteristics. It can be noticed that all five observed roughness parameters have similar behaviour in dependence of varied parameters. In other words, change from one set of processing conditions' values to another is causing the same trend of changes but with different intensity.

From Tables 3-7 also can be deducted that, considering just main exposure time, resulting plates surface roughness after 8 minutes of main exposure are quite different from plates treated with longer main exposure period. With enhancing main exposure time fluctuations in roughness parameters are lower indicating that if changes in main exposure time should be done and are directed toward lower bound, negligible changes in surface roughness cannot be expected.

Results presented in Table 8 show that different rotation number of developing drum caused the smallest difference between corresponding roughness parameters for the exposure time of 10 minutes. For all other exposure periods, the influence of developing condition on surface topography should not be ignored.

6. CONCLUSION

Every change of printing plate's surface roughness has an impact on the ink transfer from the ink tray to the imprint, and consequently on the imprint quality. In the domain of flexographic printing, the key factors which define the adequate plate processing are optimal lasting of all processing phases which will provide acceptable plate quality and high plate production speed at the same time. The only way to achieve repeatable and controlled plate processing production in the flexo systems with same configuration is by conducting experiments in order to define those optimal processing conditions.

This paper relates to a method of tailoring surface roughness of flexographic printing elements upon thermal processing. The present invention relates to a method of tailoring surface roughness of flexographic printing elements upon thermal processing. Obtained results showed the level of significance in changes of surface roughness parameters in dependence of applied different main exposure time and different rotations of developing drum during thermal processing. It was shown that neither main exposure time nor developing conditions have negligible influence on flexo plate surface roughness. Conclusions deducted from the obtained results about influence level of the main exposure time and the rotation number of developing drum and their interaction represent first step in predicting surface roughness of printing plate. With further investigation of these and other plate processing parameters the plate making process can be significantly upgraded.

Acknowledgments

This work was supported by the Serbian Ministry of Science and Technological Development, Grant No.:35027 "The development of software model for improvement of knowledge and production in graphic arts industry".

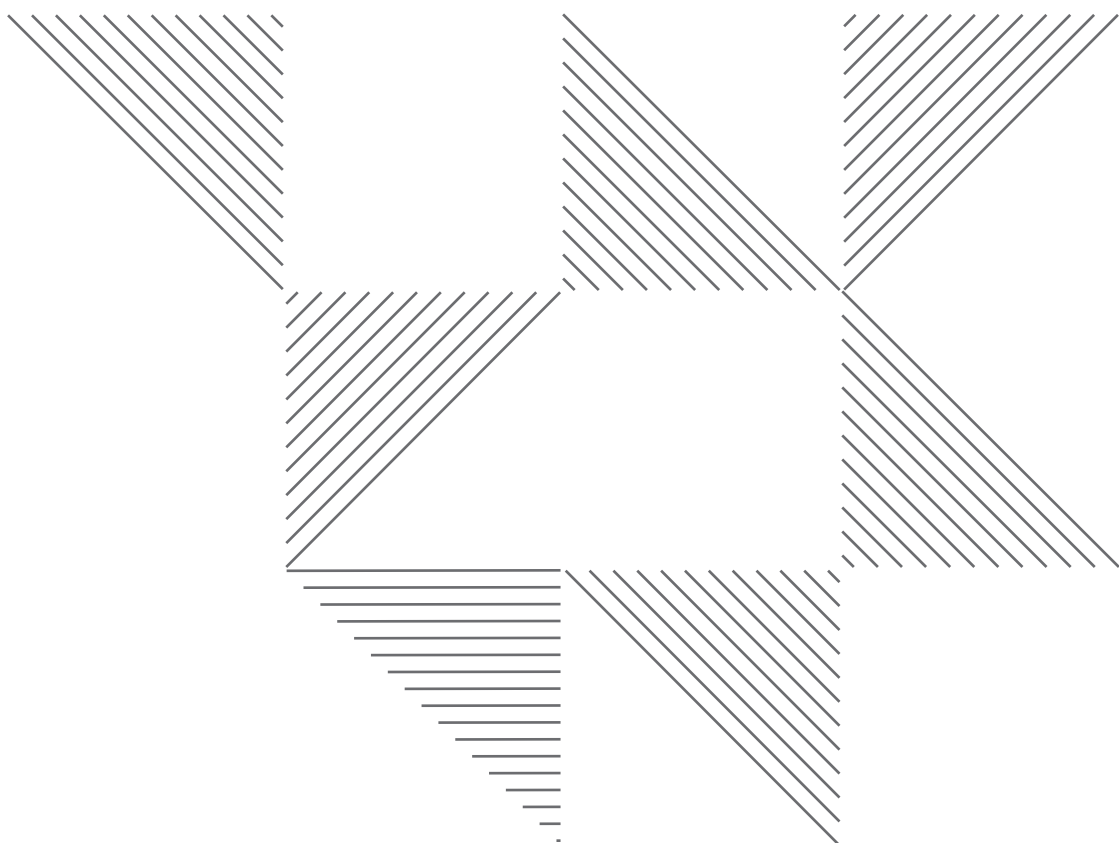
7. LITERATURE

- [1] Barros, G.G., Fahlcrantz, C.M., Johansson, P.A. (2005) Topographic distribution of uncovered areas (UCA) in full tone flexographic prints, TAGA Journal, vol.2, no.1, pp. 43-57
- [2] Chappard, D, Degasne, I, Huré, G, Legrand, E, Audran, M, Baslé, MF. (2003) On image analysis measurements of roughness by texture and fractal analysis correlate with contact profilometry, Biomaterials, vol.24, no.8, pp. 1399-1407
- [3] Choi, J., O'Brate, K. (2010) Method of Controlling Surface Roughness of a Flexographic Printing Plate, US patent 2010/0173135 A1, [Online] Available from: <http://www.google.com/patents?id=QCXSAAAAEBAJ&printsec=abstract&zoom=4&hl=sr#v=onepage&q&f=false>, [Accessed: 3rd April 2012]
- [4] Dedijer, S., Novaković, D. (2010) Determination of surface roughness factors of solid printing areas on different flexo printing plates, Proceedings of International Symposium on Novelties in Graphics, Ljubljana, Slovenia, pp. 806-812.

- [5] Mahović, S. (2007) Karakterizacija površinskih struktura ofsetnih tiskovnih formi, doktorska disertacija, 38-50, Sveučilište u zagrebu, grafički fakultet
- [6] Pallant, J. (2007) Postupni vodič kroz analizu podataka pomoću SPSS-a za Windows (verzija 15), prevod 3. izdanja, Allen&Unvin, Mikro knjiga, Beograd
- [7] Pavlović, Ž., Cigula, T., Novaković, D., Apro, M. (2010) Influence of printing process on printing plate`s surface characteristics, Proceedings of International Joint Conference on Environmental and Light Industry Technologies, Budapest, Hungary, pp. 135-142.
- [8] Pavlović, Ž. Novaković, D., Dedijer, S., Apro, M. (2010) Changes in the surface roughness of aluminium oxide (non-printing) areas on offset printing plate depending on number of imprints, Journal of graphic engineering and design, vol.1, no.1, pp. 32 -38
- [9] Ramon-Torregrosa, P.J, Rodríguez-Valverde, M.A., Amirfazli, A., Cabrerizo-Vílchez, M.A. (2008) Factors affecting the measurement of roughness factor of surfaces and its implications for wetting studies", Colloids and surfaces a: physicochemical and engineering aspects, vol.323, no.1, pp. 83–9
- [10] Risović, D., Mahović – Poljaček, S., Gojo, M. (2009) On correlation between fractal dimension and profilometric parameters in characterization of surface topographies, Applied Surface Science, vol.255, no.7, pp 4283-4288.



Print Quality



THE SIGNIFICANCE OF COLOUR AND ITS COLOUR CHARACTERISTICS ON PRINTED FLEXIBLE PACKAGING

Petra Balaban

Higher Education Technical School of Professional Studies Novi Sad

Corresponding author: Petra Balaban

e-mail: balaban@vtsns.edu.rs

1. ABSTRACT

This paper is a segment of multiple criteria study of flexible printed packaging. Its value is affected, among others, by non-verbal criteria (colour, size, material, shape, image, graphics). Those criteria have a major impact on making decisions when buying any packaged product. The overall quality of print is greatly influenced by colour characteristics. This paper deals with subjective assessment of those characteristics and influence of printing inks viscosity and speed on colour variations in polymer packaging foils (polyethylene, polypropylene). The study was carried out in a local printing office mostly producing packaging for granary and powdery foodstuffs. The study revealed colour variations of prints at different viscosity and speed. However, the issue here is different subjective assessment of colour characteristics within the rest of requirements for flexible packaging by producers, buyers and the author of this paper respectively.

Key words: flexographic printing, packaging foils, colour characteristics

2. INTRODUCTION

Flexible printed packaging, plays a communicating part when deciding what product to buy. Apart from maintaining the brand's visual identity and other non-verbal criteria involved when deciding what to buy, it is important to keep certain tolerance for colour variations of prints in flexible printed packaging. Too visible discrepancies i.e. poor quality of print, may lead buyers to think that the quality of product itself has dropped.

This paper attempts to ascertain the value of colour quality within the overall visual quality of printed packaging, based on subjective assessment.

Prints on printed polymer packaging polyethylene and polypropylene foils are also discussed, with special reference to colour variations at different viscosities and speeds.

3. EXPERIMENTAL PART OF STUDY

3.1. Measurement preparation

- Flexographic stack press (Figure 1), type ZBS 450 with 6 printing aggregates, print width 460 mm, length 210 mm - 460 mm, max belt speed 50 m/min, drying temperature range 60 °C – 75 °C.
- Anilox Rolls 800 l/in and 300 l/in.
- Photopolymer printing form thickness 1,14 mm, type Cyrel Fast, 58 l/cm, test form- (Figure 1), with full tone and halftone patches for each colour.
- Termoflex solvent-based inks by Colorprint
- Printing materials: transparent polyethylene thickness 40 µm and transparent polypropylene thickness 30 µm, with surface tension of approx. 38 Nm/m.
- Measuring gauge: X-Rite spectrophotometer under standard measuring conditions.

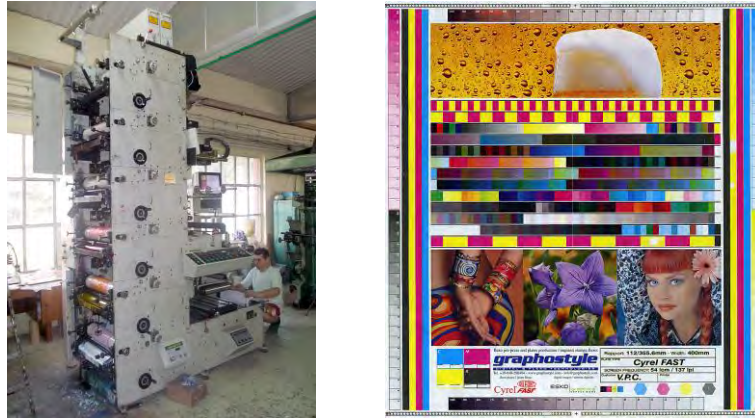


Figure 1: Printing machine ZBS 450 with camera and screen for print control and test form with full and halftone patches, and test pictures

3.2. Print testing

Test form prints were studied to compare density, tonal value increase and Lab- parameters at different viscosity and speed rates.

After optimum settings adjustment of the machine (pressure, speed, etc), prints were made at colour viscosity of 35 s and speed of 20 m/min, followed by printing speed of 35 m/min. The same procedure was repeated for printing at ink viscosity of 20 s.

Viscosity was adjusted by adding solvent while cylinder pressure was kept constant.

Thirty prints were made per each material. Five samples each were measured for deviation of colour characteristics at various speeds and viscosities.

Figure 3 shows influence of printing speed on optical density at varying viscosity readings.

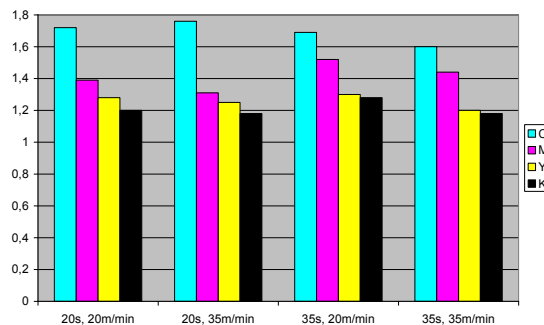


Figure 3: Readings of optical densities of full colour tones at various ink viscosities and speeds for polyethylene

The hypothesis that optical density increases with increased viscosity was not confirmed for all colours. There was no point in assessing tone value increase (TVI) in order to control prints since tone value is not known for print form. Tone values were measured relative to test form (Figure 1), for the sake of comparison between various viscosities.

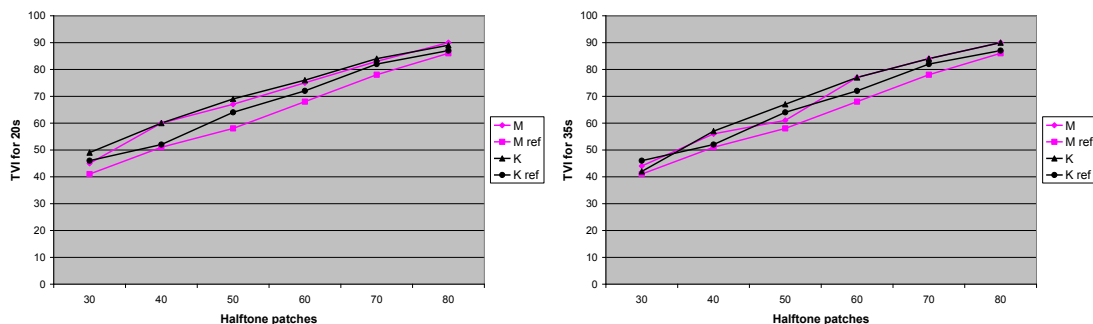


Figure 4: Tone value increase on polyethylene prints for ink viscosities 20 s i 35 s

Tone value increase discrepancies at various viscosities for magenta and black are displayed in the Figure 4 for raster areas of 30 %, 40 %, 50 %, 60 % and 80 % respectively. Some colours display lower TVI at higher viscosity. Consequently, lowering viscosity enhances printability of a surface, and increases tonal value. Figure 5 shows influence on colour discrepancies in prints in Lab-system (print speed of 28 m/min).

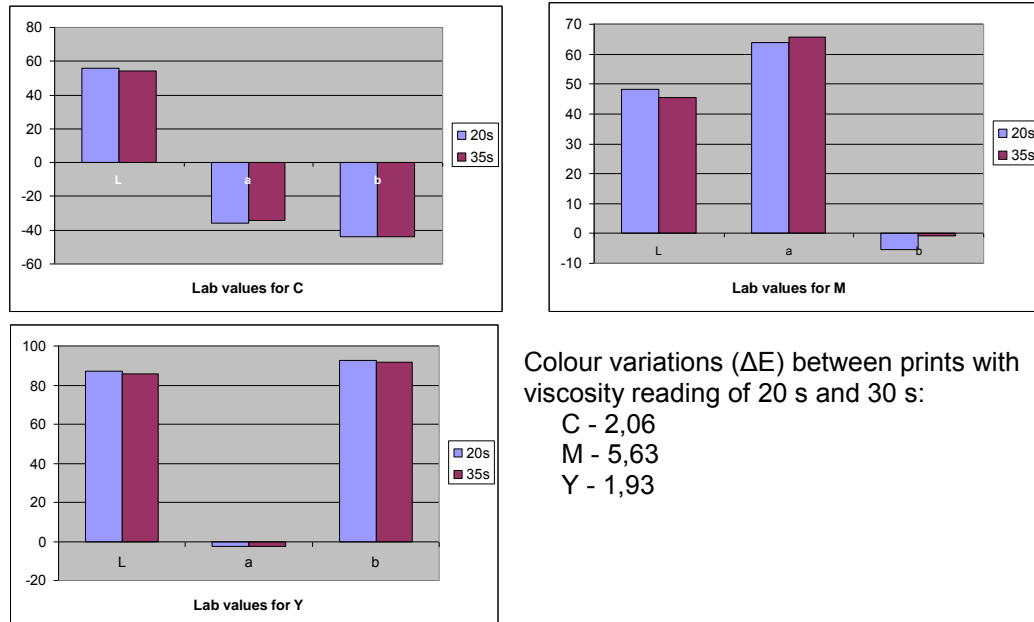


Figure 5: Lab values at different ink viscosities for polyethylene

The degree of whiteness is not a very suitable parameter for practical print quality testing in print shops. However, to achieve quality colour characteristics, the degree of whiteness is important when picking printing materials. Findings for printed PP foils showed the same trend and were not shown here.

4. THE VISUAL IMPORTANCE OF COLOUR

The degree of importance factors of some requirements for flexible packaging depends on contents/products. The factors are compared to each other and assessed in various ways, starting from simple score-based comparisons (Table 1), more complex tests and assessments based on objective (measured) evaluations which take longer and more expensive to perform. A number of studies were carried out to research different target customers and packaging types, using questionnaires, e.g. [1,2].

Research [3] suggests that in impulse buys, non-verbal influences (Figure 6) at work at first sight comprise up to 93 % for milk, 90 % for chewing gum and shampoo. The importance of packaging colour for the same items amounts to 28 %, 31 % and 25 % respectively, hence averaging 28%.

Table 1 indicates importance of factors with simple breakdown of major criteria assessed by print office experts, buyers and author of this paper.

Table 1: Major Criteria Importance Factors Score

Requirements	Importance factor
Barrier	0,10
Passage ability	0,25
Hardness	0,30
Package Colour Effect	0,20
Production Cost	0,15

The table suggests that hardness and passage ability were most important criteria for packaging to meet, while others played a less important role. On the other hand, the importance of production cost can be altered in the changing market, hence all other requirements, including visual impact, can fall behind. Visual effects are interesting as information that can manipulate consumers. Colour is a major non-verbal criterion but its significance is, however, very difficult to determine. These percentages of visual impact somewhat differ from those shown in Table 1.

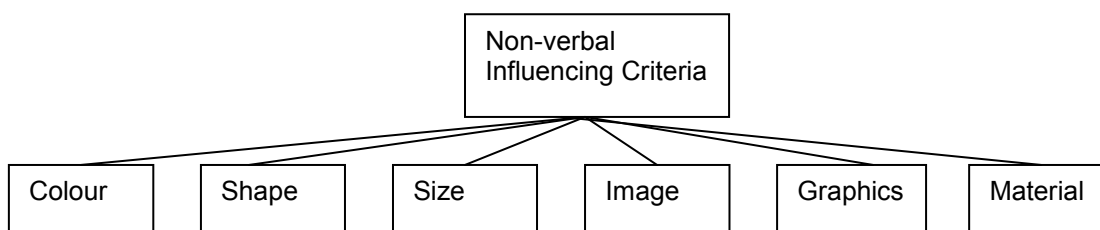


Figure 6: Non-verbal influencing criteria of printed packaging importance

5. CONCLUSION

Our study results suggest that the influence of speed on colour differences in prints was negligible. The influence of viscosity differences (20s and 35s) of colours indicated that the range of those differences in certain colours was 1.93 – 5.63.

Since the influence on colour characteristics of prints depends on a number of other factors (printing press, printing plate, anilox rolls, and especially printing pressure), our results can only point to a trend in specific conditions of a printing office.

The evaluation of factors of importance of visual and colour characteristics shown was the result of the mean value arrived at by assessment by producers, buyers of flexible packages tested, and the author of this paper. Their views in examples shown here and in other examples differed from one another and there was uncertainty about them.

It can also be concluded that colour plays more important role in the first phase of decision making than in final phase, when all visual impressions are taken into account.

6. LITERATURE

- [1] Jurečić, D.: „Evaluacija elemenata vizualne informacije na grafičkoj opremi ambalaže”, Magistarski rad, Sveučilište u Zagrebu, Fakultet organizacije i informatike Varaždin, 2004.
- [2] Balaban-Đurđev, P, Maletić, V.: „Visual Impact of Graphic Information in the Package”, Informing Science and IT Education 2011 Joint Conference, Novi Sad, 2011.
- [3] Butkeviciene, V., Stravinskiene, Rutelione, A: „Impact of Consumer Package Communication on Consumer Decision Making Process”, Engineering Economics, 2008. No 1.
- [4] Foundation of Flexographic Technical Association: „Flexography: Principles & Practices”, Foundation of Flexographic Technical Association, Inc., 1999.
- [5] Bould, D., Claypole, T., Galton, David.: „Process parameters in flexography: effects on ink transfer and image quality characteristics”, Journal of Print and Media Technology Research, March 2012.
- [6] Szentgyörgyvölgyi, R., Novotny, E.: „Investigation of flexographic printing on PE and BOPP foils”, The Fifth International Symposium, GRID 2010.
- [7] Borbély, A., Szentgyörgyvölgyi, R.: „The effect of flexographic process parameter on the properties of prints on nonabsorbing substrates”, 2nd International Joint Conference on Environmental and Light Industry Technologies, 21 – 22 November 2011, Budapest, Hungary Óbuda University.
- [8] Olsson, R.: „Some aspects on flexographic ink-paper and paperboard coating interaction”, Dissertation, Karlstad university studies, 2007.
- [9] Buchner, N.: „Verpacken von Lebensmitteln”; Springer Verlag; Heidelberg, 1999.
- [10] Ahlhaus, E. O.: „Verpackung mit Kunststoffen”, C.Hanser, 1997.

DETERMINING THE CORRELATION BETWEEN TOTAL HARDNESS OF WATER AND SPECTRO-DENSITOMETRIC CHARACTERISTIC OF PRINTING QUALITY

Zoran Gazibarić¹, Predrag Živković², Dragana Živojinović²

¹Faculty of Graphic Arts, University of Zagreb

²Faculty of Technology and Metallurgy, University of Belgrade

Corresponding author: Zoran Gazibarić

e-mail: zorangazibaric@gmail.com

1. ABSTRACT

The wetting solution plays significant role in offset printing process, helping in separation of printing from non-printing areas of the printing form. The wetting solution is characterized by the share of isopropyl alcohol, pH value, electrical conductivity, temperature and water hardness, which is a direct consequence of the presence of various salts in water.

It is proved that setting the optimal total hardness of water, which is recommended to be kept from 8°d to 12°d of German hardness, could extend the service life of metal components and machine parts in contact with the wetting solution, because of reduced corrosion and lime scale sedimentation. It also extends the life of the rubber rollers in contact with the wetting solution. However, there is an issue of particular owner's and management's interest: would they get prints of higher quality if they install system for regulation of the water hardness?

In this paper an attempt was made to determine the correlation between the total hardness of water and some characteristics of print quality (tone value increase, range of reproduced tonal values, maximum screen ruling at which it is possible to get a clear image without defects).

In the experimental part a single color sheet fed offset printing machine will be used, on which all printing conditions will be kept constant, except the hardness of water to be used in the wetting solution. Soft, medium hard and hard water will be used.

Key words: wetting solution, water hardness, print quality

2. INTRODUCTION

It is well known that the wetting solution (also known as dampening or fount solution), which enables separation of printing from non-printing elements, which are practically positioned in the same level on the offset printing form, plays one of the key roles in the offset printing. [1]

Wetting solution in modern offset printing is a multicomponent water solution, consisting of some components that are deliberately added (IPA - Isopropyl Alcohol, buffer solution, anticorrosive additives, biocides), but there are some components (inorganic salts) that come with water which is used as a solvent.

Wetting solution is usually characterized by following parameters. [2]

- IPA amount;
- pH value;
- specific electrical conductivity,
- total water hardness.

IPA reduces surface tension of solution and contact angle. The smaller is contact angle the wetting of non-printing elements with wetting solution is better, even with reduced amount of wetting solution and ink cannot cover non-printing elements. However, too much IPA could prevent drying of the printed ink.

The function of buffer solution is to keep pH value at optimum level, which is considered to be 4.7-5.2, which is necessary for maintaining stabile hydrophilic properties of aluminum-oxide, and enabling water absorption on non-printing elements during printing.[3]

Out of this pH range wetting is reduced (too acid) or increased (to alkaline), which could cause further problems in printing.[4]

Specific electro conductivity depends on concentration of ions, and in this case represents the amount of impurities dissolved in dampening solution. The impurities come mostly from the paper and surrounding, and could affect pH value and surface tension of wetting solution.

Hardness of water is caused by presence of dissolved Calcium (Ca^{2+}) and Magnesium (Mg^{2+}) salts. Hardness of water is expressed as content of CaCO_3 in mg per one dm^3 of water, or in German degrees ($^\circ \text{dH}$). Total hardness of water consists of carbonate and non-carbonate hardness, and for offset printing purposes should be kept in the range 8°dH (German hardness degree) – 12°dH ($143 - 215 \text{ mg CaCO}_3/\text{dm}^3$), [5] in order to reduced limestone sedimentation on parts of the press that are in contact with dampening solution, and to reduce corrosion of metal parts. Using too hard or too soft water could cause problem of depositing. If water with a high total hardness is used, ink rollers may tend to strip, because of depositing of poorly soluble calcium compounds in the pores of the rubber rollers, which then clog up, becoming increasingly hydrophilic, and greatly disrupt ink transfer in the inking unit. [6]

Considering the investing in water conditioning system, managers of printing houses frequently set a question - would quality of prints be affected by changing total hardness. The main goal of this work is to determine an influence of total water hardness to some densitometric and spectrophotometric print quality parameters.

3. EXPERIMENTAL

In order to investigate an influence of total hardness of water to quality of prints for small runs, the following works was carried out:

- creating the test form;
- manufacturing the offset printing form;
- preparing the three water samples with controlled total hardness;
- preparing three wetting solutions with water of different total hardness;
- perform experimental printing on two different presses, using three different wetting solutions;
- measuring and comparing some quality parameters on samples printed on the same press, but with different wetting solutions.

3.1. Creating the test form

Test form was prepared using software for vector graphics. Test form was monochromatic and composed of:

- wedge with different tints (1, 2, 3, 4, 5, 10, 20, 30, 40, 50, 60, 70, 80, 85, 90, 92, 94, 95, 96, 97, 98, 99, 100%);
- micro lines, positive and negative, 4, 6, 8 and $10 \mu\text{m}$;
- small text, positive and negative, 1, 2, 3, 4, 5 and 6 pt;
- isolated round dots, positive and negative, 0.02, 0.04, 0.06, 0.08, 0.10, 0.12, 0.14, 0.16, 0.18 and 0.20 mm;
- three photographs.

3.2. Manufacturing the offset printing form

The first experimental printing was performed with positive offset thermal printing form CINKARNA CELJE, which was exposed at screen ruling 175 lpi by LUSHER X-pose 130 plate setter and developed in HAASE SYSTEMTECHNIK Peter Haase GmbH processor. The plate was developed in P-71+ CINKARNA CELJE developer.

The second experimental printing was performed with positive offset thermal printing form Agfa Azura TS Processless, which was exposed at screen ruling 175 lpi by Presstek plate setter and washed in Washer Presstek processor.

After developing, both offset printing forms were checked for reproducing the smallest details in both positive and negative. Absolute tone values and absolute dimensions of tiny elements were not measured, since the aim of this experiment was to find difference between prints made with the same printing form, but with different wetting solution.

3.3. Preparing the water samples

In this experiment three water samples with different total hardness were prepared. The sample 1 was prepared by ion exchange process, which extracts Ca^{2+} and Mg^{2+} ions. Water was treated in TEHNOLAB-BP with R.O. PASTER ion exchanger, and after treatment the total hardness of water was less than 1 °dH and specific electrical conductivity was less than 1 μS . The sample 2 was prepared by reverse osmosis process with bypass. Water was treated in OSMOHOM SPECIAL reverse osmosis system. In order to achieve desired total hardness, the treated water was mixed with tap water that was only treated against microorganisms. The total hardness of water sample 2 after mixing was 11 dH, and electrical conductivity was 371 μS . The sample 3 was taken directly from the water supply. Without any treatment the total hardness was 18° dH and specific electrical conductivity was 576 μS .

3.4. Preparing wetting solutions

In this experiment three different wetting solutions were prepared. The only difference between three wetting solutions was total hardness of water that was used as a solvent. The wetting solutions were prepared by adding IPA (P-43 CINKARNA CELJE) and buffer solution (P-56 CINKARNA CELJE) in water samples 1, 2 and 3. Final composition of all three solutions was 8 vol. % of IPA and 3 vol. % of buffer solution.

All three wetting solutions were characterized by pH value, total hardness, electrical conductivity and temperature (table 1.) Specific electrical conductivity and pH values were measured by Cyberscan PC510 measuring unit.

Table 1 Characteristics of wetting solutions

Wetting solution:	1	2	3
Total hardness, °dH	0.5	11	18
pH	4.95	5.31	5.37
Specific electrical conductivity, μS	911	968	1008
Temperature, °C	19	19	20

3.5. Printing conditions

Experimental printing was performed on two presses and two similar stocks:

- MAN Roland Practica - mat coated 150 g/m², and
- Heidelberg GTO - mat coated 250 g/m².

Printing conditions were maintained exactly the same like in normal production, except wetting solution that was prepared with water of specific total hardness. In both cases black offset ink was printed.

3.6. Experimental printing

Printing form with test form was loaded onto form cylinder. Pressman manually set the press until he got visually correct prints. During this make-ready period pressman utilized commercial wetting solution that is regularly used in the printing house. Then the commercial wetting solution was replaced with one of wetting solution prepared in this experiment. After 200 prints the wetting solution was replaced with next wetting solution and another 200 prints were made. Finally, 200 prints were made with third wetting solution.

Replacing the wetting solution was the only change in printing conditions during experimental printing. All other printing parameters were considered to remain unchanged: temperature, pressure, type of blanket, printing ink, printing speed, amount of ink per ink zones, printed stock, printing form...

All prints were dried naturally during 24 hours and then analyzed.

3.7. Analyzing the quality of prints

Two methods were used for analyzing prints that are printed in this experiment:

- Optical microscopy and
- Spectrodensitometry.

Optical microscope Olympus CX41 with digital camera Olympus UC30 was used for comparison of appearance of microelements on prints that are printed with different wetting solutions. All analyzed control elements were recorded by camera at magnification of 100 times.

In order to quantitatively determine and express differences in print quality between prints made with different wetting solutions, spectrodensitometer Spectrolino Easy Gretag Macbeth was used for measuring tone and Lab values of some control patches of the test form. Spectrodensitometer was set to standard illumination D50, standard observer 2°, calibration to absolute white and to measure without filter.

Control patches were measured on last five prints of each series. An average tone value of the certain control patch was calculated, as well as standard deviation. Density of solids as well as lab values were also measured and averaged between last five prints in each series.

Then the standard deviation amongst average tone or density values of certain patch on three series of prints was calculated, in order to compare deviation in one series with deviation between series.

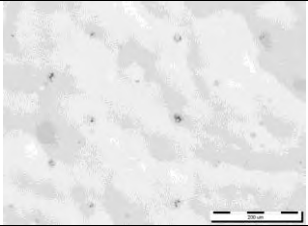
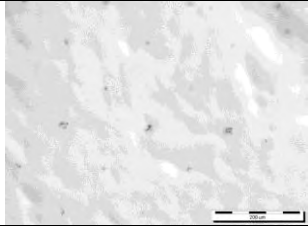
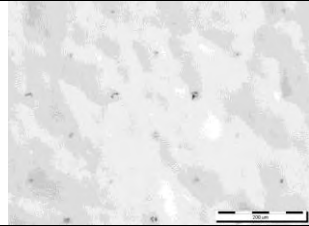
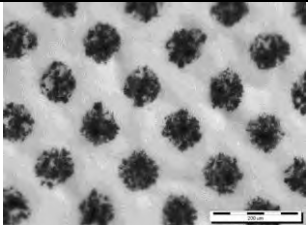
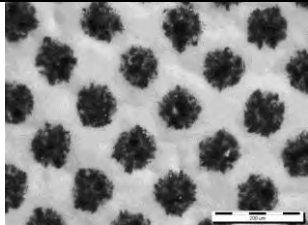
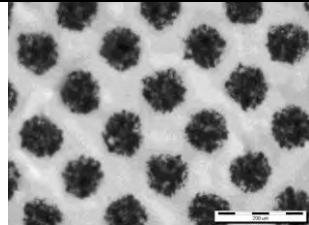
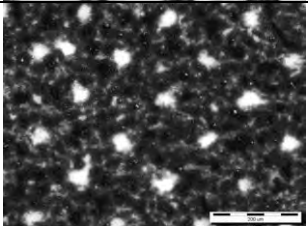
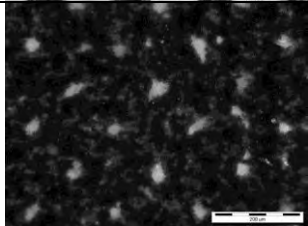
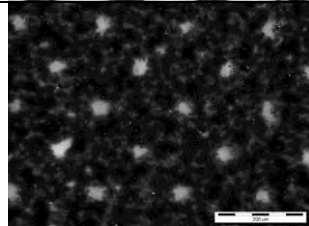
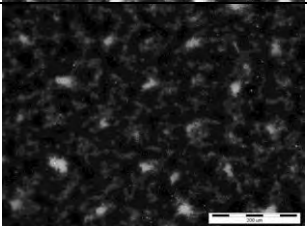
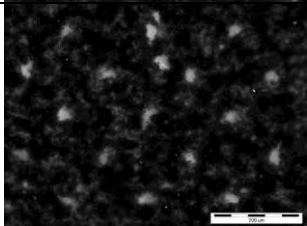
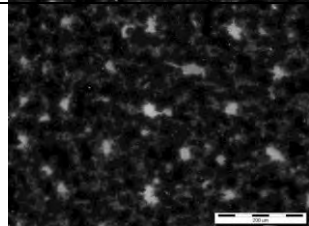
The color difference between printed patch and standard CIE $L^*a^*b^*$ values for black ink according to ISO 1247-2 standard ($L^* = 16$, $a^* = 0$, $b^* = 0$) were also calculated.

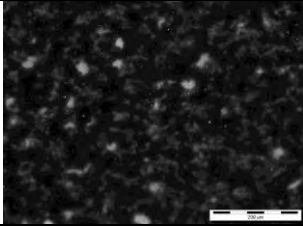
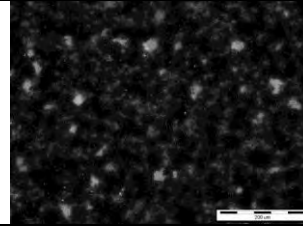
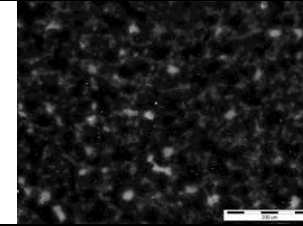
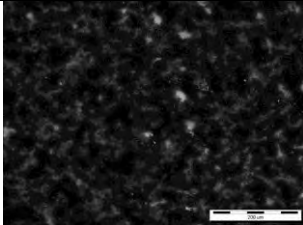
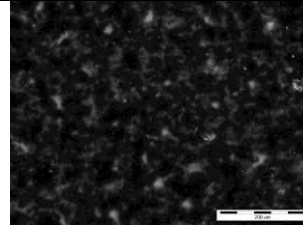
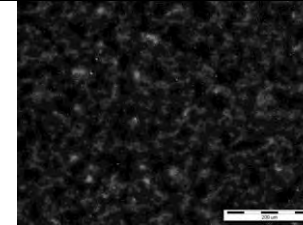
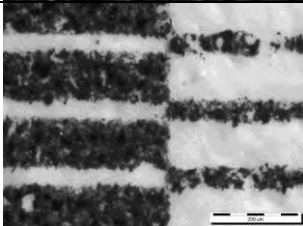
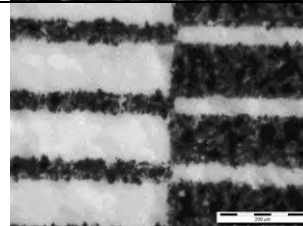
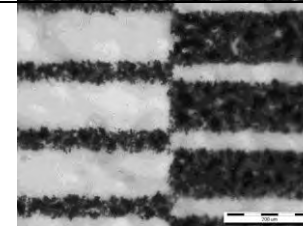
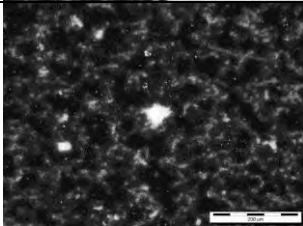
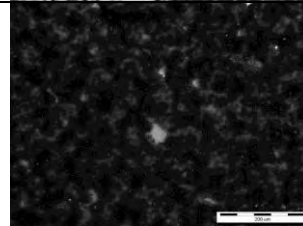
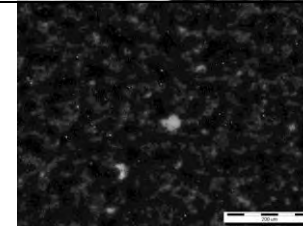
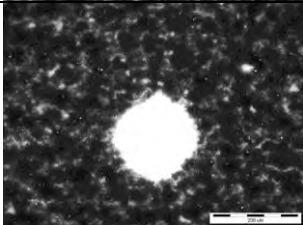
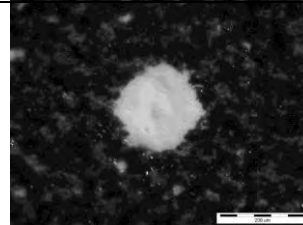
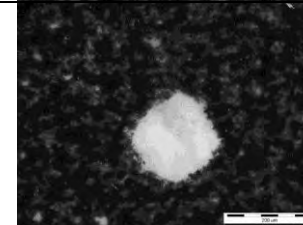
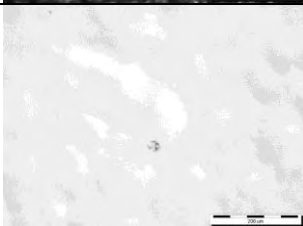
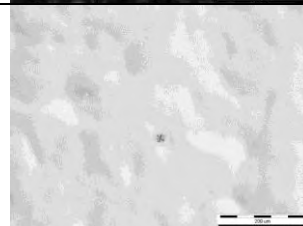

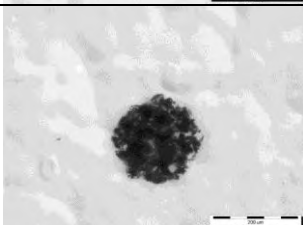
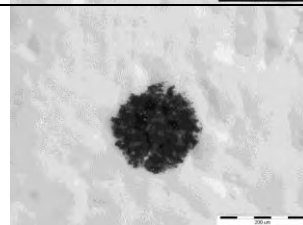
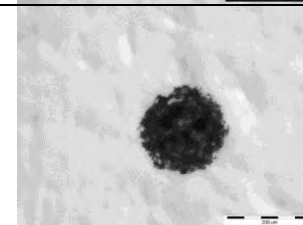
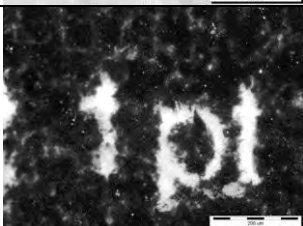

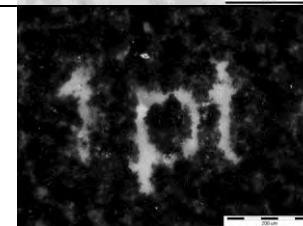
4. RESULTS AND DISCUSSION

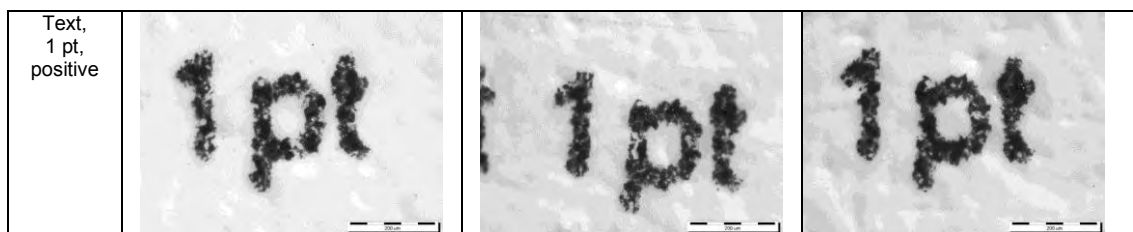
4.1. Analysis of microphotographs

Microphotographs of some control elements printed on MAN Roland Practica with three wetting solutions are presented in Table 2.

Table 2. Microphotographs of some control elements printed on MAN Roland Practica with three wetting solutions. Magnification 100x.

Control patch	1	2	3
1 %			
50 %			
97 %			
98 %			

99 %			
Solid			
Microlines			
Isolated dot, 0.04 mm, negative			
Isolated dot, 0.20 mm, negative			
Isolated dot, 0.02 mm, positive			
Isolated dot, 0.20 mm, positive			
Text, 1 pt, negative			



The smallest reproduced isolated positive dot was 0.02 mm in all three cases. The smallest reproduced isolated negative dot was 0.04 mm in all three cases. All other control elements seems to be the same, so it was impossible to determine differences between prints made with different wetting solution at magnification of 100 times.

The very same conclusion was obtained analyzing prints made on Heidelberg GTO.

4.2. Results of spectrophotometric measurements

Results of spectrodensitometric measurements of some control patches on prints that were made with three different wetting solutions are presented in Table 3.

Table 3. Results of spectrodensitometric measurements of some control patches on prints that were made with three different wetting solutions

	Series 1	Series 2	Series 3	Sdev for series 1, 2 and 3
Tone value (TV) at 50%	51.2	50.7	50.1	
	50.2	49.7	50.2	
	50.1	50.8	50.4	
	51.3	50.7	50.3	
	51.2	50.9	51.4	
Average TV, %	50.8	50.6	50.5	0,12
Sdev	0.55	0.42	0.48	
D _{100%}	1.29	1.29	1.23	
	1.25	1.26	1.28	
	1.26	1.30	1.22	
	1.25	1.30	1.19	
	1.24	1.31	1.23	
Average D _{100%}	1.26	1.29	1.23	0.03
Sdev	0.02	0.02	0.03	
ΔE	11.0	11.3	13.1	
	12.6	12.1	11.6	
	12.2	10.7	13.4	
	12.6	10.7	14.5	
	12.8	10.5	13.1	
Average ΔE	12.2	11.1	13.1	0.85
Sdev	0.65	0.59	0.93	

According to data presented in the table 3, it is not possible to find any dependence between hardness of water that is used for preparing the wetting solution and quality of prints. Average values for the three series are very similar. Standard deviation (Sdev) of values from each series is similar to Sdev calculated for three average values from three series that are printed in this experiment. For instance, Sdev of TV at 50% in first series is 0.55, in the second series is 0.42 and in the third series is 0.48. If Sdev for three average values from series 1, 2 and 3 is calculated, obtained value is 0.12, which is in this case smaller than Sdev for each series. Prints made on Heidelberg showed the similar results.

5. CONCLUSION

According to performed experimental printing and analyzes of prints obtained with three different wetting solutions, with all other printing parameters unchanged, it could be concluded that for short runs and single color prints total hardness of water has no influence to quality of prints itself.

6. LITERATURE

- [1] *T. Cigula, Ž. Pavlović, M. Gojo, D. Risović*, Wetting of offset printing plate's non-printing areas as a function of print run, Proceedings of 5th International Symposium on Graphic Engineering and Design, University of Novi Sad, Faculty of Technical Sciences, Graphic engineering and Design, 2011, p. 211
- [2] *G. Golob, B. Zajc, M. Gojo*, Usporedba kemijskih parametara otopina za vlaženje u ofsetnom tisku, Zbornik radova Četvrtog naučno-stručnog simpozijuma grafičkog inženjerstva i dizajna, Univerzitet u Novom Sadu, Fakultet tehničkih nauka, Grafičko inženjerstvo i dizajn, 2008, s. 3
- [3] *J. Kiurski*, Fizičko – hemijske osnove izrade štamparskih formi , FTN – Novi Sad, 2006.
- [4] Dampening solutions in Offset Printing, Print Media Academy, Heidelberg, 2001, p. 4
- [5] *W. J. Johnstone*, The Influence Of Water Hardness on the Performance of Ink and the Printability of Coated Paper by the Lithographic Process, Independent Ink Technologies, 2003, p.3
- [6] Fount solution in offset printing, Technical information 45.01 E, Hubergroup, 2003, p. 2

INFLUENCE OF INK LAYERS AND DIFFERENT MATERIALS ON THE COLOUR FASTNESS TO RUBBING

Nemanja Kašiković, Gojko Vladić, Neda Milić, Darko Avramović
Faculty of Technical Sciences, Graphic Engineering and Design, Novi Sad

Corresponding author: Nemanja Kašiković
e-mail: knemanja@uns.ac.rs

1. ABSTRACT

Textile materials printed with screen or digital printing during the exploitation can be under the influence of various environmental elements and treatments. This paper presents research regarding influence of ink layers and different type of materials on colour fastness to rubbing. Research was done on three different types of textile materials composed of 100 % polyester. Test chart consisted of four colour fields each 100% of one of process colours (CMYK) and was printed on substrates. Printing machine Mimaki JV22-160 with J-eco Subly nano inks was used. Apart from substrates, variable factor was number of ink layers applied, textile materials were printed with one, two, three, four and five layers of ink. The analysis of rubbing treatment influence on prints was done according to ISO 105-X12 standard. Total of 120 samples were analyzed. Resistance of colour to rubbing treatment (dry and wet staining) was determined by usage of the grey scale.

Key words: ink layer, type of materials, polyester, rubbing, ink jet

2. INTRODUCTION

The mostly used technique for textile printing is screen printing (Horrocks, 2000), but it should be noted that digital ink jet printing is rapidly expanding in the textile markets. Ink jet process, more possibilities for creativity, flexibility, as well as speed and environmental protection (Choi, 2005, Masaru, 2010). Also, designers are not limited in length of print formats which gives opportunity for new ideas (Chun, 2011).

During the last few years, the great progress was made in the field of textile materials. Textile materials have different characteristics like fabric weight, thread count and material composition. Those characteristics can be influential factors on colour reproduction in printing process. With pre-treatment the manufactures can improve some basic characteristic of materials and the results could be better quality of textile products (Chepelyuk, 2011).

After printing process, textile materials can be under the influence of different treatments such as washing, heat, light, as well as rubbing. Colour fastness to rubbing is very often a topic in new research (Mongkhorrattanasit, 2011, Sánchez, 2010, Mongkhorrattanasit, 2010, Avinc, 2010, Xie, 2010, Kasikovic, 2012). Standard ISO 105-X12 can be used to examine influence of rubbing treatment on changes in printed material. After rubbing treatment according to ISO 105-X12 standard the colour resistance to dry and wet staining is determined according to gray scale (Figure 1). The treated material is graded from 1 to 5. Value 5 represents the best result for colour fastness to rubbing which means that least amount of pigments is rubbed off. While value 1 represents the worst result for colour fastness to rubbing, which means that biggest amount of pigments is rubbed off.



Figure 1: Grey scale

The aim of this research is to determine influence of quantity of ink layers and different types of materials on the colour fastness to rubbing of printed textile materials.

3. METHODS

In the experiment three types of materials were used. All materials were composed of 100% polyester (determined using standard SRPS F.S3.112), but with different fabric weight and thread count. Generally, all polyester textile materials are well known for their strong fastness and durability (Zhang, 2009) and that was the reason why polyester materials were used in research. Properties of materials used in experiment are presented in Table 1.

Table 1: Characteristics of material used in testing

Tests	Material composition (%)	Fabric weight (g/m ²)	Thread count p/10cm	
			Warp	Weft
Material 1	Polyester 100 %	110,6	170	120
Material 2	Polyester 100 %	101,5	160	100
Material 3	Polyester 100 %	141,3	260	120
Methods	ISO 1833	ISO 3801	ISO 7211-2	

Test chart consisted of four colour fields each 100% of one of process colours (CMYK) was printed on substrates by digital inkjet printing machine Mimaki JV22-160 and J-eco Subly nano inks. The volume of ink transferred to the material was varied, by printing different number of layers; five different ink volumes were applied to material and used in analysis. For 120 samples we determined the colour fastness to rubbing according to ISO 105-X12 with grayscale.

4. RESULTS AND DISCUSSION

In this experiment, we determined colour fastness to rubbing for all samples. We compared how change of ink layer numbers and type of materials influenced the resistance of colour to dry and wet rubbing.

In case of cyan values for dry staining for material 1 was 5 (sample printed with one ink layer), 4-5 (sample printed with two ink layers) and 4 (samples printed with three, four and five ink layers). Samples printed on material 2 had a lower resistance in comparison to material 1. Value 3 was determined for samples printed with one and two ink layers. Samples printed with three and four ink layers had value 2-3 for colour fastness to rubbing. The lowest value for samples printed on material 2 was value 2 (sample printed with five ink layers). The material 3 showed the least resistance to rubbing. Sample printed with one ink layer had value 2-3 for colour fastness. Value 2 was determined for samples printed with two and three ink layers. The worst results were determined for samples printed with four and five ink layers. Those values were 1-2. All results for the assessment of dry staining according to grey scale for samples printed with cyan are shown in figure 2.

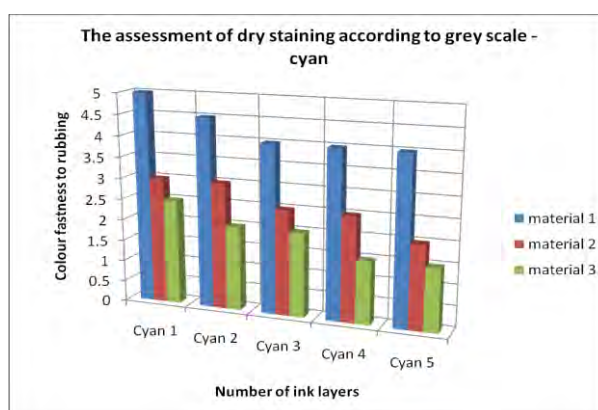


Figure 2: The assessment of dry staining according to grey scale - cyan

Colour change values for wet staining are shown in figure 3. Like in first case, when we analyzed the assessment of dry staining the best results were on samples printed using material 1. The worst resistance were determined for samples printed using material 3. Values for material 1 was 4-5 (sample printed with one ink layer), 4 (sample printed with two ink layers), 3-4 (samples printed with three and four ink layers) and 3 (sample printed with five ink layers). Colour change values for wet staining was 2, when samples were printed with one, two, three and four ink layers on material 2. The value for wet staining was 1-2 when sample was printed with five ink layers on material 2. Colour fastness to rubbing for wet staining was the lowest when we were printing with cyan ink on material 3. When we printed with one, two, three, as well as four ink layers colour fastness were 2. The value 1 was determined when we tested sample printed with five ink layers.

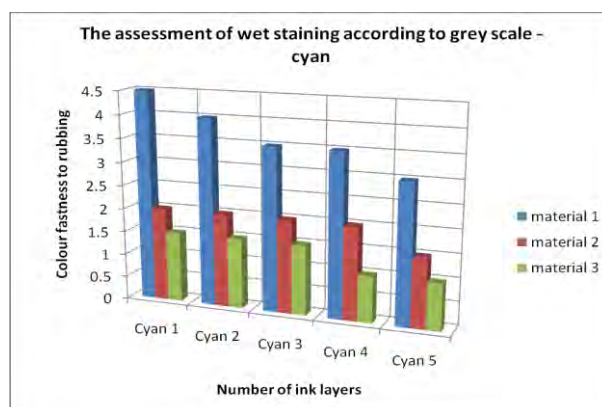


Figure 3: The assessment of wet staining according to grey scale - cyan

When we analyzed colour fastness to rubbing (dry and wet staining) for samples printed with magenta ink, we found the same behaviour like in previous analyze. The best resistance was for samples printed in material 1 and the worst was for samples printed on material 3. With increasing number of ink layers, colour fastness to rubbing was lower.

In figure 4, we showed the assessment of dry staining according to grey scale for samples printed with magenta.

For samples printed on material 1 values were: 4-5 (samples printed with one and two ink layers), and 4 (samples printed with three, four and five ink layers). Values for colour fastness to rubbing (material 2) were: 4 (sample printed with one ink layer), 3-4 (sample printed with two ink layers), 3 (samples printed with three and four ink layers) and 2-3 (sample printed with five ink layers). The lowest values were for samples printed in material 3: 4 (sample printed with one ink layer), 3 (samples printed with two, three and four ink layers) and 2-3 (sample printed with five ink layers).

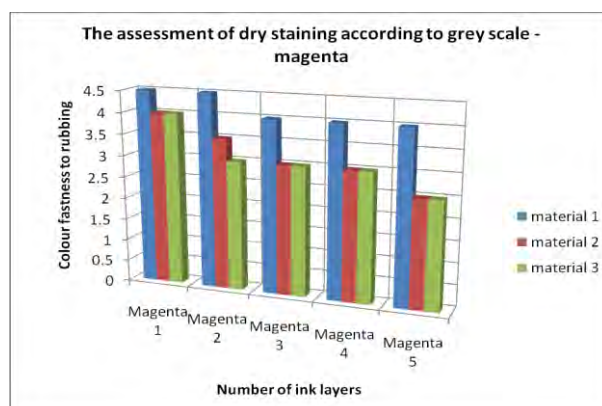


Figure 4: The assessment of dry staining according to grey scale - magenta

Samples exposed to wet staining had lower values to colour fastness. The values were 4 (samples printed with one, two, three and four ink layers), 3-4 (sample printed with five ink layers) for samples printed on material 1. The assessment of wet staining according to

grey scale for samples printed on material 2 and material 3 were: 3 (samples printed with one and two ink layer), 2-3 (samples printed with three and four ink layers) and 2 (sample printed with five ink layers) - material 2; 2-3 (samples printed with one, two, three and four ink layers) and 2 (sample printed with five ink layers) - material 3.

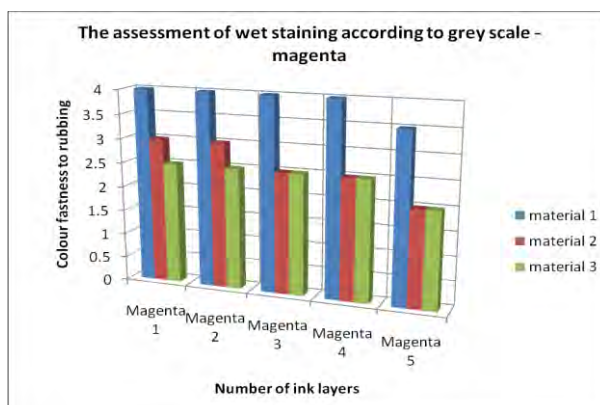


Figure 5: The assessment of wet staining according to grey scale - magenta

Samples printed with yellow ink, exposed to rubbing were graded better than samples printed with cyan and magenta inks.

In figure 6, we showed assessment of dry staining according to grey scale. Like in previous analyze, samples printed in material 1 were most resistant to rubbing. Those values were 5 (samples printed with one, two and three ink layers) and 4-5 (samples printed with four and five ink layers). Samples printed in material 2 were less resistant to rubbing. For these samples, values were: 4-5 (samples printed with one and two ink layers), 4 (samples printed with three and four ink layers) and 3-4 (sample printed five ink layers). Analyze showed that samples printed in material 3 were the least resistant to rubbing. Those values were: 4 (samples printed with one, two, three and four ink layers) and 3 (sample printed with five ink layers).

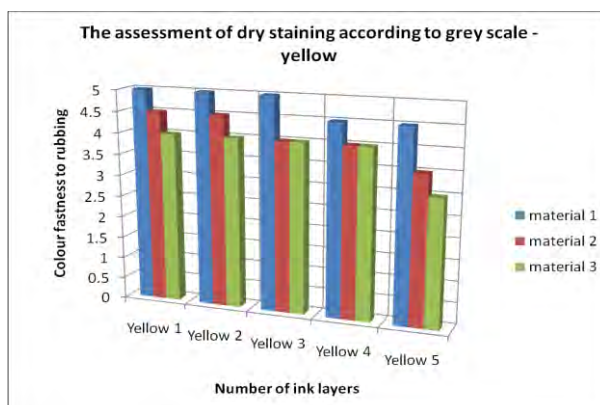


Figure 6: The assessment of dry staining according to grey scale - yellow

After exposing materials to wet staining lower values to colour fastness were noticed (figure 7). For samples printed on material 1 values were always 4-5 and these samples were the most resistant. Samples printed in material 2 were better on comparing to samples printed on material 3. Values were 4-5 (sample printed with one ink layer), 4 (sample printed with two ink layers), 3-4 (samples printed with three and four ink layers) and 3 (sample printed with five ink layers). Like in all cases, samples printed on material 3 were the least resistant. Those values were 3-4 (sample printed with one ink layer), 3 (samples printed with two, three and four ink layers) and 2-3 (sample printed with five ink layers).

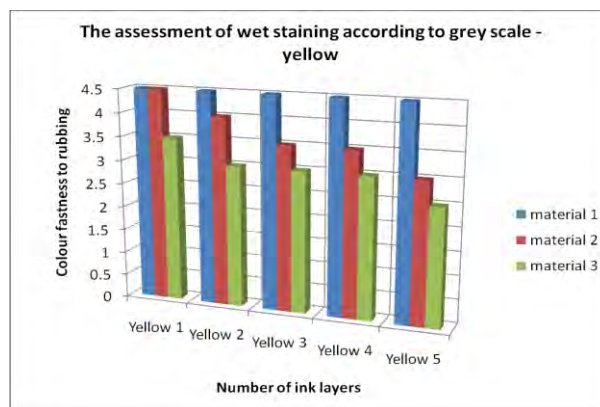


Figure 7: The assessment of wet staining according to grey scale - yellow

Samples printed with black ink, exposed to rubbing had same behaviour like samples printed with other inks. The best results for colour fastness to rubbing were in case when we printed samples on material 1 and the worst results for colour fastness to rubbing were when we printed samples on material 3. Also, after exposition to wet staining lower values to colour fastness were noticed.

In figure 8, we showed assessment of dry staining according to grey scale. Results for samples printed in material 1 were: 4-5 (samples printed with one, two and three ink layers) and 4 (samples printed with four and five ink layers). Lower values for colour fastness to rubbing were determined for samples printed in material 2. Those values were 4-5 (sample printed with one ink layer), 4 (sample printed with two ink layers), 3-4 (sample printed with three ink layers) and 3 (samples printed with four and five ink layers). For samples printed on material 3 values were: 3 (samples printed with one and two ink layers), 2-3 (sample printed with three ink layers), and 3 (samples printed with four and five ink layers).

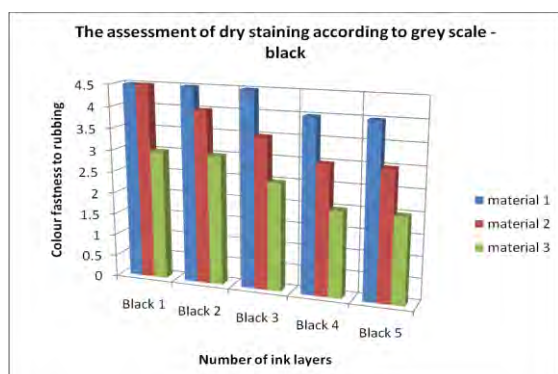


Figure 8: The assessment of dry staining according to grey scale - black

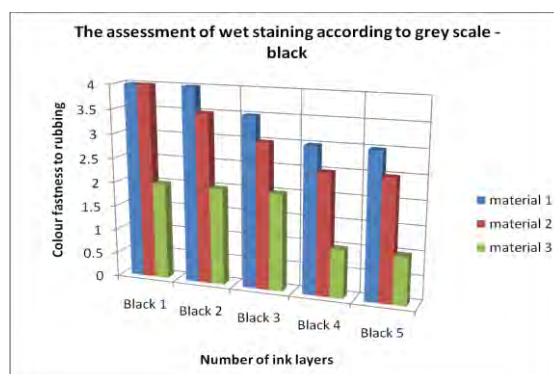


Figure 9: The assessment of wet staining according to grey scale - black

In figure 9, we showed assessment of wet staining according to grey scale - black. Values for colour fastness to rubbing (wet staining), when we analyze samples printed on material 1, were: 4 (samples printed with one and two ink layers), 3-4 (sample printed with three ink layers), and 3 (samples printed with four and five ink layers). Samples printed on material 2 were of a lower resistant. Those values were: 4 (sample printed with one ink layer), 3-4 (sample printed with two ink layers), 3 (sample printed with three ink layers) and 2-3 (samples printed with four and five ink layers). The lowest resistant were determined for samples printed on material 3. Those values were: 2 (samples printed with one, two and three ink layers) and 1 (samples printed with four and five ink layers).

When we analyze all results, we can say that samples have higher colour fastness to dry staining in comparison to results to wet staining. Also, increasing the number of ink layers reduces a colour fastness to rubbing. Another influential factor was material. The worst colour fastness to rubbing was for samples printed on material 3. Material 3 had the biggest fabric weight and thread count. Material 1 and material 2 had a similar behaviour although material 1

had a bit better colour fastness. They had similar fabric weight as well as thread count. When we compared all materials in case that we want to have samples more resistant to rubbing, it is better to use material with lower fabric weight and lower thread count.

5. CONCLUSION

It can be concluded that with increasing number of ink layers, it is not possible to improve colour fastness to rubbing, because there is larger amount of inks on the surface of material. When materials printed with greater number of ink layers are exposed to rubbing, larger amount of inks will be removed. With right choice of material it is possible to improve colour fastness to rubbing because some materials can receive pigments of ink into fibres and that is the reason why they are more resistant to rubbing.

Acknowledgements

This work was supported by the Serbian Ministry of Science and Technological Development, Grant No.:35027 »The development of software model for improvement of knowledge and production in graphic arts industry«

6. LITERATURE

- [1] Avinc O., Wilding M., Bone J., Phillips D., Farrington D. "Evaluation of colour fastness and thermal migration in softened polylactic acid fabrics dyed with disperse dyes of differing hydrophobicity", *Coloration Technology*, 126, 353–364, 2010
- [2] Chepelyuk E. V. , Choogin V. V., Hui D., Cousens J. "Method of determining key parameters of thread arrangement in structure of single-layer woven fabric for reinforcement of composite textile material", *World Journal of Engineering*, 8 (3), 209-216, 2011
- [3] Choi P. S. R. , Yuen C. W. M. , Ku S. K. A. , Kan C. W. "Digital Ink-jet Printing for Chitosan-treated Cotton Fabric", *Fibers and Polymers*, 6 (3), 229-234, 2005
- [4] Chun J. H. "A review of the characteristics of digital art expressed in contemporary fashion", *International Journal of Fashion Design, Technology and Education*, 4 (3), 161 – 171, 2011
- [5] Horrocks, A.R. "Handbook of Technical Textiles", (The Textile Institute, 2000.)
- [6] Kašiković N., Novaković D., Vladić G., Avramović D. "Influence of ink layers on the colourfastness to rubbing of printed textile materials", *Tekstilna industrija*, 60 (2), 28 – 32, 2012
- [7] Masaru O. , Kazuhide Y., Yukio A. "Textile Printing by the Ink-Jet Printer", *Nihon Gazo Gakkaishi/Journal of the Imaging Society of Japan*, 49 (5), 417-423, 2010
- [8] Mongkholrattanasit R., Kryštůfek J., Wiener J. "Dyeing and fastness properties of natural dye extracted from eucalyptus leaves using padding techniques", *Fibers and Polymers Journal*, Vol. 11 (3), 346-350, 2010
- [9] Mongkholrattanasit R., Kryštůfek J., Wiener J., Studničková J. "Properties of Wool and Cotton Fabrics Dyed with Eucalyptus, Tannin and Flavonoids", *FIBRES & TEXTILES in Eastern Europe*, 85 (2), 90-95, 2011
- [10] Sánchez P., Sánchez-Fernandez M. V., Romero A., Rodríguez J. F., Sánchez-Silva L. "Development of thermo-regulating textiles using paraffin wax microcapsules", *Thermochimica Acta*, 498, 16–21, 2010
- [11] Xie K., Wang Y., Xu L. "Modification of cellulose with reactive polyhedral oligomeric silsesquioxane and nano-crosslinking effect on color properties of dyed cellulose materials", *Carbohydrate Polymers*, 80, 480–484, 2010
- [12] Zhang C, Fang K, "Surface modification of polyester fabrics for inkjet printing with atmospheric-pressure air/Ar plasma", *Surface and Coatings Technology*, 203 (14), 2058-2063, 2009

INFLUENCE OF DIGITALLY PRINTED SELF ADHESIVE FOILS ON PRINT QUALITY PARAMETERS

Mladen Stančić¹, Igor Karlović², Ivana Jurič²

¹Faculty of Technology, Graphic engineering, Banja Luka,

²Faculty of Technical Sciences, Graphic Engineering and Design, Novi Sad

Corresponding author: Mladen Stančić
e-mail: mladenstancic@yahoo.com

1. ABSTRACT

Printing substrate and its characteristics has a significant impact on print quality. Essential characteristic of substrates is the substrate surface. Substrates with different surface have various reflection of light, which leads to various print quality. Print quality itself is a complex term that includes desired colour reproduction and satisfactory reproduction of image elements. Important print quality attributes are sharpness, mottle and line quality. In this paper we have focused on ink-jet printed PVC self adhesive substrates. Three PVC substrates (enlightened and nonenlightened) have been measured and based on image analysis it can be concluded that the substrate surface and enlightening affects the print quality.

Key words: print quality, modulation transfer function (MTF), mottle, line perimeter, line area

2. INTRODUCTION

A common way to analyze the print quality is to quantitatively assess the tone and colour of an image. This, however, is not enough to define overall, perceived quality as stated by Pedersen et al. (Pedersen et al., 2011). Evaluation of print quality is dependent on a number of Quality Attributes, which are terms of perception, such as colorfulness, contrast and sharpness. These Quality Attributes influence the overall print quality differently, and knowledge about their importance can be used to achieve an optimal reproduction of an image (Fedorovskaya et al., 1993). These factors are directly related to line and dot quality, which are elements of any image, and are not easily identified by visual inspection alone. In order to obtain the bigger picture of print quality it is necessary to estimate the reproduction of image elements. It can be said that the line and dot structure reproducible by a particular printing process substantially influence the appearance of an image (Dhopade, 2009), which is why it is important to evaluate reproduction of these elements, together with the colour reproduction control.

In work by Pedersen et al. the Quality Attributes found in the literature are reduced to the following six (Pedersen et al., 2009): Colour, Lightness, Contrast, Sharpness, Artifacts (such as noise and banding) and Physical Quality Attributes (such as paper properties and gloss).

A group of engineers from Torrey Research Group (Torrey Pines Research, 2003) investigated influence of different attributes on print quality in ink-jet printing, stating that attributes they emphasized could be used to evaluate quality of any imaging systems. As the most critical to the evaluation of prints authors defined permanence, edge quality, artifacts, resolution/addressability, linear tonescale/colour reproduction and solid area quality. Some of these parameters are also accentuated by Dalal et al. (Dalal et al., 1998). Authors divided quality attributes in two groups: fundamental quality attributes and stability and material quality attributes. Attributes from the first group are visually relevant and could be assessed for both coated and uncoated substrates. Some of the addressed are: text and line quality, micro-uniformity, macro-uniformity, adjacency, gloss uniformity, effective resolution etc.

PVC substrates can be printed by screen printing, offset printing and digital ink-jet printing. Nowadays, PVC substrates are mostly printed by digital ink-jet printing technology, with UV or so called Latex inks. Latex inks are pigmented, water-based inks designed for commercial and industrial printing. Water-based inks offer environmental, health and safety advantages over eco-solvent/low solvent inks. Latex Inks consist of a liquid ink vehicle that carries latex polymer and pigment particles to the surface of the print media. Physical and chemical properties of the ink vehicle are critical both for drop ejection performance and control of ink-media interactions. Prints printed with these inks are fully dried inside the printer and do not require external dryer or drying time.

Latex inks enable printing on low-cost ucoated papers and foils with excellent image sharpness, while solvent inks require more expensive coated substrates to achieve the same results. These inks achieve excellent image quality- produce high-resolution prints up to 1200 dpi, with dense, saturated colours and offer display permanence and scratch-, smudge- and water resistance. Latex Inks have excellent flexibility and can stretch with the foils during mounting without cracking. In addition to this Latex inks soften, rather than dissolve, the surface of the print medium, providing better long-term adhesion and elasticity.

3. METHODS AND MATERIALS

Image quality attributes are primarily defined for ink-jet printing and had been evaluated for other digital printing techniques and offset printing. In this paper focus was placed on reproduction of image elements in ink-jet printing. The aim of this work was to evaluate the influence of substrate surface properties on quality of image elements in ink-jet printing. Three PVC self adhesive substrates with different surface properties were used. We chose to evaluate some of the basic print quality attributes – mottle, line quality and sharpness. Sharpness was estimated by measuring modulation transfer function. Reproduction of lines was estimated by measuring line area and perimeter. Mottle was chosen to measure non-uniformity in ink application. Analyses were performed on enlightened and non-enlightened substrates.

Printed test image was created with Adobe Illustrator CS5 software, containing different elements used for print quality control as shown in Figure 1. Test image dimension was 200 x 210 mm. Elements we used for obtaining the results were the ISO 12233 test chart, area for macro non- uniformity control, horizontal and vertical lines with width from 1/8 to 2 point and positive/ negative lines in cycles from 5 to 0,5 line pairs per mm.

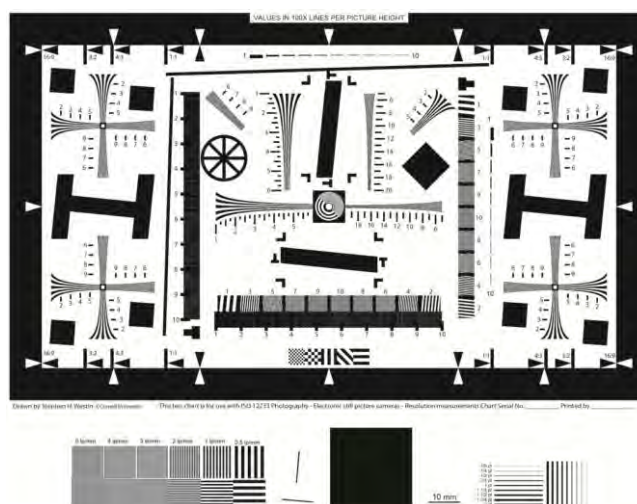


Figure 1. Test image used to evaluate print quality

Test image was printed on HP Designjet L65500 ink-jet printer, with HP Latex inks. Printing was performed at predefined 600 dpi resolution for printing materials. After printing, test image was digitalized by Canon EOS 20D digital camera, and the imaging resolution was set as 600 ppi. Recorded image was saved as separate tiff file.

Three PVC self adhesive materials were chosen for printing substrates, Neschen Solvoprint 80 GP (gloss surface), Neschen Solvoprint 80 GP Nolite (gloss surface), Neschen Solvoprint 80 MP (matte surface). All materials had a thickness of 80 µm. Neschen Solvoprint 80 GP Nolite had dark grey adhesive back side; the other two materials had transparent adhesive back side. Substrate specifications are given in Table 1.

Table 1. Printing substrates specifications

	Neschen Solvoprint 80 GP	Neschen Solvoprint 80 GP Nolite	Neschen Solvoprint 80 MP
Thickness (μm)	80	80	80
Gloss (graduations)	> 50 (20°measuring angle)	> 50 (20°measuring angle)	15 to 30 (85°measuring angle)
Adhesive type	Polyacrylate dispersion, transparent	Polyacrylate dispersion, black	Polyacrylate dispersion, transparent
Roughness Ra (μm)	0,414	0,578	2,767

Print sharpness was assessed by measuring modulation transfer function (MTF). The ability of a system to reproduce details is captured in its modulation transfer function (Bonnier and Lindner, 2010). MTF was measured by slanted edge method. The slanted edge method is often used to measure the MTF of a scanner or any capture device and can be adapted to measure the MTF of a printing system (Bang et al., 2008). During the analysis, one edge of digitalized test image is selected as the region of interest (ROI). The analysis is visualized in Figure 2. In each line of the ROI is a transition from black to white- a step function (Figure 2 a). The position of the transition of each step function is estimated and the lines are shifted, so that the transitions are all vertically aligned. Then the average of all the shifted step functions is calculated along this vertical line to reduce the influence of noise (Figure 2 b). The derivative of this mean step function is ideally a Dirac delta function, but in reality it is a peak of a certain width (Figure 2 c). The absolute value of the Fourier transform of this peak is the MTF (Figure 2 d) (Bonnier and Lindner, 2010).

In this work we used MTF50 parameter. MTF50 is spatial frequency where MTF is 50% of the low frequency MTF. Print quality of observed image could be established based on MTF50 parameter. It is necessary to divide MTF50 value (in LW/PH unit) with image height (inch as unit). In this work image height was 5 inch – printed ISO 12233 test chart height. To determine print quality obtained values are compared with reference values. Table 2 is guide to quality requirements.

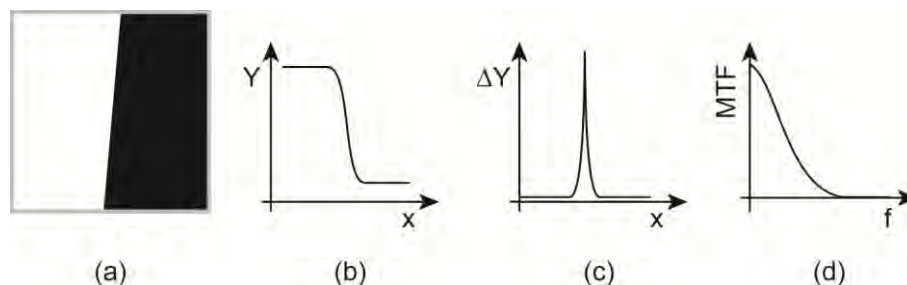


Figure 2. Basic principle for the MTF measurement with the slanted edge method: (a) region of interest, (b) average of Y values from shifted lines, (c) derivative with noise suppression, and (d) Fourier transform and normalization resulting in an estimation of the MTF

Table 2. Print Quality level according MTF50 parameter and image height

	Quality level
150	Excellent — Extremely sharp at any viewing distance
110	Very good — Large look excellent, though they won't look perfect under a magnifier. Small prints still look very good.
80	Good — Large prints look OK when viewed from normal distances, but somewhat soft when examined closely. Small prints look soft (adequate, perhaps, for the "average" consumer).

In a study by Lindberg was concluded that print quality can be defined by mottle and colour gamut (Pedersen et al., 2009). Mottling can be defined as undesired unevenness in perceived print density, or more precisely as nonuniformity occurring on a scale greater than 1.27 mm (Sadovnikov et al., 2005). Degree of mottling can be defined by mottling index, which ideally should be 0. Mottling index or so called non-uniformity number (NU) is calculated from average of dots intensity above median (U_x) and those under median (L_x) by following equation (Muck et al, 2009):

$$NU = U_x - L_x \quad (1)$$

By evaluating lines appearance on printed material quality of image reproduction can be determined. Ink bleeding tends to make lines wider; hence estimating the line width changes could determine the bleeding degree.

Line quality was assessed by measuring area and perimeter of 2 point thick black line. Lines were compared with the same elements from original test image. In this manner we determined degree of bleeding for black ink.

Sharpness of printed test images was analyzed by Imatest SFR software. Line quality and mottling index were determined by ImageJ software. In order to determine visual deviations, 2 point thick lines were captured with Sibress Pit camera (elements were magnified 40 times).

4. RESULTS AND DISCUSSION

4.1. Mottle

The degree of mottle was defined with non-uniformity number. Figures 3-4 show change in mottle on different substrates. The minimum values of non-uniformity number were obtained at Neschen Solvoprint 80 GP Nolite substrate (substrate with dark gray adhesive back side, gloss surface). The highest values of non-uniformity number were obtained at Neschen Solvoprint 80 MP (matte surface). On glossy substrates the higher NU values occur when substrates are non-enlightened, on matte substrates the higher NU values occur when substrates are enlightened.

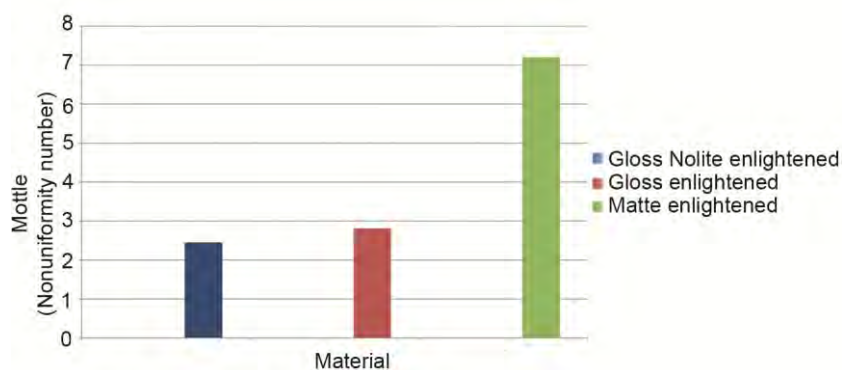


Figure 3. Degree of mottle (enlightened substrates)

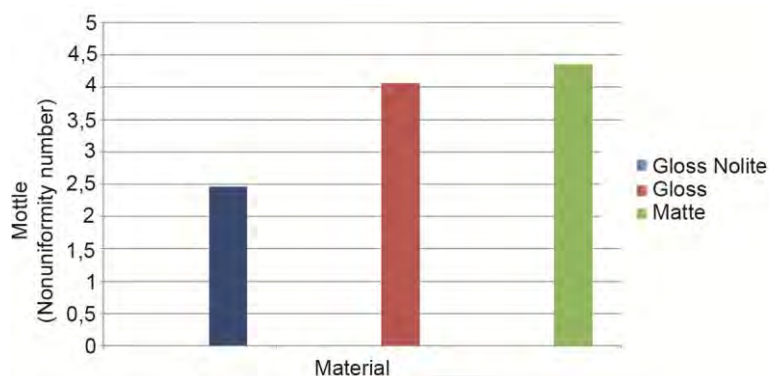


Figure 4. Degree of mottle (non-enlightened substrates)

As we can see in Figure 3 and 4 the matte material had the highest values of non-uniformity number and the gloss substrate with dark gray adhesive back side had the lowest values of non-uniformity number, in each case (enlightened and non-enlightened substrate). Substrate enlightenment caused increased values of non-uniformity number on matte substrate. The values of non-uniformity number on gloss substrate decreased by substrate enlightenment. The material with dark gray back side had approximately the same values of non-uniformity number in each case.

Figure 5 compares the magnified visuals of the extreme qualities with the sample image on the left having high percentage of the mottle.

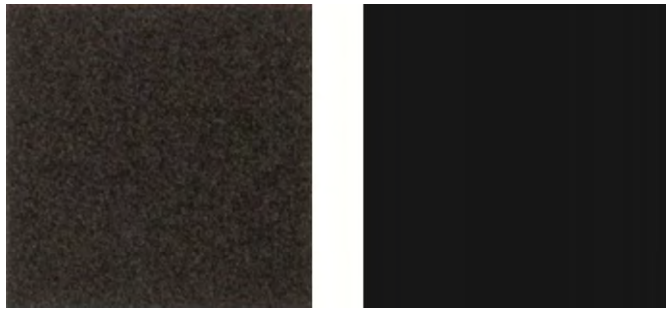


Figure 5. Mottle seen on enlightened matte substrate (left) vs. ideal simulation (right)

4.2. Line assessment

The line assessment as an important quality factor was obtained by digital image analysis of line area and line perimeter. Results obtained from the PVC substrates, where the 2pt thick lines were measured, are presented in Figure 6-7.

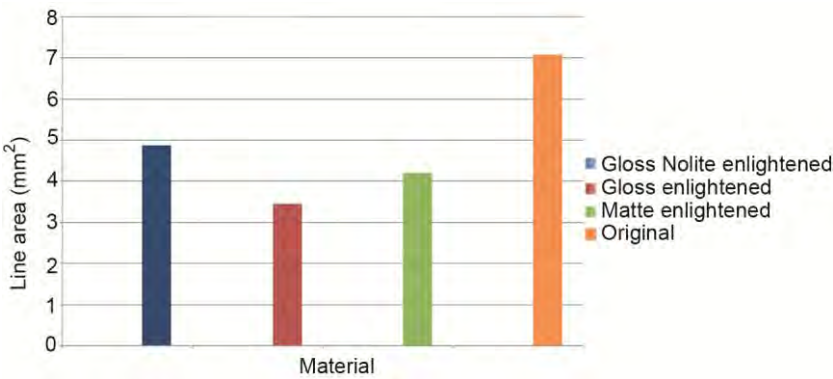


Figure 6. Areas of 2 pt thick lines (enlightened substrates)

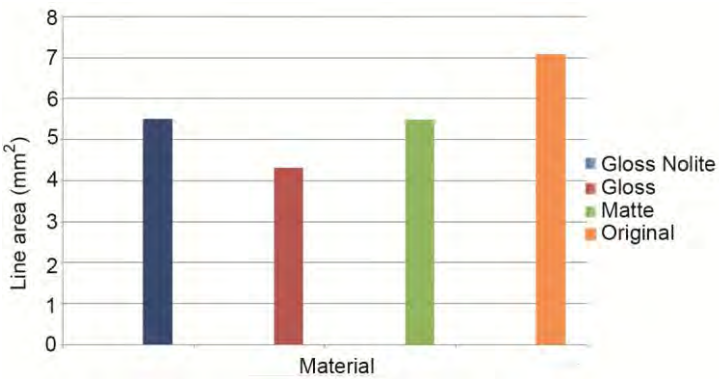


Figure 7. Areas of 2 pt thick lines (non-enlightened substrates)

Substrate enlightenment leads to a higher deviation in line area, as seen on Figures 5-6. Comparing glossy and matte substrates, higher line area deviations were obtained on glossy substrates. Results obtained from measuring 2 pt thick line perimeters are given on Figures 8-9.

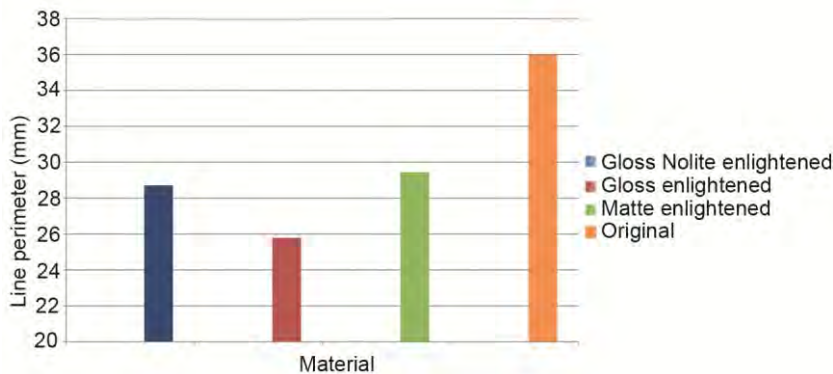


Figure 8. Perimeter of 2 pt thick line (enlightened substrates)

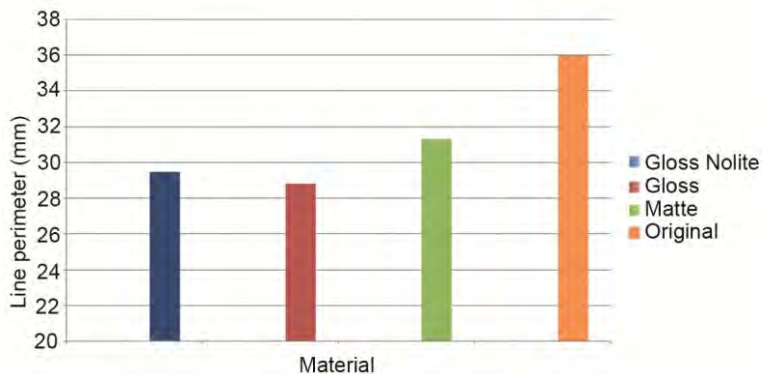


Figure 9. Perimeter of 2 pt thick line (non-enlightened substrates)

Similar to the line area deviations, substrate enlightenment leads to a higher deviation in line perimeter. Comparing glossy and matte substrates, higher line perimeter deviations were also obtained on glossy substrates. Figures 10 compares 2 pt thick lines printed on different substrates.

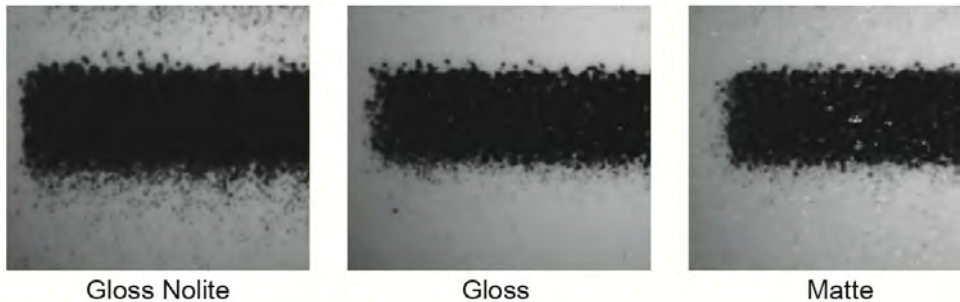


Figure 10. 2 pt lines on non-enlightened substrates

4.3. Sharpness assessment

The print sharpness was assessed by measuring modulation transfer function (MTF). Results obtained from the PVC substrates, where the MTF was measured on the ISO 12233 test chart by slanted edge method, are given in Table 3.

Table 3. MTF50 parameter value

	MTF50 (LW/PH)	
	Enlightened substrate	Non-enlightened substrate
Gloss Nolite	560,7	593,5
Gloss	812,2	770,8
Matte	799	902,8

Observing the enlightened substrates, the prints printed on gloss substrate (with transparent adhesive back side) have the highest value; while the prints printed on gloss substrate (with dark grey adhesive back side) have the lowest value. Hence, the prints printed on gloss substrate (with transparent adhesive back side) have the best quality level, the prints printed on matte substrate have a slightly lower quality level, and the prints printed on gloss substrate (with dark gray adhesive back side) have the lowest quality level, at the same distance.

On the non-enlightened substrate, the prints printed on matte substrate have the highest value. Hence, the prints printed on matte substrate have the best quality level, the prints printed on gloss substrate (with transparent adhesive back side) have a slightly lower quality level, and the prints printed on gloss substrate (with dark gray adhesive back side) have the lowest quality level, at the same distance.

Substrate enlightenment caused increased MTF50 values on gloss substrate. The MTF50 values on matte substrate decreased by substrate enlightenment. The material with dark gray back side had approximately the same MTF50 values in each case.

Print quality of observed images was established by dividing MTF50 value with image height 5 inch (Table 4).

Table 4. Quality level obtained by the MTF50 parameter and observed image height

	MTF50	
	Enlightened substrate	Non-enlightened substrate
Gloss Nolite	112,14	118,7
Gloss	162,44	154,16
Matte	159,8	180,56

The resulting quality level indicates that the prints printed on matte and gloss surface possess an excellent quality level, while prints printed on substrate with dark gray adhesive back side possess a very good quality level (in both cases, enlightened and non-enlightened substrate).

Figure 11 show positive/negative lines in cycles from 5 to 0,5 pairs per mm printed on enlightened gloss substrate (with dark gray adhesive back side) and enlightened matte substrate, as indicators of sharpness.

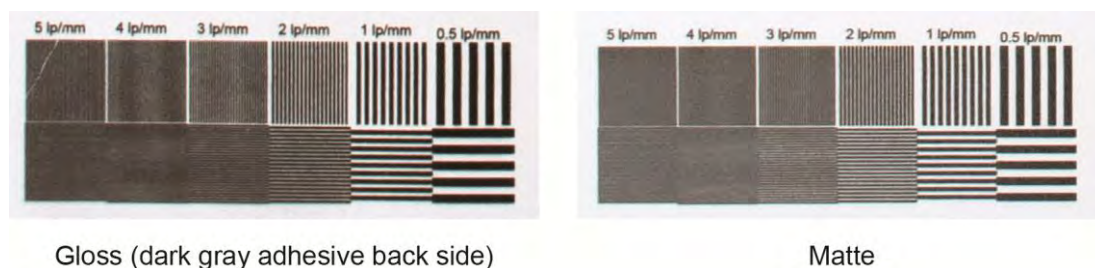


Figure 11. Positive/negative lines in cycles from 5 to 0,5 pairs per mm

5. CONCLUSIONS

In this work assessment of influence of substrate surface properties on quality of image elements in ink-jet printing was conducted. We performed printing of test image on three PVC self adhesive substrates with different surface properties. Using image analysis we evaluated mottle, line quality and sharpness on enlightened and non-enlightened substrates.

From changes in nonuniformity number it was concluded that mottle was more noticeable for matte substrate. Gloss surface enlightenment decreases mottle index, while matte surface enlightenment increases mottle index.

Line quality assessment showed that line areas and perimeters decreased from ideal case for all substrate used. Higher deviations were obtained on gloss substrates. Comparing two gloss substrates, line deviations were less noticeable for substrate with dark grey adhesive back side. Sharpness assessment showed that quality level on enlightened substrate was higher on gloss substrate, while on non-enlightened substrate quality level was higher on matte substrate. Lowest quality level was reached on substrate with dark grey adhesive back side. Taking all results into account it can be concluded that substrate surface properties affects the print quality attributes. It was also noticed that substrate enlightenment and adhesive back side properties also has some influence on the print quality. In order to confirm these findings further testing should be performed, where more substrates with the different adhesive back side type and thickness should be evaluated.

6. LITERATURE

- [1] Bang, Y., Kim, S., Choi, D.: "Printer resolution measurement based on slanted edge method", URL <http://144.206.159.178/ft/CONF/16408531/16408537.pdf> (last request: 2012-07-10).
- [2] Bonnier, N., Lindner, A.: "Measurement and compensation of printer modulation transfer function", URL http://nicobonnier.free.fr/research/publications/JEI_2010_Bonnier (last request: 2012-07-05).
- [3] Dalal, E., Rasmussen, D., Nakaya, F., Crean, P., Sato, M.: "Evaluating the overall image quality of hardcopy output" Proceedings of Image Processing, Image Quality, Image Capture, Systems Conference 1998, (IS&T: Portland, Oregon, USA, 1998), pages 169-173.
- [4] Dhopade, A.: "Image Quality Assessment According to ISO 13660 and ISO 19751", URL http://cias.rit.edu/~gravure/tt/pdf/pc/TT9_image_quality_assessment.pdf (last request: 2012-06-12).
- [5] Fedorovskaya, E., Blommaert, F., De Ridder, H.: "Perceptual quality of color images of natural scenes transformed in CIELUV color space" Proceedings of Color Imaging Conference 1993, (IS&T/SID: Scottsdale, Arizona, USA, 1993), pages 37-40.
- [6] Muck, T., Hladnik, A., Stanić, M.: „Analiza tiskovne kakovosti z orodjem ImageJ = Analysis of print quality with ImageJ“, URL <http://www.ot.ntf.uni-lj.si/simpozij2009/zbornik.pdf> (last request: 2012-06-15).
- [7] Pedersen, M., Bonnier, N., Hardeberg, J., Albregtsen, F.: "Attributes of a New Image Quality Model for Color Prints" Proceedings of Color Imaging Conference 2009, (IS&T/SID: Albuquerque, New Mexico, USA, 2009), pages 204-209.
- [8] Pedersen, M., Bonnier, N., Hardeberg, J.: „Image quality metrics for the evaluation of print quality“, URL <http://colorlab.no/content/download/30728/366341/file/ISQP2011.pdf> (last request: 2012-07-11).
- [9] Sadovnikov, A., Salmela, P., Lensu, L., Kamarainen, J., Kälviäinen, H.: „Mottling Assessment of Solid Printed Areas and Its Correlation to Perceived Uniformity“, URL http://www2.it.lut.fi/kurssit/04-05/010976000/mottling_scia.pdf (last request: 2012-06-15).
- [10] Torrey Pines Research: "Inkjet Print Image Quality Considerations: PEARLS", URL <http://www.tpr.com/PDFFiles/Pearls-white-paper-tpr.pdf> (last request: 2012-06-25).

PRINTING OF FOLDING CARTON BY DIGITAL TECHNOLOGIES

Rozália Szentgyörgyvölgyi, Óbuda University, Rejtő Sándor
Faculty of Light Industry and Environmental Engineering

Corresponding author: Rozália Szentgyörgyvölgyi
e-mail: szentgyorgyvolygi.rozsa@rkk.uni-obuda.hu

1. ABSTRACT

*The market share of the digitally printed packaging materials in the world is in constant rise. The reason for this is the rapid improvement of the quality and efficiency of these printing technologies, as well the increase in demand of small print run packaging by the producers. In this paper we have researched prints made with electro photographic and inkjet which were made on cardboard substrates. Four different cardboard substrates which differed in surface properties were printed with Xerox Docucolor 12, Xerox iGen3, Canon ImagePress C1 and Canon Pixma iX6550. On the prints we have measured the optical properties (TVI, ΔE^*_{ab} , reproducible gamut). The largest TVI on all cardboards was found with the Canon Pixma iX6550 inkjet printer and also the largest colour offsets were measured on these samples. The reference for the samples was the ISO 12647/2: 2004. The smallest colour difference was achieved on Canon ImagePress C1 electro photographic prints while the largest colour difference was measured on the prints made by Canon Pixma iX6550 inkjet printer.*

Key words: folding carton, electro photography, inkjet, colour gamut

2. INTRODUCTION

The market share of the digitally printed packaging materials in the world is in constant rise. The reason for this is the rapid improvement of the quality and efficiency of these printing technologies, as well the increase in demand of small print run packaging by the producers.

The increase in the demand for small print run packaging with special effects is driven by the marketing and sales opportunities in the beverage and other consumer markets. High end color print on demand (POD) digital presses, are now well established and growing in the packaging industry. Approximately 1150 these types of installations were running in the world in 2009. 85% of these systems were based on electro photography [1]. Color digital folding cartons are mostly printed by color electro photographic POD presses. About 1150 such systems were operated worldwide in the beginning of 2009 [2]. Folding cartons are much more difficult to print and convert with POD equipment. The size of the printed image is often a problem and finishing for each of these applications involves specialized equipment. Also the media are in often challenging. Folding cartons produced by digital printing in offset quality is the most important for the folding carton manufacturers.

Our work focuses on digital printing characteristics on cardboard substrates. We investigated quality of test prints printed by electro photographic and inkjet technologies, different types of cardboard substrates, with varies thickness and surface properties.

3. METHODS

In our studies, four different types of cardboard substrates were used. Duplex 2 layer coated chromo carton, with grey backing (#1), Grafopak 3 layer coated chromo carton, with grey backing (#2), GC2-235 3 layer coated chromo carton, with grey backing (#3) and GC2-250 3 layer coated chromo carton, with grey backing (#4) (Table 1).

Table 1: Printing substrates

cardboard	#1	#2	#3	#4
type	Duplex	Grafopak	GC2-235	GC2-250
property	2 layer coated chromo-carton, grey backing	3 layer coated chromo-carton, grey backing	3 layer coated chromo-carton, light backing	3 layer coated chromo-carton, light backing

In the first phase of the studies, the physical properties of the cardboards have been examined. Surface smoothness was measured with the use of a Beck smoothness tester and we measured the caliper of the cardboards (Table 2).

Table 2: Substrate properties

Property	#1	#2	#3	#4
caliper, mm	0,393	0,309	0,333	0,312
g/m ²	250	250	235	250
smoothness, s	50,3	105,7	65,54	210,0

The test image was designed with the use of the Adobe Indesign CS2 program. It contained the measuring fields, as well as the test stripes to be used for the purpose of our measurements and it included visual, densitometric and spectrophotometric test elements. It has been printed on A4-sized substrates (Figure 1).

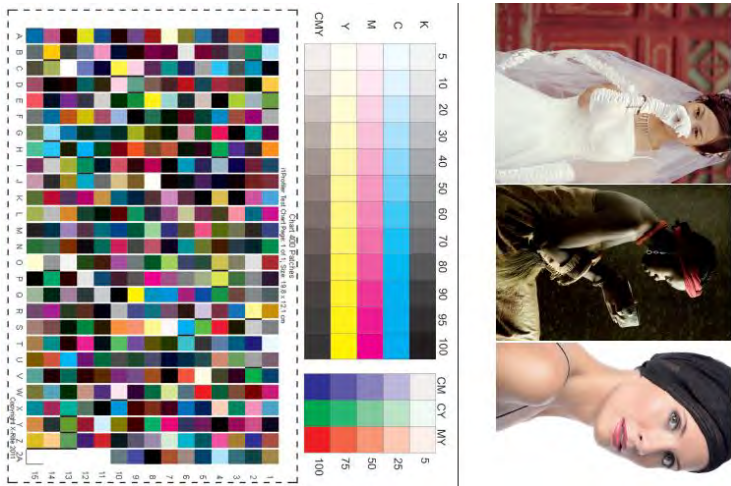


Figure 1: Test image

Four different cardboard substrates were printed with three different types of electro photographic printers and an inkjet printer. Each test print was made in one copy, with the use of electro photographic and inkjet printers, under identical circumstances and conditions. Test printing was performed under normal operating conditions as follows: printing machines: Xerox Docucolor 12, Xerox iGen3, Canon ImagePress C1 electro photographic printers and Canon Pixma iX6550 inkjet printer, T=21-22 °C, RH 39-44%. Substrate #4 (GC2-250) was not printed by Canon ImagePress C1 electro photographic printer, because of surface problems.

4. RESULTS AND DISCUSSION

The reproducible color gamut increases together with ink coverage but ink spreading will also increase together with TVI. All properties influence print quality. The objective is to achieve the largest gamut along with keeping the TVI in an acceptable range [3] [4]. Our research focused on the digital print quality on cardboard substrates. To perform optical properties on the test prints, an X-Rite SpectroEye spectrophotometer was used. The conditions of measurements were as follows: 380-780 nm spectral range, 0°:45°a measurement geometry, 4.5 mm aperture diameter, D65 filter. Surface smoothness of the substrates, and optical characteristics (optical density, tone values increase, colour difference) of the prints were determined.

4.1. Tone value increase of CMYK prints

CMYK print optical density values (D) were the highest in the case of Docucolor 12 (C: D=1,19-2,26; M: D=1,62-1,81; Y: D=1,71-1,79; K: D=2,37-2,51), the lowest were produced by Canon Pixma iX6550 printer (C: D=0,91-1,01; M: D=0,88-1,16; Y: D=0,76-0,94; K: D=0,83-1,00).

All substrates produced the highest TVI values with Canon Pixma iX6550 inkjet printer on the 40%-os halftone patch (TVI_{40} =18-45%, for all process colours). A lowest TVI values were measured on Canon ImagePress C1 electro photographic printer (TVI_{40} =5-20%, for all process colours) (Table 3). The highest TVI values were seen in case of the cyan process colour (Figure 2).

Table 3: TVI values on a 40% halftone patch

Printer	TVI_{40} , %			
	#1	#2	#3	#4
Docucolor 12	10-18	6-19	11-23	13-27
iGen	12-23	13-22	16-24	18-26
Canon Pixma iX6550	36-44	32-44	32-45	18-42
Canon ImagePress C1	5-16	13-18	15-20	-

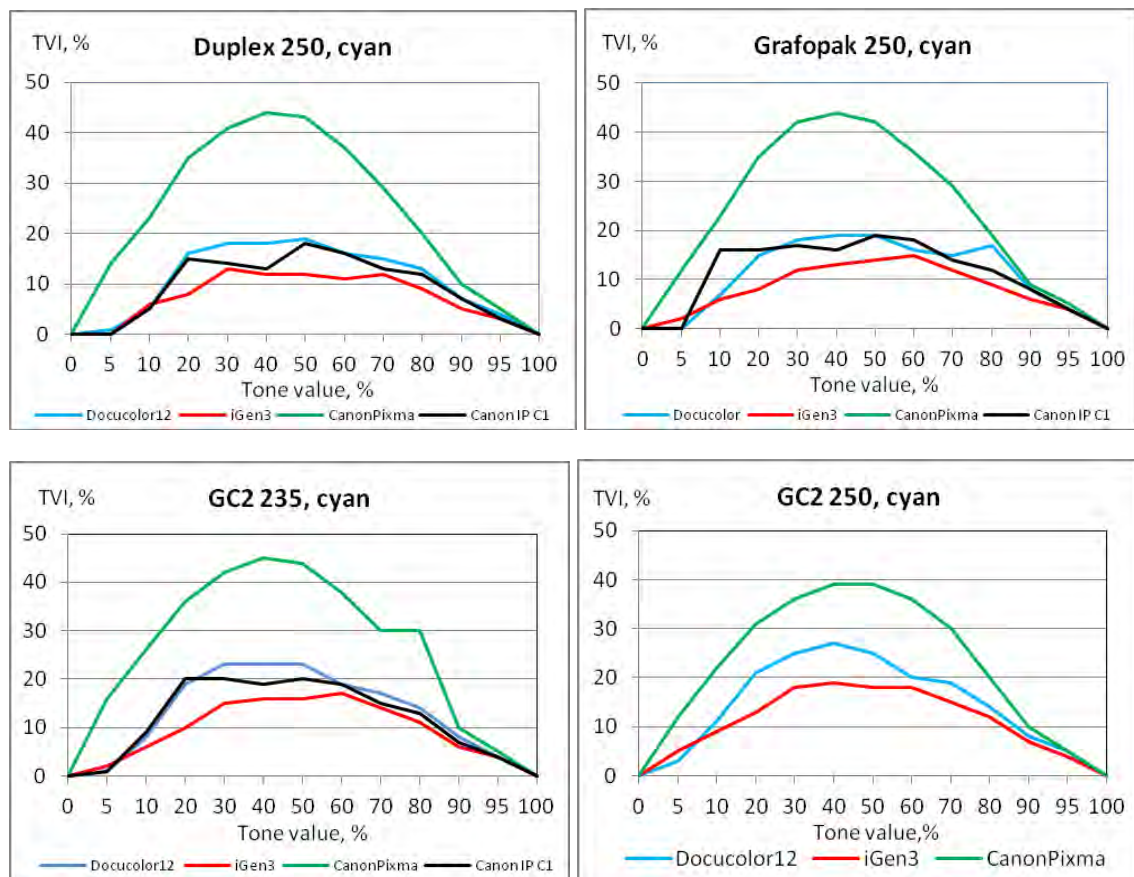


Figure 2: TVI curves of cyan prints

4.2. Colour differences

Tone value increase will influence color which makes it important to investigate colour differences on the prints. The measurements were performed on color control patches of CMYK and RGB, with the use of the X-rite SpectroEye spectrophotometer. The $L^*a^*b^*$ colour coordinates were measured on the prints, and ΔE^*_{ab} colour differences in relation to the reference print were calculated. It was chosen sample #4 as the etalon ($L=96,17$).

The highest color differences were found on prints produced by Canon Pixma iX6550 inkjet printer, on both sets of the process (CMYK) and secondary (RGB) colours (Figure 4 and 5).

Table 4: ΔE^*_{ab} colour differences of the CMYK prints

Printer	ΔE^*_{ab}											
	#1				#2				#3			
	C	M	Y	K	C	M	Y	K	C	M	Y	K
Docucolor 12	2,5	4,2	3,0	3,5	1,4	2,5	0,4	1,9	0,9	0,9	0,4	0,6
iGen	2,2	2,0	1,8	3,2	0,5	1,3	1,0	2,0	1,8	1,1	1,1	0,6
Canon Pixma iX6550	2,7	4,5	3,4	7,5	1,6	2,9	6,8	0,4	4,1	5,0	3,6	3,2
Canon ImagePress C1	2,4	3,7	6,6	3,0	1,6	1,0	0,5	0,8	-	-	-	-

Table 5: ΔE^*_{ab} colour differences of the RGB prints

Printer	ΔE^*_{ab}								
	#1			#2			#3		
	R	G	B	R	G	B	R	G	B
Docucolor 12	1,7	4,1	3,4	1,4	1,7	1,6	2,2	2,1	1,4
iGen	5,8	7,5	6,7	0,9	3,7	3,7	3,1	2,3	1,6
Canon Pixma iX6550	8,2	6,2	6,1	5,1	4,3	2,4	2,4	3,2	3,0
Canon ImagePress C1	4,0	5,5	2,9	2,0	2,3	1,2	-	-	-

Colour differences were compared to the ($L^*a^*b^*$) values of the ISO 12647-2: 2004 offset standard. All ΔE^*_{ab} values exceeded the tolerance ranges. The smallest CMYK colour difference ($\Delta E^*_{ab}=3,3-7,7$) és RGB colour difference ($\Delta E^*_{ab}=3,3-9,3$) were produced by Canon ImagePress C1 press. The highest colour differences were found on samples printed with Canon Pixma iX6550 ($\Delta E^*_{ab}=19,0-45,4$).

4.3. Colour gamuts

The range of reproducible colors (gamut) depends on the printing process and the substrate and other printing materials used. We used a software tool commonly applied in proofing color workflows to visualize and compare the color gamut achievable on the substrates investigated. First, printer profiles were generated using X-Rite EyeOne Pro measurement device and profiling software. A standard CMYK test chart with 323 patches was printed on the substrates of this study, by both printing presses to sample the printable color solid. The profiles were loaded to the gamut visualization tool, which calculated printable gamut in CIELAB color space volume units. Relative printable gamut sizes are shown in table 6, the largest gamut is taken as reference for every ink-printer combination. The maximum colour range reproduced in the print that have been made with the Canon ImagePress C1 printer on GC2 (250 g/m²) cardboard and the minimum colour range reproduced with the Canon PIXMA iX6550 printer on Duplex cardboard. Considerable differences (approx. 80%) can be observed in between the gamut volumes in the case of inkjet and electro photography printers (Figure 3). We experienced less than 13% colour gamut shrinking in case of all substrates printed with electro photographic technology.

Table 6: Relative values of computed printable gamut volumes on cardboard substrates using two types of printers, based on spectral measurements of a CMYK test chart containing 323 halftone patches

Printer	Relative values of computed printable gamut			
	#1	#2	#3	#4
Docucolor 12	0,90	0,91	0,94	0,97
iGen	0,82	0,86	0,87	0,90
Canon Pixma iX6550	0,17	0,25	0,20	0,23
Canon ImagePress C1	0,91	0,95	1,00	-

The largest gamut was produced on substrate #3 printed by Canon ImagePress C1 electro photographic printer, the smallest was produced on substrate #1 by Canon Pixma iX6550 inkjet printer (Figure 3).

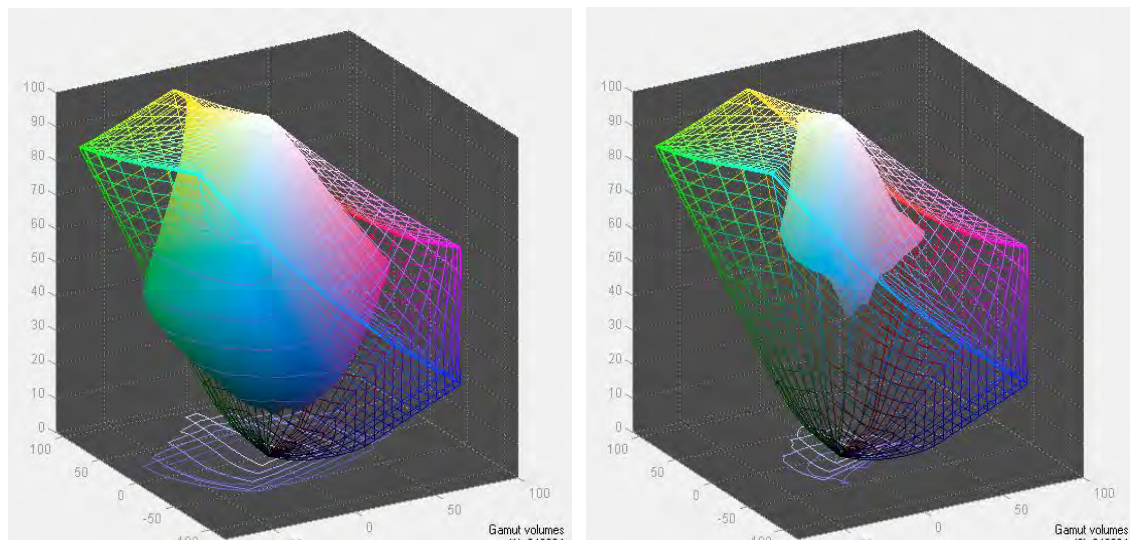


Figure 3: Colour ranges that can be presented in the CIELAB colour space on cardboard substrates, wherein the spatial mesh body represents the standard sRGB colour space (left: maximum: Canon ImagePress C1/GC2-1; right: minimum: Canon Pixma iX 6550/Duplex)

5. CONCLUSIONS

Our research focused on electro photographic and inkjet print quality on cardboard substrates. The test prints have been made on four types of cardboard substrates with the use of the electro photographic Docucolor12, Xerox iGen, Canon ImagePRESS C1 and inkjet Canon PIXMA iX6550 printers. The optical properties of the test prints (tone value increase, and reproducible colour range) have been measured.

In the light of the results, it can be stated that the Docucolor12 printer has produced prints of higher optical density on all the cardboards.

The largest TVI value and most outstanding reproducible colour range have been found for the GC2-250 cardboard for all devices. In the case of the GC2-235 cardboard, the inkjet technique has resulted in the smallest reproducible colour gamut, whereas the electro photographic of Canon ImagePress C1 printer procedure has yielded the largest reproducible colour gamut. The smallest TVI values were also measured in the case of Canon ImagePress C1.

The highest colour difference values were experienced on prints produced by Canon Pixma iX 6550 inkjet printer for the process colours and the secondary colours as well. Colour gamut of Canon PIXMA iX6550 inkjet printer was 75-80% smaller on every substrates. Generally 9-13% colour gamut reduction was experienced on electro photographic prints on all substrates of the study.

6. LITERATURE

- [1] „Insight Report Highlights Importance of Greater Customer Communication“, Canon Europe, 2012
- [2] „Color Digital Printing in Packaging and Prime Labels: A Multie-Client Report“, InfoTrends, 2010
- [3] K. Smith, S. Moriarty, G. Barbatsis, K. Kenney: „Handbook of Visual Communication - Theory, Methods, And Media“ (601s), LEA, London, 2005
- [4] Novotny, E.:Colour management with standard colour profiles. Proceedings of GRID'08, Novi Sad, Serbia, pages 165-171.



Colour Science



CASE STUDY CARBON BLACK SEPARATION EXTENDED FEATURES

Agić, D., Rudolf, M., Agić, A., Stanić-Loknar, N., Faculty of Graphic Arts, Zagreb

Corresponding author: Darko Agić
e-mail: darko.agic@grf.hr

1. ABSTRACT

Case study in work is determining extended black separation in current graphic arts, in infra red properties. Graphic reproduction is generally based on screening system, principles of subtractive synthesis and separation with mostly added black, with infrared Z absorption. Subtractive ternary color combinations could be partially substituted with black, that can lead to achromatic way of reproduction, with various extended possibilities. The aim is to prove stability of achromatic system, and operating in NIR domain, as wide acceptance is desirable.

Key words: subtractive, carbon black separation, achromatic, NIR

2. INTRODUCTION

One of the differences of color photography and graphic arts printing is that photography utilizes subtractive primaries in layers. Graphic arts technology mainly practices fourth, black channel or separation. Some of the reasons are that color photography generates colorants during chemical development, according to optical sensitivity of layers. Besides that, density (or saturation) of obtained dyestuffs in layers is enough high, that in subtractive mixing process experience of "black" is obtained (fig.1) (1). Graphic reproduction usually reaches lower values (lower high density and density range), so trichromatic achieved black is often rather not satiable according to density, as well not neutral hue. For that, and some other reasons, fourth separation "color" as black separation or printer is added to the reproduction system (2). If utilization in NIR part of the spectrum is also demanded, so that the second image can be imaged, preparing the system has to be maintained through visual management.

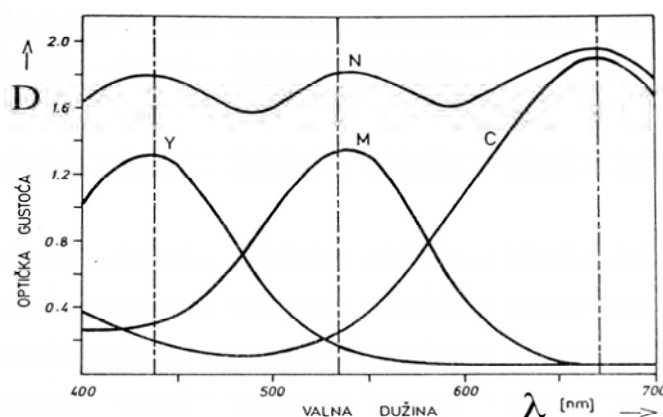


Fig.1. Forming neutral experience from three subtractive primaries (3)

3. BLACK SEPARATION

There were various ways for achieving the black separation. In photomechanical technology usage of (red, green and blue) filters "narrow or wide" meaning spectral response were in use, although some other colored filters (yellowish, pink, etc.) could be utilized according the light source used, depending of the color temperature of the source and spectral (panchromatic) characteristic of the photographic material used.

Program aided systems generate black separation applying RGB/CMYK color system tables for dedicated profile. Also programmed systems apply appropriate profile for the output system, so pure PS (postscript) equations could not be used directly.

Basically, reproduction curves (CMY+K) could fit the coverage range from 0 to 100 (%, coverage), but according the output system these values mostly differ, meaning they mostly in practice are downsized. In that step two elementary facts still impact that: TAC (total area coverage) would get till 400% value, what is most practical purposes is not acceptable, and gray balance is not taken in respect at that moment. TAC and gray balance, between other parameters are incorporated in ISO specification, although often some parameters such as screening system and BRC (basic reproduction curves) are suggested from various equipment suppliers (4).

Basic black separation can be carried out in two ways: full tonal range (FTR black) and skeleton range (SR black), Fig 2. They differ in highlight/midtone range. Standard situation question is, if two different black separation systems in various reproduction systems have to be used, how to achieve the same visual perception as well same density. That leads to program (or generate) customized CMY BRC to compensate in highlights/midtones missing part of skeleton k coverage. Sometimes non standard screening systems are suggested (5).

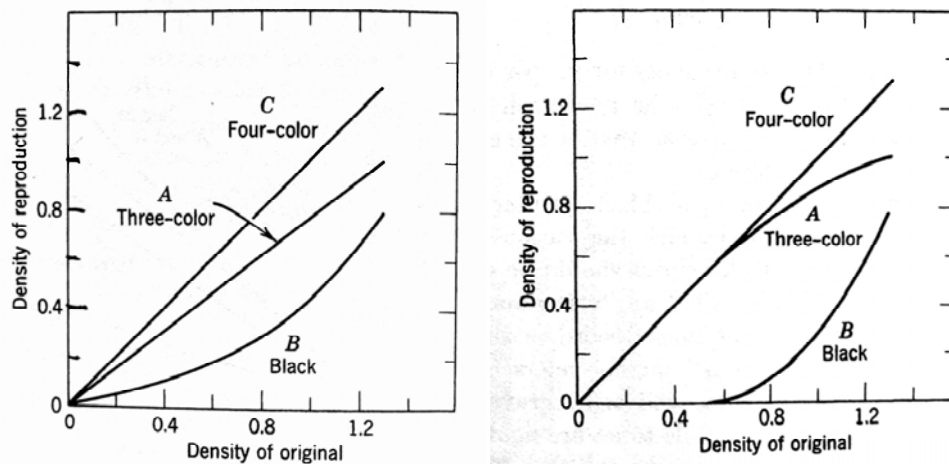


Fig. 2. BRC (full tone range black left, SR black, right)

4. ACHROMATIC REDUCTION

As standard “color”, meaning CMYK reproduction would, as mentioned, have high entire coverage (total CMYK coverage could reach till $\hat{a}=4$), for practical/technical and financial reasons achromatic reduction is applied enabling various possible benefits (6). This covers the situation that in some CMY combination representing a color, common CMY part according to principles of subtractive synthesis can be substituted with K. Unfortunately, the additive failure (7) and other light catching, scattering and similar effects can lead to decreasing of overall density, lower gamut and can impact grayness. ISO (7) regulates TAC for standard reproduction systems conditions.

Photomechanical systems and analog scanners practically were applying UCR (under color reduction, Farbrücknahme) according to their suitability, meaning substituting in gray scale common or possible content of CMY component (in separations) with black, raising (rather) proportionally black coverage in black separation. Digital systems distinguish gray parts and other parts consisting trichromatic CMY combination, forming CCR (complementary color reduction), PCR (polychromatic color reduction) converting/reducing program module. Basic display of a possible reduction, Fig 3. presents a CMY combination achieving come colored output (impression), and possible reductions that should achieve the same visual output. Reduced combinations consist of lower CMY content and higher K content, lowering ultimate TAC. Final reduction situation would be only two chromatic components, in this case yc and black. The question besides technical and visual benefits, is it advisable to apply high or maximum reduction (100% possible reduction) has no simple answer, as it depends on dyes-substrate interactions and whole printing system.

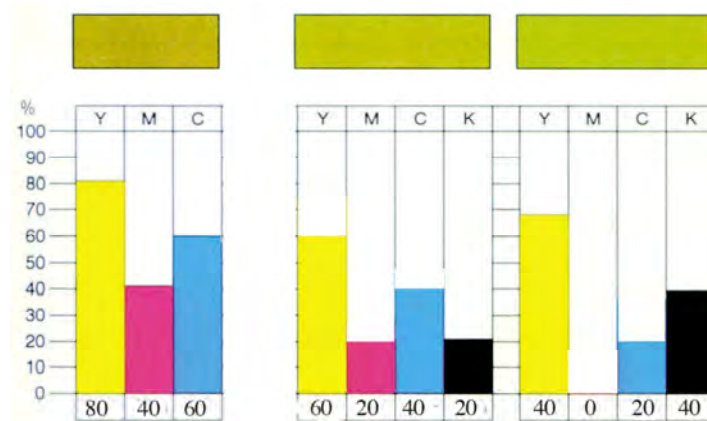


Fig.3. possible achromatic reductions for a trichromatic color patch

ISO (7) regulation suggests a reasonable amount for the system applied. Some authors treat these achromatic reduction possibilities as an advanced black separation (8) practically not distinguishing chromatic or neutral part of image. It has to be mentioned by programmed reproduction (9), if high yield of achromatic reduction is applied and ultimate reduction is performed, density and gamut features could be lowered, and BRC as well reproduction properties are probably cut down.

5. NIR RESPONSE

Common color management encloses visual response, meaning wavelengths approximately from 400-700 nm. It covers separation principles, RGB to CMYK conversion, BRC, black generation, achromatic systems, implementation of input and output properties (gamuts) of devices used, illuminants characteristics, rendering intent systems, and other features. Special colors as, UV (security), can be visualized by usage of black (UV) light and then imaged and valued and valued by standard imaging means (11). Further wavelengths, near infra red (NIR) till 1000 nm are not directly human visible, but have interesting features in response. In reproduction most standard colorants (dyes) are organic origin, while black component is often carbon black. It appears that most standard chromatic dyes render relative high response (reflection), while carbon black has rather low response, Fig 4, so differentiating can be performed in NIR during preparing visual preferences, and second image is fulfilled within black separation.

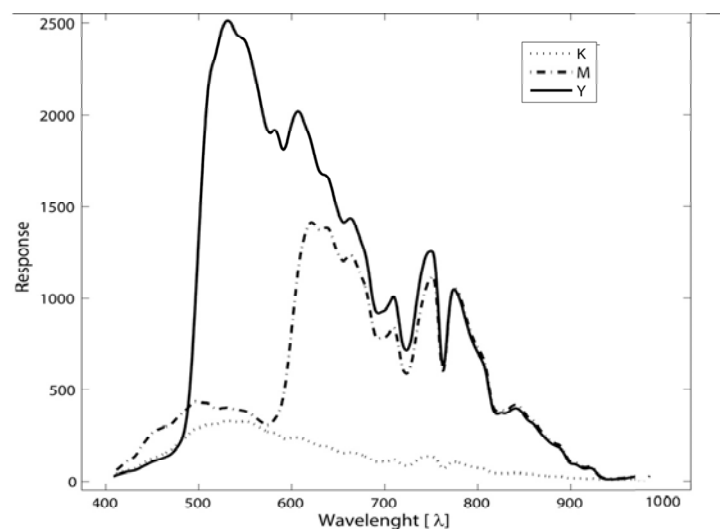


Fig.4. response of magenta, yellow and black in visual and NIR spectrum (Ocean Optics radiometer S2000)

This response can be treated and considered as relative reflection or absorption, recounted as relative density or quantified and valuated as proposed Z value for NIR design purposes. (12) Visualization is mainly simple. Many common, often used light sensitive devices (with CCD chip) in a variety of usual devices such as standard amateur cameras covers this wavelength area also (night shot function), Fig 5. The “cut off” effect is performed by common IR filters, while chip function “cuts” above 1000 nm, and filter under 700 nm, or any desired value. (Fig. 6). (13)

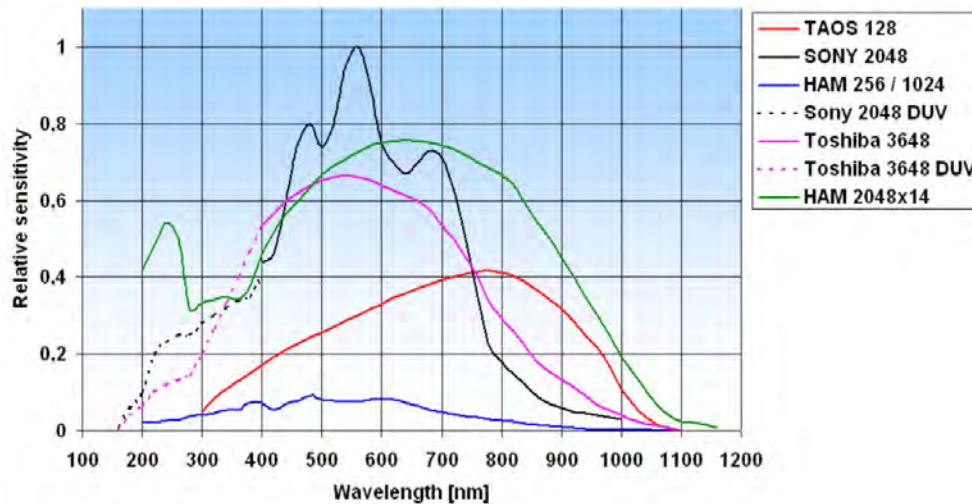


Fig 5. Visual and NIR response of various CCD chips

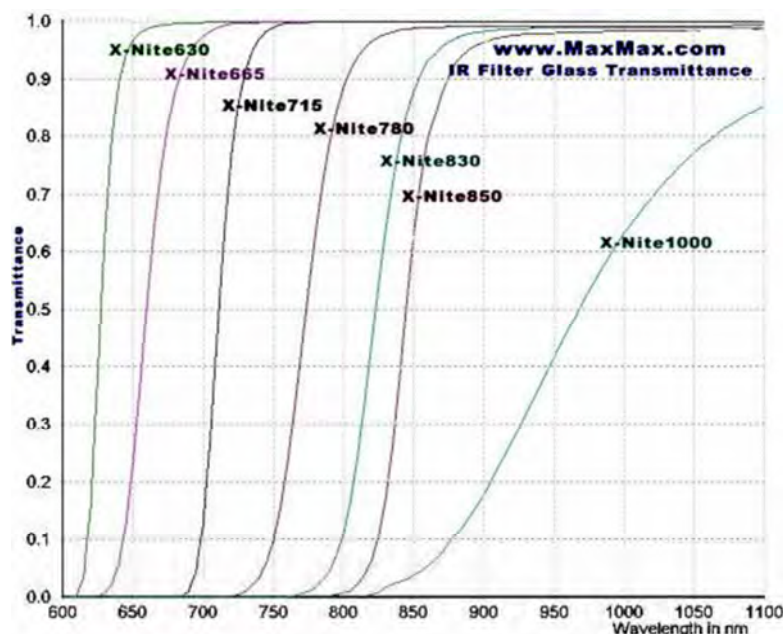


Fig.6. Transmittance of various IR filters

All these situations can lead to very interesting, moreover usable situations in various reproduction fields, but are also very sensible to deployed working conditions. The fact is that visible and IR part become one unity, although they cannot be observed direct simultaneously, already IR part needs a IR device support. Significant is, that through management of visible colors IR properties are assessed.

In visible it is possible to generate metameric pairs of color (patches), one in “pure” CMY combination, other in preferred CMYK. On the level of pixel graphics or dedicated screening system, some elements (steganographic) can be “hidden” in K channel, and be observed only with NIR system. Repeating the process through scanning discards the effect.

6. CASE STUDY FOR ACHROMATIC COMBINATIONS

For a presumed demand to get desired colors (in this case colored patches) possible to be enforced in various reproduction systems, series of combinations were generated (Fig. 7). The screen system was set to 5500K and sRGB gamut. Each patch was separated in two parts and generated as a CMY and medium reduction CMYK combination, sustaining the same Lab values.



Fig.7. Generated patches (Mediaware substrate)

The output was performed on quality substrate (output Epson Stylus 3800 on Mediaware Pearl Gloss Super). In this stage is advisable to check out, for assumed viewing conditions e.g. daylight and artificial light, possible viewing changes by means of some difference measure such as metameric index (MI) or similar, and manage output profiles with rendering intent mode that could fit optimal for various conditions. Rather simple tool for this purpose was Tiffen (similar to Kodak guide) separation color chart (14) (Fig. 8) and Tiffen gray scale. Patches are calibrated, so simplified but usable examination of overall colorimetric properties on reproduction could be performed on realized images. During determining that card values were used for preliminary gamuts and color positioning.

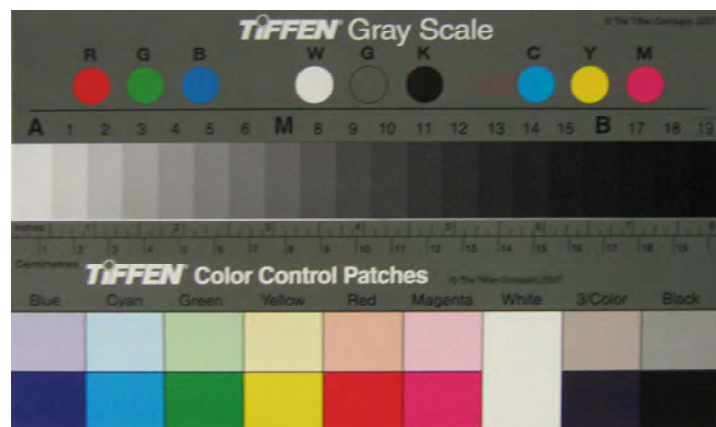


Fig.8. Control wedge

Table 1: colorimetric values of calibrated wedge (D50 2 deg)

	L*	a*	b*
Blue (light)	70.21	7.76	-17.45
Cyan (light)	83.75	-14.39	-14.39
Green (light)	81.36	-19.58	12.76
Yellow (light)	95.39	-2.65	32.14
Red (light)	78.16	23.4	19.62
Magenta (light)	80.04	25.27	-3.11
White (top)	97.54	0.18	1.098
3/Color (light)	69.39	3.57	1.81
Black (light)	69.31	0.19	2.17
Blue (dark)	29.38	16.77	-43.51
Cyan (dark)	60.56	-38.15	-43.71
Green (dark)	53.21	-62.01	26.74
Yellow (dark)	91.64	-2.46	89.91
Red (dark)	49.07	68.83	38.51
Magenta (dark)	50.95	72.63	-3.11
White (bottom)	97.54	0.18	1.098
3/Color (dark)	28.21	-0.22	-9.15
Black (dark)	23.97	0.18	1.21

Patches for reproduction were so chosen that fit the proposed, but not to large gamut of output device. Their chromaticity and saturation are not to high, and they can form complete CMYK combination, Table 2. The black content was through black generation set to medium.

Table 2: basic values for examined patches

	E2	E3	F3
Lab	44 17 16	42 57 12	39 48 2
RGB (profile)	176 64 80	159 50 91	181 42 83
CMY (profile)	35 88 61	46 92 52	33 95 68

The rendering intend (abs) colorimetric was applied, so it supposed that various output systems could fit. For testing patches F3 E3 and E2 were chosen for determination, as they don't differ a lot in hue, the difference between CMY and CMYK combination doesn't exceed colorimetric difference above 6 Observed in the light boot (D50 illuminant and artificial light) did not show significant difference.

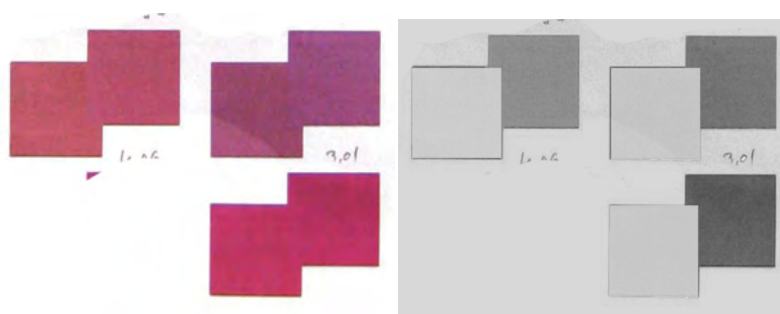


Fig.9. Selected patches F3 E3 and E2 for visual and NIR reproduction

Several usual substrates were chosen, to testify the stability of achromatic reduction system and the possibility of stable NIR image.

NIR estimation

For NIR investigation preliminary step contained metameric pairs for desired color patches that were programmed with the same Lab value. The part with "K" component was prepared with

high achromatic amount, but as lightness changes within the patches various shades in NIR are expected. In advance the gamut was determined, and proved that chosen colors patches are within the proposed system. Besides primary chosen substrate, several other usual were experienced with or without simple standardization of the system. For NIR purposes snapshot was taken in visible light, followed by adjusted NIR system camera (15).

Differentiation between "pure" CMY and (reduced) CMYK was by standard means visualized, so that difference between responses can be visualized.

7. DISCUSSION

On tested materials, differentiation between CMY and reduced combination in acceptable, although reduced combination has lower TAC, that is mainly wanted. Visually they are mainly similar in both viewing conditions. As on fig. 9 colorimetric difference for a quality substrate is from 5.86 (patch E2) to 2.98 (patch F3). Less quality materials by higher reductions show some more colorimetric difference, as saturation decreases, particular. Reduced patches (colors) appear rather stable than trichromatic, gain better gray balance features, render shades and details, reach faster drying and lower printing problems. That leads to answer what is the importance of reduced achromatic way of reproduction, where stability of reproduction, not only in one printing system is improved, and changing of optical properties is lowering. This is not an universal condition for any possible color, as technical and mechanical properties (gamut, densities, lightness, profiles, properties of colorants, ink absorption/soaking, drying and other technological impacts) must be taken in consideration. Also is advisable to count black amount instead of program generating. Financial aspect is interesting too, profit by black ink usage.

Reflection properties of standard dyes used in reproduction in visual and NIR are very interesting. The situation that most colored dyes (pigments) have relative high reflectance (output) in NIR similar to white reflection, and carbon black relative low (fig 4), allows extended role of managing from visual to NIR, where in NIR various (gray) shades can be reached. This principle is also applied to a color image (visual) and another in NIR (16)

Managing through standard color management, chromatic components and black, it is possible to get a broadened visual output through carbon black carrying a additional information. Image (color) observed in visual exposes one information, and the extended part introduced by NIR system utilized by simple IR camera exposes another. On fig 9. there are just dark squares rather different shade, but supported by pixel graphic and dedicated screening system it can display very different effects and information.

Managing with colors ensured good "color" reproduction, additional black is a factor that can improve reproduction, enhance visual and technical parameters, and lead to new features as NIR system.

8. LITERATURE

- [1] Theory of Photographic Process, Macmillan publishers London, 1977, 335-339
- [2] Wentzel, F., Graphic Arts Photography-Color, GATF Pittsburgh, 1985, 94-96
- [3] Yule, J., A., C., Principles of Color Reproduction, GATF Press, Pittsburgh 2000, 286-289.
- [4] Dr. Ing. R. Hell: DC 350/399 Chromograph, User manual; setting reproduction properties/
- [5] Morgenstern, D., Rasterungstechnik, Photomechanisch und Elektronisch, Polygraph Verlag 1985, 68-71
- [6] Hunt, R., G., W., The Reproduction of Color, Fountain Press, 1995, 679-682
- [7] Lythock, G., Exploration of Hue Error and Grayness, X-rite doc#GA 0034a, www.xrite.com/documentation/manuals, 96, accessed 2007.
- [8] ISO 12646-2: Graphic Technology: process control for halftone color separations, ISO12647/2 -1996
- [9] Enoksson, E., Compensation by Black: a new separation, KTH publication, www.scientificcommons.org/44629123, accessed 2008
- [10] Cholewo, T., J., Conversion between CMYK color spaces preserving black separation, Lexmark Inc, Lexington KY, Color Imaging Conference, IS and T (2000) Science and Technical report 257-261, (accessed 2006)
- [11] Žiljak I., Grafika dokumentata sa spot bojama iz UV područja, Magistarski rad Grafički Fakultet, Zagreb 2005, 21-25
- [12] Žiljak, V. Pap, K., Žiljak-Stanimirović, I., Žiljak-Vujić, Jana. Managing dual color properties with the Z-parameter in the visual and NIR spectrum. // Infrared physics & technology. 55 (2012) ; 326-336 (journal article)

- [13] IR Filters specification, [www. Max.com/support/documentation/ir/filters](http://www.Max.com/support/documentation/ir/filters): accessed 2010.
- [14] Puglia, S., National archives and record administration, creation of master files, [www.NARA/archive/tutorials/tech. guides](http://www.NARA/archive/tutorials/tech_guides), accessed 2009
- [15] Žiljak, V., Pap, K., Žiljak-Stanimirović, I., DEVELOPMENT OF A PROTOTYPE FOR ZRGB INFRAREDESIGN DEVICE. // Technical Gazette. 18 (2011) , 2; 153-159 (journal article)
- [16] Žiljak, V. Pap, K., Žiljak, I., Infrared hidden CMYK graphics. // Imaging science journal. 58 (2010) , 1; 20-27 (journal article)

A PRELIMINARY PERCEPTUAL SCALE FOR TEXTURE FEATURE PARAMETERS

Ana Gebeješ¹, Ivana Tomić², Rafael Huertas³, Mladen Stepanić²

¹Color in Informatics and Media Technology - Erasmus Mundus Master, University
Jean Monnet, Saint-Etienne

²Faculty of Technical Sciences, Graphic Engineering and Design, Novi Sad

³Dpto. Optica, Facultad de Ciencias, Universidad de Granada, Granada

Corresponding author: Ana Gebeješ
e-mail: ana.gebejes@gmail.com

1. ABSTRACT

Texture, along with colour, is one of the most important characteristics of a material defining the appearance of its surface. While colour had been studied for a long time and continues being a hot topic, the analysis of texture has traditionally been postponed. However, in the last years texture is being more and more considered, for example in image analysis and processing to detect regions of interest in images or recognize objects. In the fields of image analysis and processing different ways to manage texture are proposed, where almost all of them are based on the so called texture features computed from the image. The following parameters, describing some of the texture features, are the most widely used: Contrast, Homogeneity, Dissimilarity, Energy and Entropy. If these parameters characterize a texture, then they must be related with the perceived sensation texture produce. The aim of this paper is to perform a preliminary visual experiment in order to scale each of these parameters according to human texture perception. The five above parameters are computed for 10 greyscale images, which differ in their texture strength. The obtained values are then correlated with the results of the perceptual test, indicating the scale and the applicability of these parameters in describing texture perception.

Keywords: texture, image analysis, perceptual scale

2. INTRODUCTION

Texture perception is shown to be one of the early steps towards identifying objects and understanding the scene (Bergen and Landy, 1991; Julesz, 1962). In 1925 Katz proposed that perception of texture depends of two cues: spatial and temporal (Goldstein, 2010). Spatial cues are determined by the size, shape and distribution of surface elements, while temporal are described by the rate of vibration detected with the skin. Over the years a variety of theories have been developed to understand the mechanisms of human texture perception. Some of them incorporate statistical approach which characterizes a texture by image statistical features (Julesz, 1962). Structural approach, defined within the texton theory (Julesz, 1981), extracts texture primitives as local features for texture description, while the filter-bank model decompose a texture using filters and extend texture analysis into the spatial, frequency and joint spatial/spatial-frequency domain (Xie, 2008).

The very first steps toward computational texture analysis were conducted by Julesz and his associates (Julesz et al., 1981). They empirically investigated the perceptual significance of various image statistics of texture patterns in order to determine how the human low-level visual system responds to the variation of a particular order statistic. Examples of order statistics include contrast (first-order), homogeneity (second-order) and curvature (third-order). The initial work (Julesz, 1962) suggested that human observers cannot distinguish between textures with identical second-order statistics. It was proven to be false by Julesz himself (Julesz, 1973), but these works lead to the idea that texture might be modelled using low-order statistics. The Julesz conjecture inspired the statistical approach to texture analysis which characterizes a texture by image statistical features. Due to limited computing power, many of the today's available approaches in texture analysis still rely on first and second-order signal statistics.

In digital images, texture is another expression of the local spatial structure. One class of image characteristics used for determining texture is first-order statistics of local areas (Ferro, 2002). These include mean, entropy, and variance (Jensen, 1996). Second order statistical

measurements are based on Grey-Level Co-occurrence Matrix (GLCM), which have been the cornerstone of image texture analysis since they were proposed by Haralick in the 1970s. Features presented by Haralick and his co-workers (Haralick et al., 1973) are based on the assumption that the texture information in an image is contained in the overall spatial relationship which grey levels of neighbouring pixels have to one another. As Haralick states, to find these features it is necessary to follow the way the human visual system treats texture. This relationship can be represented by a grey tone spatial-dependence probability matrix also called as grey-level co-occurrence matrix (GLCM). GLCM contains information about the frequency of occurrence of two neighbouring pixel combination in an image. Two perceptual studies conducted by Julesz's (Julesz, 1962) had proven that GLCM matches the human perception response to textures the best.

Many authors investigated the usability of features proposed by Haralick (or derived from its work) (Mallard, 2003), where the focus is placed in texture discrimination and object recognition (Haddon and Boyce, 1990; Sali and Wolfson, 1992; Hay et al., 1996; Soh and Tsatsoulis, 2009; Clausi and Zhao, 2002). Each of these works is oriented toward evaluating the statistics in remote image analysis, used mainly for classification of defined datasets and texture extraction. Yet, there is no available information on how all these parameters can be related to the actual perception of texture. Also, there is no available scale or value that will define e.g. what a high contrast texture is, or when a random noise becomes a texture for the human visual system.

Therefore the purpose of this paper is to estimate whether some of the low order statistics can be used to define the response of human to texture perception with certain degree of accuracy. We chose to evaluate five of the most commonly used statistics: Contrast, Homogeneity, Dissimilarity, Energy and Entropy. If significant degree of correlation is obtained for certain parameter, this particular one will be assessed more in depth in future studies. In order to define the scale for the defined parameters, 22 observers were asked to arrange a set of textured samples according to the texture visibility. Their responses are compared with the computed values of the defined parameters.

3. METHOD

3.1. Samples

For this study 10 images were considered – 9 greyscale images of cross-hatched textile fabrics and 1 solid colour image. Images of textile fabrics were chosen so that they differ visually in their texture strength, while fibre orientation and weaving type were kept constant. For the solid sample colour was set to grey with $L^*=70$. In order to minimize colour differences between texture images, they were modified using the LCH mapping method (Milic et al., 2010). This method enables altering L^* , C^*_{ab} and h_{ab} value of each pixel in an image in order to change its appearance. Mapping was performed by taking into account the pixel deviation to the mean chroma and luminance values (Milic et al., 2010). C^*_{ab} and h_{ab} values were set to 0, while L^* value was altered to obtain 70. Furthermore, texture images were adjusted so that the mean histogram value was 165 (with a maximum deviation of 0.10). All the images had normal or close to normal tonal distribution.

Figure 1 shows an image of the employed images, with the notation that had been used.

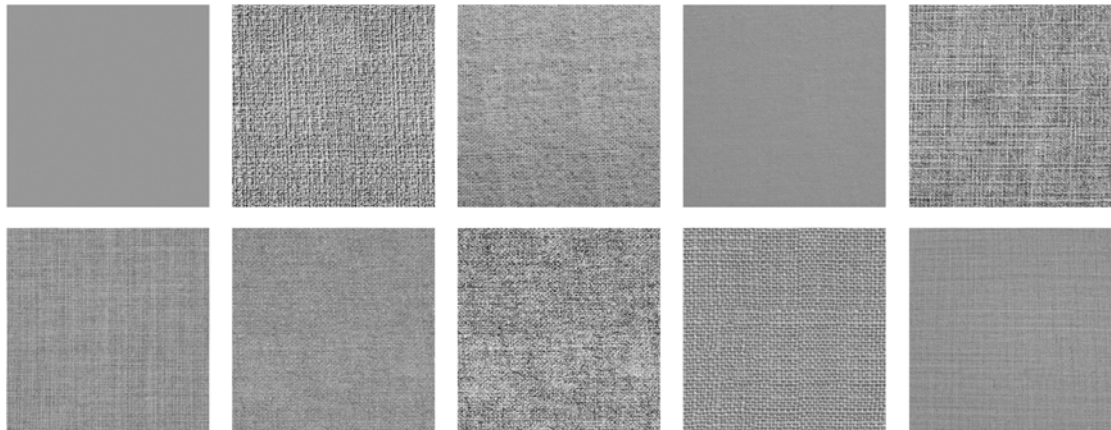


Figure 1. Images used in the experiment noted with letters a, b, c, d, e, f, g, h, i, j, respectively

3.2. Display and laboratory setup

Images were presented on calibrated EIZO CG241W monitor, where white point was set to 6505 K (chromacity coordinates – 0.3127, 0.3290) with a luminance of 100 cd/m². Black point luminance was 0.08 cd/m². All the values were measured with an Eye-One Pro spectrophotometer. Monitor resolution was set to its native, 1920 x 1200.

JavaScript code was written in order to display the test. Images were presented in two rows on a grey background ($L^*=53$) covering the whole screen. Both rows were positioned at the centre of the screen, like shown in Figure 2. Each image sample subtended 9.1° of the visual angle from the position of the observers, which was approximately 50 cm from the display. Experiment was carried out in a complete dark room eliminating the influence of ambient illumination.

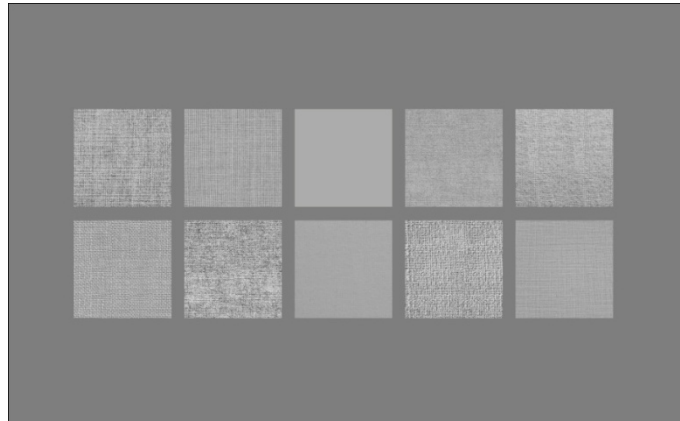


Figure 2. Layout of a test presented to the observers

3.3. Observers

A panel of 22 observers (13 experienced and 9 naive) with normal colour vision (tested with Ishihara test) and normal or corrected vision participated in the experiment.

The observer adapted to the grey background for 2 min before each session. Observers were instructed to arrange presented images according to their texture visibility, where the first in order should be image with no texture (solid colour). Accordingly, the last one should be an image where texture is most noticeable. Observers were allowed to drag and drop images, changing their position in the rows. They were not time-limited, each observer took as much time as needed in order to create the desired order. Next sequence was presented when assessor hovered over a previously hidden "Next" button in the low left corner of the screen. The current order was stored in a database using AJAX call to Ruby on Rails application. Database system used was PostgreSQL. Each observer performed the test four times, where first attempt was regarded as trial. Overall, 60 sequences were recorded.

3.4. Calculating the texture feature parameters

Once the GLCM matrix is constructed with the selected parameters, texture features can be calculated from it. When building the GLCM, parameters like number of grey levels (N_g), displacement of the GLCM (d) and orientation (θ) should be taken into account. In this experiment a 256 grey level image representation was used. The displacement, which represents the distance (d) between two pixels whose repetition is examined, was selected to 6 pixels. Chen (Chen, 1989) used displacement values of $d=1, 2, 3, 4, 8, 16, 32$ and found that single displacement value cannot be deducted because it depends on the type of the texture that is being investigated. In this paper we decided to use the displacement value that gives the highest contrast for the majority of the samples because it suggests that only one texture element is enclosed within the defined neighbourhood. For the orientation the average of the possible four ($0^\circ, 90^\circ, -45^\circ$ and 45°) was taken since the main goal was to create an underlying experiment that can be expanded by analysing the effect of orientation in the future.

Calculations were performed in MATLAB software with a code proposed by Uppuluri in 2010. With this code it is possible to obtain 22 features highlighted in different papers (Haralick et al., 1973; Soh et al., 1999; Clausi et al., 2002). From those, as parameters of importance we

defined Contrast, Homogeneity, Dissimilarity, Energy and Entropy, as stated above. Thus, only these five were taken into account for further analysis. Calculations were performed for all 10 texture samples in the CIELAB colour space on the L^* channel. The L^* channel was selected because several works stated that the majority of texture information is located on this channel (Xin et al., 2003; Xin et al., 2005; Milic et al., 2010).

Below are described all the features used in the experiment and the meaning of each one of them in the actual texture analysis case is explained (Haralick et al., 1973; Soh et al., 1999; Clausi et al., 2002). In all the formulas $p(i; j)$ stands for $(i; j)^{\text{th}}$ entry or value in a normalized GLCM.

3.4.1. Contrast

Contrast is a local grey level variation in the grey level co-occurrence matrix. It can be thought of as a linear dependency of grey levels of neighbouring pixels (Haralick et al., 1973).

$$Contrast = \sum_{i,j} |i - j|^2 p(i, j) \quad (1)$$

In Equation (1) i and j are the horizontal and vertical cell coordinates and p is the cell value. If the neighbouring pixels are very similar in their grey level values then the contrast in the image is very low. In the case of texture, the grey level variations show the variation of texture itself. High contrast values are expected for heavy textures and low for smooth, soft textures. The range of the Contrast is $[0 \text{ (size (GLCM, } 1)-1)^2]$ where Contrast is 0 for a constant image.

3.4.2. Homogeneity

Homogeneity measures the uniformity of the non-zero entries in the GLCM (Clusi, 2002). It weights values by the inverse of contrast weight (Soh et al., 1999).

$$Homogeneity = \sum_{i,j} \frac{1}{1 - (i - j)^2} p(i, j) \quad (2)$$

The GLCM homogeneity of any texture is high if GLCM concentrates along the diagonal, meaning that there are a lot of pixels with the same or very similar grey level value. The larger the changes in grey values, the lower the GLCM homogeneity making higher the GLCM contrast. The range of homogeneity is $[0-1]$ where homogeneity is 1 for a diagonal GLCM. If the image has little variation it has high homogeneity and if there is no variation homogeneity is 1. Therefore, strong homogeneous textures contain ideal repetitive structures, while weak homogeneity refers to variation in texture elements in their spatial arrangements. An 'inhomogeneous texture' mostly refers to an image where repetition and spatial self-similarity are absent.

3.4.3. Dissimilarity

Dissimilarity is a measure that defines the variation of grey level pairs in an image. It is the closest to Contrast with a difference in the weight – Contrast unlike Dissimilarity grows quadratically (Soh et al., 1999).

$$Dissimilarity = \sum_{i,j} |i - j| p(i, j) \quad (3)$$

It is expected that these two measures behave in the same way for the same texture because they calculate the same parameter with different weights. Contrast will always give slightly higher values than Dissimilarity. Dissimilarity ranges from $[0-1]$ and obtain maximum when the grey level of the reference and neighbour pixel is at the extremes of the possible grey levels in the texture sample 4.

3.4.4. Entropy

Entropy in any system represents disorder, where in the case of texture analysis entropy is a measure of spatial disorder in an image (Haralick et al., 1973; Soh et al., 1999).

$$Entropy = - \sum_{i,j} p(i, j) \log(p(i, j)) \quad (4)$$

A completely random distribution would have very high entropy because it in its sense represents chaos. Solid tone image would have an entropy value of 0. This feature can be useful to tell us if entropy is bigger for heavy textures or for the smooth textures giving us information about which type of texture can be considered statistically more chaotic.

3.4.5. Energy

Energy is a measure of local homogeneity and therefore it represents the opposite of the Entropy. Basically this feature will tell us how uniform the texture is (Haralick et al., Soh et al., 1999).

$$Energy = \sum_{i,j} p(i, j)^2 \quad (5)$$

The higher the Energy value, the bigger the homogeneity of the texture. The range of Energy is [0-1], where Energy is 1 for a constant image.

All the features discussed within this section are connected in certain manner. Contrast and Dissimilarity both calculate the variation of grey level pairs, but with a different weight. Homogeneity weights values by the inverse of Contrast weight, which means lower the homogeneity, higher the contrast. Energy is actually local homogeneity and entropy is the opposite of energy. These correlations are very easy to find and very useful because they relate through Contrast to the question posed to the observers. This explains the selections of the chosen features.

4. RESULTS AND COMMENTS

For each image, the defined parameters of importance (Contrast, Homogeneity, Dissimilarity, Energy and Entropy) have been computed from the GLCM matrix. For computing the GLCM matrix it is necessary to define a value for the displacement, d . The criterion was to use the displacement value that maximizes the contrast for majority of samples. Table 1 shows the contrast for each texture at different d values. Please, note that maximum contrasts are in bold.

Table 1. Contrast for each image at different displacements

Contrast\image	a	b	c	d	e	f	g	h	i	j
Contrast ($d=4$)	0.000	2.800	0.901	0.012	2.235	1.335	0.420	2.346	0.935	0.372
Contrast ($d=6$)	0.000	2.682	0.991	0.012*	2.765	1.021	0.444	2.559	0.989	0.440
Contrast ($d=10$)	0.000	2.815	1.033	0.012	2.237	1.522	0.435	2.469	0.929	0.373
Contrast ($d=12$)	0.000	2.776	1.028	0.012	2.700	1.145	0.455	2.638	0.985	0.416

*contrast for $d=6$ is higher when values are observed at four decimal places

As can be seen, a displacement of 6 pixels maximizes the contrast for the majority of images so it is considered further on. The whole set of featured for each image is summarized in Table 2.

Table 2. Texture parameters for each image

Feature\image	a	b	c	d	e	f	g	h	i	j
Contrast	0.000	2.682	0.991	0.012	2.765	1.021	0.444	2.559	0.989	0.440
Dissimilarity	0.000	1.225	0.715	0.012	1.311	0.690	0.417	1.215	0.725	0.419
Energy	1.000	0.071	0.142	0.975	0.055	0.117	0.327	0.062	0.131	0.375
Entropy	0.000	2.959	2.250	0.077	3.108	2.340	1.417	3.043	2.277	1.231
Homogeneity	1.000	0.525	0.670	0.994	0.486	0.688	0.794	0.522	0.664	0.792

For each image, the position that observers assessed can be seen in Table 3. The values are the average position of the tree repetitions for each observer and the average of the observers' answers. The average for observers' standard deviation between the tree repetitions (intra-observers variability) is shown in third row. The standard deviation between observers' answer (inter-observers variability) is shown in forth row.

Table 3. Average position for each image

Feature\image	a	b	c	d	e	f	g	h	i	j
Position	1	9.48	5.80	2.03	7.41	5.12	4.30	7.26	9	3.59
SD (Repetition)	0	0.16	0.52	0.03	0.46	0.40	0.45	0.39	0.23	0.26
SD (Observers)	0	0.48	0.71	0.14	1.15	1.23	0.86	1.33	1.14	1.16

As is probe in Table 3, textures of the images e and f are the most difficult to order both between observers and between repetitions.

In order to assess the agreement among the observers, Kendall's coefficient of concordance was also calculated by taking into account mean value for each image position given by each observer. Kendall's W ranges from 0 (no agreement) to 1 (complete agreement). Value of 0.889 obtained for our set of data indicated very good agreement between observers, so all the results were included in further evaluation.

For assessing the possible relationship between calculated texture feature values and the rates observers gave to each image, we found the mean value for each image position (considering all the responses for each observer). Mean rating for each image are correlated with the texture feature values by calculating Pearson correlation coefficient for linear relation. Strong correlation was obtained for each parameter used, as can be observed in Table 4.

Table 4. Pearson correlation coefficients between texture feature values and observers ratings

Texture feature	Correlation coefficient
Contrast	0.809 (p=0.005)
Dissimilarity	0.880 (p=0.001)
Energy	-0.861 (p=0.001)
Entropy	0.901 (p<0.0005)
Homogeneity	-0.899 (p<0.0005)

From the results presented in Table 4 it can be concluded that highest degree of correlation with visual rankings is obtained if Entropy values are considered. High Entropy values are found in samples with high texture strength and high contrast (Table 2, Figure 1). If image is categorized through high degree of local contrast, texture is well defined, but it is clearly not enough to state the perceived texture conspicuousness. The random noise images can also obtain high Contrast values, lacking the perceived order of texture elements. Hence, the measure of spatial disorder (Entropy) is better indicator of texture perception than Contrast. High negative correlation values are obtained for Energy too, which is expected since it represents the opposite of Entropy.

It is also clear that Dissimilarity and Homogeneity gave better correlation with visual rankings than Contrast. Dissimilarity is, due to the different weight used for calculating the parameter, more sensitive to grey level variations, while the Homogeneity weights values by the inverse of Contrast weight so negative correlation value is expected.

5. CONCLUSIONS

In this paper a first attempt to relate the low order statistical texture features with the judgements human observers made when evaluating texture images of a textile samples were presented. Initial experimental results are promising, which is proven by the very good correlation coefficients for each parameter used (0.8 and higher). It can be concluded that the selected features are well correlated with the human perception. At this point it is possible to state that Entropy parameter (and consequently Energy) performs better than others, suggesting that it might be used to describe human texture perception with high degree of confidence. High Contrast value of texture image implies greater grey level difference between neighbouring pixels, but this parameter is not enough to state that texture is more or less conspicuous. However, if the Entropy value is high, particular texture becomes more visible and easier to notice. Therefore it can be concluded that higher Entropy value suggests stronger texture pattern making it easier to perceive. In this paper images of textile fabrics with constant

orientation were used. In order to generalize these conclusions, further studies that will include texture samples of different types and orientations had to be performed. Future research could also include defining which Contrast and Entropy values characterises strong or weak textures and connect them with the size of a texture element. Additionally, a possible scale for these features can be formed.

Acknowledgments

This work was supported by the Serbian Ministry of Science and Technological Development, Grant No.:35027 "The development of software model for improvement of knowledge and production in graphic arts industry".

6. LITERATURE

- [1] Bergen, J.-M., Landy, M.-S.: "Computational Modelling of. Visual Texture Segregation" in Computational Models of Visual Processing (M. S. Landy and J. A. Movshon, eds.), (Cambridge, MA: MIT Press, 1991). pages 253-271.
- [2] Chen P.-C., Senguota S.-K., Welch R.-M.: "Cloud field classification based upon high spatial resolution textural features, 2. Simplified vector approach", J. Geophys. Res, 94, 1989.
- [3] Clausi D.-A.: "An analysis of co-occurrence texture statistics as a function of grey level quantization", Can. J. Remote Sensing, vol. 28, no. 1, pp. 45-62, 2002.
- [4] Clausi, D.-A. Zhao, Y. "Rapid co-occurrence texture feature extraction using a hybrid data structure", Computers and Geosciences, 28 (6), 763 - 774, 2002.
- [5] Ferro, C.-J.-S., Warner, T.: "Scale and texture in digital image classification", Photogrammetric Engineering and Remote, Sensing 68(1), 51–63, 2002.
- [6] Goldstein, E.-B.: "Sensation and Perception", 8th Ed. (Belmont, CA: Wadsworth, 2010). page 338.
- [7] Haddon, J.-F., Boyce, J.-F.: "Image segmentation by unifying region and boundary information," IEEE Trans. Pattern Anal. Machine Intell., 12, 929–948, 1990.
- [8] Haralick R.M., Shanmugam K., Dinstein: "Textural Features of Image Classification", IEEE, 3(6), 1973.
- [9] Hay, G.-J., Niemann, K.-O., McLean, G.-F.: "An object-specific Image-texture analysis of h-resolution forest imagery", Remote Sensing of Environment, 55, 108–122, 1996.
- [10] Jensen, J.-R. "Introductory Digital Image Processing: A Remote Sensing Perspective", (Upper Saddle River, New Jersey: Prentice Hall, 1996), page 316.
- [11] Julesz B.: "Visual pattern discrimination", IRE Trans. Inform., Theory, 8, (1962)
- [12] Julesz, B., Gilbert, E.-N., Shepp, L.-A., Frisch, H.-L.: "Inability of humans to discriminate between visual textures that agree in second order statistics—Revisited," Perception, 2, 391–405, 1973.
- [13] Julesz, B.: "Textons, the elements of texture perception, and their interactions", Nature, 290, 91-97, 1981.
- [14] Maillard, P.: "Comparing texture analysis methods through classification", Photogrammetric Engineering and Remote Sensing, 69(4), 357–367, 2003.
- [15] Milic N., Slavuj R., Milosavljevic B.: "The colour mapping method based on the LCH colour space for simulating textile printed texture images", Proceedings of the 5th International Symposium on Graphic Engineering and Design 2010 (Faculty of Technical Science/GRID: Novi Sad, Serbia, 2010), pages 167-172., (2010)
- [16] Sali, E., Wolfson, H.: "Texture classification in aerial photographs and satellite data", International Journal of Remote Sensing. 13 (18), 3395–3408, 1992.
- [17] Soh L., Tsatsoulis C.: "Texture Analysis of SAR Sea Ice Imagery Using Grey Level Co-Occurrence Matrices", IEEE Transactions on Geoscience and Remote Sensing, 37(2), 1999
- [18] Soh, L.-K., Tsatsoulis, C.: "Texture Analysis of SAR Sea Ice Imagery Using Grey Level Co-Occurrence Matrices", CSE Journal Articles. Paper 47, 2009. URL <http://digitalcommons.unl.edu/csearticles/47/> (last request: 2012-09-01)
- [19] Uppuluri, A.: "GLCM_Features4-Calculates the texture features from the different GLCMs" URL <http://www.mathworks.com/matlabcentral/fileexchange/22354-glcmmfeatures4-m-vectorized-version-of-glcmmfeatures1-m-with-code-changes> (last request: 2012-07-01)

- [20] Xie, X.: "A Review of Recent Advances in Surface Defect Detection using Texture analysis Techniques", *Electronic Letters on Computer Vision and Image Analysis*, 7(3), 1-22, 2008.
- [21] Xin J.-H., Shen H.-L.: "Computational model for mapping on texture images", *Journal of Electronic Imaging* 12(4), 697-704, 2003.
- [22] Xin J.-H., Shen H.-L.: "Computational models for fusion of texture and: a comparative study", *Jurnal of Electronic Imaging* 14(3), 033003, 2005.

THE POSSIBILITY OF USING G7 METHOD FOR CALIBRATION AND CHARACTERIZATION OF XEROX DOCUCOLOR DIGITAL PRESS

Ivana Jurič, Igor Karlović, Ivana Tomić

Faculty of Technical Sciences, Graphic Engineering and Design, Novi Sad

Corresponding author: Ivana Jurič

e-mail:rilovska@uns.ac.rs

1. ABSTRACT

G7 method introduces gray balance control as the key to achieve consistent colour reproduction, instead of controlling optical density and tone value increase (TVI). This method was originally intended for commercial offset printing, but it is also applicable to virtually any CMYK imaging process and has been successfully tested on a wide range of processes, including coated and uncoated offset, newsprint, gravure, flexography, digital printing, as well as a wide range of AM and FM screening methods.

This study is focused on the validation and efficiency of G7 method in calibrating Xerox DocuColor 252 digital press that is based on electrophotographic process. By following the guidelines of G7, the quality of gray and colour reproduction was compared to factory calibration. The results indicate the need to make additional adjustments in addition to the basic G7 method. G7 method alone is not sufficient to calibrate the toner based printing press.

Key words: G7 calibration method, gray balance, digital press

2. INTRODUCTION

For successful colour management the stages, calibration, characterization, control and visualization are of equal importance. The calibration or linearization of a device serves to maintain a consistent colour reproduction – an essential process, particularly with digital proof systems (Homann, 2009). Calibration is performed for many reasons, but for colour management, the most important reason is to make the device behave consistently so that the profile that describes it remains accurate. In addition to calibration, devices are usually characterized. While calibration changes the way a device behaves, characterization or profiling only describes how the device was behaving at the time the profile was created, it just records how device makes colour and what colours it can (and cannot) reproduce (Fraser, 2005).

Printer calibration and characterization continues to be a challenging problem due to the complex nonlinear colour characteristics of these devices. According to Sharma there are two common approaches of calibration: channel-independent and gray-balanced calibration (Sharma, 2003). First type of calibration implies linearization of each channel independently.

Gray-balanced calibration, an alternative approach to calibration is to gray balance the printer so that amounts of C, M, Y processed through the calibration result in a neutral (i.e., $a^* = b^* = 0$) response. There are two main motivations for this approach. First, the human visual system is particularly sensitive to colour differences near neutrals. Hence, it makes sense to carefully control the state of the printer in this region. Second, gray balancing considers interactions between C, M, and Y that are not taken into account in channel-independent calibration. In addition to determining the relative proportions of C, M, Y that generate neutral colours, gray balancing can also achieve a specified tone response along the neutral axis (Sharma, 2003).

So far, there are defined two methods of calibration: FOGRA/ISO 12647-2:2004 and G7 (GRACoL/SWOP). There are fundamental differences between them. The aim of the FOGRA method is to achieve the best possible tone value increase (TVI) in ISO 12647-2:2004. This method calibrates the press by matching the specified tone values with the use of four one-dimensional curves. GRACoL breaks with tradition by raising gray balance to a more important status than TVI. The aim of the G7 methodology is to achieve the most visually similar result possible, in terms of gradation and gray balance, with the most different of printing processes and paper types.

G7 is a new calibration method developed to support the GRACoL 7 specification. The 'G' refers to calibrating gray values, while the '7' refers to the seven primary colour values defined in the ISO 12647-2:2004 printing standard: Cyan, Magenta, Yellow, Black (K), Red (M+Y), Green

(C+Y) and Blue (C+M). Although originally intended for commercial offset printing, the G7 method can also be applied to every type of printing process (Idealliance, 2006).

The basis of the G7 method is a K and a CMY scales called "*Neutral Print Density Curves*" or NPDC, which, measured in print in respect of the gray balance in the CIE Lab colour space and the gradation in optical density, should fulfill certain specifications. NPDC is the relationship between measured optical density and original halftone percentages on a printed gray scale (Idealliance, 2006). Because optical density is an absolute value, while TVI is a relative function, NPDC ensures a better contrast and optical density match between multiple devices.

Two NPDC curves are specified, one for a combined CMY gray scale and one for a black-ink gray scale. NPDC calibration compares a printed gray scale to a reference scale and calculates RIP correction values in dot percentage terms that force the press (or other imaging device) to the desired NPDC shape. Curve correction values are calculated either manually by plotting graphs on special graph paper (Figures 2 and 3), or automatically in the *IDEALink™* Curve software.

Although this method is primarily intended for offset printing, Rong demonstrated its ability in calibrating a printing press other than offset (Rong, 2008). Wang also compared TVI and G7 calibration method by simulating them and concluded that it is possible to use both methods for calibrating offset printing press (Wang, 2011).

G7 method has its benefits and limitations, which are listed below.

Benefits:

- The primary advantage of the G7 calibration method is that the visual appearance of neutral tones and near-neutral tones is more effectively controlled by gray tones from the shadows to the highlights than by traditional TVI-based methods.
- The G7 method and values are equally valid in proofing or printing, unlike TVI-based calibration, which requires different aim values for proofing systems than for presses.
- G7 relies on measuring colour with a spectrophotometer rather than measuring the thickness of dots of ink on paper using only a densitometer. GRACoL's research indicates that the measurement of dots of ink on paper is not the best basis producing a consistent visual appearance from device to device. G7 breaks from tradition by focusing on colorimetric data rather than on densitometric aims, i.e. dot gain, for each colour (Kennedy, 2006).

Limitations:

- Gray balance is generally harder to control on a typical offset press than single-ink performance, due to wet trapping and other issues. But that's really the whole point - focusing on the most unstable variable helps stabilize the whole process.
- If the average job contains few gray areas, gray balance control may not be worth the effort.
- Calibrating an unstable device with different CMY curves may solve a one-time gray balance error but cause a different gray balance problem on subsequent work, if the calibration test was not typical. The use of 'smoothed' gray correction curves helps reduce this problem (Idealliance, 2006).

In this study we investigated the possibility and efficiency of using G7 method for calibrating an electrophotographic printing press. The research was conducted following the guidelines prescribed by the G7.

3. MATERIALS AND METHODS

The used electrophotographic printing press for calibration and characterization was the Xerox DocuColor 252 which utilizes dry toner (cyan, magenta, yellow and black). Substrate *Biomat paper 115g/m²* was used for entire study. The colorimetric values of this substrate and optical properties are presented in Table 1. G7 defines ISO Paper type 1 with as little fluorescence as possible and a nominal white point of 95 L* (+/- 3), 0 a* (+/- 2), -2 b* (+/- 2) (measured with white backing) which corresponds to the selected substrate (Idealliance, 2006).

Table 1: Optical paper properties of selected substrate

Paper properties	L* a* b* values	CIE Whiteness	TAPPI Brightness %	TAPPI Opacity %
<i>Biomat paper</i>	92.82 / 1.58 / -4,34	101.9	88.7	100.2

A test target was built following G7 guidelines (Figure 1). This target includes *P2P25x* target which was used for calibration, *Gray Finder 2.2* for calibration control and *ECI2002* for characterization of the device.

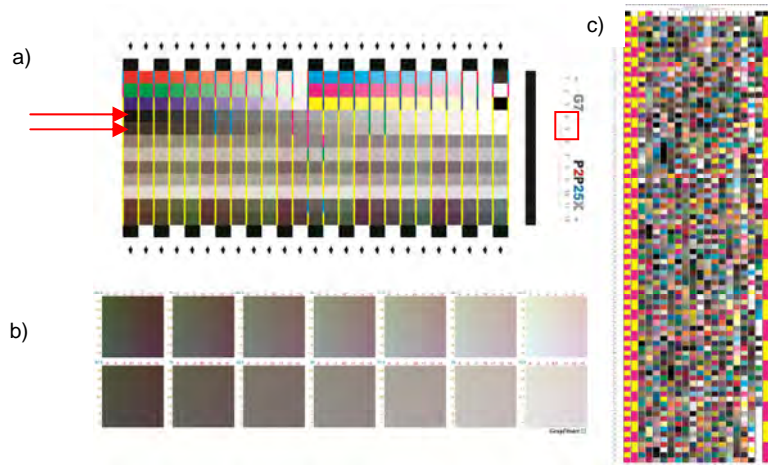


Figure 1: Test target for a) *P2P25x*, b) *Gray Finder 2.2* and c) *ECI2002*

In the first step the *P2P25x* and *ECI 2002* test targets were printed and measured. The printing was done with no adjustments on the used *Creo Spire CX260* RIP which drives the digital press. Measurements were done using a spectrophotometer *Eye - One (i1) Pro* with 45°/0° measurement geometry, under conditions *D50* illuminant and observer angle 2°. The spectral data of *ECI2002* target was used to build profile for further testing. From the *P2P25x* target we determined the RIP correction values that force the printing device to match the specified *G7* NPDC curves. Then the RIP curves were adjusted based on the measured data. The test target was printed again with RIP adjustment. The *P2P25x* and *ECI2002* were measured again to compare them with the original print, which had no RIP adjustment and no profile embedded. For determining the colourimetric differences, ICC profiles were created in *GM Profile Maker 5*. The profiles were compared and the generated colour gamut from the *ECI 2002* spectral data was analyzed using *Patch Tool* and *ColorThink Pro* softwares. The generated ICC profiles were also assigned to test image for visual evaluation of the calibration processes.

4. RESULTS AND DISCUSSION

For *G7* calibration we only need information about optical density of gray balance patches (column 4 – *K* and column 5 – *CMY*, 0 – 100% tone value), marked with red arrows in Figure 1. These measured optical density values were plotted in *GRACoL 7 NPDC FanGraph* for each colour separately. In Figures 2 and 3 are presented graphs (curves) for all separations which are the relationship of optical density and dot percentage. Based on these curves can be seen that optical densities of magenta and black are higher than the ideal numbers, while optical densities of cyan and yellow do not deviate much from the reference. According to Target and Sample Curve from *NPDC FanGraph* we manually calculated correction values for RIP adjustment. These new aim values are presented in Table 2.

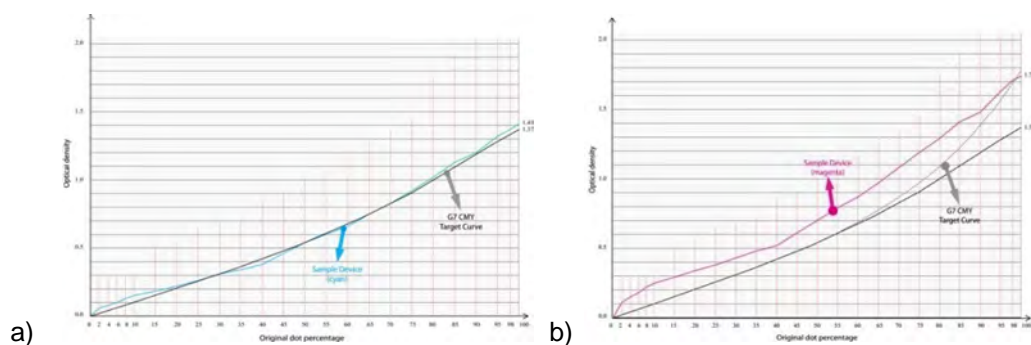


Figure 2: NPDC Curve a) cyan and b) magenta

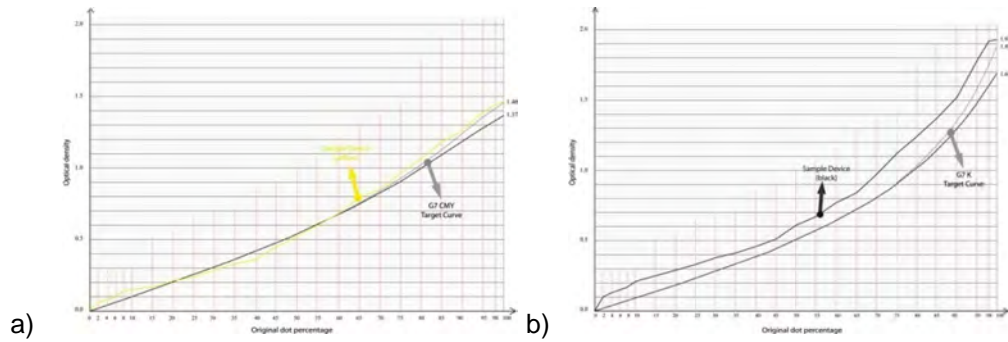


Figure 3: NPDC Curve a) yellow and b) black

Table 2: New Aim Values for adjusting RIP curves

New Aim Values					New Aim Values				
Patch	C	M	Y	K	Patch	C	M	Y	K
0	0	0	0	0	50	50	41	51	45
2	1	0	1	0	55	56	45	56	47
4	1	0	1	1	60	61	49	60	53
6	2	1	2	1	65	65	54	63	58
8	4	2	4	2	70	70	60	69	63
10	6	2	6	2	75	74	65	74	68
15	10	4	11	5	80	79	71	78	73
20	18	7	20	9	85	84	77	83	78
25	25	11	27	13	90	89	84	89	84
30	30	17	32	19	95	94	93	93	91
35	38	23	40	25	98	96	97	96	95
40	43	29	44	32	100	100	100	100	100
45	47	35	47	38					

These calculated correction (aim) values are applied to RIP to adjust printing press. Corrected curves are presented in Figure 4.

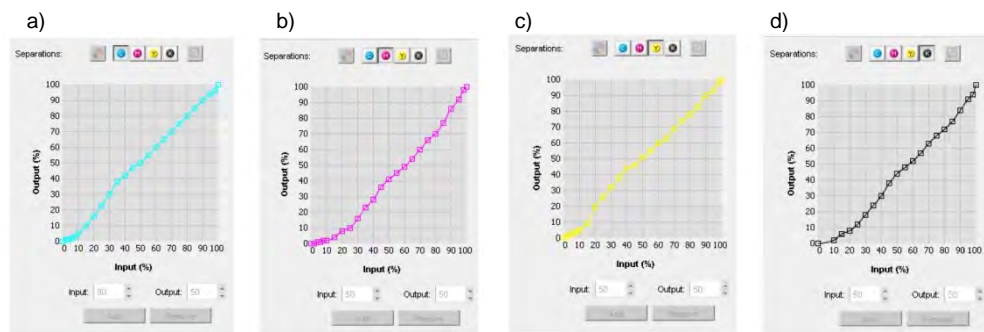


Figure 4: Corrected curves in RIP a) cyan, b) magenta, c) yellow and d) black

After correction we printed again test target with RIP adjustment. The colorimetric values of gray balance were measured to compare them with the reference values suggested by the G7 specifications (Idealliance, 2006). Comparison results showed large deviations from reference a^* and b^* values for all patches, what also could be seen on the printed test target that had a dominant green tone. These values can be compensated by adjusting the yellow and

magenta curves. To determine the exact percentage by which to increase or decrease the drift of the two colours, we used test target *GrayFinder* (Figure 1c). However, measuring the patches of test target we found that all values deviate from the reference. It was not possible to find a patch whose $L^*a^*b^*$ values meet the reference. So, it was not possible to determine the percentage values of correction for magenta and yellow. Although these results were not satisfactory, they are considered to be the final outcome of the application of the G7 method. But, an attempt was made to arbitrary correct curves. Correction values were chosen arbitrarily, and without a reference value. The goal was to get the calorimetric values that are within reference. Test target was printed again with new RIP curve adjustment. Although it was expected that there will be improvements, green tone was still dominant, and the visual assessment showed that Lab values will not be attained. Moreover, some of the values were even deteriorated. The cause of this problem lies in the fact that the exact amount of any process colour cannot be unambiguously defined and kept under control. In fact, moving e.g. cyan curve, will not only affect that colour, but it will also affect the other two. For this reason, this attempt to manually configure all three curves is not correctly and accurately. Unlike offset printing, where colours are separate and could be manipulated separately, in digital printing shifting one colour affects all colours.

To find some reasons for colour deviation from the recommended values we captured the gray balance patches with microscope SibressPit. In some patches are clearly identified yellow spots that appear randomly (Figure 5a). From Figure 5c can be seen that patch contains a black, although it should only contain cyan, magenta and yellow. Also, except for the black (which should be the only one in patches in fourth column), presence of other colours were noticed, as it could be seen in the Figure 5b. According to these figures we can see that digital printing press uses a proprietary halftoning method which is adjusted by the RIP itself and no direct control over separate colours is possible.

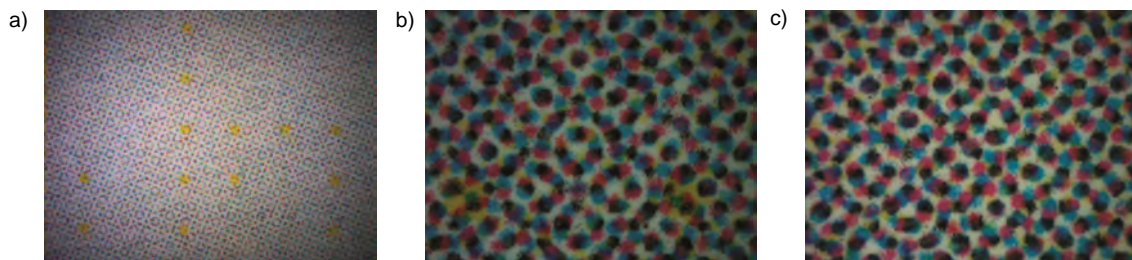


Figure 5: a) Patch with random yellow spots, b) 50% patch of column 4 and c) 50% patch of column 5

To assess the obtained gamut, the generated ICC profiles were measured after every step during the investigation and 3 profiles (1 - without calibration, 2 - after G7 method and 3 - after additional adjustments) were obtained. Profiles were compared with each other in order to calculate the difference between them. As could be concluded from the previous results, there is a large difference between them. By comparing the first with second or third profile, the difference is massive ($\Delta E = 10$). Difference between second and third profile is much smaller ($\Delta E = 2.16$). Color gamut of all three prints is presented in Figure 6. G7 method improved color gamut only in green and yellow parts, which does not mean improvement of overall print quality.

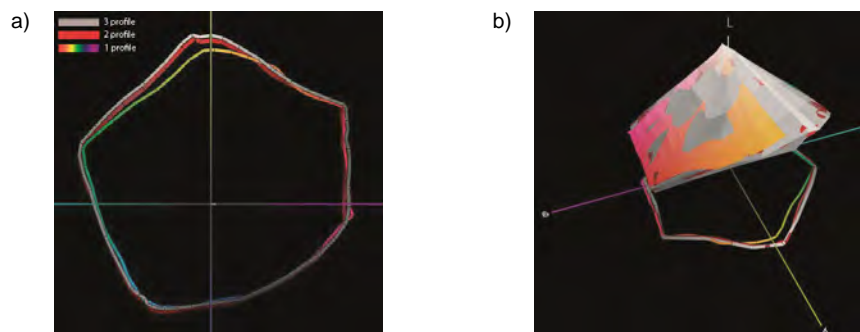


Figure 6: Color gamut comparison a) 2D and b) 3D

The profiles of different calibration steps were also embedded to test image for visual evaluation (Figure 7). After the first step, print without RIP adjustment had a dominant tone of magenta. To compensate that, RIP was adjusted which led to an increase in green tone, as can be seen from Figure 7c and 7d.



Figure 7: Test image a) original, with embedded profile b) without calibration, c) with G7 method and d) with additional adjustments

5. CONCLUSIONS

The G7 calibration method presented in this paper controls the press by colorimetric values of gray to achieve a better visual match. Theoretically, it can be applied to any printing process. But, on the basis of obtained results we can conclude that this is not entirely accurate. The G7 calibration method was not fulfilled one of its aims, gray balancing and elimination of tonal cast for an electrophotographic printing press. Moreover, after calibration, prints had dominant green tone. This is unexpected, because one of the aims of the G7 calibration method is correcting tonal cast, making the reproduction appear neutral over the tonal range. The reason of this lies mostly in the inability to directly control separate colours, because this digital press uses halftoning method defined by the device manufacturer.

Our future work will be to examine the halftone algorithm used by toner-based digital press to get the desired tone. How that algorithm uses, varies and places the dots. The aim will be to achieve as regular distribution of dots as possible.

Acknowledgments

This work was supported by the Serbian Ministry of Science and Technological Development, Grant No.: 35027 "The development of software model for improvement of knowledge and production in graphic arts industry".

6. LITERATURE

- [1] Fraser, B., Murphy, C. and Bunting, F.: "Real World Color Management", Second Edition, Peachpit Press, Berkeley, ISBN 0-321-26722-2, 2005
- [2] Homman, J.: "Digital Color Management Principles and Strategies for the Standardized Print Production", Berlin Heidelberg: Springer-Verlag, ISSN 1612-1449, 2009
- [3] Idealliance: "Calibrating, Printing and Proofing by the G7™ Method", URL [http://www.aptec.vtc.edu.hk/idealliance-china/resource_centre/free_resources/08-G7_how-to_v6\[final\].pdf](http://www.aptec.vtc.edu.hk/idealliance-china/resource_centre/free_resources/08-G7_how-to_v6[final].pdf) (last request: 2012-08-15), 2006
- [4] Kennedy, D.: "Why You Should Employ G7™, the New Proof-to-Print Process", Idealliance, 2006.
- [5] Rong, X.: "G7 Method for Indigo Press Calibration and Proofing", Proceedings of NIP24 and Digital Fabrication 2008 (California Polytechnic State University, San Luis Obispo)
- [6] Sharma, G.: "Color Fundamentals for Digital Imaging - Digital Color Imaging Handbook", CRC Press, 2003
- [7] Wand, Y.: "Comparing TVI and G7 Calibration Methods by Simulation", Test Target, Vol. 10, pages 36 – 47, 2011

COMPARISON OF INDUSTRIAL AND NON AUTOMATED COLOR CALIBRATION CREATED COLOR PROFILES

Krisztián Samu, Zsuzsanna Veres

Budapest University of Technology and Economics – Department of Mechatronics,
Optics and Engineering Informatics, Budapest

Corresponding author: Krisztián Samu
e-mail: samuk@mogi.bme.hu

1. ABSTRACT

To use color management systems the condition is to use appropriate color profiles to the device. There are two ways to get to these appropriate color profiles. We can use industrial color profiles or we can create our own color profiles by color calibration. The great advantage of the industrial profiles is the easy access, however arising from manufacturing and other uncertainties these reliability is in question. Creating our own color profiles is lengthy and requiring expertise and even this is no guarantee of perfect color profile, because during the calibration we can make different types of measurement errors. These errors can be significant mainly in the case of manual (non automated) calibration. In this paper, the question we would like to provide answer is that industrial or non automated calibration should we use to an inkjet printer?

Keywords: ICC color management, inkjet printing, color measurement

2. INTRODUCTION TO ICC COLOR MANAGEMENT

In 1993, eight companies specified to color management and they founded the International Color Consortium (ICC). Their aim was to develop an opened, platform-independent color management system that provides color accurate function of several image transferring and image display devices [1]. ICC color management system includes the following items:

a. Device-independent color model, which ensures that the device-independent color spaces (gamut) can be converted into each other. For example, color accuracy is not obtained if RGB color coordinates of a scanner displayed directly on an LCD monitor. However, if we convert the input RGB values into an intermediate color space (for example CIE Lab), while the colorimetric characteristics of the devices are known, then the correct output RGB values can be set from this intermediate color space (Fig. 3.).

b. The color profile is a digital data file that describes the color management abilities of a device. The profiling shall consist in measuring (calibrating) the radiometric, photometric and colorimetric properties of the input and output devices.

c. The Color Management Module (CMM) is a calculating and converter part of the color management system. In general, it is a part of the operating system, but there are individual CMMs used by image-editing programs - like Adobe (ACE) that is the CMM of the Photoshop. The CMM is able to using several color profiles. It establishes equivalences so called gamuts (color spaces) of two devices and mathematical connection between two device-dependent color spaces. During operation it uses the color profiles and the so called rendering intents (RI). RIs - described by mathematical model – defining the color transfer, between the devices, optimized for what kind of visual effect. If the color stimulus which is need to be converted not contained of the gamut of the target device, then the RI determines the compliance of the transforming so as to the current color coordinates transform to the gamut of the other device [2]. There are four types of RI in color management (Fig.2.):

- The perceptual RI is striving to a faithful reproduction of the perceived color while conversion.
- The most important property, converting saturation RI, is the color saturation.
- The absolute colorimetric RI is optimizing to the colorimetric same displaying
- The relative colorimetric RI is compounding to the previous method, nevertheless takes account to the source parameters while converting the white color stimuli.

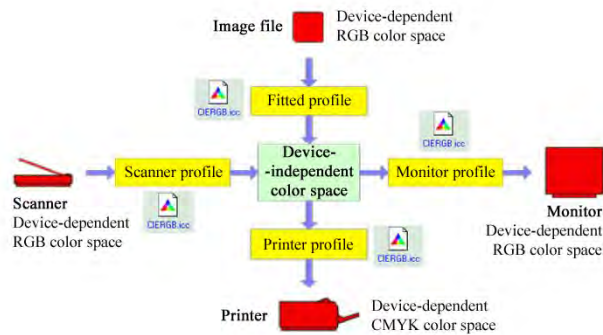


Fig.1. The operation of the color management system

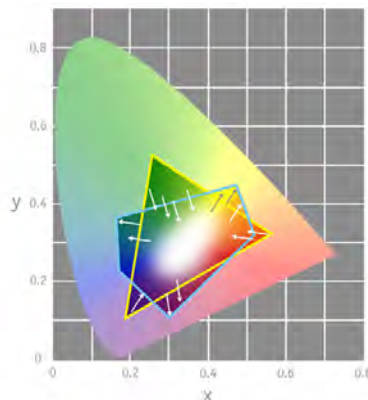


Fig.2. Explanation of RI in the case of a printer with five primary colors and an RGB monitor

3. USING COLOR PROFILES IN PRINTING

A decisive step of a designing, architectural, CAD or DTP (printing preparation) work process is to color the product according to the corresponding design. During designing usually this operation is carried out by a computer while the output is generally a color printer or printing machine. The key questions are that the stimuli could see on the monitor how to appear on the output side or even can we display them on the monitor within a specific color tolerance. If we don't use color management, the result is totally random and we can experience significant color fidelity and quality problems. Therefore it is obvious to use color management, because all the operating systems and design software including color management modules. Using color management has two conditions: application skills and having ICC color profile files. The first condition can be met by appropriate courses or knowing the literature however creating ICC color profiles is technically more complex and a costly process. Using the most simple color management – where we want to print a color-stimuli-perfect copy of a monitor displayed picture – we need at least two ICC color profile files: one monitor input and one printer output files. Creating ICC profile of a monitor is simple: an automatic calibrating software and a spectrophotometer or for the cheaper version a colorimeter with a color filter array are required. Fixing the optical aperture of the instrument to the monitor and starting the automatic software the ICC color profile file (containing the color display properties of the monitor) is ready in minutes. Printer calibration (profiling) is more complex, more time-consuming and more costly [3]. For measuring only expensive reflectance spectrophotometer is able to use. Primary color patches of printed test figures with certain number of patterns should be measured one by one. The results are analyzed by software and the ICC color profile is creating from these data. Hundreds of color patterns has to measure to create color profiles with appropriate quality (accuracy) and this is a time- and patience-consuming process even if investing in a costly X-Y coordinate moving table. It should be known that the manufacturer provides ICC profile files to the output devices (such as monitors or printers). These devices can be accessed on supplied CDs or on the manufacturer's website. A good question therefore, that why are expensive and time-consuming calibrations required, if these files are as easy to get? To decide a color profile of a printer and several manual calibrated ICC profiles were compared.

4. CREATING ICC PROFILE OF AN INKJET PRINTER

The investigated printer was an upper mid-range Canon Pixma iX5000 4 headed (CMYK) inkjet printer. The profile, created to this printer, was available on the website of the manufacturer. Because the color profile carries the properties of the paper therefore No. MP101 Canon paper and ink (included in the specification of the ICC color profile) were used. 343, 729 and 1728 colorpatterns were printed on these papers without color management. Our aim was to compare the color profile of the manufacturer against small, medium and large numbers of calibrating patterns. The color spots were measured by an X-Rite Eye-One Pro reflectance spectrophotometer (Fig.3.) Measuring small series takes 1,5 hour, the medium takes 3 hours and the large one takes 8 hours. Measuring with coordinate-board would take tenth of this. To create these three ICC profiles MonacoPROFILTER was used.



Fig.3. Calibration pattern and device using for calibration

5. CREATING THE COLOR STIMULI OF THE INKJET TEST

Table 1. The CIE Lab values of the 25 control color stimuli

No.	color stimulus (notation)	coordinates of color stimulus		
		L*	a*	b*
1.	Normal red (np)	43	57	39
2.	Light red (vp)	74	30	12
3.	Dark red (sp)	36	51	24
4.	Normal blue (nk)	53	-21	-34
5.	Light blue (vk)	76	-18	-19
6.	Dark blue (sk)	36	-10	-33
7.	Normal green (nz)	62	-49	31
8.	Light green (vz)	82	-27	20
9.	Dark green (sz)	40	-34	20
10.	Pink (p)	64	37	-9
11.	Turquoise (t)	70	-39	-8
12.	Light blue 2 (vk2)	85	-22	-4
13.	Greenish blue (zk)	56	-46	-9
14.	Normal yellow (ns)	82	16	79
15.	Greenish yellow (zs)	82	-3	47
16.	Orangish yellow (nrs)	78	24	51
17.	Normal brown (nb)	46	15	14
18.	Beige (b)	84	7	12
19.	Dark brown (sb)	31	8	9
20.	Light grey (vsz)	79	0	2
21.	Dark grey (ssz)	47	0	0
22.	Normal purple (nl)	60	20	-20
23.	Light purple (vl)	79	12	-14
24.	Dark purple (sl)	39	22	-22
25.	Orange (n)	70	37	60

To compare the color profile files testpatterns were printed by a printer set for 3 calibrated and 1 manufacturing profiles. These testpatterns containing 25 reference color stimuli (fig 4), which are compiled from specific color stimuli of NCS colorpatterns [4, 5]. Colorsamples are printed by Adobe Photoshop using the available 4 (3+1) color profiles and all the several RI, defining with CIE Labcoordinates of color stimuli - belonging to NCS color samples - in the Table 1. Thus, a total of 16x25 colorsample were measured. In order to objectivity, the control-measuring - also in CIE Lab color space [6] - were carried out using an other colorimeter (AvantesSpectrocam).



Figure 4: Reference test patterns

6. RESULTS AND EVALUATION

Theoretically, because of using color management, color-stimuli coordinates - measured with 25 colorsamples printed by four different profiles - should agree with values in the Table 1. Of course it is not the case, due to the inaccuracies of the profile of manufacturer and the numbers of the profiles. To adjudicate the quality of the profiles CIE $\Delta E^*_{a,b}$ color stimulus difference [7] were calculated, between each of measured color samples and the - theoretically- correct color stimuli from the Table 1. Using this method the color fidelity of the printed color sample can be shown. The high color fidelity belongs to a small color differences, and the small color fidelity conversely. Table 2. shows, considering for example the relative colorimetric RI, increasing the number of samples (343→729→1728) the $\Delta E^*_{a,b}$ color stimulus difference is reducing, deviating (not specified trend) or increasing.

Table 2: Trend of color stimuli in the case of absolute colorimetric RI

Trend	Abbreviation of color stimulus	Nr. of pieces
reducing $\Delta E^*_{a,b}$	nk, vp, ns, nlvk, zs, sb, b, sz, vsz, p, ssz, sl, nrs,	16
deviating $\Delta E^*_{a,b}$	sk, nz, vz, t, vk2, zk, nb, vl	7
increasing $\Delta E^*_{a,b}$	np, sp, n	2

Result, similar to the above, appeared in the case of the other three RIs as well. Thus our logical expectation is justified: increasing the number of the calibration patches is resulting ICC profiles with better color fidelity. Then let us see how the ICC profile of the factory was related to the three color profiles we created. This was examined that we were looked for that in how many cases were better or worse the color differences calculated with the profile of the manufacturer as color differences made without calibration carried out with the maximum number of elements (1728). In the case of the 4 RIs this number on average was 16, thus the profile of the manufacturer performed better result than the profile executed by hand and calibrated carrying out with the maximum number of elements.

At the beginning of the measurements, it was expected that the calibration carried out with large number of elements resulting better color fidelity than the calibrating by the manufacturer, because we had that experiences about monitors [8]. However following the results of our measurements we can trust in an ICC profile of a reputed manufacturer in the case of the printers. Probably, the color fidelity measured by the profile of the manufacturer is due to the original paper, the ink and this profile is presumably created using thousands of samples. This large number of elements is compensating the commercial quality changes of paper and the ink well. It can be possible, that using aftermarket-commodity causes much more worse results. Better color fidelity can be achieved with own calibration, if possibly the number of the elements by the calibration is even larger (more than 1728). Mechanized XY coordinate-table is need to this, otherwise we should calibrate for several days.

7. LITERATURE

- [1] Tim Grey: Color Confidence: The Digital Photographer's Guide to Color Management. SYBEX, London, 2004
- [2] Green P., Holm J., Li W.: Recent Developments in ICC Color Management. COLOR RESEARCH AND APPLICATION Vol. 33(6), pp. 444-448. 2007
- [3] FarkasZoltan:
Színmenedzsmethodszerekhatékonyágánakvizsgálatatintasugarasnyomtatókesetében . diplomaterv, BME-MOGI, 2010
- [4] Derefeldt G, Hedin Ce., Sahlin C.: Ttransformation of NCS data into cieluv color space, DISPLAYS Vol. 8(4), pp. 183-192, 1987
- [5] K Wenzel, K Samu: Pseudo-Isochromatic Plates to Measure Colour Discrimination. ACTA POLYTECHNICA HUNGARICA 9:(2) pp. 185-195. 2012
- [6] Dr. ÁbrahámGyörgy: Optika, Panem–McGraw-Hill, Budapest, 1998
- [7] LukácsGyula – Színmérés, MűszakiKönyvkiadó, Budapest, 1982
- [8] Samu K: A színhelyesszámitógépesmegjelenítésbiztosítása. ELEKTROTECHNIKA 100:(1) pp. 11-12., 2007

COLOR DIFFERENCES OF PROCESS COLORS AS PREDICTORS OF SECONDARY MIXTURES, RED, GREEN, AND BLUE IN DIGITAL TEXTILE PRINTING

Gojko Vladić, Nemanja Kašiković, Drako Avramović, Neda Milić
Faculty of Technical Sciences, Graphic Engineering and Design, Novi Sad

Corresponding author: Gojko Vladić
e-mail: vladicg@uns.ac.rs

1. ABSTRACT

Color printing of textile is achieved by subtractive color mixing of four process colors cyan, magenta, yellow, and key (black), also called CMYK color model. Real textile products are usually colored by wide variety of colors achieved by mixing of the process colors. The process colors are not often used in pure form. Great majority of research regarding the color of textile products and various influences on the color is dealing with process colors; therefore it is needed to gain insight in correlation between results for color differences of process colors and colors in real application. This paper focuses on correlation between color differences of process colors and secondary mixtures, red, green, and blue varying textile substrates in digital textile printing. Four different materials were printed with pure process colors and their mixtures using printing machine Mimaki JV22-160 with J-eco Subly nano inks, colors were measured and differences calculated. Comparison was made between color differences of process colors and their mixtures. The results of the research show strong correlation between color differences, it can be concluded that results of research on process colors can be good predictors for other colors achieved by mixing the process colors, although some inconsistencies were noticed and require further investigation.

Key words: textile printing, color differences, process color, color mixtures

2. INTRODUCTION

The market of textile products today is very diverse. Textile materials are used in fashion, furniture, packaging and many other industries. Each of the industries having its own specific needs and demands, thus using specific textile materials or their combinations. Great number of artificial and natural textile materials present in the market today can satisfy most of the demands. Textile materials are usually colored or printed during manufacturing process. All textile materials have distinctive properties and those properties can have influence on final color of colored or printed textile material. Dominant technique for printing textile is screen printing (Horrocks, 2000), although digital printing is taking greater share of the market every day. Digital ink jet printing is a relatively new technology for textile printing and it is increasingly attracting attention of the textile industry. Ability to quickly adapt to the market demands, ability to print on wide variety of materials and ability to produce satisfactory quality are main reasons for market success of digital ink jet printing technique (Novaković, 2010). Ink jet process offers more possibilities for creativity, flexibility as well as speed and environmental protection (Choi, 2005, Masaru, 2010). Also, designers are not limited in length of print formats and that gives opportunity for new ideas (Chun, 2011). Digital printing is more cost effective technique for small print runs, i.e. the circulation below 20 pieces, for higher circulations than that it is more profitable to apply screen printing (Novaković, 2010). Recent studies have proven that material characteristics have an influence on final color reproduction (Kašiković, 2012). Polyester, which is a hard, tough, synthetic material and it can be produced in various colors, shapes and sizes. It is made from chemical substances found in petroleum and is produced in forms of fibers and later compose textile materials. Silk which is natural material and it also can be produced in many variations as a textile material. Other materials have their own characteristics which make them suitable for specific products. Color printing of textile is achieved by subtractive color mixing of four process colors cyan, magenta, yellow, and key (black), also called CMYK color model. Real textile products are usually colored by wide variety of colors achieved by mixing the process colors. The process colors are not often used in pure form. Researchers in the field of textile printing are mainly

concentrated on the examination of various influences on process colors. Having that in mind, it is needed to gain insight in correlation between results for color differences of process colors and colors in real application.

For the purpose of determining color differences ΔE are computed using the Euclidean distance between the two stimuli. First color $[L_1, a_1, b_1]$ and second color $[L_2, a_2, b_2]$. The color difference between them is given by equation 1.

$$\Delta E = [(\Delta L)^2 + (\Delta a)^2 + (\Delta b)^2]^{1/2} \quad (1)$$

Focusing attention on process colors alone is not enough as the mixtures of these colors are used more often. This paper focuses its attention on correlation between color differences of process colors and secondary mixtures, red, green, and blue varying textile substrates in digital textile printing. Comparison between color differences of process colors and their mixtures printed on different textile materials are important in order to determine the values of color differences of process colors good predictors for color differences of secondary mixtures.

3. METHODS

3.1. Sample preparation

Test chart was created using appropriate graphic software. Test chart consisted of six color fields 150 mm by 150 mm, three fields of process colors, cyan, magenta and yellow all of them printed with 100 % coverage and three fields of secondary colors resulting from mixing process colors. Red as a result of mixing 100% magenta and 100% yellow, green as a result of mixing 100% cyan and 100% yellow and blue as a result of mixing 100% magenta and 100% cyan, as shown in the figure 1. Four different materials were printed with pure process colors and their mixtures using printing machine Mimaki JV22-160 with J-eco Subly nano inks. Materials chosen were three materials composed of 100% with different thread count and one silk material in order to insure color differences between prints, characteristics of the materials are shown in table 1.

Table 1. Characteristics of the materials

Tests	Material composition (%)	Fabric weight (g/m ²)	Thread count p/10cm	
			Warp	Weft
Silk	Silk 100%	120,3	N/A	
Polyester 1	Polyester 100 %	110,6	170	120
Polyester 2	Polyester 100 %	101,5	160	100
Polyester 3	Polyester 100 %	141,3	260	120



Figure 1: Test chart

3.2. Procedure

Samples were folded in four layers to achieve an opaque sample and avoid reflection off the backing material. Rotation and reposition of the samples was done to reduce measurement variability due to fabric construction, directionality of threads and unlevel dyeing. Sample conditioning was done in order to avoid variations in measurement data. Multiple measurements were done on the spectrophotometer HP 200 using d/8 measurement geometry with 16 mm

aperture, with D65 standard illuminant and 10° standard observer. Results gathered by measurement were stored to data base. Before data was analyzed average values for CIELab color coordinates were calculated. After the average CIELab color coordinates were calculated, color difference was determined between colors printed on different materials using equation 1. In order to determine whether color differences of process colors are good predictors of color differences of resulting color, correlation coefficient with statistical significance was calculated for color differences of process colors and resulting colors.

4. RESULTS

Average values for CIELab color coordinates for all four materials: unprinted substrate color, printed three process colors and printed secondary mixtures of process colors are shown in table 2.

Table 2. Average CIELab color coordinates of process and secondary colors printed on textile materials

	Silk			Polyester 1			Polyester 2			Polyester 3		
	L	a	b	L	a	b	L	a	b	L	a	b
Substrate	89.28	2.68	-5.8	89.75	1.25	-3.14	88.35	2.18	-4.57	89.36	1.17	-0.16
Cyan	40.37	-2.13	-24.19	29.74	-1.65	-23.31	34.76	-3.6	-21.84	32.05	-2.3	-19.46
Magenta	40.48	38.71	-0.58	34.2	45.91	4.9	36.05	41.23	2.42	34.46	40.49	2.52
Yellow	72.85	5.64	55.38	67.49	7.47	57.1	69.35	7.91	53.08	68.29	8.04	55.14
Red	42.38	41.18	8.81	35.55	51.27	10.7	37.34	46.18	9.23	35.27	48.52	10.63
Blue	29.22	5.39	-12.71	21.75	1.75	-8.91	26.24	1.23	-9.88	22.51	2.91	-8.02
Green	37.9	-9.65	1.34	28.23	-7.79	-1.3	32.7	-8.34	-0.21	29.88	-7.4	1.62

Results shown in figures 1, 2 and 3 represent color differences determined between process colors and secondary mixtures printed on different materials. Vertical axis showing value of ΔE , while horizontal axis shows which of the materials where compared: S/P1: Silk – Polyester 1, S/P2: Silk – Polyester 2, S/P3: Silk – Polyester 3, P1/P2: Polyester 1 – Polyester 2 P1/P3: Polyester 1 – Polyester 3 P2/P3: Polyester 2 – Polyester 3.

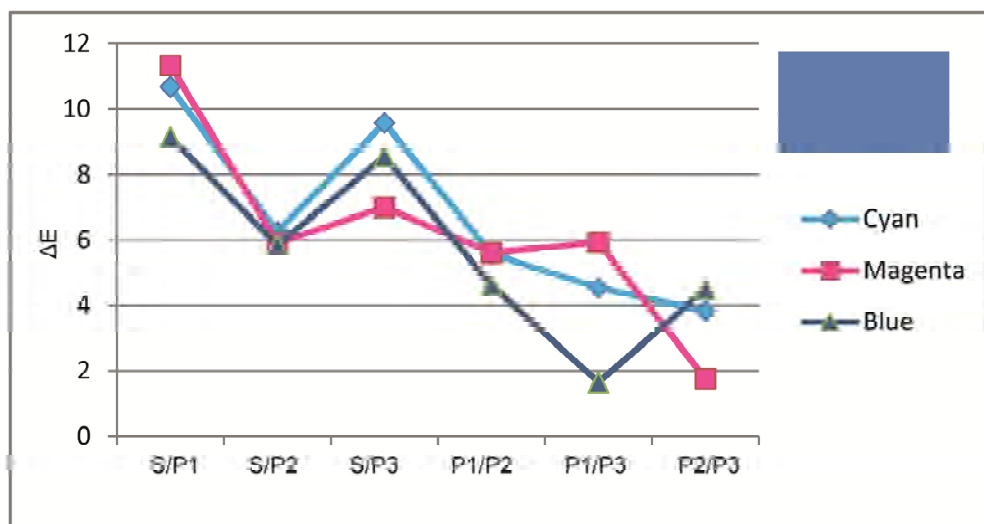


Figure 1. Color difference value between Cyan, Magenta and resulting Blue colors printed on different materials



Figure 2. Color difference value between Cyan, Yellow and resulting Green colors printed on different materials

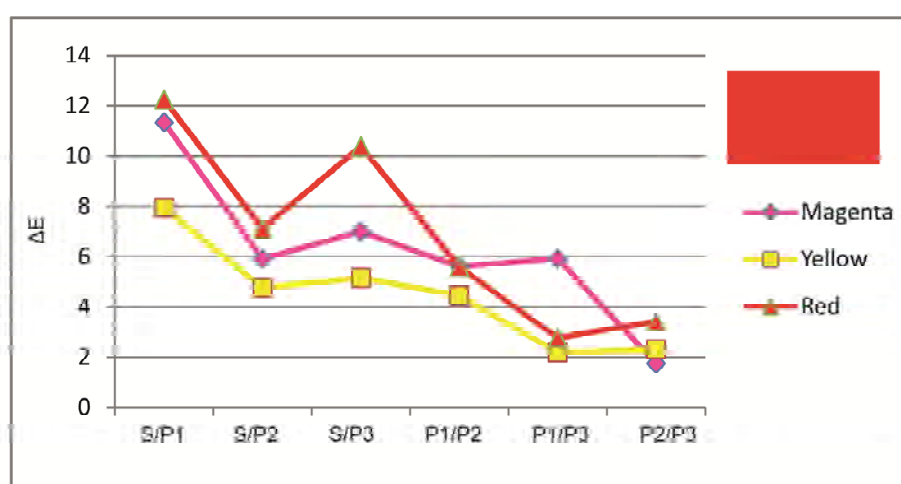


Figure 3. Color difference value between Magenta, Yellow and resulting Red color printed on different materials

Value of correlation coefficient calculated for color differences between materials printed with cyan and magenta is 0.867, between cyan and blue color value of correlation coefficient was 0.91 both statistically significant at $p < 0.05$. Value of correlation coefficient calculated for color differences between materials printed with blue and magenta was 0.629 and not statistically significant at $p < 0.05$.

Value of correlation coefficient calculated for color differences between materials printed with cyan and yellow is 0.912, between cyan and blue color value of correlation coefficient was 0.991 and value of correlation coefficient between materials printed with yellow and green was 0.937, all of them statistically significant at $p < 0.05$.

Value of correlation coefficient calculated for color differences between materials printed with magenta and yellow is 0.875, between magenta and red color value of correlation coefficient was 0.817 and value of correlation coefficient between materials printed with yellow and red was 0.946, all of them statistically significant at $p < 0.05$.

5. DISCUSSION

Color differences are determined by CIELAB equation 1, although some of the other color difference equation, such as CMC, M&S, BFD, and CIE 94, might give other results. Analysis of the results show strong correlation between process colors printed on all materials thus it can be noticed that reproduction quality is very dependent on the characteristics of textile material. In case of color differences between materials polyester 1 and polyester 3 from figures 1 and 3

it can be noticed that both blue and red color significantly differ from results of ΔE for magenta and it causes of low correlation coefficient between magenta and blue color. This high value of ΔE for magenta while retaining low value of ΔE for blue color can be caused by some material characteristic, other than composition which is the same 100% polyester. Significantly higher thread count that can be noticed, specially the warp, 260 for polyester 3 and 170 for polyester 1. This is not enough to come to conclusion and it must be further examined.

Yellow color showed smallest color differences between all materials. Color differences for secondary mixtures in which yellow color is included, red and green, are significantly higher. In case of green color figure 2 clearly showed dependence on cyan component of mixture and very high correlation coefficient of 0.991 statistically significant at $p < 0.05$ proves that as a fact. Red color as a result of mixing yellow and magenta shows stronger correlation coefficient to yellow but that can be explained by the differences between materials polyester 1 and polyester 3 which is already mentioned. Blue color as a resulting mixture of magenta and cyan is only color that did not show statistically significant correlation at $p < 0.05$, once again differences between materials polyester 1 and polyester 3 can be explanation, specially having in mind high correlation coefficient 0.91 with cyan color.

6. CONCLUSIONS

It can be concluded that color differences of process colors can be a predictor for color differences of secondary mixtures, but quality of those prediction is influenced by the characteristics of the material, or some other factor that is to be examined. Although this requires further investigations differences which are noticed in case of magenta printed material polyester 3 are good indicators of this. On the other hand strong correlations between color differences of secondary mixtures to the process colors that created them are good enough reason to take noticed inconsistencies as an exemption to the rule. Further research on subject of process colors usage as predictors of secondary mixtures will put emphasis on the inconsistencies noticed in this research.

Acknowledgments

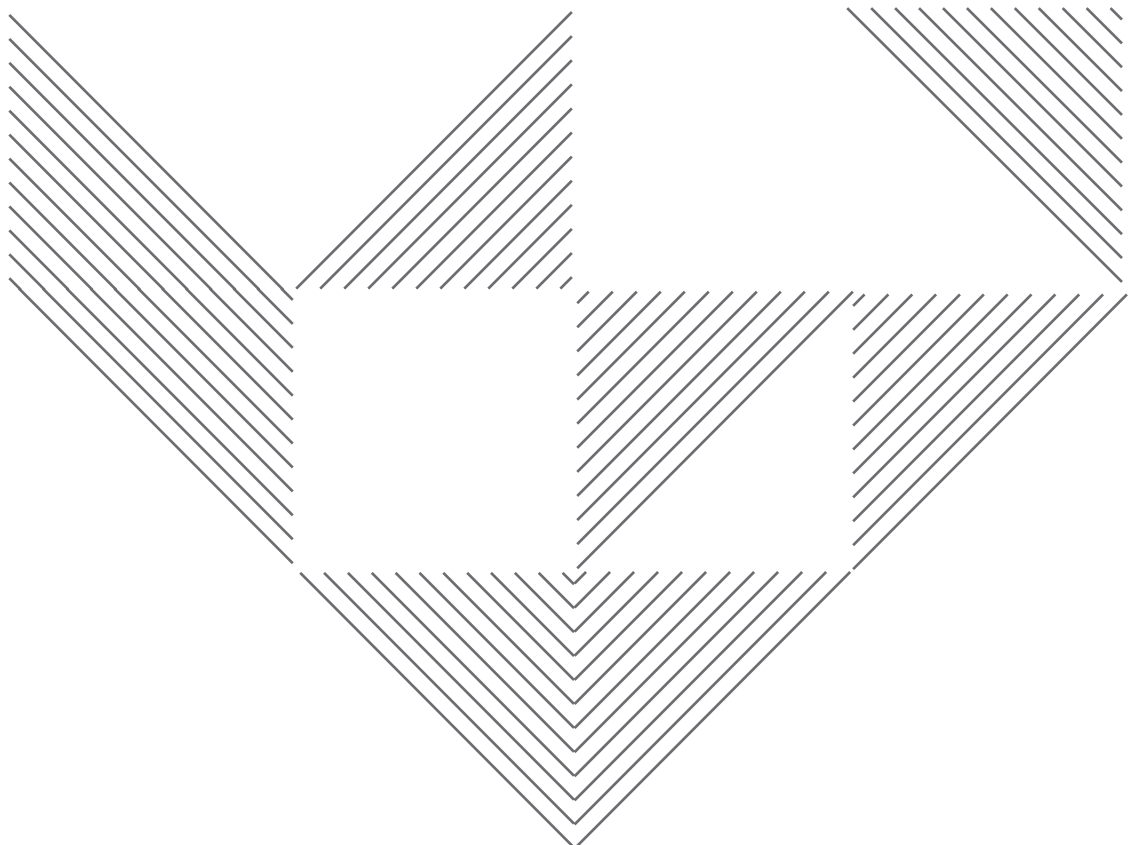
This work was supported by the Serbian Ministry of Science and Technological Development, Grant No.:35027 "The development of software model for improvement of knowledge and production in graphic arts industry".

7. LITERATURE

- [1] Choi P. S. R. , Yuen C. W. M. , Ku S. K. A. , Kan C. W. "Digital Ink-jet Printing for Chitosan-treated Cotton Fabric", *Fibers and Polymers*, 6 (3), 229-234, 2005
- [2] Chun J. H. "A review of the characteristics of digital art expressed in contemporary fashion", *International Journal of Fashion Design, Technology and Education*, 4 (3), 161 – 171, 2011
- [3] Ebner M., *Color Constancy*, (John Wiley & Sons Ltd, England, 2007)
- [4] Horrocks, A.R. *Handbook of Technical Textiles*, (The Textile Institute, 2000.)
- [5] Kašiković N., Novaković D., Karlović I, Vladić G.. "Influence of Ink layers on the quality of ink jet printed textile materials", *TEKSTIL ve KONFEKSIYON*, 22(2), 115 – 124, 2012
- [6] Masaru O. , Kazuhide Y., Yukio A. "Textile Printing by the Ink-Jet Printer" *Nihon Gazo Gakkaishi/Journal of the Imaging Society of Japan*, 49 (5), 417-423, 2010
- [7] Novaković D., Kašiković N., Vladić G.: "Analiza promene na digitalno štampanom pamučnom materijalu izloženom toplotnom dejstvu" *Tekstilna industrija*, 58 (1), 32-37, 2010
- [8] Novaković D, Kašiković N, Vladić G.: "Integrating Internet application in to the workflow for costumisation of textile products", *International Joint Conference on Environment and Light Industry Technologies*, Budapest, Hungary, Obuda University, Faculty of Light Industry and Environmental Engineering, 978-615-5018-08-4, 471 – 476, 2010



Digital and Web Media



HTML5 AND SVG DRIVEN METHODS FOR DATA PRESENTATION IN SCIENTIFIC PUBLISHING

*Darko Avramović, Nemanja Kašiković, Gojko Vladić, Željko Zeljković
Faculty of Technical Sciences, Graphic Engineering and Design, Novi Sad*

*Corresponding author: Darko Avramović
e-mail: adarko@uns.ac.rs*

1. ABSTRACT

This paper proposes certain methods of displaying scientific results to public. Instead of common data carrier format types like Adobe PDF, HTML5 and SVG offer alternative way of graphic presentation of data. The paper shall present methods of generating dynamic graphs, plots, color palettes and other sorts of graphic objects used for displaying science results. Nevertheless, performance tests were conducted to determine common browsers performances while creating such objects. Individual and mixed objects patterns were used. The browsers ran inside specially created test environment including dedicated chamber application for performance measurements. The data gathered was statistically processed and based on that conclusions were made.

Key words: *html5, svg, graphics, browser, performance*

2. INTRODUCTION

Scalable Vector Graphics or SVG is language developed for purposes of describing two-dimensional graphics in XML (W3C, 2012). SVG presents new XML based format of describing scalable 2D graphics which is commonly used inside Web based applications. These applications are often rendered by common web browser clients (Peng, 2000). Scalable Vector Graphics format or SVG allows three different types of graphic objects to be operated with: scalable vector graphics (paths that consists of lines or curves, etc), images and text.

The content of an Scalable Vector Graphic document is pure XML data. The data can be easily created by any kind of server based or client based technology. Other advantage of SVG is that it is fully scalable and not pixel based and therefore there is not data loss during image editing or scaling operations (Avramović et al., 2012).

Also, Scalable Vector Graphics are widely used for displaying scientific information and data. The data can be easily represented using SVG graphs, diagrams and other types of data presentation which is applicable by SVG (Kim, E.N. et al., 2012)

3. RELATED WORK AND MOTIVATION

Similar researches were conducted by Moreno and de Olivera in 2008. They measured system CPU and Memory utilization as well as web application response times. The tests were performed using simple and complex SVG graphics patterns. Browsers used during tests were Internet Explorer version 6 (dates from year 2001), Firefox 1.5 (dates from year 2005) and Opera 9.02 (dates from year 2006). Platform used during tests was Microsoft Windows. The browsers used for testing are out dated and the results presented do not give the information usable today (Avramović et al., 2012) (Release Histories for all Major Browsers [Online], 2012).

Another research has been conducted by Avramović et al. 2012 which presented information about browser performances and CPU and Memory states. The browsers that were used during the research were: Google Chrome 18.0, Mozilla Firefox 12.0, Opera 11.64 and Apple Safari 5.1.7 (due to lack of support Internet Explorer was excluded from research). Platform that was used during tests was Microsoft Windows. Apple Safari achieved the best results in terms of SVG generating speed while Opera did not perform that well. CPU utilization and bottleneck situations were observed and the tests returned significant results.

Also, motivation to conduct this type of research was development of highly sophisticated web based applications used during print production. Scalable Vector Graphics are frequently used as crucial component of such systems. Web-To-Print applications also known as Web2Print presents commercial prepress process that bridges a gap between digital content online and

commercial print production (Avramović et al., 2012). This process allows client to create from scratch, edit or approve online templates during prepress process. The core part of these processes is SVG graphics and these facts served as motivation for this research.

4. EXPERIMENT AND EXPERIMENTAL ENVIRONMENT

Experiments were conducted using latest versions of popular web browsers: Google Chrome Version 22.0.1229.94, Mozilla Firefox Version 16.0.1 and Opera Version 12.02. Platform used was Linux 3.2.0-23-generic #36-Ubuntu x86_64 GNU/Linux. Due to platform limitations Microsoft Internet Explorer and Apple Safari were omitted from the research. Table 1 presents hardware specification of the environment used for testing applications.

Table 1: Testing environment hardware specification

Hardware used	
CPU	Intel i3 2.5GHz
Memory	4GB DDR3
GPU	1GB DDR5 DirectX 11 compatible

Software supporting this research consists of several specially made scripts. The scripts were executed and relevant data has been recorded. Tests were performed inside specially designed chamber application environment used to measure script execution times.

The scripts mentioned were used to generate different number of SVG objects. Depending on number of objects and average amount of data generated, conclusions shall be made.

First SVG object type was called “graphImage” and it represents simple graph generated using random data (Figure 1).

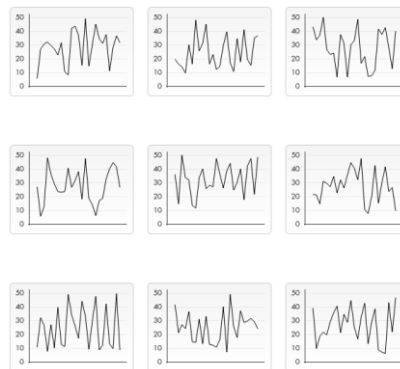


Figure1: “graphImage” SVG object sample

These objects were generated using a following pseudo source code:

```

Cv0 = getCanvas()
Ct0 = Cv0.getContext(ctx2d)
call Cv0.moveCursorToStart()
for i = {1..24}
  Pi = MATHFLOOR(MATHRAND()+Lu-LI-1)+LI
  call Ct0.addPoint(50i+5, Pi)
  call Ct0.drawLine()

```

Cv0 – canvas object
Ct0 – context
Pi – point
Lu – upper limit
LI – lower limit

Second SVG object type was called “draw5x5”. The object consists of certain number of color palettes. Figure 2 displays such example.

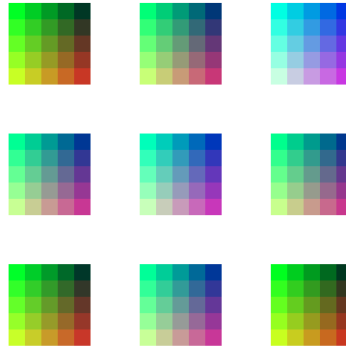


Figure 2: "draw5x5" SVG object sample

These objects were generated using a following pseudo source code:

```
Cv0 = getCanvas()
Ct0 = Cv0.getContext(ctx2d)
for i = {0..4}
  for j = {0..4}
    Cr = MATHFLOOR(50*i)
    Cg = MATHFLOOR(255-50*j)
    Cb = MATHFLOOR(MATHRAND()*255)+1
    call Ct0.fill(rgb(Cr, Cg, Cb))
    call Ct0.drawRectangle()
```

Cv0 – canvas object
Ct0 – context
Cx – colour component

Third SVG object type was called "transGradient" and it consists of four process colors gradient scales. Figure 3 presents example script output. These objects were generated using a following pseudo source code:

```
Cv0 = getCanvas()
Ct0 = Cv0.getContext(ctx2d)
call Ct0.fillRectangles(colorInformationType)
for i = {0..9}
  for j = {0..3}
    call Ct0.fillStyle(rgba(255,255,255,i+1/10))
    call Ct0.fillRect(5+i*14,5+j*37.5,14,27.5)
```

Cv0 – canvas object
Ct0 – context

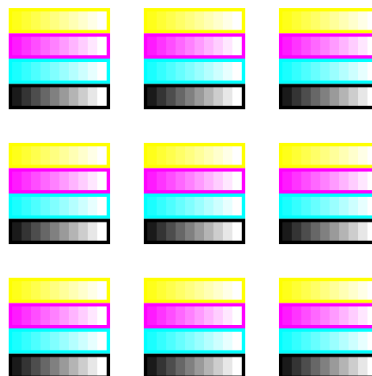


Figure 3: "transGradient" SVG object sample

The fourth SVG object type is called "transCircles" and it consists of transparent circles inscribed into four color fields which is presented in Figure 4.

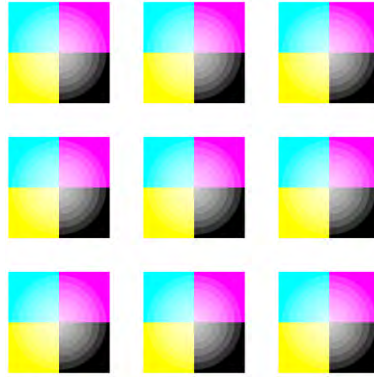


Figure 4: “transCircles” SVG object sample

SVG objects presented in Figure 4 were generated using following pseudo source code:

```
Cv0 = getCanvas()
Ct0 = Cv0.getContext(ctx2d)
call Ct0.fillRectangles(colorInformationType)
Ct0.globalAlphaProperty = 0.2
for i = {0..6}
call Ct0.drawArc(75,75,10+10*i,0,2π,true)
call Ct0.fill()
```

Cv0 – canvas object
Ct0 – context

At the end, the fifth SVG object has been called “circle5x5” and is consisted of 25 circles with colored strokes. The object is presented in Figure 5.

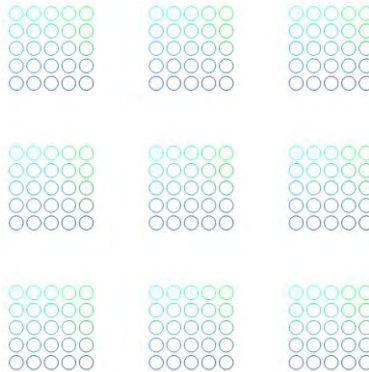


Figure 5: “circle5x5” SVG object sample

The object was created using following pseudo source code:

```
Cv0 = getCanvas()
Ct0 = Cv0.getContext(ctx2d)
for i = {0..4}
for j = {0..4}
Ct0.strokeStyle = rgb(0, MATHFLOOR(255-50i), MATHFLOOR(255-50j))
Ct0.drawArc(12.5+j*25,12.5+i*25,10,0,2π,true)
```

Cv0 – canvas object
Ct0 – context

The objects were chosen against shape complexity parameters, number of colors, methods of generation, and amount of bytes generated by the particular script execution. There were four tasks (cases) of script execution. For each task each script generated different

number of objects. For the first task number of objects was 50, for the second it was 100, for the third it was 150, and for the fourth task the number was 200 objects. For each task of each browser 50 samples of time were taken and recorded. That means that each browser has been tested 200 times for each script. Total amount of measurements for all browsers and scripts taken is 3000 samples.

5. RESULTS AND DISCUSSION

After performing scripts efficiency measurements, the following results were obtained. Figures 6a to 10a present average generation times for each SVG object type generated using scripts described earlier. Average amount of generated bytes per object is presented in Table 2. “circle5x5” script generates the largest amount of output bytes. “graphImage” script on the other hand generates the least data.

Table 2: Average amount of data generated by SVG object types

SVG object type	Amount of data
circle5x5	6239 bytes
transGradient	4313 bytes
draw5x5	2909 bytes
transCircles	1262 bytes
graphImage	687 bytes

As it is visible from Figures 6a to 10 Google Chrome browser performed the best in comparison to other browsers. Google chrome achieved best results no matter the amount of output data created. Firefox performed the worst in 4 out of 5 tests. The only test where Firefox performed better than opera was during generation of “draw5x5” SVG objects.

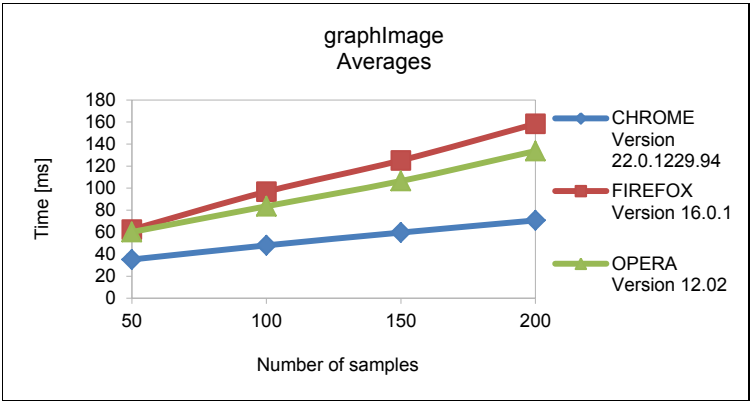


Figure 6a: “graphImage” SVG object type average generation times depending on number of samples

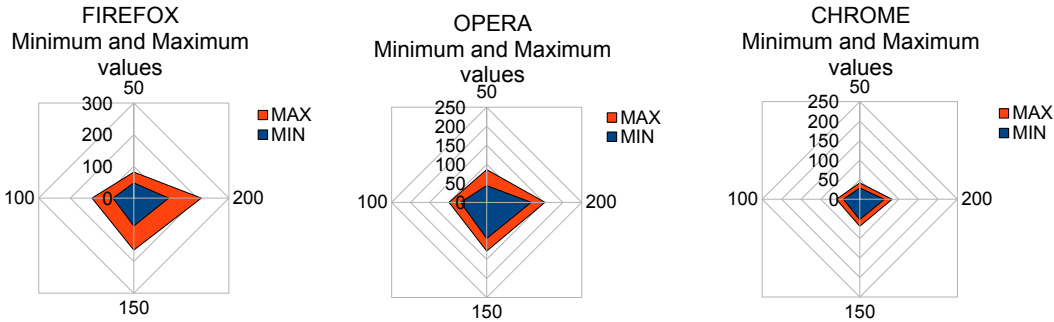


Figure 6b: “graphImage” SVG object type minimum versus maximum generation times per browser

In case of “graphImage” SVG object, from Figure 6a, we can see that the difference between test completion times is not so great between browsers. In case Chrome and Opera, curve up growth is almost linear. Firefox presented slight oscillations and the curve deviates from linearity. The true difference between browsers performances is obvious if the diagrams from Figure 6b are analyzed. The diagrams show the difference between minimum and maximum generation times for each of four tasks. Greater difference between minimum and maximum values indicates the level of performance drop after adding more objects to be generated.

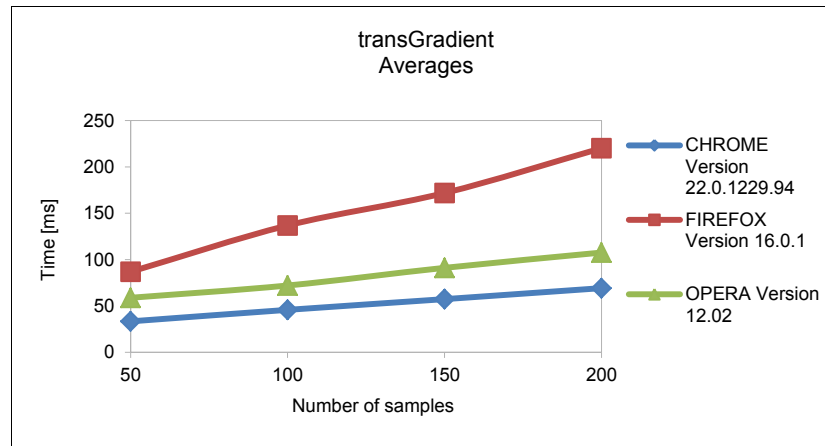


Figure 7a: “transGradient” SVG object type average generation times depending on number of samples

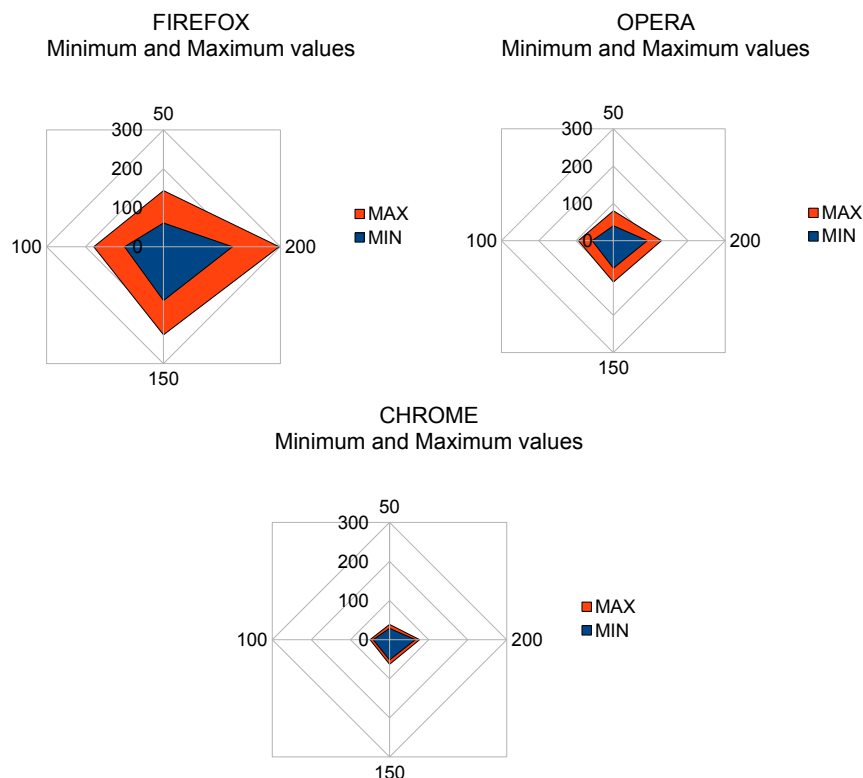


Figure 7b: “transGradient” SVG object type minimum versus maximum generation times per browser

The second SVG object type that was tested was “transGradient”. The results gathered emphasize the differences between browsers even more. Opera performance was slightly better than in case of previous test, but Firefox performance dropped. Curves strive to linear state in case of all browsers but Firefox where slight oscillations are present. Figure 7b shows even

bigger differences between Firefox and the other two browsers. Opera and Chrome present small performance drop. On the other hand, performance drop in case of Firefox is significant.

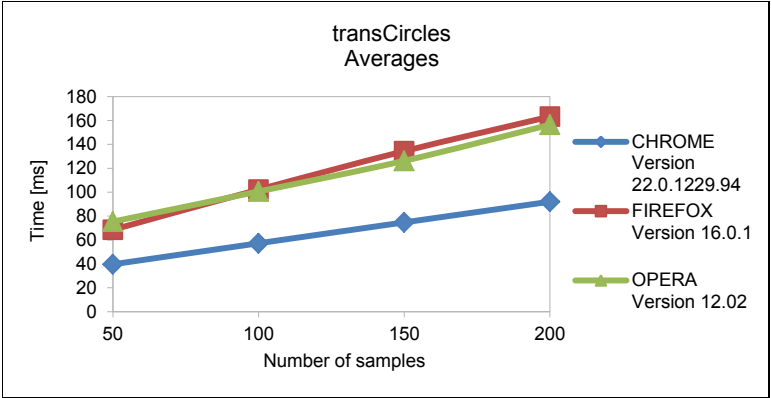


Figure 8a: “transCircles” SVG object type average generation times depending on number of samples

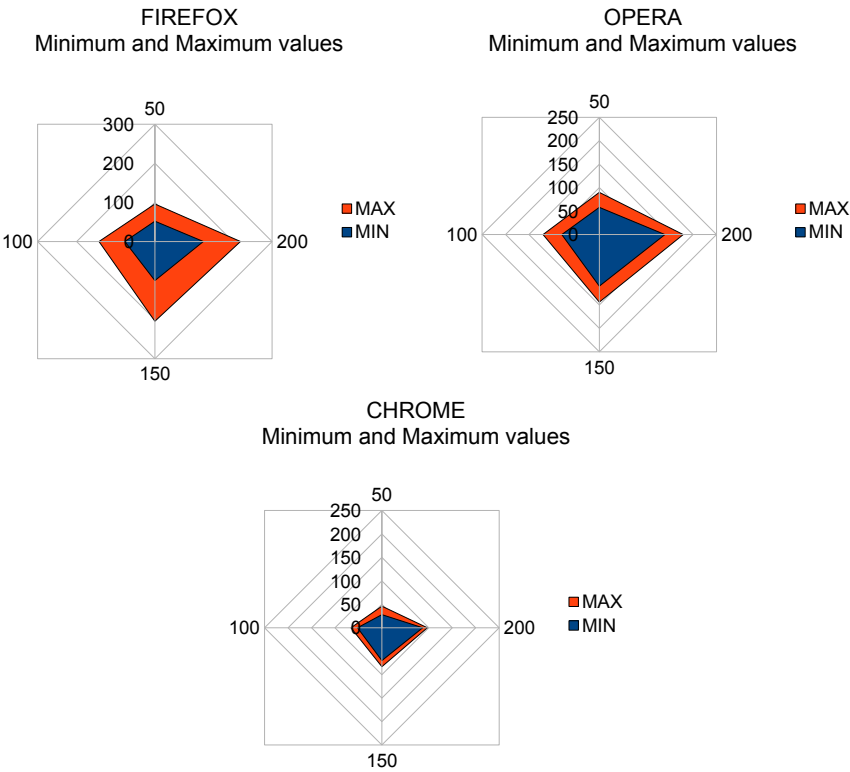


Figure 8b: “transCircles” SVG object type minimum versus maximum generation times per browser

The third test, “transCircles”, gave us slightly different picture. In this case, Opera and Firefox performance levels are almost the same. Opera achieved slightly worse results during 50-samples test case. Figure 8b shows that Opera minimum values are greater than minimum values Firefox achieved, but the difference between minimum and maximum values in case of Firefox are especially emphasized.

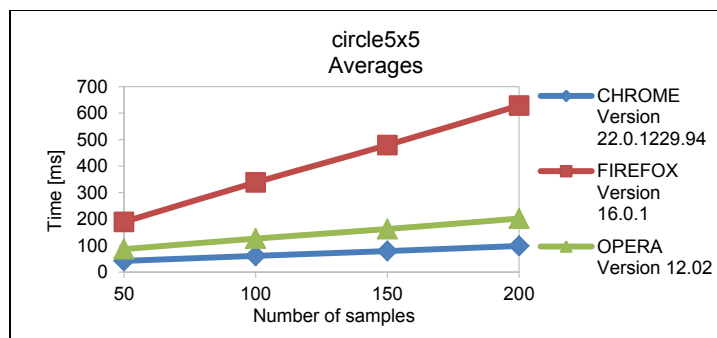


Figure 9a: "circle5x5" SVG object type average generation times depending on number of samples

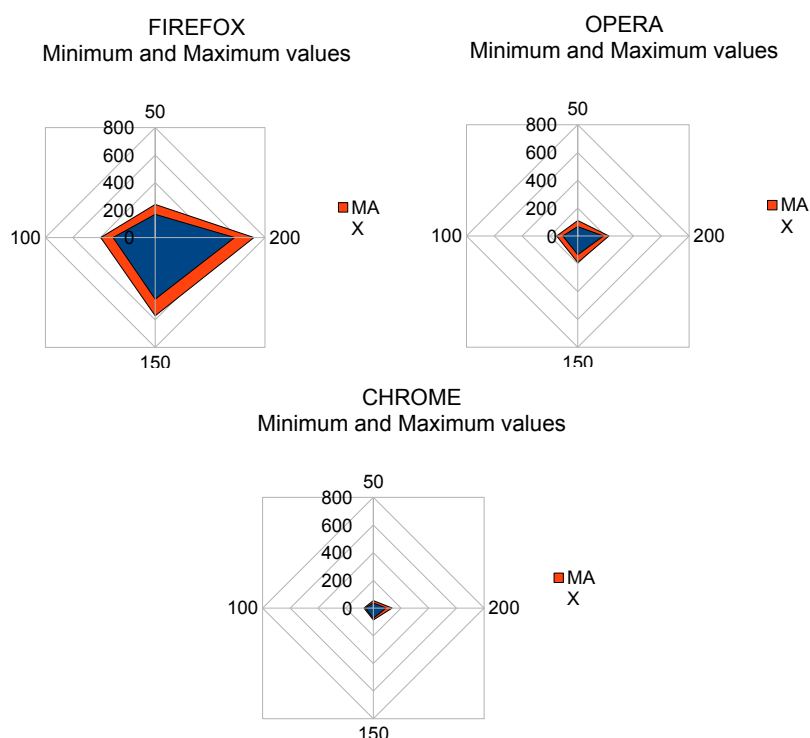


Figure 9b: "circle5x5" SVG object type minimum versus maximum generation times per browser

SVG object type "circle5x5" deepened the differences between Firefox browser and the other two. Significant performance drop is obvious both from Figure 9a and 9b. Minimum and maximum object generation times are way worse than results achieved by Opera and Chrome. Firefox maximum object generation times go as high as 719ms, which is bad in comparison to other two web browsers.

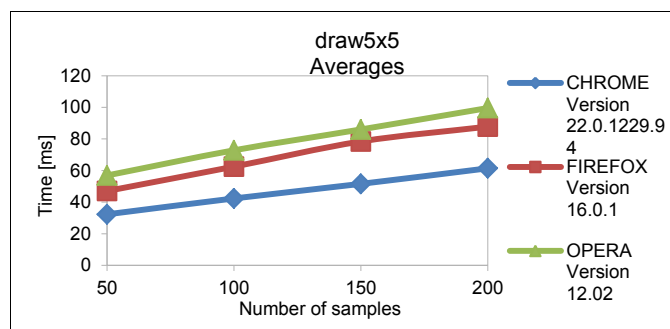


Figure 10a: "draw5x5" SVG object type average generation times depending on number of samples

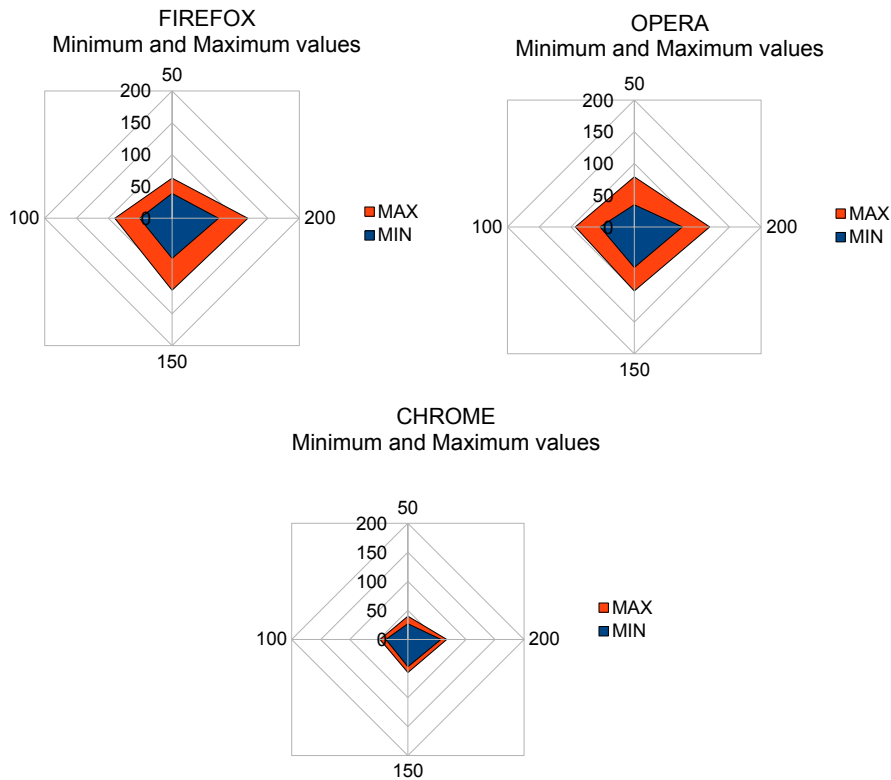


Figure 10b: “draw5x5” SVG object type minimum versus maximum generation times per browser

The last test gave the results that were announced during “transCircles” SVG object generation tests. In this case Opera achieved worst results of all three browsers. Also, Firefox curve deviates from linear trend, oscillations are present. Figure 10b reveals that minimum to maximum relations are similar for Opera and Firefox. Average values presented in figure 10a reveals slightly worse results.

If the amount generated data is taken into consideration, not all results are expected. Results gathered reveal that test completion time is not always directly related to amount of data created. It means that if the time needed to complete one test is x and the amount of generated data is y , and on the other hand time needed to complete other test is q , and the amount of generated data is w , possible result is that $q < x$ and in the same time $w > y$. The situation is present in case of “draw5x5” SVG object type.

6. CONCLUSIONS

It can be concluded that describing scientific data is possible using Scalable Vector Graphics. SVG is very good replacement for popular data exchange formats like PDF. Also, one more good thing that comes with SVG is the thing that it is fully exportable into many other formats because SVG inside is pure XML which is widely readable and widespread today. SVG proved to be convenient and reliable graphic format which has been proved today considering its wide usage as a core part of sophisticated web-to-print systems. Each user needs stability and efficiency and this paper also gives a clue which browser is best to use in cases of creating objects mentioned. Opposite to Avramović et al. 2012 results, Opera web browser improved its performance and here has nice advantage over Firefox web browser. Depending on complexity of objects generated, web browser performance drops are present with increasing number of objects to be generated. The drops are more distinctive in case of Firefox browser, and least distinctive in case of Chrome browser. Chrome browser proved to be best optimized for SVG based tasks and SVG in general.

Acknowledgments

This work was supported by the Serbian Ministry of Science and Technological Development, Grant No.:35027 "The development of software model for improvement of knowledge and production in graphic arts industry"

7. LITERATURE

- [1] Avramović, D., Zeljković, Ž., Milić, N., Vladić, G.: "Evaluating Web browser graphics rendering system performance by using dynamically generated SVG", *Journal of Graphic Engineering and Design*, Volume 3 (issue 1), 15-22, (2012.)
- [2] Peng, C, SCALABLE VECTOR GRAPHICS (SVG), Tik-111.590 Research Seminar on Interactive Digital Media, (2000)
- [3] World Wide Web Consortium (W3C), SVG 1.1 (Second Edition) [Online], URL <http://www.w3.org/TR/SVG/intro.html> (last request 15th October 2012).
- [4] Impressive Webs, Release Histories for all Major Browsers [Online], URL <http://www.impressivewebs.com/release-history-major-browsers/> (last request 15th October 2012)
- [5] Kim, E.N., et al. Web-based (HTML5) interactive graphics for fusion research and collaboration, *Fusion Eng. Des.* <http://dx.doi.org/10.1016/j.fusengdes.2012.03.041> [Article in press], (2012)
- [6] Moreno, E. D, de Oliveira, J. I. F., Architectural impact of the SVG-based graphical components in web applications, *Computer Standards & Interfaces* 31 1150–1157, (2009)

JDF-PDF PREFLIGHT SOFTWARE

Vivien Bareis, Iryna Artemieva, Barbara Dörsam, Thomas Hoffmann-Walbeck
Stuttgart Media University, Stuttgart

Corresponding author: Iryna Artemieva
e-mail: ia009@hdm-stuttgart.de

1. ABSTRACT

Software is presented that analyses inconsistencies in the definition of trim boxes and bleed boxes for a job. For that the PDF-file and the related JDF-file are examined.

Key words: Preflight, PDF, JDF, Trim box, Bleed box

2. INTRODUCTION

Preflighting in Workflow Management Systems is usually based on PDF only and not in the context of product and production definitions written in JDF. But it is obvious that it can be quite powerful to check inconsistencies in the page definition of PDF with the job definition of JDF. Those can easily occur, in fact, since JDF often is generated when calculating the costs with the help of a print shop's MIS, while PDF is created independently by an advertising agency.

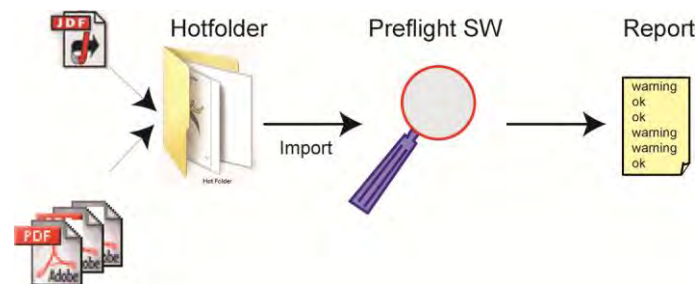


Figure 1: Software architecture

The program that we present here checks such differences with respect to trim boxes, bleed boxes and implicitly page sizes and number of pages.

Trim boxes and bleed boxes are optional entries in the dictionaries of the *Page*-object within a PDF-file [2]. Trim boxes are mandatory for PDF/X-files, but bleed boxes are not. The default value for the bleed box is the value of the cropbox, the default value of the cropbox is the value of the mediabox, which is a required entry. We comply with this consent, while we assume the existence a trim box entry for each page. In our software we access these entries processing the usual object tree in PDF, which is sketched in figure 2.

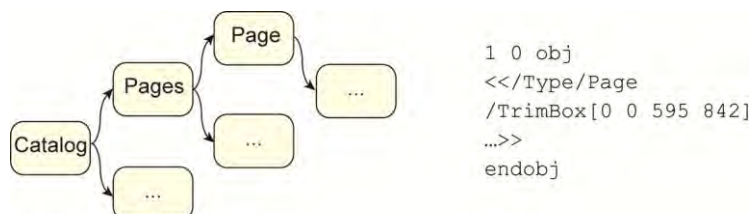


Figure 2: Object tree in PDF and Example of PDF-Object Page

The situation is more complex with JDF metadata, mainly because such files get modified permanently during the production process. This is so, because each software module that reads the JDF file normally also updates it with new details concerning processes that are further upstream in the workflow as well as about the execution result of the module. Therefore,

for example, the JDF file issued by a MIS looks quite different after the sheet layout software has been applied on it. We assume that the latter is the case, that is, one or more *Layout*-resources are available in the JDF-file [1]. In other words, we are going to preflight the PDF/JDF-files just before the imposition process (=combining PDF content on to a surface) is due. The situation gets even more obscure because the resources need not to be written inside the JDF-node that is responsible for the imposition process, but can be stored in any JDF-node that is closer to the root. Therefore, we have to import all nodes of the entire JDF-file and have to scan each *ResourcePool* (if there is one) for the *Layout*-resource. A *Layout*-resource contains or references one or more abstract elements called *PlacedObject* in the form of *ContentObjects*. Those have the two optional attributes *TrimSize* and *ClipBox*.

3. METHODS

The program is written in Java. Furthermore, the JDFLib-J-2.1.4a62 library of the CIP4 organization (see www.cip4.org) and the *PDFBox* from the Apache Software Foundation (see <http://pdfbox.apache.org>) are used.

4. RESULTS

The software compares information from a JDF and the related PDF files. Without loss of generality we are assuming that one single PDF-file only is present (we always could combine several files to a singleton). The result of the preflight check is issued as text message. Possible inconsistencies are outputted as an error or warning.

Figure 3 gives an overview of the crucial part of the software. First the PDF-file is imported, then the JDF. The following methods are checking the number of pages, the trim boxes and the bleed boxes in PDF and JDF. Inside these methods warnings or approvals are created and returned. The method *output* collects these and returns them to the calling method, which output the messages in the GUI.

```
public String output() {

    // import PDF file
    PDDocument pdf = null;
    PDFHelper pdfhelper = new PDFHelper();

    try {
        pdf = PDDocument.load(Constants.inputFilePDF);}
    catch (IOException e) { e.printStackTrace(); }

    // import JDF file and create JDF-document / KElements
    JDFDoc jdfDocument = null;
    jdfDocument = JDFDoc.parseFile(Constants.inputFileJDF);
    JdfHelper jdfHelper = new JdfHelper();
    List<JDFNode> jdfNodeKElements = jdfHelper.storeAllJdfNodes(jdfDocument);

    String msg1 = checkNumberOfPages(pdf, jdfNodeKElements, jdfHelper);
    String msg2 = checkTrimBox(pdf, pdfhelper);
    String msg3 = checkBleedBox(pdf);

    try { pdf.close(); }
    catch (IOException e) { e.printStackTrace(); }

    return(msg1+msg2+msg3);
}
```

Figure 3: Overview of the programm's source code

The examination of the trim boxes are fairly straight-forward. First of all, it should be checked if the PDF-file contains as many pages as needed in the JDF job description, i.e. if the number of references inside the *Pages*-object to different *Page*-objects in the PDF-file equals to the number of the *ContentObjects* in the JDF-file. Next, one has to find out if all PDF pages have the same dimensions. Similarly one needs to check if all JDF templates in the sheet layout have the same size. If both are true, then finally one should determine, if both these rectangles have the same widths and heights. Figure 4 shows the flow chart.

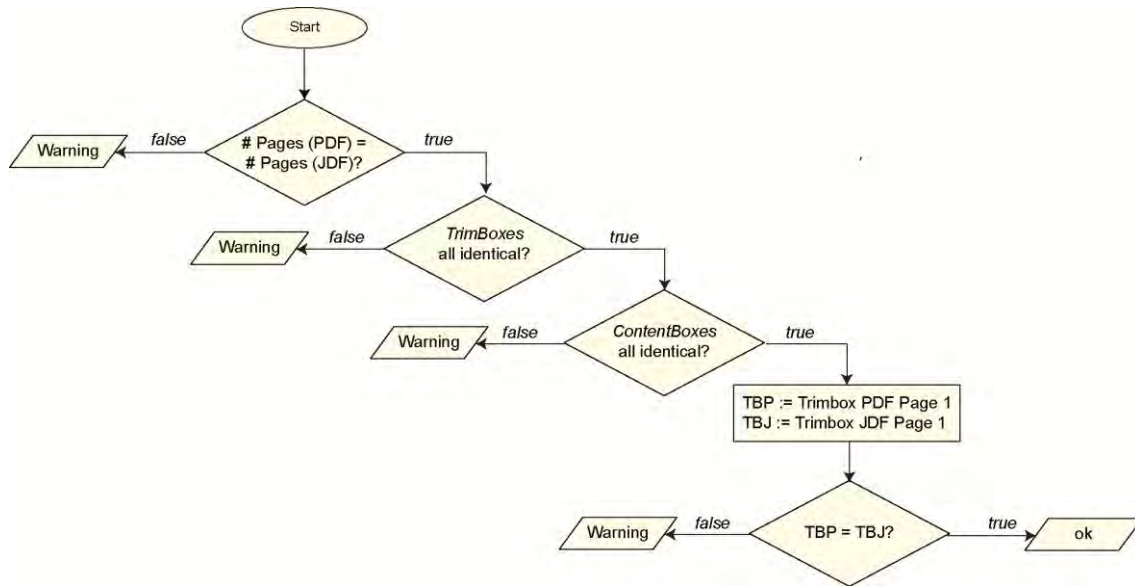


Figure 4: Flow chart for checking trim boxes

The output results of the first two conditional symbols can be seen in figure 5 for a sample run.

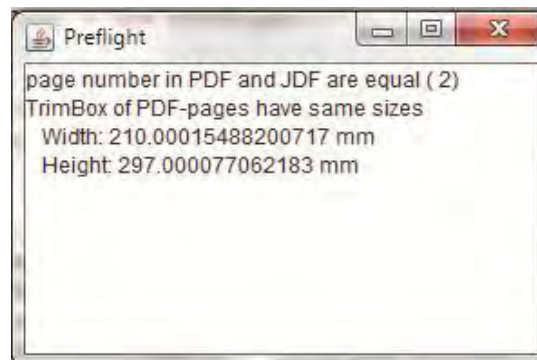


Figure 5: Page numbers (PDF, JDF) and trim boxes (PDF)

In order to find the number of *ContentBoxes* in the JDF-file, we need to parse the entire JDF-file and find all JDF-nodes recursively. Figure 3 shows that the parsing of the file is simply done by the CIP-method *parseFile* in the class *JDFdoc*. The code in Figure 6 shows the method *findJDFNodes* that looks for all JDF-kids of a JDF-Node, writes them into the *JDFNodeKElements* -list and executes the methods on all the kids.

```

public void findJDFNodes(KElement parentKe, List<JDFNode> jdfNodeKElements){
    if(parentKe != null) {
        KElement[] kidsKElementArray = parentKe.getChildElementArray();

        for (int i = 0; i < kidsKElementArray.length; i++){
            KElement kidKEL = kidsKElementArray[i];
            if(kidKEL instanceof JDFNode) {
                JDFNode jdf = (JDFNode) kidKEL;
                jdfNodeKElements.add(jdf);
                findJDFNodes(kidKEL, jdfNodeKElements);
            }
        }
    }
}
  
```

Figure 6: Parsing a JDF-File and scanning the nodes

Note, that the sizes of the PDF-TrimBoxes and the JDF-TrimSizes need not be equal necessarily. That is, due to rounding errors during the calculation the absolute difference of these two values need not to be exactly zero but rather “fairly small”. One is tempted to set up the preflight check concerning bleed boxes in a similar fashion. The situation, however, is quite different. One only has to realize that

- depending on the design one does not need any bleed at all,
- there is no need that the bleedboxes in JDF and PDF must be equal. The minimum of the two values should be larger than a given number (typically 3 mm) if and only if a bleed is needed at all.

No bleed is needed, if the minimal distance d between all colored object (vector graphic, text or image) inside of the trim box to the four edges of the trim box is larger than some defined minimum. Let's call this distance d_{\min} . Typically, one sets d_{\min} to be at least three millimeters, but the value depends not only on the accuracy of the folding, cutting and trimming processes, but also on the design of the page. If the distance d gets smaller than this value, inaccurate postpress processes could lead to visible flaws. That is why this case usually is considered to be a fault in the design. But if colored objects reach right to the trim box edge, i.e. the distance d equals zero, then a certain bleed is needed. We denote the minimal width of the bleed with bw_{\min} . Again, bw_{\min} often is set to be two or three millimeters. In this case not only the bleed-sizes in the PDF and JDF should both be larger than bw_{\min} , but also there should be colored pixels outside the trim box with a distance to the trim box larger or equal bw_{\min} (as a minimal requirement). This yields to the following relations:

$$\begin{aligned} d &\geq d_{\min} && \Rightarrow \text{no bleed necessary} \\ 0 < d < d_{\min} && \Rightarrow \text{design fault} \\ d &= 0 && \Rightarrow \text{bleed must larger than } bw_{\min}. \end{aligned}$$

Figure 7 shows the flow chart concerning the check of the bleed box. We assume that each PDF-page has been transformed to an image, which can have a low resolution. The transformation can be carried out easily by using the class *PDFImageWriter* of the *PDFBox*-library. Then we have to check for each page and each edge of the trim box the minimal distances as described above. The corresponding flow chart is shown in figure 7.

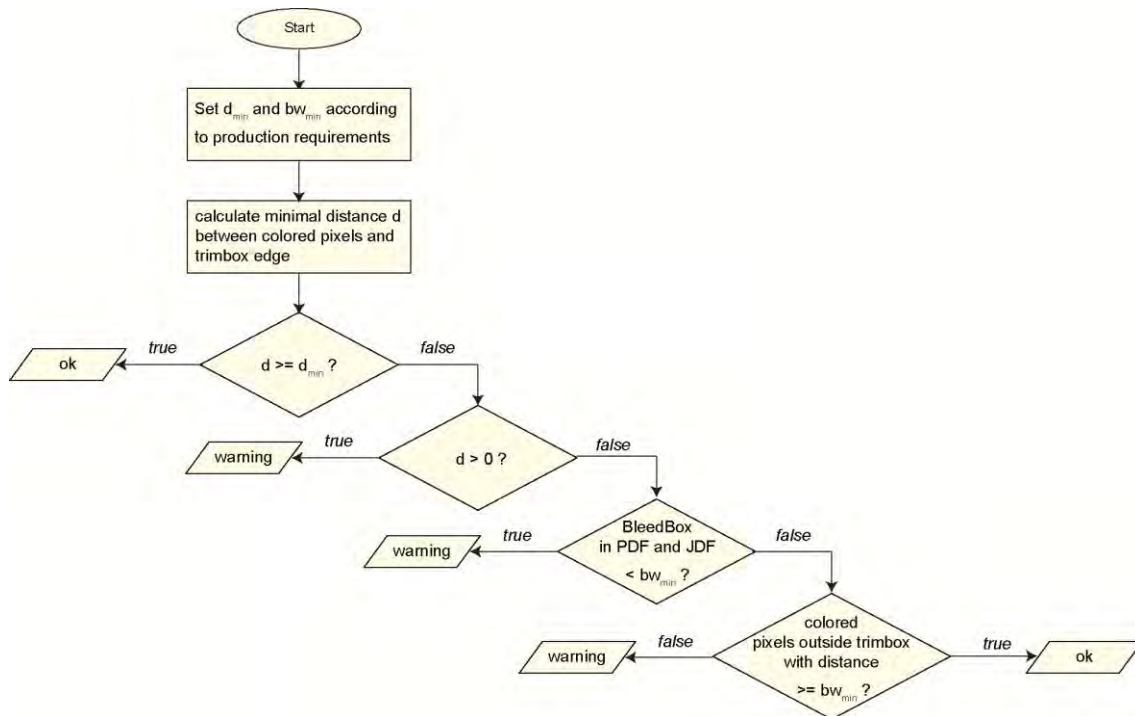


Figure 7: Flow chart for checking bleed boxes

The core of this algorithm is the calculation of the distances of colored pixels to the trim box edges. The value concerning the edge on the right-hand side, for example, equals to the difference between the image width and the maximal column of the image, in which colored pixel are occurring. The method *searchMaxInColumns* is calculating the latter value.

```
public int searchMaxInColumns(BufferedImage image, int column) {
    int max = -1;

    boolean found = false;
    int i = image.getHeight() - 1;
    while(!found && i >= 0) {
        if(image.getRGB(column, i) != Constants.Color.NOCOLOR) {
            max = i;
            found = true;
        }
        i--;
    }
    return max;
}
```

Figure 8: Calculation of the maximal coloured column of an image

This algorithm, however, checks only if there are colored pixels with a certain distance to the trim box edge. This could be enhanced by an evaluation if all colored pixels on the edge of the trim box are connected with colored pixels outside the trim box with distance larger or equal bw_{min} .

5. DISCUSSION

The value bw_{min} does not only depend on the tolerances of the postpress processes mentioned above, but possibly also on the shingling. This denotes a translation of the page content on the pages orthogonally to the spine. Alternatively the page content might get scaled. The reason for doing this is the compensation of movement of the inner folding sheets away from the spine. Therefore the contents of those pages are moved in the opposite direction. This practice is common for saddle-stitched jobs, but sometimes also for perfect bound products if many folds are involved. The shingling value depends on the paper thickness. But if page content is moved closer to the spine and needs a bleed in the same time, the bleed zone must be enlarged. Again, in order to preflight this situation one needs the information about binding details and materials (JDF) as well as about page content (PDF).

6. CONCLUSION

This software is being developed during a technological course about integration of production processes at Stuttgart Media University. A prototype is produced under the supervision of Prof. Dr. Thomas Hoffmann-Walbeck, teaching production integration, and Prof. Dr. Barbara Dörsam, software engineering for media applications.

The preflight program is still under development and expansions are planned, such as color details in PDF and JDF files.

7. LITERATURE

- [1] Cooperation for the Integration of Processes in Prepress, Press, and Postpress (CIP4): JDF-Specification, version 1.4 (2009)
- [2] Adobe Systems Incorporated: "PDF reference" version 1.7 (2006)

DIGITAL IMAGE COMPRESSION USING PRINCIPAL COMPONENTS ANALYSIS

Aleš Hladnik

*Faculty of Natural Sciences and Engineering,
Chair of Information and Graphic Arts Technology, Ljubljana*

*Corresponding author: Aleš Hladnik
e-mail: ales.hladnik@ntf.uni-lj.si*

1. ABSTRACT

Data compression plays a crucial role in various modern digital photography and video applications. Its main goal is to reduce irrelevant and/or redundant image data while keeping relevant information intact as much as possible. There are numerous international as well as industry standards available that are based on either lossless or lossy compression of images. While a lossy compression standard such as JPEG offers a tradeoff between the image quality and the file size, in lossless compression methods – run length encoding, LZW, Chain codes and others – no information reduction takes place, but the image file size may be prohibitively large.

Principal components analysis (PCA) is an established multivariate statistical tool that linearly transforms a number of possibly correlated variables into a smaller number of new variables, known as principal components. Since a digital image can be regarded as a two – or more – dimensional function of pixel values and represented as a 2D (grayscale image) or 3D (color image) data array, PCA can be performed on such an $m \times n$ matrix. The presentation will demonstrate how to implement PCA for image compression on different digital images and, in particular, how the choice of the number of extracted PCs affects the image compression ratio and consequently the image quality.

Key words: *Principal components analysis, image compression, digital image processing*

2. INTRODUCTION

Image compression can be seen as an intersection of two seemingly not so closely related technical fields: digital image processing and multivariate statistics. As we will try to demonstrate below, these two disciplines can be successfully combined when one is interested in a lossy compression of digital images.

2.1. Image compression

Due to the large amount of data encountered in modern still- and video image applications, compression is an almost inevitable step towards the reduction of the image storage space or transmission time requirements. While *lossy* compression standards such as JPEG offer a tradeoff between the image quality and the file size, in *lossless* compression methods – run length encoding, LZW, Chain codes and others – no information reduction takes place, but the image file size may be prohibitively large.

Three types of redundancy typically exist in a digital image and are exploited in image compression techniques: coding, interpixel (spatial) and psychovisual redundancy. In practice, both non-redundant and relevant information are discarded to achieve a higher compression ratio (CR) and reduced file size (Brower, 2012). CR can be computed according to the following formula:

$$\text{CR} = \text{size of original image} / \text{size of compressed image} \quad (1)$$

While in lossless (reversible) compression typical CR is approximately 2:1 for natural scenes and somewhat higher for document images, this ratio is much higher with lossy compression schemes, such as lossy JPEG.

2.2. Principal components analysis

Principal components analysis (PCA) is a widely implemented multivariate statistical technique often used in exploratory data analysis and for making predictive models. PCA is based on a construction of a new set of variables, referred to as principal components (PCs), which are completely uncorrelated – orthogonal – to each other. Technically speaking, PCA can be accomplished by eigenvalue decomposition of a data covariance (or correlation) matrix or by singular value decomposition (SVD) of a data matrix, usually after mean centering and normalization (Abdi, 2010).

A score s_{ip} is a projection of sample (observation) i along a principal component PC p and is a linear combination of original variables (Massart, 1997):

$$s_{ip} = \sum_j v_{jp} \cdot x_{ij} \quad (1)$$

where v_{jp} denotes the loading of variable j on PC p and x_{ij} is the i -th object for original variable j . In matrix notation one can write:

$$\mathbf{S} = \mathbf{X} \cdot \mathbf{V} \quad (2)$$

where \mathbf{S} , \mathbf{X} and \mathbf{V} denote the matrices of scores, original data matrix and loadings, respectively. Upon rearranging one obtains:

$$\mathbf{X} = \mathbf{S} \cdot \mathbf{V}^T \quad (3)$$

The data matrix \mathbf{X} can therefore be decomposed into a product of two matrices, one containing information about the samples (\mathbf{S}), the other about the variables (\mathbf{V}). Calculation of these new matrices, i.e. extraction of PCs, proceeds successively so that each new PC captures as much as possible of the variation which has not been explained by the former PC.

Figure 1 shows this decomposition schematically. The \mathbf{S} matrix contains the scores of m samples on n PCs. The square \mathbf{V}^T matrix consists of the loadings of the n original variables on the n PCs. The number of extracted PCs equals the number of original variables n , but by retaining only the first few significant PCs (PC1, PC2 and PC3 in Figure 1), one discards irrelevant information since higher components often contain data noise only (grey parts of matrices).

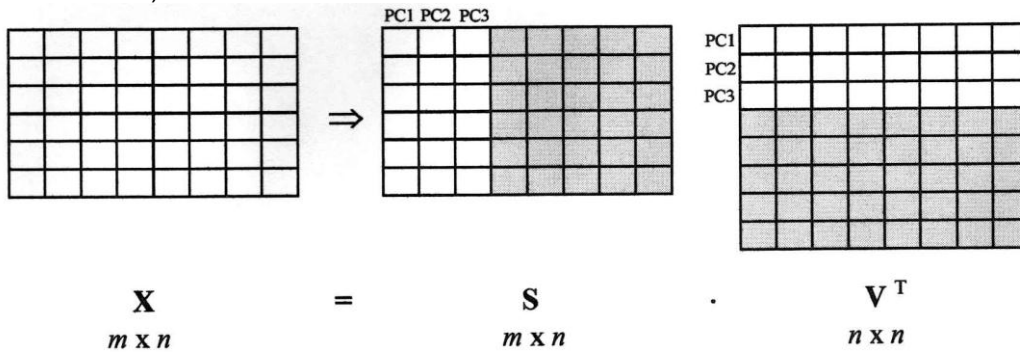


Figure 1. PCA: Decomposition of matrix \mathbf{X} into matrices \mathbf{S} and \mathbf{V}^T .

The calculated scores and loadings can be displayed in a coordinate system of the first few PCs. Such interpretation enables visualization of patterns in the data and reveals similarities and dissimilarities between individual samples as well as the relationship between original variables. Another frequent approach, the one implemented in our study, is to use PCA as a data reduction tool.

2.3. Image quality assessment

In order to quantify, i.e. numerically express, visually perceived differences between the original and the reproduced or distorted – e.g. compressed – image, numerous image quality metrics have been proposed (Lin and Jay Kuo, 2011). These can be subdivided into full-, half- and no-

reference metrics, depending on whether or not the reference, i.e., original, image is present. Structural similarity (SSIM) index (Wang, 2004) is a full-reference metric that measures the similarity between two images and can be seen as a quality measure of one of the images being compared when the other one is considered as the reference, i.e. of perfect quality. The basic idea of SSIM is that the structural distortion can be related to perceived image quality and is calculated as follows:

$$SSIM = \frac{\sigma_{ab}}{\sigma_a \cdot \sigma_b} \cdot \frac{2\sigma_a \cdot \sigma_b}{(\sigma_a)^2 + (\sigma_b)^2} \cdot \frac{2\bar{a} \cdot \bar{b}}{(\bar{a})^2 + (\bar{b})^2} \quad (4)$$

where a and b denote the original and the test images, \bar{a} and \bar{b} are their means, σ_a and σ_b are the corresponding standard deviations, and $\sigma_a \cdot \sigma_b$ is the cross covariance. The three terms in Eq. (4) measure the loss of correlation, contrast distortion and luminance distortion, respectively. SSIM values can range from -1 to +1; SSIM = +1 is achieved only when $a = b$, i.e. when the two images are identical.

SSIM index does not take into account characteristics of the human visual system (HVS), but was nevertheless proved to be strongly correlated with the subjective image quality assessment results.

Calculation of SSIM also generates a map, which provides a measurement of local image quality over space thus making it possible to compare different regions in the images and to observe their (dis)similarities. This feature was also used in our study as demonstrated below.

3. MATERIALS AND METHODS

Individual steps of our experimental work are presented in Figure 1. Three 24-bit RGB images – referred to as 'Hedgehog', 'Man' and 'Building' – taken with Canon digital camera EOS 400D were converted to 8-bit grayscale images, trimmed to a square region and downsampled to 1024x1024, 512x512 and 256x256 pixel size, respectively. Each image was subject to PCA procedure. The degree of image reconstruction, i.e. image quality, when using an increasing number of PCs was assessed using SSIM index along with the conventional image quality metric peak signal-to-noise-ratio (PSNR). Corresponding compression ratios (CR) were also calculated. All image processing routines and computations were performed with MATLAB®. PCA implementation was based on this paper (Richardson, 2009).

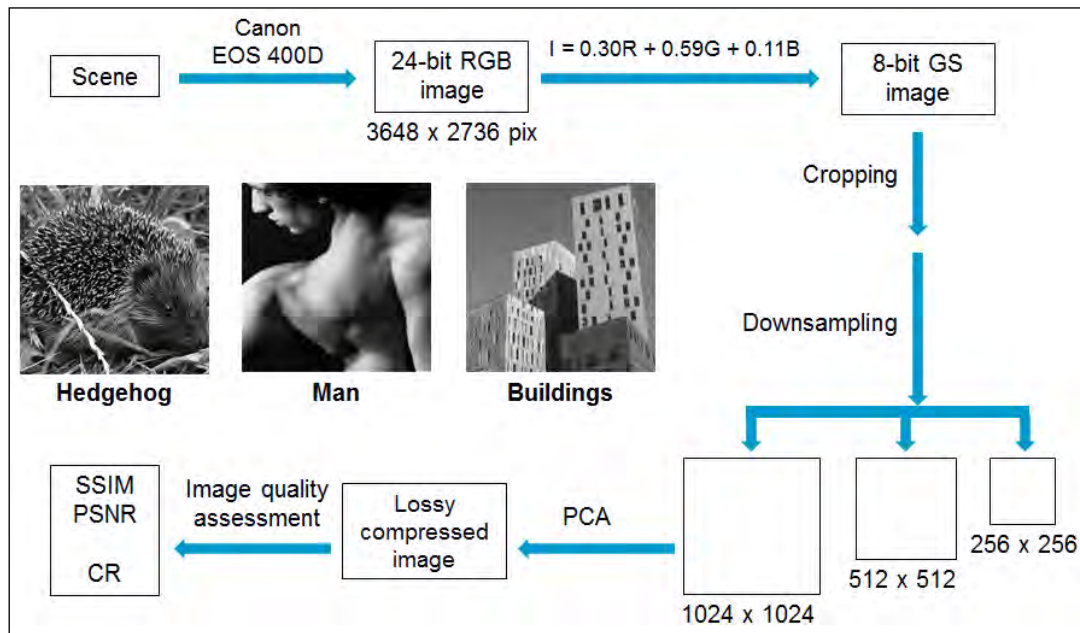


Figure 1: Image processing workflow

4. RESULTS AND DISCUSSION

As Figure 2 demonstrates, the higher the number of PCs used in the reconstruction of the 'Hedgehog' image, the better its quality – as indicated by progressively higher SSIM and PSNR values – but, on the other hand, the lower the compression ratio and, consequently, the file reduction gain. The corresponding SSIM maps provide additional information on the location of image regions with poor (black) or good (white) quality with respect to the original image. It can be seen that the most pronounced differences are in the facial area, which corresponds very well to the visual, subjective, perception of these images.

Table 1 shows that SSIM index, unlike CR, depends on the type of image under investigation. With the same number of PCs used for reconstruction, the image with the largest amount of details, i.e. high-frequency components – in our case the 'Hedgehog' image – results in the lowest quality and, consequently, the lowest SSIM index when compared to the other two images. This finding is again in a very good agreement with the human-based perception of these images.

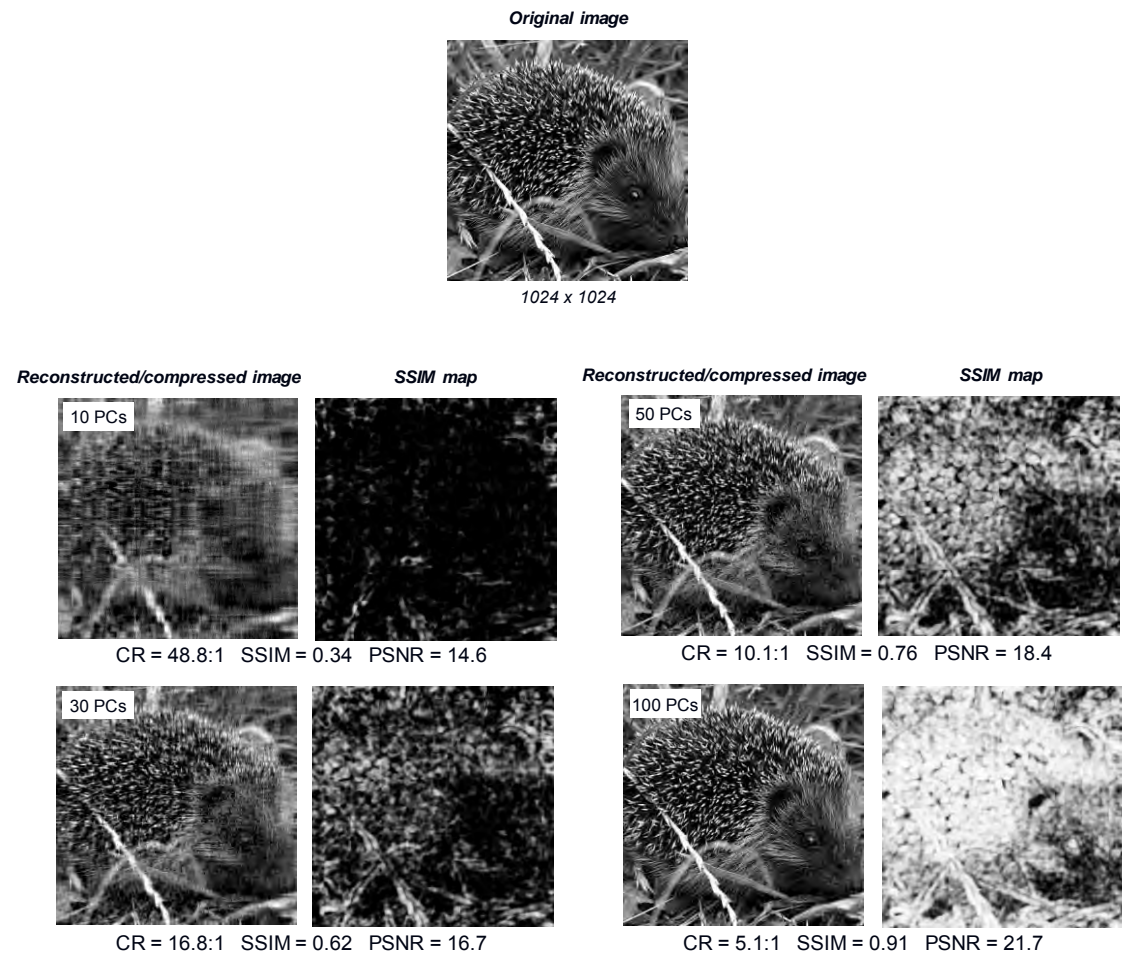


Figure 2: Results of the 'Hedgehog' image compression using 10, 30, 50 and 100 PCs

Table 1: Comparison of the three 1024 x 1024 test images in terms of the number of PCs, compression ratio, SSIM index and PSNR

No. of PCs	CR	SSIM index			PSNR		
		Hedgehog	Buildings	Man	Hedgehog	Buildings	Man
10	48.8	0.34	0.64	0.77	14.6	21.5	26.0
20	25.0	0.50	0.76	0.88	15.7	24.4	30.9
30	16.8	0.62	0.85	0.92	16.7	26.4	33.6
40	12.6	0.70	0.89	0.95	17.6	27.7	35.5
50	10.1	0.76	0.91	0.96	18.4	28.7	37.0
...
100	5.1	0.91	0.97	0.99	21.7	32.3	41.2
200	2.6	0.98	0.99	1.00	27.0	37.2	45.3
512	1.0	1.00	1.00	1.00	41.6	48.8	53.9

5. CONCLUSIONS

It is a well-known fact that the choice of the best compression method always depends on the application. Among the most important factors to consider are input image characteristics (data type, previous processing), desired output (compressed) image quality, compression scheme computational complexity and presence of artifacts (blocks, blur, edge noise). PCA is one of the many possible approaches used to reduce image file size at the expense of its perceptual quality. The tool has also been successfully implemented in other advanced image processing and pattern recognition applications such as face detection and recognition so in the future we intend to focus our research on these topics.

6. LITERATURE

- [1] Abdi, H., Williams, L.J. (2010): "Principal component analysis". Wiley Interdisciplinary Reviews: Computational Statistics, 2: 433–459.
- [2] Brower, B. (2012): "Image Compression Basics", URL: <http://www.lokminglui.com/CompressionTutorial.pdf> (last request: 12.9.2012).
- [3] Lin, W., Jay Kuo, C.-C. (2011): "Perceptual visual quality metrics: A survey", URL: <http://dx.doi.org/10.1016/j.jvcir.2011.01.005> (last request: 15.9.2012).
- [4] Massart, D. L., Vandeginste, B. G. M., Buydens, L. M. C., De Jong, S., Lewi, P. J., and Smeyers-Verbeke, J. (1997): "Principal components". In Handbook of Chemometrics and Qualimetrics: Part A (Amsterdam: Elsevier), pp. 519-535.
- [5] Richardson, M. (2009): "Principal Component Analysis", URL: <http://people.maths.ox.ac.uk/richardsonm/SignalProcPCA.pdf> (last request: 12.9.2012).
- [6] Wang, Z., Bovik, A. C., Sheikh, H. R., Simoncelli, E. P. (2004): "Image quality assessment: From error visibility to structural similarity," IEEE Transactions on Image Processing, vol. 13, no. 4, pp. 600-612.

ANALYZING DIFFERENT ELEMENTS OF WEB GALLERIES

Andrej Iskra, Klemen Možina

University of Ljubljana, Faculty of Natural Sciences and Engineering,
Department of Textiles, Chair of Information and Graphic Art Technology, Ljubljana

Corresponding author: Andrej Iskra
e-mail: andrej.iskra@ntf.uni-lj.si

1. ABSTRACT

Web galleries are one of most used elements of web sites. They are framework for presenting images. Images are very important elements in web sites in the sense of carrying information. Good images show concepts, carry information, invoke positive feelings, etc. All this aspects contribute to positive user experience. On the other hand, bad images waste space, are usually ignored, or even worse, are confusing for the users. Images in web galleries can have additional elements, like image index and image captions. Index helps users to realize the size of the web gallery and where they are at certain image. Image captions increase informational value of the images. In this study we tested three web galleries with different combination of these additional elements. Testing was performed with eye tracking system. Eye tracking technology allows us to analyze how people look and use certain test form (i.e. web gallery). We can also create AOI (area of interest), which was, in our case, used in research of image index and image captions.

Keywords: web galleries, image index, image captions, eye tracking, area of interest

2. INTRODUCTION

There are four fundamental forms on the web sites: text, graphic, moving elements (animations or movies) and sound. Out of these four elements images are the strongest to present information. Images are also very natural and fastest way of interacting with users (1). Talking about eye tracking users respond to web image in just few fixation (total less that a second). Web gallery on a web site is collection of images or photos that is uploaded to a web site and available for web site visitors to view.

Important aspect in web galleries is informatively of web gallery and images within. For that purpose we use image index and image captions. Image index helps users realize the size of the gallery and where in the gallery user actually is. Image captions are formed as phrase or short sentence that explains the content of image and give additional information to the image (2). Some designers make huge mistake thinking they have to fill the gallery with certain number of images regardless what they present. It turns out that web gallery has a lot of meaningless images that carry no information and users ask themselves what the designer wanted to tell him. Users spent some time reading this image captions, and total time of using gallery is slightly larger, but this increase is irrelevant compared to larger informatively.

Navigation in the galleries was implemented with navigation buttons same way for all three galleries. Designers should pay attention at their placement and informatively. Placement must always be at the same spot, regardless different image orientations (portrait or landscape) and different image dimensions (although we tend to have same dimension for the whole gallery).

3. THEORETICAL PART

Eye tracking has recently become more and more popular in the studies of usability of web sites (3). Eye tracking is the process of measuring two values: position of a gaze and movement of the eyes. Most recent eye trackers use technology of reflection of infrared light from a cornea (4). This reflection is received by infrared camera. We can divide eye movement into fixations and saccades. Fixation means that eye gaze stops in a certain position, whereas saccades are quick moves to another position. Fixations typically last from 200 ms (reading text) to 350 ms (viewing images) (5). The result is series of fixations and saccades that is called gazeplot. Sample of part of a gazeplot is shown in figure 1.



Figure 1: Gazeplot from eye tracking system

4. EXPERIMENTAL PART

4.1. Web galleries design

We tested three different web galleries in terms of use of image index and image captions. First gallery doesn't have any of these additional elements, second gallery has only image index, and third gallery has image captions.

Each gallery has twelve images. All of them landscape orientation with dimensions 800×600 pixel. Each gallery has images from certain country and images were equally divided by content (landscape, architecture, people and funny). Obligating this requirements make use of the galleries independent from the image content as much as possible. Galleries were made in Adobe Flash with the use of simple animation techniques. All three galleries have only full size images and two navigation buttons. Navigation was made as unlimited gallery. That means button forward (>) was also active at the last image, so user could start gallery again from the first image. Usually designers exclude button backward (<) at the first image and button forward at the last image, so user immediately know when he reached the end of the gallery. In that case gallery is limited.

We decided to make galleries unlimited for the purpose of testing image index. Because our galleries was unlimited, we tested how long does it take for user to realize that he went though all images. Without image index that happened when they again saw first image in the gallery, because they don't have any information about the size and their position in the gallery.

On the other hand image index indicates the number of the image (e. g. 3/12). Therefore index is element which defines the size of the gallery and can help user to see when he has reached last image (index 12/12) and stop there.

Testing was done on Eye tracking system Tobii x120 with Tobii Studio 3.0 software (6).

4.2. Gallery 1

Gallery 1 is without any additional elements. It has only full size images and two navigation buttons. Figure 2 shows gallery 1.

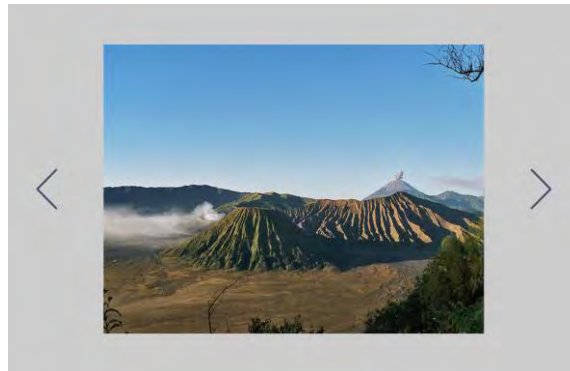


Figure 2: Gallery 1

4.3. Gallery 2

Second gallery was made has image index placed at bottom right corner. Gallery 2 is shown on figure 3.



Figure 3: Gallery 2

4.4. Gallery 3

Third gallery has image captions written at the bottom of the image. They are short sentences with average length of 3.8 words. Figure 4 shows implementation of gallery 3.

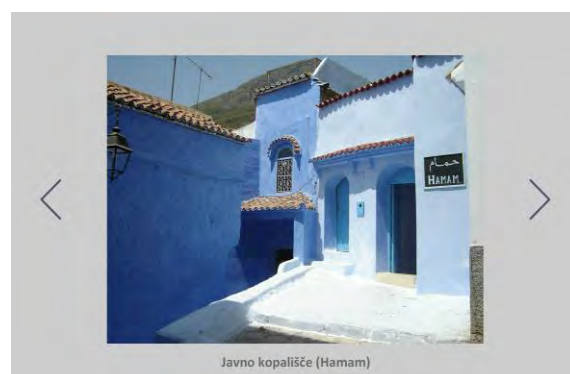


Figure 4: Gallery 3

4.5. Testing methodology

During testing we focused on two common elements of web galleries: image captions and image index. We measured total number of fixation and the total time of observing each gallery. In gallery 1 which doesn't have any additional elements, we measured only total time of observing gallery. That was almost equal to the sum of observing images. Only few fixations at the first image was needed to locate button forward (>), and the users mostly didn't look it again and just use it. That is the guideline for designers to put all buttons (menu buttons, navigation buttons, etc.) at exactly same positions.

Gallery 2 has image index. Our interest was to find out how many times users looked it, how much time they spent for that and if image index was at any use. The purpose of image index is to indicate size of the gallery and for the users to realize when they reach the last image (12/12), so they don't click button forward (>) and go to the first image in the gallery, which they already saw.

With Gallery 3 we analyzed captions of images. Again we measured how many times users read them, how much time spent and also when they read image captions. They can be read before, during or after observing image. We assume that most common case is that users first briefly look at the image then carefully read image caption and when they got more information about image they look image again for longer time. At the end of the test we try, with the informal discussion, to find out how useful image captions are in the frame of increasing informatively.

Because the eye tracking can not record all gazes from the users (blinks of eyes, side looks) we analyzed nine test users who all has more than 90 % of recording success (at least 90% of total time of observing was recorded).

To insure independent results from the order for the galleries we used Latin square. It means that not all users started with gallery 1, but it was shifted for all users equally. Sample of Latin square in shown at table 1.

Table 1: order of the galleries for test users

	Order of galleries		
Test user 1	Gallery 1	Gallery 2	Gallery 3
Test user 2	Gallery 2	Gallery 3	Gallery 1
Test user 3	Gallery 3	Gallery 1	Gallery 2

Eye tracking software allows us to set AOI (area of interest). AOI are useful for analyzing gazes and use of certain elements on the web sites (icons, buttons, text, etc.). We used these in image index in Gallery 2 and image captions in Gallery 3. Figure 5 shows the use of AIO for the image index.

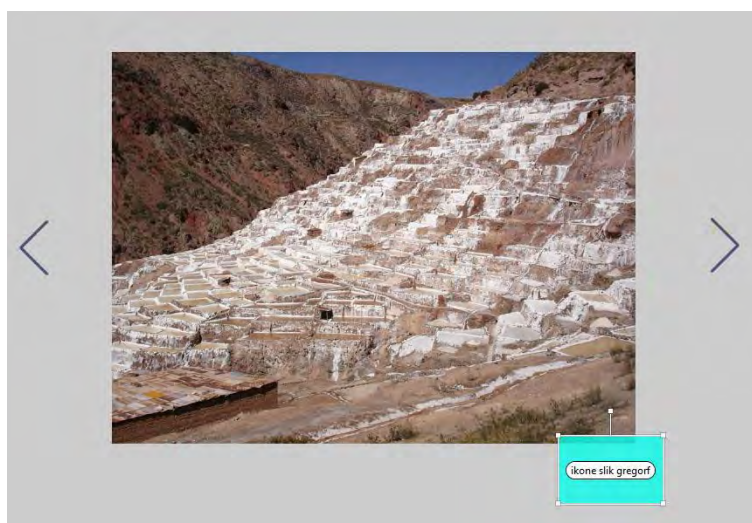


Figure 5: use of AOI

Eye tracking software also allows us to track many events during the use of web sites. We tracked mouse click, which indirectly told us the time clicking button forward (>) and therefore time of observing image and use of additional elements.

5. RESULTS

As written in the previous chapter we analyzed total number of fixation and total time of using different galleries. Table 2, 3 and 4 shows results for nine test users.

Table 2: Results for Gallery 1

Gallery 1	Total time of test (s)	Average time for one image (s)
Test user 1	41,4	3,5
Test user 2	43,0	3,6
Test user 3	89,7	8,3
Test user 4	31,0	2,6
Test user 5	39,7	3,3
Test user 6	43,8	3,6
Test user 7	53,9	4,5
Test user 8	69,6	5,8
Test user 9	73,5	6,1
Average	54,0	4,59

Table 3: Results for Gallery 2

Gallery 2	Total time of test (s)	Average time for one image (s)
Test user 1	41,8	3,48
Test user 2	52,6	4,39
Test user 3	92,1	6,84
Test user 4	38,9	3,24
Test user 5	45,3	4,19
Test user 6	46,0	4,25
Test user 7	54,8	4,56
Test user 8	70,8	5,90
Test user 9	73,5	6,12
Average	57,3	4,77

Table 4: Results for Gallery 3

Gallery 3	Total time of test (s)	Average time for one image (s)
Test user 1	52,8	4,40
Test user 2	46,1	3,84
Test user 3	142,1	11,84
Test user 4	49,1	4,09
Test user 5	47,4	3,95
Test user 6	81,4	6,79
Test user 7	66,1	5,50
Test user 8	76,6	6,38
Test user 9	88,3	7,36
Average	72,2	6,02

Table 5 shows results from observing image index. We measured number of fixations and visits, average time of fixation and visit and total time spent observing image index.

Table 5: Analysis of use of image index in Gallery 2

Image index in Gallery 2	Number of fixations	Average fixation time (s)	Total time (s)	Number of visits	Average visit time (s)
Test user 1	8	0,23	1,8	7	0,26
Test user 2	3	0,18	0,55	3	0,18
Test user 3	14	0,24	3,31	11	0,30
Test user 4	8	0,27	2,15	5	0,43
Test user 5	6	0,21	1,27	5	0,25
Test user 6	3	0,20	0,6	3	0,20
Test user 7	5	0,23	1,13	3	0,38
Test user 8	4	0,25	1	4	0,25
Test user 9	5	0,19	0,93	5	0,19
All Recordings	56	0,23	12,74	46	0,28
Average	6,22		1,42	5,11	

Table 6 shows results from observing image index. Again we measured number of fixations and visits, average time of fixation and visit and total time spent observing image index.

Table 6: Analysis of time division in Gallery 2

Image subtitles Gallery 3	Number of fixations	Average fixation time (s)	Total time (s)	Number of visits	Average visit time (s)
Test user 1	51	0,31	15,79	17	0,93
Test user 2	49	0,29	14,02	15	0,93
Test user 3	79	0,30	24,05	28	0,86
Test user 4	66	0,33	21,93	23	0,95
Test user 5	47	0,40	18,94	15	1,26
Test user 6	52	0,27	13,79	15	0,92
Test user 7	54	0,29	15,84	19	0,83
Test user 8	51	0,27	13,91	15	0,93
Test user 9	48	0,26	12,55	15	0,84
All Recordings	497	0,30	150,82	162	0,93
Average	55,22		16,76	18,00	

Some problems appear during the interpretation of results. At gallery 2 and gallery 3 it was hard to tell which fixations were real look at the image index and image captions or was just side glint when observing image. So, defining AOI in both cases required some manual monitoring of video recordings from eye tracker.

6. DISCUSSION

First of all, we should compare results from tables 2, 3 and 4. Total time for observing gallery is the shortest for gallery 1, which include only images and no additional elements. At gallery 2 total observation time is slightly longer (2.2 s). We can consider that as the approximately additional time when users look image index. At the same time table 5 shows that total time for observing image index was measured 1.42 s. This two results, of course, are not the same, because it is one calculation is based on difference of total observation time (time of observing only images for two galleries is not exactly the same), the other time is measured by the AOI, which in the correct result. The first result (difference in total observation time), in one way, just confirm our assumption that gallery 2 is longer observed, because of some slight time spent for looking image index. Correct result can only be measured by AOI, and show just slightly more time (2.5 %) spent for gallery with image index than the gallery without it. Table 5 shows also those users don't look every image index, but just occasionally glance at image index. They looked 12 image indexes on average 5.11 times and made 6.22 fixations. Image index is just a short number label so, in most cases, just one fixation is needed to "read" it (on average 1.22 fixations per visit). Table 5 shows that average fixation time looking at image index is 0.23 s. For observing images average fixation time is 0.34 s (it is not stated in the results). That also confirm assumption that images are more attracted than text and looking at image index is just

a glance. As for the use of image index to realize the end of the gallery it failed completely. None of the users take in consideration that at image index 12/12 they have reached the end of the gallery and they should not use button forward (>). All of the test users realized they have gone through all images of the gallery only when they saw first image again.

Table 6 shows that total observation time in gallery 3 is much longer than in gallery 1 and 2. The reason is in image captions, which were carefully read by all test users. Table 6 shows that total time spent for reading image captions is 16.76 seconds on average per user. That is 23.2 %, which is quite a lot. That means that image captions in this case attracted a lot of attention and were read carefully. Reason for that is the content of the images in the gallery. Images were from exotic places so they were not known to the users. So the users always read the captions to get additional information about images, regardless it took them longer to go through the gallery. Manual video replay has confirmed our assumption that in most cases users first just quickly glint the image, then carefully read image caption and then observe image for longer time. Here is also difference in correct result of time spent for image captions gained from measurement AOI (16.76 s) and difference in total observation time in gallery 1 and 3 (17.1 s). Reason was explained above. Table 7 also shows that 12 image captions were observed 18 times. During reviewing we noticed that some users after reading image caption look image and then read caption again. That was strictly done by test user 3, who read every image caption twice. Average time to read image captions was 0.93 s, and was done with average 3.1 fixations. Average fixation time for reading captions is 0.3 s, which is slightly less than fixation time for observing images. At informal interview at the end of the test all test users confirmed that image caption was very useful in terms of carrying information of images.

7. CONCLUSION

Based on results we can recommend using both additional elements that were investigated: image index and image captions. Image index takes just fraction time to look at it, but contribute to useful knowledge of the size of the gallery and the user current position in the gallery. Also the use is quite undisturbed for the users.

An image caption takes more user time (almost $\frac{1}{4}$ of time of observing images). But in our case of pretty exotic content of images which were unknown to users, image captions are highly recommended. They contribute a lot to informativity of the images. That can also be confirmed from the results, because all users read all image captions, some of them even twice. Image captions lose the primal purpose with common and well known content of images (well known persons, natural attractions, buildings). We can conclude, that more exotic content of images we have, more useful image captions are.

8. LITERATURE

- [1] Nielsen, J.; Pernice, K.: "Eyetracking Web Usability", (Barkeley CA, USA: New Riders, 2010.), page 196.
- [2] Halpern, D.: "The Biggest Mistake Every Blogger Makes (And How to Avoid It)", URL <http://socialtriggers.com/biggest-blogger-mistake/> (last request: 2012-08-21).
- [3] Iskra, A.; Franken, G.: "Measuring web usability with eyetracking system", Proceedings of 6th International Symposium on Novelties in Graphics, (UL NTF-OT: Ljubljana, Slovenija 2010) pages 277-291.
- [4] Henderson, J.M.: "Human gaze control during real-world scene perception", Trends in Cognitive Sciences 7 (11), 498-504, 2003.
- [5] Rayner, K.: "Eye movements in reading: Perceptual and cognitive processes", Canadian Psychology 36 (1), 57-58, 1995.
- [6] "Usability testing and eye tracking", URL <http://www.tobii.com/en/eye-tracking-research/global/research/usability/> (last request: 2012-08-11).

DIGITAL PUBLISHING FORMATS

Vladimir Zorić, Branko Milosavljević

Faculty of Technical Sciences, Graphic Engineering and Design, Novi Sad

Corresponding author: Vladimir Zorić

e-mail: zoric@uns.ac.rs

1. ABSTRACT

In recent years the Internet has become the main source of information. The increasing presence of wireless signal transfer allows us to via mobile devices: smartphone or tablet device, get the information immediately. The viewing and manipulation of these informations are possible with the use of different software and document formats. One such format is EPUB.

EPUB is the format used for viewing and manipulating electronic publications. This format is standardized by the organization called IDPF. In 2011, IDPF presented the third improved version of the EPUB. This format beside text can contain meta data, audio and video recording, linking, and other multimedia forms. This format offers a completely new understanding of learning, reading books, magazines, daily news.

The increasing environmental awareness, economic aspects, the emergence of mobile devices, access to information, the ability to manipulate, enables that digital publishing gets used by the wider public and business users. Publishing today includes not only printing and publishing books, magazines and other publishing material, but publishing all them also in some digital form.

Key words: IDPF, EPUB, digital publishing, tablet devices, software, Internet

2. ELECTRONIC PUBLISHING

Electronic publishing, also called digital publishing or, ePublishing, includes the digital publication of e-books, EPUBs, and electronic articles, and the development of digital libraries and catalogues. Electronic publishing has become common in scientific publishing, it is also becoming common to distribute books, magazines, and newspapers to consumers through tablet devices. This market is growing by millions each year, generated by online vendors such as Apple's iTunes bookstore, Amazon's bookstore for Kindle, and books in the Android Market. Market research suggests that half of all magazine and newspaper circulation will be via digital delivery by the end of 2015 and that half of all reading in the United States will be done without paper by 2015. Although distribution via the Internet (also known as online publishing or web publishing when in the form of a website) is nowadays strongly associated with electronic publishing, there are many non network electronic publications such as Encyclopedias on CD and DVD, as well as technical and reference publications relied on by mobile users and others without reliable and high speed access to a network. Electronic publishing is also being used in the field of test- preparation in developed as well as in developing economies for student education (thus partly replacing conventional books) - for it enables content and analytics combined - for the benefit of students. The use of electronic publishing for textbooks may become more prevalent with iBooks from Apple Inc. and Apple's negotiation with the three largest textbook suppliers in the U.S. Electronic publishers are able to provide quick gratification for late-night readers, books that customers might not be able to find in standard book retailers. [Yu, A. (2012)]

While the term "electronic publishing" is primarily used today to refer to the current offerings of online and web-based publishers, the term has a history of being used to describe the development of new forms of production, distribution, and user interaction in regard to computer-based production of text and other interactive media. [Yu, A. (2012)]

There is an increase in e-book sales, according to statistics released by The International Digital Publishing Forum and the Association of American Publishers. The numbers only represent wholesale revenues from 12-15 trade publishers in the United States and do not include library, educational or professional sales but consumers are buying more e-books. Figure 1. [Yu, A. (2012)]

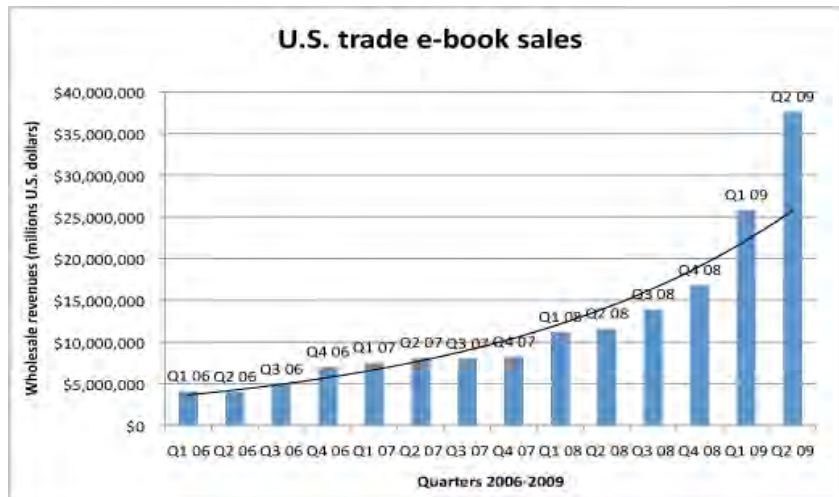


Figure 1

3. HISTORY

The inventor and the title of the first e-book is not widely agreed upon.

The first e-book may be the Index Thomisticus, a heavily annotated electronic index to the works of Thomas Aquinas, prepared by Roberto Busa beginning in the late 1940s. However, this is sometimes omitted, perhaps because the digitized text was (at least initially) a means to developing an index and concordance, rather than as a published edition in its own right.

Alternatively, electronic books are considered by some to have started in the early 1960s, with the NLS project headed by Doug Engelbart at Stanford Research Institute (SRI), and the Hypertext Editing System and FRESS projects headed by Andries van Dam at Brown University. Augment ran on specialized hardware, while FRESS ran on IBM mainframes. FRESS documents were structure-oriented rather than line-oriented, and were formatted dynamically for different users, display hardware, window sizes, and so on, as well as having automated tables of contents, indexes, and so on. All these systems also provided extensive hyperlinking, graphics, and other capabilities. Van Dam is generally thought to have coined the term “electronic book”, and it was established enough to use in an article title by 1985. In 1992, Sony launched the Data Discman, an electronic book reader that could read e-books that were stored on CDs. One of the electronic publications that could be played on the Data Discman was called The Library of the Future. Early e-books were generally written for specialty areas and a limited audience, meant to be read only by small and devoted interest groups. The scope of the subject matter of these e-books included technical manuals for hardware, manufacturing techniques and other subjects. In the 1990s, the general availability of the Internet made transferring electronic files much easier, including e-books.[Anone, (2012)]

4. E BOOK FORMATS

Numerous e-book formats emerged and proliferated, some supported by major software companies such as Adobe with its PDF format, and others supported by independent and open-source programmers. Multiple readers followed multiple formats, most of them specializing in only one format, and thereby fragmenting the e-book market even more. Due to exclusiveness and limited readerships of e-books, the fractured market of independent publishers and specialty authors lacked consensus regarding a standard for packaging and selling e-books.

However, in the late 1990s a consortium was formed to develop the Open eBook format as a way for authors and publishers to provide a single source document that could be handled by many book-reading software and hardware platforms. Open eBook defined required subsets of XHTML and CSS; a set of multimedia formats (others could be used, but there must also be a fallback in one of the required formats); and an XML schema for a “manifest”, to list the components of a given ebook, identify a table of contents, cover art, and so on. Google Books has converted many public-domain works to this open format. [Anone, (2012)]

5. IDPF

The International Digital Publishing Forum (IDPF) is a trade and standards association for the digital publishing industry, that has been set up in order to establish a reliable and complete standard for ebook publishing.

Starting from the Open eBook Publication Structure or “OEB” (1999), which was created loosely around HTML, it then defined the OPS (Open Publication Structure), the OPF (Open Packaging Format) and the OCF (Open Container Format). These formats are the basis for the common EPUB and Mobipocket ebook file formats (Comparison of e-book formats). [Anone, (2009)]

The goals of the IDPF are to:

- Promote industry-wide adoption of electronic publishing through standards development, conferences, best practices, and demonstrations of proven technology.
- Develop, publish, and maintain common standards (e.g. EPUB) relating to electronic publications and promote the successful adoption of these specifications.
- Encourage interoperable implementations of EPUB publications and reading systems and provide a forum for resolution of interoperability issues.
- Identify, evaluate, and recommend standards created by other bodies related to electronic publishing.
- Provide a forum for the discussion of issues and technologies related to electronic publishing.
- Accommodate differences in language, culture, reading and learning styles, and individual abilities. [Anone, (2012)]

6. EPUB

EPUB 2 was initially standardized in 2007 as a successor format to the Open eBook Publication Structure or “OEB”, which was originally developed in 1999. A maintenance release, EPUB 2.0.1, was approved in 2010. In October, 2011, EPUB 3 was approved as a final Recommended Specification. [Anone, (2012)]

EPUB defines a means of representing, packaging and encoding structured and semantically enhanced Web content — including XHTML, CSS, SVG, images, and other resources — for distribution in a single-file format. EPUB allows publishers to produce and send a single digital publication file through distribution and offers consumers interoperability between software/hardware for unencrypted reflowable digital books and other publications.

[Anone, (2007)]

EPUB 3, the third major release of the standard, consists of a set of four specifications, each defining an important component of an overall EPUB Publication:

- EPUB Publications 3.0, which defines publication-level semantics and overarching conformance requirements for EPUB Publications.
- EPUB Content Documents 3.0, which defines profiles of XHTML, SVG and CSS for use in the context of EPUB Publications.
- EPUB Open Container Format (OCF) 3.0, which defines a file format and processing model for encapsulating a set of related resources into a single-file (ZIP) EPUB Container.
- EPUB Media Overlays 3.0, which defines a format and a processing model for synchronization of text and audio.

EPUB has been widely adopted as the format for digital books. These new specifications significantly increase the format’s capabilities in order to better support a wider range of publication requirements, including complex layouts, rich media and interactivity, and global typography features. The expectation is that EPUB 3 will be utilized for a broad range of content, including books, magazines and educational, professional and scientific publications.

This document provides a starting point for content authors and software developers wishing to understand these specifications. It consists of non-normative overview material, including a roadmap to the four building-block specification documents that compose EPUB 3. [Anone, (2011)]. At in most basic level, an EPUB publication is a collection of resources that can be reliably and predictably ingested by an EPUB Reading System in order to present its contents to a user. Some of these resources, facilitate the discovery and processing of the

EPUB publication, while others make up the content of the source publication. The latter, EPUB Content Documents, are described in Content Documents and are fully defined in.

A Publication's resources are typically bundled for distribution as a ZIP-based archive with the file extension .epub. As conformant ZIP archives, Publications can be unzipped by many software programs, simplifying both their production and consumption. The container format is introduced in Container and defined in. [Anone, (2011)]

An EPUB Publication is transported and interchanged as a single file (a "portable document") that contains the Package Document, all Content Documents and all other required resources for processing the Publication. The single-file container format for EPUB is based on the widely adopted ZIP format. An XML manifest that specifies the location in the ZIP archive of the Package Document must be found at a well-defined location within the archive.

This approach provides a clear contract between any creator of an EPUB Publication and any system which consumes such Publications, as well as a reliable representation that is independent of network transport or file system specifics. [Anone, (2011)]

HTML5 supports a number of new elements intended to make markup more semantically meaningful and introduces more clearly defined semantics for some HTML4 elements. These elements, in conjunction with best practices for authoring well-structured Web content, should be utilized when creating EPUB XHTML Content Documents. These additions allow content to be better grouped and defined, both for representing the structure of documents and to facilitate their logical navigation. XHTML Content Documents also natively support the inclusion of ARIA role and state attributes and events, enhancing the ability of Assistive Technologies to interact with the content. [Anone, (2011)]

EPUB 3 further introduces the epub: type attribute, which is meant to be functionally equivalent to the W3C Role Attribute. This attribute allows any element in an XHTML Content Document to include additional information about its purpose and meaning within the work, using controlled vocabularies and terms. Refer to Semantic Inflection for more information. [Anone, (2011)]

The design center of EPUB is dynamic layout: content is typically intended to be formatted on the fly rather than being typeset in a paginated manner in advance (i.e., expecting a particular sized "page"). This core capability is useful, for example, for optimizing rendering onto different sized device screens or window sizes, and it facilitates and simplifies content accessibility.

While it is possible to incorporate more highly formatted content in EPUB — for example via bitmap images or SVG graphics, or even use of CSS explicit positioning and/or table elements to achieve particular visual layouts — Authors are strongly discouraged from utilizing such techniques. They are not reliable in EPUB since many Reading Systems render content in a paginated manner rather than creating a single scrolling Viewport and since each Reading System may define its own pagination algorithm. If these techniques are required to convey the content of the publication (for example, for graphic novels), fallbacks should always be included.

In general, it is preferable to achieve visual richness by using EPUB Style Sheets without absolute sizing or positioning. [Anone, (2011)]

We can add interactivity to an EPUB book using either the <object> or <script> elements. Currently object has the best support, especially using Flash in Adobe Digital Editions.

The script element is specifically discouraged (though not disallowed) in EPUB 2.0.1, and no major reading system supports it. However, all browsers do.

The primary advantage of interactivity using script is that the content creator has the ability to manipulate every part of the ebook: all of the text, its layout, even potentially the user interface of the reading system itself. With object you can apply interactivity to just an arbitrary rectangle. There is a great deal of interesting animation and even interactivity possible using CSS3, which is allowed in EPUB 2.0.1 and is supported by iBooks and other WebKit-based ereaders. Interactivity is also possible using JavaScript combined with the HTML5 canvas element, though canvas is not part of EPUB 2.0.1. [Anone, (2011)]

With access to JavaScript on mobile devices, ebooks can potentially gain access to information about the reading device itself, such as the location of the reader in the physical world, or the device's orientation, or even add photos and video from the device's camera.

Any ereader that allows JavaScript provides the ability for ebooks to access live data on the web. The primary blocker for extremely rich interactive ebooks is ereader support, but by embedding browser-based reading systems like Monocle, content creators can distribute such ebooks today. It remains to be worked out how to handle JavaScript in larger ereading systems both safely and with proper fallbacks to non-interactive content.

7. CREATING EPUB FORMAT

To create an ebooks we need a software. Right now we have software and computer that can create ePub files. We create ebooks, digital scrapbooks, photomontages, brochures, school year books, journals, catalogues, manuals, magazines, cards and more.

To create ebook we can use diferet softwares platforms such is Adobe InDesign, Open Office, Sigil, Calibre and more. Some of these are open formats, some not, but all of them are able to create EPUB format.

7.1. Exporting from InDesign & Open Office

For example, InDesign is capable of exporting to the ePub format. This is very convenient, because InDesign is pretty much mandatory in the publishing world; most people who putting together books, are probably already using it.

If we want to use only free software to get the EPUB format, we can use plugin for Open Office. When we download this plugin we can use Open Office's "Export" function to create ePub documents on Windows, Mac and Linux computers. It's not perfect (no chapters) but it works. In this days, there's no such plugin for Microsoft Word, but we can open Word documents using Open Office.

7.2. Creating From Scratch Or Editing (Sigil)

Sigil is handy if we want to create an ePub from scratch. Sigil also have ability to edit existing ePub files. This means that if the exported results from one of the above tools doesn't quite look right we, can easily use Sigil to make changes. We can also use Sigil to create an ePub from scratch, but its usefulness as a repair tool is hard to overstate. Formatting errors will come up if we are exporting, so Sigil is good cleanup tool.

It's also possible to edit these files manually, as an ePub is essentially a .zip file containing a series of HTML files. Sigil is a free and open sorce ebook editor. This is multi platform editor who can runs on Windows, Linux and Mac.

7.3. Calibre: Convert Almost Anything To ePub

Calibre is the ultimate ebook manager. This program can convert many different formats to ePub. Calibre is free and open source e-book computer software that organizes, saves and manages e-books, supporting a variety of formats. It also supports e-book syncing with a variety of popular e-book readers and will, within DRM restrictions, convert e-books between differing formats. Calibre helps to organize the personal e-book library by allowing the user to sort and group ebooks by metadata fields. Metadata can be pulled from many different sources (ISBNdb.com, Google Books, Amazon, LibraryThing). Full-text search, including the whole library, is possible.

8. READING EPUB FORMAT

EPUB can be read on all computer platforms, but it is best suited for a tablet devices. EPUB format is independent of performas of the device. To read simple e books we do not have to use expensive tablet computers. If we want to run videos and photos at high resolution, work smoothly, and use all potencial of EPUB format we need better hardware platforms. This segment of the market is constantly advancing, both, hardware and the software sense.

Currently in this segment, the most prevalent operating systems OS (Apple) and Android in various versions and the latest Windows 8 for mobile devices.

Platform, which is currently under developement, and its architecture is very interesting is B2G (Boot to Gecko, Mozilla). B2G is a completely new view of the operating system, for now only for mobile devices. It includes HTML5 language in the background, and the main engine is Linux core operating system. This, according to the developers B2G gets much simpler and more open platform that can be used on priceless mobile devices, with performance of much more expensive devices. Figure 2.



Figure 2

There are much software solutions to read and review the document. They are depend on the model of tablet PCs, and there are many.

Each offers a variety of software options. Besides just reading, we can zoom in and out text, increase or decrease contrast, crawl, watch multimedia content, listen, link to.

All described belongs to the present and the near future, and the possibilities EPUB format (currently) on this computer platforms are great.

One of more interesting solution is the Samsung tablet, that has a stylus for writing and drawing. The pen is pressure sensitive and offers the possibility of writing, drawing, and every experience that we can achieve by manipulating a pencil on paper.

Tablet becomes a multimedia platform for reading, writing, watching, listening ... and any content in book format.

9. CONCLUSION

The press in the last few years faced a number of difficulties that threaten their survival. Last year was the world record number of newspaper readers, but newspapers were also recorded a decline in ad revenue, as a result of the reduced circulation of many newspapers around the world. The last number printed American magazine Newsweek will appear on newsstands 31st December 2012. years, after which the magazine will come out only on the Internet.

A similar fate is expected soon, and the Guardian. U.S. magazine Newsweek cease after 80 years to be published in print form since the beginning of 2013, there will be only in digital format, which will involve layoffs. [Anone, (2010)]

The last print edition of Newsweek in the U.S. will appear on newsstands 31st December. Considering that more and more readers read the news on their mobile phones and tablets, the media are increasingly turning to digital format, or the Internet. [Anone, (2010)]

The main reason for canceling the printed edition of the printed editions perennial losses and rising income from marketing on the Internet. [Anone, (2012)]

Books previously printed on paper are now available on computer screens, mobile phones and other ebook devices. One of the greatest benefits brought about by ebooks software is the ability for anyone to create professional ebooks without having to fork out thousands of dollars to design and publish a book. People can easily become authors overnight and earn income from selling online ebooks. [Anone, (2010)].

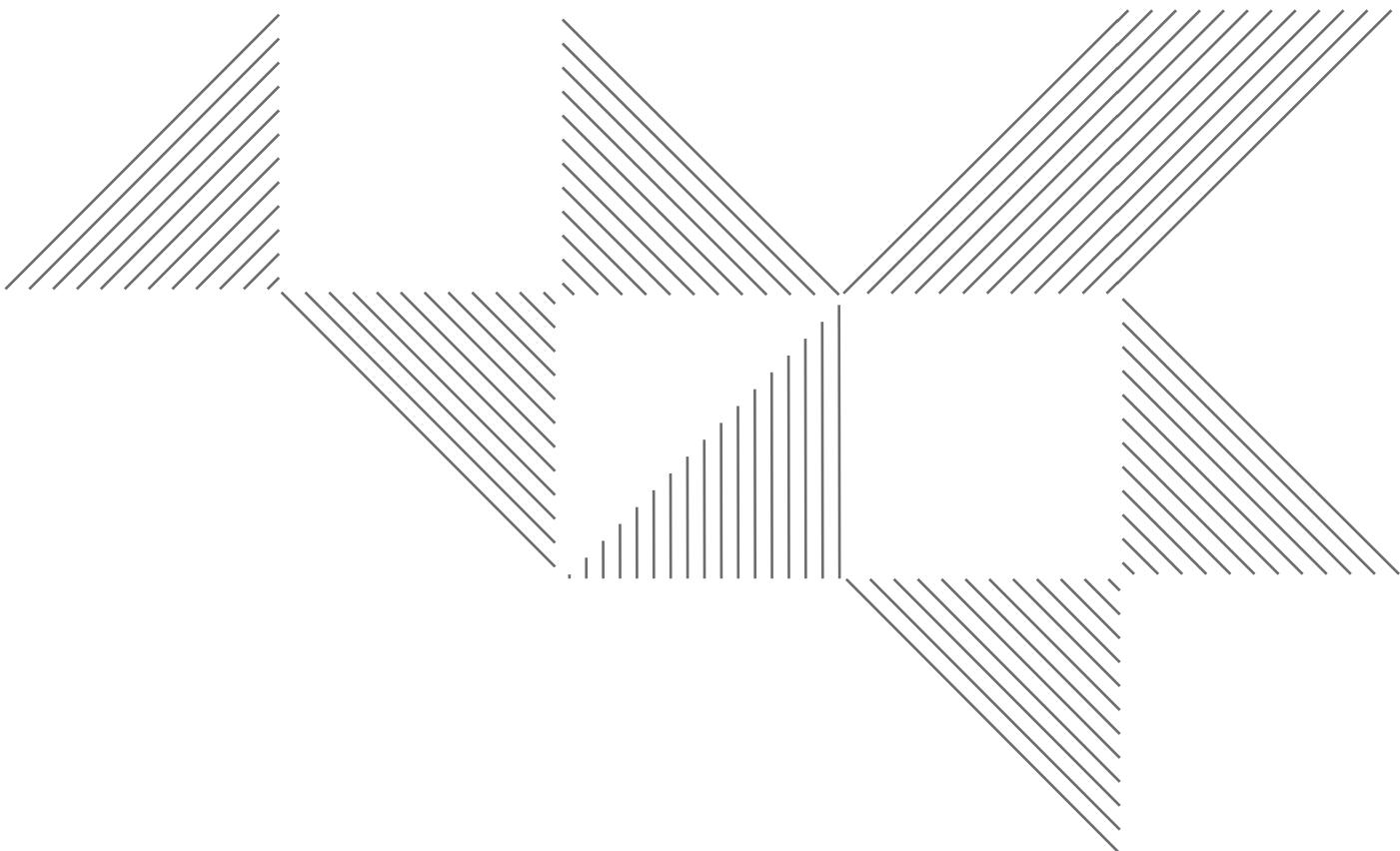
The wide opportunities such is circulation, availability, and interactivity of ebooks, changed the way of publishing we know, and the future is in front of us. Who knows, maybe the abstract for GRID 2014 will be publish in EPUB format, and only in electronic form.

10. LITERATURE

- [1] Yu, A. (2012) The future of e-books?. Writing beyond the byline, [blog] 23 03, URL: <http://al-anyu039.wordpress.com/2010/03/23/the-future-of-e-books/> [Accessed: 09 10 2012]
- [2] Anon. En.wikipedia.org (2012) E-book - Wikipedia, the free encyclopedia. [online] Available at: <http://en.wikipedia.org/wiki/E-book> [Accessed: 21 Oct 2012].
- [3] Anone, En.wikipedia.org (2009) International Digital Publishing Forum - Wikipedia, the free en- cyclopedia. [online] Available at: http://en.wikipedia.org/wiki/International_Digital_Publishing_Fo- rum [Accessed: 21 Oct 2012].
- [4] Anone, Idpf.org (2012) About Us | International Digital Publishing Forum. [online] Available at: <http://idpf.org/about-us> [Accessed: 21 Oct 2012].
- [5] Anone, Idpf.org (2007) EPUB | International Digital Publishing Forum. [online] Available at: <http://idpf.org/epub> [Accessed: 21 Oct 2012].
- [6] Anone, Idpf.org (2011) EPUB 3 Overview. [online] Available at: <http://idpf.org/epub/30/spec/epub30-overview.html> [Accessed: 21 Oct 2012].
- [7] Anone, Cbsnews.com (2010) How e-Books Are Changing the Printed Word - CBS News. [on- line] Available at: <http://www.cbsnews.com/stories/2010/01/10/sunday/main6079170.shtml> [Accessed: 21 Oct 2012].
- [8] Anone, Bizlife.rs (2012) Gase se štampana izdanja Newsweeka i Gardiana. [online] Available at: <http://www.bizlife.rs/vesti/vest/49379/gase-se-stampana-izdanja-newsweeka-i-guardiana.html> [Accessed: 21 Oct 2012].



Design and Typography



EMPIRICAL FINDINGS ON FEATURE DISTINCTIVENESS: LEGIBILITY BASED ON DIFFERENTIATION OF CHARACTERS

Uroš Nedeljković, Bojan Banjanin, Irma Puškarević, Ivan Pinčjer
Faculty of Technical Sciences, Graphic Engineering and Design, Novi Sad

Corresponding author: Uroš Nedeljković
e-mail: urosned@uns.ac.rs

1. ABSTRACT

After a series of empirical findings from the first half of the last century, and a stream of empirical findings in the field of legibility and readability of typefaces, little research has sustained a grounding theory. Since the majority of psychologists do not possess sufficient knowledge of typography, their studies lacked internal validity (Lund, 1999), whereas typography scholars have published numerous ungrounded work in their attempt to base the discourse stylistically and ideologically. Seen from our hindsight, providing the theoretical framework for this field was less probable without the cognitive information processing theory. Numerous research regarding word superiority effect support different hypothesis (Cattell, 1886; Reicher, 1969; Wheeler, 1970; McClelland & Johnston, 1977)) but only with the advancement of the eye tracking and the neural network modeling in the '80s scholars were able to obtain precise answers to the question: How we recognize words? (Rayner & Pollatsek, 1989; McClelland & Rumelhart, 1981; Seidenberg & McClelland, 1989). The findings that the bottom-up processing in parallel distribution (PDP) starts from feature level indicates that if we want to progress the legibility of the typeface we need to explore the feature level ie. feature distinctiveness. Therefore, this paper analyzes key findings on legibility of letters within type which have been perceived as meaningful for designers and type practitioner.

Key words: *legibility, feature, distinctivnes, typefaces*

2. LETTER PERCEPTION

A decade ago, a consensus has been reached in favor of a more liberally interpreted analogy between the pattern and its representation, therefore, the recent empirical research research are based on the structural approach of the feature detection theory. Instead of observing the entire pattern, the essence of feature detection is in the assumption that the brain decodes distinctive features that separate one pattern from the other. Type designers, graphic designers and other practitioners are familiar with the notion that all of the glyphs of the alphabet are defined according to this limited number of strokes (the vertical, the horizontal, the conjoining, the diagonal, the curved). The strokes that compose them represent their distinctive features. The computer model representing the central hypothesis that the letters are recognized according to their features was devised by Oliver Selfridge, in 1959. under the name *Pandemonium*¹. It was one of the first computer models for pattern recognition that represented a few levels of parallel processing. Though it wasn't perfect, the program was very influential for the development of other computer models and the development of artificial intelligence.

The support for the detection theory came from neurological and physiological studies. Two Nobel laureates, Hubel and Wiesel, determined that certain neurons in the visual cortex respond only to specific stimuli presented on the part of the retina that these neurons cover. Generally, retinal neurons don't respond to a simple illumination, though they do respond to 'specifically oriented line segments' (Hubel & Wiesel, 1979, as cited in Sternberg, et al. 2008).

¹ The group of Pandemonium models can process patterns in four levels. Every level of findings procession obtains detectors of different graphemic pattern. Selfridge metaphorically calls these levels "the demons". The first image demon receives sensory stimuli. The processing starts at feature demons level, the activation is produced at the cognitive demons level that "scream" when they receive certain feature combinations. The assemblies with the largest number of activations received from the feature detection level, and also make cognitive demons scream the loudest, generate up to the decision demon level. The decision making level is comprised of memorised assembled strokes that make up letter signs and some other signs.

In the study of Ulrich Neisser(1964) the results support the theory of feature detection. Assuming that recognition starts with identification of distinctive features, the recognition will be more difficult if the targeted pattern (targeted letter) is amongst other patterns that share large number of distinctive features². The subject that participated in this study found it less difficult to point target letter in the matrix of letters with different distinctive features. In other words, identifying target letter in the matrix of letters with similar distinctive features took longer and was followed by numerous mistakes (Neisser, 1964, 1967, as cited in Kostić, 2010; Balota, Yap, & Cortese, 2006). The pattern recognition approaches described here imply the bottom up processing. In other words, they move from the basic units towards the more complex. However, if the patterns that we have observed are put into context i.e. we use letters to compose words and sentences that convey meaning, we are faced with an actual observation. Like any other pattern in nature, the letters are rarely seen individually within actual observation, but rather in a context that induces their meaning. The researchers and typographers are faced with a key question and problem; In what way do we recognize words? Are the properties of the letters themselves a key factor for word recognition or are the words patterns we recognize by their distinct features, in this case the graphemes, or is the word and letter recognition within the word happening on a much higher level – the top-down processing.

3. VISUAL WORD RECOGNITION

In the attempt to explain the reading process, the cognitive psychologists have assumed a number of models of visual word recognition. From whole word recognition (Huey, 1908; Reicher, 1969; Haber & Schindler, 1981), bigram or supraletter features (Wheeler, 1970; Monk & Hulme, 1983); from Serial Letter Recognition to Parallel Letter Recognition (Wheeler, 1970; Monk & Hulme, 1983). A famous researcher in the field of psycholinguistics, James Cattell was the first to discover the intricate effect known today as the Word Superiority Effect WSE. The basis of the experiment was to display words to the participants in a very short time interval (5-10ms), thereby discovering a more accurate recognition of letters. From this experiment Cattell deduced that words are better recognized since they present whole units that we can discern. The same effect was repeated in Reicher's (1969) and Wheeler's (1970) research. The results showed that letters were more easily and more accurately recognized if they are within a context rather than within a pseudoword or isolated. Based on the results a hypothesis was established that word recognition includes long-term memory and word pattern recognition, as well as the word shape or individual parts (familiar letter units – *supraletterfeature*)³. However, despite the convictions of many psychologists and typography practitioners, that word and letter patterns are of essential importance for word recognition, in recent decades a new favored model that points out that along with the causality of the semantic, syntactic and phonological restrictions of recognition, grapheme recognition occurs through Parallel Letter Recognition within the word itself.

The results of the Word shapes in poor shape for the race to lexicon study (Paap, Newsome, & Noel, 1984) show that the demonstrations of the word shape effect (Haber & Schindler, 1981) and the supraletter effect (Monk & Hulme; 1983; Wheeler, 1970) from the previous studies Revising the earlier and analyzing the newly obtained research results, Paap and others assume that the fast, automatic word recognition is mediated by the activation of abstract letter identities (Coltheart, 1981; Paap et al., 1982). Because the bottom-up activation of abstract letter units would have to be driven by the detection of infraletter features, supraletter features like length and shape may have no influence on automatic word recognition.

² Neisser determined capital letter 'Z' as target letter within two matrix of letters: the matrix of letters with similar distinctive feature (I, V, M, X, E, W), and the matrix of letters with different distinctive features in comparison to the target letter (O, D, U, G, Q, R, C).

³ For example, rounded strokes of the letter pair CO or the square strokes of the letter pair NI.

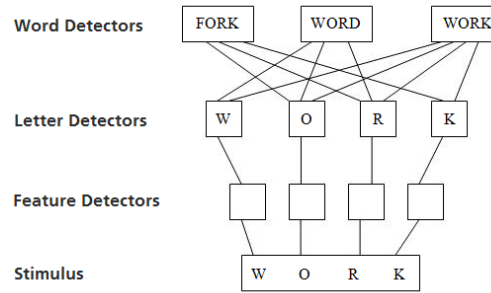


Figure 1. The letter "W", for example, triggers activation of all the words that have this letter as their first letter, the letter "O" of all the letters that have this letter as their second letter, etc. If a certain word has the most activations from the letter detection level (among the displayed words), that word is postulated as predefined, in this example the word "WORK".

According to the PLR model, the letters within words are recognized at the same time, and the letter information (i.e. the characteristic glyph features) are used for word recognition (McClelland & Rumelhart, 1981; Rayner & Pollatsek, 1989). For example, a participant was displayed the word "WORK". The first step is the letter feature detection (the horizontal, vertical and diagonal strokes, etc.). These features are then sent to the level where every letter from a word is recognized simultaneously. After this comes the word detector level (Image 1). So the final level involves the word detectors that function in the same way as the letter detectors, identifying features, in this case letters and combining them into words.

What happens at the word detector level is not exactly identified or clear. However, it is clear that there is a secondary process occurring parallel with the bottom-up processing at the word detector level that consists of the top-down lexic stimulus processing depending on the context (McClelland & Rumelhart, 1981). The parallel distributed processing – PDP in the PLR model explains the WSE. While the letters individually need to be exclusively identified by the information gained from the letter detection level, words gain information from both word and letter detector levels, which gives the words a greater advantage to be recognized than and individual letter (McClelland & Rumelhart, 1981; Rayner & Pollatsek, The Psychology of Reading, 1989).

4. EMPIRICAL FINDINGS ON DIFFERENTIATION OF LETTERS

One of the most constructive/beneficial researchers from the early stages of legibility research, Miles Tinker, in his book *Legibility of print* (1964, as cited in Beier, 2009) he summarized the findings from the research concerning relative legibility of the letters of the alphabet from 1885 up to 1928. The relative legibility of the letters of the alphabet during this period had been researched by many methods (short exposure, distance, parafoveal vision) whereby the results acquired were expected to be different. However, Tinker grouped the findings that were consistent with seven studies. Among the most legible letters, the following were selected: 'd', 'm', 'p', 'q', 'w'; letters of mediocre legibility: 'j', 'r', 'v', 'x', 'y'; least legible letters: 'c', 'e', 'i', 'n', 'l' (Tinker, 1964; as cited in Beier, 2009). After examining the studies, Tinker concludes that some letter features affect the legibility of the typeface. In his view, ascenders i.e. descenders of letters 'd', 'b', 'p', 'q', i 'k' make these letters the most distinguished. His findings differ from recent findings which will be discussed later in the paper (cf. Courrieu, Farioli, & Grainger, 2004). Word recognition research, in other words feature distinctiveness, gained popularity with the emergence of the information processing theory. The confusion matrix is a traditional method of research of the distinctive letter features. A typical experiment for generating confusion matrix consists of isolated letters which are presented in the constricted conditions (short exposure and/or energy masking) and that can lead to the problem of identification. Error rate (e.g. reporting letter F when letter E is displayed) indicates that visual similarities are the result of the common features where analyzing confusion patterns the group of features that help identify letters is revealed (e.g. Bouma, 1971; Geyer, 1977; Gilmore, et al. 1979). Among the 70 studies of this subject published so far, feature lists for Roman letters have been formed, that usually consist of lines of different directions or curvature (Grainger, Rey, & Dufau, 2008). The first accurate description of distinct features of the capital letters of the Roman alphabet was given by Eleanor Gibson at the end of the 1960' (Gibson, 1969, according to Kostić, 2010). Gibson

discusses a list of 12 distinct features through four descriptive factors: the straights, the curves, redundancy, discontinuity (Gibson, 1969, as cited in Geyer & DeWald, 1973). In an attempt to provide more accurate descriptions Geyer and DeWald state the 12 distinct features. Keren and Baggen (1981) discover 14 distinct features of the capital Roman letters, according to the confusion matrix reported by Gilmore (1979). The features are differentiated by the value of the legibility of the graphemes. The different estimated values are for the following features: (3) parallel vertical lines, (6) single straight vertical line, (10) diagonal lines that are not diagonal lines (excluding those that are between parallel straight lines), (14) nonclosed letterstanding on a broad base. However, none of the above mentioned feature lists (Gibson, Geyer & DeWald, Keren & Baggen) can be considered widely applicable because each one of them is only valid for a specific stimulus i.e. a font used in the research, making the findings of these researchers inconsistent in a good measure, which is the subject of discussion in this paper.

In the legibility study of the Cyrillic and Roman letters, Rot and Kostic (1987) have conducted four experiments in which the legibility of individual capital and lowercase letters was explored. In their work Rot and Kostic emphasize that during the consideration and definition of the recognizability factors of a typeface, they start with the assumption that the factors need to be mutual for both letterforms in other words they have focused on discovering the global parameters. A study was conducted in the quest to answer the two basic questions: a) Are there letters in both Cyrillic and Roman alphabets that are relatively consistently legible, i.e. less legible than others, b) which grapheme characteristics influence their legibility?

Measuring the response times for a given stimulus, the authors have concluded that the most legible lowercase letters can be categorized by the following order: 'л', 'ж', 'ш', 'ь', 'т', 'к', 'и', 'ц', 'о'; while the least legible would be 'б', 'в', 'р', 'ч', 'с', 'з'. The most legible Roman lowercase letters are: 'j', 'k', 'c', 'i', 'o', 'z', 'r', 's', 'f', 'e', 't'; and the least legible: 'b', 'g', 'd', 'u', 'dz', 'h', 'v', 'l', 'a'.

The results of the legibility studies of the capitals show that the most legible capital letters of the Roman alphabet range in the following order: 'Š', 'O', 'A', 'K', 'E', 'L', 'S', 'M', 'R', 'T'; and the least legible are 'H', 'C', 'B', 'P', 'Dž', 'Lj', 'F', 'Č', 'V', 'J'. The most legible Cyrillic capitals are 'Ш', 'Л', 'Ь', 'А', 'Е', 'М', 'О'; and the least legible are 'Х', 'Ц', 'У', 'Ф', 'Н', 'З', 'В', 'Б', 'И', 'Р', 'Б', 'Н'.

Making a qualitative analysis of the results of this study⁴, Rot and Kostic (1987), draw a conclusion that the legibility of the letters greatly depends on their graphemic characteristics, and the most important difference determinant of the legibility is defined by the dimension of the straight and curved lines. "The straight lines, especially the vertical ones and with them the straight and sharp corners, are the most important factor of greater legibility" (Rot & Kostić, 1987). Alongside this, the legibility is influenced by the special letter parts perceived as additions, such as the diacritic symbols found in the letters 'č', 'š', 'ž', and the letters with a point above them like 'j', 'i', and the lateral additions of the letters 'ь', 'л', 'ц'. Therefore, the discontinuity of the line as a factor and the factor of the asymmetric form, as well as the factor of the unusual form compared to the other letters (for example 'ж', 'ш', 'Ш', 'S'). The given results are somewhat in accordance with the Keren & Baggen results (1981). These authors also emphasize the presence of the straight vertical lines as the necessary characteristics for discerning of the graphemes. Rot and Kostic state that the factors that decrease the letter identification are the curved strokes and graphemic similarity (found in letters such as 'b' and 'd'), that is the decreased legibility is pronounced by graphemic complexity (the doubled graphemes characteristic of the Serbian and Croatian Roman alphabet: 'lj', 'nj', 'dž') a weaker pronunciation of the discernable parts (for example: 'l', 'v', 'č'). which is in a manner of speaking in accordance with the findings of recent studies. (cf. Courrieu, Farioli, & Grainger, 2004).

Courrieu et al. (2004) exemplify a simple, precise and mathematically based method of measurement of the similarities of the letter pairs based on the response time of the participant to these stimuli. The participants had a task to respond by pressing a button each time they were presented with a different stimulus, and not to respond each time they were presented a same or similar stimulus (go/no-go task). All of the lowercase Roman letters were shown in Arial size 12pt and with them a 27x27 matrix was formed so that all of the combinations of letters

⁴ Rot and Kostic in this study (1987) confirmed the findings from the previous research (The readability of the Cyrillic and Latin alphabet (1986) where the results indicated that printed lowercase letters of the Cyrillic alphabet (reviewed as alphabet altogether) are more legible than the printed lowercase letters of the Latin alphabet whereas capital letters of the Latin alphabet (reviewed as alphabet altogether) are more legible than Cyrillic capital letters.

were made. Each participant was displayed all of the possible pairs only once ($27 \times 26 / 2 = 351$) and 13 times of only one character ($27 \times 13 = 351$), which is 702 pairs in total. These 702 displayed images were divided into 3 blocks (each by 234 pairs) with a short pause between the blocks.

The authors of this work Principal component analysis (PCA) come to a categorization of the letter characters into classes of similarity of letter properties, contrast classes as well as the most characteristic features of the class.

The authors define 25 dimensions, for each of the dimensions a single main class of feature similarity and a contrast class with the prominent similar feature for each main class. A contrast class encompasses a character set that do not share a similar feature as the main class.

Courrieu et al. (2004) present the following classes:

1. main class of feature similarity ('b', 'd', 'g', 'p', 'q')
2. opaque strokes class ('a', 'c', 'e', 'o', 's')
3. repeating vertical strokes class ('m', 'n', 'u', 'w')
4. a subclass of the first class with ascenders ('b', 'd')
5. v-shaped class ('v', 'y')
6. an ascending stroke that cuts the horizontal stroke class ('f', 't')
7. n-shaped class ('h', 'n')
8. four corners and square diagonal class ('x', 'z')
9. i-shaped class ('i', 'j')
10. character that can be created by rotation or extension of another character class ('a', 'g')
11. the upper left rounded segment class ('c', 'r')
12. the character with the same but interrupted stroke class ('i', 'l')
13. a sigmaesque characters class ('s', 'z')
14. the subclass of the first class with the left rounded segment ('b', 'p')

The remainder of the 11 classes refer to the other distinct features of the individual characters (i.e. letters). Using the Bubbles Classification Image Technique Fiset, et al. (2008) discover which parts of the individual glyphs are most important for their recognition. The studied typeface was Arial. Their study provides evidence that the terminals of the glyphs are the features most important for letter recognition. The authors also emphasize that it is exactly these terminals that assist the reader to differentiate between the visually similar characters. The logics behind the Classification Image Technique is simple. If we deprive the observer of the visual information necessary to perform a task by masking them, this will greatly diminish his performance. In contrast, if we deprive him of information non-essential for performing a task, his performance will be undisturbed. For example: to make a difference between the letters 'F' and 'E', the information necessary is contained within the lower part of the letter. If we conceal the lower part of the letter 'E', there will be no difference between these two letters. However, if we conceal the upper part of the letter 'E' the difference will be visible, and the observer will clearly recognize the difference and which letter is in question. The authors have made 213 masks containing the following 10 features for each of the letters of the alphabet: (1) verticals, (2) horizontals, (3) Slants Tilted Left, (4) Slants Tilted Right, (5) Curves Opened Top, (6) /Curves Opened Bottom, (7) Curves Opened Left, (8) Curves Opened Right, (9) Intersections and (10) terminations.

Sofie Beier has summarized the findings of five studies in her dissertation *Typeface Legibility: Towards defining familiarity* (2009) with the focus on the misrecognition of the lowercase letters. Comparing the findings of Sanford, Bouma, Tinker, Geyer, Dockeray, she states that the different typographic alphabets were used as stimuli, therefore, the misrecognition of the letter pairs were inconsistent between the compared findings. Other than that, Beier points out that with the review of the data an error repetition pattern is noticeable with the two main groups of the problematic letters. One group is the letters whose x-height and standard width are the same, different only by their straight and curved strokes (e-c-a-s-n-u-o); the other group consists of the narrow letters with one vertical stroke and small width (i-j-l-t-f) (Beier, 2009). These differentiated groups of letters will be the subject of her further research.

Inspired by the differentiation theory given by Legros & Grant (1916)⁵, Beier considers the shapes of the skeleton variations as the subject of her study (Beier & Larson, 2010; Beier, 2009). For research purposes, she designs three typefaces: a serif, a sans serif and a pseudo-serif (*Pyke*, *Ovink*, *Spencer*) with the same skeleton. Beier and Larson (2010) have tested numerous hypotheses with these two carefully prepared experiments: short exposure and distance. With the short exposure experiment in the conditions when the stimuli were placed within the foveal area of vision, no recognition errors were detected, which made the subject of their study the conditional identification errors at the parafoveal area. In the effort to discover the most optimal differentiation of letters with a similar skeleton, they tested the following hypotheses with designed stimuli:

- Serif on a lowercase sans serif letter 'i' used to emphasize the division of the stem from the dot, which made them expect a better legibility in comparison to the sans serif letters. The hypothesis was confirmed for distance viewing.
- Greater differentiation of the letters 'u' and 'n' should provide better legibility. To test this hypothesis Beier designs variants for these letters: tailless 'u' and variations for both letters with a pronounced difference in the height of the junction stroke. This hypothesis was not confirmed.
- According to the Gestalt psychology, our perceptive system tends to close the incomplete shapes by filling the gaps (The Law of Closure). Guided by this theory it might be expected that the smaller aperture of the letters 'c' and 'e' increases the risk of an error, by closing the gaps and recognizing them as the letter 'o'. The closed apertures hypothesis was tested with many other versions of the letters 'e' and 's' and the two-storey 'a'. The closed apertures hypothesis was only confirmed in the case of the letter 'e', where the stimulus 'e₄' recorded far greater identification errors than the other letters. The authors think that the hypothesis isn't confirmed in case of the letter 's', they assign considerable differences between the variants of the letters to the difference in the spine of the letter. The variant of the letter 's₁' has a diagonal spine and a big closed aperture while the variant 's₂' has a rounded spine and a closed aperture. The authors state that this finding is inconsistent with the earlier findings of the typography researcher G.W. Ovink (cf. 1938, as cited in Beier, 2009), which increases the doubt in the precision of the interpretation of this result.
- For the one-storey 'a' a lower legibility was expected compared to a two-storey 'a' and a misrecognition of the letter 'o'. The hypothesis was confirmed and frequent identification errors were recorded, i.e. the confusion between the one-story letter 'a' with the letter 'o' and the letter 'q'.
- The narrow letters 'l', 'f', 't', 'j' i 'i' take up little width. If their image was to expand, greater legibility would be expected. For these letters there is a wide and a narrow variation. This hypothesis was confirmed for the letters 'j', 'l' i 't', in the case of the pseudo-serif font (*Spencer*) it was confirmed for the letter 'f' while the letter 'i' has no clear value in a widened form.

⁵ Legros and Grant examined the amount of overlap between similar letter pair of different fonts (letter to letter, e.g. . c-o-e, n-u, b-h, s-a, i-l). The fonts with the largest area of overlap have been defined as less legible from the fonts with smaller overlapping area.

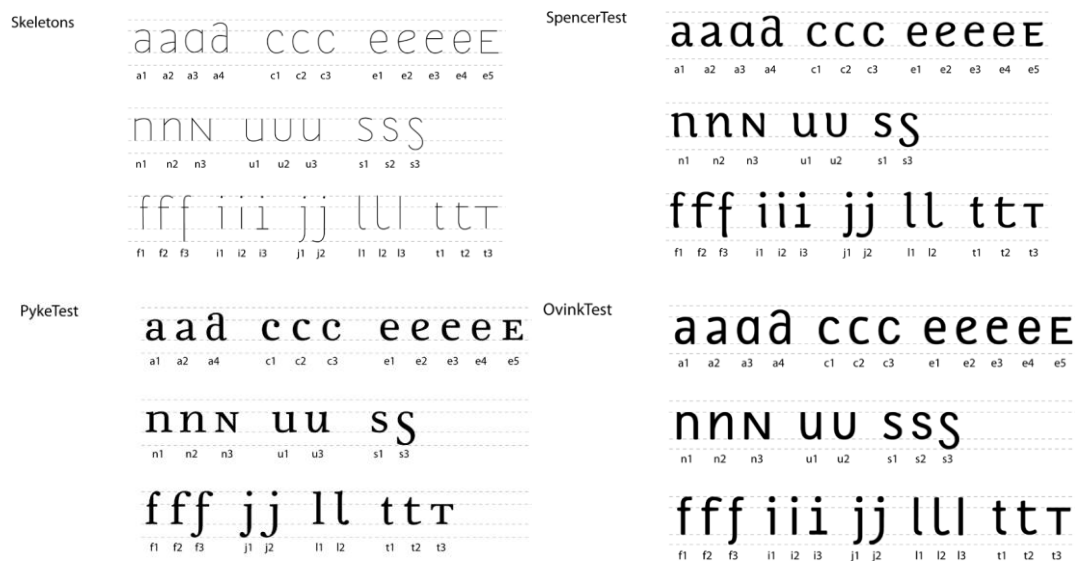


Figure 1. The skeleton and the variations of the skeleton viewed in three different fonts designed by Sofi Beier Beier (Reproduced, from Beier & Larson, 2010).

5. DISCUSSION

In the first epistemological study of the construction of the typographical knowledge, Ole Lund (1999) discovers that according to 26 viewed studies on legibility (of the approximately 72 that have been published up to that point) every one of them lacks internal validity among other methodological errors. The most commonly spotted errors are inappropriate manipulation of the typographic stimulus which can, according to the author, due to the insufficient education in the field of the typographic design. Lund concludes from 72 studies that the effort to explore typeface legibility base on different operational methods was not so successful. Therefore, we cannot recognize that knowledge about typography has been expanded, nor we are to consider that certain theories have been simplified or established based upon this research. However, the benefits of the revised studies differ in quality according to Lund. In his opinion, the studies that are rational, interesting but not without its faults, are those of English 1944, Zachrisson 1965, Harris 1973, Vanderplas and Vanderplas 1980, and de Lange (as cited in Lund 1999). Additionally, Lund extricates Tinker and Peterson as fruitful researchers with remarkable results. The choice of different types of stimulus (typefaces), and yet again their inadequate manipulation in the studies of feature detection with confusion matrix method have lead to inconsistencies among the results between numerous studies. Consequently, this has slowed down the progress of finding the ultimate list of distinctive features of the letters – the key to letter recognition. Even though many scholars were aware of this, some still compared their results to the results of others and published their findings with inconsistencies neglecting the fact that their stimulus was different (cf. Geyer, 1977; Bouma, 1971). Nonetheless, oversights of this kind have caused scholarly discussions and qualitative analysis of the confusion matrix findings. In his study, Geyer (1977), argues that previous results of the confusion matrix even for the lowercase of the alphabet in the Bouma study (1971) unconvincing. He suggests that we must consider comparison of the results of the foveal and eccentric field of vision, based upon the performance of the identification, as an empirical question. In the attempt to present the answer to this question, Geyer compared confusion matrix of the eccentric field of vision published by Bouma (1971) to the confusion matrix of the foveal vision from his findings (Geyer 1977). Besides the differences in the data analysis exemplified in the commentary section of this study (Milloy 1978) there is detailed review based on a drastic difference in the choice of stimulus. Milloy points out obvious difference between typefaces Courier 10, used by Bouma in his study, and Tactype Futura demi 5424, used by Geyer. The differences such as: the amplified serif typical for the Courier typeface, and the lack of the serif in the Futura typeface; the two-storey 'a' in contrast to one-storey 'a'; noticeable similarities of the one-storey letter 'a' with the letter 'o' of the Futura typeface; and many other not listed by Milloy but mentioned by Beier (2009) are sufficient enough not to consider the findings related to this matter and published by Geyer as fully grounded.

Analyzing the findings of five studies with the focus on the misrecognition of lowercase, Sofie Beier manages to single out the pattern of the repeated error for the two main groups of the problematic letters, besides the inconsistency in the findings as noted in her work. The deviations in confusion matrix findings of Baume (1971) and Geyer (1977), as well as the deviations of these two authors in comparison to the findings of Sanford, Tinker and Dockeray, are very appealing for detailed analysis. Namely, Beier argues that the characteristics such as amplified serifs and monospaced characters of the tested typeface (Courier) in the Boume study (1971) had been crucial for errors in some letter pairs for which other studies do not recognise any deviations. This observation logically explains that the uniform width of the character may have been the cause in the misidentification of the letter 'n' with the letter 'm', as well as the letter 'v' with the letter 'w'. Contrary to this finding, we recognize the serif feature as oversight which caused misidentification of the letter 'g' with the letter 'q', considering these two characters have very similar skeleton of the letter i.e. in this typeface the letter 'g' is one-storey (figure 3). That does not exclude the effect of the amplified slab-serif, yet certainly this is not considered as the feature that had caused the error in the first place, and we can find the confirmation in the findings of Courrieu, Farioli, & Grainger (2004). Similarities that caused the error should be perceived as essential for further scholarly research, but also for the research of type design practitioners. In their study Courrieu, Farioli, & Grainger (2004) applying the factor analysis to the main components (PCA) have arranged the letter 'g' into the main similarity class along with the letters 'b', 'd', 'q', 'p', where the common feature is specified as 'a circle with an ascender or descender'. Thereby, Courrieu, et al. in the tested font (Ariel) identify that „the graphic realisation of the letter 'g' is the one that looks like 'q' and the digit '9' (in other words one-storey 'g')". The findings of Courrieu et al. along with most common misrecognition (31% confusion) of the letter 'g' and 'q' in the study of Boume (1971) imply an inquiry to why Beier and Larson (2010) didn't find interest in testing skeleton variability of the two-storey and one-storey letter 'g' allograph. We believe that this issue must be considered as empirical.



Figure 2. Lowercase 'g' and 'q' of the typeface Courier

Faced with the inconsistencies among the findings of other scholars, Beier considers certain findings of Geyer (1977). Beier implies that the straight stem (without typical curving at the bottom) had probably increased chances why subjects misrecognized the letter 't' during short exposure with the letters 'i' and 'l'. As stated before, the unusual choice of the tested typeface (Tactype Futura demi 5424) in this study had caused different errors in letter recognition. The unusual character of the letter 't' of this typeface had been highly reduced presenting kind of an idiom or "idiosyncrasy". Geyer was aware of the fact that there is variability in the configuration of different lowercase letters, and that is actually a function of certain typographic style. He believed that the cause of this variability is the level of "ornateness". Therefore, he tried to find appropriate stimulus for his experiment which in his opinion would "minimised the influence of any particular type style idiosyncrasy" and chose Tactype Futura demi 5424. Futura typeface (designed by Poul Renner) is the typical example of the elementary-constructivist early German modernism which would explain why this typeface, in its idiosyncrasy, among other things, is aesthetically different. In his book "New Typography", Tschichold (1928/1995) pointed out: "All the attempts up to now to produce a type for our time are merely 'improvements' on the previous sans serifs: they are still too artistic, too artificial, in the old sense, to fulfil what we need today". This was generalised comment on typeface designed in this manner. Like many experimental psychologists before him, Geyer was not educated properly in the field of typography in order to deal with this problem. Still, his findings are considered interesting for examining this group of sans serif typeface that have a new shape of the skeleton as their common feature, besides the listed features – one-storey letter 'a' i.e. allograph of this character, and one-storey letter 'g' (previously mentioned allograph). Sanford, Dockeray and Tinker in their research used Antiqua typefaces as stimulus which made their findings more consistent according to which Beier (2009) was able to define a pattern of continuous letter misrecognition.

6. CONCLUSIONS

After a breakthrough in information processing theory, researchers were able to present significant findings on letter recognition i.e. letter distinctive features within a typeface – alphabet. Numerous research consulting confusion matrix (Bouma, 1971; Geyer, 1977; Gilmore, Hersch, Caramazza, & Griffin, 1979; Keren & Baggen, 1981; Geyer & DeWald, 1973) provided qualitative and significant findings which were helpful in many ways – with the development of eye tracker device and neural network modeling (Bouma, 1971; Geyer, 1977; Gilmore, Hersch, Caramazza, & Griffin, 1979; Keren & Baggen, 1981; Geyer & DeWald, 1973) these findings were beneficial in presenting precise answer to the question: How do we recognize words?

Further research provided groundwork for the pattern recognition theory. However, foundation for the theory of readability and legibility of typefaces fundamental for typographers and type designers was made possible with the findings of Rot and Kostic (1987), supported by the study of Courrieu et al. (2004); epistemological study of typographic design knowledge by Ole Lund (1999); the findings most prominent for type designers were in the studies of Beier and Larson (2010; 2009) which propose new approach to legibility research of the type letters, and they also, in great extent, certify some feature styles as more legible than others. Not in the least less interesting within this field were the findings of familiarity, commonality, and font tuning (Sanocki, 1987; Sanocki, 1992; Walker, 2008) which by its nature could not be included in the focus of this research (see Sanocki & Dyson, 2012).

Acknowledgements

This work was supported by the Serbian Ministry of Science and Technological Development, Grant No.:35027 »The development of software model for improvement of knowledge and production in graphic arts industry«

7. LITERATURE

- [1] Balota, D. A., Yap, M. J., & Cortese, M. J. (2006). Visual Word Recognition : The Journey from Features to Meaning (A Travel Update). In M. Traxler, & M. A. Gernsbacher (Eds.), *Handbook of Psycholinguistics* (2 ed., pp. 285–375). Academic Press.
- [2] Beier, S. (2009, May). Typeface Legibility:Towards defining familiarity. *PhD thesis* . London: The Royal College of Art.
- [3] Beier, S., & Larson, K. (2010). Design Improvements for Frequently Misrecognized Letters. *Information Design Journal*, 18 (2), 118-137.
- [4] Bouma, H. (1971). Visual recognition of isolated lower-case letters. *Vision Research*, 11 (5), 459–474.
- [5] Cattell, J. M. (1886). The Time Taken up by Cerebral Operations. *Mind*, 11 (44), 524-538.
- [6] Courrieu, P., Farioli, F., & Grainger, J. (2004). Inverse discrimination time as a perceptual distance for alphabetic characters. *Visual Cognition*, 7 (11), 901–919.
- [7] Fiset, D., Blais, C., Éthier-Majcher, C., Arguin, M., Bub, D., & Gosselin, F. (2008). Features for Identification of Uppercase and Lowercase Letters. *Psychological Science*, 19 (11), 1161-1168.
- [8] Geyer, L. H. (1977). Recognition and confusion of the lowercase alphabet. *Perception & Psychophysics*, 22 (5), 457-490.
- [9] Geyer, L. H., & DeWald, C. G. (1973). Feature lists and confusion matrices. *Perception & Psychophysics*, 14 (3), 471-482.
- [10] Gilmore, G. C., Hersch, H., Caramazza, A., & Griffin, J. (1979). Multidimensional letter similarity derived from recognition errors. *Perception & psychophysics*, 25 (5), 425–431.
- [11] Grainger, J., Rey, A., & Dufau, S. (2008). Letter perception: from pixels to pandemonium. *Trends in Cognitive Sciences*, 12, 381-387.
- [12] Haber, R. N., & Schindler, R. M. (1981). Error in proofreading: Evidence of syntactic control of letter processing? *Journal of Experimental Psychology: Human Perception and Performance*, 7 (3), 573-579.
- [13] Hebb, D. O. (1989). The first stage of perception: Growth of the assembly. In J. Anderson, & E. Rosenfeld (Eds.), *Neurocomputing: Foundations of Research* (pp. 54-56). The Mit Press.

- [14] Huey, E. (1908). *The Psychology and Pedagogy of Reading*. New York: The Macmillan Company.
- [15] Keren, G., & Baggen, S. (1981). Recognition models of alphanumeric characters. *Perception & psychophysics*, 29 (3), 234-46.
- [16] Kostić, A. (2010). *Kognitivna psihologija* (Drugo ed.). Beograd: Zavod za udžbenike.
- [17] Larsen, A., & Bundesen, C. (1996). A template-matching pandemonium recognizes unconstrained written characters with high accuracy. *Memory & Cognition*, 24 (2), 136–143.
- [18] Larson, K. (2005). The science of word recognition. *Typo*, 2–11.
- [19] Legros, L., & Grant, J. (1916). *Typographical printing surfaces: the technology and mechanism of their production*. London: Longmans, Green, and Co.
- [20] Lund, O. (1999). Knowledge construction in typography: the case of legibility research and the legibility of sans serif typefaces. *PhD Thesis*. The University of Reading, Department of Typography & Graphic Communication.
- [21] McClelland, J. L., & Johnston, J. (1977). The role of familiar units in perception of words and nonwords. *Attention, Perception, & Psychophysics*, 22 (3), 249-261.
- [22] McClelland, J. L., & Rumelhart, D. E. (1981). An interactive activation model of context effects in letter perception: Part 1. An account of basic findings. *Psychological Review*, 88, 375–407.
- [23] Milloy, D. G. (1978). Comment on Recognition and confusion of the lowercase alphabet. *Perception & Psychophysics*, 22 (2), 190–191.
- [24] Monk, A. F., & Hulme, C. (1983). Errors in proofreading: Evidence for the use of word shape in word recognition. *Memory & Cognition*, 11 (1), 16-23.
- [25] Paap, K. R., Newsome, S. L., & Noel, R. W. (1984). Word shape's in poor shape for the race to the lexicon. *Journal of Experimental Psychology: Human Perception and Performance*, 10 (3), 413-428.
- [26] Rayner, K. (1998). Eye Movements in Reading and Information Processing : 20 Years of Research. *Psychological Bulletin*, 124 (3), 372-422.
- [27] Rayner, K., & Pollatsek, A. (1989). *The Psychology of Reading*. New Jersey: Lawrence Erlbaum Associates.
- [28] Reicher, G. M. (1969). Perceptual recognition as a function of meaningfulness of stimulus material. *Journal of Experimental Psychology*, 81 (2), 275-280.
- [29] Rot, N., & Kostić, A. (1986). Čitljivost ćirilćnog i latinićnog alfabeta. *Psihologija*, 19 (1–2), 157–171.
- [30] Rot, N., & Kostić, A. (1987). Čitljivost slova latinice i ćirilice i njihove grafemske karakteristike. *Psihologija*, 20 (1–2), 3–19.
- [31] Rumelhart, D. E., & McClelland, J. L. (1982). An interactive activation model of context effects in letter perception: II. The contextual enhancement effect and some tests and extensions of the model. *Psychological Review*, 89 (1), 60-94.
- [32] Sanocki, T. (1992). Effects of font- and letter-specific experience on the perceptual of letters processing. *American Journal of Psychology*, 105 (3), 435-458.
- [33] Sanocki, T. (1987). Visual Knowledge Underlying Letter Perception: Font-Specific, Schematic Tuning. *Journal of Experimental Psychology Human Perception and Performance*, 13 (2), 267-278.
- [34] Sanocki, T., & Dyson, M. C. (2012). Letter processing and font information during reading: Beyond distinctiveness, where vision meets design. *Attention, Perception & Psychophysics*, 74 (1), 132-145.
- [35] Seidenberg, M. S., & McClelland, J. L. (1989). A Distributed, Developmental Model of Word Recognition and Naming. *Psychological review*, 96 (4), 523-568.
- [36] Sternberg, R. J., & Mio, J. (2008). *Cognitive Psychology* (5 ed.). Wadsworth Publishing Company.
- [37] Tschichold, J. (1928/1995). *The New Typography/ The First English Translation of The Revolutionary 1928 Document*. London: University of California Press.
- [38] Walker, P. (2008). Font tuning: A review and new experimental evidence. *Visual Cognition*, 16 (8), 1022-1058.
- [39] Wheeler, D. (1970). Processes in Word Recognition. *Cognitive Psychology*, 1, 59-85.

PRINCIPLES OF ART NOUVEAU AND IT'S REFLECTION ON CONTEMPORARY TYPE FORMS

Slobodan Nedeljković¹, Ivan Pinčjer², Uroš Nedeljković²

¹ Academy of Arts, Novi Sad, Novi Sad

² Faculty of Technical Sciences,

Department of Graphic Engineering and Design, Novi Sad

Corresponding author: Ivan Pinčjer

e-mail: pintier@uns.ac.rs

1. ABSTRACT

This paper analyzes the new Art Nouveau typeface by Slobodan Nedeljković - Zaharius Neo-Secession. It is very difficult to determine whether this typeface follows the continuity of this typographic form, or is it a hybrid sub-form of some kind. Therefore, it is necessary to look back at some of the influential classical typefaces, such as Schwabacher, Behrens and Fette Eckmann whose authors have instilled them with a personal touch corresponding to the period in which they had been designed. Neo-secession type forms are celebrating its 100th birthday, but it is evident that this style holds up extremely well, because of both its artistic and functional appearance. This paper studies the Jugendstil groups and their specific characteristics that have made way for interpretations by new authors, as well as the process of designing a typeface and its morphological development. Finally, we have considered the typographic characteristics and the practical applications according to the latent, dynamic rhetoric of our new typeface.

Key words: Neo-Secession, Fraktur, Hybrid typeface

2. INTRODUCTION

Secession is the last generally accepted movement in art that have left an artistic mark on every aspect of life in the beginning of the 20th century. Although Secession has been known under different names in the different parts of Europe, it has made a new style in the world of fashion and has imposed a certain style of life altogether. Secession is a movement that made its mark in architecture and painting, while in the art of sculpture it influenced the decorative and applied arts.

The movement had a variety of names throughout Europe. In Austro-Hungarian monarchy it was known as *Viennese Secession* (ger. *Wiener Secession*), in Germany it has been *Jugendstil* (after the name of the „Jugend“ magazine), in France and Belgium *Art Nouveau*, in Britain and U.S.A. it bore the name of *Modern Style* or *Liberty*, in Spain *Catalonian modernism* (cat. *Modernisme catalonie*), in Italy, it was known as *Floral stile* (ita. *Stile floreale*), while in imperial Russia they called it *The World of Art* (rus. *Mup uckyccmea*).

In the field of graphic design, Secession made a more important influence than in the world of Arts. The most particular mark it left on typographic letters which had deformation in glyphs design that they had got from the earlier GOTHIC types, according to the majority of typeface theorists, and the most elements of the glyphs design came from the later Gothic forms, Schwabacher and Fraktur.

3. RESEARCH

Within the eclipse of linear writing and molding, Jeffery Keedy pointed out that in typographic circles it is common to refer to traditional values as though they were permanently fixed and definitely not open to interpretation. He thinks that exactly that kind of view is the source of the misguided fear of new developments in type design and that new technology is the beginning of the end of traditional typographic standards. In fact, just the opposite is true, more and more typographic standards are being challenged by designers than ever before (Keedy, J, 1993.).

With the beginning of the desktop era that new device composed by postscript language encourages designers to treat typography as imagery. That has brought the communication to a higher level whereas readers were simply invited to interpret messages on their own terms

(Zelman, S., 2000.). Without any attempt at controversy, and in personal opinion of the author, the glyphs were taken from the Unical script. The fact that the glyphs are close to the Gothic features in terms of time is not the advantage of these typefaces, quite the opposite, they as well as the typefaces of Secession sprouted from the same roots. Because of the fact that the common belief is that the starting point of the Secession design is in the Gothic typefaces, we have presented a review of some historic designs – the lowercase letters only – with the uppercase letters of Eckmann's and Bahrens's secession in order to recognize in them the TRANSITIONAL FORMS. That is the reason why we are going to look at the glyphs that show this mark more obviously – that being letters from the span from D to T:

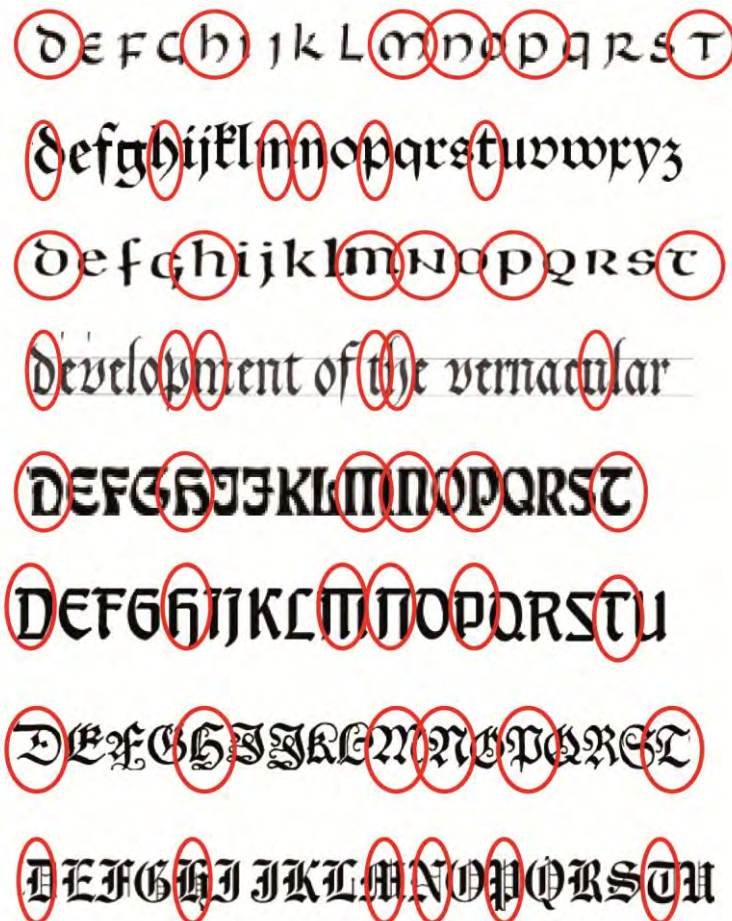


Figure 1. Glyphs of transitional forms.

As for lowercase letters, their source is the same, but the glyphs were taken from later Gothic lowercase letters because, let us remember, uppercase Gothic letters are extremely illegible and often unrecognizable.

Therefore, to be able to talk about the influence of the Gothic uppercase letters on the Secession letters we can only observe that they are similar to one another in a sense of decorativeness and nothing more. If we have a look at the Schwabacher and Fraktur letters shown herein, it is clear that those couldn't have possibly been any kind of model, because they show nothing beside sheer decorativeness and unnecessary meticulousness, which lovely as it is still has no practical use. Not until later, with the uppercase FRACTUR, there has been given the shape to the letters of American daily newspapers and for those it could be said that they have been useful in some degree.

The letters of the Secession period were under the strong influence of the couple of German designers, Otto Eckmann (1865-1902) and Peter Behrens (1868-1940). The Rudhardschen type foundry had been casting Eckmann's glyphs in the size of 16 pt even in 1900. It is important to point out that the author of the most popular typeface of that period, the one that first comes to mind when one thinks of the Secession style, *hadn't gain a long and prosperous*

life. Eckmann had not had time to enjoy the popularity of his invention – he died a year and a half after the promotion of his typeface.

His letter was a huge novelty in the typography of that time. The letters are drawn with a brush and they show in the equal measure the influence they had received from both GROTESQUE and ANTIQUE. In the wake of the first version of NORMAL went the version with a pronounced „distortion“ which led to extra bold, i.e. FET version. Beside the decorative form that explains its purpose, the real value of the cut-off had been that it was exclusively used for headlines and it was usually utilized for shaping the elements of the ACCIDENCE – book titles and wallpapers. The floral motifs were very common in Eckmann's painting and they besieged him, as well as they did the French painters, with their stylized form and simplicity similar to the Japanese graphic which initiated this style in a significant measure throughout Europe. Unfortunately, Eckmann abandoned painting and focused exclusively on applied arts and consequently on the shaping TYPOGRAPHIC letters.

His work was comprehensive; the originals of the typeface drafts as well as his paintings, drawings and illustration were sold at the Auction that took place in 1904, after his death. Eckmann made his design in a way that there is a sense of „economy“ between BLACK LETTERS and WHITENESS of a letter cut-off allowing the surface of the letters in the FET version to rise to 50-60% of the surface.

On the other hand, Bahrens also was a painter but he had studied architecture and had made remarkable results in that field. He started working on his own typeface a year later than Eckmann, although not as bold as a painter would have done but in a hard way, from the position of ANGULAR CALLIGRAPHY, which probably set the mind of the theorist who claim that, Secession is a product of deformation of the Gothic letters. However hard Bahrens tried, he never could be »natural« in the free style of shaping the letters and their only real frame was a CAPTURE in the SHAPE OF RECTANGLE.

Eckmann's and Bahrens's graphic design was modeled on the work of the prerafaelian English genius *William Morris*. The two, as well as Morris, had a wide range of interests: from the jewelry and furniture design to the design of textile and typefaces. Eckmann's most famous SINGJET is the LETTERHEAD of the Di Woche magazine „7“, which will be designed later by Peter Bahrens as well as typefaces for Karl Klingspor the owner of the type foundry, who employed Bahrens to work in the foundry as an consultant.

Since 1902, Bahrens designs a series of typefaces BAHRENS – BAHRENS Schrift, BAHRENS Italic and two forms of the historic typefaces – BAHRENS Roman and BAHRENS Medieval. Later, same as Eckmann, he also works for AEG, since 1907.

In one thing he was different that Eckmann – he had the ability to assert himself especially in press projects where he established himself as a leader in the contemporary CORPORATIVE design. Art Noveau provided opportunities for many of the German TYPO DESIGNERS as well as Viennese professor Rudolf von Larisch with his EX Libris and INTERNATIONAL designers such as Georges Auriol, Paris; Max Barlage, Amsterdam; Charles Mackintosh from Glasgow and many others.



Figure 2. Eckmann schrift, Behrens schrift, Edelgotisch

However, there had been a designer whose name is almost never mentioned in the History of creating of Secession and whose work is more than present in the beginning of the century – Albert Knab, who shaped his own version of Secession typeface only a year after the presentation of Eckmann's typeface – it was Edel Gothic (Edelgotisch). At a glance, Knab's design suffered the influence of the GOTHIC letters (the very name of the typeface states the obvious). However, unlike Eckmann's design which shows the remainder of the past serifs in Knab's typeface there is no sign of serifs (except for so called "roof lines") so that it can only be linked to a, at that time very popular, typeface of the GROTESQUE form – Accident-Grotesque.

A B C D E F G H I J K L a b c d e f . X Y Z . g h i j k l
M N O P Q R S T U V W m n o p q r s t u v w x y z
1 2 3 4 5 6 7 8 9 0

Fig 3. Edel-Gothic – 1901, Albert Knab (The Noble Gothic).

A B C D E F G H I J K L M N
O P Q R S T U V W X Y Z A
Å Ê Æ abcdefghijklmn
opqrstuvwxyz à á â ã
1 2 3 4 5 6 7 8 9 0 (\$ % . , ! ?)



Figure 4. Arnold Bocklin

Arnold Bocklin is a display letter that was created by the type foundry Schrift Giesernei OTTO VEISERT in 1904. It was named after Arnold Bocklin the Swiss painter and symbolist who died in 1901. This is the one of the most famous typefaces of Secession. The font had his rebirth during 60's and 70's of the 20th century when the RENAISSANCE of the whole Art Nouveau took place.

4. APPLICATION IN CONTEMPORARY TERMS

By the ending of the Word War I this »vibrant« artistic movement reaches its end which, as a rule, gives way to the SIMPLE, extremely rational typefaces and the corpus of GROTESQUE typefaces can be called simple and rational. Still, a part of the Secession continues to exist through decorative form of typefaces such as the Art Deco and similar.

HOBBO is a typeface a whole decade younger than extraordinary designs of the German typographs from the beginning of the century. Typefaces Eckmann and Bahrens Gothic, Edel Gothic and Veisert foundry – Arnold Bocklin, were all created merely 6 or 8 years before the HOBBO.

Although the title may suggest otherwise, Benton's typeface was not inspired by the word HOBBY. However, it is a kind of a typeface for diversion and DRIFT. Nowadays, with 100 years of hindsight we can say in all honesty that this Morris Fuller Benton's font in its appearance, but before all in its CREATION, is the American Art Nouveau, a response to "the foolish period of European Secession".

Probably the world's most prolific typo designer Morris Fuller Benton, now graduate mechanic engineer and in his most creative years (1910), had to shape the typeface at his father's - Linn

Boyd Benton - ATF, where he became a designer-in-chief in the first decade of his practice. He created more than 200 FONTS from 1900 to 1937.

It is only fair to point out that if there wasn't for Linn Boyd's establishing of the ATF, the association for registry, acquisition, distribution and promotion of typefaces and especially for the invention of PANTOGRAPH (which was used for much faster and more precise engraving of the moulds) there wouldn't have been possible for the art of typography to rise so rapidly.

Morris created his first typeface before his 18th birthday which only the French genius Firmin Didot had managed to do in the whole history of typography when he shaped the early version of his Didot style in typography.

Morris Fuller Benton is an example of creativity because of a huge number of designs out of which at least twenty are being used even today and in the full capacity. To name a few, Franklin Gothic and News Gothic belong to the group of modern Grotesque typefaces. Hobo and Broadway belong amongst typefaces that affirm Art Nouveau and Art Deco, while Bank and Agency fall into the pool of purposeful letters for the organizations with the need for specifically created letters.

ABCDEFGHIJKLM
NOPQRSTUVWXYZ
abcdefghijklm
nopqrstuvwxyz

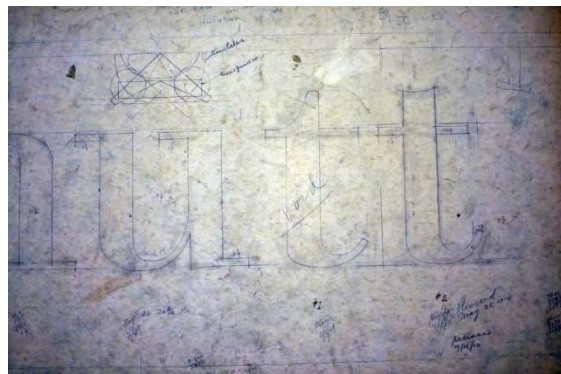


Figure 5. The Hobo font and the draft that was characteristic for the beginning of the 20th century, Bodoni and Garamond fonts Morris reshaped for the ATF. The example shows how much energy and how many drafts were being spent and used to shape only one cut-off of the typeface.

Interestingly, HOBO is the only significant typeface that came from another continent and into the sphere of the Secession modeling. His typeface has no descenders, lowercase g, p, k and l are being brought to the level of lower writing line. HOBO font looks somewhat straightforwardly, making a positive impression at a first look. It recommends itself for a variety of usage in a time when a possible user seeks to immerse in their HOBBY. If we cast a look around it will become clear that Hobo is being used for the promotion of products for HUNTING and ANGLING, for leisure activities, tourist advertisement for TOUR-OPERATORS, agencies for fun, birthday celebrations, New Year Eve's celebrations and other "happy" dates. Naturally, the font is also useful for packaging, protective signs and similar.

**This typeface has
no descenders!**



Figure 6. One of the main characteristic of Hobo type

5. RENDITION OF THE CYRILLIC AND LATIN TYPEFACE IN THE STYLE OF SECESSION, ORIGINAL WORK

Almost 100 years after the end of the movement, prof. Nedeljkovic has formed a typeface of NEO-SECESSION after a long and painstaking work on drafting the first group of the selected material in uppercase CYRILLIC and LATIN. He is determined to devote the next few months on observation of the glyphs so that he can make notes on the matter of how much, if any, particular glyphs »stand-out« or are being »blended« into the typeface comprehensiveness. In the essence, the work has been done simultaneously on the several typefaces that were supposed to be observed separately, without the influence of one typeface on another, and the notes have been made which are in their own right the »fresh« observations necessary to bring the »Cyrillic uppercase« and »Latin lowercase« into harmony.

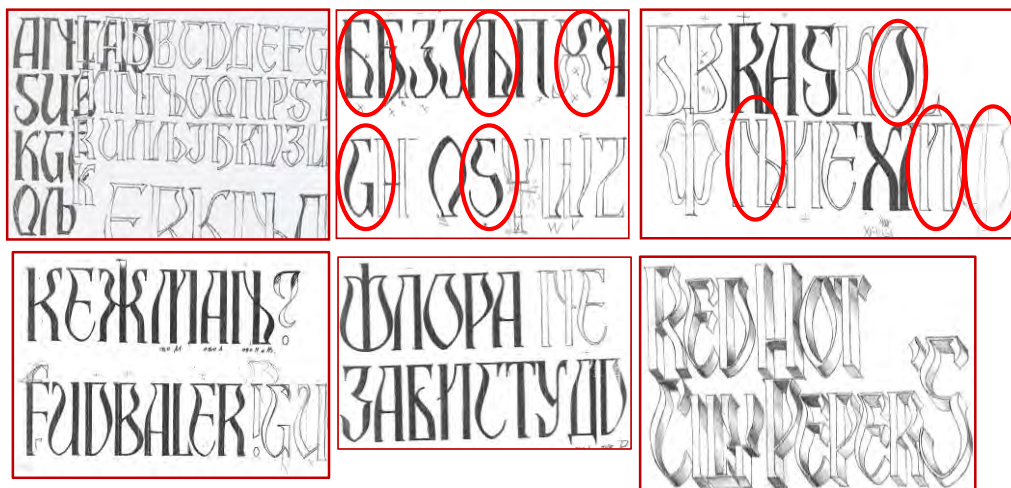


Figure 7. The plans for Zaharius Neo-secession typeface show a remarkable transition from the early drafts to the Letter ready for distribution on the market.

In the first sketch from this series, the glyphs only give a hint of elements of the future typeface in every sign of Secession; what has certainly given the basic direction to the latter typeface is an upper horizontal line which is going to decide the entire sequence of letters to use the horizontal line to render "layout" of the Secession typeface.

The next two drawings show the development of the forms of Cyrillic letters B, LJ, X, G and S, the third drawing show letters R, A, S and O, and then again Cyrillic NJ, M and F. As it may be seen, the letters are done on the same sheet of paper deliberately, forsaking the fact that some of them are Cyrillic and some Latin. By this act the author has managed to diminish the differences of the two Alphabets in some degree.

After three months of observation, the author decided that some of the glyphs are "overstrained" while the others are "too static". This should have been rendered more even with the benefit of hindsight, but the time was too short for a more elaborate work to be done. The author managed to make the glyphs to look more »exciting« than before. The overall intention in designing the typeface was to subjugate the glyphs to the entirety of the typeface so that their »beauty« or »ugliness« per se gets ABSTRACTED and to try to equalize the typeface which will get its real value only after the transmission of the letter into words and sentences. Getting a typeface with a couple of beautiful letters and 20-odd accompanying ones was not an option.



Figure 8. Uppercase after first harmonization of Cyrillic and Latin form

The first solution of the complete Cyrillic and a good deal of Latin letters is (and is being) simpler and more elegant than the final form is, and being as it is – it has not been abandoned because of the possible omissions in the forms of the glyphs. At a moment, the author had a feeling that he might have been “led on” by Miša Nedeljković’s design of 2001, which he named “CaR Dušan” (“Dusan the EmperoR”) and designed only in Cyrillic uppercase version. It was completed in 2001.



Figure 9. Font “CaR Dušan” from Miodrag Miša Nedeljković, 2001.

Wanting to have all glyphs to look a little bit “excited” at least at a first glance, the author destroyed the glyphs that seemed “calm”. This almost painting-like approach to TYPOGRAPHIC letter was supposed to contribute to the basic goal – to produce the letters that seem coherent, subdued to the unity.



Figure 10. Painting-like approach to TYPOGRAPHIC

In the spirit of “Mega Zaharius” typeface, all has been done that the typeface can deliver the basic elements of the both forms that must be respected while creating of a writing form, regardless of the time distance.



Figure 11. The numbers represent the basic principle of the letter very well.

The layout is being marked exclusively by a thin horizontal line, which is one of the elements that are always present, almost in every sign.



Figure 12. Lowercase “Mega Zaharius Neo-Secession” from May 2008.

6. CONCLUSION

Lowercase typeface “Mega Zaharius Neo-Secession” is significantly different from Eckmann’s and Bahrens’s design. The difference alone is not what is most important though – it is much more substantial and at a same time difficult to retain the spirit of the Secession from the dawn of the 20th century. It was necessary to give a contemporary element to the typeface that would enable it to become competitive and to raise an interest in its application.

If we would like to find the basic elements in which contemporary solutions of Neo-Secession, defer from typefaces from the beginning of the 20th century it is clear that we can do that by the ways chronological examination of sketches. The major difference between historic models and the typefaces under the name of Neo-Secession is in the layout, which is being rendered on either the upper or the lower writing horizontal line. Such a principle is not a product that has already been seen and borrowed from the earlier Secession typefaces. It is a step forward in finding a building block of the glyphs through which we are also reaching a harmony.

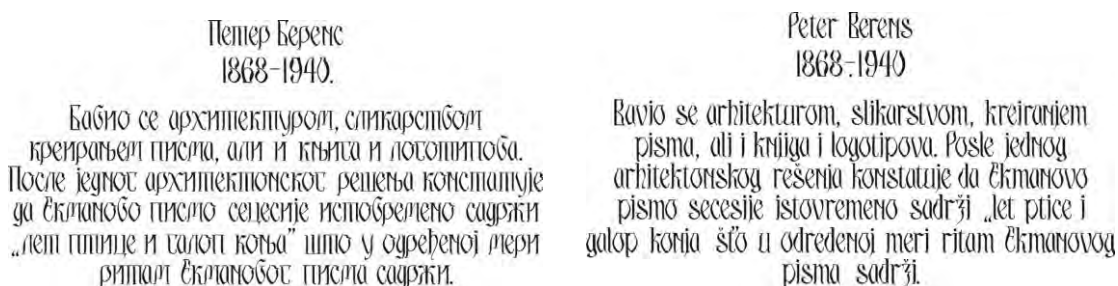


Figure 13. Text in Mega Zaharius Neo-Secession typeface

Observed individually, glyphs that belong to neo-secession seem satisfactory harmonious, especially in lowercase version. With this in mind, we laid out the text of a longer passage to observe findings stated herein.

Acknowledgements

This work was supported by the Serbian Ministry of Science and Technological Development, Grant No.:35027 »The development of software model for improvement of knowledge and production in graphic arts industry«

7. LITERATURE

- [1] Keedy, J. (1993). The rules of typography according to (crackpots) experts. Looking Closer 2, (Ed.) Michael Beirut, Pages (27–31), Allworth Press., ISBN 1880559560, New York, 1997 (Originally published in Eye, Vol 3, No. 11, November 1993)
- [2] Zelman, S. (2000). Looking into Space, Graphic Design and Reading, (Ed.) Gunnar Swanson, Pages (51–59), Allworth Press., ISBN 1581150636, California
- [3] Nedeljkovic, S (2009) PhD thesis: Tipografije ćirilčnih baroknih pisama transponovane u savremenu tipografsku formu, Faculty of Technical Sciences, Department of Graphic Engineering and Design, (august 2009)
- [4] Kapr, A. (1971). Schriftkunst, Veb Verlag der Kunst, LSV 8102 Best.-Nr. 500 132 2. DDR 60 M, Dresden.
- [5] Blackwell, L. (1992). Twentieth-CenturyType, ISBN: 978-0847815968, Rizzoli New York.
- [6] Nedeljković, S. (2005). Pismo i tipografija, ISBN: 86 85211 60 3, FTN Novi Sad
- [7] Luc Devroye (2012) Otto Weisert [online] Available from <http://luc.devroye.org/fonts-25066.html> [Accessed 9th August 2012.]

COMPARISON OF PROCESSING WORDS PRESENTED AT VARIOUS POSITIONS ON DISPLAY

Nace Pušnik¹, Klementina Možina¹, Anja Podlesek²

¹Faculty of Natural Science and Engineering, University of Ljubljana, Ljubljana

²Faculty of Arts, University of Ljubljana, Ljubljana

Corresponding author: Nace Pušnik
e-mail: nace.pusnik@ntf.uni-lj.si

1. ABSTRACT

Television production of broadcasts is developing. Graphic design is mainly based on previous (successful) broadcasts. In many cases, this is the correct procedure, but it can lead to the loss of design diversity. Inverse colour combination is an aspect that should be integrated into television design, as darker colours for backgrounds make lighter colours of typeface more visible and for this reason easier to read and remember. In the present study, we examined if the positioning of the text on a display is also important. Various meaningful and meaningless three- and five-letter words were set in the Bank Gothic typeface. Words were presented at four different positions on the television screen (in four corners of the screen) for a short time, with the presentation intervals ranging from 240 to 360 ms. To compare various technologies that are available in the market, we also varied picture size to assess the contribution of display size on the speed of word processing. Results showed that the left side of the television display was more convenient for users, regardless of upper or lower position. However, variations between upper and lower position were obtained for the right side of the display. When placed to the left side of the display, use of three- and five-letter meaningful and meaningless words did not affect visibility or legibility and recognition of words. We conclude that placing titles to the left side may lead to better title intelligibility.

Key words: broadcasting, legibility, duration, position, display.

2. INTRODUCTION

Broadcasts, which are daily presented on television displays, use generally accepted colour combinations that are more or less appropriate [1–3]. The duration of titles is based on an unofficial rule that the title should be broadcasted statically for 5 seconds. We made a comparison of five different television broadcasts by the Slovenian national television station that mainly cover the area of news channels. Every time, titles were statically broadcasted for 5 seconds, so according to this data, we predict that the 5 second interval is long enough for the user to read and comprehend written words. Commonly, prior to that interval another 2 seconds are reserved for fading-in of the broadcasted text, and after that interval, 2 seconds are reserved for fading the text out. Texts may appear in various places on the screen, but usually they appear in one of the four corners (lower left, lower right, upper left, or upper right) for the central area with important visual information to remain included as much as possible [4, 5].

In general, there are two aspects that should be distinguished: text legibility and readability [6].

Typefaces that have serifs are more readable and consequently more appropriate for books. Serifs lead us from one to another letter, and this is the reason for faster reading. On the other hand, legible typefaces are useful for short texts, for example traffic information, sales discounts, commercial purpose and titles on television screens. The sign should be observed, read and understood as quickly as possible [7]. Both concepts are very important, but when exploring the properties of texts to be presented on the display, legibility is more important [8, 9]. For use on displays (i.e. television, computer, mobile), legible typefaces have the following features: greater x-height, distinctive character features (counter shape) and sans serif style [10, 11].

At present, the use of mobile displays such as laptops, iPads or telephone displays is increasing [12]. Due to the smaller visual area covered by such screens, it is becoming more and more important that the presentation of visual information on the screen is optimal for quick and efficient processing by the observers [13]. This also relates to text such as titles, names and social functions of the speakers, etc., that the editor wishes to be detected and processed

quickly without errors [14, 15]. Various stimuli may attract attention when they suddenly appear in the visual area, but paying attention to many details in a different visual area may leave the stimulus unnoticed [16]. Stimuli that attract attention may have properties that are processed pre-attentively, such as a different colour, size, motion, etc. [16]. Some studies have shown an anisotropy of visual field [17] that might affect the processing of the text on the display. However, the letter case in which the text should be presented on the display in order to be processed efficiently has not been studied extensively.

The aim of our study was to compare various positions of titles and the efficiency of processing them on a small and big picture (in the corners of the screen) to see if some guidelines for the position of the text on the display during broadcasting could be developed.

3. METHOD

Titles were presented on a computer display that was comparable to a television screen. Display dimensions were 1920 × 1080 pixels. Viewers were sitting in front of the display at a distance of 65 cm. According to the object size on the display, the angular sizes were 9.40° (small picture) and 23.00° (big picture). Visual angle for small and big objects was calculated on the basis of the equation [18] for calculating visual angle, which is the following:

$$V = 2 \arctan\left(\frac{S}{2D}\right) [^\circ] \quad (1)$$

S – size of object (picture)

D – distance from viewer to object

□

In the study, 20 observers participated. Their mean age was 35 years. They had normal or corrected-to-normal vision and reported no visual disorders. The viewers' task was to closely observe broadcasted video that consisted of a black background where white-letter words appeared. This presented the biggest contrast possible [1, 3].

We used a 4 (text positions, repeated measures) × 2 (word length, repeated measures) × 2 (display size, repeated measures) experimental design. The text was presented either in the lower left, lower right, upper left, or upper right corner of the visual display. The size of the central area on the display in which the video was presented varied between the groups. Participants were divided into two groups. One group started with three-letter words and continued with five-letter words, and for the other group the order was the opposite.

Viewers had to observe a white spot that was positioned in the middle of the display (regardless of small or big picture). Every time the title appeared in one of four corners, the viewer had to try to observe the word and remember it. The distance from the centre of the display to the centre of the title in each of the four corners was the same every time: for the small picture size the distance was 8 cm and for the big picture size it was 20 cm, regardless of three- or five-letter words.

In our experiment, we decided to use both meaningful and meaningless words to examine the contribution of word meaningfulness to processing speed and to compare the size of this effect to the size of effects of other studied variables. The decision to use a three- or a five-letter word was based on the length of presented words. The visual field of presented letters in various corners of screen was not too big and viewers could easily track the word when moving their gaze from the centre of the display to the corners on right and left side of the display. On average, the length of three-letter words was 1.5 cm and five-letter words 3.5 cm (for the small picture size). Lengths of words for the big picture size were 4.5 cm for three-letter words and 6.5 cm for five-letter words. The typeface sizes we used were 16 pixels (12 pt) for the small picture and 32 pixels (24 pt) for the big picture [19]. To enhance the variability of processing speed to study the effects of various variables, all words were written in Bank Gothic capital letters, which are less legible than lower-case letters when used on a screen [7, 10, 20].

To examine what time is needed for word recognition, we used the method of constant stimuli [21]. Words were presented on the screen for either 240, 280, 320, or 360 ms. No fading-in or fading-out effect was used. The text appeared suddenly on the display, remained presented for a certain amount of time and then suddenly disappeared. A black screen was presented for 500 ms, and then two words were presented on the screen, one being exactly the same as the target stimulus and another one differing from the target stimuli in one letter only. In case of meaningful words, we selected such words that the change in one letter resulted in another

meaningful word. Similarly, the change of a letter in each meaningless word resulted in a new meaningless word. The position of the word that was the same as the target was randomly varied between the first or second position in pair. In each pair, the participant had to read aloud the word which in his opinion was the same as the target stimulus, and the experimenter recorded if the answer was correct or not. For each experimental condition, we counted how many participants (out of 20) responded correctly.

4. RESULTS AND DISCUSSION

Comparisons were made between duration and position for each test. The first part of the study was for comparison of three-letter words in all four positions at small picture size. When comparing meaningful and meaningless words (small picture), there is a deviation of remembering the words, which were shown to persons, when titles were displayed for short times (240 and 280 ms) regardless of position (Table 1). With longer broadcasting time answers were more comparable. The difference between the meaningful and meaningless words was small. On average, at longer time intervals, meaningless words were recognized slightly better than the meaningful words. This is somewhat surprising, but the reason for this could perhaps be found in our attention. When words are not familiar, our alertness is higher (according to the results). When observing the left upper position, the deviation between meaningful and meaningless words was the smallest (Figure 1).

Table 1: Comparison of three-letter words (small picture)

	Lower left		Upper left		Lower right		Upper right	
	m-ful*	m-less*	m-ful*	m-less*	m-ful*	m-less*	m-ful*	m-less*
240	9	14	18	18	14	16	11	16
280	12	20	19	19	17	12	15	20
320	20	17	19	20	20	19	20	20
360	19	19	20	20	15	19	20	20
\bar{x}	15.00	17.50	19.00	19.25	16.50	16.50	16.50	19.00

* m-ful (meaningful), m-less (meaningless)

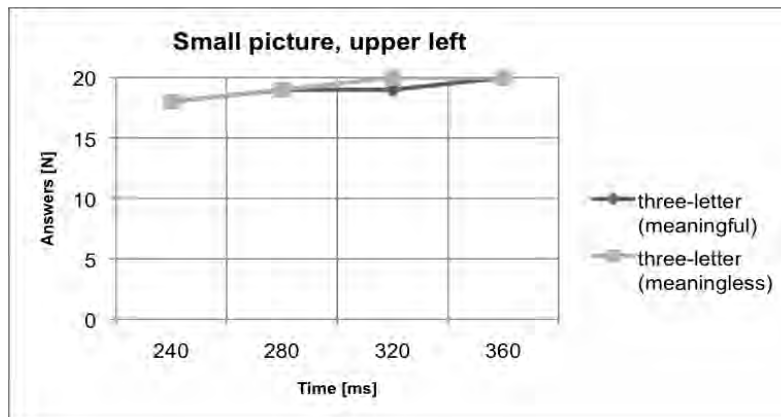


Figure 1: Comparison of upper left position for three-letter words (small picture).

Table 2: Comparison of five-letter words (small picture)

	Lower left		Upper left		Lower right		Upper right	
	m-ful*	m-less*	m-ful*	m-less*	m-ful*	m-less*	m-ful*	m-less*
240	15	13	16	17	13	18	20	10
280	15	19	18	17	20	19	18	19
320	18	18	17	19	20	19	20	19
360	20	19	20	19	20	19	20	17
\bar{x}	17.00	17.25	17.75	18.00	18.25	18.75	19.50	16.25

* m-ful (meaningful), m-less (meaningless)

The second comparison (Table 2) was between meaningful and meaningless five-letter words (small picture). In this case, the strongest difference between the two types of words could be found in cases where titles were presented for 240 ms (for all four positions). The differences among other broadcasting times were small. It turned out again that for the left upper position (Figure 2) the difference between meaningful and meaningless words was small (at a relatively high correctness of answers).

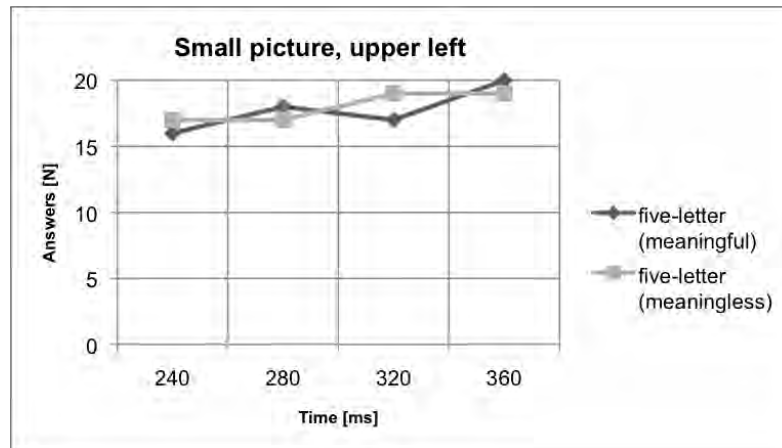


Figure 2: Comparison of upper left position for five-letter words (small picture).

With three-letter words broadcasted on a big picture (Table 3) the difference between the meaningful and meaningless words was noticeable for short broadcast times. At longer broadcasting times, the difference was smaller, with meaningless words having higher correctness in three of four cases. Again, the upper left position stands out (similar to first two compared examples), but this time the reason is correctness of answers for meaningful words (Figure 3).

Table 3: Comparison of three-letter words (big picture)

	Lower left		Upper left		Lower right		Upper right	
	m-ful*	m-less*	m-ful*	m-less*	m-ful*	m-less*	m-ful*	m-less*
240	14	17	17	13	9	15	14	11
280	14	20	18	16	17	15	14	20
320	20	20	18	20	19	18	19	19
360	19	19	20	19	15	20	19	19
\bar{x}	16.75	19.00	18.25	17.00	15.00	17.00	16.50	17.25

* m-ful (meaningful), m-less (meaningless)

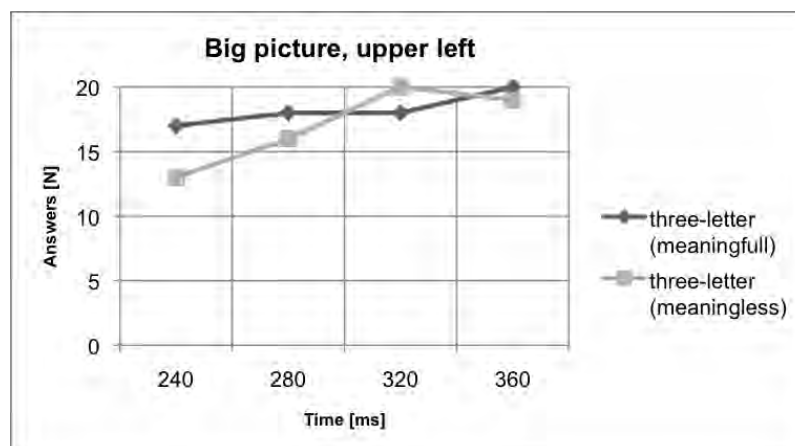


Figure 3: Comparison of upper left position for three-letter words (big picture).

In five-letter words (Table 4), the trend of correct answers rises with longer broadcasting times. The difference between the meaningless and meaningful words can be noticed for the lower-left position. If we take a closer look at the upper left position, the results on average are not the highest but are the same (meaningful and meaningless words).

Table 4: Comparison of five-letter words (big picture)

	Lower left		Upper left		Lower right		Upper right	
	m-ful*	m-less*	m-ful*	m-less*	m-ful*	m-less*	m-ful*	m-less*
240	19	17	12	15	15	11	17	14
280	12	15	18	16	20	19	19	20
320	20	16	19	20	19	19	20	19
360	20	19	19	17	20	18	19	20
\bar{x}	17.75	16.75	17.00	17.00	18.50	19.25	18.75	18.25

Figure 4 shows the movement of curves for meaningful and meaningless words. The curve for meaningful words rises with longer display time, while the curve for meaningless words is unstable.

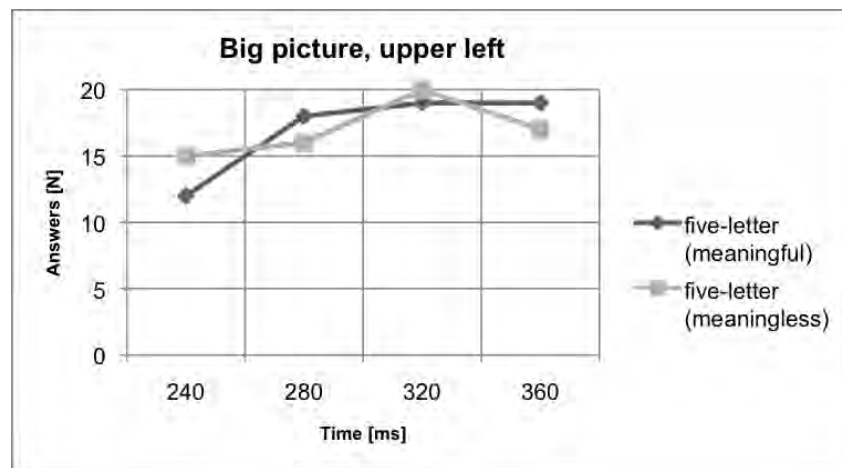


Figure 4: Comparison of upper left position for five-letter words (big picture).

5. CONCLUSIONS

The study shows that the left side of the display is on average better accepted when placing titles there. On average, recognition is better when viewers have to decide what was written on the display in the lower left or upper left position. The reason for this may be the simple fact that we are used to reading from left to right (e.g. in books) and moving our attention to the left side of the screen fast may be more efficient than moving it to the right side of the screen. Another reason may also be the established practice of putting titles at the left bottom position of the television display. However, at this point we have to stress that the text presented at the lower left position was not recognized as well as the one presented at the upper left position. The results show high correctness of answers when texts were put in the upper left. Another issue for viewers was broadcasting time. When titles were on the screen for 240 and 280 ms, viewers were really not sure what they read (based on the reactions of test subjects during the test and also the lower accuracy of their responses). Thus in many cases they were just guessing. At shorter times of stimulus presentation the recognition was slightly above chance, but for longer times (320 and 360 ms) the recognition was already close to perfect. It would probably be even higher if lower case letters were used instead of capital letters, as there is a big differentiation between letter shapes that affect our memory [22]. To sum up, our results show that the left side of the display is more appropriate for title position and that display time, if shorter than 320 ms, is not appropriate for a one-word title.

6. LITERATURE

- [1] Götz, V.: "Color & type for the screen", Crans, RotoVision, 1998.
- [2] Možina, K.: "Barva v tipografiji", Interdisciplinarnost barve, Maribor: Društvo koloristov Slovenije, pp. 341–364, 2001.
- [3] Baetens, J., "Colour as visual signifier in screen typography: less means more", Visual Studies, Vol. 23, No. 3, pp. 267–274, 2008.
- [4] Dyson, M. C.: "How physical text layout affects reading from screen", Behaviour & Information Technology, Vol. 23, No. 6, pp. 377–393, 2004.
- [5] Wheildon, C.: "Type & Layout", How typography and design can get your message across – or get in the way, Berkeley, Strathmoor Press, 2005.
- [6] Možina, K., "Mikrotipografija", Ljubljana, Faculty of Natural Science and Engineering, Department of Textiles, 2009.
- [7] Josephson, S.: "Keeping your readers' eyes on the screen: An eyetracking study comparing sans serif and serif typefaces", Visual Communication Quarterly, Vol. 15, No. 1, pp. 67–79, 2008.
- [8] Franz, L., "Is the Font Easy to Read? Anatomy and Legibility", 2010, [cited, 16. 4. 2012], http://www.typographicwebdesign.com/pdf/legibility_twd.pdf.
- [9] Pušnik, N., Možina, K.: "TV programme typeface legibility", Proceedings of 13th International conference of printing, design and graphic communications Blaž Baromić, pp. 145–149, 2009.
- [10] Reynolds, L.: "Legibility of type", Baseline, International Typographic Journal, Vol. 10, No. 26, pp. 26–29, 1988.
- [11] Gaultney, V.: "Balancing Typeface Legibility and Economy: Practical Techniques for the Type Designer", research essay, University of Reading, Reading, pp. 1–9, 2001.
- [12] Oyama, H., Shiramatsu, N.: "Smaller and bigger displays", Displays, Vol. 23, pp. 31–39, 2002.
- [13] Dyson, M. C.: "How physical text layout affects reading from screen", Behaviour & Information Technology, Vol. 23, No. 6, pp. 377–393, 2004.
- [14] Wheildon, C.: "Type & Layout, How typography and design can get your message across – or get in the way", Berkeley, Strathmoor Press, 2005.
- [15] Dyson, M. C.: "How do we read text on screen", Lawrence Erlbaum Associates, Vol. 115, No. 3, pp. 279–306, 2005.
- [16] Sternberg, R. J., "Cognitive Psychology", International student edition, 5th edition, Belmont (CA): Wadsworth, pp. 74–175, 2008.
- [17] Luccio, R., Caporusso, G., "The effect of the context on the anisotropy of the visual field", Review of Psychology, Vol. 17, No. 1, pp. 7–11, 2010.
- [18] Legge, G. E., Bigelow, C. A., "Does print size matter for reading? A review of findings from vision science and typography", Journal of Vision, Vol. 11, No. 5, pp. 1–22, 2011.
- [19] Reed, R.: "Reeddesign", 2012, [cited, 16. 5. 2012], <http://reeddesign.co.uk/test/points-pixels.html>.
- [20] Tinker, M., A.: "Bases of effective reading". Minneapolis, University of Minnesota Press, 1996.
- [21] Podlesek, A., Brenk, K.: "Osnove psihološkega merjenja: psihofizikalna metodologija", Ljubljana, Znanstvena založba Filozofske fakultete, pp. 40–61, 2009.
- [22] Arditi, A., CHO, J.: "Letter case and text legibility in normal and low vision", Vision Res, Vol. 47, No. 19, pp. 2499–2505, 2007.

COMMUNICATION THROUGH DESIGN: TRANSFER OF IDEAS - CREATION OF CONTEXT

Radoš Radivojević, Sonja Pejić
Faculty of Technical Sciences, Novi Sad

Corresponding author: Radoš Radivojević
e-mail: rados@uns.ac.rs

ABSTRACT

In order for something to be understood it does not have to be said. An image that provides information on surroundings, which is simultaneously an idea being realized and an idea that is going to become materialized, is just enough. Coding of ideas, information and attitudes by using commonly accepted patterns, styles and models that are interesting enough to draw attention, represents new form of communication in the era of virtual society. Design is a medium through which an idea or object is sent, but it is also a medium which becomes the message. This paper problematizes the possibility of a successful transfer of ideas by means of design, as well as the limits of perception of visual contents. Since design is one of the factors that affects the shape of social reality and contexts, it raises the question of whether reality created by design is a real manifestation of artist's idea or it distorts the initial ideas of its creator when in contact with socio-cultural factors of society.

Key words: *design, medium, message, virtual society.*

Art is and it should be a part of everyday life. Different manifestations of art tell us about the lives we live and offer the possibility of seeing the nuances in our experiences, feelings. We experience the years that will not be a part of us, either because those years are the future or long gone centuries. Art shapes our reality by imposing latently some patterns and forming paths and ways of life. Its liveliness retains the moment of spiritual harmony; it is a piece of work that one enjoys and feels awe at it. In the past, art was alienated from the world which was its muse, it had no contact with people and it did not seek any attention of those who brought it to life. In the capitalistic age of mass production, art is demystified and artists have a chance to express themselves in the field of entertainment and decoration, their work is instrumentalized in order to achieve efficient production. This is what makes art and design so related but at the same time so incompatible because our interaction with objects that are around us, the objects that we have created or found, the functions we assign to them and the way we understand their nature affects the decision to classify a piece of work as a design or artistic work. A work of art is self-sufficient, it exists regardless of the society needs, aspirations of clients; it is a static presentation of the way an artist experiences the world and it does not have instrumentalized dimension. Although there is no clear distinction between design and art, which is incorporated in the design, design cannot be free from utility, need for instrumentalization, dependence upon the clients, social community and socio-cultural conditions. Design is functional, it can be artistic but it is not art. John Thackara said that modern art is not interesting but the design is. It is real, capable of changing lives and solving problems, thus creating a materialized form of the way we live our lives (Thackara, 2005; Kendall, 2011). Pierre Bernard believes that a graphic designer has social responsibility which is based on the desire to participate in the creation of a better world (v. Bernard, 1997). Design represents an aesthetic intervention in the world achieved by visual forming and materialization of one's aesthetic experience of the world. In contrast to art which has the primary goal of expressing one's emotional experience of the world, the primary goal of design is to form the world according to one's emotional experience. Just as science explains the world and technology changes it, so does art express emotional experience of the world and design changes it from an aesthetic point of view. In declining design's artistic value as the domination of form over content it is overseen that the domination of design in modern society is not only the expression of market instrumentation of art but also the need of the people who live in the modern society and are free from material and emotional misery of a traditional society, who want to turn art into their real life and their life into art and an emotionally exciting, free and fulfilled artistic experience of the world. The situation is often not what it seems to be, it is not the designers who bring novelties into this world and improve it, but the demands they respond to and which force them to impose standardized patterns through

their work. Design decisions are often the cause of many problematic situations in the world. "Design decisions shape the processes behind the products we use, the materials and energy required to make them, the ways we operate them on a daily basis and what happens to them when we no longer need them" (Thackara, 2005: 1). If we were the ones who designed the way that led us to the problematic situations we are facing, then it means that we can also design the way to overcome them.

Modern society is focused and depends on the technology. In XXI century innovation means implementation of technology in a design solution, and technology always gives promises about future success and advancement. The problem of implementation of new technologies is the lack of ability to foresee the consequences of their use. In the age of technological innovations designer's awareness is necessary in order to make the right design decisions and, according to John Tachara, it means that prior to making a design decision we should consider natural, industrial and cultural systems that make the context within which designing action is taken; we should treat the contents as something that is worked on and not only as something that is to be sold; place, time and cultural differences should be considered as positive values and not obstacles. Skepticism about technology does not imply the rejection of technology but only the awareness of its influence on individuals, groups, institutions and organizations and their mutual interaction. Interdependence of design and technology gave birth to a wide scope of possibilities and opportunities for the design to change the socio-cultural context and to remain authentic, variable, creative answer to social demands when compared to other forms of communication mediated by technology. With respect to advertizing, which is a form of visual communication where the possibility of creative expression and innovative development is lost and which tends to be centralized, international and generalized, graphic design continues to create and shape itself in an autonomous and different way (v. Bernard, 1997). The ability to communicate clearly is a universal characteristic of design, but successful communications between clients and designers, designers and viewers and consumers of the design depend on the type of design and the function it has to fulfill in the society.

We interact with people every day and we will continue to share and create sociability with them, a feeling we instinctively have, but which is actuated only if there is the possibility of a feedback, that is, the possibility of communication accompanied by reflection. Our comprehension of the world is clearly marked by all types of communication we have in relationships, that is, a network of relationships with people which can be weak, strong, responsive, unresponsive, temporary or permanent. This does not mean that every interaction changes it entirely, but some surface, and sometimes even deep marks of interaction are left. In modern times, direct contact between people is not the only means of communication and is often replaced by the industrialized communication via mass media. This type of communication makes the understanding and acceptance of ideas and concepts easier, but it would not be so efficient if coding of information and ideas was not previously done by using different patterns and models that were both understandable and interesting to large number of people. Still, interaction that a man is capable of is not only with people but with material things that a man created himself and the symbols he incorporated in his work, thus establishing indirect communication with people and direct communication of his design, "an inanimate being", with human actors. Therefore, design represents a complex activity whose results infiltrate in every sphere of the society because most of the objects, spaces, and products are created esthetically and symbolically by large number of designers. By entering the commodity market the design is no longer a purpose for itself, it is not just a realized idea of an artist; it gains double purpose: design is a medium which is the message. "On the one hand, a medium (meaning the design, prim. aut. Radivojević and Pejić) presents something that is an instrument for one product, with respect to another product, to show clear purpose in the material culture" (Conway, 1991: 103), and it is a medium which develops our understanding of an object, book, events, etc. The aim of a design is to consolidate the form and meaning of a product into one whole. The visuals are essential part of a product image which can add more value even to some less qualitative contents. At present times, form is more important than the contents and quality. The name has become the criterion of quality and not only of good design. Conversation made between the design and social actors for whom the design was made is sometimes accidental, but often intentional. A good design is characterized by its intentionality and ability to draw attention, to communicate and to convince. Utility is not the only virtue a design has, even though it may be one of the most obvious aspects of a designer's work. The objective is to send the message clearly, directly, and without delay, but a work of design also aims to fascinate. Design sensationalism alone is not enough to fulfill the communicational

function, but it is a precondition for this function to be fulfilled. Under the circumstances of changed cultural-historical situations, when design can no longer be understood from cultural aspect, it continues to fascinate with its simplicity, innovativeness, clarity and refinement.

Visual language of design has become an instrument for presenting ideas and affecting our everyday life, but at the same time, it has become an instrument for manipulation because " [if] we think of communication as a characteristic (...) of the design, than we should be aware that it is a social rather than a technical category" (Conway, 1991: 103). Interaction with individuals or groups through art, in our case through the design, gives not only the opportunity to send ideas and influence the society, but also a path where the process of reflexivity will take place. In designing, reflection means reconsideration of some ideas and experiences based on the information collected either from individuals or groups who were directly or indirectly related to the design and who experienced it in a certain way.

The shaping function of design is primarily marked by two-way communication between the designer and user, and after the design is "consumed" the designer is no longer present as an important figure and the communication is established between the materialized idea and the consumer. Successful communication of a design depends on the type of design which can, according to the time criterion, be: graphic design characterized by continuity, and ephemeral graphic design; and according to the space criterion: graphic design integrated with physical structure or identity, and independent graphic design characterized by temporariness (v. Bernard, 1997). From the aspect of society, the most influential design is the integrated design whose message (form and contents) is in accordance with the dominant moral and esthetic values of the society. This is why this type of design is long-lasting and plays major part in the ideological integration. When compared to the integrated, long-lasting design, the independent short-term design sends a message related to the specific situation. It attracts the attention, but with the end of the situation it was made for, the design disappears. The idea remains in spite of the disappearance of design which goal was to send the idea to the viewers and consumers. Once the design is made its message will remain, providing the design has the power to deliver the message while the situation it has been created for is still taking place. When the design is gone, there are still people who received the message and there are other designers who will use the realized, disappearing idea as the base for their own future research and creative designing work. Thus, the death of a design work becomes the idea and material for new message and new change of the reality. If temporary design succeeded in fulfilling its function and influencing the interactive design users with audio-visual contents, then duration of a situation ceases to be adequate criterion of significance of a design. The clarity of a design, whether long-lasting or ephemeral design, will reduce the communication to the essential parts of the design which are universally understandable and permanent.

In the process of communication through a design there are two sides which act as message transmitters and those are client and graphic designer. A client is a person who belongs to one social class and for him a design is an instrument for solving the problem of competitiveness on the market, and for a designer it is an idea developed from a dominant ideology. It is obvious that the roles of designer and client are in conflict, but consensus can be achieved. Graphic design has to be recognized by its technical, artistic and intellectual dimensions, that is, clients have to accept esthetic and intellectual qualities of the design and a designer has to be aware of and has to accept the client's ideology during the creative process. Finally, a message that graphic designer sends through his work has to be adjusted to social, cultural, economic and global context before it is transmitted. The designer's work has to arise from social situations – their specific dynamics and elements of humane dimensions since culture is the base for all decisions made in the design (v. Young, 2008). Bernard believes that the use of small communication units can enable the development of creative works which will visually regenerate and develop the wealth of a society (Bernard, 1997). The interaction between people and objects is neither one-way nor simple interaction since all objects or products of designer's work contain information which cannot be revealed by simply watching it or using it only once. Objects can communicate with people while designers are mediators who enable us to develop and improvise the dialogue. Since the communication through design is possible it means that the design criticism is also possible. The criticism offers the design interpretation, contextualization, abstraction and questioning in order to create the opportunities for designers to improve everyday life and conduct research on the ways to fulfill their roles as people who change and shape the world (v. Bardzell et al., 2010). There is also a possibility for designers to explain social and cultural complexity of their designing work and to explain that the product of

artistic work is not just a commodity in modern society but an inanimate factor which changes the world and space-time frameworks within which people communicate with each other. The main categories of criticism: creator (author, designer, composer, painter), artifact (text, movie, product, poster), user (reader, observer, user) and social context (community, sculpture, job) are the categories used for the explanation of interaction. All these categories should not be observed separately because their clear connection provides us with an explanation of interaction. For example, a text does not exist as a cultural material until it is read by a reader (text is actualized through reading) (v. Bardzell, 2009). The communication through design is no different because the interaction between the observers and users of design artifacts confirms their importance and significance and stimulates innovations.

Clarisse de Souza believes that the communication between a person and technology can be considered as a communication with technology. However, technology represents a medium which enables the communication between the design and a person. Quality of the design becomes the criterion for the product quality or something that product should represent. The freedom that designers implement signs and signals into artifacts is their freedom to perceive the world. Perception of design is not gained by recognizing individual parts, since "[w]e never see figures alone (...), only dynamic "figure-ground" relationships" (Behres, 1998:300). A designer should not develop his own idea without taking into account the users' mental models and the ability of people to perceive images and attach significance to them. A designer has a task to create a general image of a product which will evoke the same feeling in people of different social classes, with different education, different physical and mental abilities and different perception. This image will also attract people to buy or use the product, witness an event or choose, for example, certain law office just because they like the business card more. One should understand mass psychology when the communication is established through artifacts and designs. The design should be adjusted to the society if larger mass distribution of the product that design represents is to be achieved and the receptor of a message is to be started by the ideas which are part of the design. The experience of design from esthetic and emotional aspects depends greatly on the physiology of human body, especially on the brain functions and eye condition. Although eyesight is very important for the perception of the design, senses of hearing and touch should not be neglected. Brain controls all our thoughts, emotions, experience; its functions enable all coded impulses from the body and surroundings to be decoded. We never perceive the surroundings as individual images, instead we develop certain "movie in the brain", which is a "metaphor for the integrated and unified composite of diverse sensory images which constitute the multimedia show which we call mind" (Damasio, 2000: 459). During the perception of the design, "physiology comes before ideology and communication is secondary to seduction" (Kendall and Hannan, 2011). The design is not perceived only from the aspect of physiology since the way we see things around us depends on the knowledge and experience that we have gained so far in our lives. Without that knowledge design would not make sense because clarity and reduction of its contents could not be connected with social, cultural, economic and political events. It enables the associative function of the design to be fulfilled since the design has to be and it already is a society presented by symbols, words, colors and textures. Instrumental and symbolic functions of the design are rarely separated due to the fact that semiocosmos¹ and sociocosmos² cannot be presented as two separate units. The products of the design are mediators in the communication between an individual (user, designer) and technocosmos, biocosmos, sociocosmos and semiocosmos. Design can solve possible problems but it requires technical-technological knowledge of the society. Every successful design is necessarily followed by new technologies, but a design user, as an actor who is placed into a certain context, that is, a symbolically rich identity who participates in social context, is often unable to perceive the design as a unit or at least in the way the artist imagined it. Every design is made of symbols and signs and every sign has its connotation and denotation. Sign denotation represents its general concept and sign connotation represents ideas and associations which can be provoked in the interpreters through signs. When design comes into contact with people and society as a whole, it is interpreted in different ways and its meaning is then changed. If a design with universal meaning causes the same emotional reaction in every individual, regardless of his

¹ Semiocosmos is the symbolic world, world of culture.

² Sociocosmos is the world of human geography created from the unit of human collectivity.

social background, then it leaves the deepest marks on the society. However, the universality of human experience is just a fiction. Considering the fact that the relationship between reality and fiction has no longer been balanced, the age of new technologies enables its replacement. "We live in a world ruled by fictions of every kind—mass merchandising, advertising, politics conducted as a branch of advertising, the preempting of any original imaginative response to experience by the television. We live inside an enormous novel. For the writer in particular it is less and less necessary to invent the fictional content of his novel. The fiction is already there. The writer's task is to invent the reality." (Balard, 2011: 5-6). The ideas of James Balard, a postmodern writer, are presented in literature but they can easily be applied to the design as well. Barriers of modernity are difficult to overcome, but design as well as literature offer numerous possibilities and imaginative solutions, that is, according to Marshall McLuhan "we live mythically and integrally, but we continue to think in the old, fragmented space and time patterns of the pre-electric age" (McLuhan, 2008 :11). The McLuhan's thesis, if transferred to the domain of design, implies that technological innovations create numerous channels and space for communication and that there are possibilities to communicate ideas, but our social "underdevelopment", moral and ethic incorrectness, and lack of responsibility eliminate the possibility to develop, perceive and implement the design. Past seems to be grasped tightly, and hands seem to be petrified with wonder, the wonder of innovation. New media and new ways of communication, as the extensions of man, have caused inexplicable mortification in individuals and society (v. MacLuhan, 2008). There was no reaction to the design, debates continued but there are still debates about war, nationalism, political correctness, economic development and instrumentalization of everything and everyone in order for constant and balanced rate of progress to be achieved in the future. Design is present and able to shape its own world, it is a language spoken by small number of people but understood by many. Postmodernism, if it can exist as reality, represents *"the stage where the commodity is immediately produced as a sign, as a value/sign, and where signs (culture) are produced as commodities"* (Baudriillard, 2001:8). Mystery of creative processes becomes simple procedure for the production of commodities and design is used for trade and not for enjoyment. The main task for designers is to develop strategic production of the design which represents the commodity and has the role to sell the commodity on the global "market of works of art". Designer, as a person, is needed only to understand the indistinct structures of society, to understand how it functions and to be an eminent psychologist of the society who is able to recognize the needs and aspirations of people.

Design alone is no longer valuable. It gives us the power to deconstruct the society and shape our surroundings as biological and social beings, thus the design becomes the decisive factor which remains invisible. Lack of recognition of the design does not imply mental rejection of the design because it is created in such a way to stimulate the creativity and intuition of a user and to make the user think about something without being influenced by the design. Postmodernism gives freedom to the design; form does not have to comply with the function. Functional design continues to be used since the main reasons for its survival are its functions. However, if numerous functions have to be fulfilled by something it does not mean that it has to be boring. The reason of existence of colors, textures, models, symbols and signs is not only to make us become interested emotionally but to show the instrumental function of the design as well.

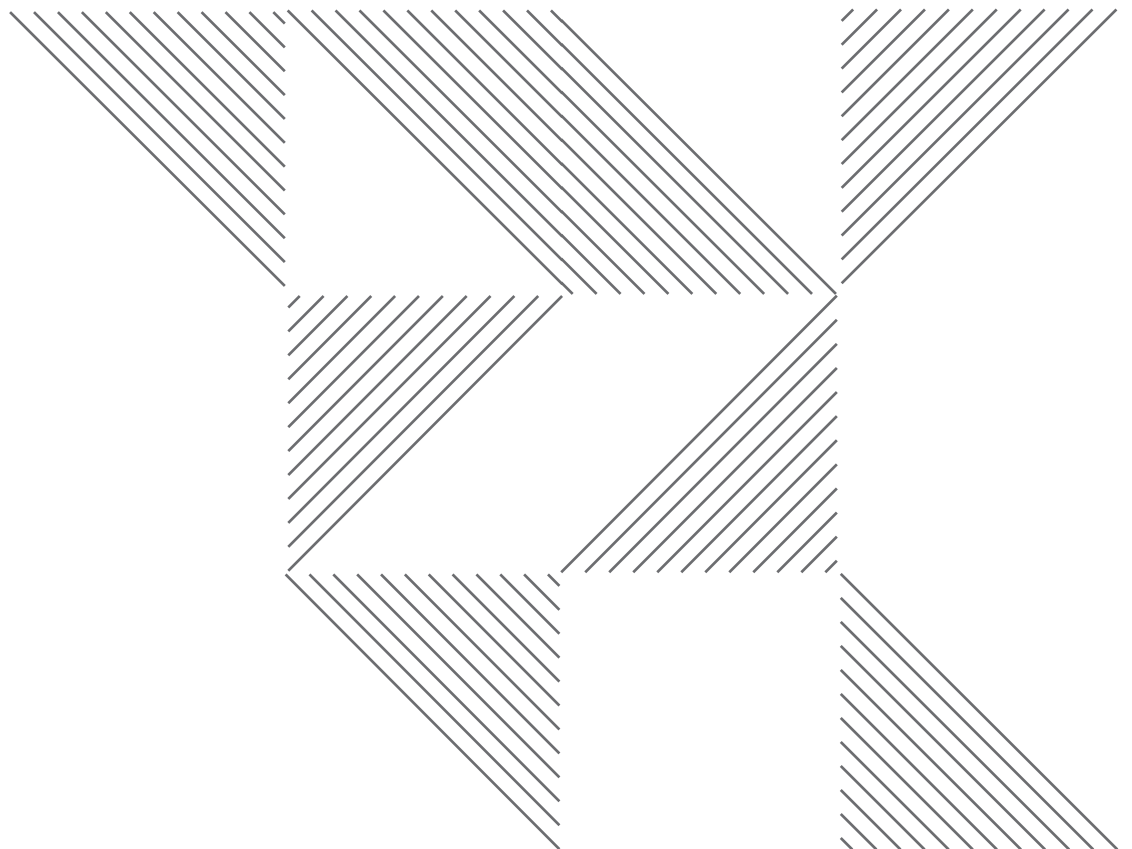
With regard to the development of technology, design limits cannot be imagined. However, the society provides the framework for the design by imposing the requirements so that design can meet its needs for utility. This means that the design has to be both functional and esthetic. Design is a fundamental and communicational process which is dependent upon the context regardless of the fact that the potential of new technologies can enable direct and independent communication with users, that is, contextual independence can be possible (Brown and Duguid, 1994). Decontextualized purity can cause numerous practical problems, and that is why the design requires a certain contextual support. '[F]undamental connection and inseparability of the object and its context' enable their understanding, application and fulfillment of a socially recognized role of the design (Brown and Duguid, 1994: 7). Although the design has some contextual limits, it has to make contributions so that better and sustainable society can be created by suggesting solutions which will have influence on the long term development and which will improve the quality of life.

LITERATURE

- [1] Balard, Dž. G. (2011). *Sudar*. Beograd: Čarobna knjiga.
- [2] Bardzell, J. (2009). Interaction criticism and aesthetics. *Proc. CHI'09*. New York: ACM Press, pp. 2357-2366.
- [3] Bardzell, J., J. Bolter and J. Löwgren (2010). Interaction criticism. *Interactions* XVII.2, March/Apr.
- [4] Baudriillard, J. (2001). *Simulacija i zbilja*. Zagreb: Naklada Jesenski i Turk.
- [5] Behrens, R. (1998). Art, design and gestalt theory. *Leonardo* Vol. 31, No. 4: 299-303.
- [6] Bernard, P. (1997). The social role of graphic designer. In. Marsack, R. (ed.) *Essays on Design 1: AGI's Designers of Influence*. London: Booth-Clibborn Editions.
- [7] Brown, J.S. and P. Duguid (1994). Borderline issues: Social and material aspects of design. *Human-Computer Interaction*, Vol.9: 3-36.
- [8] Conway, H. (ed.) (1991). *Design History*. London: Routledge.
- [9] Damasio, A. (2000). The fabric of the mind: A neurobiological perspective. *Progress in Brain Research* 126: 457-466.
- [10] Findeli, A. (1994). Ethics, aesthetics and design. *Design Issues* Vol. 10, No.2: 49-68.
- [11] Kendall, S. and V. Kannan (2011). Aesthetics and the ideology of design. 15. Oct 2012. <<http://www.stuartkendall.com/?p=46>>
- [12] Kendall, S. (2011). The dialectics of Art and Design. 13. Oct 2012. <http://www.stuartkendall.com/?cat=3>
- [13] MacLuhan, M. (2008). *Razumijevanje medija*. Zagreb: Golden Marketing.
- [14] Quayle, M. and D. Paterson (1989). Techniques for encouraging reflection in design. *Journal of Architectural education* Vol. 42, No. 2: 30-42.
- [15] Thackara, J. (2005). *In the Bubble: Designing in a Complex World*. London: The MIT Press.
- [16] Tully, R. (2012). Narrative imagination: a design imperative. *Irish Journal of Academic Practice* Vol.1, Issue 1: 1-21.
- [17] Young, P. (2008). The culture based model: A framework for designers and visual ID languages. *Educational Technology & Society* 11(2): 107-118.
- [18] www.jnd.org/dn.mss/design_as_communicat.html
- [19] www.doorsofperception.com



Packaging and Enviromental Protection



ELECTROCOAGULATION/ELECTROFLOTATION TREATMENT OF OFFSET PRINTING DEVELOPERS

Savka Adamović¹, Ljiljana Rajić², Miljana Prica¹, Rastko Milošević¹,
Irma Puškarević¹, Vladimir Zorić¹

¹Faculty of Technical Sciences, Graphic Engineering and Design, Novi Sad

²Faculty of Sciences, Department of Chemistry,
Biochemistry and Environmental protection, Novi Sad

Corresponding author: Savka Adamović
e-mail: adamovicsavka@uns.ac.rs

1. ABSTRACT

In this study we investigated the electrocoagulation/electroflotation as a purification treatment of fresh and waste offset printing developers. Electrochemical treatment was studied in a bipolar batch reactor with four plate aluminum electrodes at a constant distance of 0.5 cm. Electrocoagulation/electroflotation process was carried out at a current density of 2 mA cm⁻². Temperature, pH and electrical conductivity were measured before and after electrocoagulation/electroflotation treatment, while the content of organic substances in terms of UV₈₁₃ and turbidity was used to evaluate treatment efficiency. The results indicated electrocoagulation/electroflotation as reliable, safe and cost effective method that can be successfully applied to treating fresh and waste offset printing developers.

2. INTRODUCTION

The companies for reasons of secrecy do not reveal the full-scale chemical structure of the fresh offset printing developers produced, thus the composition of the outgoing wastewater solutions after photoplate development remains unknown. Furthermore, in the plate development process, the offset printing developer undergoes changes per se, as well as enrichment by the chemicals that are present on the plate surface, i.e. various organic binders, photosensitive compounds and dyes (Vengris, 2004). The waste offset printing developer needs to be suitably treated before being discharged into water and soil recipients.

Various treatment techniques and processes have been used to remove the pollutants from the contaminated liquid waste. Each treatment method has its advantages and disadvantages. Ion exchange, for example, while highly effective in removal of certain charged contaminants, requires resin regeneration or replacement at a high cost (Escobar, 2006). The costs of adsorption, ultrafiltration, reverse osmosis and ozonation exceed that of chemical coagulation. While chemical precipitation is a simple process, it does generate a high volume of sludge. When chemical coagulation is used to treat wastewater, the pollution may be caused by a chemical substance added at a high concentration. Excessive coagulant material can be avoided by electrocoagulation/electroflotation process (Merzouk, 2009). An alternative to the conventional coagulation process is electrocoagulation/electroflotation, which consists of the in situ generation of coagulants by electrodisolution of a sacrificial anode, usually of aluminum or iron. In both coagulation processes (conventional and electrochemical), aluminum or iron reagents are commonly used as coagulants (Akbal, 2010).

Electrocoagulation/electroflotation is not a new technology. In fact, the literature indicates that it has been regularly found over the last hundred years or so both in batch and continuous applications (Holt, 2005). It has been employed previously for the treatment of many types of wastewater with varying degrees of success (Parga, 2005). Electrocoagulation/electroflotation has been successfully used for the treatment of wastewaters such as electroplating wastewater, chemical mechanical polishing wastewater, textile wastewater, olive mill wastewater, laundry wastewater, tannery wastewater, pulp and paper mill industry wastewater, baker's yeast wastewater, slaughterhouse wastewater, potato chips manufacturing, restaurant wastewater and wastewater with phosphate, chromium (VI), arsenic or other heavy metals (Akbal, 2010; Can, 2010; Parga, 2005). Furthermore, the electrocoagulation/electroflotation systems can be effective in removing suspended solids, dissolve metals, tannin and dyes (Merzouk, 2009). On the other hand, the literature survey shows that the electrocoagulation/electroflotation

treatment has not yet been taken into consideration for the treatment of fresh and waste offset printing developers.

Electrochemical technique has attracted, in this case, a great deal of attention because of its versatility, safety, selectivity, amenability to automation, environmental compatibility and low operational and investment costs (Escobar, 2006; Mouedhen, 2008). The characteristics of the electrocoagulation/electroflotation process are simple equipment and easy operation, brief reactive retention period, decreased or negligible equipment for adding chemicals, and the decreased amount of sludge (Merzouk, 2009; Mouedhen, 2008).

The electrocoagulation/electroflotation process operates on the principle that makes the cations produced electrolytically from iron and/or aluminum anodes enhance the coagulation of contaminants from an aqueous medium. Electrophoretic motion tends to concentrate negatively charged particles in the region of the anode, and positively charged ions in the region of the cathode. The consumable, or sacrificial, metal anodes are used to continuously produce polyvalent metal cations in the vicinity of the anode. These cations neutralize the negative charge of the particles carried toward the anodes by electrophoretic motion, thereby facilitating coagulation. The production of polyvalent cations from the oxidation of the sacrificial anodes (Fe and Al) and the electrolysis gases (H_2 and O_2) work in combination to flocculate the coagulant materials. As mentioned earlier, gas bubbles produced by the electrolysis carry the pollutant to the top of the solution where it is concentrated, collected and removed. The removal mechanisms in electrocoagulation/electroflotation may involve oxidation, reduction, decomposition, deposition, coagulation, absorption, adsorption, precipitation and flotation (Chen, 2004; Parga, 2005).

In this study, the efficacy of decontamination of the fresh and waste offset printing developers by the electrocoagulation/electroflotation treatment has been investigated for the developer purification before its disposal into the environment. Relevant wastewater characteristics, such as content of organic substances in terms of UV_{813} and turbidity of pollutants, and process variables, such as temperature, pH, electrical conductivity and operating time, will be considered as relevant indicators in assessing the process performance in terms of removal efficiency.

3. METHODS

3.1. Experimental apparatus

A 250 cm³ glass was used as a batch reactor, or an electrocoagulation cell. Four plate aluminum electrodes with the same dimensions of 10 cm × 5 cm × 0.1 cm were used and placed vertically in the reactor. The total electrode area was 100 cm² and the distance between electrodes was 0.5 cm. The electrodes were connected at the bipolar parallel mode to a digital DC power supply (DF 1730LCD) equipped with potentiostatic or galvanostatic operational options.

The electrical conductivity of solutions was measured using a Cond 3210 conductimeter (Wissenschaftlich Technische Werkstätten, Germany). Turbidity was determined by HI 93703 microprocessor turbiditymeter (HANNA Instruments, Portugal) and pH was measured by using EC30 pH meter. The solid phase of samples was separated by centrifugation (Centrifuge Tehnica Železniki, Slovenia). The content of organic substances in terms of UV_{813} was determined by spectrophotometer (UV/VIS spectrophotometer UV-1800 SHIMADZU) at 813 nm.

3.2. Experimental procedure in batch mode

All experiments were performed at room temperature (25 °C). Before each experiment, the aluminum electrode surface was first mechanically polished with abrasive paper in order to ensure surface reproducibility, rinsed with distilled water, and dried prior to immersion in the electrolyte. The oxide and passive layers on the surfaces of aluminum were removed by dipping the electrodes for 10 min in a 5 M solution of hydrochloric acid.

In each experiment, 220 cm³ of the fresh and waste offset printing developers decanted into the electrocoagulation cell. The effective area of each electrode used for electrolysis was 40 cm². The electrodes were connected to a digital DC power supply with potentiostatic or galvanostatic operational options providing constant current density of 2 mA cm⁻². The total time duration of electrolysis was 60 minutes. 15 cm³ of electrolyte samples were taken at a certain operating

time (0, 5, 10, 20, 40 and 60 minutes). All collected samples were centrifuged for 10 minutes at 2000 rpm. Supernatant was then used for the analyses.

4. RESULTS AND DISCUSSION

The fresh and waste offset printing developers used in this research were taken from the printing facility in Novi Sad, Republic of Serbia. In the plate development process, fresh offset printing developers are dispensed in quantities of 100 cm³ per m² of plate.

Temperature, pH and electrical conductivity of fresh and waste offset printing developers were measured before and after the electrocoagulation/electroflotation (EC/EF) treatment (later on 60 minutes). The values of the parameters above are summarized in the Table 1.

Table 1: The parameters of offset printing developers before and after the EC/EF treatment

Offset printing developer	Parameter	Before EC/EF	After EC/EF
Fresh	t [°C]	25.4	25.9
	pH	12.44	12.49
	Electrical conductivity [mS/cm]	16.31	16.33
Waste	t [°C]	25.3	25.9
	pH	12.15	12.17
	Electrical conductivity [mS/cm]	16.27	16.28

The values of temperature, pH and electrical conductivity in Table 1 show that the EC/EF treatment does not lead to changes in these parameters. The OH⁻ ions produced at the cathode and H⁺ ions produced at anode maintain constant pH values during the EC/EF treatment. The electrical conductivity was controlled by adding solid sodium chloride, which prevented the passivation of the aluminum electrodes.

The electrochemical treatment was studied in a bipolar batch reactor with four plate aluminum electrodes at a constant distance of 0.5 cm. The EC/EF process was carried out at a current density of 2 mA cm⁻². The samples of electrolytes (fresh and waste offset printing developers) were sampled at a certain operating time during the EC/EF treatment. Relevant wastewater characteristics such as content of organic substances in terms of UV₈₁₃ and turbidity of fresh and waste offset printing developers are taken as assessment tools in the terms of removal efficiency of the EC/EF treatment. The values of turbidity, UV₈₁₃ and removal efficiency of electrolyte samples during the EC/EF treatment are summarized in the Table 2.

Table 2: The turbidity, UV₈₁₃ and removal efficiency of fresh and waste offset printing developers during the EC/EF treatment

Offset printing developer	Parameter	Operating time [min]						Removal efficiency [%]
		0	5	10	20	40	60	
Fresh	Turbidity [NTU]	183.4	13.0	9.2	5.8	1.6	0.4	99.8
	UV-VIS ₈₁₃	1.222	0.510	0.354	0.244	0.182	0.094	92.3
Waste	Turbidity [NTU]	934.2	548.0	251.4	156.7	112.4	74.2	92.1
	UV-VIS ₈₁₃	48.550	29.081	23.255	18.691	11.202	7.185	85.2

The obtained results of turbidity, content of organic substances in terms of UV₈₁₃ and removal efficiency during the EC/EF treatments of offset printing developers are presented in the Table 2. Removal efficiency of turbidity and content of organic substances for fresh offset printing developer ranged from 92.9 to 99.8% and from 58.3 to 92.3% respectively, whereas removal

efficiency of turbidity and content of organic substances ranged from 41.3 to 92.1% and from 40.1 to 85.2% respectively for waste offset printing developer.

The turbidity removal for fresh offset printing developer was 92.9% after 5 minutes of EC/EF. In case of turbidity removal in waste offset printing developer efficiencies was 83.2% after 20 minutes of EC/EF. At the end of the EC/EF treatment of waste offset printing developer, turbidity removal (92.1%) was the same as the turbidity of fresh developer after 5 minutes. Removal efficiency of UV_{813} for fresh and waste offset printing developers was achieved after 40 minutes (85.1%) and 60 minutes (85.2%) respectively. Different operating times for the removal of turbidity and content of organic substances are the consequences of contamination by chemicals that are present on the plate surface.

5. CONCLUSIONS

The results obtained in this study provide an opportunity for the application of electrocoagulation/electroflotation technology as a purification process of offset printing developers. The conclusion that the treatment of offset printing developers by electrocoagulation/electroflotation is effective, can be drawn based on the following:

- The application of the electrocoagulation/electroflotation treatment to fresh offset printing developer showed a removal turbidity of 99.8% and content of organic substances of 92.3% at a current density of 2 mA cm^{-2} and interelectrode distance of 0.5 cm.
- The application of the electrocoagulation/electroflotation treatment to waste offset printing developer showed a removal turbidity of 92.1% and content of organic substances of 85.2% at a current density of 2 mA cm^{-2} and interelectrode distance of 0.5 cm.
- The electrocoagulant produced by electrodisolution of a sacrificial aluminum anode showed high adsorption capacity.
- Based on the results obtained for the effective removal of turbidity and content of organic substances, electrocoagulation/electroflotation proves to be a very promising technology for removal of wide range of organic and inorganic pollutants, with emphasis on heavy metals from offset printing developers.

The electrocoagulation/electroflotation treatment has been investigated in this study predominantly to point out to the treatment's removal efficiency, and not so much with respect to its fundamental aspects. Electrocoagulation/electroflotation is still empirically optimized process that requires more fundamental studies to be conducted and fully exploited in case of the offset printing developers treatment.

Acknowledgements

The authors acknowledge the financial support of the Ministry of Education and Science of the Republic of Serbia (Project No. 34014) and Provincial Secretariat for Science and Technological Development (Project No. 114-451-1985).

6. LITERATURE

- [1] Akbal, F., Camcı, S.: "Comparison of electrocoagulation and chemical coagulation for heavy metal removal", *Chemical Engineering and Technology* 33 (10), 1655-1664, 2010.
- [2] Can, O.T., Bayramoglu, M.: "The effect of process conditions on the treatment of benzoquinone solution by electrocoagulation", *Journal of Hazardous Materials* 173 (1-3), 731-736, 2010.
- [3] Chen G.: "Electrochemical technologies in wastewater treatment", *Separation and Purification Technology* 38 (1), 11-41, 2004.
- [4] Escobar, C., Soto-Salazar, C., Tiral, M.I.: "Optimization of the electrocoagulation process for the removal of copper, lead and cadmium in natural waters and simulated wastewater", *Journal of Environmental Management* 81 (4), 384-391, 2006.
- [5] Holt, P.K., Barton, G.W., Mitchell, C.A.: "The future for electrocoagulation as a localised water treatment technology", *Chemosphere* 59 (3), 355-367, 2005.

- [6] Merzouk, B., Gourich, B., Sekki, A., Madani, K., Chibane, M.: "Removal turbidity and separation of heavy metals using electrocoagulation-electroflotation technique: A case study", *Journal of Hazardous Materials* 164 (1), 215-222, 2009.
- [7] Mouedhen, G., Feki, M., Wery, M.D.P., Ayedi, H.F.: "Behavior of aluminum electrodes in electrocoagulation process", *Journal of Hazardous Materials* 150 (1), 124-135, 2008.
- [8] Parga, J.R., Cocke, D.L., Valenzuela, J.L., Gomes, J.A., Kesmez, M., Irwin, G., Moreno, H., Weir, M.: "Arsenic removal via electrocoagulation from heavy metal contaminated groundwater in La Comarca Lagunera Mexico", *Journal of Hazardous Materials* 124 (1), 247-254, 2005.
- [9] Vengris, T., Binkiene, R., Butkiene, R., Nivinskiene, O., Melvydas, V., Manusadzianas, L.: "Microbiological degradation of a spent offset-printing developer", *Journal of Hazardous Materials* 113 (1-3), 181-187, 2004.

ASSESSING PRINT PRODUCTION PROCESS CAPABILITY

Diana Milčić, Davor Donevski, Mladen Šefer
Faculty of Graphic Arts, Zagreb

Corresponding author: Diana Milčić
e-mail: diana.milcic@grf.hr

1. ABSTRACT

Process capability refers to the proportion of units conforming to specification that a process is able to produce. In print production, process control standards specify aimed and tolerance values for specific process control parameters. However, producers and customers have to agree on the acceptable quality level (AQL), i.e. tolerated proportion of nonconforming units. In order to agree on the AQL, the producer has to know the capability of his process. In addition, process capability can be determined in a number of different ways, depending on how the data is collected and analyzed. The experiment presented in this paper shows how different ways of data analysis affect the assessed process capability. In order to avoid confusions and arguments between producers and customers, it is necessary to agree on the way of data analysis (determination of proportion of waste). This part is not covered by process control standards as they can only serve to determine whether a given unit conforms to them or not.

Key words: *print production, process capability, process control*

2. INTRODUCTION

Process control standards for print production define aimed values and tolerances for certain process control parameters. In addition to adjusting different processes so that they behave similarly, they are useful for producers and customers when they have to agree on which quality parameters are binding and what are their aimed and tolerance values. However, in practice, this can cause confusions and arguments between producers and customers if some produced units are found to be nonconforming to specifications. The reason for this is that both parties often neglect one very important quality measure, and that is the acceptable quality level (AQL). In addition to defining the quality parameters, their aimed and tolerance values, parties have to agree on the allowed fraction of nonconforming units, with respect to given tolerance. This allowed fraction of nonconforming units is called the acceptable quality level. When agreeing to a certain AQL, the producer has to know the fraction of nonconforming units that is being output from his process. The AQL should generally be higher than the fraction nonconforming being output from the process in order to protect the producer in cases of slightly higher variations or shifts in the process. If the producer's process isn't able to meet the quality requirements, i.e. outputs the fraction nonconforming higher than the AQL demanded by customer, then the job should be turned down to avoid damage caused by complaints. The measure of the fraction of units output from a process that meet the specification is referred to as process capability. It is expressed using different indexes. These measures provide the possibility to determine whether the process can meet the requirements and whether the finished lot is acceptable. However, printed sheets consist of a number of zones and data can be collected and analyzed in a number of different ways, resulting in different assessed process capabilities. This paper investigates these different ways of data collection and analysis and differences in their results on one offset printing process. Another important aspect is that process capability indexes suppose that the underlying process parameter distribution is normal. In this study, it was found that the observed process parameters were not normally distributed which is, in addition to data collection and analysis, a very important consideration.

3. METHODS

For the purpose of this study, the output of one offset printing process was analyzed. A regular print job in a small print shop was chosen in order to reflect the results achieved in this rather large market segment. The Heidelberg Speedmaster 74-2 press was used to print a circulation of 600 sheets of matte coated paper. A sample of 30 sheets, evenly distributed throughout the

circulation was taken for inspection. Cyan solid ink densities (SID) were measured on a control strip patches in five zones of 30 prints. The measurements were taken with an X-Rite i1Pro spectrophotometer. Measurement data was used to analyze process behavior in each of the five zones and altogether. FOGRA aimed and tolerance SID value recommendations were used. Fractions of nonconforming units and process capability indexes were calculated under the assumption that the underlying parameter distribution is normal. However, the histograms of data clearly showed that parameter distribution was not normal. Therefore, fractions of nonconforming units were also calculated from the data and compared to those calculated under the assumption of normal distribution.

4. RESULTS

As it can be seen from figures 1-6, the process parameter (cyan ink solid ink density, D_c) did not follow normal distribution. This could also have been confirmed by Kolmogorov-Smirnov or Shapiro-Wilk test, but there was no need as histograms display it quite clearly. Figure 1 shows the distribution of all results, i.e. measurements from all five zones together. It can be seen that the process was shifted toward the upper specification limit, i.e. its mean $\mu=1,49$ was higher than the nominal value $X_0=1,45$ which results in higher proportion of nonconforming units. The amount of variation was rather high as can be seen from the histogram width. A considerable proportion of results falls outside the specification limits, indicating a rather high proportion of waste. The shape of the histogram is bimodal as two groups of results appear to be dominant. This would generally be less important if the variations were smaller and the results fell within the specification limits. However, it would make the calculation of process capability indexes less accurate as they suppose normal distribution.

Figure 2 shows the distribution of cyan ink SID measured on thirty sheets in zone 1. It can be seen that in this zone, the process was centered as its mean equals the nominal value, $\mu=X_0=1,45$. This means that the fraction of nonconformities is reduced as the process is well centered. The amount of spread (histogram width) was rather high as the results spread wide outside the specification limits. This, however, does not necessarily mean high proportions of waste (relative to other cases in this study) as the distribution is not normal, but leptokurtic.

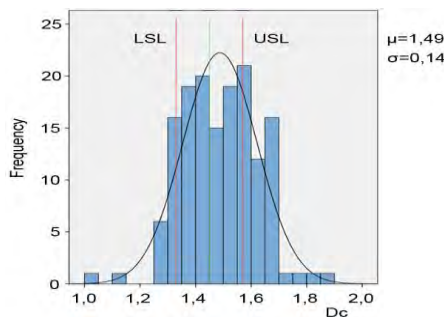


Figure 1: All results

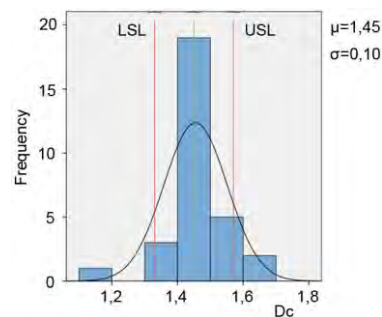


Figure 2: Zone 1

Figure 3 displays the distribution of cyan ink SID in zone 2. The process was only slightly shifted toward the lower specification limit as the shift was $1/12$ of X_0 -LSL range. The spread of results was high as one result appeared far below the LSL. The fraction of nonconformities cannot be evaluated from the histogram as two largest groups overlap with specification limits and we cannot tell how many fall within the limits. The shape of the distribution is not normal.

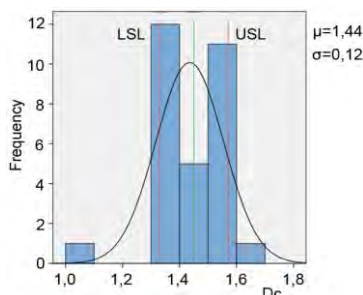


Figure 3: Zone 2

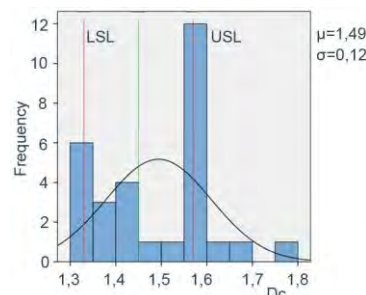


Figure 4: Zone 3

Figure 4 displays the distribution of cyan ink SID in zone 3. The process was shifted toward the USL. The shift was rather large as it equaled $1/3$ of $USL-X_0$ range. It can be seen that this caused a part of the largest group of results to appear outside the USL. The spread of results was the least among the results in this process, but still quite high as all of the groups should fall within the specification limits as they do on well-adjusted processes. The shape, like in other cases, does not follow normal distribution.

Figure 5 shows the distribution of cyan ink SID in zone 4. The process was not centered as its mean shifted more than half the $USL-X_0$ range toward the USL. This, as can be seen in the histogram, caused the largest group of results to appear above the USL. The spread, like in other cases, was quite large as the data range is wider than the specification limits range. Apart from the spread, the variability was second highest in this zone as $\sigma=0,15$. The shape does not follow normal distribution.

Figure 6 shows the distribution of cyan ink SID in zone 5. As can be seen in the histogram, the mean value shift was largest in this zone and equaled $3/4$ of the $USL-\mu$ range. The spread was also largest, as was the amount of variation, $\sigma=0,17$. The shape does not follow normal distribution.

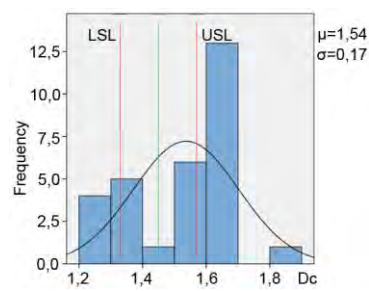
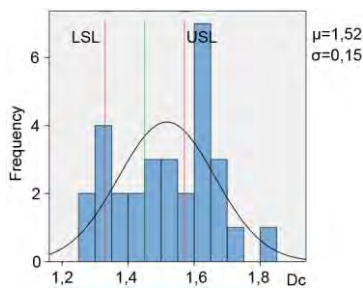


Table 1: Process capabilities by zones

$x_0=1,45$ LSL=1,33 USL= $x_2=1,57$	All values.	Zone 1	Zone 2	Zone 3	Zone 4	Zone 5
n	150	30	30	30	30	30
Min	1,02	1,11	1,02	1,33	1,28	1,26
Max	1,86	1,68	1,69	1,76	1,80	1,86
μ	1,49	1,45	1,44	1,49	1,52	1,54
σ	0,14	0,10	0,12	0,12	0,15	0,17
C_p	0,29	0,40	0,33	0,33	0,27	0,24
C_{pk}	0,19	0,40	0,31	0,22	0,11	0,06
C_{pm}	0,28	0,40	0,33	0,32	0,24	0,21
p_{normal}	41,14	23,02	31,89	34,32	47,27	53,61
p_{Cp}	38,44	23,02	31,74	31,74	42,38	47,16
p_{Cpk}	56,86	23,02	35,76	50,28	74,14	85,72
p_{real}	38,00	13,33	13,33	30,00	66,67	66,67

Table 1 displays the process capability indexes, proportion of nonconformities calculated from approximation with normal distribution and the proportion of nonconformities calculated from the data for all measurements and each of the zones. As it can be seen from the table, the C_{pk} index is lower than C_p index in all of the cases except for zone 1 where process mean equaled the nominal values. This is expected as the C_{pk} index was designed to correct the inherent flaw of C_p of assuming that process mean equals the mean between two specification limits (nominal value). The C_{pm} index was designed to correct the flaw of C_{pk} of overestimating waste by focusing on the range where the process shifted. When compared to C_p and C_{pk} , it can be seen that in this case the C_p index, although it underestimates waste, made smaller errors than the C_{pk} index.

The approximation with normal distribution, as expected, did not align with results from the empirical data as the data did not follow normal distribution. However, it is interesting to note where and how the approximation failed. In zones 1 to 3, where the proportion of nonconformities was relatively small compared to zones 4 and 5, the approximation predicted higher proportion of nonconformities than calculated from the data. In zones 4 and 5 it predicted lower proportion of nonconformities than calculated from the data. The approximation was most accurate for all results put together. This is expected as the sample size is larger, $n=150$, while for single zones the sample size is only $n=30$. However, the approximation of all results together is not particularly useful if the parties agree to follow the ISO process control standard which tolerates 10% SID difference along the sheet. If the customer agreed to assess quality by inspecting overall results, it could happen that some zones contain high amounts of error, but overall results are still acceptable.

The proportion of nonconformities calculated from the empirical data, as stated previously, differs from approximations made with normal distribution. The data was not normally distributed. However, apart from that, it should be pointed out that the proportion of nonconformities calculated from the data holds for a given sample and does not represent the population as approximations with theoretical distributions do. From the results, it can be seen that proportions of nonconformities increase from zone 1 to zone 5. This indicates that the press operator tends to control left side of the sheet more often, neglecting the right side.

5. CONCLUSIONS

Process capability is a very useful mark on well-adjusted processes as it can serve as a starting point for agreements between producers and their customers. However, on unadjusted processes such as one presented in this paper, it can be very misleading if non normal data is assumed to be normally distributed. Furthermore, due to a larger number of measuring parameters (zones) and the demand to keep them equalized within 10% tolerance, the units should be treated as attributes (conforming or nonconforming) and process output modeled by binomial or hypergeometric distribution. Another important aspect is defining a clear quality control procedure. The results in this paper showed how random, undefined control procedure, lead to high proportions of waste because right hand side zones were neglected during inspection.

6. LITERATURE

- [1] ISO 12647-2:2004
- [2] Montgomery, D.: "Introduction to Statistical Quality Control", (Wiley, 2008)
- [3] Engineering Statistics Handbook, URL <http://www.itl.nist.gov/div898/handbook/>

MECHANICAL MODELS FOR CREASING AND FOLDING BEHAVIOUR OF PAPERBOARD AND CARDBOARD: STATE-OF-THE-ART

Rastko Milošević

Faculty of Technical Sciences, Graphic Engineering and Design, Novi Sad

e-mail: rastko.m@uns.ac.rs

1. ABSTRACT

During the process of paperboard and cardboard converting, the board's top ply can break as it folds. To prevent this from happening and to prepare the material for folding, the process of creasing is applied, which defines folding lines and deforms the material plastically. Thus, some delamination occurs in the creasing zone, as a result of which paper plies bend inwards during folding and, therefore, the top ply is not stretched to its failure. There are a few criteria that define a good quality crease: the shape of a creasing zone and the existence of a bending moment-angle curve peak, which must occur before a certain angle is reached. The aim of this paper is to give better understanding and deeper insight into different behaviour of paperboard and cardboard materials during creasing and folding processes. The existing mechanical models for creasing and folding behaviour of these materials are surveyed. Comparisons of the related testing methods are made as well as the assessment of the levels of their reliability. The mechanical models discussed are categorized with respect to its accuracy, complexity and materials on which they can be applied.

Key words: mechanical models, creasing, folding, paperboard, cardboard

2. INTRODUCTION

The topic of this survey is the examination of mechanical characteristics and behaviour of mono-ply graphic materials, paper, as well as laminate (multi-ply) materials: paperboard and corrugated board during creasing and folding processes. This mostly refers to research of out-of-plane (ZD) mechanical response of these materials under various loading states. One of the main problems in paperboard processing is cracking of the top ply of the paperboard or cracking of the printed layer of ink on paperboard's surface during folding operation (Sappi Fine Paper Europe, 2006). With mechanical models which describe creasing and folding behaviour of paperboard, it is possible to overcome this problem because it enables examination of the most influential parameters without a need of making any experiment.

To be able to better understand the mechanical properties of paper based materials, it is very important to have them minutely described in respect of their structure. Paper structure consists of multiple intertwined cellulose fibers which are linked with different adhesive substances. Paperboard is usually multi-ply structures also formed of fibers, connected with the adhesive material. Corrugated board consists of at least two straight plies between which there is a wavy ply that enables high resistance to folding and wear. Due to their structure and manufacturing technology, these graphic materials show complex mechanical behaviour, mostly with highly anisotropic, linear-elastic response under moderate mechanical load and non-linear plastic response under high load. In principle, paper is heterogeneous fiber structure made of different polymers (cellulose, hemicellulose and lignin). Today three basic directions of the materials are recognized which are shown in the Figure 1. and those are: machine direction MD, cross-fiber-direction CD and out-of-plane direction ZD. Fibers enable stiffness and strength via bonds, mutual friction and interweaving between fibers, which is predominantly present in MD that leads to the greater paper stiffness in this direction than in other two principle directions (Beex, 2007).

Mechanical behaviour of paper materials is highly moisture and temperature dependant (due to hydrogen bonds between fibers which can be extended with H₂O molecule chain and as a result they become more flexible). Because of H₂O molecule penetration from ambient air into paper which is in function of temperature, consequently paper features are in function of temperature. Among other things, mechanical characteristics of paper materials depend on history of their elastic-plastic strains. One more aspect of paper which can affect creasing and folding process is the fact that paper behaviour is also time dependent. Arvidsson and Grönvall (2004) cited

by Beex (2007) conducted creep tests upon paper. The creep in paper happens in time framework from a minute or even an hour, however, creasing process time framework is less than one second.

3. CREASING AND FOLDING PROCESSES

Creasing is a mechanical process of producing a linear depression to enable the material to be folded along the line of the crease. This process defines folding lines of a paperboard material in order to reduce its bending moment and prepare it for subsequent process of folding, thus providing graphic products without cracked edges. During folding, the printing substrate is subjected to considerable mechanical stresses and printed areas over the fold may split open (Sappi Fine Paper Europe, 2006). It is considered that good quality crease produce delaminations only in the creasing zone. There are also other parameters affecting the crease quality such as: geometry, penetration depth and speed of the male die, depth and width of the creasing channel, disturbances, strength of ply bonds, structure and thickness of the paperboard, moisture content, history of the material and material properties of the paper and coating. According to Doeve (2007) cited by Beex (2007) creasing zone must be semi-circular, which is called “belly”. Another criterion for a good crease is that the bending moment-angle curve must have peak, and that the peak of bending moment-angle curve must happen before reaching the angle of 30°. But the most decisive factor is a paperboard thickness that is why crease width and depth must correlate the thickness and compressibility of paperboard in order to achieve accurate folding line and limit delaminations only to the creasing zone. Permanent damage, in the form of multiple delaminations, appears as a result of a creasing process whose extent depends on intensity of the process. This type of damage occurs due to interlaminar shear forces as a supplement to in-plane and compressive out-of-plane plastic deformation of the plies.

Nagasawa et al. (2003) cited by Giampieri et al. (2011) carried out an extensive experimental research of coated paperboard creasing, trying to estimate mechanical effects of the creasing parameters. As a first step towards characterization of the creasing process, they defined “nominal initial shearing strain” γ :

$$\gamma = \frac{2h}{W} \quad (1)$$

where h denotes the rule penetration depth and W is the groove width, γ is a nondimensional parameter related to the initial shearing deformation imposed to the paperboard which rise along with the intensity of creasing process.

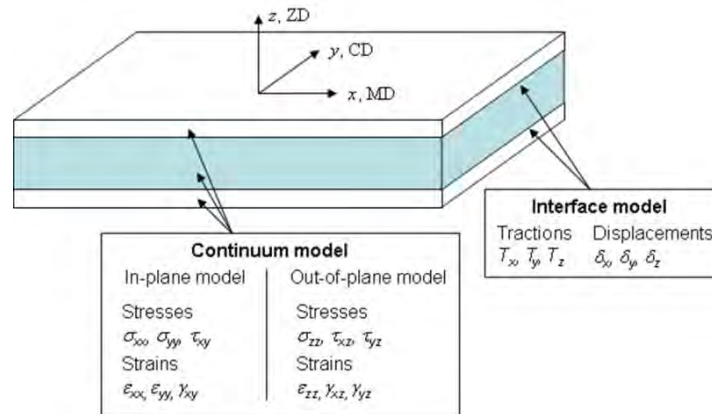


Figure 1: Paperboard numerical model concept with principle material directions, from Huang (2011)

The out-of-plane shear strength is one of the most important material properties for quality control related to creasing and folding. The most common shear test method is the rigid support shear method. Nygård et al. (2007) cited in Huang (2011) proposed the double notch shear test method (DNS) which does not rely on gluing. It uses tensile loading to induce shear failure because of two fabricated notches, one on each side of paperboard. Tensile failure can be induced by the notches when the shear zone is too large and the remaining ligaments are too

thin. To avoid this drawback, the laminated notch shear test (NST) was proposed in Nygård et al. (2009) cited in Huang (2011). The notched test piece is laminated by plastic foil so that tensile failure is avoided, Figure 2.

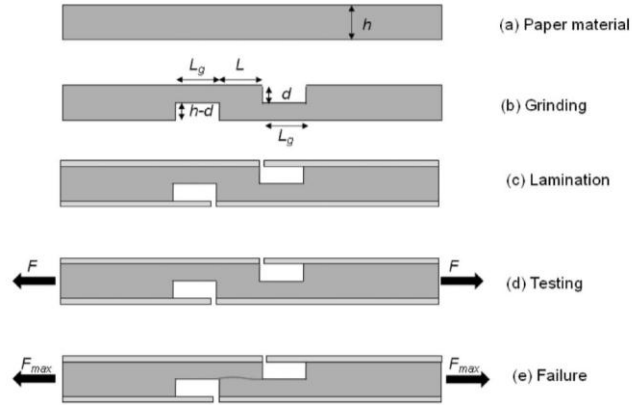


Figure 2: Manufacturing and testing procedure for the laminated notch shear test. (a) Paperboard with thickness h , (b) two grooves are ground, (c) the paperboard is laminated with plastics, (d) tensile testing procedure, (e) failure occurs between the two grooves, from Nygård et al. (2009) cited in Huang (2011)

Alberius and Gerstner (2011) examined the effect of crease depth and displacement, as an unwanted factor, on crease quality of single and four-ply paperboards. Displacement is a measure of distance from the center line of the male die to the edges on the female die, Figure 3. They used the nonlinear finite element method for their model.

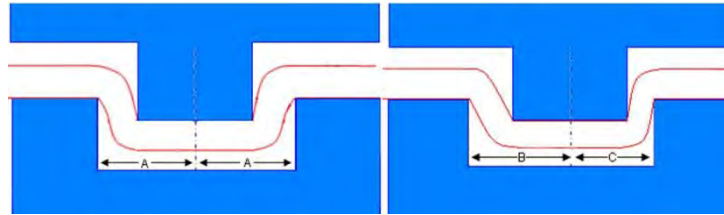


Figure 3: Male and female die centered (left), male and female die with a displacement (right), from Alberius and Gerstner (2011)

They introduced the RCS-value (relative crease strength) which is the relation between the maximum bending force at or below 30 degrees of the creased sample divided by the maximum bending force at or below 30 degrees of the uncreased sample.

$$RCS = \frac{\text{Bending force creased sample}}{\text{Bending force uncreased sample}} \quad (2)$$

For the creasing tests a hydraulic pull tester MTS 858 Table Top System was used, which enabled controlling the web tension, creasing depth and the creasing speed. Afterwards samples were tested in a creasability/bending tester, Lorentzen & Wettre.

Beex and Peerlings (2009) presented finite element mechanical model to describe mechanical response of three-layer laminated paperboard creasing and folding operations. This mechanical model defines mechanism responsible for cracking of paperboard's top ply under too shallow creasing settings. They combined continuum model which describes paperboard behaviour and delamination model which explains delamination processes between different plies. Isotropic plastic behaviour (strain hardening) is described by following stress and strain function:

$$\sigma_y = \sigma_{y0}(1 + A\bar{\varepsilon}_p)^m \quad (3)$$

where:

σ_{y0} - initial reference yield stress,

$\bar{\varepsilon}_p$ - equivalent plastic strain,

A and m - dimensionless hardening parameters.

They also presented cohesion zone model which describes irreversible material behaviour in terms of damage where friction model causes permanent deformation and leads to increasing of maximal shear stress under increasing normal compression. This formulation is characterized by two initially closed surfaces whose opening is governed by traction vector and a separation vector.

$$\lambda = \sqrt{(\delta_n)^2 + \beta^2 \delta_s^2} \quad (4)$$

where:

λ - effective separation,

δ_n , δ_s - normal and tangential component of separation vector,

β - ratio between maximum tangential traction and maximum normal traction.

Curve which shows force change with crease depth enables comparing model prediction with experimentally obtained response results, Fig. 4 a).

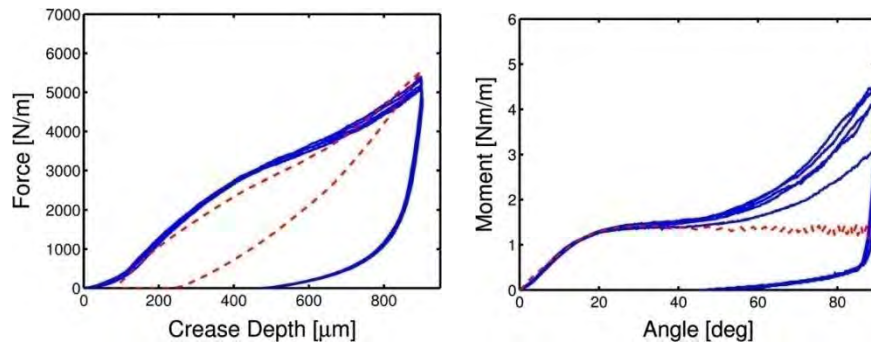


Figure 4: a) The normalized force–crease depth curves obtained from the experiments (solid) and from the numerical analysis of the mechanical model (dashed). b) The normalized moment–angle curves of the experiments (solid) and of the numerical analysis of the mechanical model (dashed), from Beex and Peerlings (2009)

Figure 4. a) shows that matching between mechanical model results and experimental data during unloading is not accomplished. Folding test was conducted by four-point-bending. Until the angle of 40 degrees, calculated response match experimental data perfectly, Figure 4. b). Gooren (2006) investigated three-ply corrugated board behaviour under CD direction creasing process in three different positions of the creasing tool. He used orthotropic (hypo) – elastic model, as well as anisotropic plastic deformation criteria by Hill. In the research, creasing and tensile tests were conducted using SEM method, and DIC (Digital Image Correlation) was used to determine Poisson's coefficients. When the deformation is purely elastic, $D_p=0$, which implies that $D_e=D$.

$$\overset{\circ}{\sigma} = {}^4C : D_e \quad (5)$$

where:

$\overset{\circ}{\sigma}$ - Cauchy stress tensor,

D_e – elastic deformation rate,

4C – the fourth order stiffness tensor.

The yield stress is defined as:

$$\sigma_y = \sigma_y(\sigma_{y0}, \overline{\varepsilon_p}) \quad (6)$$

Hardening modulus H is:

$$\frac{\partial \sigma_y}{\partial \varepsilon_p} = H(\bar{\varepsilon}_p) \quad (7)$$

Effective plastic deformation is:

$$\bar{\varepsilon}_p = \int_{\tau=0}^t \dot{\varepsilon}_p d\tau; \quad \dot{\varepsilon}_p = \sqrt{\frac{2}{3} D_p : D_p} \quad (8)$$

Exponential relation describes this post-yield behaviour in MD well ($A=3900$; $m=0.37$):

$$\sigma_y = \sigma_{y0}(1 + A\bar{\varepsilon}_p)^m \quad (9)$$

Giampieri et al. (2011) presented constitutive, material model of creasing lines mechanical response, which is implemented into final element interface for simulation of the crease presence in the curved shell structure. Model is aimed for full-scale simulation process of making package and also for optimization of different materials creasing process. They paid attention especially to crease depth penetration and material parameters dependence. In the research three types of multi-ply paperboard in MD direction were creased. The optimal creasing proved to be for the initial strain, γ value between 0,610 and 0,880, Figure 5.

The constitutive model is formulated starting from the definition of a Helmholtz free energy density potential ${}^\gamma\psi$ (where the superscript γ on the left of the symbol means that reference is made to a crease line obtained by a creasing process of intensity γ) in the form:

$$\begin{aligned} {}^\gamma\psi = & \frac{1}{2}k_c\eta_c^2 + \frac{1}{2}k_t\eta_t^2 + \frac{1}{2}k_n^+(\eta_n - \eta_n^p)_+^2 + \frac{1}{2}{}^\gamma k_n^-(\eta_n - \eta_n^p)_-^2 \\ & + \frac{1}{2}(1-d){}^\gamma k_{\vartheta c}(\vartheta_c - \vartheta_c^p)^2 + \frac{1}{2}k_{\vartheta n}\vartheta_n^2 \end{aligned} \quad (10)$$

where k_i , $i = c, t, \vartheta_n$ denotes the generalized elastic stiffness, ${}^\gamma k_{\vartheta c}$ and ${}^\gamma k_n^-$ denote the elastic bending and membrane compression stiffnesses which are assumed to be affected by the preceding creasing process, the superscript p denotes the plastic part of the generalized strains and the symbols $(.)_+$ and $(.)_-$ denote the positive and negative parts, respectively, of the contained quantity.

Huang (2011) performed a simple two-dimensional creasing simulation on four-ply paperboard. In the model paperboard was modeled as a combination of an anisotropic elastic-plastic continuum model with isotropic hardening and a softening cohesive interface model.

Huang and Nygård (2011) presented a two-dimensional finite element simulation of four-ply paperboard that was creased and folded. The tilted double notch shear test technique was used to measure the shear strengths for the paperboard interfaces. Creasing simulations were done with a laboratory creasing device, which consists of a female die, a male ruler and two clamps. The folding experiment was executed on the L&W creasability tester (Lorentzen&Wettre).

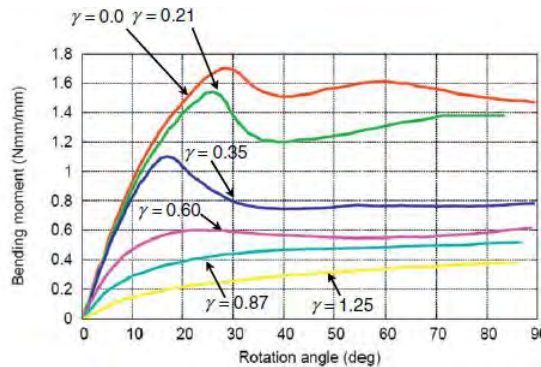


Figure 5: $M_c-\vartheta_c$ – bending tests response for different γ values, from Nagasawa et al. (2003) cited by Giampieri et al. (2011)

To represent deformation and delamination in paperboard a combination of anisotropic continuum and interface models can be used. The continuum model used is an elastic-plastic model with orthotropic linear elasticity, Hill's yield criterion and isotropic hardening. The elastic

model was defined by three elastic moduli E_x , E_y , E_z , three Poisson's ratios ν_{xy} , ν_{xz} , ν_{yz} , and three shear moduli G_{xy} , G_{xz} , G_{yz} .

$$f(\sigma) = \sqrt{F(\sigma_{yy} - \sigma_{zz})^2 + G(\sigma_{zz} - \sigma_{xx})^2 + M(\sigma_{xx} - \sigma_{yy})^2 + \frac{(\sigma_{xx}^0)^2}{(\sigma_{yz}^0)^2} \sigma_{yz}^2 + \frac{(\sigma_{xx}^0)^2}{(\sigma_{xz}^0)^2} \sigma_{xz}^2 + \frac{(\sigma_{xx}^0)^2}{(\sigma_{xy}^0)^2} \sigma_{xy}^2} \quad (11)$$

where σ_{ij}^0 represent the initial yield stresses in the different material directions, and F , G and M values are the constants.

The interface model was described by an orthotropic elastic-plastic cohesive law which relates the interface tractions to the opening and sliding of the interface. Damage initiation was governed by:

$$f^{cohesive}(t) = \max \left\{ \frac{\langle t_n \rangle}{t_n^0}, \frac{t_s}{t_s^0}, \frac{t_t}{t_t^0} \right\} = 1, \quad (12)$$

where t_n^0 , t_s^0 and t_t^0 are the maximum stresses needed to initiate damage in the respective directions, and $\langle \rangle$ indicated that purely compressive stress does not initiate damage. The damage evolution D was defined as:

$$D = 1 - \left\{ \frac{\delta_m^0}{\delta_m^{max}} \right\} \left\{ 1 - \frac{1 - e^{-\alpha \left(\frac{\delta_m^{max} - \delta_m^0}{\delta_m^f - \delta_m^0} \right)}}{1 - e^{-\alpha}} \right\} \quad (13)$$

where α is a non-dimensional parameter that defines the rate of damage evolution, δ_m^{max} is the maximum value of effective displacement during loading history, and δ_m^f is the effective separation at complete failure. The effective displacement δ_m

$$\delta_m = \sqrt{\langle \delta_n \rangle^2 + \delta_s^2 + \delta_t^2}, \quad (14)$$

describes the evolution of damage under a combination of normal and shear separations across the interface. In the model, the stiffness and traction components are deteriorated as the damage evolves according to:

$$K_{nn} = \begin{cases} (1 - D)K_{nn}^0 & t_{nn} \geq 0 \\ K_{nn} & \text{Otherwise} \end{cases}, \quad (15)$$

$$K_{ss} = (1 - D)K_{ss}^0,$$

$$K_{tt} = (1 - D)K_{tt}^0,$$

$$t_{nn} = \begin{cases} (1 - D)t_n^0 & t_{nn} \geq 0 \\ t_n & \text{Otherwise} \end{cases},$$

$$t_s = (1 - D)t_s^0, \quad (16)$$

$$t_t = (1 - D)t_t^0,$$

Nygårds et al. (2009) presented finite element analysis of the three-ply paperboard creasing with the laboratory creasing device. The paperboard was modeled as a multilayered structure with cohesive softening interface model connecting the paperboard plies. The paperboard plies were modeled by an anisotropic elastic-plastic material model. Paperboard exhibits an exponential behavior when it is compressed. Elastic part of the out-of-plane model is linear in tension, at least until the onset of delamination. Therefore, the normal stress, σ_{zz} , was divided into separate compressive and tensile behaviors.

$$\sigma_{zz} = \begin{cases} E_z \varepsilon_{zz}^e & \text{if } \varepsilon_{zz}^e > 0 \\ E_c (1 - e^{-C_c \varepsilon_{zz}^e}) & \text{otherwise} \end{cases} \quad (17)$$

where ε_{zz}^e was the elastic strain in the Z-direction, E_z , E_c , C_c and G were elastic material constants.

4. DISCUSSION

For shallow crease depth the bending moment has a maximum peak value. Also, by increasing the crease depth the peak decreases, and consequently the folding profile becomes smoother (Huang and Nygård, 2011). Both the shear strength values and the through-thickness shear strength profiles are shear zone length dependent. The longer shear zone gave lower shear strength values and more steady profiles, while the shorter shear zones gave higher strength values and more pronounced shear strength profiles (Huang, 2011). The peak moment governs the folding resistance. A reason for lower and sharper peak in the experiments comparing to simulation data is probably because in the simulation all delaminations occurred during creasing, while some creasing zones delaminated only during folding (Xia, 2002). Sometimes a simulation model match the beginning of the creasing tests well, but misses the large crease force peak, which can be due to the fact that simulation does not simulate rising friction between the plies when pressure is added. The two factors affecting the initiation of cracks in the paperboard the most are crease depth and displacement (Alberius and Gerstner, 2011). Unloading part of the creasing behaviour curve is more difficult to capture than loading. In certain cases the experimental data are initially stiffer, which results in bad predictions of the residual indent. It is believed that was due to geometrical description and the friction between the paperboard and the female die. The paperboard properties that have the most influence on creasing response are the out-of-plane shear, out-of-plane compression and the friction between the laboratory creasing device and the paperboard (Nygård et al. 2009). The enormous difference in reload stiffness between numerical and experimental results was noticed, which was probably caused by the fact that the behaviour in ZD was modeled as purely elastic instead of elasto-plastic. The force-displacement curve changes its trend in respect to different crease channel width settings (higher stiffness is achieved using wider creasing channel and for smaller creasing depth settings) (Beex, 2009). For very shallow creasing extensive damage occurs on the tensile side. For very deep creasing, delamination occurs throughout the paperboard depth and extends beyond the width of the initial creasing region (Giampieri et al., 2011). A material model has been proposed to describe the out-of-plane behaviour of paper and found that paper can withstand higher shear loads when it is subjected to compressive loads (Stenberg, 2003).

5. CONCLUSION

Analyzed mechanical models for paperboard and cardboard behaviour during creasing and folding processes accurately capture certain segments of the stress-strain and bending moment-angle curves. On the other hand they are incapable to match the other parts of the curves, especially unloading segments. Beside accuracy of the presented mechanical models, very important property is simplicity (number of required parameters).

Most surveyed mechanical models are projected for the mechanical behaviour description of similar materials, multi-ply paperboard (usually three or four plies). Concerning the experimental methods applied to conduct the tests, most authors use the same commercially available testing equipment for both creasing and folding processes, with a few exceptions, who use laboratory developed devices and certain improved techniques (e.g. laminated notch shear test).

The most suitable material model to describe creasing and folding seem to be the one created by Gooren (2006). This material model uses relatively few material parameters, which speaks in favour of simplicity, and still describes the mechanical behaviour accurately. The other positive aspects are its presence in available software (e.g. ABAQUS) and focusing more on combining material and delamination model, so that the simulations of creasing and folding are correctly predicted.

Acknowledgement

The author would like to thank professor Ivana Kovačić for the support and guidance through the research and also for the valuable advice on the manuscript.

6. LITERATURE

- [1] Alberius D., Gerstner F.: "Investigation of Creases - How the crease is affected by displaced crease plates", <http://lup.lub.lu.se/luur/download?func=downloadFile&recordId=1939973&fileId=1939975>, (2012-19-09)
- [2] Beex L. A. A.: "Creasing and folding of paperboard - LITERATURE SURVEY MT 07.46", <http://www.mate.tue.nl/mate/pdfs/8702.pdf>, (2012-19-09)
- [3] Beex L. A. A., Peerlings R.H.J.: "An experimental and computational study of laminated paperboard creasing and folding", *International Journal of Solids and Structures*, 46, 4192–4207, 2009
- [4] Giampieri A., Perego U., Borsari R.: "A constitutive model for the mechanical response of the folding of creased paperboard", *International Journal of Solids and Structures*, 48, 2275–2287, 2011
- [5] Gooren L.G.J.: "Creasing behaviour of corrugated board: An experimental and numerical approach - Report MT06.06", <http://www.mate.tue.nl/mate/pdfs/6342.pdf>, (2012-19-09)
- [6] Huang H.: "Numerical and Experimental Investigation of Paperboard Creasing and Folding", (Licentiate Thesis No. 111, KTH Royal Institute of Technology, 2011), page 28
- [7] Huang H., Nygård M.: "Numerical and experimental investigation of paperboard folding", *Nordic Pulp & Paper Research Journal* 26 (4), 452–467, 2011
- [8] Nygård M., Just M., Tryding J.: "Experimental and numerical studies of creasing of paperboard", *International Journal of Solids and Structures*, 46, 2493–2505, 2009
- [9] Sappi Fine Paper Europe: "Folding and Creasing - Finishing of Coated Papers after Sheet-Fed Offset Printing", 2006
- [10] Stenberg N.: "A model for the through-thickness elastic-plastic material behaviour of paper", *International Journal of Solids and Structure* 40, 7483–7498, 2003
- [11] Xia Q.S., Boyce M.C., Parks D.M.: "A constitutive model for the anisotropic elastic-plastic deformation of paper and paperboard", *International Journal of Solids and Structures* 39, 4053–4071, 2002

CHARACTERISATION OF FOLD-CRACK RESISTANCE OF COATED PAPERS BY TENSILE AND MULLEN BURST TEST

Magdolna Pál¹, László Koltai², Dragoljub Novaković¹,
Sandra Dedijer¹, Srđan Draganov¹

¹Faculty of Technical Sciences, Graphic Engineering and Design, Novi Sad
²Rejtő Sándor Faculty of Light Industry and Environmental Protection Engineering,
Óbuda University, Budapest

Corresponding author: Magdolna Pal
e-mail: apro@uns.ac.rs

1. ABSTRACT

The folding process is usually resulting in more or less visible cracks along the folding line on the outer side of the coated papers and boards. The basic mechanism of cracking is laying in the appearance of higher stresses on the surface layers when a sheet is folded. These high stresses can lead not only to decrease of the aesthetic feature, but to complete loss of functionality of the final product. Improving the fold-crack resistance of coated papers and boards is one of the basic tasks for paper manufacturers. This study has been conducted in order to analyze the correlation between two basic physical parameters of the folded coated paper: residual tensile strength and bursting strength. The residual tensile strength testing is one of the most commonly used fold-crack resistance testing methods, but since the specimens during the bursting strength testing have curved configuration, the bursting strength of unfolded and folded coated papers may provide additional relevant information about stress states on the outer layers of the paper.

Key words: coated papers, fold-crack resistance, residual tensile strength, bursting strength

2. INTRODUCTION

The folding process is a commonly used post-press operation in the graphical production. It is applied in the production of books, magazines, brochures, leaflets, etc. The fold behaviour of printed substrates is of great importance for the visual appearance of the printed products as well as for their mechanical behaviour (Annon, 2006). A good fold is expected to be at the right position and free of damage on the surface and in the paper. In the folding process, papers or other substrates are subjected to very high tensile stresses on the outer layers and these stresses can lead to surface cracks (annoying white lines on the folding lines). Coated papers are more sensitive to surface cracking than uncoated papers, since the coating layer is not as flexible as the base paper. In extreme cases of surface damages the base stock fibre itself may be weakened and a significant loss of tensile strength can be observed (Barbier et al., 2002; Eklund et al., 2002; Rättö and Hornatowska, 2010).

There are many factors that influence surface cracking during the folding process which are related to the paper manufacturing, to printing and converting processes. Although the surface cracking is an important phenomenon (the surface damaging in the folding process, it's experimental and numerical analysis were subject of several papers published in the last 40 years which are summarized by Barbier (Barbier, 2004) just a few methods are available to quantitatively characterize the amount of cracking (Rättö et al., 2011). The residual tensile strength of coated papers after the folding process is one of the most widely used test methods for fold-crack resistance evaluation and prediction. It has been developed based on a simple subjective assessing method, mostly used in the newspaper pressroom: after the folding process, the machine operator opens up the folded sheet and places it flat on a table, and applies tension on either side of the folded region with hands to assess the strength of the fold (Barbier, 2004; Salminen et al., 2008; Alam et al., 2009; Yang and Xie, 2010). As a new testing method, the modified Mullen burst test was proposed by Popil (Popil, 2010) for white top linerboards, which was suggested based on the measurement of stretch-to-break for specimens tested in curved configuration, accordingly to the paper's shape during the folding process. The concept of the proposed method has been verified by the obtained results from other testing

methods described by Popil (Popil, 2010). However, the applicability of proposed method for the fold-crack resistance measurement of coated paper remains to be investigated. Therefore, the aim of this investigation was to experimentally determine and evaluate the correlation between the residual tensile strength and stretch-to-break of coated papers.

3. MATERIALS AND METHODS

3.1. Samples of coated papers

The experiment was performed on commercially used glossy coated papers for offset printing with five different basis weights: 90 g/m², 115 g/m², 130 g/m², 150 g/m² and 170 g/m² (Fedrigoni, Italy). The sample papers were selected with the same base stock composition (fibre mixture of the coated paper's core), coating weight and composition in order to simulate the increasing tendency of the surface damages. All samples were printed in solid tone on KBA Rapida 75 offset machine using standard cyan ink (Sun Chemical). The printing was applied in order to measure the damaged surface area in the second phase of the planned investigation and has no direct function in this work. The folding process was performed on Horizon AFC546AKT folding machine, using one buckle folding unit with standard fold rollers (combination of soft polyurethane foam rubber and steel roller) and roller gap adjustment. 50 samples of each paper grade were folded in machine and cross direction of paper grain at standard conditions (temperature of 23 °C, relative humidity of 55%) 48 hours after printing.

3.2. Residual tensile strength

The fold-crack resistance was evaluated as the residual tensile strength after the coated paper has been folded. The residual strength test method was developed to measure the ratio of tensile break-up-strength of paper after and before the folding. The residual tensile stress of the samples is determined by the loss of the strength at the folding process and defined as :

$$RTS = FTS / UTS * 100 (\%) \quad (1)$$

Where: RTS - *residual tensile strength*,
 FTS - *folded tensile stress at break*,
 UTS - *unfolded tensile stress at break*.

Four groups of specimens were prepared. Two groups were cut to a size 15x100 mm in both directions of the paper grain: one in machine and the other one in cross direction (according to the ISO standard ISO 1924-1:1983). The other two groups of samples were first folded in both grain directions and then cut to the specimen's size defined above, while the folding line on the samples was always parallel with the shorter side of the specimens (i.e. the tensile stress at break was measured perpendicular to the folding line). The tensile strength tests were performed on Frank tensile testing machine (type 800A, No. 10, Karl Frank GMBH), at room temperature and standard relative air humidity, with constant speed of traction displacement (30 and 40 mm/min). Fifteen samples were measured for each grain, folding line and paper grade combination. It has to be mentioned, that the tensile strength measured in paper industry is not a true tensile strength, since it measures the breaking load per unit width rather than per unit of area. It is due to the porosity of paper structure and for the ordinary purposes tensile strength as measured in paper industry is indicative enough of the utility of the paper, since the paper is generally used in sheet forms.

3.3. Stretch-to-break measurement using Mullen burst method

The stretch to break measurement of specimen in curved geometry is based on the analysis of the theoretical relationships between bursting strength and tensile properties of the paper. Although the bending and shear stresses are induced in the specimen deformation as well as direct tension stresses (due to stretching in the middle plane of the specimen), but for thin sheets at relatively large deflections the bending and shear stresses are small in comparison to the direct tension stresses and may be neglected. Hence, bursting strength is primarily dependent on the tensile strengths and stretches of the sheet in the machine - and cross-

directions. With suitable approximation the strain on the sample's surface could be used to relate bursting strength to tensile strength and stretch. Based on Van den Akker unpublished work, the following relation was proposed by Popil (Annon., 1963; Annon., 1966; Popil, 2010):

$$\varepsilon \approx \left(\frac{rP}{T_{CD} + T_{MD}} \right)^2 \quad (2)$$

where: T_{MD} – tensile strength in MD (machine) direction,
 T_{CD} – tensile strength in CD (cross) direction,
 r – radius of rubber diaphragm orifice.

Equation (2) suggest that the combination of the measurements of Mullen burst pressure P and tensile strength in both grain directions of paper could be used to measure the stretch-to-break for a specimen in curved geometry. The tensile strengths in MD and CD direction were derived by standard tensile testing method (defined in previous section). The bursting strength measurements were measured according to the TAPPI standard (T 403 om-97), using a Mullen BURST-O-MATIC apparatus (Lorentzen & Wettre, Sweden) with bursting time of 10 sec, compressor pressure of 8-12 kp/cm^2 . Ten samples were measured for each paper grade.

4. RESULTS

The obtained results for tensile strength of folded and unfolded samples in machine and cross directions are presented in Figure 1a and 1b, respectively.

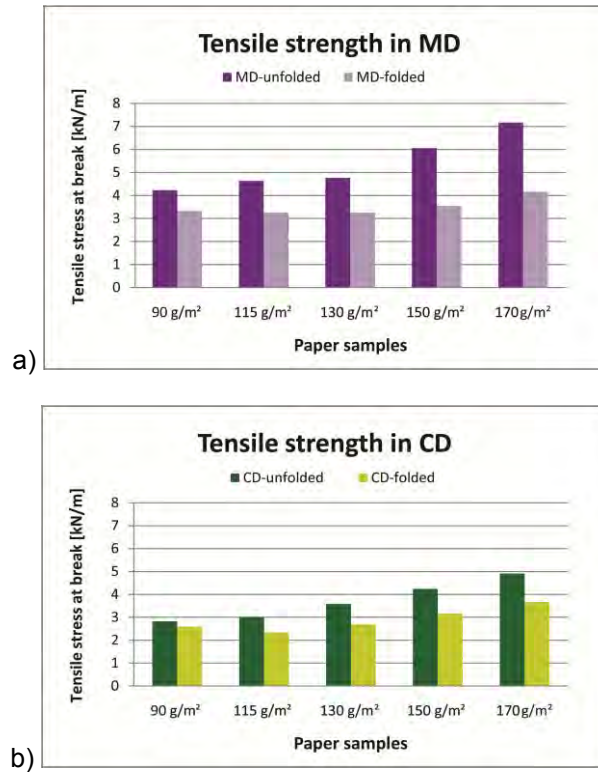


Figure 1: The tensile stress at break in machine (a) and cross (b) direction of paper grain

As it was expected based on the literature findings (Barbier et al., 2002; Salminen et al., 2008; Alam et al., 2009; Yang and Xie, 2010) the tensile strength of unfolded paper is increasing with the basis weight of the samples and it has higher value in machine then cross direction. Similar situation can be noticed for the folded samples: the tensile strength has higher values in machine direction and has increasing tendency with the basis weight. However, the differences between the folded and unfolded samples in machine and cross directions were diverse: on the samples tested in machine directions, a folding line is perpendicular to paper grain direction and therefore suffered greater surface damages and had greater loss of strength than the samples

folded parallel with machine direction and tested in cross direction. These differences in tensile strength loss are presented in Figure 2a and 2b by the residual tensile strength against the basis weight of the samples. Samples folded in cross direction have linear trend with correlation coefficient of 0.948, where the residual tensile strength has decreasing tendency with increasing of the basis weight. Whereas, samples folded in machine direction have lower correlation coefficient (0.681) for linear trend, which could induce that the folds made parallel to machine direction of the paper grain cause less damage for lower basis weights. The correlation is expected to be more significant for paper or paperboard with higher basis weight.

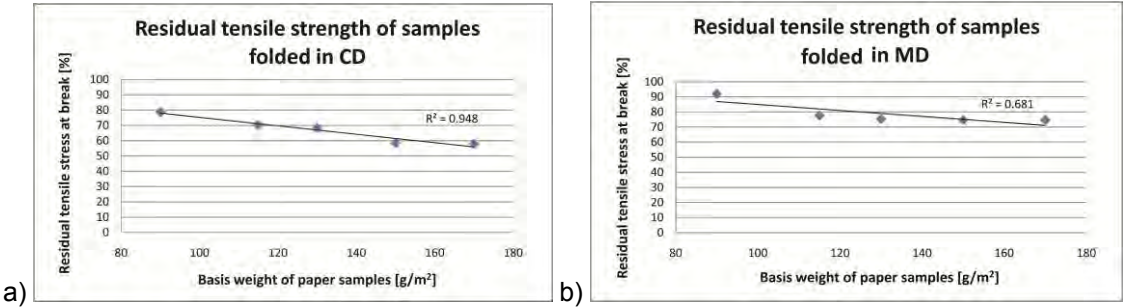


Figure 2: Residual tensile strength of samples folded in cross (a) and machine (b) direction of paper grain

Figure 3 shows the results of Mullen burst strength testing in function of the basis weight of the examined papers. As it was expected the burst strength has increasing tendency with increasing of basis weight. These values in combination with the tensile strength were used in equation (2) to obtain the stretch-to-break values, which are shown in function of the basis weight in Figure 4. The obtained results have similar tendency as Mullen burst strength, however, there is less differences between the values by changes in basis weight and therefore the correlation coefficient of linear regression is lower too.

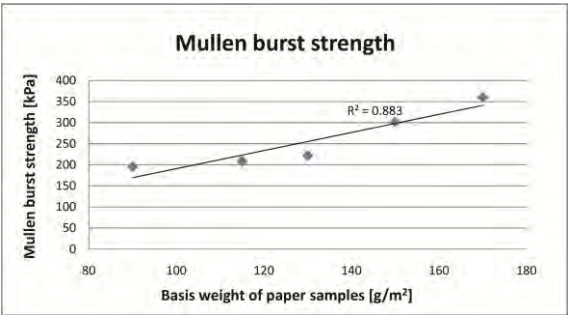


Figure 3: Mullen burst strength of samples

In Figure 5a and 5b are the plots of stretch-to-break values calculated from the Mullen burst test results versus residual tensile strength of samples folded in cross and machine directions, respectively.

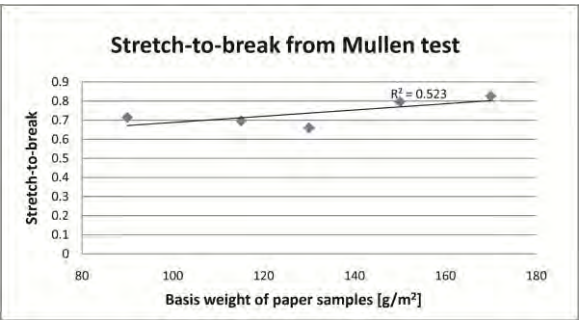


Figure 4: Stretch-to-break from Mullen test

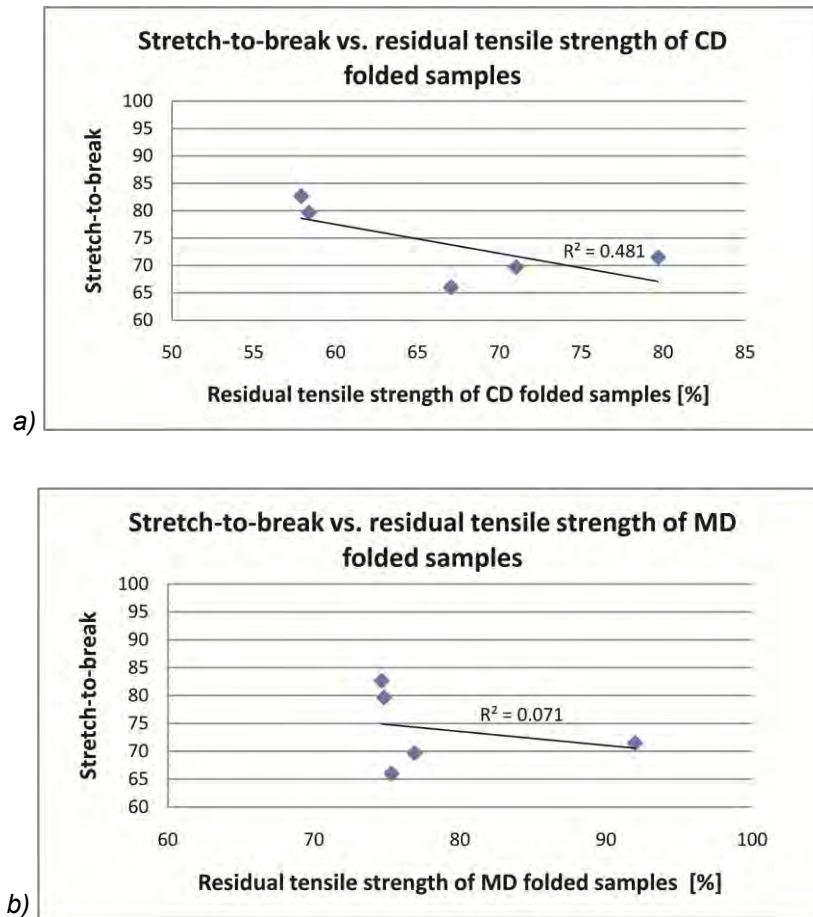


Figure 5: Stretch-to-break vs. residual tensile strength samples folded in cross (a) and machine (b) direction of paper grain

From the linear regression of data points it can be seen that for samples folded in cross direction the stretch-to-break correlate well with the residual tensile strength, except of one outlying value which is derived for sample of basis weight of 130 g/m². Opposed to cross direction folded samples, the samples folded in machine direction show a fairly low correlation, since for similar values for residual tensile strength, the stretch-to-break varies very significantly.

5. CONCLUSIONS

The folding process is one of the most common operations in the graphical production and the fold behaviour of printed substrates is of great importance for the visual appearance of a printed product. There are many factors that influence surface cracking during the folding process which are related to the paper manufacturing and to printing and converting processes. Although the surface cracking is an important phenomenon just a few methods are available to quantitatively characterize the amount of cracking. The residual tensile strength of coated papers after the folding process is one of the most widely used test methods for fold-crack resistance evaluation and prediction. A new testing method, based on Mullen burst test was proposed for white top linerboards. The aim of this investigation was to experimentally determine and evaluate the correlation between the residual tensile strength and stretch-to-break of coated papers. The derived results showed well correlation for samples folded in cross direction with exception of one outlying value which should be further investigated. Opposed, the results for machine direction folded samples showed almost no correlation. As a conclusion it can be conducted that the stretch-to-break measurement based on the pressure from Mullen burst test can be used for fold-crack resistance evaluation, but with limitations.

Acknowledgments

This work was supported by the Serbian Ministry of Science and Technological Development, Grant No.: 35027 "The development of software model for improvement of knowledge and production in graphic arts industry".

6. LITERATURE

- [1] Anon., 1963. Investigation of an improved device for evaluating the cracking potential of linerboard, Preliminary Report, Project 1108-28, The Institute of Paper Chemistry, Appleton, Wisconsin, USA
- [2] Anon., 1966. An investigation of linerboard cracking, Summary Report, Project 1108-28, The Institute of Paper Chemistry, Appleton, Wisconsin, USA
- [3] Anon., 2006. Folding and creasing, Sapp's Technical brochures, 2nd, revised edition, [Online] Available from: <http://www.sappi.com/NR/rdonlyres/F3F8F3B0-89B8-4528-9684-7D40C7A5817A/0/FoldingandCreasing.pdf> [Accessed 20th April 2008].
- [4] Alam, P., Toivakka, M., Carlsson, R., Salminen, P., Sandås, S., 2009. Balancing between Fold-crack Resistance and Stiffness, *Journal of Composite Materials*, Vol. 43, No. 11, pp. 1265-1283.
- [5] Barbier, C., Larsson, P.-L., Östlund, S., 2002. Experimental investigation of damage at folding of coated papers, *Nordic Pulp and Paper Research Journal*, Vol. 17, No. 1, pp. 34-38
- [6] Barbier, C. (2004) On Folding of Coated Papers, Doctoral Thesis no. 56, Royal Institute of Technology, Department of Solid Mechanics, Stockholm, Sweden, [Online] Available from: http://www.t2f.nu/s2p2/S2P2_MS_9%20.pdf [Accessed: 18th April 2008].
- [7] Eklund, J., Österberg, B., Eriksson, L., Eindenvall, L., 2002. Finishing of digital prints – a failure mapping, *Proceedings of the International Congress on Digital Printing Technologies, IS&T NIP 18*, San Diego, California, USA, pp. 712-715, [Online] Available from: www.t2f.nu/t2frapp_f_56.pdf [accessed: 5th May 2008].
- [8] International Standard Office, 1983. ISO 1924-1:1983 - Paper and board -- Determination of tensile properties - Part 1: Constant rate of loading method, ISO.
- [9] Popil, R. E., 2010. Prediction of Fold-Cracking Propensity through Physical Testing, In *Tappi PaperCon Conference*, Atlanta, GA, USA, [Online] Available from: <http://www.tappi.org/Downloads/Conference-Papers/2010/PaperCon-2010-Conference/10PAP101.aspx> [Accessed 19 August 2011].
- [10] Rättö, P., Hornatowska, J., 2010. The influence of coating colour composition on the crack area after creasing, *Nordic Pulp and Paper Research Journal*, Vol. 25, No. 4, pp. 488-494.
- [11] Rättö, P., Hornatowska, J., Changhong, X., Terasaki, O., 2011. Cracking mechanisms of clay-based and GCC-based coatings, *Nordic Pulp and Paper Research Journal*, Vol. 26, No. 4, pp. 485-492.
- [12] Salminen, P., Carlsson, R., Sandas, S., Toivakka, M., Alam, P., Roper, J., 2008. Combined Modeling and Experimental Studies To Optimize The Balance Between Fold Crack Resistance And Stiffness For Multilayered Paper Coatings – Part 2: Pilot Coater Experimental Studies, In *Tappi PaperCon Conference*, Dallas, TX, USA.
- [13] Technical Association of the Pulp and Paper Industry, 1997. T 403 om-97-Bursting strength of paper, Physical Properties Committee of the Process and Product Quality Division, TAPPI.
- [14] Yang, A., Xie, Y., 2011. From Theory to Practice: Improving the Foldcrack Resistance in Industrially Produced Tripple Coated Paper, In *Tappi PaperCon Conference*, Covington, Kentucky, USA, pp. 1845-1858.

POSSIBILITY OF USING CARDBOARD MILL SLUDGE IN IMMOBILIZATION OF COPPER FROM CONTAMINATED SEDIMENT

Miljana Prica¹, Božo Dalmacija², Vesna Pešić², Rastko Milošević¹, Bojan Banjanin¹,
Vladimir Zorić¹, Savka Adamović¹

¹Faculty of Technical Sciences, Graphic Engineering and Design, Novi Sad

²University of Novi Sad, Faculty of Sciences and Mathematics, Department for
Chemistry, Biochemistry and Environmental Protection,
Section for Chemical Technology and Environmental Protection, Novi Sad

Corresponding author: Miljana Prica
e-mail: miljana@uns.ac.rs

1. ABSTRACT

Pulp, paper and cardboard mills typically generate significant quantities of non-hazardous solidwaste which requires management as a waste material or as a by-product. Most of these solids are removed after primary mechanical treatment, resulting in a sludge that contains large quantities of fibers, papermaking fillers, or both. Although this primary sludge is commonly landfilled, it could be recycled into on-site production, reused in other pulp and paper mills, or used in other products. In this study the use of cardboard mill sludge as stabilizing agent in the stabilization treatment of copper polluted sediment was examined. Semi-dynamic leaching test was conducted to assess the effectiveness of stabilization treatment with cardboard mill sludge and long-term leaching behavior of copper. A diffusion-based model was used to elucidate the controlling leaching mechanisms. It appears applied treatment was effective in immobilizing copper, with diffusion being the controlling mechanism. This indicates that slow leaching of Cu could be expected when the cardboard mill sludge as stabilizing agent was applied.

Key words: copper, cardboard mill, sludge, contaminated sediment

2. INTRODUCTION

Paper and cardboard mill sludge is generated by various processes in the production of paper and cardboard, and increasing quantities produced make the disposal of this sludge a problem (Calace et al., 2005). Waste is mainly generated from pulping, deinking unit operations and wastewater treatment. The amount and the composition of the waste depends on the paper and cardboard grade produced, the raw materials used, the process techniques applied and the properties achieved.

Pulp, paper and cardboard mill wastewater treatments typically include a primary treatment consisting of neutralization, screening, and sedimentation to remove suspended solids, which are then dewatered into a sludge that requires disposal (European waste catalogue code 03 03, 94/3/EC no. L 5/15). Less frequently, secondary and tertiary treatments are included to reduce the organics content of wastewater and destroy toxic organics and color. Pulp, paper and cardboard mill primary sludge contains wood fibers as the principal organic component, as well as papermaking fillers (inorganic materials such as kaolin, CaCO₃, TiO₂, etc.), pitch (wood resin), lignin by-products, inert solids rejected during the chemical recovery process, and ash. This primary sludge is managed as a waste material or as a by-product (World Bank, 2007). Mills produce varying amounts of primary sludge, and the sludges they produce are distinctly different in composition, even between mills using the same manufacturing process. Although the industry uses in-mill loss-control measures as the primary means of recovering raw materials, the production of dry sludge is approximately 4.3% of the final product, increasing to 20–40% in the case of recycled paper mills. The primary methods of disposal for this type of sludge have been land application and landfilling. Landfilling costs in the EU are rising because of increasingly stringent regulations, taxes, and declining capacity (Ochoa de Alda, 2008).

With landfill space becoming scarce and expensive, some sludges are being burned or incinerated to reduce their volume and to recover part of the energy they contain.

Recommended wastewater reduction methods include the recycling of wastewater with simultaneous recovery of fibers (World Bank, 2007). The most common technique for reclaiming fiber is to recycle primary sludge back into the fiber-processing system of the mill. Some

recycled paper and cardboard mills and some manufacturers of unbleached and bleached pulp, paper and cardboard have reduced sludge volume by reclaiming the fiber, fillers, or both in sludge to be reused within their pulp, paper and cardboard making processes. Effluents from machines, bleach plants, and various cleaning and screening operations are also targets for fiber reclamation. Other wastewaters such as those from wood handling or chemical recovery systems usually contain non-fibrous contaminants which can become problematic in fiber-recovery systems unless cleaning systems are used. Bark, lime solids, dregs, grits, and dirt are some examples of contaminants, which should be avoided whenever possible. Because the presence of sludge can decrease the quality of the final product, the reuse of sludge in pulp, paper and cardboard making processes is not always possible in the same company where it is generated, and consequently a management alternative is required vicinity of the pulp, paper and cardboard mills, which in turn will determine the cost of the different options. An increase in the number of management alternatives will improve the feasibility of reusing sludge in a more sustainable manner.

In this study cardboard mill sludge was used as a stabilizing agent in the immobilization of copper from contaminated sediment. Currently in Serbia, dredged sediment, contaminated or non-contaminated and cardboard mill sludge are mainly deposited in landfills.

Use of paper and cardboard mill sludges could be a good practice for sediment remediation with this treatment. The paper and cardboard mill sludge's could be effective because of their organic matter, silicate and carbonate content. Organic matter is able to form stable complexes with several metals; the silicates are materials of high cation exchange capacity (CEC) and the bicarbonate/carbonate system is able to increase the pH value of soil. These chemical features were able to reduce the harmful mobile metals in polluted soils when the paper mill sludge was added to them (Calace et al., 2005).

The mechanisms governing heavy metals leachability of contaminants from waste forms and evaluation of the long-term behaviors of wastes can be effectively examined using the American Nuclear Society's (ANS) semi-dynamic leaching test (ANS, 1986). Based on the results of this test the controlling leaching mechanisms of copper in untreated and treated sediment samples could be defined.

3. MATERIALS AND METHODS

Pseudo-total copper concentration in sediment was $316 \pm 12 \text{ mg kg}^{-1}$. According to the Dutch regulation standards, sediment is polluted with copper (class 4). Class 4 sediments are of unacceptable quality and need most urgent actions, dredging, disposal in special storage reservoirs, and, if possible, sediment clean-up measures (Ministry of Housing, Spatial Planning and Environment Directorate, 2000).

Chemical characterisation of cardboard mill sludge used was: pH 8.6 ± 0.3 , CEC $14.8 \text{ (cmol kg}^{-1}\text{)}$, water content 19%, organic matter 31%, carbonates 25%, silicates 47%, Cu 1.2 mg kg^{-1} . The sludge was dried, crushed and passed through a 2.0 mm sieve, then characterised and used in the experiment.

Sediment and cardboard mill sludge were dried at 105°C to a constant mass. The sediment and cardboard mill sludge were mixed in proportion of 95:5 (M1), 90:10 (M2), 80:20 (M3), 70:30 (M4) and 50:50 (M5) by wt. Samples were prepared in the form of monolithic cubes ($(3 \pm 0.1) \times (3 \pm 0.1) \times (3 \pm 0.1) \text{ cm}$) by compaction. The compaction was performed according to ASTM D1557-00 (2000), providing a compactive effort of 2700 kN m m^{-3} . Samples were cured for 28 days at 20°C in sealed sample bags and then subjected to the ANS 16.1 leaching test. Deionized water (DI) was used as a leachant.

Copper concentration was determined on ICP-MS (Perkin Elmer Sciex Elan 5000) according to standard procedures (NEN 5758:1990).

4. RESULTS AND DISCUSSION

The long-term leachability of copper from the sediment-cardboard mill sludge mixtures was evaluated using the ANS method 16.1 (ANS, 1986). By applying this test we get the cumulative fraction of copper leached versus time. The ANS has standardized the Fick's law-based mathematical diffusion model as follows:

$$D_e = \pi \left[\frac{\frac{a_n}{A_0}}{(\Delta t)_n} \right]^2 \left[\frac{V}{S} \right]^2 T_n \quad (1)$$

where a_n is the contaminant loss (mg) during the particular leaching period with subscript n ; A_0 is the initial amount of contaminant present in the specimen (mg); V is the specimen volume (cm^3); S is the surface area of specimen (cm^2); Dt_n is the duration of the leaching period in seconds; T_n is the time that elapsed to the middle of the leaching period n (s), and D_e is the effective diffusion coefficient ($\text{cm}^2 \text{s}^{-1}$).

The relative mobility of copper can be evaluated by this coefficient, which varies from $D_e = 10^{-5} \text{ cm}^2 \text{s}^{-1}$, (very mobile) to $D_e = 10^{-15} \text{ cm}^2 \text{s}^{-1}$ (immobile).

Diffusion coefficients D_e for treated samples, computed by Eq. (1), are listed in Table 1. The mobility of copper in this study was reduced by treatment. The diffusion coefficients for metals in treated samples ranged from $10^{-11} \text{ cm}^2 \text{s}^{-1}$ to $10^{-12} \text{ cm}^2 \text{s}^{-1}$ (low mobility). The treatment employed is considered efficient.

Table 1. Diffusion coefficient D_e ($\text{cm}^2 \text{s}^{-1}$) for untreated (SO) and treated sediment samples (M1, M2, M3, M4, M5) after ANS 16.1 test completion

	SO	M1	M2	M3	M4	M5
$\overline{D_e}$	$5.54 \cdot 10^{-7}$	$6.21 \cdot 10^{-11}$	$5.37 \cdot 10^{-11}$	$4.61 \cdot 10^{-12}$	$3.81 \cdot 10^{-12}$	$2.77 \cdot 10^{-12}$

The type of leaching mechanism that controls the release of metals can be determined based on the values of the slope of the plot of the logarithm of cumulative fraction release, $\log(B_t)$, versus the logarithm of time, $\log(t)$:

$$\log(B_t) = \frac{1}{2} \log(t) + \log \left[U_{\max} d \sqrt{\left(\frac{D_e}{\pi} \right)} \right] \quad (2)$$

where D_e is the effective diffusion coefficient in $\text{m}^2 \text{s}^{-1}$ for component x ; B_t is the cumulative maximum release of the component in mg m^{-2} ; t is the contact time in seconds; U_{\max} is the maximum leachable quantity in mg kg^{-1} , and d is the bulk density of the product in kg m^{-3} .

When the slope of the plot of the logarithm of cumulative fraction release, $\log(B_t)$, versus the logarithm of time, $\log(t)$ is close to 1 (0.60-1), the process is defined as dissolution. In that case, the dissolution of the material proceeds faster than the diffusion. If the slope of the plot of the logarithm of cumulative fraction release, $\log(B_t)$, versus the logarithm of time, $\log(t)$ is around 0.50 (0.40-0.60), the release of heavy metals will be slow and diffusion will be the controlling mechanism. If the slope is less than 0.40 the release of metal will be probably due to surface wash-off (de Groot and van der Sloot, 1992).

All slopes of the plot of the logarithm of cumulative fraction release, $\log(B_t)$, versus the logarithm of time, $\log(t)$ and R^2 (correlation coefficient) values obtained from the diffusion model are presented in Table 2.

Table 2. Slope and R^2 values obtained from the diffusion model for untreated (SO) and treated sediment samples (M1, M2, M3, M4, M5)

	SO	M1	M2	M3	M4	M5
Slope	0.22	0.41	0.42	0.59	0.48	0.51
R^2	0.99	0.98	0.96	0.99	0.99	0.96

The slope values of the plot of the logarithm of cumulative fraction release, $\log(B_t)$, versus the logarithm of time, $\log(t)$ for mixtures were in the range from 0.41 to 0.59 for all treated samples. That indicates diffusion is the dominant leaching mechanism. Further research should be focused on a more detailed analysis aiming at the elucidation of the encapsulation of copper into

the structure and its leaching mechanism, relying on the studies of mineralogy (qualitative and quantitative X-ray diffraction) as well as micromorphology (scanning electron microscopy and optical microscopy).

5. CONCLUSION

The immobilization treatment with cardboard mill sludge applied appeared to be efficient in the remediation of sediment contaminated with copper based on the diffusion coefficients. In all samples the controlling leaching mechanism of copper upon the treatment appeared to be diffusion. Hence, only small amounts of copper could be expected to leach into the environment over time.

Managing cardboard mill sludges in a sustainable manner requires the availability of a wide spectrum of recycling alternatives and treatment methods to enable the determination of the most economically feasible solution. We should keep in mind that all the sludges cannot be managed in the same way because their characteristics differ depending on the industrial process and mill that produced them. The management options should be considered on a case-by-case basis because various sludges can be added to various paper and cardboard grades.

Cardboard mill sludge utilization to “remediate” a contaminated sediment could be an interesting approach as a management option especially in combination with some materials that could develop the final product potentially useful in some areas.

Acknowledgement

The authors acknowledge the financial support of Provincial Secretariat for Science and Technological Development No. 114-451-1985.

6. LITERATURE

- [1] ANS (American National Standard) ANSI/ANS 16.1. American National Standard for the Measurement of the Leachability of Solidified Low-Level Radioactive Wastes by a Short-Term Tests Procedures, American National Standards Institute, New York, NY, 1986.
- [2] ASTM D1557-00 Standard test method for laboratory compaction characteristics of soil using modified effort American Society for Testing Materials, Annual Book of ASTM standards: ASTM D1557-91, ASTM, Philadelphia, 4.08, 2000.
- [3] Calace N., Campisi, T., Iacondini, A., Leonia, M., Petronio, B.M., Pietroletti, M.: “Metal contaminated soil remediation by means of paper mill sludges addition: chemical and ecotoxicological evaluation”, *Environment Pollution*, 136, 485-492, 2005.
- [4] de Groot G.J., H.A. van der Sloot: “Determination of leaching characteristics of waste materials cadmiuming to environmental product certification, in: T.M. Gilliam, C.C. Wiles (Eds.), *Stabilization and Solidification of Hazardous, Radioactive, and Mixed Wastes*”, ASTMSTP 1123, American Society for Testing Materials, Philadelphia, PA, 2, 149–170, 1992.
- [5] Ministry of Housing, Spatial Planning and Environment Directorate-General for Environmental Protection: “Circular on target values and intervention values for soil remediation”, *Netherlands Government Gazette* No. 39, 2000.
- [6] NEN 5758:1990 – “Determination of copper content by atomic absorption spectrometry (flame technique)”
- [7] Ochoa de Alda, Jesus A.G.: “ Feasibility of recycling pulp and paper mill sludge in the paper and board industries”, *Resources, Conservation and Recycling* 52, 965–972, 2008.
- [8] World Bank. Environmental, health, and safety guidelines for pulp and paper mills. Draft technical document. Washington, DC: Environment and Social Development Department, International Finance Corporation; 2007.

